2015-06-15

Novel toll-like receptor 4 ligands: synthesis, biological studies and applications in molecular vaccines

Lewicky, Jordan David

Novel Toll-Like Receptor 4 Ligands: Synthesis, Biological Studies & Applications in Molecular Vaccines

Jordan David Lewicky

Lakehead University
Thunder Bay, Ontario

A dissertation submitted in partial fulfillment of the requirements of the degree of Doctor of Philosophy in Biotechnology

ABSTRACT

Lipid A, a unique disaccharide glycolipid, is the active principle of Gram-negative bacterial lipopolysaccharide in activating the innate immune response via Toll-like receptor 4 (TLR4). Given the important role that TLR4 plays in innate immunity, and ultimately, the development of an adaptive immune response, ligands that can modulate TLR4-mediated signalling have great therapeutic potential as both vaccine adjuvants, and anti-sepsis agents. In attempting to develop novel ligands which can successfully modulate TLR4-mediated signalling in a well defined fashion, simplified structures which aim to mimic the natural lipid A structure have shown great promise.

The notion of cancer immunotherapy, in which the vast power of the immune system is tapped to prevent and/or eradicate the disease has begun to garner considerable attention. Tumour associated carbohydrate antigens, carbohydrate containing epitopes which are either unique of over-expressed by cancer cells, are viable targets of said immunotherapy. A major limitation, however, is the low antigenicity displayed by these carbohydrate epitopes. Studies have shown that the inclusion of adjuvant structures, especially when directly chemically conjugated to the antigen, improve the success of anti-cancer vaccination efforts.

The primary goal of this study has been aimed at the development of novel vaccine adjuvants, specifically the design of novel molecular frameworks to mimic the structure of lipid A in the activation of TLR4. A secondary goal of this study has aimed at the

application of successful novel lipid A mimics as the immunostimulatory component of self-adjuvanting carbohydrate antigens for use in therapeutic cancer vaccines.

One novel molecular framework that has been designed and synthesized employs a flexible, acyclic diethanolamine-based scaffold to mimic one of the sugar moieties natural to the lipid A disaccharide. Several structural variations of this framework were generated for structure-activity relationship studies in an effort to maximize immunostimulatory potency. The mimics were evaluated *in vitro* for their ability to induce TLR4-mediated cytokines. All variations showed confirmed TLR4 stimulatory activity, the potency of which was dependent on the functionalization of the terminal ethanol moiety of the diethanolamine-based acyclic scaffold. *In vivo* studies evaluating the adjuvant potential of this novel family of lipid A mimics are currently underway.

As part of an industrial partnership aimed at the development of novel vaccine adjuvants, a second lipid A mimic framework was designed and synthesized, in which an aromatic residue has been incorporated into the structural backbone. Two structural variations of the framework were generated which vary in the functionalization of the phenolic hydroxyl of the aromatic-based backbone. Several *in vivo* studies have shown that both mimics exhibit potent TLR4 immunostimulatory activity, and successful adjuvant properties.

In an effort to construct a fully synthetic, self-adjuvanting tumour associated carbohydrate antigen for eventual use in therapeutic cancer vaccines, the immunostimulatory activity of the diethanolamine-based lipid A mimic framework designed herein, was tapped. As such, a conjugate structure in which the lipid A mimic

framework and the Thomsen-Friedenreich carbohydrate antigen are directly linked via a flexible chemical linker was designed and synthesized. Future studies will determine the ability of the conjugate to induce an effective antibody response towards the carbohydrate epitope.

ACKNOWLEDGEMENTS

Firstly, I wish to express the utmost gratitude to my supervisors, Dr. Marina Ulanova and Dr. Z-Hua Jiang, for their support and guidance throughout this study. I am also very grateful to Dr. Chris Phenix for serving on my examination committee. A special thanks goes out to all of the members of both the Lakehead University department of chemistry and biotechnology program. In addition, a debt of gratitude is owed to entire group of technicians at Chemistry Stores for their support and technical expertise.

I would like to extend my appreciation to the staff at the Lakehead University Instrumentation Laboratory, especially Mr. Mike Sorokopud, for their technical aid in various forms of chemical analyses.

Financial support from the National Sciences and Engineering Research Council is gratefully acknowledged.

Finally, my deepest gratitude goes out to my parents, for without their support, encouragement, and sacrifice, none of this would have been possible.

LIST OF ABBREVIATIONS

Ac	acetate
AGP	aminoalkyl glucosaminide-4-phosphate
APC	antigen presenting cell
Ar	aromatic
BAIB	bis(acetoxy)iodobenzene
BAP	2-bromoacetophenone
BCR	B cell receptor
Bn	benzyl
Boc	*tert*-butyloxycarbonyl
Boc_2O	di-*tert*-butyl dicarbonate
br	broad
Bz	benzoyl
COSY	correlated spectroscopy
d	doublet
dd	double doublet
DAMP	danger associated molecular pattern
DEA	diethanolamine
DC	dendritic cell
DCC	*N*, *N*'-dicyclohexylcarbodiimide
DCM	dichloromethane
DIC	*N*, *N*'-diisopropylcarbodiimide
DMAP	4-dimethylaminopyridine
DMSO	dimethylsulfoxide
DMF	*N, N*-dimethylformamide
DPX	DepoVax™
ELISA	enzyme-linked immunosorbent assay
ESI	electrospray ionization
g	gram

HBTU	*O*-benzotriazole-*N*, *N*, *N*', *N*'-tetramethyl-uronium-hexafluorophosphate
HR	high resolution
Hz	hertz
ICAM-1	intercellular adhesion molecule-1
IBCF	*iso*-butyl chloroformate
IF-β	interferon β
γ-IFN	γ-interferon
IL	interleukin
IRAK	interleukin-1 receptor kinases
IRF-3	interferon regulatory factor 3
J	coupling constant
LBP	lipopolysaccharide binding protein
LPS	lipopolysaccharide
m	multiplet
Mal	MyD-adapter-like protein
MALDI	matrix-assisted laser desorption/ionization
m-CPBA	*m*-chloroperbenzoic acid
MHC	major histocompatibility complex
mg	milligram
MLA	monophosphoryl Lipid A
MyD88	myeloid differentiation primary response gene 88
mol	mole
mmol	millimole
NEMO	NFκB essential modulator
NHS	*N*-hydroxysuccinimide
NFκB	nuclear factor kappa-light chain-enhancer of activated B cells
NLR	NOD-like receptor
NMM	*N*-methylmorpholine
NMR	nuclear magnetic resonance
PAMP	pathogen associated molecular pattern

PMA	phorbol 12-myristate 13-acetate
PRR	pattern recognition receptor
q	quartet
t	triplet
TACA	tumour associated carbohydrate antigen
TBDPS	*tert*-butyldiphenylsilyl
TBK1	TANK binding kinase 1
TCR	T cell receptor
TEMPO	(2, 2, 6, 6-tetramethylpiperidin-1-yl)oxyl
T_F	Thomsen-Friedenreich antigen
THF	tetrahydrofuran
TIR	Toll/Interleukin-1 Receptor
TLC	thin layer chromatography
TLR	Toll-like receptor
TMS	tetramethylsilane
TMSOTf	trimethylsilyl trifluoromethane sulfonate
TNF-α	tumour necrosis factor-α
TRAF6	tumour necrosis factor receptor associated factor 6
TRAM	TRIF-related adapter molecule
TRIF	TIR-domain-containing adapter-inducing interferon-β
Troc	2,2,2-trichloroethoxycarbonyl
Troc-Cl	2,2,2-trichloroethoxychloroformate

TABLE OF CONTENTS

1 INTRODUCTION & OBJECTIVES

1.1 The Immune System

1.1.1 An Introduction to Immunity

Immunity is a biological term describing a state in which sufficient biological defences are present to avoid infection or disease. The immune system is a complex, multilayered system comprising two separate arms: (i) innate immunity, and (ii) adaptive immunity. The innate and adaptive immune responses, although separate, work in concert to protect the host [1].

The innate immune system represents the first line of defence against pathogens that have entered the body. Characteristic to innate immune responses are rapid kinetics, providing almost immediate protection, in addition to the lack of both antigen specificity, and the learning process that ultimately generates immunological "memory". The primary role of the innate immune system is the induction of an inflammatory response that serves to control the spread, and eliminate much of the invading pathogen. The second, equally important role that the innate immune response serves is the induction of the adaptive immune system [1].

Adaptive immunity provides a second line of defence, often at later stages of pathogenic infection. Adaptive immune responses are characterized by slow kinetics, and effector mechanisms which are highly antigen specific. After elimination of the pathogen, the adaptive immune response ultimately establishes a state of immunological "memory", thus allowing for a much more rapid, and stronger immunological response if the

pathogen is encountered further. This "memory" is the hallmark of the adaptive immune response, and is the basis of preventative vaccination strategies [1].

1.1.2 The Innate Immune System

Cells of the innate immune system represent a very diverse set of cells, comprising both tissue-residing cells such as macrophages and dendritic cells, in addition to non-tissue-residing, rather, "moving" cells, such as neutrophils, eosinophils and monocytes that patrol the body via the blood and lymph circulation [2].

The cells of the innate immune system are able to detect an invading pathogen through a limited set of innate immune receptors often referred to as pattern recognition receptors (PRRs). PRRs recognize a series of conserved structural motifs found throughout the pathogenic world known as pathogen-associated molecular patterns (PAMPs). Some examples of common PAMPs include bacterial products such a peptidoglycan, lipoteichoic acid, lipopolysaccharide (LPS), flagellin, as well as viral RNA. Among PRRs, Toll-like receptors (TLRs) have garnered considerable attention as pivotal components of the innate immune system. These receptors are capable of sensing a wide spectrum of organisms including bacteria, viruses, and parasites [2]. TLRs will be discussed in detail in the coming sections.

In addition to the TLR family, another family of intracellular PRRs have been identified. The NOD-like receptor (NLR) family of cytoplasmic receptors comprises over 20 members able to react to intracellular pathogen-derived structures [3]. Remarkably, the NLR family can also sense cellular damage, even in the absence of a pathogen-derived

trigger, via natural ligands referred to as danger associate molecular patterns (DAMPs). These DAMPs can include normal intracellular constituents that are released upon cell lysis. The discovery of the NLR family has altered the notion of the innate immune system as that being only able to detect infectious events, to that which is now able to detect both infectious events and the consequences of said infections [4].

Phagocytosis represents the primary effector mechanism of innate immune response, in that nearly all cells of the innate immune system are effective phagocytes [5]. Efficient elimination of pathogens via phagocytosis requires the rapid recruitment of effector cells to the site of infection, a process knows as the inflammatory response. Upon pathogen recognition, innate immune cells secrete a series of chemokines and cytokines that both attract phagocytes from the blood circulation, and also increase their phagocytic capacity. Elevated secretion of cytokines and chemokines leads to the recruitment of cells and plasma proteins to the infection site through increased vessel permeability, ultimately resulting in the classical signs of inflammation such as swelling, redness, heat, and pain [6].

1.1.3 The Adaptive Immune System

Due to the limited diversity of the PRRs of the innate immune system, the detection and elimination of those pathogens displaying a high mutation rate, or those pathogens, such as viruses, that are able to replicate intracellularly, is particularly challenging. The adaptive immune system is a highly sophisticated response involving antibodies and T-lymphocytes that has evolved in response to these challenges [7].

Antibodies are proteins that are produced by B lymphocytes. Characteristic to antibodies is an almost infinite diversity, from which virtually all known molecular structures, whether biological or synthetic, can be recognized. Each B lymphocyte expresses numerous copies of a unique antibody as a receptor on the cellular surface known as the B cell receptor (BCR). Upon encounter with it's particular antigen, the respective B cell is stimulated to divide and differentiate into plasma B cells and memory B cells. Most plasma B cells return to the bone marrow, where they produce large amounts of soluble antibodies of their respective specificity that are released into the blood and other fluids. The binding of an antibody to its target is often sufficient to render the antigen harmless. However, more often the antigen-antibody complex is able to recruit additional effector mechanisms that ultimately lead to pathogen destruction [8, 9].

Although antibodies allow the immune system to react with a large variety of antigens, these large proteins cannot cross the cellular membrane, thus rendering them ineffective at detecting and eliminating intracellular pathogens. To achieve this seemingly difficult task, T lymphocytes exploit the fact that nearly all cells display peptide fragments derived from intracellular proteins at their cellular surface. These intracellular peptides are presented to T lymphocytes bound to transmembrane presenting molecules encoded by the major histocompatibility complex (MHC) genes in humans. Similar to B lymphocytes, T lymphocytes express a unique antigen-specific receptor on their cell surface called the T cell antigen receptor (TCR), which is a specialized receptor able to recognize the molecular complex made up of a given intracellular peptide fragment and accompanying MHC molecule. T lymphocytes that react to protein fragments of

cytoplasmic origin are identified by the expression of the CD8 cell surface marker, and react to peptide fragments presented by the class I MHC subset. In contrast, those T lymphocytes expressing the CD4 cell surface marker react to protein fragments bound by the class II MHC subset of presenting molecules, the likes of which are formed in the endocytic vesicles and are derived from proteins in the extracellular milieu. It is important to note that MHC class II molecules are only expressed by cells of the immune system known as antigen presenting cells (APCs). The complex mechanism of antigen presentation via MHC restriction allows the immune system to scan and detect intracellular proteins while maintaining cellular integrity [10].

In terms of effector mechanisms, CD8+ lymphocytes possess the ability to inhibit intracellular pathogen replication through the secretion of soluble mediators which interfere with pathogen replication and induce the death of infected cells. Similarly, CD4+ lymphocytes secrete soluble mediators which can affect pathogen survival, however, the more important action of these cells is the regulation of other cells of the adaptive immune system. Thus, CD4+ T lymphocytes are commonly referred to as helper T cells, regulating the activity of other immune cells through the secretion of cytokines [11, 12].

With an almost infinite number of possible antigens, lymphocytes of a particular specificity are too infrequent to mount an effective immune response on their own. When a TCR or BCR of a lymphocyte binds to its respective antigen, in a process known as clonal selection, it induces its multiplication and therefore, increase in relative abundance

before, and after the immune response. Immunological memory is a consequence of this permanent alteration of the components of the immunological system, whereby a fraction of those now overrepresented lymphocytes is maintained during the life of the host, ultimately allowing for a faster and stronger response upon future encounter with the same pathogen [8, 13].

1.1.4 Dendritic Cells: The Link Between Innate & Adaptive Immunity

The selection and control of the complex array of effector mechanisms of the adaptive immune system requires the cooperation between various cell types. Activation of CD4+ helper T cells is an early and important step in the initiation of an immune response. The ability to activate naive helper T cells is a specific property of the rare class of APCs known as dendritic cells (DCs) [14, 15, 16].

DCs are members of the innate immune system, and as such, express members of the TLR family. DCs also express receptors to several of the cytokines produced during an innate immune response in their environment. Signalling through these receptors leads to DC maturation. Maturation is characterized sequentially by the accumulation of high numbers of peptide antigen loaded MHC class II complexes at the cellular surface, loss of adherence of the DC with surrounding tissue and subsequent migration to the lymphoid organs, and finally, expression of the cytokines and costimulatory signals required for the optimal activation of naive CD4+ helper T cells. DC maturation represents a confirmation signal, effectively linking the development of an adaptive immune response to the previous recognition of an invading pathogen mediated by the innate immune

system. Moreover, DCs function as a "lens", in that they highlight certain pathogenic characteristics, thus indicating the correct adaptive immune effectors [17, 18].

1.1.5 The Humoral Response & The Role of Helper T Cells

Antigens able to directly activate the BCR of B lymphocytes, induce their differentiation into antibody secreting cells independent of helper T cell influence. These response are characterized by slow kinetics, and the secretion of low levels of mainly low affinity IgM antibodies. Overall, this type of primary response is most often inefficient for the elimination of invading pathogens. The typical secondary antibody response, characterized by rapid kinetics, and a higher, more sustained secretion of higher affinity IgG antibodies, only occurs under the control of helper T cells [19, 20, 21].

1.1.6 Basic Principles of Modern Vaccination

Vaccination rests on the premise of immunological memory, whereby the second encounter with a particular pathogen induces an enhanced immune response. An ideal vaccine should therefore represent an innocuous form of a given pathogen, able to elicit a strong and adequate immune response. The challenge for modern vaccinology is to be able to elicit all of the required steps leading to immune activation *in vivo*. Antigen presentation and DC maturation are currently thought of as the limiting step in the development of vaccines [22].

Vaccine adjuvants are defined as compounds that modulate or increase the intrinsic immunogenicity of a particular antigen. Adjuvants allow the use of lower doses of antigens, thus minimizing the potential of adverse reactions. Recognizing the link

between the innate and adaptive immune response has led to a reappraisal of the role of adjuvants in vaccination, in that the ability to activate the innate immune system represents an obligatory property for an effective adjuvant. Recent observations have clearly indicated that most efficient adjuvants, including the widely used aluminium-based salts, are able to activate an innate immune response by either directly activating DCs, or by inducing the release of those cytokines able to activate DCs. Greater understanding of the signals involved in the innate immune response has led to the rational design of immunological modulators as potential vaccine adjuvants [23].

1.2 Toll-Like Receptors

1.2.1 Discovery

The discovery of a protein named Toll in *Drosophila* has revolutionized our understanding of the innate immune system. Toll was discovered as a membrane bound protein which was initially implicated in the development of polarity in the *Drosophila* embryo, and later shown to be responsible for anti-fungal defences in the adult fly. A genomic search resulted in the discovery of homologous proteins in mammals, which were called TLRs [24]. Characteristics to these receptors is a defined amino acid homology with the interleukin-1 (IL-1) receptor. The Toll/IL-1 (TIR) domain has been shown to regulate intracellular signalling pathways through the interaction with intracellular adaptor proteins which differentially regulate the expression of the inflammatory cytokines associated with the innate immune response [25]. To date, 13 mammalian members of the TLR family have been identified, and 10-or-more distinct TLRs have been identified in humans [26].

1.2.2 Ligand Specificity

Although all members of the TLR family share a large degree of sequence homology, growing evidence suggests specificity in their recognition and response. The TLRs involved in the recognition of bacterial ligands are transmembrane proteins with leucine-rich, horseshoe shaped extracellular domains that play a major role in PAMP based pathogen detection. TLR4 and TLR5 recognize LPS and bacterial flagellin respectively, while TLRs 1, 2, and 6 work cooperatively in the recognition of lipoproteins and glycolipids from Gram-positive bacteria. In contrast, the other members of the TLR family are restricted to intracellular compartments and recognize mostly viral products and nucleic acids; TLRs 3, 7, and 8 are involved in the detection of viral RNA, while TLR9 is specific to the recognition of unmethylated DNA common to both bacteria and viral sources [27].

1.2.3 Signalling

Activation of a TLR by its respective ligand leads to a conformational change in the TLR that ultimately results in the recruitment of intracellular adaptor proteins that initiate one of, or in the case of TLR 4, both of two separate intracellular signalling pathways (**Figure 1**). One signalling pathway is mediated by the adaptor protein myeloid differentiation primary response gene 88 (MyD88), whereas the other signalling pathway is mediated in concert by the adaptor proteins TIR-domain-containing adapter-inducing interferon-β (TRIF) and TRIF-related adapter molecule (TRAM) [28].

The adaptor protein MyD88 is a member of the TIR family, with the primary effect of the MyD88 signalling cascade being the activation of the nuclear factor kappa-light chain-

enhancer of activated B cells (NFκB). All TLRs, with the exception of TLR3, utilize the MyD88 signalling cascade. Upon interaction with the TIR domain of the TLR, MyD88 recruits interleukin-1 receptor kinases (IRAKs) 1, 2, and 4, which subsequently phosphorylate and activate the protein tumour necrosis factor receptor associated factor 6 (TRAF6). TLRs 1, 6, 2, and 4 accomplish this task with the help of the MyD88-adapter-like (Mal) protein. TRAF6 serves to activate the NFκB essential modulator (NEMO), which in turn phosphorylates IκB, causing its degradation, thus allowing NFκB to diffuse into the nucleus, ultimately resulting in the transcription and induction of inflammatory cytokines such as tumour necrosis factor-α (TNF-α), IL-6, and IL-1β [28].

Both TLR3 and TLR4 utilize the other TLR-induced intracellular signalling cascade, in which the adaptor proteins TRIF and TRAM are first recruited to the TIR domain of the activated TLR. TRIF activates the TANK binding kinase 1 (TBK1), which in turn activates the interferon regulatory factor 3 (IRF3), allowing for its translocation into the nucleus, and final induction of interferon β (IF-β) [28].

In all, TLR signalling ultimately leads to the induction or suppression of thousands of genes that make up the inflammatory response. Although TLR signalling is highly pleiotropic, it also one of the most tightly regulated signalling pathways. Interestingly, TLR4 is the only TLR, which upon activation, induces both the MyD88 and TRIF/TRAM dependent signalling pathways [28].

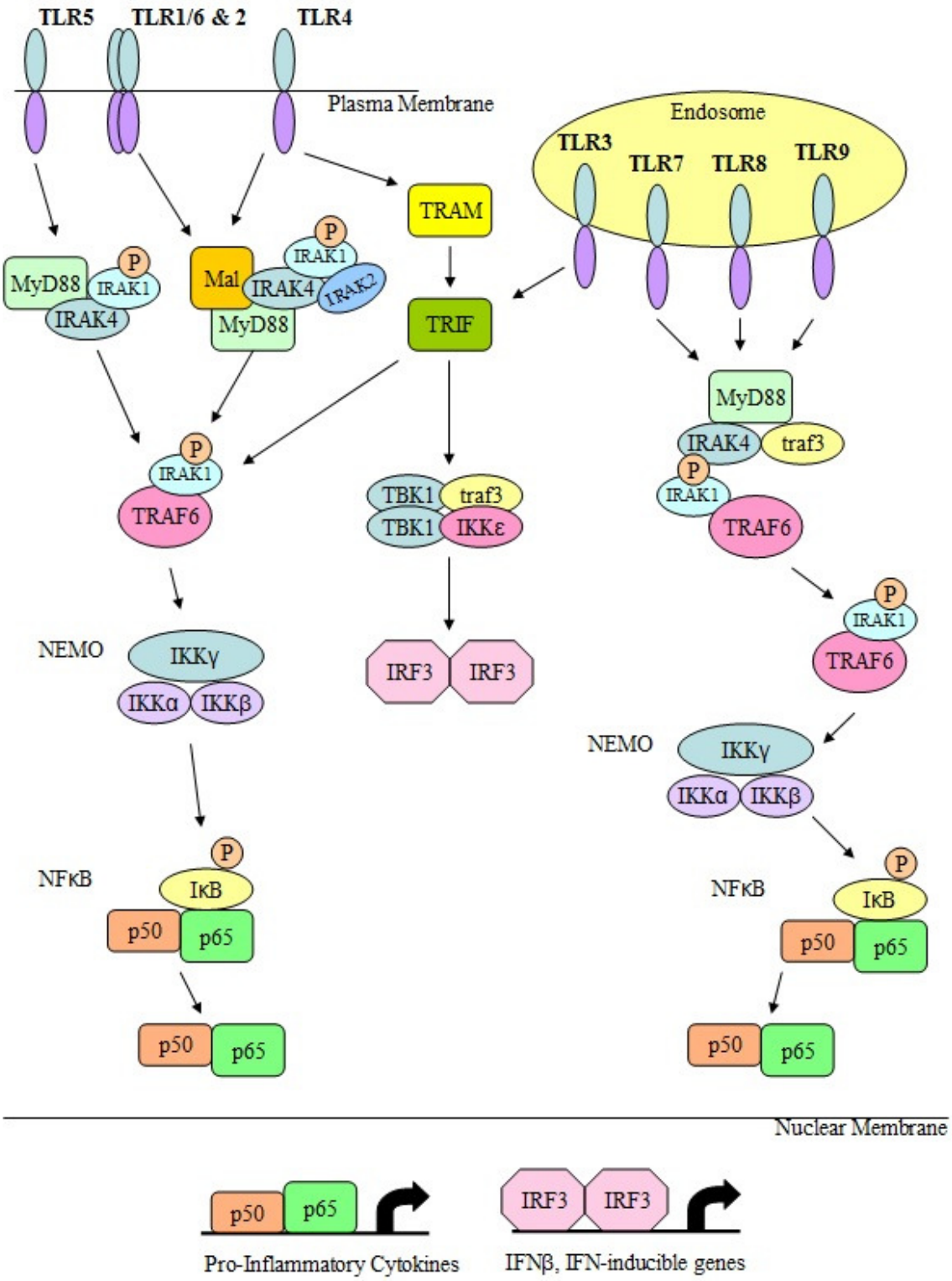

Figure 1. Intracellular TLR Dependent Signalling (Adapted from Reference 28)

1.2.4 Therapeutic Potential

Given the direct link between TLR activation and the maturation of DCs, which is thought to be the key step in the development of an adaptive immune response, TLR signalling has been pegged for its vaccine adjuvant potential. The identification of the natural ligands of the TLR family has led to the development of purified and synthetic ligands which can activate TLR signalling pathways in a well defined manner. The end goal of this research is the maximization of antigen immunogenicity while minimizing systemic inflammatory effects [29].

Inhibition of pathogen induced TLR signalling is also an area of intense research. The inflammatory response induced by prolonged TLR activation can ultimately be harmful to the host. As our knowledge of the molecular basis of TLR activation increases, effective competitive inhibitors are being designed to alleviate the undesired effects of pathogen induced TLR activation [29].

1.3 Toll-Like Receptor 4

1.3.1 LPS as Trigger of TLR4

LPS has been identified as the primary ligand of TLR4. LPS is a unique glycolipid molecule ubiquitous to Gram-negative bacteria where it is found in the outer portion of the outer membrane, which is the second lipid bilayer outside of the cytoplasmic membrane characteristic to this type of bacteria [30]. Pffeifer first described this material firmly bound to the cells of *Vibrio cholerae* in 1892, and given its toxicity, aptly named the material endotoxin [31]. LPS is, perhaps, the most effective trigger of the innate

immune response, with its potent toxicity causing high fever, tissue damage, and even death in experimental animals. A serious clinical syndrome in humans known as septic shock, which can ultimately become fatal, occurs if LPS levels remain elevated for an extended period of time [32].

Structurally, LPS consists of three distinct, covalently linked segments: the O-polysaccharide, the core oligosaccharide, and a terminal glycolipid lipid A (**Figure 2**). The O-polysaccharide at the distal terminal is composed of repeating oligosaccharide units, the structure of which varies between bacterial species and strains. In contrast, the core oligosaccharide is comprised of more conserved structures. Finally, the glycolipid lipid A, located at the proximal terminal, anchors the molecule via hydrophobic interactions to outer membrane of the Gram-negative bacteria [31, 33].

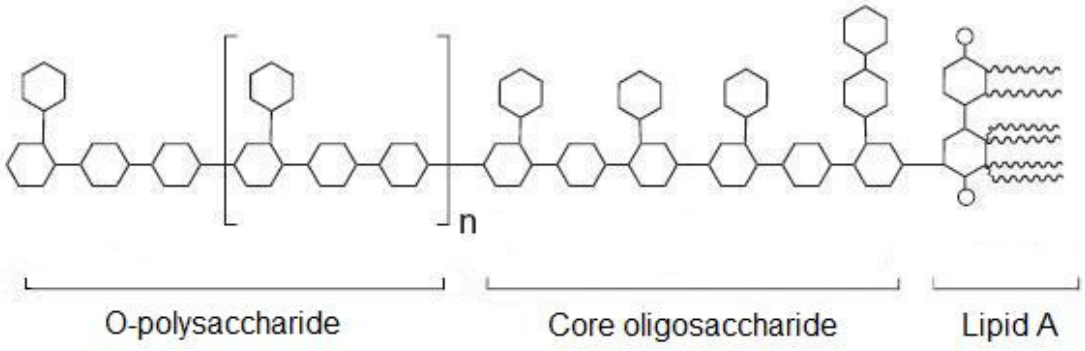

Figure 2. Schematic Representation of LPS

1.3.2 Lipid A as Endotoxic Principle of LPS

Westphal and Lüderitz noted that the mild acid treatment of LPS allowed for the cleavage of the bond between the core oligosaccharide and the glycolipid Lipid A. Lipid A was later shown to be solely responsible for the endotoxic activity of LPS [34]. As such, the

chemical structure of Lipid A became an area of intense investigation. However, due to its amphipathic nature, extensive purification was inhibited. Therefore, the structure of the hydrophilic backbone and the presence of *O*- and *N*-linked acyl moieties were only proposed, with the exact structural details not known [35, 36]. The first successful isolation of a single molecular species of Lipid A from *Escherichia coli* (*E. coli*) was reported by Imoto *et al*, and its chemical structure was elucidated by spectroscopic and chemical analysis [37]. The backbone of Lipid A consists of a β-(1-6) linked disaccharide of glucosamine, which is bisphosphorylated at the 1- and 4'-hydroxyl groups (**Figure 3**). This disaccharide backbone is common to all lipid A molecules, regardless of bacterial species or strain. However, significant variability in the number, length, and composition of the acyl lipid chains exists between species. This structural variability has been proposed as one of the mechanisms responsible for the highly variable degree of toxicity associated with different bacterial strains [38]. The *E. coli* Lipid A molecule was also synthesized by Imoto *et al* [38, 39], and shown to be identical with its natural counterpart in terms of both *in vitro* and *in vivo* activities [40].

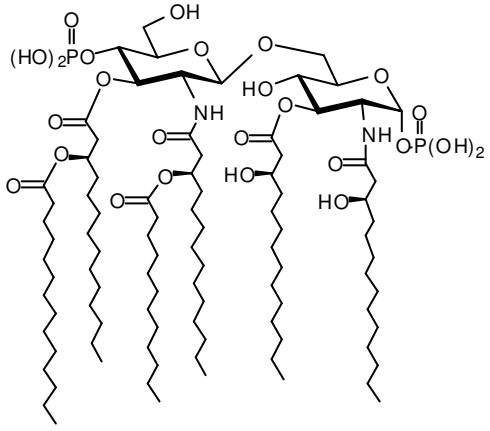

Figure 3. Structure of Lipid A From *E. coli*

1.3.3 Mechanism of TLR4 Activation

The interaction between TLR4 and LPS/lipid A has been, perhaps, the most studied of all mammalian TLRs, with significant effort gone into the delineation of the precise molecular events that ultimately lead to the profound biological response generated. Several obligate accessory proteins have been discovered that are critically involved in the recognition of LPS/lipid A. Lipopolysaccharide binding protein (LBP), found in serum, binds aggregate forms of LPS and facilitates the transfer of monomeric LPS to CD-14 [41]. CD-14 exists as both a serum soluble or as a membrane bound protein [42]. Either form of CD-14 has been shown to be responsible for the transfer of monomeric LPS to a third accessory protein, MD-2 [43]. MD-2 is a protein which lacks any intracellular domain and has been shown to bind to the extracellular domains of TLR4 [44]. The TLR4-MD-2 complex is expressed as a heterodimer on the surface of immune cells. Transfer of LPS from CD-14 to MD-2 is thought to bring about a reorganization of the cytoplasmic TIR domain of TLR4, enabling the induction of the two separate signalling pathways associated with TLR signalling [45].

1.3.4 TLR4 Signalling Antagonism

Antagonism of the TLR4 signalling pathway has also been reported. Several natural antagonistic Lipid A structures have been isolated from various bacterial sources. For example, Lipid A structures from *Rhodobacter sphaeroides* and *Rhodobacter caspulatas* show potent antagonism of *E. coli* lipid A induced TLR4 activation (**Figure 4**) [46].

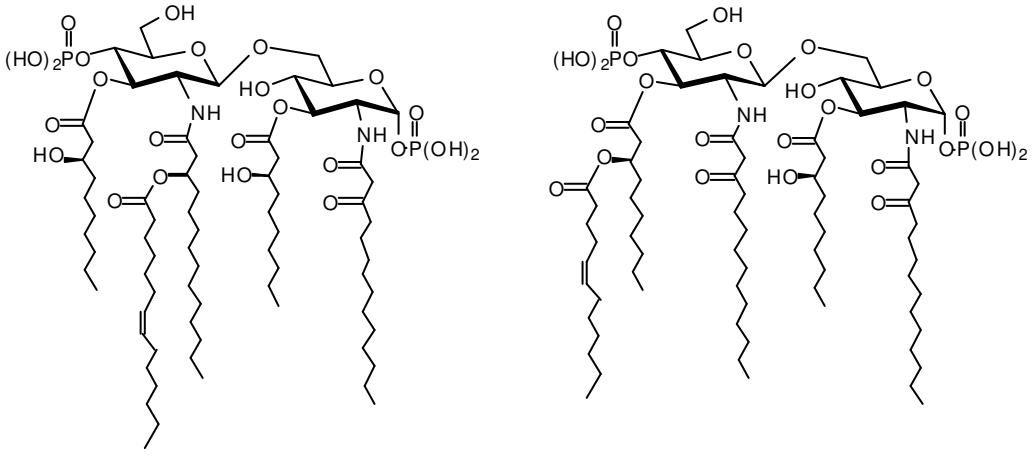

R. sphaeroides Lipid A *R. capsulatas Lipid A*

Figure 4. Natural Lipid A TLR4 Antagonists

Lipid IVa, the tetra-acyl biosynthetic precursor of the *E. coli* Lipid A molecule, which lacks the two β-acyloxy lipid chains was proposed and synthesized (**Figure 5**) [46, 47]. Lipid IVa was shown to have full endotoxic activity as compared to *E. coli* lipid A when tested using murine cells [48]. However, it was also shown to behave as an antagonist when tested in human cells, inhibiting the endotoxic activity of *E. coli* lipid A [49].

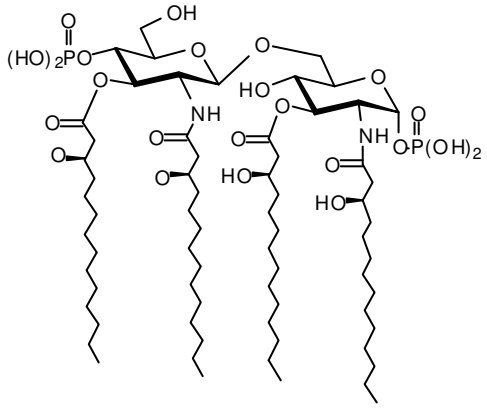

Figure 5. Lipid A Biosynthetic Precursor lipid IVa

Biochemical investigations have confirmed that murine MD-2 binds both lipid A and lipid IVa similarly, ultimately leading to TLR4 dimerization and activation with either ligand. The same combination of human MD-2 and TLR4 was found to also effectively bind lipid IVa, but neither a conformational change, or the dimerization of TLR4 occurs. Furthermore, a chimeric complex of murine TLR4 and human MD-2 behaves in the same manner. It was therefore concluded that MD-2 is responsible for this species-specific recognition difference [50]. The antagonism of the TLR4 signalling cascade in the human system is viewed as a promising approach to the treatment of bacterial sepsis, a topic which is discussed in detail in the coming sections.

1.3.5 Therapeutic Potential of TLR4 Signalling

Given the far reaching impacts of the TLR4 signalling pathway, it is not a surprise that it has been targeted for its possible therapeutic potentials. The focus, thus far, has centered on three main areas of therapeutic potential: anti-sepsis treatment, vaccine adjuvants, and anti-cancer therapies [51]. With an ever increasing knowledge of the biochemical pathways of TLR4 signalling, the manipulation of this pathway for potential beneficial effects is becoming a more realistic possibility.

The secretory products released as results of bacterial LPS induced TLR4 activation serve to assist the host in eradicating, and preventing the spread of the infecting pathogen. Unfortunately, as previously mentioned, the continued presence of elevated levels of bacterial LPS in the blood, having been released from dead or dying bacteria, can lead to a biological over-reaction which results in the release of toxic levels of these cellular mediators. This reaction is referred to as the systemic inflammatory response syndrome,

and is commonly referred to as sepsis. Characteristic to sepsis are life threatening responses such as tissue damage, vascular leakage, hypotension, organ dysfunction and eventual failure resulting in death. The antagonistic action in humans of lipid IVa and various other natural lipid A molecules could potentially be employed for the treatment of sepsis. The competitive inhibition of these antagonists could serve to not only treat sepsis once it has developed, but also prevent the bacterial infections that ultimately cause the condition [51].

Given the strong immunological responses that result from the activation of the TLR4 signalling cascade, there has been significant effort in terms of employing it for its vaccine adjuvant potential. However, as will be discussed in detail in the next section, an underlying concern is the strong inflammatory response associated with TLR4 activation. In order to serve as a successful adjuvant system, the ability to stimulate the adaptive immune system must be uncoupled from the strong inflammatory cytokine response [52].

Chemotherapy and radiation can successfully delay the progression of cancer, yet in many cases, the cancer can relapse. TLR4 agonism is a promising molecular treatment against chemotherapy and radiation relapsing cancer metastases. The potent anticancer action of microbes or microbial products has been known since the beginning of the 18th century when Deider reported that infection in cancer patients was concomitant with disease remission [53]. This anti-tumour effect was later found by Shear *et al* to be due to LPS [54]. It is now known that the TNF-α cytokine that results from TLR4 activation selectively increases the permeability of tumoural neoangiogenic vessels to cytotoxic

drugs [55]. Moreover, nitric oxide derived from TLR4 activation participates in local tumouricidal activity against many different tumour types, the likes of which was later found to be associated with apoptosis [56, 57]. Unfortunately, because of the toxicity associated with LPS, the treatment of cancer patients has been limited to the local application of small amounts of bacterial LPS, those doses being too low to obtain any beneficial anti-tumour effects [58].

1.3.6 TLR4 Therapeutic Concerns

In order for the modulation of TLR4 signalling to be practical for immunotherapeutic purposes, certain issues need to be addressed. The most important concern is the high toxicity associated with naturally derived Lipid A molecules. Therefore, an important issue for the design of safe immune modulators is a detailed knowledge of structure-activity relationships (SARs), which could ultimately allow for the maximization of the beneficial effects, and the minimization of the undesired toxicity. This information has been difficult to obtain using naturally isolated compounds, a direct result of the inhomogeneity encountered with natural lipid A preparations. Natural preparations suffer from a lack of consistency in both composition and performance, even when derived from the same bacterial strain, Moreover, possible contamination with other inflammatory components is also of prime concern [59].

Recent work has focused on the preparation of single molecular species by way of chemical synthesis. Chemical synthesis not only provides single, pure molecules, but also allows for the creation of structural analogs of the natural lipid A structure. By modifying the natural structure, those structural details that are beneficial to desired therapeutic

purposes may be separated from those details that are associated with the undesired toxicity.

1.3.7 Lipid A Structure Activity Relationships

Structure-activity analysis of LPS isolates from different bacterial species, and of synthetic lipid A derivatives indicate that both the length, and number of acyl chains are critical in the activation of TLR4. Studies indicate that the hexa-acylated lipid A from *E. coli* (**Figure 3**) maximally stimulates TLR4 [60]. Lipid A molecules with five or seven acyl chains are ~100 fold less active, while lipid IVa, the biosynthetic precursor with four acyl chains, lacks any agonistic activity, and is in fact, antagonistic to human TLR4 activation [60, 61]. Even among those hexa-acylated lipid A molecules, acyl chain length is strongly linked to TLR4 activation. It has been demonstrated that the optimum acyl chain length is 12-14 carbons, with a rapid decline in activity noted with chain lengths less than 10 or greater than 16 carbons [62, 63].

The two phosphate groups in the lipid A structure also greatly influence TLR4 stimulatory activity. Deletion of either phosphate reduces endotoxic activity ~100 fold, while deletion of both abolishes all agonistic activity [64]. It appears that phosphates specifically are not required, as substitution of the phosphate groups with other negatively charged groups has only minor effects [65, 66].

1.3.8 Molecular Basis of TLR4 Activation

Our understanding of the molecular basis of the LPS/lipid A activation of the TLR4 receptor complex has increased significantly as of late, thanks largely to several crystal

structures. For instance, the crystal structure of human MD-2 was obtained in both its native form, as well as bound to the antagonistic lipid IVa. A large, deep hydrophobic cavity is reported, in which all four acyl chains of the ligand are found. No direct contacts are made between the lipid IVa ligand and TLR4. Moreover, the conformational change of MD-2 upon binding of lipid IVa was noted to be minimal [67].

More recently, the crystal structure of the TLR4-MD-2 receptor complex bound to LPS has been reported. The structure shows the lipid A portion of LPS binding to two copies of TLR4, with the dimerization facilitated through hydrophilic and hydrophobic interactions with LPS. Five of the six acyl chains of lipid A are found within the hydrophobic pocket of MD-2, with the remaining chain exposed to the surface where it forms hydrophobic interactions with phenylalanine residues on TLR4. The binding of LPS is noted to cause structural changes within a loop region of MD-2 (Phe 126), leading to hydrophilic interactions between TLR4 and MD-2 that further stabilize the complex [68]. This structural change in the Phe 126 loop region of MD-2 following LPS binding is essential for the formation of the receptor complex dimers, and subsequent downstream signalling. This is supported by mutation analysis of Phe 126 in MD-2, which shows that alterations to this key amino acid prevents receptor complex dimerization [69]. The two phosphate groups of lipid A form medium range ionic interactions with positively charged residues on both TLR4, and MD-2, as well as with the adjacent TLR4 of the dimer complex. This explains the phosphate-activity relationship discovered in the structure-activity studies mentioned in earlier sections, and why the phosphates can be replaced with other negatively charged groups [64, 65, 66]. Moreover, in comparison to the

binding of the antagonistic lipid IVa, the extra lipid chain inserted into the binding pocket of MD-2 when LPS is bound results in the displacement of the di-glucosamine backbone of lipid A, such that the phosphate groups can form such key associations [68].

1.3.9 Disaccharide Lipid A Analogs

Over the past decade, a great deal of research has gone into the synthesis of analogs of the lipid A disaccharide structure, with hopes that the beneficial immunostimulatory properties can be separated from the associated high toxicity. One notable discovery is that through the removal of the anomeric phosphate and the 3-*O* acyl chain of the reducing sugar of lipid A derived from *Salmonella minnesota* RC595, a significant decrease in endotoxicity is achieved while immunostimulatory activity is still maintained [69]. The resulting structure has been named as monophosphoryl lipid A (MLA) (**Figure 6**), and has been synthesized along with numerous structural analogs [70]. Certain MLA structures have shown excellent adjuvant characteristics, and have been approved for use in therapeutic vaccines [70, 71].

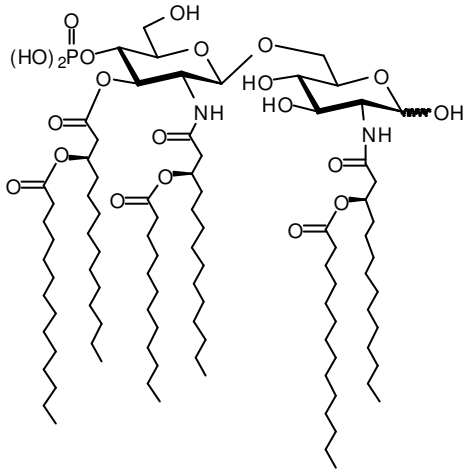

Figure 6. MLA structure derived from *Salmonella minnesota* RC595 Lipid A

Recently, it has been reported that the MLA somehow engages the TLR4-MD-2 receptor complex differently than those lipid A molecules which possess high endotoxicity. MLA has been shown to selectively activate only the TRIF-TRAM dependent arm of the TLR4 signalling pathways. The failure of MLA to engage the Myd88 pathway, which controls the expression of inflammatory cytokines, appears to account for the lack of harmful toxic effects normally associated with TLR4 signalling activation. These findings have provided an empirical basis supporting the use of MLA as a vaccine adjuvant, in that it shows that it is not simply weakly endotoxic [72]. It has also been suggested that the lack of pro-inflammatory activity of MLA may be due its ability to stimulate higher levels of the anti-inflammatory cytokine IL-10 [73], or due to its inability to activate caspase-1, which is involved in the maturation of several pro-inflammatory cytokines such as IL-1β and IL-18 [74].

Two highly promising TLR4 antagonist have been synthesized based on the naturally occurring antagonistic structures of Lipid A derived from *R. capsulatas* and *R. sphaeroides* mentioned earlier (**Figure 4**). E5531, a structural mimic of *R. capsulatas* lipid A, is a potent antagonist of TLR4 (**Figure 7**) [75, 76, 77, 78]. E5564, based on *R. sphaeroides* lipid A, has shown similar activity with a notable increase in potency. Currently, E5564 is in clinical trials as an anti-sepsis treatment under the name Eritoran [79, 80, 81]. The crystal structure of E5564 bound to the murine TLR4-MD-2 receptor complex was reported. Similar to the binding of the antagonistic lipid IVa, the four lipid chains of E5564 are noted to be found in the hydrophobic cavity of MD-2, and no interaction between the ligand and TLR4 is observed [82].

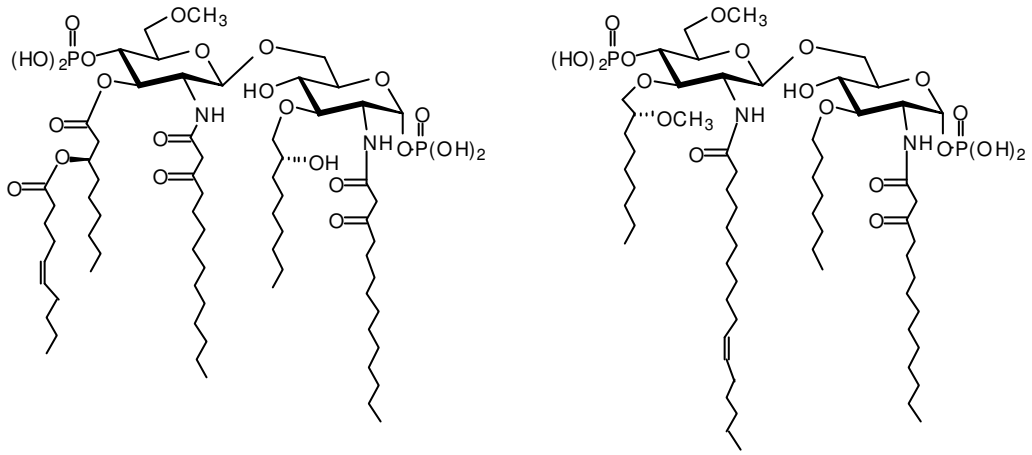

E5531 E5564

Figure 7. Synthetic Disaccharide TLR4 Antagonists

Another notable discovery in terms of disaccharide lipid A analogs is the tri-acyl OM-174 (**Figure 8**). This compound has shown significant promise as both a vaccine adjuvant, and a molecular treatment of chemotherapy and radiotherapy relapsing cancers. The toxicity of OM-174 was noted to be more than 100 times lower than that of LPS [83]. The immunostimulatory properties of OM-174 are not only being targeted for their anti-tumour effect, but also as a palliative for chemotherapy induced immunosuppression, which has the potential to result in fatal opportunistic infections [55].

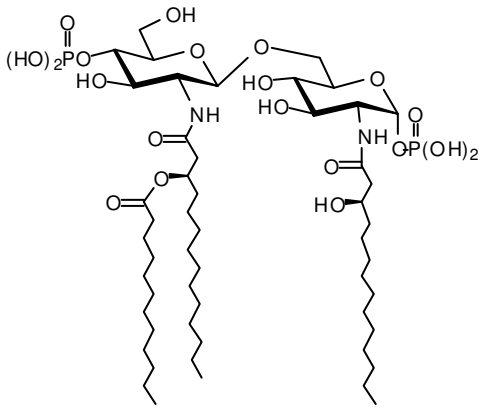

Figure 8. Synthetic Adjuvant & Anti-Cancer Agent OM-174

1.3.10 Monosaccharide Lipid Analogs

Numerous subunit derivatives of bacterial lipid A have been synthesized. These molecules have typically been synthetic analogs of either the reducing or non-reducing glucosamine functionalities of lipid A, or analogs in which one of the glucosamine units has been replaced with an acyclic scaffold. These subunit analogs provide a structural motif more amenable to systematic SAR investigations than more complex disaccharide analogs. Synthetic analogs of either the reducing or non-reducing glucosamine moieties of lipid A which contain up to five acyl chains typically exhibit very low biological activities. Moreover, monosaccharide analogs of the reducing glucosamine often exhibit TLR4 antagonistic activities. However, certain monosaccharide derivatives, mainly of the non-reducing subunit which possess three lipid chains show an elevated level of immunostimulatory power with low toxicity compared to natural lipid A [84]. For example, GLA-60 has shown the best adjuvant properties among various non-reducing subunit analogs (**Figure 9**) [85].

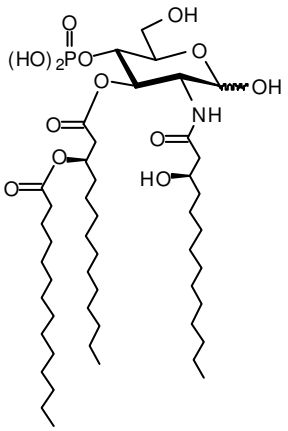

Figure 9. Monosaccharide Lipid A Based Adjuvant GLA-60

A novel class of monosaccharide lipid A mimics known as aminoalkyl glucosaminide 4-phosphates (AGPs), in which the reducing sugar has been replaced with an *N*-acyl aglycon unit have been developed (**Figure 10**). Certain analogs of the AGP generic structure show significant promise as both TLR4 agonists and antagonists [86].

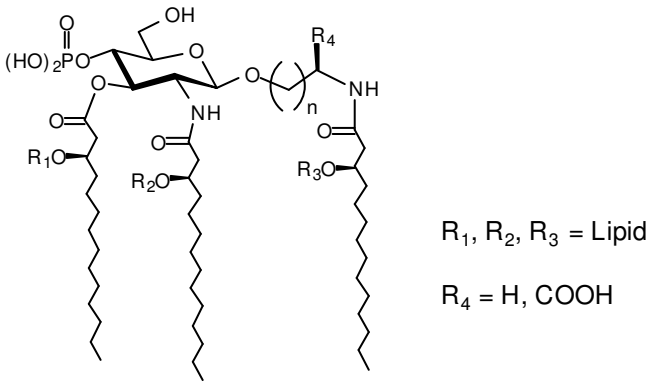

Figure 10. Generic Structure of AGP Class of Lipid A Mimics

In the AGP class of Lipid A mimics, adjuvant potential shows a profound dependence on both the acyl chain, and the aglycon chain length, as well as on the nature of the of the

aglycon α-substituent. The highest levels of immunostimulatory activity are noted when the secondary acyl chains (R_1, R_2, R_3, **Figure 10**) are 10 to 12 carbons in length, the aglycon is 2 carbons long (n = 1), and the aglycon α-substituent (R_4) is a carboxyl group, as exemplified by CRX-527 (**Figure 11**). Immunostimulatory activity is abolished in TLR4 antagonist CRX-526, in which the length of the secondary acyl chains has been reduced to 6 carbons [86]. RC-520, in which the α-carboxyl moiety has been eliminated shows an even greater activity to toxicity profile, and has been investigated for uses as a paediatric vaccine [71]. Interestingly, selective TRIF-dependent signalling has recently been reported for an analog of CRX-527 in which the stereochemistry of the α-carboxyl moiety has been inverted [87].

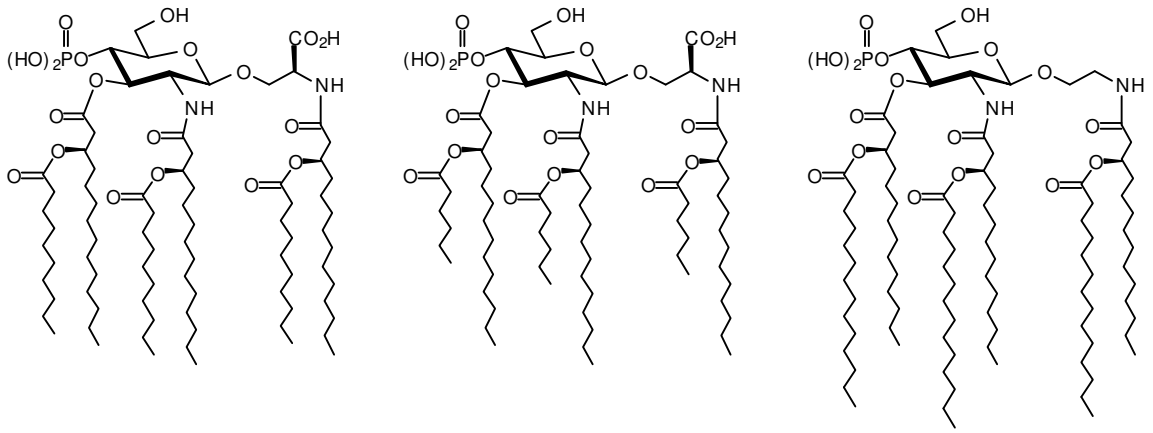

CRX-527 CRX-526 RC-529

Figure 11. Notable members of the AGP Class of Lipid A Mimics

As a further testament to the AGP approach of adjuvant design using synthetic monosaccharide derivatives of lipid A, a set of analogs in which the reducing glucosamine has been replaced with an *N*-acylated pentaerythritol aglycon unit have been

synthesized (**Figure 11**). These compounds were noted to exhibit a biological activity similar to that of natural lipid A, inducing the secretion of high levels of inflammatory cytokines. In a totally synthetic liposomal vaccine system, these mimics were noted to exhibit strong immunostimulatory adjuvant properties [88].

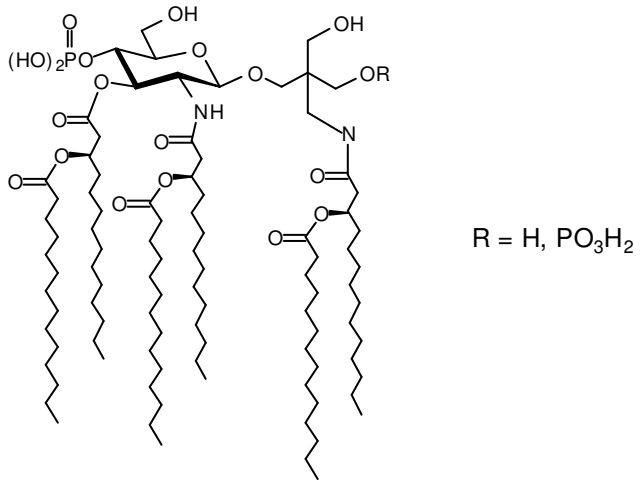

Figure 12. Pentaerythritol Based Monosaccharide Lipid A Mimics

1.3.11 Acyclic Lipid A Analogs

In an extension of the approach in which one of the glucosamine residues of the natural lipid A disaccharide framework is replaced with an acyclic scaffold, several lipid A mimics in which both of the glucosamine residues have been replaced by acyclic scaffolds have been reported. The premise behind this approach to generating lipid A mimic structures is to simplify the structure of the mimic, preserving only those elements which have been shown to be critical for TLR4 activation, namely the acyl chains and the phosphate moieties. For instance, E6020 is a lipid A mimic containing a hexa-acylated acyclic backbone (**Figure 13**), and is being developed as a vaccine adjuvant [89, 90]. OM-294 is based on the structure of the synthetic adjuvant OM-174 (**Figure 8**), and contains a

tri-acylated pseudo-dipeptide acyclic backbone. This class of lipid A mimics show potent immunostimulatory activity, practically devoid of any toxicity [91].

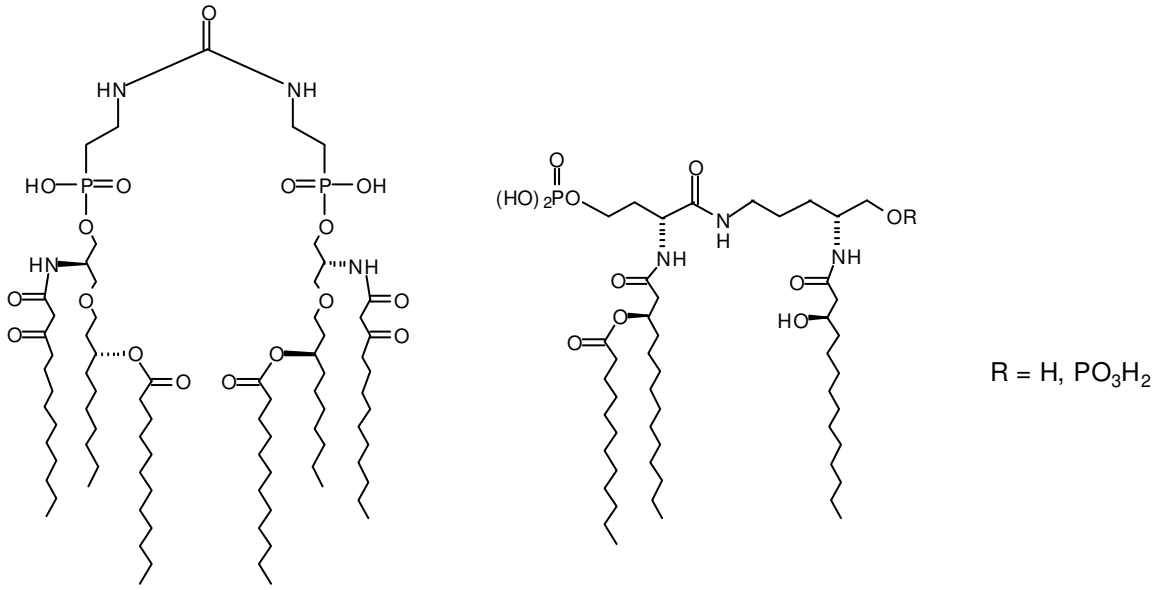

E6020 OM-294

Figure 13. Acyclic Lipid A Mimics

1.4 Cancer Immunotherapy

1.4.1 Background

The traditional treatment options for cancer, which include surgery, chemotherapy, and radiation, are generally unselective. Not only do they suffer from many undesired side reactions, they may not be able to eliminate cancer cells that have metastasized. In an effort to overcome these problems, significant effort has been directed towards employing the human immune system to selectively remove cancerous cells. The concept of cancer immunotherapy was first employed over 100 years ago by Coley, where it was found that the injection of a mixture of bacterial toxins into a tumour was able to initiate an immune response that led to its complete eradication [92]. Given our current

understanding of the molecular mechanisms of human immune system, it is now generally regarded that LPS molecules in the bacterial mixture activated the innate immune system, leading to the release of cytokines that ultimately resulted in the induction of the protective effects of the adaptive immune system.

It has been shown that antibodies which target tumour-associated antigens have the ability to eliminate circulating tumour cells [93, 94, 95]. Antibodies against tumour-associated antigens can mediate elimination of cancerous cells by various mechanisms, including complement dependent cytotoxicity and antibody-dependent cellular toxicity. Moreover, antibodies have been shown to interfere with receptor-mediated signalling, adhesion, and metastasis of tumour cells [96].

Traditionally, vaccines are employed to provide protection against invading pathogens. However, the concept of cancer immunotherapy utilizes a vaccination to evoke an immune response which can eradicate an already existing disease [97]. In addition to eradicating a pre-existing tumour, anti-cancer vaccination can protect the host against the common relapses of the same cancer [98].

1.4.2 Tumour-Associated Carbohydrate Antigens

The first efforts to develop a cancer vaccine utilized the patient's own tumour cells, which when removed, inactivated, and re-injected into the patient, initiated a tumour-specific immune response. This approach has been refined over time, however, major drawbacks of this approach include the cost and labour intensiveness of such personalized medicine [99].

The identification of tumour-associated carbohydrate antigens (TACAs) has made it possible to develop general anti-cancer vaccination strategies. It has been known for a long time that the majority of human cancers are characterized by abnormal glycosylation [100, 101, 102, 103]. Cancerous cells may over-express truncated versions of oligosaccharides, and unusual terminal oligosaccharide sequences. Mechanistically, several theories have been proposed to account for the formation of TACAs, including an altered metabolism of cancerous cells, changes in the tumour microenvironment, and changes in the glycosylation genetic code [104, 105, 106].

The oligosaccharides found on the surface of cells are involved in many biological processes. It is not a surprise that cancerous cells, which display abnormal glycosylation, also display differences in cell adhesion and mobility [107, 108, 109]. In addition to being membrane bound, many TACAs are secreted into the serum by the cancerous cells, thus providing viable targets for the development of both diagnostic evaluations, and selective vaccinations.

TACAs can be linked to lipids, such as gangliosides. The glycosphingolipids GM2, GD2, and GD3 are highly expressed on human melanoma cells, and have received considerable research in terms of vaccine development (**Figure 14**) [110]. Globo-H has been identified as TACA for ovary, colon, prostate, lung, and small-cell lung cancers [111].

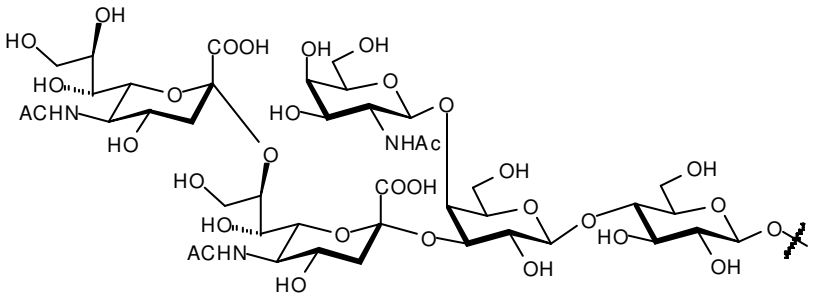

GD2

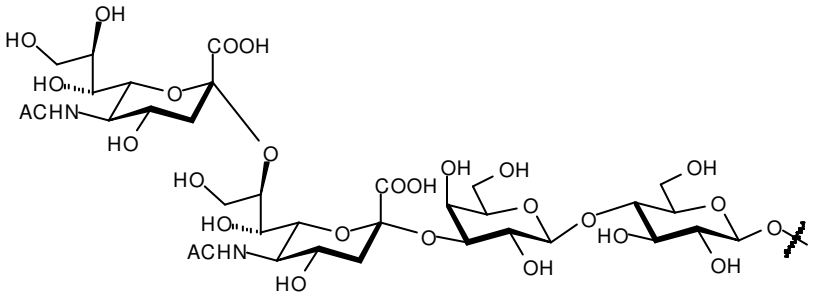

GD3

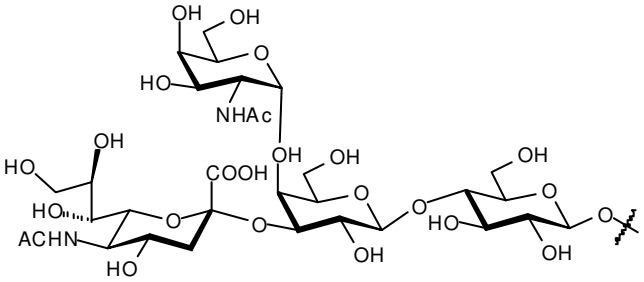

GM2

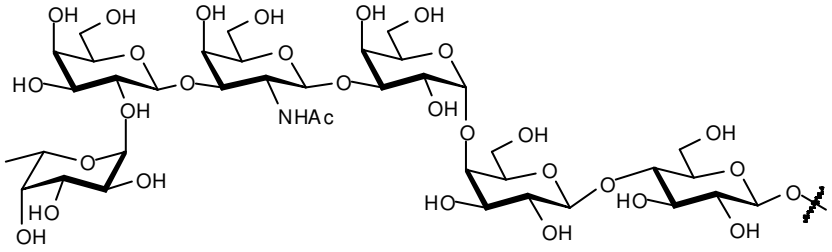

Globo-H

Figure 14. Glycosphingolipid TACAs

Several tumour-associated glycosphingolipids have been identified as adhesion molecules, and thus have been shown to promote tumour cell invasion and metastasis [112]. For instance, the Lewis antigen Le^y is over-expressed on ovary, breast, colon, prostate and non-small cell lung cancers (**Figure 15**) [113]. The KH-1 antigen is found on human colon cancer cells, and has never been isolated from normal colonic tissue. This makes this TACA a highly specific target for vaccination strategies [113, 114, 115].

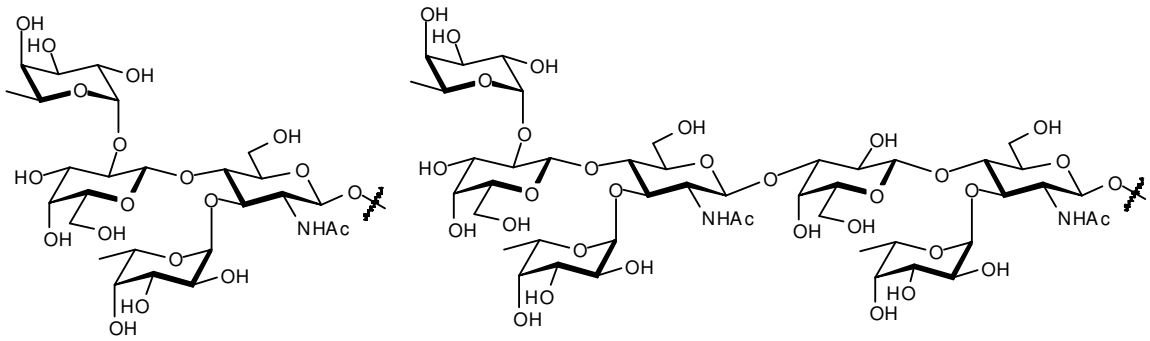

Figure 15. Tumour-Associated Carbohydrate Adhesion Molecules

TACAs can also be linked to proteins, such as mucins, which are a family of densely glycosylated high molecular weight proteins implicated in epithelial cancers. For example, MUC-1, a membrane-bound mucin, is noted to be over-expressed in almost all breast carcinomas, as well as being associated with ovarian, lung, colon, and pancreatic carcinomas [116]. The tumour-associated MUC-1 displays the truncated blood group antigens Tn, sialylated Tn (STn) and T_F (**Figure 16**), which all result from incomplete *O*-glycan synthesis. In addition, both the Globo series (**Figure 14**) and Lewis antigens (**Figure 15**) can be found linked to proteins [117].

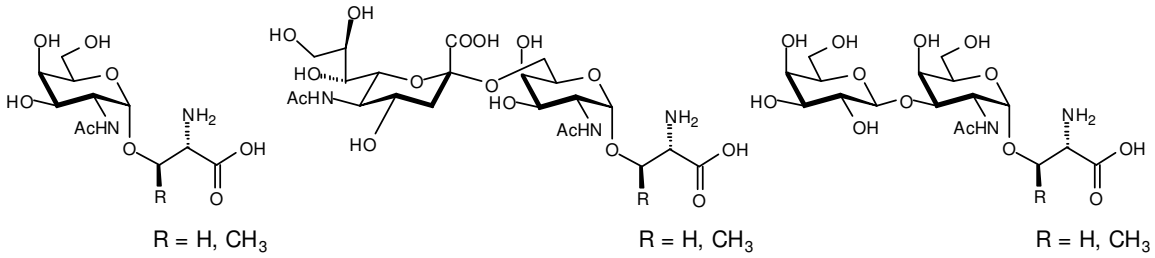

Tn STn T_F

Figure 16. Glycoprotein TACAs

1.4.3 Difficulties Associated With Carbohydrate Vaccine Development

Although TACAs offer a promising target for cancer immunotherapy, several issues complicate their use as the target of vaccination strategies. For instance, generating an appropriate immune response to a carbohydrate antigen in a vaccination setting is highly difficult, owing to their inherently T-cell independent nature. As such, immune responses to carbohydrate antigens are often only short-lived, generating only low affinity IgM antibodies which ultimately lack immunological memory. In addition, several TACAs are found on normal cells as well, albeit in low abundance, and therefore receive tolerance from the immune system. The TACAs are often shed into the blood stream by growing tumours, further reinforcing the tolerance of the immune system toward these antigens. Consequently, the induction of high affinity IgG antibodies against TACAs has proven to be much more challenging than inducing the same response against viral or bacterial carbohydrates [118].

1.4.4 Protein Conjugate Vaccines: The Classical Approach

Given the challenges associated with generating an appropriate immune response to TACAs, considerable efforts have been focused on better presenting these antigens, such

that specific and relevant antibody responses are generated. The classical approach for carbohydrate-based cancer vaccination strategies involve the conjugation of the antigen to a carrier protein, such as keyhole limpet hemocyanin, bovine serum albumin, and tetanus toxoid. The premise behind this approach is that the carrier protein contains helper T-cell epitopes, which ultimately lead to the activation of this vital class of lymphocyte. In addition, the protein carrier can possess adjuvant-like properties that stimulate the innate immune response to provide the necessary signals for the generation of the desired adaptive immune response. However, most often, the protein conjugate is administered with an external adjuvant to stimulate the desired innate immune response [119].

A critical issue for carbohydrate-protein conjugate vaccine development is the conjugation chemistry employed to attach the carbohydrate antigen to the carrier protein. Carbohydrate antigens isolated from natural sources are often conjugated to the protein carrier via reductive amination, which has the potential to destroy vital recognition elements and result in the complete loss of immunogenicity. Organic chemistry has allowed for the synthesis of TACA which incorporate a linker that has functional groups which allow for selective conjugation to the carrier protein without affecting the carbohydrate epitope. The results of several studies indicate that the choice of protein carrier, adjuvant, and linker chemistry can greatly influence the immune response generated to the TACA. For instance, in many cases, immune responses against the linker are generated, the likes of which ultimately suppress the desired immune response against the carbohydrate [120, 121, 122, 123].

Several carbohydrate-protein conjugate vaccine constructs have been examined in various stages of clinical trials. The results indicate that the vaccines are well tolerated, and appear most effective when used in conjunction with a potent adjuvant. However, even with optimized immunization protocols, high titers of high affinity IgG antibodies have remained elusive. One major problem noted is that the carrier proteins are highly immunogenic, eliciting strong immune responses themselves which ultimately lead to the suppression of the desired immune response against the TACA [120, 121, 122, 123, 124].

1.4.5 Synthetic, Two-Component, Self-Adjuvanting Cancer Vaccines

The attachment of a TACA to a carrier protein represents a problematic aspect of conjugate vaccine development. The conjugation chemistry is often difficult to control, resulting in conjugates with differences in composition and structure. In addition, the linkers that are employed for the conjugation can be immunogenic, leading to suppression of the desired immune response against the TACA.

One approach to improve the presentation of TACAs to the appropriate immune cells is to synthetically attach the antigen to a receptor ligand that activates the desired immune cells. Such vaccine candidates are advantageous as they incorporate only those elements required for the desired immune response, and can be produced in a reproducible fashion. For example, the TLR2 ligand Pam_3Cys has been covalently attached to TACAs, with the hope that the cytokines produced from TLR2 stimulation would lead to the activation of dendritic cells. An example utilizing this approach was reported by Toyukuni *et al*., in which a dimeric Tn-antigen was covalently linked to Pam_3Cys. Although low titers of IgG antibodies were found, the study was monumental in that it showed that an immune

response against a small synthetic carbohydrate antigen could be generated devoid of a protein carrier [125, 126].

Several other attempts at covalently linking a TACA to the TLR2 ligand Pam_3Cys have been reported. In general, mainly low affinity IgM antibodies are noted, even with the use of an external adjuvant [121, 127, 128]. These results highlight the T-cell independent nature of the TACAs, in that without the inclusion of a helper T-cell epitope, the desired antibody class switch and affinity maturation cannot be achieved.

1.4.6 Synthetic, Multi-Component, Self-Adjuvanting Cancer Vaccines

The lack of T-helper cell involvement in the two-component synthetic vaccine approaches lead to the notion of a tri-component synthetic vaccine that incorporates the TACA, a helper T-cell epitope, and a potent immune activator, such as a TLR ligand. Such a vaccine construct constitutes the minimal subunits necessary to evoke the desired immune response against the carbohydrate [129, 130, 131]. For example, a fully synthetic three-component vaccine construct consisting of the Tn-antigen, a helper T-cell epitope derived from *Neisseria meningitis*, and the TLR2 ligand Pam3Cys was designed and synthesized by Boons *et al*. Moderate titers of IgG antibodies against the Tn-antigen were found, thus validating the concept of a fully synthetic anti-cancer vaccine [130].

The influence of the covalent attachment of the various components of the vaccine construct on the immune response has been studied. Uptake and processing of the construct is necessary for the presentation of the helper T-cell epitope. It could be argued that by incorporating the three components of the vaccine construct into a liposome,

processing of the vaccine construct would be rendered unnecessary, and a more robust immune response would be expected. However, it has been shown that covalent attachment of the three components is critical in achieving good antibody titers. One possible explanation is that the covalent attachment of the adjuvant ensures that the cytokines induced are produced locally at the site where the vaccine interacts with the desired immune cells. [131].

1.4.7 A Self-Adjuvanting MLA-TACA Conjugate

Previous efforts towards developing a synthetic, self-adjuvanting TACA have primarily focused on the use of TLR2 ligands as the immunostimulatory component. In a paradigm shifting experiment, the adjuvant power of the TLR4 ligand MLA has recently been employed in a self-adjuvanting vaccine conjugate. MLA from *Neisseria meningitidis* was synthetically conjugated to a modified form of the GM3 TACA (**Figure 17**) [132]. Vaccination studies indicate that a robust, high affinity IgG antibody response is elicited by the construct, thus indicating T-cell mediated immunity [133]. Interestingly though, the construct lacks any helper T-cell epitopes. The exact nature through which T-cell mediated immunity is induced by the construct is still to be determined.

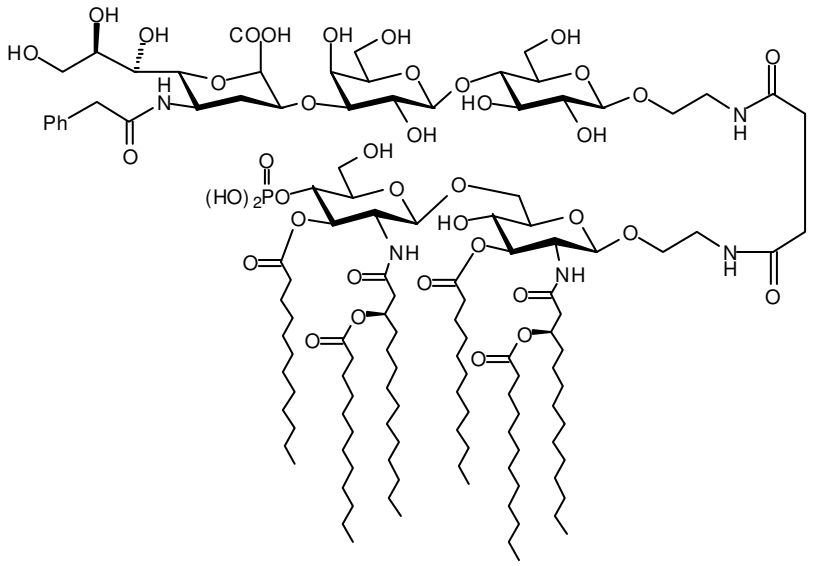

Figure 17. MLA-GM3 Conjugate

1.5 Objectives of Thesis Project

1.5.1 Novel Lipid A Mimic Frameworks

Given our current understanding of the molecular basis of the activation of the TLR4 receptor complex by LPS/lipid A, the design of potent immunostimulatory lipid A mimic structures as potential vaccine adjuvants is possible. The primary goal of the current study is the design and synthesis of novel molecular frameworks to mimic the disaccharide structure of natural lipid A in the activation of the TLR4 receptor complex. The novel frameworks will be tested for their potential to activate TLR4 mediated signalling. Moreover, efforts will focus on maximizing the immunological response generated by the novel frameworks in an effort to generate a potential vaccine adjuvant candidate.

1.5.2 Fully Synthetic Self-Adjuvanting Carbohydrate Antigens

Based on the results achieved with the MLA-TACA vaccine conjugate discussed earlier, other TLR4 ligands have potential for being employed as the immunostimulatory component of synthetic, self-adjuvanting antigens. The secondary goal of the current study is therefore, the application of the adjuvant potential of the novel molecular lipid A mimic frameworks designed herein for the construction of self-adjuvanting carbhydrate antigens. Those antigens generated will be tested as potential synthetic, self-adjuvanting anti-cancer vaccine candidates.

2 DIETHANOLAMINE-CONTAINING LIPID A MIMICS

2.1 Initial Studies

2.1.1 Design

Simplified lipid A structures with various acyclic molecular frameworks to mimic one, or both of the D-glucosamine residues of the natural lipid A disaccharide backbone have been reported to display interesting immunostimulatory activities.[134-141] In those lipid A mimics in which the reducing glucosamine residue has been replaced by an acyclic acylated aglycon, it appears that the location of the fatty acyl chain on the aglycon is directly related to immunostimulatory activity, in that optimal immunostimulatory activity is observed when the aglycon acyl chain is separated from the glycosyl residue by a two or three carbon linker.[136, 139, 141] In addition, SAR studies have also indicated that the position of any aglycon phosphate residues aiming to mimic the distal (reducing sugar) phosphate of the natural disaccharide lipid A structure is not strictly required.[142]

In an effort to design and synthesize novel molecular frameworks to mimic the disaccharide structure of natural lipid A in the activation of the TLR4 receptor complex, diethanolamine (DEA) has been envisioned as an acyclic scaffold to replace the reducing glucosamine residue of the natural lipid A disaccharie. As such, two different DEA-containing lipid A mimic structures were initially targeted (**1** & **2**, **Figure 18**). DEA was envisioned as an simple, efficient acyclic molecular framework capable of replacing the reducing glucosamine residue of the natural lipid A structure based on several considerations: (a) a conservation of essential functional groups involved in TLR4/MD-2 activation, namely the phosphate groups and fatty acid chains; (b) a conservation of the glycosidic linkage; (c) the appropriate location of each functional group in the DEA

acyclic molecular framework. Compounds **1** and **2** are both monophosphorylated lipid A mimics with different numbers of fatty acyl chains. Compound **1** carries six fatty acyl chains, and has been designed to directly mimic the structure of *E. coli* Lipid A (**Figure 3**). In an effort to examine the effect of lipid content on activity in this novel family of lipid A mimics, Compound **2** carries eight acyl chains, and is likely the first example of a lipid A analog, either natural or synthetic, with more than seven fatty acyl chains.

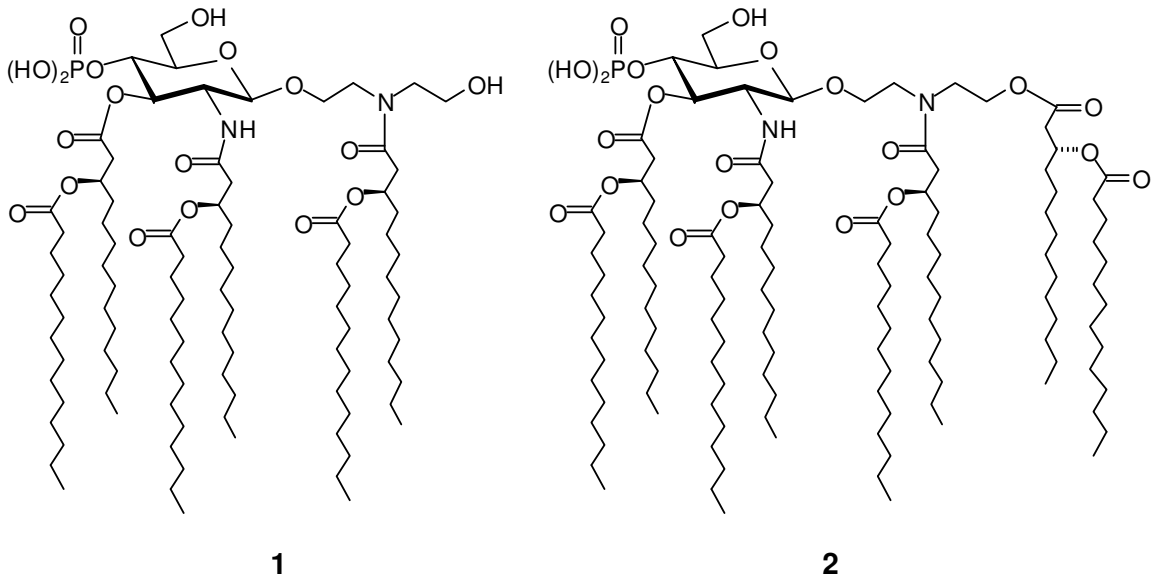

1 **2**

Figure 18. Targeted DEA-Containing Lipid A Mimics

2.1.2 Retrosynthetic Analysis

Beginning with compound **2**, elimination of the terminal fatty acyl chain on the acyclic scaffold yields compound **1** and dilipid acid **3** (**Scheme 1**) [143]. The benzyl (Bn) protecting group was then employed to protect all glycosyl hydroxyl residues, the likes of which would ultimately allow for global deprotection via hydrogenolysis. Elimination of the amide bound fatty acyl chain resulted in the free glucosamine moiety, which was subsequently protected as the 2,2,2-trichloroethoxycarbonyl(Troc). The Troc protecting

group was employed for its proven β-glycoside directing ability through neighbouring group participation.[144] Cleavage of the glycosidic bond yielded readily available trichloroacetimidate glycosyl donor **4** [136], and DEA based glycosyl acceptor **5**. Finally, elimination of the fatty acyl chain on compound **5**, ultimately yielded DEA as the starting point of the synthesis.

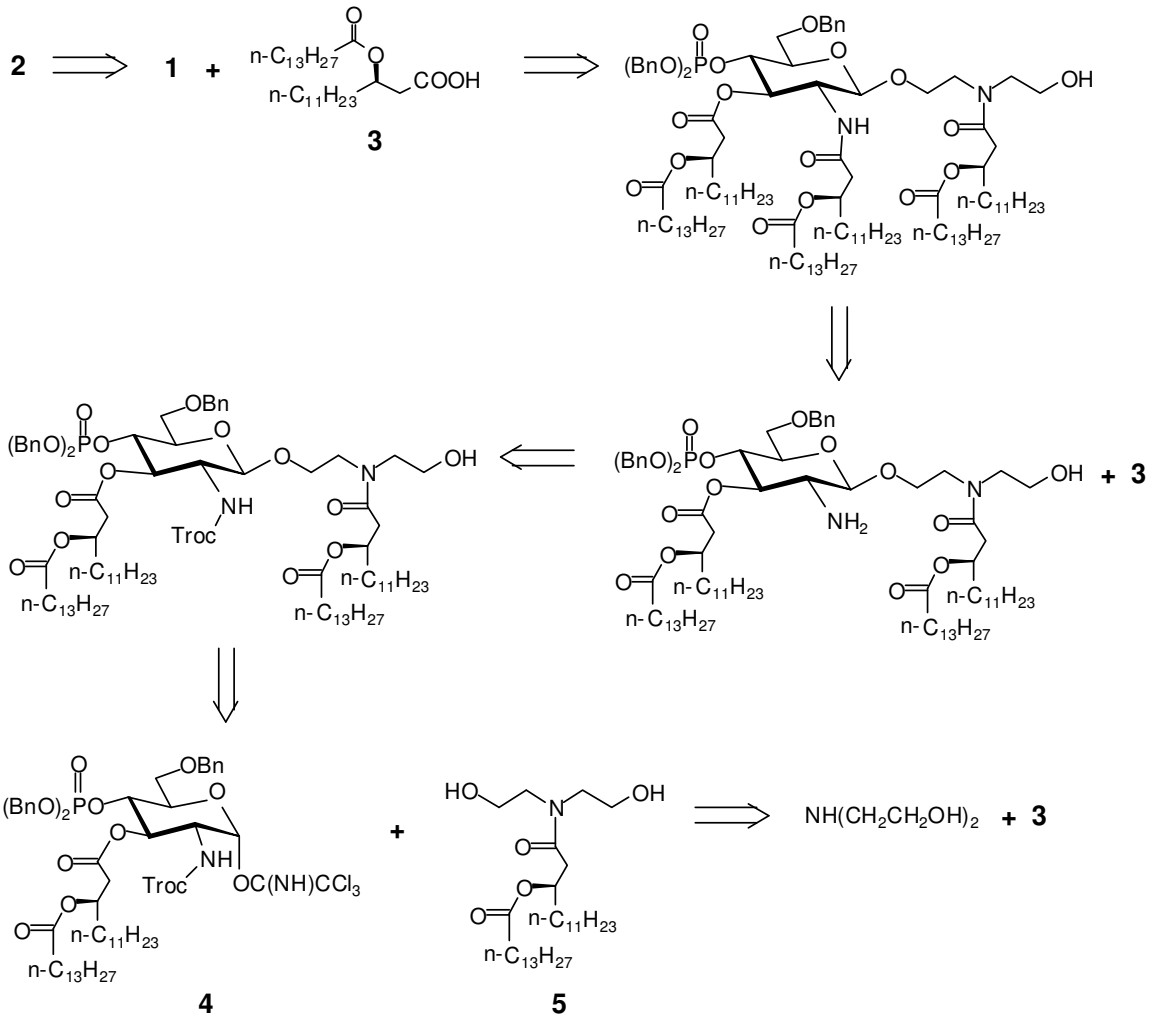

Scheme 1. Retrosynthetic Analysis of Targeted DEA-Containing Lipid A Mimics

2.1.3 Synthesis of Dilipid Acid 3

Natural to the archetypical lipid A structure from *E. coli* (**Figure 3**) are enantiomerically pure lipid moieties, specifically of the (*R*) orientation. Through the retrosynthesis of targeted lipid A mimics **1** and **2** (**Scheme 1**), enantiomerically pure dilipid acid **3** [143] arose as a necessary chemical building block. As such, **3** was prepared via a known literature procedure [143]. Briefly, a Reformatsky reaction between commercially available dodecyl aldehyde and ethyl bromoacetate forms a racemate of β-hydroxy ester **I** (**Scheme 2**). Hydrolysis of the ethyl ester yields a racemate of mono-lipid acid **II**. Enantiomeric enrichment was achieved via the formation the optically pure (*R*)-salt of mono-lipid acid **II** and commercially available (+)-dehydroabietylamine through repeated recrystalization efforts. Hydrolysis of the optically pure salt provides pure-(R) monolipid acid **III**, the enantiomeric excess of which was estimated to be > 95% based on optical rotation measurements. The protection of the carboxylic acid **III** as the corresponding phenacyl ester allowed for conversion into dilipid acid based **V** (**Scheme 3**) via reaction with myristoyl chloride in pyridine. Finally, deprotection of the carboxylic acid yields desired optically pure (*R*)-dilipid acid **3**.

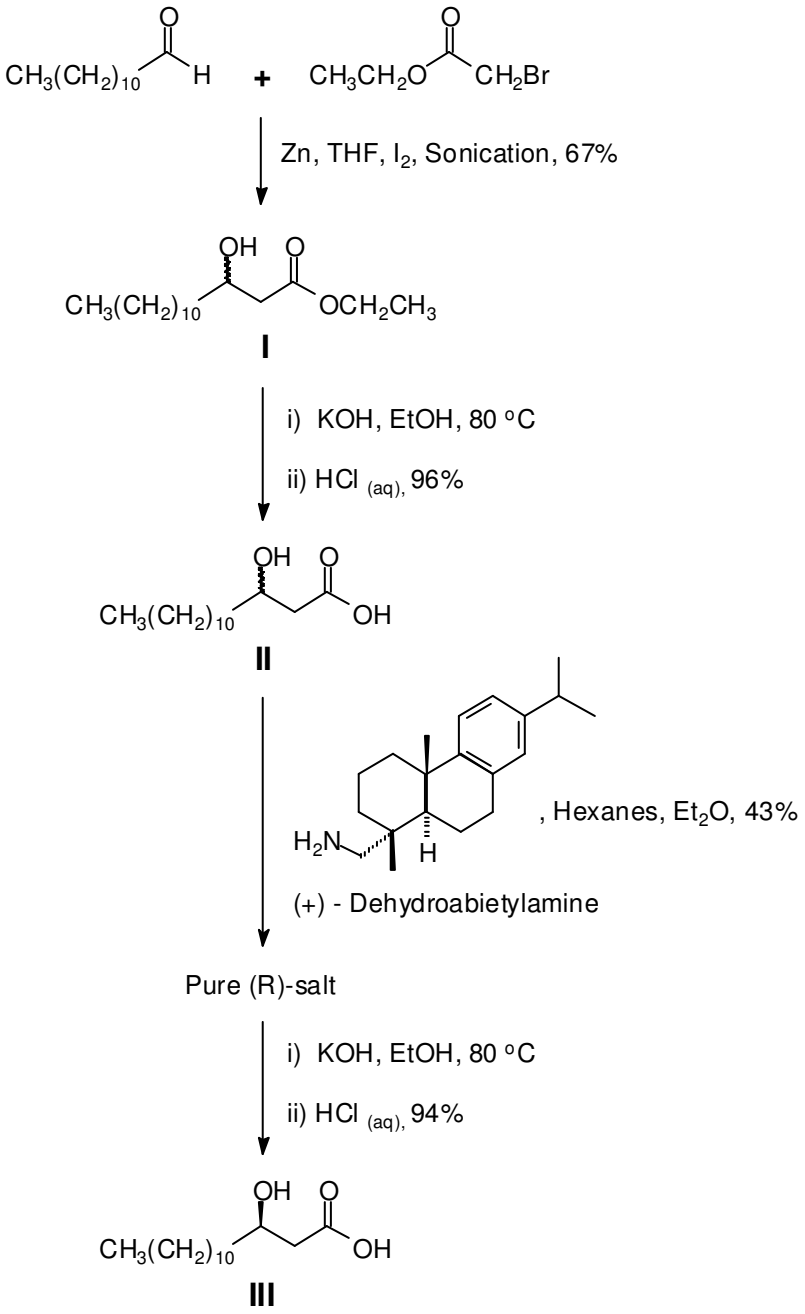

Scheme 2. Synthesis of Enantiomerically Pure Monolipid Acid **III**

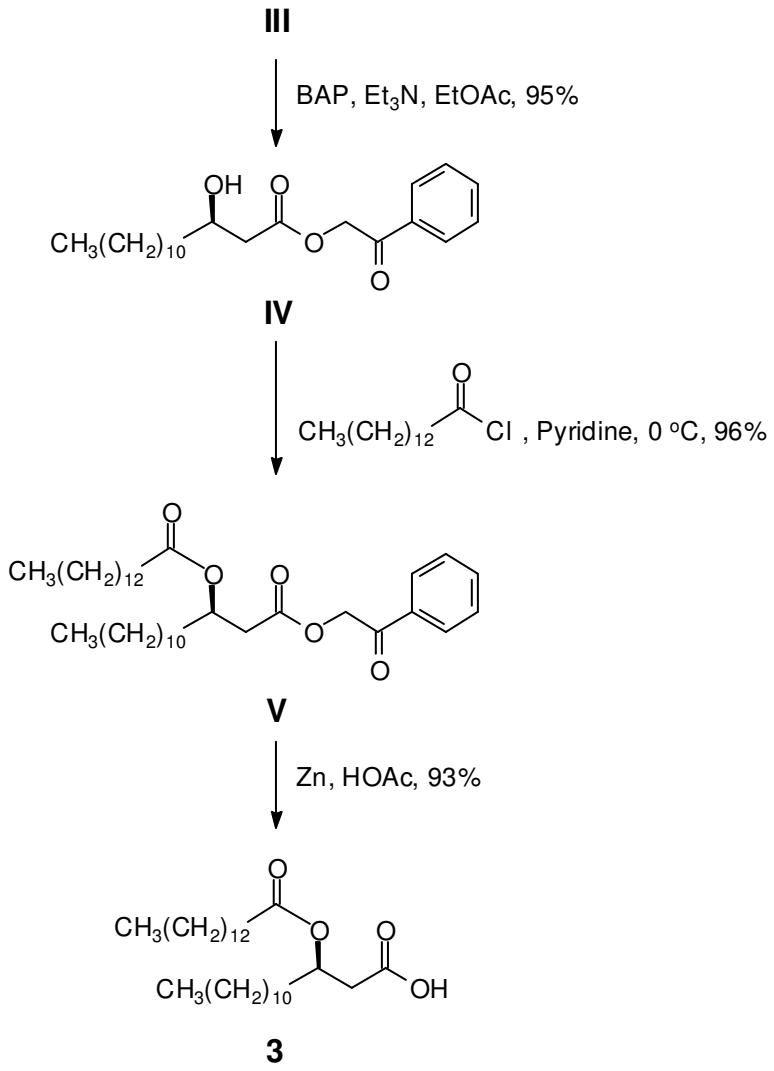

Scheme 3. Synthesis of Dilipid Acid **3**

2.1.4 Synthesis of Diethanolamine-Containing Lipid A Mimics

The synthesis of the designed lipid A Mimics **1** and **2** began with the installation of the fatty acyl chains onto the DEA acyclic scaffold (**Scheme 4**). As such, the amine moiety in DEA was selectively acylated with dilipid acid **3** [143] under the promotion of peptide coupling reagent *O*-benzotriazole-*N*, *N*, *N*', *N*'-tetramethyl-uronium-hexafluorophosphate (HBTU) to form glycosylation acceptor **5** in 68% yield. NMR spectral data indicated that the two ethanol residues in **5** were not identical, a consequence of the prohibited free rotation about the amide bond. The trimethylsilyl tirfluoromethanesulfonate (TMSOTf) catalyzed glycosylation of **5** with known imidate donor **4** [136] yielded the desired mono-glycosylation product **6** in 53% yield, along with the di-glycosylation product **7**, which was isolated in 15% yield. Compound **6** existed as a mixture of two rotational isomers in an approximate rationof 3:2 as a result of the presence of the secondary amide moiety. The desired β-glycosidic linkage in **6** was confirmed by NMR spectral data (^{1}H NMR: δ 4.78, d, *J* 8.0 Hz, H-1 from one isomer; and ^{13}C NMR: δ 100.44 and 100.87, C-1 of two isomers).

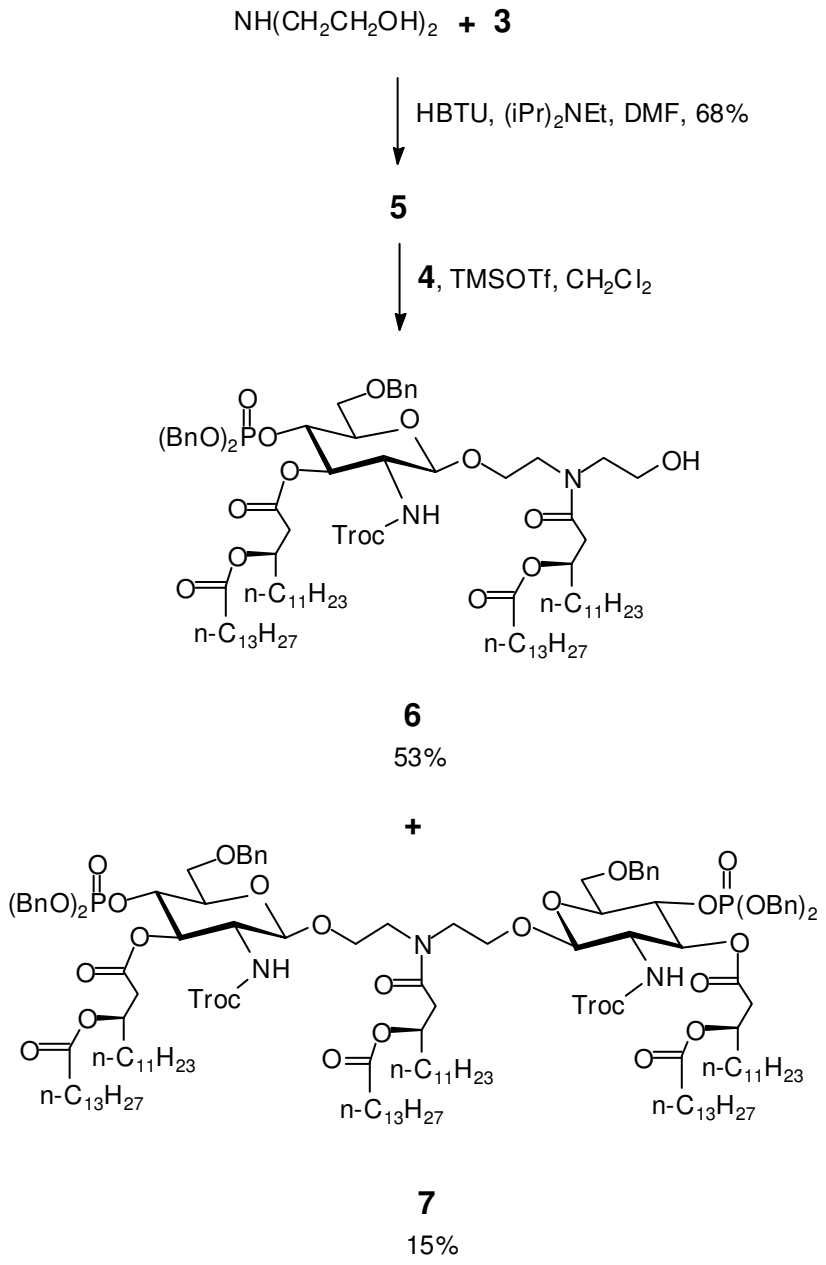

Scheme 4. Synthesis of DEA-Containing Mimic Framework

Removal of the *N*-Troc protecting group in **6** via treatment with zinc in acetic acid-THF (1:4) provided free amine **8** (**Scheme 5**), which was found to be slowly converted to a new product spot during the reaction, as visualized by TLC. This unexpected product was isolated and its MS data showed a molecular weight with and additional 72 mass units,

which corresponded to the incorporation of a THF molecule. Careful analysis of the respective NMR data led to the establishment of its structure as **9**.

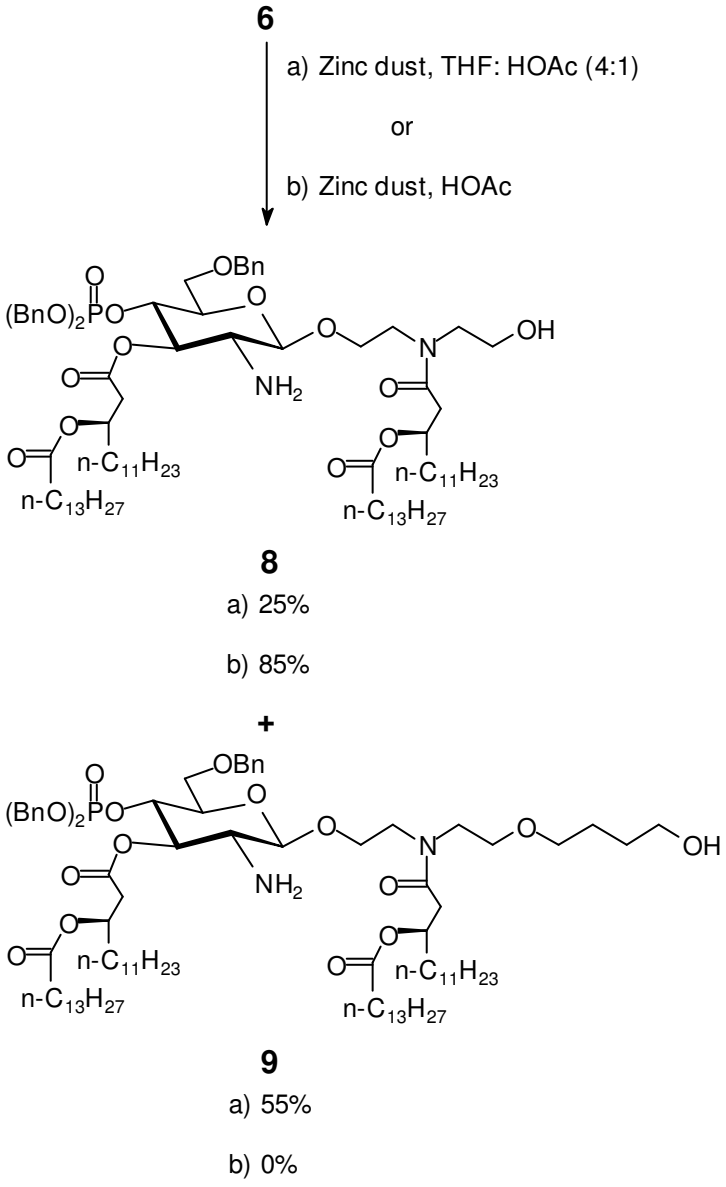

Scheme 5. Cleavage of the N-Troc Protecting Group

THF ring opening is usually initiated by a strong Lewis acid [145, 146] or an electrophilic reagent.[147, 148] With the weakly acidic reaction conditions employed for the cleavage of

the *N*-Troc protecting group, the ring opening of THF was suspected to be initiated by an electrophilic intermediate present in the reaction. Indeed, earlier studies showed that β-hydroxy alkylamides reacted with carboxylic acids via oxazolinium cation intermediates to form esters.[149, 150] Accordingly, we proposed a mechanism to account for the formation of product **9** (**Scheme 6**). Under acid catalysis, compound **8** could dehydrate to form oxazolinium cation **II**, which thereby reacted readily with nucleophiles present in the reaction mixture. Thus, the reaction of **II** with THF led to intermediate **III**, which was followed by a nucleophilic attack by water to generate compound **9**. Water was certainly present in the reaction mixture as the solvents were not dried. Accordingly, direct attack of intermediated **II** by water would regenerate compound **10**. Acetic acid was likely the weakest nucleophile present, and thus no product carrying an additional acetate functionality was observed. Supporting this proposed mechanism, was the clean conversion of compound **7** into desired amine **8** when the reaction was repeated with acetic acid as the sole solvent (**Scheme 5**).

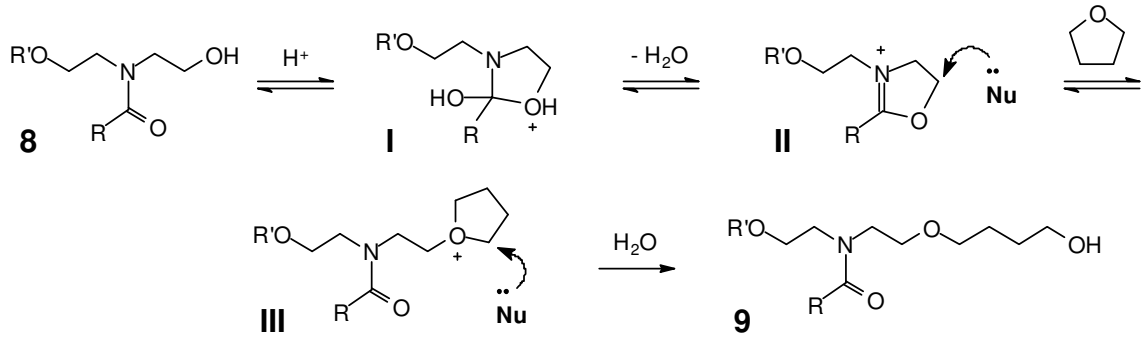

Scheme 6 Postulated Mechanism For The Incorporation of a Ring-Opened THF Residue to Form Product **9**

The *N*, *N*'-dicyclohexylcarbodiimide (DCC) promoted coupling of amine **8** with dilipid acid **3** provided both hexa-acylated **10** and octa-acylated **11** in 65% and 16% yields, respectively (**Scheme 7**). Acylation of a hydroxyl group normally does not occur under solely DCC-promoted peptide coupling condition, and typically requires the inclusion of the acyl transfer-reagent 4-dimethylaminopyridine (DMAP). Previous reports have shown that the hydroxyl group in β-hydroxy alkylamides displays higher reactivity than normal alcohols, the likes of which was noted to be likely the result of an intra-molecular hydrogen bond.[151, 152] Therefore, the formation of **11** might be due to an increased nucleophilicity of the hydroxyl group in **10** as a result of the presence of the same type of intra-molecular hydrogen bonding (**Figure 19**). Through said hydrogen bonding, resonance structure **10-B** is further stabilized and the electron density on the oxygen atom of the hydroxyl group is increased. Since enough material of **11** was obtained from this reaction, no attempt was made to prepare **11** separately through further acylation of **10** under typical hydroxyl acylation conditions.

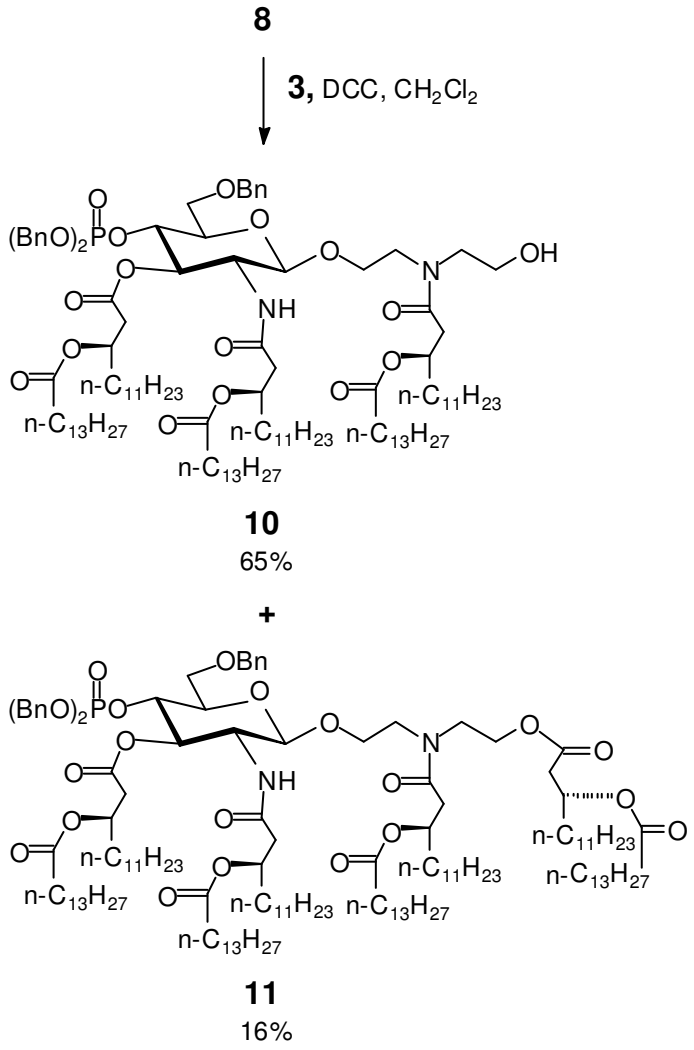

Scheme 7. Acylation of Glycosyl Amine Moiety

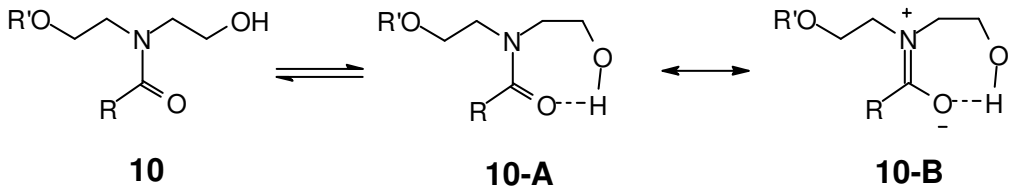

Figure 19. Intra-Molecular Hydrogen Bonding in **10** *via* a Seven-Member Ring

Global de-benzylation of **12** was furnished via catalytic hydrogenation under atmospheric pressure in the presence of palladium on charcoal. Initially the reaction was carried out in an acetic acid-THF (1 : 4) solvent system to give the desired product **1** in 44% yield, together with a side a product **12** in 21% yield (**Scheme 8**). The structures of **1** and **12** were confirmed by their ^{1}H NMR and ESI-MS data. Side product **12** contained an additional 1-hydroxybutyl group reminiscent to that of compound **9**, which was formed under similar reaction conditions (acetic acid-THF, **Scheme 3**). Thus, the formation of **12** (and other partially debenzylated precursors) was most likely through the same mechanism described for the formation of **9** (**Scheme 6**). It was also noticed that higher temperatures (even at 30 °C) could significantly increase the conversion rate of **1** to **12**. An acetic acid-THF mixture is a common solvent mixture used for the hydrogenation reactions of this type of compound.[141, 153-155] The reaction was initially tried with this solvent mixture with no concept, at the time, about the mechanistic details for the formation of side product **9**. Since the formation of the oxazolinium cation was acid catalysis dependent, the hydrogenation of **10** was repeated using THF alone as the solvent. Indeed, the side reaction could be largely suppressed without acetic acid as the co-solvent: the side product **12** was formed in less than 5% and the yield of **1** was raised to 76%. Finally, a similar global debenzylation of **11** in THF provided **2** in 85% yield, with its structure confirmed by ^{1}H NMR and high resolution ESI-MS data (**Scheme 9**).

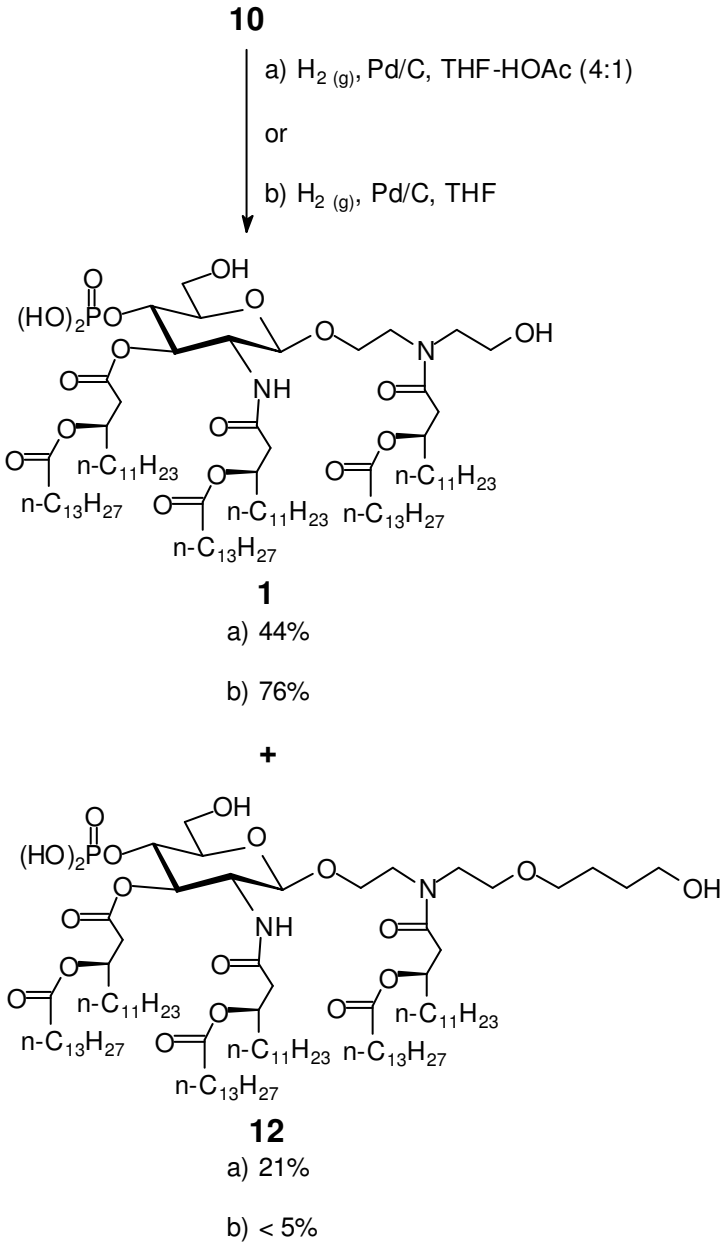

Scheme 8. Global Deprotection of **10** to Obtain DEA-Containing Lipid A Mimic **1**

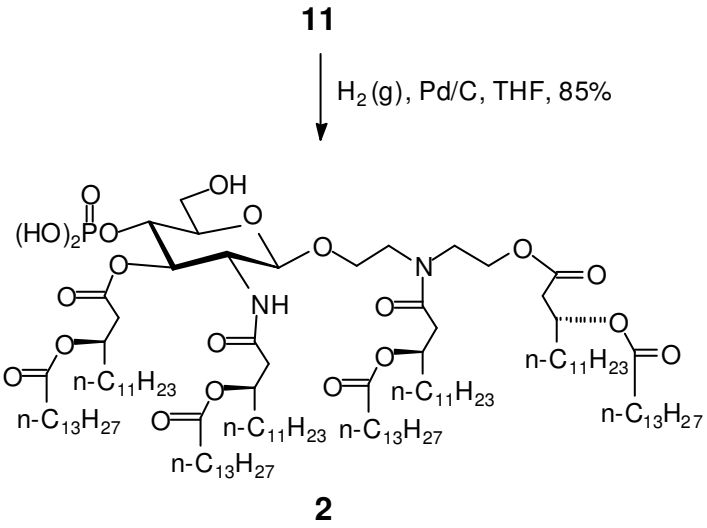

Scheme 9. Global Deprotection of **11** to Obtain DEA-Containing Lipid A Mimic **2**

2.1.5 Biological Evaluation

The activation of TLR4 by specific ligands leads to the release of pro-inflammatory cytokines and the up-regulation of cellular adhesion molecules. The Human pre-monocytic THP-1 cell line expresses TLR4 as well as other receptors [156], and LPS has been shown to induce the expression of intercellular adhesion molecule-1 (ICAM-1) in these cells.[157, 158] Our initial studies of the immunostimulatory activity of lipid a mimics **1**, **2** & **12** involved the evaluation of the molecules in affecting the expression level of ICAM-1 by pre-monocytic THP-1 cells.

Preliminary data indicates that compound **1** significantly increases the level of ICAM-1 expression in Human pre-monocytic THP-1 cells (**Figure 20**). Compound **12** also exhibits significant activity, although it is less potent than **1**. A maximum ICAM-1 expression level is achieved at a concentration of 2.0 μM for both **1** and **12**, upon which further increases in their concentrations results in a decrease in ICAM-1 expression levels. In contrast, no significant increase in ICAM-1 expression level is noted for octa-

acylated analog **2** up to the highest concentration tested (4.0 μM). Importantly, all three compounds (**1**, **2** & **12**) show no detrimental effect on cell viability at the highest concentrations tested for each, as measured through the assay of cellular Trypan Blue exclusion.

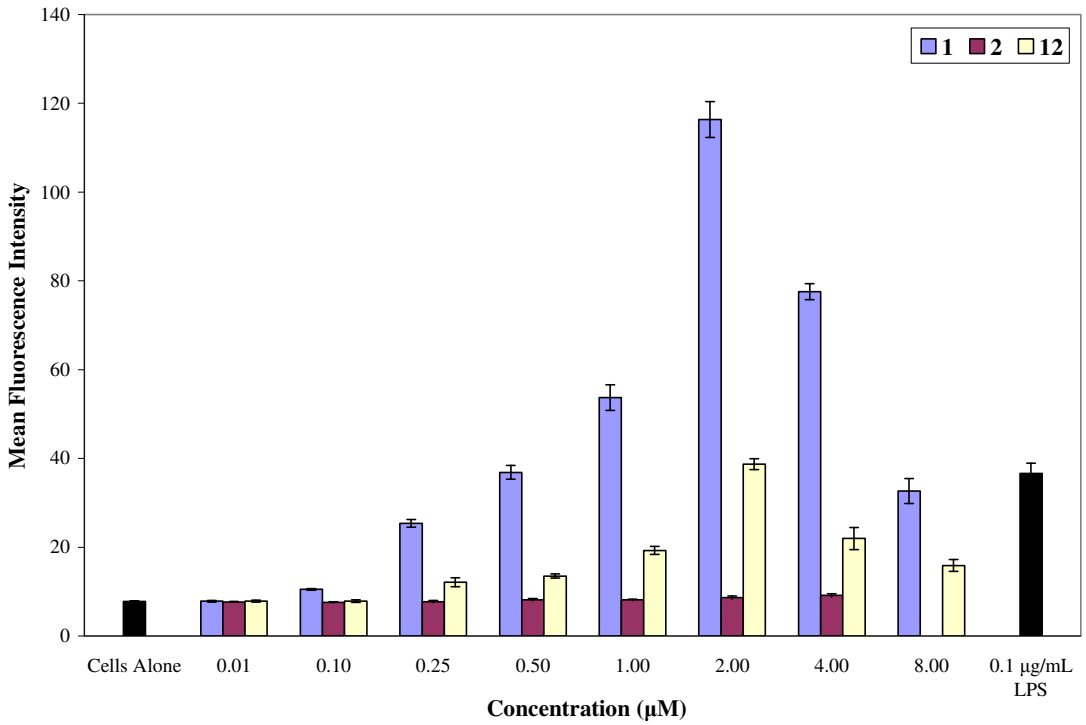

Figure 20. ICAM-1 expression by THP-1 cells after exposure to LPS & lipid A mimics (**1**, **2** & **12**). THP-1 cells were incubated for 18 h with increasing concentrations of **1**, **2** & **12**. The resulting ICAM-1 expression was measured via immunostaining and flow cytometry analysis. The results are expressed as the mean fluorescence intensity and are shown as the average of three separate experiment.

ICAM-1 expression is NF-κB-dependent, and induction of high levels of ICAM-1 occurs in response to various inflammatory mediators, including bacterial LPS, and pro-inflammatory cytokines, such as tumour necrosis factor-α (TNF-α), interleukin-1β (IL-1β), and γ-interferon (γ-IFN) [159, 160]. In an effort to further characterize the immunostimulatory properties of **1**, **2** & **12**, the direct effects of the analogs on TNF-α,

IL-6, and IL-1β cytokine production were measured via the enzyme-linked immunosorbent assay (ELISA) methodology. The pre-monocytic THP-1 cell line is weakly responsive in terms of cytokine production to immunostimulatory signals such as LPS.[161] As such, terminal differentiation of the pre-monocytes was induced via 5 ng mL^{-1} of phorbol 12-myristate 13-acetate (PMA), the concentration of which was chosen to ensure that residual cytokine expression levels would be minimal and that small responses to weak stimuli were measurable.[162]

In general, the responses measured for all three cytokines mirror that of the ICAM-1 expression response, with compound **1** showing the greatest potency, compound **12** showing a slightly decreased potency, and compound **2** inducing very little to no detectable response (**Figures 21-23**). Both **1** and **12** induce the highest level of TNF-α, IL-6, and IL-1β at the 9 μM maximum concentration tested, which is in contrast to the induction of ICAM-1 expression, which maximized at a 2 μM stimulus concentration. The IL-1β induced by **1** and **12** at the 9 μM stimulus concentration is 3-4 fold that induced by *E. coli* LPS at a concentration of 0.01 μg mL^{-1}. Interestingly, compound **2** also induces significant IL-1β expression at the 9 μM maximum stimulus concentration tested, while at lower stimulus concentrations (up to 3 μM), the level of IL-1β is hardly detectable. IL-1β contributes to host defence against infection by augmenting the antimicrobial properties of phagocytes and initiating Th1 and Th17 adaptive immune responses.[163] Production of IL-1β involves the proteolytic cleavage of pro-IL-1β by intracellular cysteine protease caspase-1[164], which is regulated by protein complexes called inflammasomes.[165] Since **2** does not show any activity in the induction of ICAM-1 expression and other pro-inflammatory cytokines including TNF-α and IL-6, it is a

possibility that the induction of IL-1β by **2** may involve a different mechanism than that of analogs **2** and **12**.

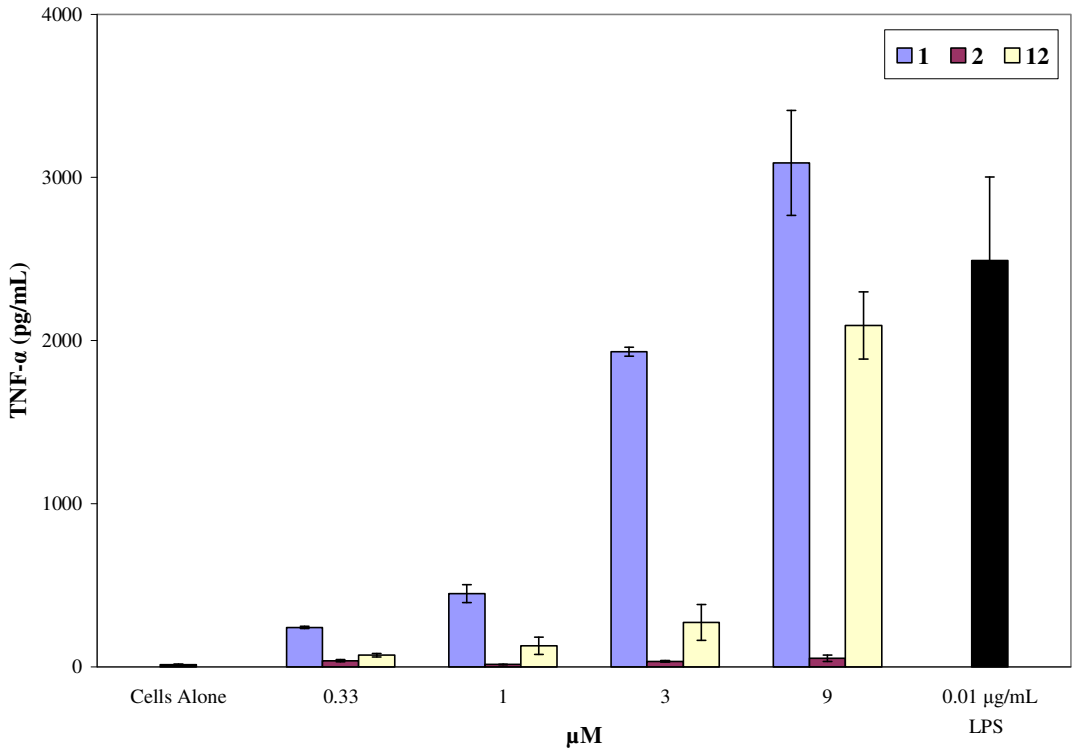

Figure 21. TNF-α production by differentiated THP-1 monocytes after exposure to LPS & lipid A mimics (**1**, **2** & **12**). THP-1 monocytes were incubated for 24 h with increasing concentrations of lipid A mimics **1**, **2** & **12**. TNF-α in cell supernatants was measured via ELISA. The results are shown as the average of two separate experiments.

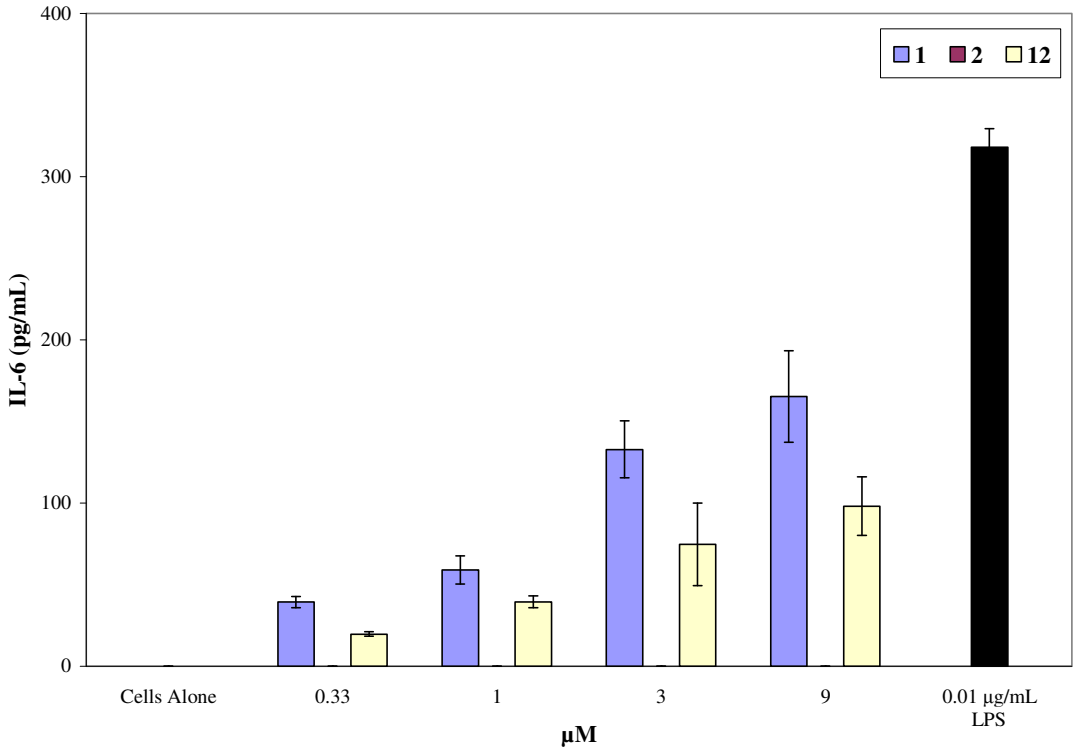

Figure 22. IL-6 production by differentiated THP-1 monocytes after exposure to LPS & lipid A Mimics (**1**, **2** & **12**). THP-1 monocytes were incubated for 24 h with increasing concentrations of lipid A mimics **1**, **2** & **12**. IL-6 in cell supernatants was measured via ELISA. The results are shown as the average of two separate experiments.

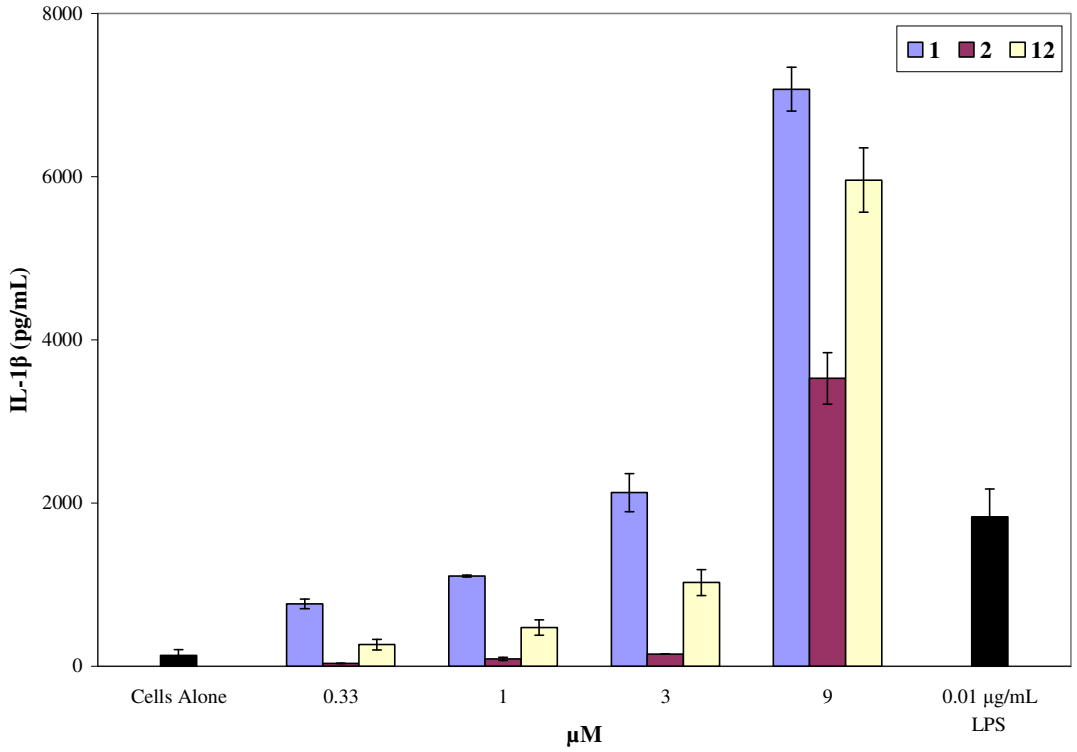

Figure 23. IL-1β production by differentiated THP-1 monocytes after exposure to LPS & lipid A Mimics (**1**, **2** & **12**). THP-1 monocytes were incubated for 24 h with increasing concentrations of lipid A mimics **1**, **2** & **12**. IL-1β in cell supernatants was measured via ELISA. The results are shown as the average of two separate experiments.

Structurally speaking, the hexa-acylated analog **1** shows the highest potency in the induction of both ICAM-1 expression and the expression of pro-inflammatory cytokines (TNF-α, IL-6, and IL-1β). This immunostimulatory activity is retained with the additional 1-hydroxybutyl group incorporated in the diethanolamine moiety of **12**, albeit with reduced potency. However, the increased number of lipid chains in octa-acylated analog **2** seems to have a more profound effect on immunostimulatory activity, as **2** appears inactive in terms of inducing ICAM-1 expression, as well as inducing TNF-α and IL-6 production up to the highest concentration tested in each assay. Although significant IL-

1β production is observed at the highest concentration of **2** tested, this may involve a different mechanism from TLR4/MD-2 activation, which is presumably the mechanism of action of analogs **1** and **12**.

2.2 Improving Immunostimulatory Potency

2.2.1 Design

The two phosphate groups in lipid A greatly affect the immunological activity of lipid A/LPS. Deletion of either of the phosphates reduces endotoxic activity ~100 fold, while elimination of both phosphates abolishes all activity.[166] Phosphate groups are not a strict requirement, however, as other negatively charged and acidic groups have been employed as bioisosteres of the phosphates, with only minor effects noted.[167, 168] In the crystal structure of the TLR4/MD-2 receptor complex bound to LPS, the two phosphate groups of lipid A have been shown to play an important role in receptor-ligand binding, and the subsequent receptor dimerization/activation. The phosphates provide ionic interactions with positively charged residues on both TLR4 and MD-2, as well as the adjacent TLR4 within the dimer complex.[68]

Given the key role the two phosphate groups of lipid A play in the dimerization and activation of the TLR4/MD-2 receptor complex, two novel analogs of the DEA-containing lipid A mimic framework (**Figure 24**) were therefore targeted in an effort to improve the immunostimulatory potency of lipid A mimic **1** (**Figure 18**). Mimic **13** includes an additional phosphate on the diethanolamine scaffold, while mimic **14** contains a terminal carboxylic acid moiety as a phosphate bioisostere.

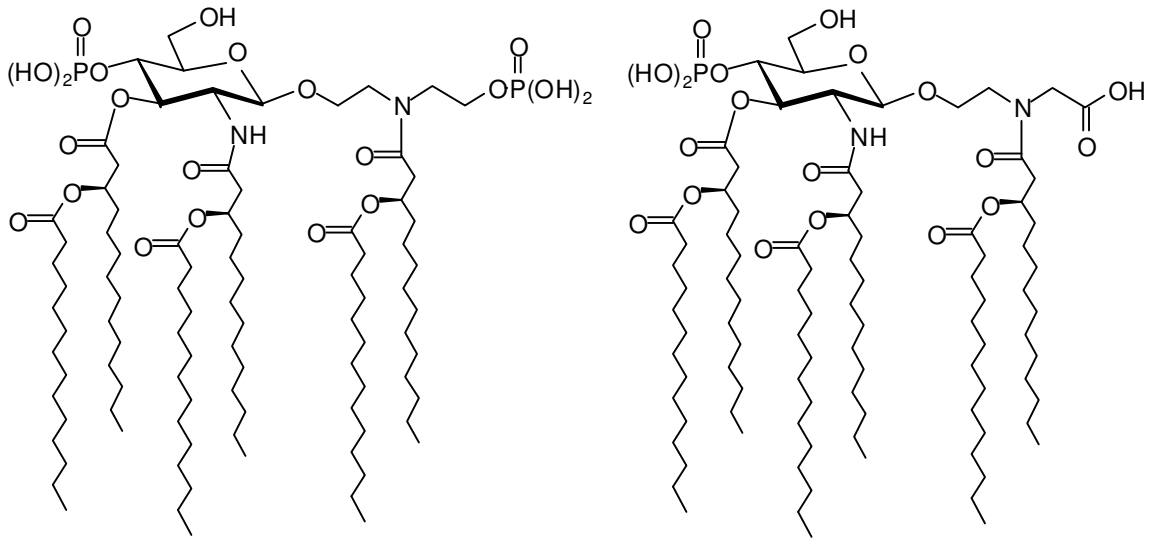

Figure 24. Novel DEA-Containing Lipid A Mimics Targeted

2.2.2 Retrosynthetic Analysis

There is significant evidence indicating that the degree, pattern, and chain length of the lipid acylation in lipid A molecules are important factors contributing to their overall biological activity.[60, 61] The previously reported synthesis of DEA-containing lipid A mimic **1** installed a defined lipid onto the DEA acyclic scaffold at the early stages, thus limiting the potential for incorporating variation in any of the above mentioned acyl characteristics. An alternate synthetic strategy was therefore employed for accessing lipid A mimics **13** and **14**, in an effort to ultimately allow for facile acyl chain variation in future structure-activity relationship investigations.

Beginning with either mimic **13** or **14**, elimination of the DEA-bound phosphate of **13** or reduction of the terminal carboxylic acid moiety of **14** into the respective primary hydroxyl yields mimic **1** (**Scheme 8**). The previous synthesis of lipid A mimic **1** left the DEA terminal hydroxyl free throughout the synthesis, which proved problematic at many

stages, including a propensity to form undesired di-glycosylated products, issues with acylation selectivity, and the interesting side reaction in which the solvent THF molecule was ring-opened to form 1-hydroxybutyl adducts. As such, the DEA terminal hydroxyl was kept protected as the *tert*-butyldiphenylsilyl ether (TBDPS) until the late stages of the synthesis. Combining this protection with the protection of the glycosyl and phosphate hydroxyl moieties as benzyl ethers yields **25**. Elimination of both amide and ester bound acyl lipid chains yields the di-amine, mono-hydroxyl framework, following which both amine moieties were protected as their Troc carbamates. Elimination of the 6-*O*-benzyl ether and the 4-*O*-phosphotriester yields **21**, following which the protection of all glycosyl hydroxyls as their respective acetates (Ac) yields **20**. Disconnection of the glycosidic bond yields glycosylation acceptor **17**, and known trichloroacetimidate glycosylation donor **19.**[169] Finally, elimination of the DEA-bound TBDPS moiety in **17** yields **15**, from which elimination of the Troc carbamate moiety again yields DEA as the starting point of the synthesis.

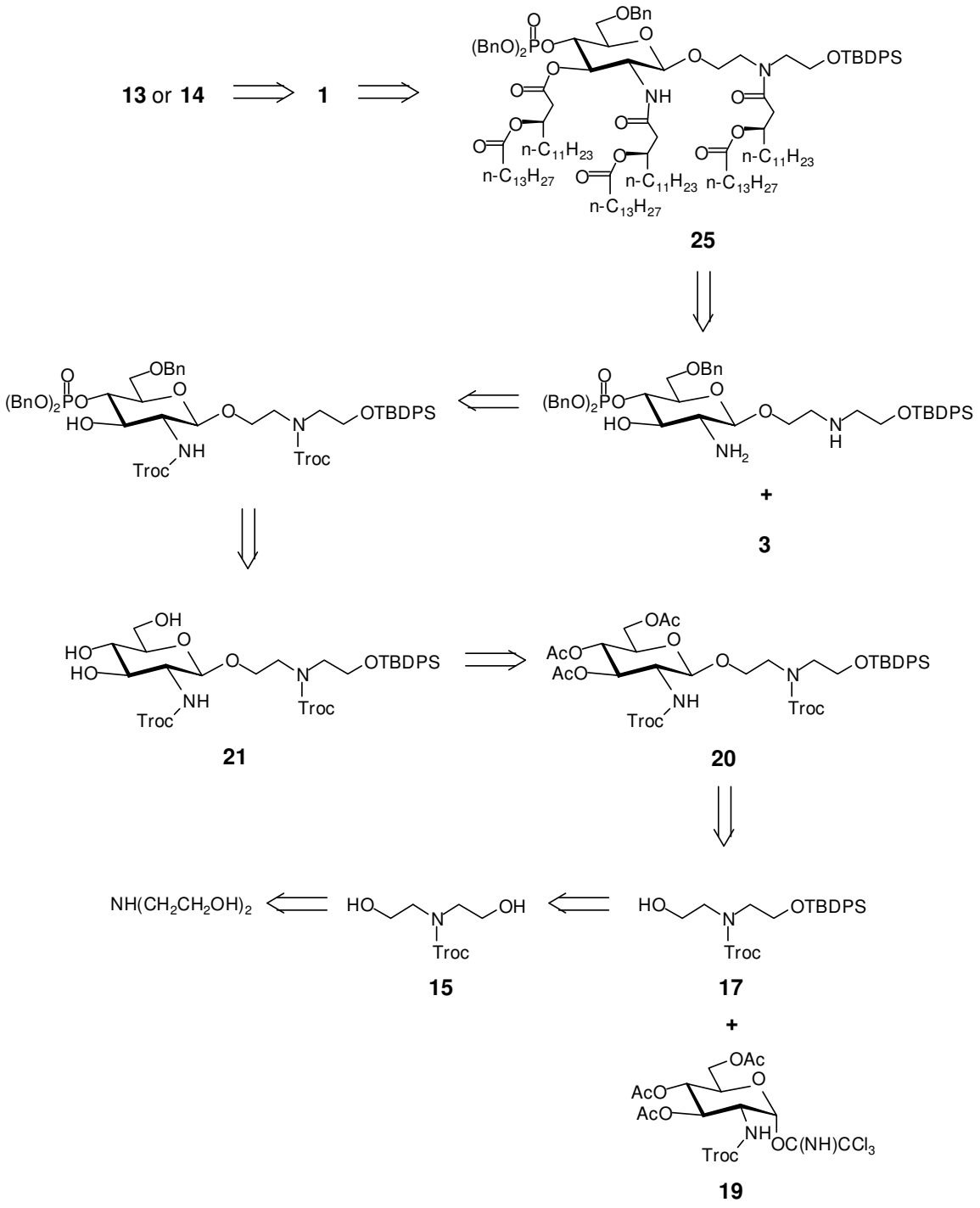

Scheme 8. Retrosynthetic Analysis of Novel DEA-Containing Mimics Targeted

2.2.3 Synthesis

The amine moiety of diethanolamine was first protected as the Troc carbamate by reaction with 2,2,2-trichloroethoxychloroformate (Troc-Cl) and sodium bicarbonate in water to furnish **15** in 78% yield, as well as **16** in a 7% yield, in which one of the β-hydroxy moieties has reacted to form the Troc carbonate (**Scheme 9**). Attempts at the protection of one of the β-hydroxy moieties of **15** as the TBDPS ether yielded mono-silylated **17**, and di-silylated **18** in 54% and 6%, respectively, with a 35% recovery of unreacted **15**.

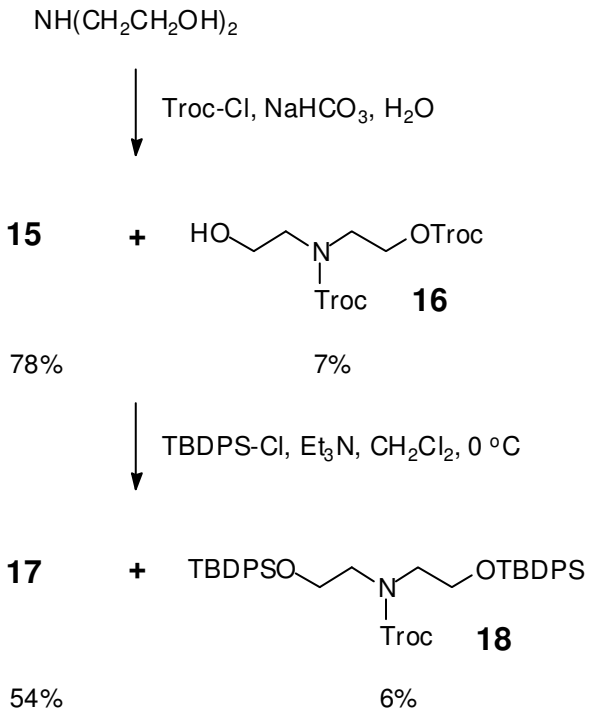

Scheme 9. Synthesis of Glycosylation Acceptor **17**

The TMSOTf catalyzed glycosylation of **17** with known imidate donor **19** [169] yielded glycoside **20** in 94% yield (**Scheme 10**). Similar to the previous synthesis of lipid A mimic **1**, compound **20** existed as a mixture of two rotational isomers in an approximate 1:1 ratio as a result of prohibited free rotation around the carbamate C-N bond. The desired β-glycosidic linkage in **20** was confirmed via NMR spectral data (^{1}H NMR: δ 4.53, d, *J* 8.5 Hz, H-1 from one isomer & δ 4.65, d , *J* 8.5 Hz, H-1 from the other isomer). Compound **20** was treated with guanidinium nitrate-sodium methoxide at room temperature to give the *O*-deacetylated product **21** in 91% yield, leaving the two *N*-Troc groups intact.[170] The acid catalyzed installation of the 4,6-di-*O*-benzylidene group furnished **22** in 87% yield. The DMAP and DIC promoted acylation of the 3-OH moiety in **22** with dilipid acid **3** yielded intermediate **23** in 93% yield.

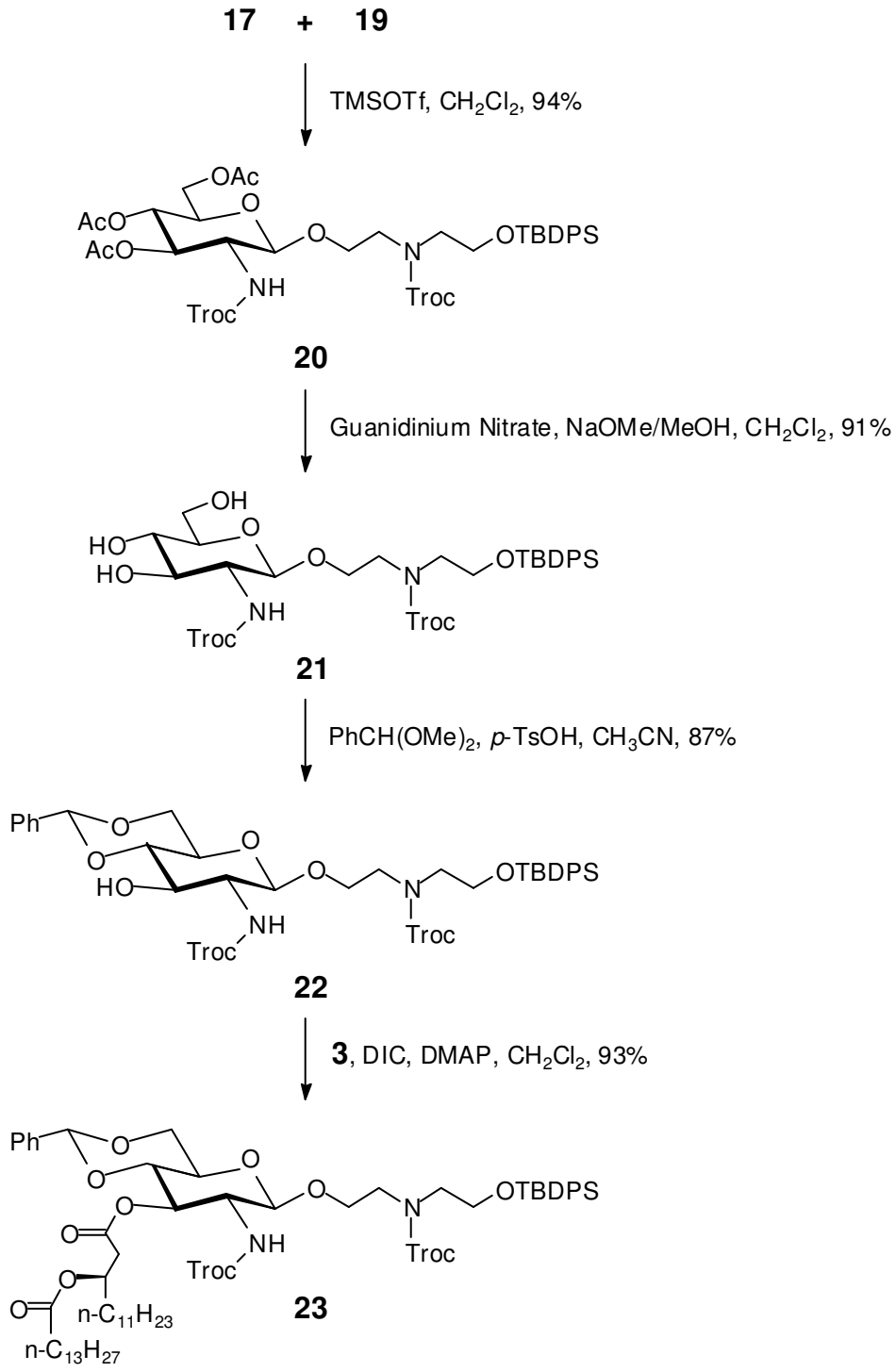

Scheme 10. Synthesis of 3-O Acyl Intermediate **23**

Regioselective benzylidene ring opening of **23** was next brought about via sodium cyanoborohydride ($NaBH_3CN$) and $HCl_{(g)}$-infused diethyl ether solution at 0 °C to give **24**, with the free 4-OH, in an 87% yield (**Scheme 11**). The installation of the benzyl protected phosphotriester at the free 4-OH position followed via the reaction of **24** with 5-phenyl tetrazole (5-Ph-tetrazole) and dibenzyl *N*,*N*-diisopropylphosphoramidite [$(BnO)_2PN(iPr)_2$], and the subsequent *m*-chloroperbenzoic acid (*m*-CPBA) promoted oxidation at 0 °C to yield advanced intermediate **25** in 85% yield. Following the removal of both *N*-Troc protecting groups, the advanced intermediate **25** would allow for chemoselective acylation of the two amine moieties, since the primary amine is anticipated to be more reactive towards an acylation reagent that the secondary amine due to the increased steric hindrance in the secondary amine.[171, 172] Thus, **25** could serve as a common precursor to accessing molecules with different acylation patterns on the two amine groups.

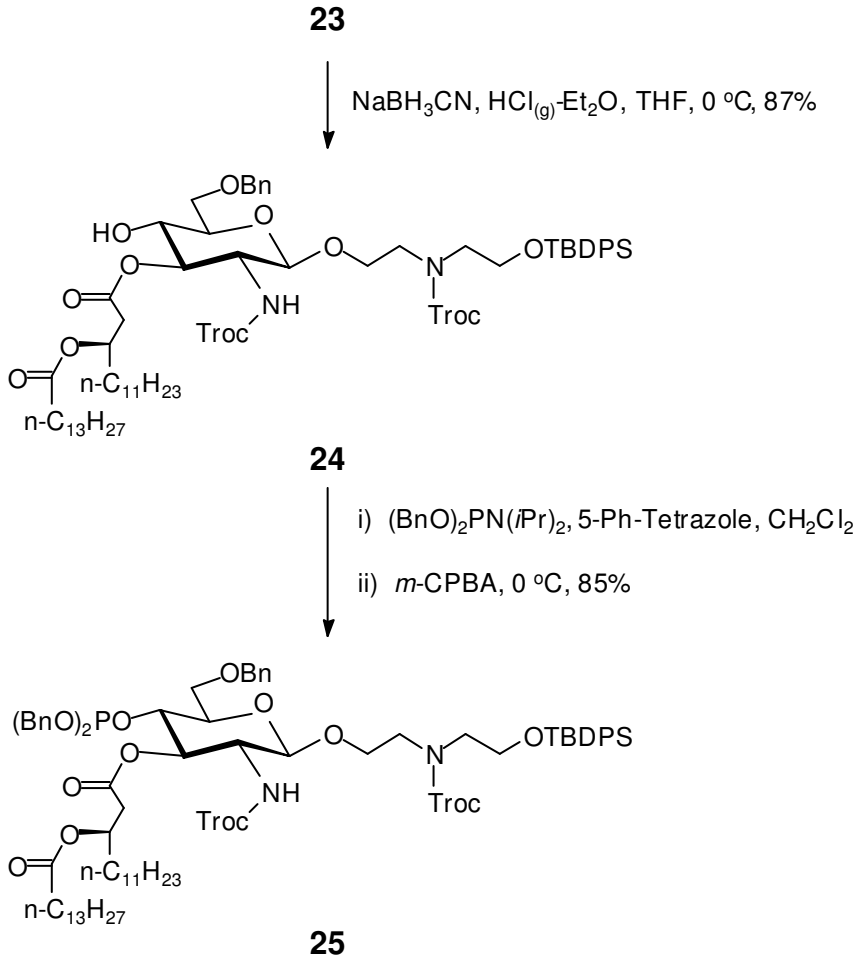

Scheme 11. Synthesis of Advanced Intermediate **25**

Compound **25** was subjected to a zinc treatment in acetic acid to furnish the di-amine, which was immediately coupled with dilipid acid **3** [143] under the promotion of the peptide coupling reagent HBTU to form **26** in 65% overall yield (**Scheme 12**). Deprotection of the acyclic scaffold hydroxyl via a tetrabutylammonium fluoride treatment furnished the previously reported intermediate **10** in 90% yield.

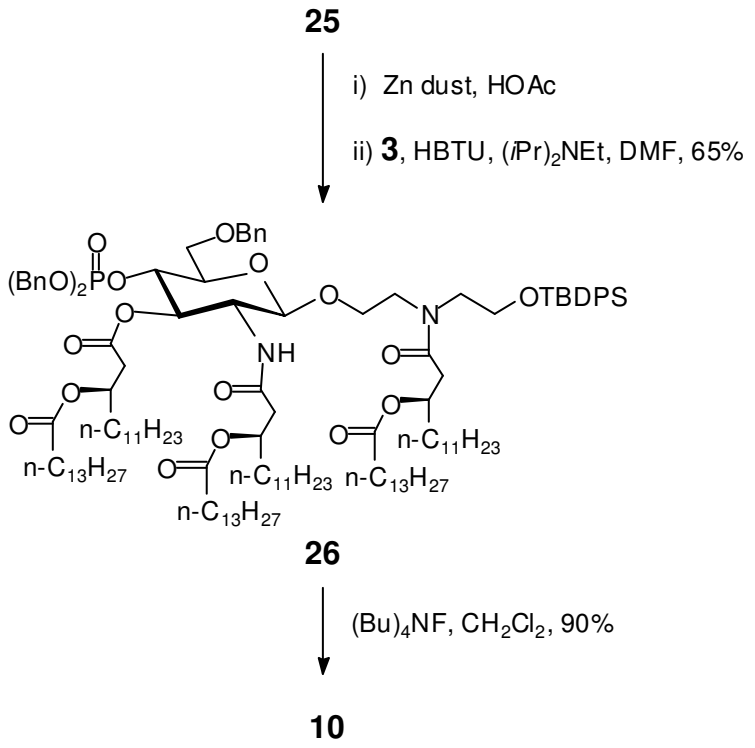

Scheme 12. Synthesis of Hexa-Acylated Intermediate **10**

To obtain the di-phosphate DEA-containing lipid A mimic **13**, compound **10** was subjected to a similar phosphoramidite treatment as **24** (**Scheme 11**) to install the desired phosphotriester functionality in **27** in 71% yield (**Scheme 13**). Compound **27** was found to be quite unstable during chromatographic purification, thus accounting for the less than ideal yield for the conversion of **10** to **27**, and was also noted to be rather unstable upon storage in the freezer. Practically, due to its relative instability, compound **27** had to be purified quickly and immediately subjected to global deprotection via catalytic hydrogenation under atmospheric pressure in the presence of palladium on charcoal to yield **13** in a 70% yield. The structure of **13** was confirmed by ^{1}H NMR and MALDI-MS data.

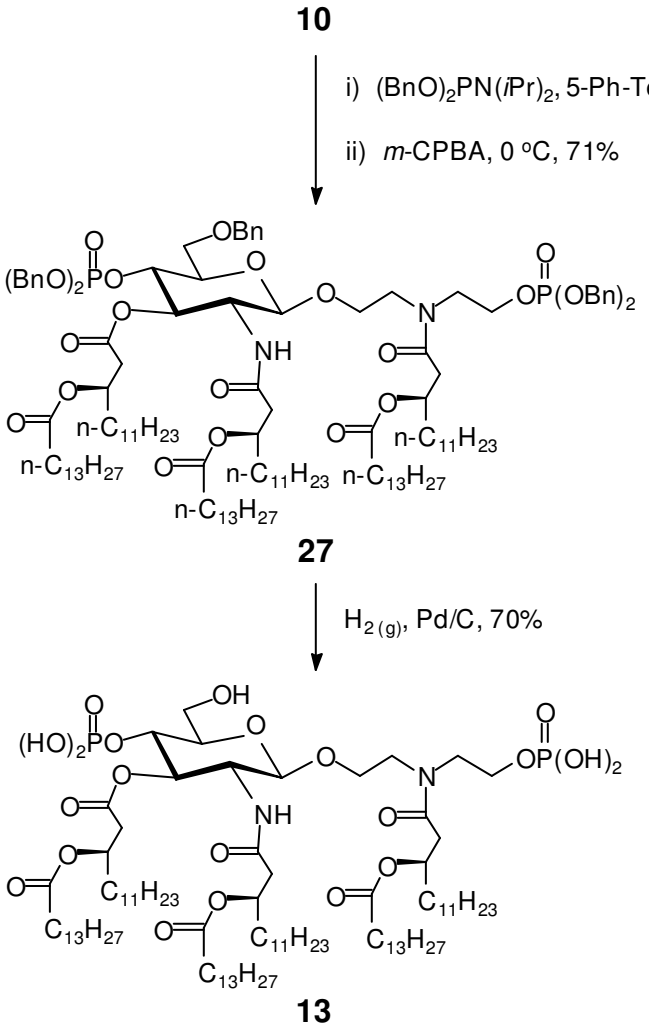

Scheme 13. Synthesis of Di-Phosphate DEA-Containing Lipid A Mimic **13**

The ready decomposition encountered with compound **27**, however problematic, was again attributed to the propensity of the DEA acyclic framework to form the oxazolinium ion, as previously noted. Thus, it is speculated that the decomposition of **27** may involve an intramolecular substitution to form the relatively stable oxazolinium ion **27-A** (**Scheme 14**).[149] Oxazolinium ions have been reported and structurally confirmed by NMR as intermediates for β-hydroxy alkyl amides, which react readily with a carboxylic acid to form esters under neutral conditions.[149] The oxazolinium ion **27-A** may undergo

nucleophilic attack or an elimination reaction leading to further decomposed products such as **27-B** to **27-D**. At this stage of the investigation, the structures of the decomposed products have not been determined.

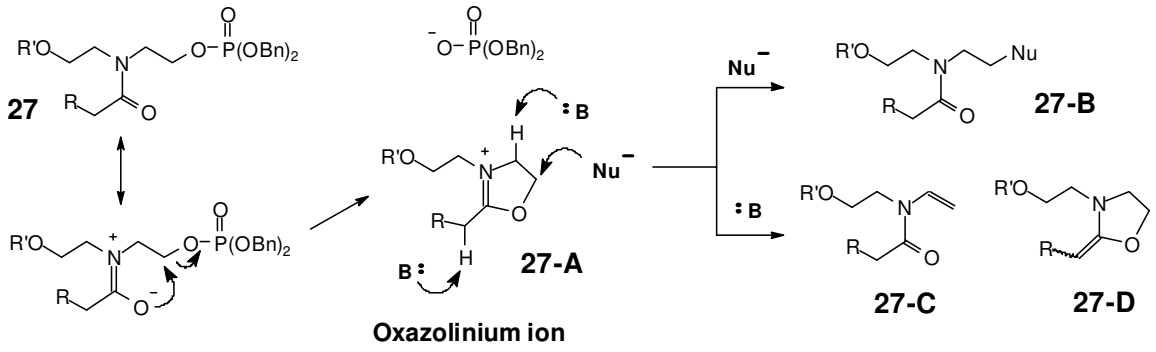

Scheme 14. Proposed Mechanism Accounting For The Ready Decomposition of **27**

To obtain the terminal carboxylic acid DEA-containing lipid A mimic **14**, the free hydroxyl of compound **10** was first subjected to a (2,2,6,6-tetramethylpiperidin-1-yl)oxyl (TEMPO) and bis(acetoxy)iodobenzene (BAIB) promoted oxidation to yield acid **28** in an 83 % yield, with which no stability issued were noted (**Scheme 15**). A similar catalytic hydrogenation to remove benzyl protecting groups in acid **28** yielded **14** in a 77% yield, the structure of which was again confirmed by ^{1}H NMR and MALDI-MS data.

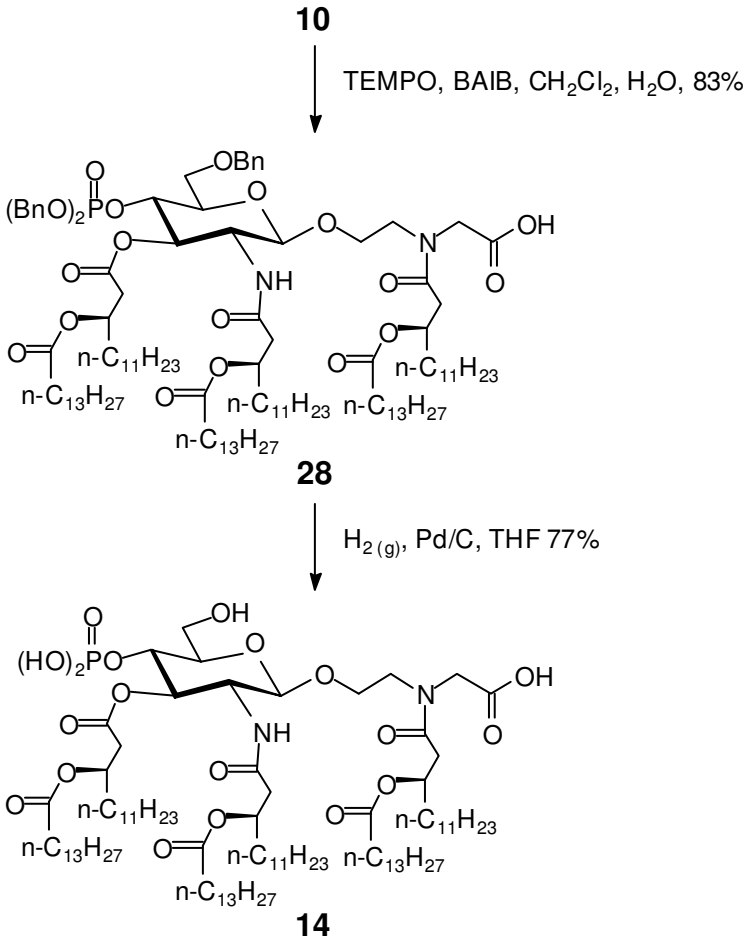

Scheme 15. Synthesis of Terminal Acid DEA-Containing Lipid A Mimic **14**

2.2.4 Biological Evaluation

To evaluate the relative immunostimulatory activity of lipid A mimics **1**, **13** & **14**, the direct effects of the mimics on TNF-α, IL-6, and IL-1β production in the PMA differentiated human monocytic cell line THP-1 was again evaluated. Initially, 5 ng ml^{-1} of PMA was employed for the differentiation process, in order to minimize residual cytokine levels, and thus allow low level responses to weak stimuli to be detected.[162] However, initial results obtained (not shown) were plagued by a both a lack of sensitivity and reproducibility. It was therefore concluded that the differentiation process was likely

incomplete, and that a greater concentration of PMA was needed to induce full differentiation. As such, all further experiments employed a PMA concentration of 25 ng mL^{-1}, a concentration which is much more in accordance with what is commonly reported for the differentiation of the THP-1 cell line.[173, 174]

Lipid A mimics **1, 13** & **14** were tested over a wide range of concentrations (10^{-4} μM-10 μM), and the cytokine responses follow a clear dose response relationship (**Figures 24-26**). A maximum response level is achieved for all three cytokines at a stimulus concentration of between 0.1 μM and 1.0 μM, after which a further increase to a 10 μM stimulus concentration results in decreased responses. Significant levels of TNF-α and IL-1β are induced by all three mimics at concentrations in the 10^{-3} μM range. Measurable IL-1β is also observed for mimic **14** at a concentration as low as 10^{-4} μM. In general, both mimics **13** and **14** show increased potency over mimic **1**, with mimic **14** showing the greatest potency for stimulating production of all three cytokines. This trend is most evident in the IL-6 response data (**Figure 25**), in which mimics **13** and **14**, in comparison to mimic **1**, exhibit an approximate 10-fold and 100-fold increase in potency, respectively. These results clearly indicate that the phosphate/phosphate bioisostere group on the DEA moiety plays an important role in the immunostimulatory potency of these lipid A mimics.

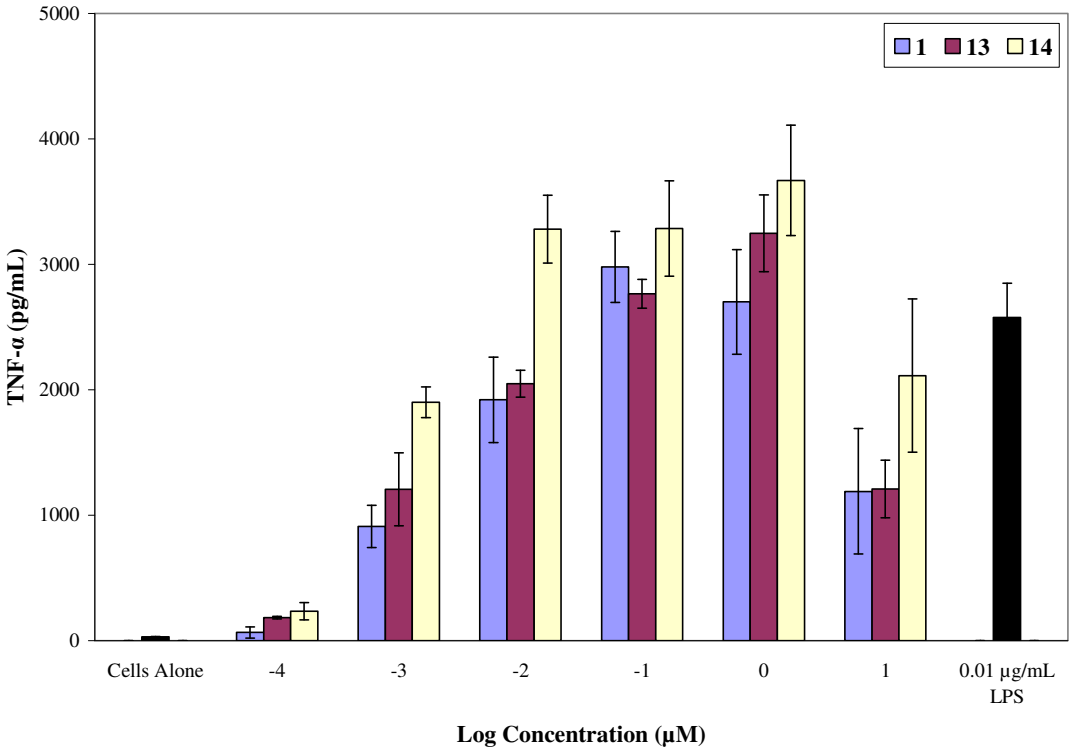

Figure 24. TNF-α production by differentiated THP-1 monocytes after exposure to LPS & lipid A mimics (**1**, **13** & **14**). THP-1 monocytes were incubated for 24 h with increasing concentrations of lipid A mimics **1**, **13** & **14**. TNF-α in cell supernatants was measured via ELISA. The results are shown as the average of two separate experiments.

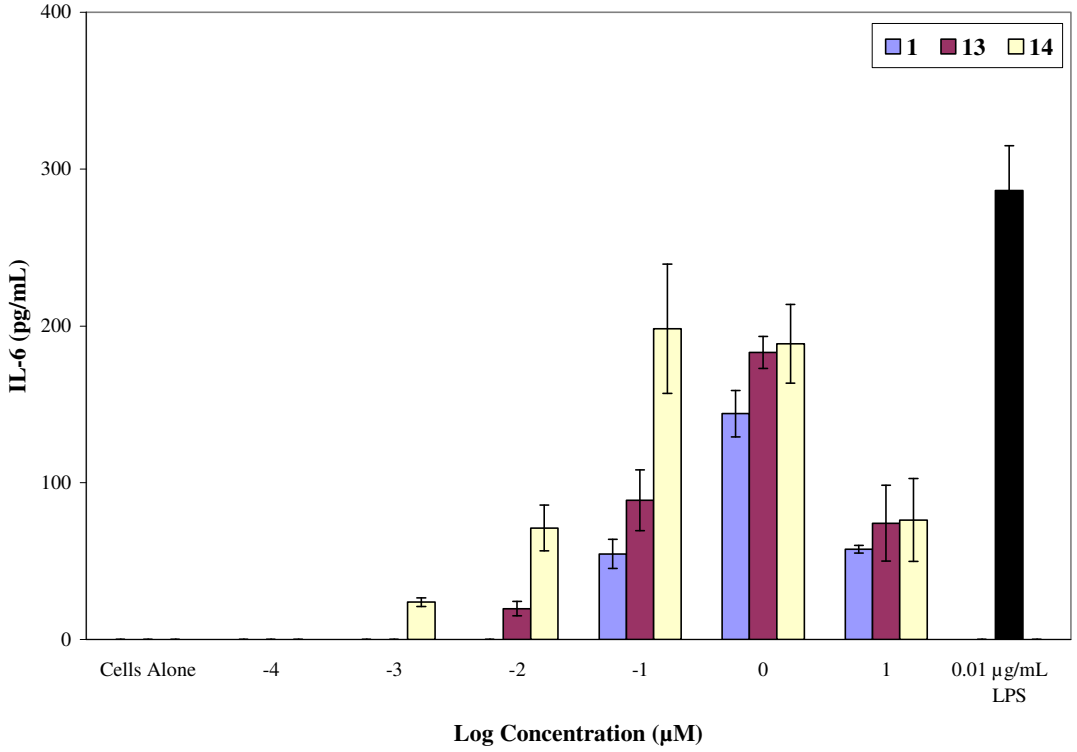

Figure 25. IL-6 production by differentiated THP-1 monocytes after exposure to LPS & lipid A mimics (**1**, **13** & **14**). THP-1 monocytes were incubated for 24 h with increasing concentrations of lipid A mimics **1**, **13** & **14**. IL-6 in cell supernatants was measured via ELISA. The results are shown as the average of two separate experiments.

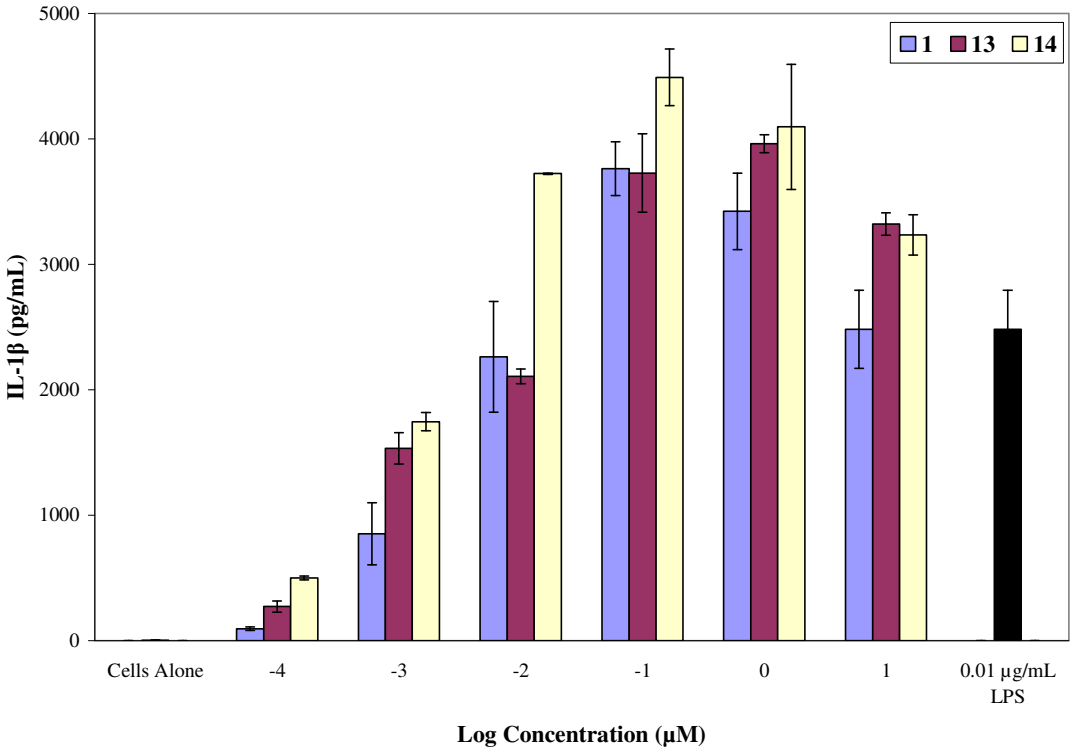

Figure 26. IL-1β production by differentiated THP-1 monocytes after exposure to LPS & lipid A mimics (**1**, **13** & **14**). THP-1 monocytes were incubated for 24 h with increasing concentrations of lipid A mimics **1**, **13** & **14**. IL-1β in cell supernatants was measured via ELISA. The results are shown as the average of two separate experiments.

The suspected mode of action of lipid A mimics **1**, **12**, **13** & **14** is stimulation of the TR4/MD-2 receptor complex. In an effort to confirm TLR4 as the target of the DEA containing lipid A mimics, a competitive inhibition study was performed with lipid IVa. As previously mentioned, lipid IVa is the tetra-acyl biosynthetic precursory of lipid A, which has been shown to bind to the human TLR4/MD-2 receptor complex, yet not induce any activation (**Figure 5**).[46-49] It follows that lipid IVa is a potent antagonist of LPS-induced TLR4 activation in the human monocytic cell line THP-1.[174] Therefore, the potential of lipid IVa to inhibit the TNF-α and IL-1β cytokine response of THP-1 cells to

lipid A mimic **14** was tested (**Figures 27** & **28**). Co-treatment with lipid IVa significantly inhibits the production of both cytokines induced by both LPS and mimic **14**. At a concentration of 0.1 μM of **14**, at which point a maximum level of cytokine induction is expected, the presence of lipid IVa at 0.5 μM appears to have completely inhibited the production of TNF-α, while the production of IL-1β is still marginally increased over residual expression levels. In contrast, the presence of lipid IVa at 0.1 μM exhibits only partial antagonism against the production of both cytokines induced by mimic **14** at a concentration of 0.1 μM. It is worth noting that complete inhibition of the production of both cytokines induced by 0.001 μM of mimic **14** in the presence of 0.1 μM lipid IVa (100-fold of **14**) is not observed, suggesting that mimic **14** may have a higher binding affinity for the TLR4/MD-2 receptor complex than lipid IVa. Based on these data, it is concluded that mimic **14** is an agonist of TLR4, and the other DEA-containing Lipid A mimics are likely ligands of TLR4 as well.

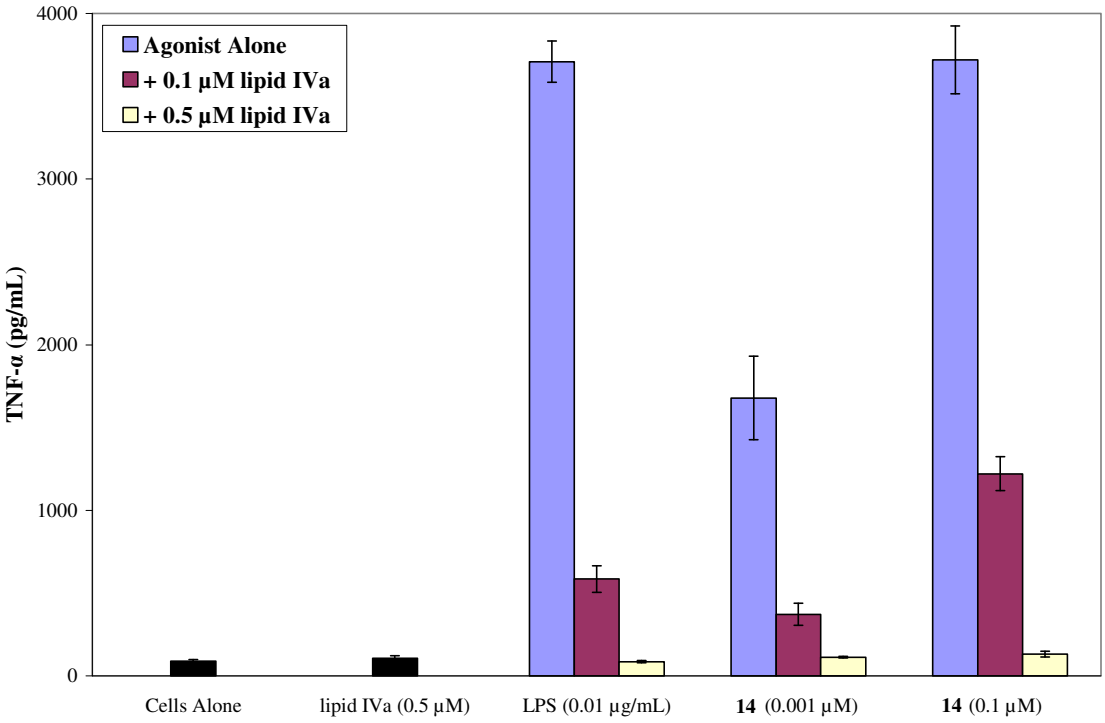

Figure 27. Inhibited TNF-α production by differentiated THP-1 monocytes after stimulation with an agonist (LPS or Lipid A mimic **14**) in the presence of lipid IVa. THP-1 cells were incubated for 24 h with either LPS or Lipid A mimic **14** in the presence of increasing concentrations of lipid IVa. TNF-α in cell supernatants was measured via ELISA. The results are shown as the average of two separate experiments.

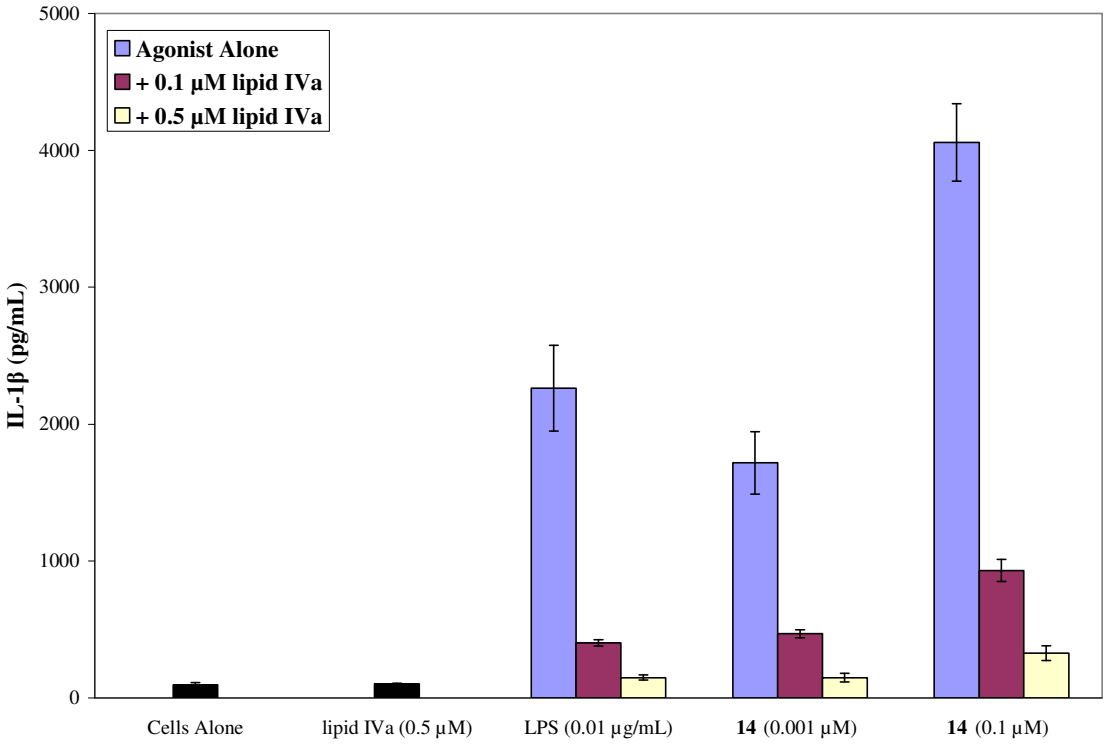

Figure 28. Inhibited IL-1β production by differentiated THP-1 monocytes after stimulation with an agonist (LPS or Lipid A mimic **14**) in the presence of lipid IVa. THP-1 cells were incubated for 24 h with either LPS or Lipid A mimic **14** in the presence of increasing concentrations of lipid IVa. IL-1β in cell supernatants was measured via ELISA. The results are shown as the average of two separate experiments.

Octa-acylated DEA-containing lipid A mimic **2** (**Figure 18**) was initially tested on THP-1 cells differentiated with only 5 ng mL^{-1} PMA, and the results showed a lack of any immunostimulatory activity except for a significant production of IL-1β at the highest concentration tested (**Figures 21-23**). Given the difficulties encountered with using only 5 ng mL^{-1} in the differentiation of the THP-1 cells encountered, the immunostimulatory activity of mimic **2** was investigated again, now in THP-1 cells differentiated using 25 ng mL^{-1} of PMA. Interestingly, a clear dose response relationship was observed for both the

production of TNF-α and IL-1β (**Figures 29** & **30**). However, in comparison to the other DEA-containing Lipid A mimics tested, mimic **2** is significantly less potent. When mimic **2** was tested with 0.1 µM of antagonist lipid IVa, a significant decrease in the production of both cytokines was observed. These results clearly indicate that DEA-containing Lipid A mimic **2**, which is likely the first ever octa-acylated lipid A mimic reported, binds and activates the TLR4/MD-2 receptor complex.

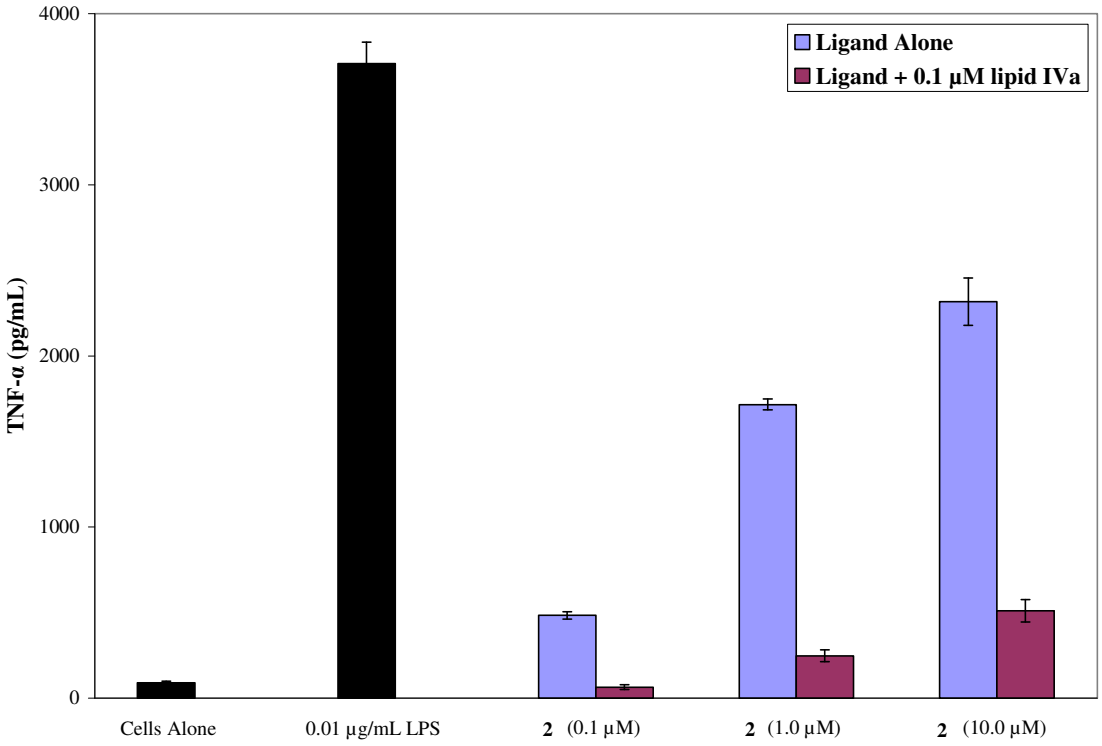

Figure 29. TNF-α production by differentiated THP-1 monocytes after exposure to lipid A mimic **2** in both the absence and presence of lipid IVa. THP-1 monocytes were incubated for 24 h with increasing concentrations of lipid A mimic **2** alone, and in the presence of 0.1 µM lipid IVa. TNF-α in cell supernatants was measured via ELISA. The results are shown as the average of two separate experiments.

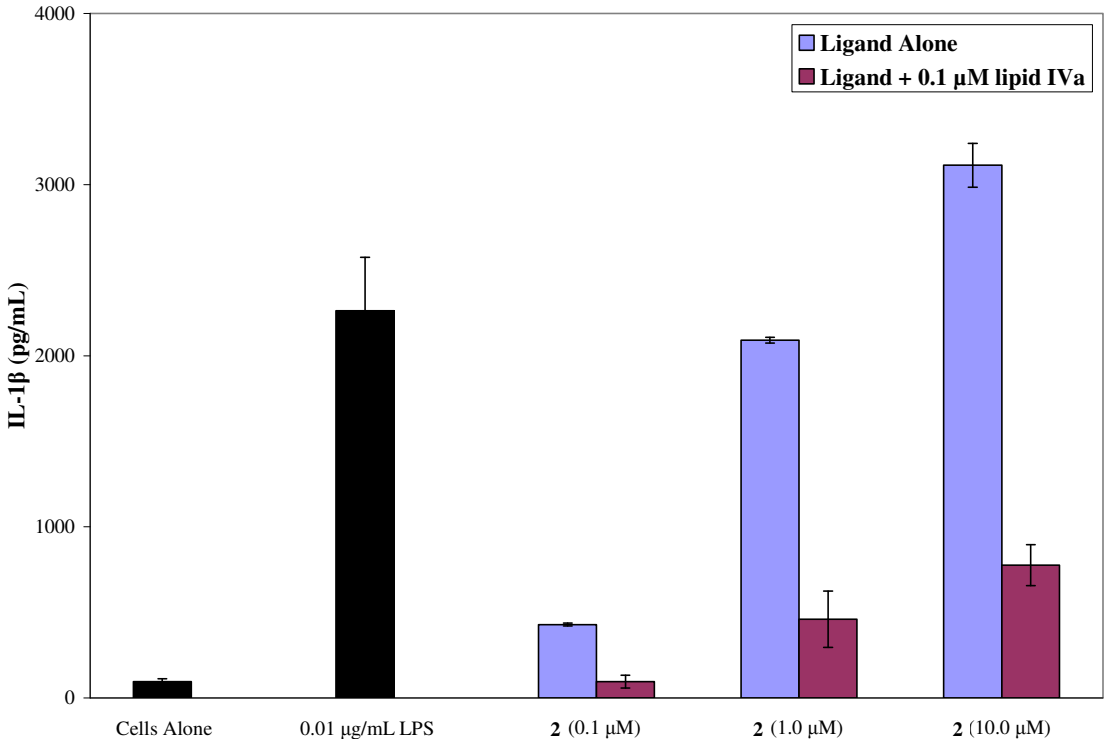

Figure 30. IL-1β production by differentiated THP-1 monocytes after exposure to lipid A mimic **2** in both the absence, and presence of lipid IVa. THP-1 monocytes were incubated for 24 h with increasing concentrations of lipid A mimic **2** alone, and in the presence of 0.1 µM lipid IVa. IL-1β in cell supernatants was measured via ELISA. The results are shown as the average of two separate experiments.

2.3 Experimental

2.3.1 General Methods

All air and moisture sensitive reactions were performed under nitrogen atmosphere. All commercial reagents were used as supplied. Anhydrous dichloromethane was distilled over calcium hydride, whereas anhydrous *N*,*N*-dimethylformamide (DMF) was purchased from Aldrich. ACS grade solvents were purchased from Fisher Scientific and used for chromatography without distillation. TLC plates (silica gel 60 F_{254}, thickness 0.25 mm) and silica gel 60 (40-63 µm) for flash column chromatography were purchased from

SILICYCLE INC., Canada. ^{1}H and ^{13}C NMR spectra were recorded on a Varian Unity Inova 500 MHz spectrometer. Tetramethylsilane (TMS, δ 0.00 ppm) or solvent peaks were used as internal standards for ^{1}H and ^{13}C NMR spectra. The chemical shifts were given in ppm and coupling constants in Hz indicated to a resolution of ± 0.5 Hz. Multiplicity of proton signals is indicated as follows: s (singlet), d (doublet), dd (double doublet), t (triplet), q (quartet), m (multiplet), br (broad). Structural assignments were made using standard gCOSY and gHSQC methodology. NMR peaks belonging to primary lipid chains are denoted with an L subscript, whereas those belonging to secondary lipid chains are denoted with an L' subscript. ESI mass spectra were measured on the Applied Biosystems Mariner Bio-Spectrometry Workstation at the University of Alberta, Canada. MALDI mass spectra were measured on the Applied Biosystems Mariner 4700 system at the University of Western Ontario. Optical rotations were measured with Perkin Elmer 343 Polarimeter at 22°C.

2.3.2 ***N,N*-Bis(2-hydroxyethyl)-3-(*R*)-tetradecanoyloxytetradecanamide (5):**

To a solution of diethanolamine (73 mg, 0.665 mmol) in DMF (3 mL), dilipid acid **3** (302 mg, 0.665 mmol), HBTU (262 mg, 0.698 mmol), and diisopropylethylamine (DIPEA, 0.24 mL, 1.40 mmol) were added. The mixture was stirred at room temperature for 16 h. The mixture was then concentrated, dissolved in water (30 mL), and extracted with EtOAc (3 x 30 mL). The combined organic layers were dried over Na_2SO_4, concentrated, and purified by flash column chromatography (hexane/EtOAc/MeOH, 1:1:0.125) to afford pure **5** (242 mg, 68%) as white solid. R_f 0.28 (hexane/EtOAc/MeOH, 1:1:0.1); $[\alpha]_D^{22}$ - 3.7 (*c* 1.0, $CHCl_3$); ^{1}H NMR (500 MHz, $CDCl_3$): δ 0.84 (t, 6H, *J* 7.0 Hz,

2 x CH_3), 1.16-1.33 (br m, 38H, 19 x CH_2 of lipid), 1.51-1.62 (m, 4H, H-4_L, H-$3_{L'}$), 2.23 (t, 2H, *J* 7.5 Hz, H-$2_{L'}$), 2.56 (dd, 1H, *J* 15.0, 7.5 Hz, H-2_{La}), 2.68 (dd, *J* 15.0, 7.5 Hz, H-2_{Lb}), 3.39-3.57 (m, 4H, $HOCH_2C\underline{H_2}NC\underline{H_2}CH_2OH$), 3.72-3.78 (m, 4H, $HOC\underline{H_2}CH_2NCH_2C\underline{H_2}OH$), 4.04-4.36 (br, 2H, OH x 2), 5.16-5.21 (m, 1H, H-3_L); ^{13}C NMR (125 MHz, $CDCl_3$): δ 14.11 (CH_3), 22.67 ($\underline{C}H_2$), 24.96 ($\underline{C}H_2$), 25.33 ($\underline{C}H_2$), 29.15 ($\underline{C}H_2$), 29.30 ($\underline{C}H_2$), 29.35 ($\underline{C}H_2$), 29.41 ($\underline{C}H_2$), 29.51 ($\underline{C}H_2$), 29.54 ($\underline{C}H_2$), 29.57 ($\underline{C}H_2$), 29.63 ($\underline{C}H_2$), 29.65 ($\underline{C}H_2$), 29.68 ($\underline{C}H_2$), 31.91 ($\underline{C}H_2$), 34.49 (C-$2_{L'}$), 38.76 (C-2_L), 50.29 & 52.39 ($HOCH_2\underline{C}H_2N\underline{C}H_2CH_2OH$), 60.44 & 60.74 ($HO\underline{C}H_2CH_2NCH_2\underline{C}H_2OH$), 71.40 (C-$3_L$), 172.36 (C=O), 174.14 (C=O); HRESI-MS (*m*/*z*) Calcd for $C_{32}H_{63}NO_5Na$ $[M+Na]^+$: 564.4587, found: 564.4588.

2.3.3 [*N*-(2-hydroxyethyl)-(*R*)-3-tetradecanoyloxytetradecanamido]-eth-1-yl 6-*O*-benzyl-2-deoxy-4-*O*-(di-*O*-benzylphosphono)-3-*O*-[(*R*)-3-tetradecanoyloxytetradecanoyl]-2-(2,2,2-trichloroethoxycarbonylamino)-β-D-glucopyranoside (6)

&

(*R*)-3-tetradecanoyloxytetradecanamido-di-(ethyl 6-*O*-benzyl-2-deoxy-4-*O*-(di-*O*-benzylphosphono)-3-*O*-[(*R*)-3-tetradecanoyloxytetradecanoyl]-2-(2,2,2-trichloroethoxycarbonylamino)-β-D-glucopyranoside) (7):

A solution of **4** (460 mg, 0.36 mmol) and **5** (194 mg, 0.36 mmol) in dry CH_2Cl_2 (4 mL) in the presence of molecular sieves (4 Å, 2.0 g) was stirred under nitrogen for 30 min at room temperature. A solution of TMSOTf (0.01 M in dry CH_2Cl_2, 0.80 mL) was added

drop wise in about 3 min. The mixture was stirred at room temperature for 1 h before a saturated sodium bicarbonate solution (10 mL) was added to quench the reaction. Solids were filtered out before the mixture was extracted with CH_2Cl_2 (3 x 25 mL). The combined organic phase was dried over Na_2SO_4, concentrated, and purified via repeated flash column chromatography (hexane/EtOAc, 2:1 and 3:4) to yield **6** (314 mg, 53%) and **7** (148 mg, 15%), both as colorless syrups.

For **6**: R_f 0.40 (hexane/EtOAc, 3:4); $[\alpha]_D^{22}$ + 0.5 (*c* 1.0, $CHCl_3$); ^{1}H NMR (500 MHz, $CDCl_3$): δ 0.89 (t, 12H, *J* 7.0 Hz, 4 x CH_3), 1.20-1.37 (br m, 76H, 38 x CH_2 of lipid), 1.46-1.81 (br m, 8H H-4_L x 2, H-$3_{L'}$ x 2), 2.20-2.31 (m, 4H, H-$2_{L'}$ x 2), 2.38-2.54 (m, 4, H-2_L x 2), 3.25-3.40 (m, 1.4H, H-2 from one isomer, H-6b), 3.42-3.52 (m, 1.6H, H-2 from one isomer, H-6a), 3.56-3.84 (m, 8H, H-5, $ROCH_2C\underline{H_2}NC\underline{H_2}CH_2O\underline{H}$, $ROCH_2CH_2NCH_2C\underline{H_2}OH$), 4.03 (m, 2H, $ROC\underline{H_2}CH_2NCH_2CH_2OH$), 4.38-4.57 (m, 3H, Troc-Ha, Troc-Hb, H-4), 4.64-4.73 (m, 2H, $PhC\underline{H_2}$), 4.78 (d, 0.4H, *J* 8.0 Hz, H-1 from one isomer), 4.85-4.92 (m, 4.6H, H-1 from one isomer, $(PhC\underline{H_2}O)_2P$), 5.08-5.21 (m, 2H, H-3_L x 2), 5.35 (dd, 0.4H, *J* 10.0, 10.0 Hz, H-3 from one isomer), 5.54 (dd, 0.6H, *J* 9.5, 9.5 Hz, H-3 from one isomer), 5.76 (d, 0.4H, *J* 8.0 Hz, NH from one isomer), 6.24 (d, 0.6H, *J* 7.0 Hz, NH from one isomer), 7.27-7.32 (m, 15H, Ar-H); ^{13}C NMR (125 MHz, $CDCl_3$): δ 14.34 (CH_3), 22.90 ($\underline{C}H_2$), 25.19 ($\underline{C}H_2$), 25.23 ($\underline{C}H_2$), 25.30 ($\underline{C}H_2$), 25.56 ($\underline{C}H_2$), 25.77 ($\underline{C}H_2$), 29.38 ($\underline{C}H_2$), 29.42 ($\underline{C}H_2$), 29.53 ($\underline{C}H_2$), 29.57 ($\underline{C}H_2$), 29.66 ($\underline{C}H_2$), 29.75 ($\underline{C}H_2$), 29.78 ($\underline{C}H_2$), 29.79 ($\underline{C}H_2$), 29.82 ($\underline{C}H_2$), 29.87 ($\underline{C}H_2$), 29.90 ($\underline{C}H_2$), 32.13 ($\underline{C}H_2$), 34.26 ($\underline{C}H_2$), 34.51 ($\underline{C}H_2$), 34.62 ($\underline{C}H_2$), 34.64 ($\underline{C}H_2$), 34.74 ($\underline{C}H_2$), 34.79 ($\underline{C}H_2$), 34.84 ($\underline{C}H_2$), 38.70 ($\underline{C}H_2$), 39.38 ($\underline{C}H_2$), 39.61 ($\underline{C}H_2$), 47.84 ($\underline{C}H_2N$), 49.54 ($\underline{C}H_2N$),

50.84 (CH_2N), 52.20 (CH_2N), 56.75 (C-2), 60.35 (C-6 from one isomer), 61.60 (C-6 from one isomer), 68.12 (OCH_2), 68.36 (OCH_2), 68.64 (OCH_2), 68.97 (OCH_2), 69.85-69.97 (m, (PhCH_2O)$_2$P), 70.24 (C-3$_L$), 70.27 (C-3$_L$), 71.70 (C-3$_L$), 71.91 (C-3 from one isomer), 72.52 (C-3 from one isomer), 72.15 (C-3$_L$), 73.63 (Troc-CH_2), 73.90 (C-4 from one isomer), 73.94 (C-5 from one isomer), 74.21 (C-5 from one isomer), 74.26 (d, *J* 5.0 Hz, C-4 from one isomer), 74.33 (d, *J* 5.0 Hz, C-4 from one isomer), 74.52 (PhCH_2 from one isomer), 74.67 (PhCH_2 from one isomer), 95.17 (Troc-CCl$_3$), 100.44 (C-1 from one isomer), 100.87 (C-1 from one isomer), 127.64 (CH-Ar), 127.98 (CH-Ar), 128.08 (CH-Ar), 128.34 (CH-Ar), 128.56 (CH-Ar), 128.57 (CH-Ar), 128.62 (CH-Ar), 135.43 (d, *J* 2.5 Hz, C-Ar), 135.68 (d, *J* 2.5 Hz, C-Ar), 137.99 (C-Ar), 138.06 (C-Ar), 154.54 (C=O Troc), 170.25 (C=O), 170.50 (C=O), 171.18 (C=O), 171.95 (C=O), 173.65 (C=O) 173.80 (C=O) 174.28 (C=O); HRESI-MS (*m/z*) Calcd for $C_{90}H_{146}Cl_3N_2O_{17}P$ $[M+Na]^+$: 1685.9282, found: 1685.9317.

For **7**: R_f 0.36 (hexane/EtOAc, 2:1); $[\alpha]_D^{22}$ + 0.5 (*c* 1.0, $CHCl_3$); ^{1}H NMR (500 MHz, $CDCl_3$): δ 0.88 (t, 18H, *J* 7.0 Hz, 6 x CH_3), 1.20-1.37 (br m, 114H, 57 x CH_2 of lipid), 1.44-1.84 (br m, 12H H-4$_L$ x 3, H-3$_{L'}$ x 3), 2.20-2.31 (m, 6H, H-2$_{L'}$ x 3), 2.38-2.54 (m, 4H, H-2$_L$ x 2), 2.68-2.77 (m, 2H, H-2$_L$), 3.26-3.43 (m, 3H, H-2 from one sugar, CH_2N), 3.51-3.70 (m, 10H, H-2 from one sugar, H-5 from one sugar, H-6a from both sugars, H-6b from both sugars, CH_2N, CH_2O), 3.74-3.92 (m, 3H, H-5 from one sugar, CH_2O), 4.36-4.54 (m, 6H, H-4 from both sugars, PhCH_2 from both sugars), 4.58 (d, 1H, *J* 8.0 Hz, H-1 from one sugar), 4.63-4.80 (m, 5H, H-1 from one sugar, Troc-Ha from both sugars, Troc-Hb from both sugars), 4.86-4.93 (m, 8H, (PhCH_2O)$_2$P from both sugars), 5.08-5.16

(m, 3H, H-3_L), 5.26 (dd, 1H, *J* 9.5, 9.5 Hz, H-3 from one sugar), 5.52 (dd, 1H, *J* 9.5, 9.5 Hz, H-3 from one sugar), 5.73 (d, 1H, *J* 8.0 Hz, NH from one sugar), 6.14 (d, 1H, *J* 8.0 Hz, NH from one sugar), 7.24-7.38 (m, 30H, Ar-H); ^{13}C NMR (125 MHz, $CDCl_3$): δ 14.17 (CH_3), 22.73 ($\underline{C}H_2$), 25.01 ($\underline{C}H_2$), 25.04 ($\underline{C}H_2$), 25.09 ($\underline{C}H_2$), 25.13 ($\underline{C}H_2$), 25.69 ($\underline{C}H_2$), 29.19 ($\underline{C}H_2$), 29.28 ($\underline{C}H_2$), 29.36 ($\underline{C}H_2$), 29.40 ($\underline{C}H_2$), 29.42 ($\underline{C}H_2$), 29.49 ($\underline{C}H_2$), 29.57 ($\underline{C}H_2$), 29.62 ($\underline{C}H_2$), 29.64 ($\underline{C}H_2$), 29.69 ($\underline{C}H_2$), 29.71 ($\underline{C}H_2$), 29.74 ($\underline{C}H_2$), 31.96 ($\underline{C}H_2$), 33.97 ($\underline{C}H_2$), 34.28 ($\underline{C}H_2$), 34.43 ($\underline{C}H_2$), 34.47 ($\underline{C}H_2$), 34.72 ($\underline{C}H_2$), 38.30 ($\underline{C}H_2$), 38.93 ($\underline{C}H_2$), 39.20 ($\underline{C}H_2$), 45.01 ($\underline{C}H_2N$), 46.83 ($\underline{C}H_2N$), 46.87 ($\underline{C}H_2N$), 48.83 ($\underline{C}H_2N$), 56.39 (C-2 from one sugar), 56.50 (C-2 from one sugar), 60.21 (C-6 from one sugar), 61.47 (C-6 from one sugar), 67.94 (O$\underline{C}H_2$), 68.37 (O$\underline{C}H_2$), 68.41 (O$\underline{C}H_2$), 68.45 (O$\underline{C}H_2$), 69.64 (m, (Ph$\underline{C}H_2O)_2$P from both sugars), 69.97 (C-3_L), 72.03 (C-3_L), 72.07 (C-3_L), 72.14 (C-3 from one sugar), 72. 44 (C-3 from one sugar), 73.38 (Ph$\underline{C}H_2$ from one sugar), 73.42 (Ph$\underline{C}H_2$ from one sugar), 73.78 (C-5 from one sugar), 73.84 (C-5 from one sugar), 73.96 (d, *J* 5.0 Hz, C-4 from one sugar), 74.05 (d, *J* 5.0 Hz, C-4 from one sugar), 74.35 (Troc-CH_2 from one sugar), 74.61 (Troc-CH_2 from one sugar), 95.51 (Troc-CCl_3 from one sugar), 95.72 (Troc-CCl_3 from one sugar), 100.57 (C-1 from one sugar), 102.03 (C-1 from one sugar), 127.61 ($\underline{C}$H-Ar), 127.67 ($\underline{C}$H-Ar), 128.01 ($\underline{C}$H-Ar), 128.03 ($\underline{C}$H-Ar), 128.11 ($\underline{C}$H-Ar), 128.15 ($\underline{C}$H-Ar), 128.36 ($\underline{C}$H-Ar), 128.40 ($\underline{C}$H-Ar), 128.58 ($\underline{C}$H-Ar), 128.61 ($\underline{C}$H-Ar), 128.65 ($\underline{C}$H-Ar), 135.56 (m, C-Ar), 137.94 (C-Ar), 138.02 (C-Ar), 154.12 (C=O Troc from one sugar), 154.51 (C=O Troc from one sugar), 170.01 (C=O), 170.46 (C=O), 170.70 (C=O), 173.28 (C=O), 173.47 (C=O), 174.11 (C=O); HRESI-MS (*m*/*z*) Calcd for $C_{148}H_{229}Cl_6N_3O_{29}P_2$ $[M+Na]^+$: 2807.3979, found: 2807.4086.

2.3.4 [N-(2-(4-hydroxybutyloxy)-ethyl)-(*R*)-3-tetradecanoyloxytetradecanamido]-eth-1-yl 6-*O*-benzyl-2-deoxy-4-*O*-(di-*O*-benzylphosphono)-3-*O*-[(*R*)-tetradecanoyloxytetradecanoyl]-2-amino-β-D-glucopyranoside (9):

To a solution of **6** (100 mg, 0.06 mmol) in THF (4 mL) and glacial acetic acid (1 mL), zinc powder (500 mg) was added. The mixture was stirred at room temperature and the progress of the reaction monitored via TLC. After approximately 30 minutes, the complete consumption of **8** was noted. However, two different product spots were noted. Interestingly, the slow conversion of one of the product spots into the other was noted as the reaction was allowed to stir further. After stirring for approximately 4 hours, the solid was filtered, washed with acetic acid (30 mL) and the filtrate concentrated *in vacuo*. The residue was dissolved in CH_2Cl_2 (100 mL) and washed with a saturated sodium bicarbonate solution (50 mL). The organic phase was dried with Na_2SO_4, concentrated, and the residue purified by flash column chromatography (hexane/EtOAc, 2:3) to obtain pure **9** (51 mg, 55%) as a colorless syrup. R_f 0.26 (4% MeOH in CH_2Cl_2); $[\alpha]_D^{22}$ + 0.2 (*c* 1.0, $CHCl_3$); ^{1}H NMR (500 MHz, $CDCl_3$): δ 0.89 (t, 12H, *J* 7.0 Hz, 4 x CH_3), 1.11-1.40 (br m, 76H, 38 x CH_2 of lipid), 1.41-1.74 (br m, 12H, H-4_L x 3, H-$3_{L'}$ x 3, $ROCH_2C\underline{H_2}C\underline{H_2}CH_2OH$), 2.18-2.31 (m, 4H, H-$2_{L'}$ x 2), 2.38-2.45 (m, 1H, H-2_L), 2.49-2.55 (m, 1.4H, H-2 from one isomer, H-2_L), 2.60-2.78 (m, 4.6H, H-2 from one isomer, NH_2, H-2_L x 2), 3.33-3.39 (m, 1H, H-6a), 3.43-3.70 (m, 11H, H-5, H-6b, $ROCH_2C\underline{H_2}NC\underline{H_2}CH_2OC\underline{H_2}CH_2CH_2C\underline{H_2}O\underline{H}$), 3.74-3.91 (m, 3H, $ROCH\underline{\textit{H}}CH_2NCH_2C\underline{H_2}OCH_2CH_2CH_2CH_2OH$), 4.01-4.06 (m, 1H, $ROC\underline{\textit{H}}HCH_2NCH_2CH_2OCH_2CH_2CH_2CH_2OH$), 4.30 (d, 0.4H, *J* 8.0 Hz, H-1 from one

isomer), 4.34-4.50 (m, 3.6 H, H-1 from one isomer, H-4, PhC$\underline{H}_2$), 4.85-4.94 (m, 4H, (PhC$\underline{H}_2$O)$_2$P), 5.04-5.14 (m, 1.4H, H-3 from one isomer, H-3$_L$), 5.19-5.24 (m, 1.6H, H-3 from one isomer, H-3$_L$), 7.22-7.37 (m, 15H, Ar-H); ^{13}C NMR (125 MHz, $CDCl_3$): δ 22.92 (CH_3), 22.73 ($\underline{C}H_2$), 25.12 ($\underline{C}H_2$), 25.17 ($\underline{C}H_2$), 25.21 ($\underline{C}H_2$), 25.24 ($\underline{C}H_2$), 25.36 ($\underline{C}H_2$), 25.62 ($\underline{C}H_2$), 25.67 ($\underline{C}H_2$), 27.76 ($\underline{C}H_2$), 28.26 ($\underline{C}H_2$), 29.36 ($\underline{C}H_2$), 29.41 ($\underline{C}H_2$), 29.42 ($\underline{C}H_2$), 29.44 ($\underline{C}H_2$), 29.53 ($\underline{C}H_2$), 29.55 ($\underline{C}H_2$), 29.59 ($\underline{C}H_2$), 29.63 ($\underline{C}H_2$), 29.67 ($\underline{C}H_2$), 29.75($\underline{C}H_2$), 29.81 ($\underline{C}H_2$), 29.87 ($\underline{C}H_2$), 29.89($\underline{C}H_2$), 29.91 ($\underline{C}H_2$), 29.93 ($\underline{C}H_2$), 31.31 ($\underline{C}H_2$), 31.89 ($\underline{C}H_2$), 31.96 ($ROCH_2CH_2\underline{C}H_2CH_2OH$ from one isomer), 32.01 ($ROCH_2CH_2\underline{C}H_2CH_2OH$ from one isomer), 32.07 ($ROCH_2\underline{C}H_2CH_2CH_2OH$ from one isomer), 32.14 ($ROCH_2\underline{C}H_2CH_2CH_2OH$ from one isomer), 34.56 ($\underline{C}H_2$), 34.60 ($\underline{C}H_2$), 34.77 ($\underline{C}H_2$), 34.82 ($\underline{C}H_2$), 38.79 ($\underline{C}H_2$), 39.23 ($\underline{C}H_2$), 40.01 ($\underline{C}H_2$), 40.06 ($\underline{C}H_2$), 45.69 (C$\underline{H}_2$N), 48.34 (C$\underline{H}_2$N), 49.44 (C$\underline{H}_2$N), 49.86 (C$\underline{H}_2$N), 51.33 (C-2 from one isomer), 52.69 (C-2 from one isomer), 60.03 (O$\underline{C}H_2$), 60.98 (O$\underline{C}H_2$), 61.40 (C-6 from one isomer), 62.24 (C-6 from one isomer), 62.43 (O$\underline{C}H_2$), 62.49 (O$\underline{C}H_2$), 67.95 (O$\underline{C}H_2$), 68.14 (O$\underline{C}H_2$), 68.56 (O$\underline{C}H_2$), 68.76 (O$\underline{C}H_2$), 69.91 (m, (Ph$\underline{C}H_2$O)$_2$P), 70.34 (C-3$_L$), 70.38 (C-3 from one isomer), 71.33 (C-3 from one isomer), 71.52 (C-3$_L$), 73.58 (Ph$\underline{C}H_2$ from one isomer), 73.62 (Ph$\underline{C}H_2$ from one isomer), 73.94 (C-3 from one isomer), 74.06 (C-3 from one isomer), 74.20 (C-5 from one isomer), 74.25 (C-5 from one isomer), 74.59 (d, *J* 5.0 Hz, C-4 from one isomer), 74.66 (d, *J* 5.0 Hz, C-4 from one isomer), 100.04 (C-1 from one isomer), 104.06 (C-1 from one isomer), 127.83 ($\underline{C}$H-Ar), 127.86 ($\underline{C}$H-Ar), 128.22 ($\underline{C}$H-Ar), 128.27 ($\underline{C}$H-Ar), 128.32 ($\underline{C}$H-Ar), 128.39 ($\underline{C}$H-Ar), 128.56 ($\underline{C}$H-Ar), 128.80 ($\underline{C}$H-Ar), 128.85 ($\underline{C}$H-Ar), 128.89 ($\underline{C}$H-Ar), 135.70 (m, C-Ar), 138.12 (C-Ar), 170.83 (C=O), 171.16 (C=O), 171.29 (C=O), 171.59 (C=O), 173.68 (C=O), 173.71

(C=O), 173.75 (C=O), 173.99 (C=O); ESI-MS (*m*/*z*) Calcd for $C_{91}H_{154}N_2O_{16}P$ $[M+H]^+$: 1563.1, found: 1563.1.

2.3.5 [N-(2-hydroxyethyl)-(*R*)-3-tetradecanoyloxytetradecanamido]-eth-1-yl 6-*O*-benzyl-2-deoxy-4-*O*-(di-*O*-benzylphosphono)-3-*O*-[(*R*)-3-tetradecanoyloxytetradecanoyl]-2-[(*R*)-3-tetradecanoyloxytetradecanamido]-β-D-glucopyranoside (12)

&

2-[N-(2-{(*R*)-3-tetradecanoyloxytetradecanoyl)-ethyl}-(*R*)-3-tetradecanoyloxytetradecanamido]-eth-1-yl 6-*O*-benzyl-2-deoxy-4-*O*-(di-*O*-benzylphosphono)-3-*O*-[(*R*)-3-tetradecanoyloxytetradecanoyl]-2-[(*R*)-3-tetradecanoyloxytetradecanamido]-β-D-glucopyranoside (13):

Method 1:

To a solution of **6** (320 mg, 0.19 mmol) in glacial acetic acid (5 mL), zinc powder (1.0 g) was added. The mixture was stirred at room temperature for 30 min and then filtered. The solid was washed with acetic acid (30 mL) and the filtrate concentrated *in vacuo*. The residue was dissolved in CH_2Cl_2 (150 mL) and washed with a saturated sodium bicarbonate solution (75 mL). The combined organic phase was dried with Na_2SO_4 and concentrated to obtain free amine **8** (244 mg, 85%) as a white solid.

A mixture of amine **8** (280 mg), **3** (160 mg, 0.33 mmol), and DCC (154 mg, 0.66 mmol) in dry CH_2Cl_2 (5 mL) was stirred at room temperature for 20 h. Water (0.50 mL) was added and the reaction mixture was stirred for a further 20 min. The solid was then

filtered through a sintered glass funnel with a bed of Na_2SO_4. The filtrate was concentrated and the residue purified by repeated flash column chromatography (hexane/acetone, 5:1 and 4.5:1) to afford **10** (203 mg, 65 % over two steps) and **11** (63 mg, 16%), both as colorless syrups.

For compound **10**: R_f 0.31 (hexane/acetone, 4:1); $[\alpha]_D^{22}$ -2.2 (*c* 1.0, $CHCl_3$); ^{1}H NMR (500 MHz, $CDCl_3$): δ 0.89 (t, 18H, *J* 7.0 Hz, 6 x CH_3), 1.21-1.39 (br m, 114H, 57 x CH_2 of lipid), 1.48-1.72 (br m, 12H H-4_L x 3, H-$3_{L'}$ x 3), 2.18-2.56 (m, 10H, H-$2_{L'}$ x 3, H-2_L x 2), 2.76 (dd, 1H, J 15.5, 7.5 Hz, H-2_{La}), 2.85 (dd. 1H, J 15.5, 5.0 Hz, H-2_{Lb}), 3.18-3.23 (m, 0.6H, H-2 from one isomer), 3.29-3.37 (m, 2H, H-6a, H-6b), 3.44 (br s, 1H, OH), 3.52-3.86 (m, 7.4 H, H-2 from one isomer, H-5, $ROCH_2C\underline{H_2}NC\underline{H_2}C\underline{H_2}OH$), 3.97- 4.08 (m, 2H, $ROC\underline{H_2}CH_2NCH_2CH_2OH$), 4.41-4.52 (m, 3H, H-4, $PhC\underline{H_2}$), 4.63 (d, 0.4H, *J* 8.0 Hz, H-1 from one isomer), 4.82-4.94 (m, 4H, $(PhC\underline{H_2}O)_2P$), 5.10 (m, 4H, H-1 from one isomer, H-3 from one isomer, C-3_L x 3), 5.64 (dd, 0.6H, *J* 10.5, 8.5 Hz, H-3 from one isomer), 6.18 (d, 0.4H, *J* 8.0 Hz, NH from one isomer), 6.80 (d, 0.6H, *J* 8.0 Hz, NH from one isomer), 7.21-7.39 (m, 15H, Ar-H); ^{13}C NMR (125 MHz, $CDCl_3$): δ 14.15 (CH_3), 22.73 ($\underline{C}H_2$), 25.05 ($\underline{C}H_2$), 25.17 ($\underline{C}H_2$), 25.20 ($\underline{C}H_2$), 25.31 ($\underline{C}H_2$), 25.38 ($\underline{C}H_2$), 25.69 ($\underline{C}H_2$), 29.21 ($\underline{C}H_2$), 29.25 ($\underline{C}H_2$), 29.26 ($\underline{C}H_2$), 29.28 ($\underline{C}H_2$), 29.32 ($\underline{C}H_2$), 29.36 ($\underline{C}H_2$), 29.39 ($\underline{C}H_2$), 29.42 ($\underline{C}H_2$), 29.45 ($\underline{C}H_2$), 29.50 ($\underline{C}H_2$), 29.52 ($\underline{C}H_2$), 29.56 ($\underline{C}H_2$), 29.62 ($\underline{C}H_2$), 29.64 ($\underline{C}H_2$), 29.66 ($\underline{C}H_2$), 29.71 ($\underline{C}H_2$), 29.73 ($\underline{C}H_2$), 29.74 ($\underline{C}H_2$), 29.76 ($\underline{C}H_2$), 29.80 ($\underline{C}H_2$), 31.96 ($\underline{C}H_2$), 31.98 ($\underline{C}H_2$), 34.19 ($\underline{C}H_2$), 34.41 ($\underline{C}H_2$), 34.47 ($\underline{C}H_2$), 34.53 ($\underline{C}H_2$), 34.60 ($\underline{C}H_2$), 34.66 ($\underline{C}H_2$), 38.24 ($\underline{C}H_2$), 38.60 ($\underline{C}H_2$), 39.25 ($\underline{C}H_2$), 39.46 ($\underline{C}H_2$), 40.85 ($\underline{C}H_2$), 41.51 ($\underline{C}H_2$), 47.60 ($C\underline{H_2}N$), 49.49 ($C\underline{H_2}N$), 51.21 ($C\underline{H_2}N$), 51.88 ($C\underline{H_2}N$),

54.77 (C-2 from one isomer), 56.40 (C-2 from one isomer), 60.15 (C-6 from one isomer), 60.97 (C-6 from isomer), 67.67 (O<u>C</u>H_2), 68.25 (O<u>C</u>H_2), 68.41 (O<u>C</u>H_2), 68.66 (O<u>C</u>H_2), 69.59 (m, (Ph<u>C</u>H_2O)$_2$P), 70.14 (C-3_L), 70.87 (C-3 from one isomer), 71.40 (C-3 from one isomer), 71.86 (C-3_L), 72.15 (C-3_L), 73.37 (Ph<u>C</u>H_2 from one isomer), 73.45 (Ph<u>C</u>H_2 from one isomer), 73.86 (C-5 from one isomer), 73.90 (C-5 from one isomer), 74.13 (d, *J* 5.0 Hz, C-4 from one isomer), 74.33 (d, *J* 5.0 Hz, C-4 from one isomer), 99.76 (C-1 from one isomer), 100.92 (C-1 from one isomer), 127.61 (<u>C</u>H-Ar), 127.66 (<u>C</u>H-Ar), 127.98 (<u>C</u>H-Ar), 128.00 (<u>C</u>H-Ar), 128.09 (<u>C</u>H-Ar), 128.11 (<u>C</u>H-Ar), 128.30 (<u>C</u>H-Ar), 128.35 (<u>C</u>H-Ar), 128.52 (<u>C</u>H-Ar), 128.54 (<u>C</u>H-Ar), 128.56 (<u>C</u>H-Ar), 128.58 (<u>C</u>H-Ar), 128.61 (<u>C</u>H-Ar), 128.67 (<u>C</u>H-Ar), 135.53 (m, C-Ar), 137.84 (C-Ar), 137.97 (C-Ar), 169.80 (C=O), 170.52 (C=O), 170.62 (C=O), 170.77 (C=O), 171.37 (C=O), 171.69 (C=O), 173.20 (C=O), 173.33 (C=O), 173.52 (C=O), 173.56 (C=O), 173.58 (C=O), 174.37 (C=O); HRESI-MS (*m/z*) Calcd for $C_{115}H1_{97}N_2O_{18}P$ $[M+Na]^+$: 1948.4144, found: 1948.4183.

For compound **11**: R_f 0.41 (hexane/acetone, 4:1); $[\alpha]_D^{22}$ -1.1 (*c* 1.0, $CHCl_3$); ^{1}H NMR (500 MHz, $CDCl_3$): δ 0.83 (t, 24H, *J* 7.0 Hz, 8 x CH_3), 1.21-1.39 (br m, 152H, 76 x CH_2 of lipid), 1.46-1.79 (br m, 16H, H-4_L x 4, H-$3_{L'}$ x 4), 2.17-2.58 (m, 14H, H-$2_{L'}$ x 4, H-2_L x 3), 2.73 (dd, 1H, *J* 16.0, 6.0 Hz, H-2_{La}), 2.85 (dd, 1H, *J* 16.0, 5.0 Hz, H-2_{Lb}), 3.12-3.17 (m, 0.6H, H-2 from one isomer), 3.23-3.41 (m, 2H, H-6a, H-6b), 3.49-3.78 (m, 6.4H, H-2 from one isomer, H-5, $R_1OCH_2C\underline{H_2}N\underline{CH_2}CH_2OR_2$, OC<u>*H*</u>H), 3.89-3.95 (m, 1H, OCH<u>*H*</u>), 4.11-4.17 (m, 2H, OCH_2), 4.39-4.51 (m, 3H, H-4, PhC<u>H_2</u>), 4.69 (d, 0.4H, *J* 8.5 Hz, H-1 from one isomer), 4.85-4.91 (m, 4H, (Ph<u>C</u>H_2O)$_2$P), 5.06-5.24 (m, 4.6 H, H-1 from one isomer, H-3_L x 4), 5.31 (dd, 0.4H, *J* 10.0, 10.0 Hz, H-3 from one isomer), 5.68

(dd, 0.6H, *J* 10.0, 10.0 Hz, H-3 from one isomer), 6.16 (d, 0.4H, *J* 8.5 Hz, NH from one isomer), 6.67 (d, 0.6H, *J* 7.5 Hz, NH from one isomer), 7.22-7.39 (m, 15H, Ar-H); ^{13}C NMR (125 MHz, $CDCl_3$): δ 14.15 (CH_3), 22.73 ($\underline{C}H_2$), 25.07 ($\underline{C}H_2$), 25.09 ($\underline{C}H_2$), 25.19 ($\underline{C}H_2$), 25.27 ($\underline{C}H_2$), 25.35 ($\underline{C}H_2$), 25.74 ($\underline{C}H_2$), 29.19 ($\underline{C}H_2$), 29.27 ($\underline{C}H_2$), 29.35 ($\underline{C}H_2$), 29.42 ($\underline{C}H_2$), 29.49 ($\underline{C}H_2$), 29.57 ($\underline{C}H_2$), 29.62 ($\underline{C}H_2$), 29.68 ($\underline{C}H_2$), 29.73 ($\underline{C}H_2$), 29.75 ($\underline{C}H_2$), 31.96 ($\underline{C}H_2$), 34.17 ($\underline{C}H_2$), 34.48 ($\underline{C}H_2$), 34.52 ($\underline{C}H_2$), 34.67 ($\underline{C}H_2$), 37.81 ($\underline{C}H_2$), 38.16 ($\underline{C}H_2$), 39.19 ($\underline{C}H_2$), 39.27 ($\underline{C}H_2$), 40.86 ($\underline{C}H_2$), 41.33 ($\underline{C}H_2$), 45.01 ($C\underline{H_2}N$), 46.00 ($C\underline{H_2}N$), 47.16 ($C\underline{H_2}N$), 48.00 ($C\underline{H_2}N$), 55.03 (C-2 from one isomer), 56.43 (C-2 from one isomer), 61.95 (C-6 from one isomer), 62.39 (C-6 from one isomer), 67.24 ($O\underline{C}H_2$), 67.29 ($O\underline{C}H_2$), 68.36 ($O\underline{C}H_2$), 68.42 ($O\underline{C}H_2$), 69.60 (m, $(Ph\underline{C}H_2O)_2P$), 70.13 ($C\text{-}3_L$), 70.69 ($C\text{-}3_L$), 71.29 ($C\text{-}3_L$), 71.78 ($C\text{-}3_L$), 72.05 (C-3 from one isomer), 72.71 (C-3 from one isomer), 73.33 ($Ph\underline{C}H_2$ from one isomer), 73.37 ($Ph\underline{C}H_2$ from one isomer), 73.82 (C-5 from one isomer), 73.89 (C-5 from one isomer), 74.01 (d, *J* 5.0 Hz, C-4 from one isomer), 74.38 (d, *J* 5.0 Hz, C-4 from one isomer), 99.53 (C-1 from one isomer), 100.88 (C-1 from one isomer), 127.57 (CH-Ar), 127.91 (CH-Ar), 128.08 (CH-Ar), 128.29 (CH-Ar), 128.36 (CH-Ar), 128.52 (CH-Ar), 128.54 (CH-Ar), 128.56 (CH-Ar), 128.58 (CH-Ar), 128.60 (CH-Ar), 128.60 (CH-Ar), 135.55 (m, C-Ar), 137.96 (C-Ar), 138.04 (C-Ar), 169.76 (C=O), 170.10 (C=O), 170.18 (C=O), 170.24 (C=O), 170.43 (C=O), 170.58 (C=O), 170.67 (C=O), 173.16 (C=O), 173.18 (C=O), 173.22 (C=O), 173.26 (C=O), 173.39 (C=O), 173.42 (C=O), 173.48 (C=O), 174.04 (C=O); HRESI-MS (*m*/*z*) Calcd for $C_{143}H_{249}N_2O_{21}P$ $[M+Na]^+$: 2384.8047, found: 2384.8032.

Method 2:

To a solution of **26** (890 mg, 0.41 mmol) in CH_2Cl (3 mL) and glacial acetic acid (0.1 mL), a tetrabutylammonium fluoride solution (1 M in THF, 0.62 mL) was added, and the mixture was stirred at room temperature for 18 h. The mixture was then poured into a saturated sodium bicarbonate solution (30 mL), extracted with CH_2Cl (3 x 50 mL), dried over Na_2SO_4, and concentrated. Flash column chromatography of the residue (hexane/EtOAc/MeOH, 3 : 1 : 0.1) yielded **10** (715 mg, 90 %) as a colorless syrup

2.3.6 [N-(2-hydroxyethyl)-(*R*)-3-tetradecanoyloxytetradecanamido]eth-1-yl 2-deoxy-4-*O*-(phosphono)-3-*O*-[(*R*)-3-tetradecanoyloxytetradecanoyl]-2-[(*R*)-3-tetradecanoyloxytetradecanamido]-β-D-glucopyranoside (1)

&

2-[N-(2-(4-hydroxybutyloxy)-ethyl)-(*R*)-3-tetradecanoyloxytetradecanamido]-eth-1-yl 2-deoxy-4-*O*-(phosphono)-3-*O*-[(*R*)-3-tetradecanoyloxytetradecanoyl]-2-[(*R*)-3-tetradecanoyloxytetradecanamido]-β-D-glucopyranoside (12):

Method 1:

To a solution of **10** (60 mg, 0.03 mmol) in freshly distilled THF (45 ml) and glacial acetic acid (5 mL), was added palladium on charcoal (5%, 25 mg). The mixture was stirred at room temperature under hydrogen atmosphere for 24 h. The mixture was filtered and the filtrate concentrated *in vacuo*, keeping the bath temperature at 20^oC. The residue was purified by flash column chromatography ($CHCl_3$/MeOH, 9:1 → $CHCl_3$/MeOH/H_2O, 4:1:0.1) to afford **1** (23 mg, 44%) and **12** (12 mg, 21%). Both **1** and **12** were freeze dried from a dioxane-$CHCl_3$ mixture (95:5) to give white fluffy solids.

For compound **1**: R_f 0.34 ($CHCl_3$/MeOH/H_2O, 4:1:0.1); $[\alpha]_D^{22}$ -0.2 (*c* 1.0, $CHCl_3$); ^1H NMR (500 MHz, $CDCl_3$:CD_3OD, 4:1): δ 0.75 (t, 18H, *J* 7.0 Hz, 6 x CH_3), 1.08-1.27 (br m, 114, 57 x CH_2 of lipid), 1.37-1.58 (br m, 12H, H-4_L x 3, H-$3_{L'}$ x 3), 2.10-2.27 (m, 8H, H-$2_{L'}$ x 3, H-2_L x 1), 2.29-2.71 (br m, 4H, H-2_L x 2), 3.17-3.29 (br m, H-2, H-6a, H-6b), 3.47-3.68 (br m, 7H, H-5, $ROCH_2C\underline{H_2}NC\underline{H_2}C\underline{H_2}OH$), 3.71-3.88 (m, 2H, $ROC\underline{H_2}CH_2NCH_2CH_2OH$), 4.03-4.15 (br m, 1H, H-4), 4.30 (d, 0.6H, *J* 8.0 Hz, H-1 from one isomer), 4.45 (d, 0.4H, *J* 8.0 Hz, H-1 from one isomer), 4.89-5.16 (br m, 4H, H-3, H-3_L x 3); HRESI-MS (*m*/*z*) Calcd for $C_{94}H_{178}N_2O_{18}P$ $[M-H]^-$ 1654.2843, found: 1654.2837.

For compound **12**: R_f 0.40 ($CHCl_3$/MeOH/H_2O, 4:1:0.1); $[\alpha]_D^{22}$ -0.2 (*c* 1.0, $CHCl_3$); ^1H NMR (500 MHz, $CDCl_3$:CD_3OD, 4:1): δ 0.75 (t, 18H, *J* 7.0 Hz, 6 x CH_3), 1.20-1.45 (br m, 114, 57 x CH_2 of lipid), 1.52-1.75 (br m, 12H, H-4_L x 3, H-$3_{L'}$ x 3), 1.81-2.03 (br, m, 4H, $ROCH_2C\underline{H_2}C\underline{H_2}CH_2OH$), 2.20-2.51 (br m, 8H, H-$2_{L'}$ x 3, H-2_L x 1), 2.29-2.71 (br m, 4H, H-2_L x 2), 3.28-3.43 (br m, 3H, H-2, H-6a, H-6b), 3.45-4.06 (br m, 13H H-5, $ROC\underline{H_2}C\underline{H_2}NC\underline{H_2}C\underline{H_2}OC\underline{H_2}CH_2CH_2C\underline{H_2}OH$), 4.41-4.65 (br m, 2H, H-1, H-4), 5.02-5.33 (br m 4H, H-3, H-3_L x 3); ESI-MS (*m*/*z*) Calcd for $C_{98}H_{186}N_2O_{19}P$ $[M-H]^-$ 1726.3, found: 1726.3.

Method 2:

To a solution of **10** (40 mg, 0.02 mmol) in freshly distilled THF (45 ml) and glacial acetic acid (5 mL), was added palladium on charcoal (5%, 15 mg). The mixture was stirred at room temperature under hydrogen atmosphere for 24 h. TLC analysis again indicated the

formation of a mixture of both **1** and **12**. However, it was observed that **1** formed in far greater abundance, with the relative abundance of **12** estimated at being < 5%. The mixture was filtered and the filtrate concentrated *in vacuo*, keeping the bath temperature at 20°C. The residue was purified by flash column chromatography ($CHCl_3$/MeOH, 9:1 → $CHCl_3$/MeOH/H_2O, 4:1:0.1) to afford **1** (26 mg, 76%) as white fluffy solid after being freeze dried from a dioxane-$CHCl_3$ mixture (95:5).

2.3.7 [N-(2-{(*R*)-3-tetradecanoyloxytetradecanoyl)-ethyl}-(*R*)-3-tetradecanoyloxytetradecanamido]-eth-1-yl 2-deoxy-4-*O*-(phosphono)-3-*O*-[(*R*)-3-tetradecanoyloxytetradecanoyl]-2-[(*R*)-3-tetradecanoyloxytetradecanamido]-β-D-glucopyranoside (2):

In a similar manner as described for the global deprotection of **10**, a solution of **11** (12 mg, 0.005 mmol) in freshly distilled THF (30 mL) and palladium on charcoal (5%, 15 mg) was stirred at room temperature under hydrogen atmosphere for 24 h. The mixture was filtered, the filtrate concentrated, and the resulting residue purified by flash column chromatography ($CHCl_3$/MeOH, 9:1 → $CHCl_3$/MeOH/H_2O, 4:1:0.1) to afford **2** (9 mg, 85%) as white fluffy solid after being freeze dried from a dioxane-$CHCl_3$ mixture (95:5). R_f 0.54 ($CHCl_3$/MeOH/H_2O, 4:1:0.1); $[\alpha]_D^{22}$ -0.1 (*c* 1.0, $CHCl_3$); ^{1}H NMR (500 MHz, $CDCl_3$:CD_3OD, 2:1): δ 0.82 (t, 24H, *J* 7.0 Hz, 8 x CH_3), 1.13-1.34 (br m, 114, 57 x CH_2 of lipid),), 1.42-1.70 (br m, 16H, H-4_L x 4, H-$3_{L'}$ x 4), 2.17-2.43 (br m, 10H, H-$2_{L'}$ x 4, H-2_L x 1), 2.45-2.77 (br m, 6H, H-3_L x 3), 3.22-3.31 (br m, 3H, H-2, H-6a, H-6b), 3.38-3.73 (br m, 7H, OCH_2, CH_2N x 2), 4.03-4.19 (br m, 2H, OCH_2), 4.36-4.48 (br m, 2H, H-

1, H-4), 4.89-5.08 (br m, 5H, H-3, H-3_L x 4); HRESI-MS (*m/z*) Calcd for $C_{122}H_{230}N_2O_{21}P$ $[M-H]^-$: 2090.6746, found: 2090.6727.

2.3.8 *N*,*N*-Bis(2-hydroxyethyl)-2,2,2-trichloroethoxymethanamide (15)

&

N-(2-hydroxyethyl)-*N*-{2-(2,2,2-trichloroethoxycarbonyloxy)-ethyl}-2,2,2-trichloroethoxymethanamide (16):

To a solution of diethanolamine (1.10 g, 10.45 mmol) and sodium bicarbonate (3.07 g, 36.58 mmol) in water (70 mL), 2,2,2-trichloroethoxychloroformate (2.88 g, 13.59 mmol) was added drop wise in about 3 min. As the mixture was stirred at room temperature, a viscous insoluble oil formed and settled to the bottom of the reaction vessel. After stirring for 3 h, the mixture was extracted with EtOAc (3 x 135 mL), after which the combined organic layers were dried over Na_2SO_4 and concentrated. Purification via flash column chromatography (hexane/EtOAc/MeOH, 1:1:0.1) yielded **15** (2.29 g, 78%) and **16** (332 mg, 7%), both as colorless syrups.

For (**15**): Rf 0.34 (hexane/EtOAc/MeOH, 1:1:0.1); ^{1}H NMR (500 MHz, $CDCl_3$): δ 3.52-3.63 (br m, 6H, NCH_2 x 2, OH x 2), 3.86-3.94 (m, 4H, OCH_2 x 2), 4.78 (s, 2H, Troc-CH_2); ^{13}C NMR (125 MHz, $CDCl_3$): δ 52.55 (N$\underline{C}H_2$), 53.26 (N$\underline{C}H_2$), 61.57 (O$\underline{C}H_2$), 62.04 (O$\underline{C}H_2$), 75.45 (Troc-$\underline{C}H_2$), 95.61 (Troc-$\underline{C}Cl_3$), 155.15 (C=O); ESI-MS (*m/z*) Calcd for $C_7H_{12}Cl_3NO_4$ $[M + Na]^+$: 301.9, found: 302.0.

For (**16**): Rf 0.65 (hexane/EtOAc/MeOH, 1:1:0.1); ^{1}H NMR (500 MHz, $CDCl_3$): δ 1.82-1.95 (br s, 0.5H, OH from one isomer), 2.20-2.34 (br s, 0.5 H, OH from one isomer), 3.58-3.61 (m, 2H, $HOCH_2C\underline{H_2}N$), 3.73-3.77 (m, 2H, $NC\underline{H_2}CH_2OTroc$), 3.82-3.88 (br m, 2H, $HOC\underline{H_2}$), 4.44-4.49 (m, 2H, $C\underline{H_2}OTroc$), 4.76-4.81 (m, 4H, Troc-CH_2 x 2); ^{13}C NMR (125 MHz, $CDCl_3$): δ 47.45 ($HOCH_2\underline{C}H_2N$ from one isomer), 48.24 ($HOCH_2\underline{C}H_2N$ from one isomer), 51.10 ($N\underline{C}H_2CH_2OTroc$ from one isomer), 51.86 ($N\underline{C}H_2CH_2OTroc$ from one isomer), 61.22 ($HO\underline{C}H_2$ from one isomer), 61.27 ($HO\underline{C}H_2$ from one isomer), 66.66 ($\underline{C}H_2OTroc$ from one isomer), 66.91 ($\underline{C}H_2OTroc$ from one isomer), 75.20 (O-Troc-CH_2 from one isomer), 75.34 (O-Troc-$\underline{C}H_2$ from one isomer), 76.86 (N-Troc-$\underline{C}H_2$), 94.24 (O-Troc-$\underline{C}Cl_3$), 95.22 (N-Troc-$\underline{C}Cl_3$), 153.82 (O-Troc-C=O), 154.52 (N-Troc-C=O from one isomer), 155.05 (N-Troc-C=O from one isomer); ESI-MS (*m*/*z*) Calcd for $C_{10}H_{13}Cl_6NO_6$ $[M + Na]^+$: 475.9, found: 475.9.

2.3.9 *N*-(2-hydroxyethyl)-*N*-{2-(*tert*-butyldiphenylsilyloxy)ethyl}-2,2,2-trichloroethoxymethanamide (17) :

&

N,*N*-Bis{2-(*tert*-butyldiphenylsilyloxy)ethyl}-2,2,2-trichloroethoxymethanamide (18):

To a cooled solution (ice water bath) of **15** (2.00 g, 7.13 mmol) and Et_3N (902 mg, 8.91 mmol) in CH_2Cl_2 (8 mL), tert-butyldiphenylsilyl chloride (2.45 g, 8.91 mmol) was added. After stirring at room temperature for 3 hours, the reaction was quenched with MeOH and concentrated. Flash column chromatography purification (hexane/acetone, 3.5 : 1)

yielded **17** (2.01 g, 54%) and **18** (321 mg, 6%), as well as recovered **15** (706 mg, 35%), all as colorless syrups.

For (**17**): Rf 0.38 (hexane/acetone, 3:1); ^{1}H NMR (500 MHz, $CDCl_3$): δ 1.09 (s, 9H, $C(C\underline{H}_3)_3$), 2.69 (br s, 0.4H, OH from one isomer), 2.94 (br s, 0.6H, OH from one isomer), 3.56-3.64 (m, 4H, NCH_2 x 2), 3.83-3.90 (m, 4H, OCH_2 x 2), 4.68 (s, 1.2H, Troc-CH_2 from one isomer), 4.78 (s, 0.8H, Troc-CH_2 from one isomer), 7.40-7.48 (m, 6H, Ar-H), 7.67-7.70 (m, 4H, Ar-H); ^{13}C NMR (125 MHz, $CDCl_3$): δ 19.10 ($\underline{C}(CH_3)_3$ from one isomer), 19.13 ($\underline{C}(CH_3)_3$ from one isomer), 26.82 ($C(\underline{C}H_3)_3$), 50.77 ($N\underline{C}H_2CH_2$OTBDPS from one isomer), 51.42 ($N\underline{C}H_2CH_2$OTBDPS from one isomer), 51.46 ($HOCH_2\underline{C}H_2N$ from one isomer), 52.44 ($HOCH_2\underline{C}H_2N$ from one isomer), 61.54 ($\underline{C}H_2$OTBDPS from one isomer), 61.72 ($\underline{C}H_2$OTBDPS from one isomer), 62.18 ($HO\underline{C}H_2$ from one isomer, 62.72 ($HO\underline{C}H_2$ from one isomer), 75.15 (Troc-$\underline{C}H_2$ from one isomer), 75.19 (Troc-$\underline{C}H_2$ from one isomer), 95.30 (Troc-$\underline{C}Cl_3$ from one isomer), 95.57 (Troc-$\underline{C}Cl_3$ from one isomer), 127.84 (CH-Ar), 127.86 (CH-Ar), 129.93 (CH-Ar), 132.92 (C-Ar), 135.58 (CH-Ar), 154.40 (C=O from one isomer), 155.45 (C=O from one isomer); ESI-MS (*m*/*z*) Calcd for $C_{23}H_{30}Cl_3NO_4Si$ $[M - C_4H_9]^+$: 460.0, found: 460.4.

For (**18**): Rf 0.67 (hexane/acetone, 3:1); ^{1}H NMR (500 MHz, $CDCl_3$): δ 1.05 (s, 18H, $C(C\underline{H}_3)_3$ x 2), 3.61-3.69 (m, 4H, NCH_2 x 2), 3.85-3.92 (m, 4H, OCH_2 x 2), 4.75 (s, 2H, Troc-CH_2), 7.43-7.52 (m, 12H, Ar-H), 7.72-7.79 (m, 8H, Ar-H); ^{13}C NMR (125 MHz, $CDCl_3$): δ 19.20 ($\underline{C}(CH_3)_3$), 26.88 ($C(\underline{C}H_3)_3$), 50.86 ($N\underline{C}H_2$), 51.32 ($N\underline{C}H_2$), 62.24 ($O\underline{C}H_2$), 62.65 ($O\underline{C}H_2$), 75.04 (Troc-$\underline{C}H_2$), 95.62 (Troc-$\underline{C}Cl_3$), 127.78 (CH-Ar), 127.82

(CH-Ar), 127.85 (CH-Ar), 129.70 (CH-Ar), 129.82 (CH-Ar) 129.84 (CH-Ar), 133.35 (C-Ar), 133.44 (C-Ar), 133.59 (C-Ar), 135.59 (CH-Ar), 135.62 (CH-Ar), 154.27 (C=O); ESI-MS (*m*/*z*) Calcd for $C_{39}H_{48}Cl_3NO_4Si_2$ $[M - C_4H_9]^+$: 698.2, found: 698.5.

2.3.10 *N*-{2-(*tert*-butyldiphenylsilyloxy)ethyl}-*N*-{2-[3,4,6-tri-*O*-acetyl-2-deoxy-2-(2,2,2-trichloroethoxycarbonylamino)-β-D-glucopyranosyloxy]-ethyl}-2,2,2-trichloroethoxymethanamide (20):

A solution of **17** (997 mg, 1.92 mmol) and imidate **19** (1.26 g, 2.02 mmol) in dry CH_2Cl_2 (8 mL) in the presence of molecular sieves (4Å, 4.0 g) was stirred under nitrogen at room temperature for 30 min. A solution of TMSOTf (0.05 M in dry CH_2Cl_2, 0.8 mL) was added drop wise in about 3 min. The mixture was stirred at room temperature for 1 h before a saturated sodium bicarbonate solution (15 mL) was added to quench the reaction. Solids were filtered out, and the filtrate was extracted with CH_2Cl_2 (3 x 30 mL). The combined organic phase was dried over Na_2SO_4 , concentrated, and purified via flash column chromatography (hexane/acetone, 2.5 : 1) to yield **20** (1.77 g, 94%) as a fluffy white solid. Rf 0.42 (hexane/acetone, 5:2); $[\alpha]_D^{22}$ + 0.9 (*c* 1.0, $CHCl_3$); ^{1}H NMR (500 MHz, $CDCl_3$): δ 1.04 (s, 9H, C(CH_3)$_3$), 2.01-2.09 (m, 9H, Ac x 3), 3.38-3.47 (m, 2H, NCH_2), 3.51-3.72 (m, 4H, H-2, H-5, NCH_2), 3.75-3.86 (m, 3H, ROCH*H*, CH_2OTBDPS), 3.94-4.04 (m, 1H, ROC*H*H), 4.08-4.13 (m, 1H, H-6b), 4.26 (dd, 0.5H, *J* 12.0, 12.0 Hz, H-6a from one isomer), 4.28 (dd, 0.5H, *J* 12.0, 12.0 Hz, H-6a from one isomer), 4.53 (d, 0.5H, *J* 8.5 Hz, H-1 from one isomer), 4.55 (d, 0.5H, *J* 12.5 Hz, Troc), 4.60 (d, 0.5H, *J* 12.0 Hz, Troc), 4.65 (d, 0.5H, *J* 8.5 Hz, H-1 from one isomer), 4.68 (d, 0.5H, *J* 12.5 Hz,

Troc), 4.72 (d, 0.5H, *J* 12.5 Hz, Troc), 4.76 (d, 1.0H, *J* 12.0 Hz, Troc), 4.89 (d, 1.0H, *J* 12.0 Hz, Troc), 4.94 (d, 0.5H, *J* 8.0 Hz, NH from one isomer), 5.05 (dd, 0.5H, *J* 9.5, 9.5 Hz, H-4 from one isomer), 5.08 (dd, 0.5H, *J* 9.5, 9.5 Hz, H-4 from one isomer), 5.22 (dd, 0.5H, *J* 9.5, 9.5 Hz, H-3 from one isomer), 5.24 (dd, 0.5H, *J* 9.5, 9.5 Hz, H-3 from one isomer), 5.31 (d, 0.5 H, *J* 8.0 Hz, NH from one isomer), 7.38-7.46 (m, 6H, Ar-H), 7.62-7.66 (m, 4H, Ar-H); ^{13}C NMR (125 MHz, $CDCl_3$): δ 19.11 ($\underline{C}(CH_3)_3$ from one isomer), 19.14 ($\underline{C}(CH_3)_3$ from one isomer), 20.69 ($C(\underline{C}H_3)_3$ from one isomer), 20.80 ($C(\underline{C}H_3)_3$ from one isomer), 26.85 ($COO\underline{C}H_3$), 48.26 ($N\underline{C}H_2$), 48.33 ($N\underline{C}H_2$), 50.22 ($N\underline{C}H_2$), 51.30 ($N\underline{C}H_2$), 61.90 ($O\underline{C}H_2$), 61.94 ($O\underline{C}H_2$), 61.98 (C-6), 62.48 ($O\underline{C}H_2$), 66.89 ($O\underline{C}H_2$), 68.50 (C-4 from one isomer), 68.58 (C-4 from one isomer), 71.79 (C-5 from one isomer), 71.84 (C-5 from one isomer), 71.89 (C-3 from one isomer), 72.39 (C-3 from one isomer), 74.32 (Troc-$\underline{C}H_2$), 74.35 (Troc-$\underline{C}H_2$), 75.01 (Troc-$\underline{C}H_2$), 75.10 (Troc-$\underline{C}H_2$), 95.38 (Troc-$\underline{C}Cl_3$), 95.45 (Troc-$\underline{C}Cl_3$), 95.51 (Troc-$\underline{C}Cl_3$), 95.68 (Troc-$\underline{C}Cl_3$), 99.61 (C-1 from one isomer), 100.99 (C-1 from one isomer), 127.80 ($\underline{C}$H-Ar), 127.83 ($\underline{C}$H-Ar), 127.84 ($\underline{C}$H-Ar), 129.83 ($\underline{C}$H-Ar), 129.88 ($\underline{C}$H-Ar), 133.11 ($\underline{C}$-Ar), 133.16 ($\underline{C}$-Ar), 133.29 ($\underline{C}$-Ar), 133.34 ($\underline{C}$-Ar), 135.56 ($\underline{C}$H-Ar), 135.57 ($\underline{C}$H-Ar), 153.97 (C=O Troc), 153.99 (C=O Troc), 154.20 (C=O Troc), 154.67 (C=O Troc), 169.49 (C=O), 170.57 (C=O). 170.64 (C=O), 170.71 (C=O), 170.73 (C=O); MALDI-MS (*m*/*z*) Calcd for $C_{38}H_{48}Cl_6N_2O_{13}Si$ $[M + Na]^+$: 1001.09, found: 1001.08.

2.3.11 *N*-{2-(tert-butyldiphenylsilyloxy)-ethyl}-*N*-{2-[2-deoxy-2-(2,2,2-trichloroethoxycarbonylamino)-β-D-glucopyranosyloxy]-ethyl}-2,2,2-trichloroethoxymethanamide (21):

Guanidinium nitrate (1.87 g, 15.32 mmol) was dissolved in MeOH:CH_2Cl_2 (9:1, 150 mL) and sodium methoxide in methanol solution (0.5 M, 6 mL) was added. **20** (1.86 g, 1.89 mmol) was dissolved in the above solution and stirred at room temperature for 3 h. The mixture was then neutralized by adding weak acidic ion-exchange resin (Amberlite IRC-64). The resin was filtered and the filtrate concentrated. The residue was purified via flash column chromatography (CH_2Cl_2/MeOH, 13 : 1) to afford **21** (1.48 g, 91%) as a white fluffy solid. Rf 0.29 (hexane/acetone, 3:2); $[\alpha]_D^{22}$ -12.5 (*c* 1.0, $CHCl_3$); ^{1}H NMR (500 MHz, $CDCl_3$): δ 1.04 (s, 9H, C(C<u>H</u>$_3$)$_3$), 3.25-3.67 (m, 8H, H-2, H-4, H-6b, H-6a, NCH_2 x 2), 3.69-3.85 (m, 5H, H-3, H-5, ROCH*<u>H</u>*, C<u>H</u>$_2$OTBDPS), 3.87-3.99 (m, 1H, ROC*<u>H</u>*H), 4.43 (d, 0.4H, *J* 8.0 Hz, H-1 from one isomer), 4.54 (d, 0.6H, *J* 8.0 Hz, H-1 from one isomer), 4.61 (d, 0.6H, J 12.0 Hz, Troc), 4.63 (d, 0.6H, J 12.0 Hz, Troc), 4.69 (d, 1H, J 12.0 Hz, Troc), 4.71 (d, 0.4 H, J 12.0 Hz, Troc), 4.74 (d, 0.4H, J 12.0 Hz, Troc), 4.78 (d, 1 H, J 12.0 Hz, Troc), 4.99 (br s, 3H, OH x 3), 6.17 (d, 0.4H, J 8.0 Hz, NH from one isomer), 6.31 (d, 0.6H, J 8.0 Hz, NH from one isomer), 7.36-7.43 (m, 6H, Ar-H), 7.61-7.64 (m, 4H, Ar-H); ^{13}C NMR (125 MHz, $CDCl_3$): δ 19.14 (<u>C</u>(CH$_3$)$_3$ from one isomer), 19.17 (<u>C</u>(CH$_3$)$_3$ from one isomer), 26.90 (C(<u>C</u>H$_3$)$_3$), 48.22 (N<u>C</u>H$_2$), 48.42 (N<u>C</u>H$_2$), 49.93 (N<u>C</u>H$_2$), 51.43 (N<u>C</u>H$_2$), 57.63 (C-2 from one isomer), 57.78 (C-2 from one isomer), 61.35 (O<u>C</u>H$_2$), 61.92 (O<u>C</u>H$_2$), 62.40 (C-6), 66.23 (O<u>C</u>H$_2$), 68.32 (O<u>C</u>H$_2$), 70.07 (C-4 from one isomer), 70.20 (C-4 from one isomer), 73.95 (C-5 from one isomer), 74.61 (Troc-CH_2), 74.72 (C-5 from one isomer), 75.09 (Troc-CH_2), 75.17 (Troc-CH_2), 75.50 (C-3 from one isomer), 75.63 (Troc-CH_2), 95.31 (Troc-CCl_3), 95.61 (Troc-CCl_3), 95.64 (Troc-CCl_3), 100.03 (C-1 from one isomer), 101.50 (C-1 from one isomer), 127.81

(CH-Ar), 127.87 (CH-Ar), 129.82 (CH-Ar), 129.90 (CH-Ar), 133.09 (C-Ar), 133.27 (C-Ar), 135.57 (CH-Ar), 154.46 (C=O Troc), 154.88 (C=O Troc), 155.17 (C=O Troc), 155.57 (C=O Troc); MALDI-MS (*m*/*z*) Calcd for $C_{32}H_{42}Cl_6N_2O_{10}Si$ $[M + Na]^+$: 875.06, found: 875.05.

2.3.12 *N*-{2-(tert-butyldiphenylsilyloxy)-ethyl}-*N*-{2-[4,6-O-benzylidene-2-deoxy-2-(2,2,2-trichloroethoxycarbonylamino)-β-D-glucopyranosyloxy]-ethyl}-2,2,2-trichloroethoxymethanamide (12):

To a solution of **21** (1.35 g, 1.58 mmol) in CH_3CN (8 mL), benzaldehyde dimethyl acetal (308 mg, 2.02 mmol) and p-toluene sulfonic acid (15 mg, 0.08 mmol) were added successively. The mixture was stirred at room temperature for 2 h before being quenched with Et_3N (0.5 mL), and concentrated. The residue was purified via flash column chromatography (hexane/acetone, 3 : 1) to yield **22** (1.29 g, 87%) as a white fluffy solid. Rf 0.46 (hexane/acetone, 5:2); $[\alpha]_D^{22}$ -17.9 (*c* 1.0, $CHCl_3$); ^{1}H NMR (500 MHz, $CDCl_3$): δ 1.05 (s, 9H, $C(CH_3)_3$), 3.33-3.66 (m, 8H, H-2, H-4, H-5, OH, NCH_2 x 2), 3.68-3.99 (m, 6H, H-3, H-6b, OCH_2 x 2), 4.27 (dd, 0.4H, J 10.0, 10.0 Hz, H-6a from one isomer), 4.29 (dd, 0.6H, J 10.0, 10.0 Hz, H-6a from one isomer), 4.45 (d, 0.4H, J 8.0 Hz, H-1 from one isomer), 4.53 (d, 0.6H, J 8.0 Hz, H-1 from one isomer), 4.61 (d, 1.4H, J 12.0 Hz, Troc), 4.69 (0.6H, J 12.0 Hz, Troc), 4.72 (d, 0.6H, J 12.0 Hz, Troc), 4.74 (d, 1H, J 12.0 Hz, Troc), 4.81 (d, 0.4H, J 12.0 Hz, Troc), 5.23 (d, 0.4H, J 8.0 Hz, NH from one isomer), 5.50 (s, 0.4H, Ph-CH from one isomer), 5.52 (s, 0.6H, Ph-CH from one isomer), 5.74 (d, 0.6H, J 8.0 Hz, NH from one isomer), 7.33-7.44 (m, 9H, Ar-H), 7.47-7.51 (m, 2H, Ar-H),

7.61-7.65 (m, 4H, Ar-H); ^{13}C NMR (125 MHz, $CDCl_3$): δ 19.15 ($\underline{C}(CH_3)_3$ from one isomer), 19.18 ($\underline{C}(CH_3)_3$ from one isomer), 26.89 ($C(\underline{C}H_3)_3$), 48.38 ($N\underline{C}H_2$), 48.45 ($N\underline{C}H_2$), 50.19 ($N\underline{C}H_2$), 51.35 ($N\underline{C}H_2$), 58.45 (C-2 from one isomer), 58.62 (C-2 from one isomer), 61.97 ($O\underline{C}H_2$), 62.51 ($O\underline{C}H_2$), 66.03 (C-5 from one isomer), 66.17 (C-5 from one isomer), 66.83 ($O\underline{C}H_2$), 68.55 (C-6), 70.74 (C-3 from one isomer), 71.81 (C-3 from one isomer), 74.66 (Troc-CH_2), 75.06 (Troc-CH_2), 75.15 (Troc-CH_2), 81.40 (C-4), 95.38 (Troc-CCl_3), 95.48 (Troc-CCl_3), 95.70 (Troc-CCl_3), 99.86 (C-1 from one isomer), 101.35 (C-1 from one isomer), 101.86 (Ph-$\underline{C}$H from one isomer), 101.89 (Ph-$\underline{C}$H from one isomer), 126.43 ($\underline{C}$H-Ar), 126.45 ($\underline{C}$H-Ar), 127.83 ($\underline{C}$H-Ar), 127.87 ($\underline{C}$H-Ar), 128.45 ($\underline{C}$H-Ar), 128.49 ($\underline{C}$H-Ar), 129.42 ($\underline{C}$H-Ar), 129.46 ($\underline{C}$H-Ar), 129.85 ($\underline{C}$H-Ar), 129.91 ($\underline{C}$H-Ar), 133.12 ($\underline{C}$-Ar), 133.14 ($\underline{C}$-Ar), 133.31 ($\underline{C}$-Ar), 133.33 ($\underline{C}$-Ar), 135.58 ($\underline{C}$H-Ar), 137.03 ($\underline{C}$-Ar), 154.05 (C=O Troc), 154.54 (C=O Troc), 154.85 (C=O Troc), 155.37 (C=O Troc); MALDI-MS (*m/z*) Calcd for $C_{39}H_{46}Cl_6N_2O_{10}Si$ $[M + Na - C_4H_9]^+$: 906.06, found: 906.12.

2.3.13 *N*-{2-(tert-butyldiphenylsilyloxy)-ethyl}-*N*-{2-[4,6-*O*-benzylidene-2-deoxy-3-*O*-((*R*)-3-tetradecanoyloxytetradecanoyl)-2-(2,2,2-trichloroethoxycarbonylamino)-β-D-glucopyranosyloxy]-ethyl}-2,2,2-trichloroethoxymethanamide (23):

A mixture of **22** (1.16 g, 1.23 mmol), dilipid acid **3** (590 mg, 1.30 mmol), *N,N*-dimethylaminopyridine (15 mg, 0.12 mmol) and *N,N'*-diisopropylcarbodiimide (235 mg, 1.85 mmol) in CH_2Cl_2 (7 mL) was stirred at room temperature for 4 h. Water (0.5 mL) was added and the mixture stirred for a further 1 h. The solids were then filtered through

a scintered glass funnel with a bed of Na_2SO_4 . The filtrate was concentrated and the residue purified by flash column chromatography (hexane/acetone, 4.5 : 1) to afford **23** (1.58 g, 93%) as a colorless syrup. Rf 0.38 (hexane/acetone, 4:1); $[\alpha]_D^{22}$ -14.1 (*c* 1.0, $CHCl_3$); ^{1}H NMR (500 MHz, $CDCl_3$): δ 0.91 (t, 6H, J 6.5 Hz, CH_3 x 2), 1.08 (s, 9H, $C(C\underline{H}_3)_3$), 1.14-1.36 (br m, 38H, CH_2 x 19), 1.53-162 (br m, 4H, H-4_L, H-$3_{L'}$), 2.16-2.23 (m, 2H, H-$2_{L'}$), 2.53-2.66 (m, 2H, H-2_L), 3.46-3.68 (m, 7H, H-2, H-4, H-5, NCH_2 x 2), 3.71-3.87 (m, 4H, H-6b, $C\underline{H}_2$OTBDPS, ROCH*H*), 3.94-4.04 (m, 1H, ROC*H*H), 4.33 (dd, 0.4H, J 10.0, 10.0 Hz, H-6a from one isomer), 4.34 (dd, 0.6H, J 10.0, 10.0 Hz, H-6a from one isomer), 4.55 (d, 0.4 H, J 12.0 Hz, Troc), 4.59 (d, 0.6 H, J 12.0 Hz, Troc), 4.61 (d, 0.4H, J 8.0 Hz, H-1 from one isomer), 4.63 (d, 0.6 H, J 12.0 Hz, Troc), 4.69 (d, 0.6H, J 8.0 Hz, H-1 from one isomer), 4.72 (d, 0.4 H, J 12.0 Hz, Troc), 4.74 (d, 0.6 H, J 12.0 Hz, Troc), 4.78 (d, 0.6 H, J 12.0 Hz, Troc), 4.80 (d, 0.4 H, J 12.0 Hz, Troc), 4.87 (d, 0.4 H, J 12.0 Hz, Troc), 5.18-5.26 (m, 1H, H-3_L), 5.32-5.38 (m, 1.4H, H-3, NH from one isomer), 5.50-5.54 (m, 1.6H, Ph-C$\underline{H}$, NH from one isomer), 7.34-7.49 (m, 11H, Ar-H), 7.58-7.69 (m, 4H, Ar-H); ^{13}C NMR (125 MHz, $CDCl_3$): δ 14.18 (CH_3), 19.13 ($\underline{C}(CH_3)_3$ from one isomer), 19.17 ($\underline{C}(CH_3)_3$ from one isomer), 22.73 (CH_2), 25.01 (CH_2), 25.09 (CH_2), 26.86 ($C(\underline{C}H_3)_3$ from one isomer), 26.88 ($C(\underline{C}H_3)_3$ from one isomer), 29.16 (CH_2), 29.33 (CH_2), 29.35 (CH_2), 29.39 (CH_2), 29.400 (CH_2), 29.56 (CH_2), 29.58 (CH_2), 29.68 (CH_2), 29.70 (CH_2), 29.71 (CH_2), 29.73 (CH_2), 33.87 (CH_2), 33.92 (CH_2), 34.37 (CH_2), 39.22 (C-2_L from one isomer), 39.32 (C-2_L from one isomer), 48.35 ($N\underline{C}H_2$), 48.69 ($N\underline{C}H_2$), 50.42 ($N\underline{C}H_2$), 51.28 ($N\underline{C}H_2$), 56.85 (C-2), 61.96 ($O\underline{C}H_2$), 62.51 ($O\underline{C}H_2$), 66.30 (C-5 from one isomer), 66.35 (C-5 from one isomer), 67.57 ($O\underline{C}H_2$), 68.55 (C-6), 68.65 ($O\underline{C}H_2$), 69.96 (C-3_L from one isomer), 69.99 (C-3_L from one isomer), 70.99 (C-3 from one isomer),

71.27 (C-3 from one isomer), 74.41 (Troc-CH_2), 74.44 (Troc-CH_2), 75.04 (Troc-CH_2), 75.09 (Troc-CH_2), 78.74 (C-4 from one isomer), 78.80 (C-4 from one isomer), 95.42 (Troc-CCl_3), 95.51 (Troc-CCl_3), 95.69 (Troc-CCl_3), 100.95 (C-1 from one isomer), 101.47 (Ph-CH), 101.84 (C-1 from one isomer), 126.16 (CH-Ar), 127.80 (CH-Ar), 127.84 (CH-Ar), 128.27 (CH-Ar), 129.18 (CH-Ar), 129.82 (CH-Ar), 129.86 (CH-Ar), 133.17 (C-Ar), 133.20 (C-Ar), 133.32 (C-Ar), 133.36 (C-Ar), 135.58 (CH-Ar), 136.82 (C-Ar), 154.01 (C=O Troc), 154.19 (C=O Troc), 154.36 (C=O Troc), 154.50 (C=O Troc), 170.01 (C=O), 170.06 (C=O), 173.41 (C=O), 173.50 (C=O); MALDI-MS (*m*/*z*) Calcd for $C_{67}H_{98}Cl_6N_2O_{13}Si$ $[M + Na]^+$: 1399.49, found: 1399.50.

2.3.14 *N*-{2-(*tert*-butyldiphenylsilyloxy)-ethyl}-*N*-{2-[6-*O*-benzyl-2-deoxy-3-*O*-((*R*)-3-tetradecanoyloxytetradecanoyl)-2-(2,2,2-trichloroethoxycarbonylamino)-β-D-glucopyranosyloxy]-ethyl}-2,2,2-trichloroethoxymethanamide (24):

A solution of **23** (1.51 g, 1.09 mmol) in dry THF (10 mL) and molecular sieves (4Å, 4.0 g) was stirred at room temperature under nitrogen for 30 min. Sodium cyanoborohydride (550 mg, 8.75 mmol) was added and the mixture cooled to 0 °C, followed by the drop wise addition of dry ethereal-$HCl_{(g)}$ until no further gas was evolved. The mixture was poured into a saturated sodium bicarbonate solution (100 mL) and solids were filtered out before removal of the THF *in vacuo*. The resulting solution was extracted with EtOAc (3 x 100 mL), with the combined organic phase dried over Na_2SO_4 and concentrated. Flash column chromatography of the residue (hexane/acetone, 4 : 1) afforded **24** (1.31 g, 87%) as a colorless syrup. Rf 0.31 (hexane/acetone, 4:1); $[\alpha]_D^{22}$ -6.6 (*c* 1.0, $CHCl_3$); ^{1}H NMR

(500 MHz, $CDCl_3$): δ 0.91 (t, 6H, J 6.5 Hz, CH_3 x 2), 1.07 (s, 9H, $C(C\underline{H}_3)_3$), 1.24-1.38 (br m, 38H, CH_2 x 19), 1.54-1.68 (br m, 4H, H-4_L, H-$3_{L'}$), 2.31 (t, 2H, J 7.5 Hz, H-$2_{L'}$), 2.48-2.61 (m, 2H, H-2_L), 3.46-3.72 (m, 8H, H-2, H-4, H-5, OH, NCH_2 x 2), 3.75-3.86 (m, 5H, H-6b, H-6a, $C\underline{H}_2$OTBDPS, ROCH*H*), 3.94-4.05 (m, 1H, ROC*H*H), 4.42 (d, 0.4H, J 8.5 Hz, H-1 from one isomer), 4.48 (d, 0.6 H, J 12.0 Hz, Troc), 4.52-4.65 (m, 2.6H, H-1 from one isomer, Ph-$C\underline{H}_2$), 4.68 (d, 1 H, J 12.0 Hz, Troc), 4.72 (d, 0.6 H, J 12.0 Hz, Troc), 4.76 (d, 0.4 H, J 12.0 Hz, Troc), 4.80 (d, 0.4 H, J 12.0 Hz, Troc), 4.89 (d, 1 H, J 12.0 Hz, Troc), 5.00 (dd, 0.4H, J 10.0, 10.0 Hz, H-3 from one isomer). 5.02 (dd, 0.6H, J 10.0, 10.0 Hz, H-3 from one isomer), 5.13-5.20 (m, 1H, H-3_L), 5.26 (d, 0.4H, J 8.0 Hz, NH from one isomer), 5.49 (d, 0.6H, J 8.0 Hz, NH from one isomer), 7.30-7.47 (m, 11H, Ar-H), 7.63-7.68 (m, 4H, Ar-H); ^{13}C NMR (125 MHz, $CDCl_3$): δ 14.14 (CH_3), 19.11 ($\underline{C}(CH_3)_3$ from one isomer), 19.15 ($\underline{C}(CH_3)_3$ from one isomer), 22.70 (CH_2), 24.98 (CH_2), 25.14 (CH_2), 26.86 ($C(\underline{C}H_3)_3$), 29.15 (CH_2), 29.30 (CH_2), 29.36 (CH_2), 29.38 (CH_2), 29.51 (CH_2), 29.53 (CH_2), 29.55 (CH_2), 29.65 (CH_2), 29.66 (CH_2), 29.68 (CH_2), 29.72 (CH_2), 31.93 (CH_2), 31.94 (CH_2), 34.51 (CH_2), 34.64 (CH_2), 40.09 (C-2_L), 48.29 ($N\underline{C}H_2$), 48.36 ($N\underline{C}H_2$), 50.22 ($N\underline{C}H_2$), 51.20 ($N\underline{C}H_2$), 55.70 (C-2), 61.89 ($O\underline{C}H_2$), 62.48 ($O\underline{C}H_2$), 66.86 ($O\underline{C}H_2$), 68.29 ($O\underline{C}H_2$), 66.71 (C-6 from one isomer), 66.73 (C-6 from one isomer), 70.10 (C-4), 71.00 (C-3_L from one isomer), 71.03 (C-3_L from one isomer), 73.69 (Ph-$\underline{C}H_2$), 74.36 (Troc-CH_2), 74.38 (Troc-CH_2), 74.51 (C-5 from one isomer), 74.63 (C-5 from one isomer), 75.03 (Troc-CH_2), 75.11 (Troc-CH_2), 75.65 (C-3 from one isomer), 76.12 (C-3 from one isomer), 95.43 (Troc-CCl_3), 95.58 (Troc-CCl_3), 95.61 (Troc-CCl_3), 95.71 (Troc-CCl_3), 100.17 (C-1 from one isomer), 101.44 (C-1 from one isomer), 127.67 ($\underline{C}$H-Ar), 127.69 ($\underline{C}$H-Ar), 127.77 ($\underline{C}$H-Ar), 127.81 ($\underline{C}$H-Ar), 128.46 ($\underline{C}$H-Ar), 129.78

(CH-Ar), 129.82 (CH-Ar), 133.20 (C-Ar), 133.36 (C-Ar), 135.57 (CH-Ar), 137.80 (C-Ar), 137.85 (C-Ar), 154.05 (C=O Troc), 154.20 (C=O Troc), 154.38 (C=O Troc), 154.58 (C=O Troc), 171.48 (C=O), 174.37 (C=O Troc); MALDI-MS (*m*/*z*) Calcd for $C_{67}H_{100}Cl_6N_2O_{13}Si$ $[M + Na]^+$: 1401.50, found: 1401.45.

2.3.15 *N*-{2-(*tert*-butyldiphenylsilyloxy)-ethyl}-*N*-{2-[6-*O*-benzyl-2-deoxy-3-*O*-((*R*)-3-tetradecanoyloxytetradecanoyl)-2-(2,2,2-trichloroethoxycarbonylamino)-β-D-glucopyranosyloxy]-ethyl}-2,2,2-trichloroethoxymethanamide (24):

A solution of **23** (1.51 g, 1.09 mmol) in dry THF (10 mL) and molecular sieves (4Å, 4.0 g) was stirred at room temperature under nitrogen for 30 min. Sodium cyanoborohydride (550 mg, 8.75 mmol) was added and the mixture cooled to 0 °C, followed by the drop wise addition of dry ethereal-$HCl_{(g)}$ until no further gas was evolved. The mixture was poured into a saturated sodium bicarbonate solution (100 mL) and solids were filtered out before removal of the THF *in vacuo*. The resulting solution was extracted with EtOAc (3 x 100 mL), with the combined organic phase dried over Na_2SO_4 and concentrated. Flash column chromatography of the residue (hexane/acetone, 4 : 1) afforded **24** (1.31 g, 87%) as a colorless syrup. Rf 0.31 (hexane/acetone, 4:1); $[\alpha]_D^{22}$ -6.6 (*c* 1.0, $CHCl_3$); ^{1}H NMR (500 MHz, $CDCl_3$): δ 0.91 (t, 6H, J 6.5 Hz, CH_3 x 2), 1.07 (s, 9H, $C(CH_3)_3$), 1.24-1.38 (br m, 38H, CH_2 x 19), 1.54-1.68 (br m, 4H, H-4_L, H-$3_{L'}$), 2.31 (t, 2H, J 7.5 Hz, H-$2_{L'}$), 2.48-2.61 (m, 2H, H-2_L), 3.46-3.72 (m, 8H, H-2, H-4, H-5, OH, NCH_2 x 2), 3.75-3.86 (m, 5H, H-6b, H-6a, CH_2OTBDPS, ROCH*H*), 3.94-4.05 (m, 1H, ROC*H*H), 4.42 (d, 0.4H, J 8.5 Hz, H-1 from one isomer), 4.48 (d, 0.6 H, J 12.0 Hz, Troc), 4.52-4.65 (m, 2.6H, H-1 from

one isomer, Ph-C$\underline{H}_2$), 4.68 (d, 1 H, J 12.0 Hz, Troc), 4.72 (d, 0.6 H, J 12.0 Hz, Troc), 4.76 (d, 0.4 H, J 12.0 Hz, Troc), 4.80 (d, 0.4 H, J 12.0 Hz, Troc), 4.89 (d, 1 H, J 12.0 Hz, Troc), 5.00 (dd, 0.4H, J 10.0, 10.0 Hz, H-3 from one isomer). 5.02 (dd, 0.6H, J 10.0, 10.0 Hz, H-3 from one isomer), 5.13-5.20 (m, 1H, H-3_L), 5.26 (d, 0.4H, J 8.0 Hz, NH from one isomer), 5.49 (d, 0.6H, J 8.0 Hz, NH from one isomer), 7.30-7.47 (m, 11H, Ar-H), 7.63-7.68 (m, 4H, Ar-H); ^{13}C NMR (125 MHz, $CDCl_3$): δ 14.14 (CH_3), 19.11 ($\underline{C}(CH_3)_3$ from one isomer), 19.15 ($\underline{C}(CH_3)_3$ from one isomer), 22.70 (CH_2), 24.98 (CH_2), 25.14 (CH_2), 26.86 (C($\underline{C}H_3)_3$), 29.15 (CH_2), 29.30 (CH_2), 29.36 (CH_2), 29.38 (CH_2), 29.51 (CH_2), 29.53 (CH_2), 29.55 (CH_2), 29.65 (CH_2), 29.66 (CH_2), 29.68 (CH_2), 29.72 (CH_2), 31.93 (CH_2), 31.94 (CH_2), 34.51 (CH_2), 34.64 (CH_2), 40.09 (C-2_L), 48.29 (N$\underline{C}H_2$), 48.36 (N$\underline{C}H_2$), 50.22 (N$\underline{C}H_2$), 51.20 (N$\underline{C}H_2$), 55.70 (C-2), 61.89 (O$\underline{C}H_2$), 62.48 (O$\underline{C}H_2$), 66.86 (O$\underline{C}H_2$), 68.29 (O$\underline{C}H_2$), 66.71 (C-6 from one isomer), 66.73 (C-6 from one isomer), 70.10 (C-4), 71.00 (C-3_L from one isomer), 71.03 (C-3_L from one isomer), 73.69 (Ph-$\underline{C}H_2$), 74.36 (Troc-CH_2), 74.38 (Troc-CH_2), 74.51 (C-5 from one isomer), 74.63 (C-5 from one isomer), 75.03 (Troc-CH_2), 75.11 (Troc-CH_2), 75.65 (C-3 from one isomer), 76.12 (C-3 from one isomer), 95.43 (Troc-CCl_3), 95.58 (Troc-CCl_3), 95.61 (Troc-CCl_3), 95.71 (Troc-CCl_3), 100.17 (C-1 from one isomer), 101.44 (C-1 from one isomer), 127.67 ($\underline{C}$H-Ar), 127.69 ($\underline{C}$H-Ar), 127.77 ($\underline{C}$H-Ar), 127.81 ($\underline{C}$H-Ar), 128.46 ($\underline{C}$H-Ar), 129.78 ($\underline{C}$H-Ar), 129.82 ($\underline{C}$H-Ar), 133.20 ($\underline{C}$-Ar), 133.36 ($\underline{C}$-Ar), 135.57 ($\underline{C}$H-Ar), 137.80 ($\underline{C}$-Ar), 137.85 ($\underline{C}$-Ar), 154.05 (C=O Troc), 154.20 (C=O Troc), 154.38 (C=O Troc), 154.58 (C=O Troc), 171.48 (C=O), 174.37 (C=O Troc); MALDI-MS (*m/z*) Calcd for $C_{67}H_{100}Cl_6N_2O_{13}Si$ $[M + Na]^+$: 1401.50, found: 1401.45.

2.3.16 *N*-{2-(*tert*-butyldiphenylsilyloxy)-ethyl}-*N*-{2-[6-*O*-benzyl-2-deoxy-4-*O*-(di-*O*-benzylphosphono)-3-*O*-((*R*)-3-tetradecanoyloxytetradecanoyl)-2-(2,2,2-trichloroethoxycarbonylamino)-β-D-glucopyranosyloxy]-ethyl}-2,2,2-trichloroethoxymethanamide (25):

To a solution of **24** (1.25 g, 0.90 mmol) in dry CH_2Cl_2 (8 mL), 5-phenyltetrazole (265 mg, 1.80 mmol) and N,N-diisopropylphosphoramidite (0.62 mL, 1.80 mmol) were added. The mixture was stirred at room temperature for 1 h and then cooled to 0 °C before the addition of m-chloroperbenzoic acid (505 mg, 77 %, 2.25 mmol). The mixture was stirred at the reduced temperature for 1 h and then poured into a saturated sodium bicarbonate solution (50 mL) and extracted with CH_2Cl_2 (3 x 50 mL). The combined organic phase was dried over Na_2SO_4, concentrated, and purified by flash column chromatography (hexane/acetone, 4 : 1) to give **25** (1.26 g, 85 %) as a colorless syrup. Rf 0.40 (hexane/EtOAc, 5:2); $[\alpha]_D^{22}$ -2.9 (*c* 1.0, $CHCl_3$); ^{1}H NMR (500 MHz, $CDCl_3$): δ 0.88 (t, 6H, J 6.5 Hz, CH_3 x 2), 1.04 (s, 9H, C(C<u>H</u>$_3$)$_3$), 1.17-1.32 (br m, 38H, CH_2 x 19), 1.43-1.56 (br m, 4H, H-4$_L$, H-3$_{L'}$), 2.18-2.25 (t, 2H, J 7.5 Hz, H-2$_{L'}$), 2.38-2.47 (m, 2H, H-2$_L$), 3.39-3.63 (m, 7H, H-2, H-5, H-6b, NCH_2 x 2), 3.68-3.82 (m, 4H, H-6a, C<u>H</u>$_2$OTBDPS, ROCH*<u>H</u>*), 3.94-4.02 (m, 1H, ROC*<u>H</u>*H), 4.40-4.54 (m, 4H, H-4, Ph-C<u>H</u>$_2$, Troc), 4.57 (d, 0.4H, J 12.0 Hz, Troc), 4.59 (d, 0.6H, J 12.0 Hz, Troc), 4.64 (d, 0.6H, J 12.0 Hz, Troc), 4.68 (d, 0.4H, J 12.0 Hz, Troc), 4.71 (d, 0.4H, J 8.0 Hz, H-1 from one isomer), 4.73 (d, 0.4H, J 12.0 Hz, Troc) 4.75 (d, 0.6H, J 8.0 Hz, H-1 from one isomer), 4.80 (d, 0.6H, J 12.0 Hz, Troc), 4.86-4.93 (m, 4H, (PhC<u>H</u>$_2$O)$_2$P), 5.14-5.23 (m, 1H, H-3$_L$), 5.34-5.40 (m, 1H, H-3), 5.43 (d, 0.4H, J 8.0 Hz, NH from one isomer), 5.55 (d, 0.6H, J 8.0 Hz, NH

from one isomer), 7.22-7.32 (m, 13H, Ar-H), 7.35-7.44 (m, 8H, Ar-H), 7.60-7.66 (m, 4H, Ar-H); ^{13}C NMR (125 MHz, $CDCl_3$): δ 14.20 (CH_3), 19.13 ($\underline{C}(CH_3)_3$ from one isomer), 19.16 ($\underline{C}(CH_3)_3$ from one isomer), 22.75 (CH_2), 25.05 (CH_2), 25.16 (CH_2), 26.88 ($C(\underline{C}H_3)_3$ from one isomer), 26.90 ($C(\underline{C}H_3)_3$ from one isomer), 29.21 (CH_2), 29.37 (CH_2), 29.41 (CH_2), 29.58 (CH_2), 29.59 (CH_2), 29.62 (CH_2), 29.68 (CH_2), 29.70 (CH_2), 29.72 (CH_2), 29.74 (CH_2), 31.97 (CH_2), 34.34 (CH_2), 34.49 (CH_2), 39.37 (C-2_L from one isomer), 39.61 (C-2_L from one isomer), 48.27 (N$\underline{C}H_2$), 48.62 (N$\underline{C}H_2$), 50.30 (N$\underline{C}H_2$), 51.17 (N$\underline{C}H_2$), 56.51 (C-2 from one isomer), 56.54 (C-2 from one isomer), 61.92 (O$\underline{C}H_2$ROCH$_2$CH$_2$NCH$_2\underline{C}$H$_2$OTBDPS from one isomer), 62.49 (O$\underline{C}H_2$), 67.44 (O$\underline{C}H_2$), 68.46 (C-6), 68.58 (O$\underline{C}H_2$), 69.61-69.73 (m, (Ph$\underline{C}H_2O)_2$P), 69.99 (C-3_L from one isomer), 70.12 (C-3_L from one isomer), 72.27 (C-3 from one isomer), 72.62 (C-3 from one isomer), 73.46 (Ph-$\underline{C}H_2$), 74.00 (d, *J* 5.5 Hz, C-4 from one isomer), 74.05 (d, *J* 5.5 Hz, C-4 from one isomer), 74.14 (C-5 from one isomer), 74.19 (C-5 from one isomer), 74.44 (Troc-CH_2), 75.01 (Troc-CH_2), 75.06 (Troc-CH_2), 95.46 (Troc-CCl_3), 95.48 (Troc-CCl_3), 95.50 (Troc-CCl_3), 95.69 (Troc-CCl_3), 99.77 (C-1 from one isomer), 100.58 (C-1 from one isomer), 127.65 ($\underline{C}$H-Ar), 127.80 ($\underline{C}$H-Ar), 127.84 ($\underline{C}$H-Ar), 128.04 ($\underline{C}$H-Ar), 128.11 ($\underline{C}$H-Ar), 128.14 ($\underline{C}$H-Ar), 128.38 ($\underline{C}$H-Ar), 128.63 ($\underline{C}$H-Ar), 128.67 ($\underline{C}$H-Ar), 129.81 ($\underline{C}$H-Ar), 129.84 ($\underline{C}$H-Ar), 133.19 ($\underline{C}$-Ar), 133.21 ($\underline{C}$-Ar), 133.34 ($\underline{C}$-Ar), 133.37 ($\underline{C}$-Ar), 135.59 ($\underline{C}$H-Ar), 138.00 ($\underline{C}$-Ar), 138.02 ($\underline{C}$-Ar), 154.02 (C=O Troc), 154.22 (C=O Troc), 154.49 (C=O Troc), 170.28 (C=O), 170.32 (C=O), 173.61 (C=O), 173.75 (C=O); MALDI-MS (*m*/*z*) Calcd for $C_{81}H_{113}Cl_6N_2O_{16}PSi$ $[M + Na]^+$: 1661.56, found: 1661.48.

2.3.17 *N*-{2-(*tert*-butyldiphenylsilyloxy)-ethyl}-*N*-{2-[6-*O*-benzyl-2-deoxy-4-*O*-(di-*O*-benzylphosphono)-3-*O*-((*R*)-3-tetradecanoyloxytetradecanoyl)-2-((*R*)-3-tetradecanoyloxytetradecanamido)-β-D-glucopyranosyloxy]-ethyl}-(*R*)-3-tetradecanoyloxytetradecanamide (26):

To a solution of **25** (440 mg, 0.27 mmol) in glacial acetic acid (5 mL), zinc powder (750 mg) was added and the mixture was stirred at room temperature for 45 min. The mixture was then filtered, and the solids were washed with acetic acid (10 mL). The filtrate was slowly poured into a saturated sodium bicarbonate solution (300 mL) and then extracted with CH_2Cl_2 (3 x 150 mL). The combined organic phase was washed with further saturated sodium bicarbonate solution (100 mL), dried over Na_2SO_4, and concentrated to give the crude di-amine (338 mg, 98 %)as a colorless syrup.

A solution of the crude di-amine (337 mg) in DMF (2 mL) was added to a mixture of dilipid acid **3** (283 mg, 0.62 mmol), HBTU (352 mg, 0.94 mmol) and DIPEA (0.16 mL, 0.94 mmol) in DMF (5 mL). The resulting mixture was stirred at room temperature for 18 h before being poured into a separatory funnel with water (50 mL), and then extracted with Et_2O (3 x 75 mL). The combined organic phase was washed with a cold saturated sodium chloride solution (3 x 8 mL), dried over Na_2SO_4, and concentrated. Flash column chromatography of the residue (hexane/EtOAc, 2.5 : 1) afforded **26** (381 mg, 67 %) as a colorless syrup. Rf 0.35 (hexane/acetone, 4:1); $[\alpha]_D^{22}$ -1.5 (*c* 1.0, $CHCl_3$); ^{1}H NMR (500 MHz, $CDCl_3$): δ 0.88 (t, 18H, J 6.5 Hz, CH_3 x 6), 1.03 (s, 9H, $C(C\underline{H}_3)_3$), 1.16-1.38 (br m, 114H, CH_2 x 57), 1.52-1.68 (br m, 12H, H-4_L x 6, H-$3_{L'}$ x 6), 2.17-2.51 (m, 11H, H-2_L x

5, H-$2_{L'}$ x 6), 2.75 (dd, 0.4H, J 15.5, 6.5 Hz, H-2_{LB} from one isomer), 2.87 (dd, 0.6 H, J 15.5, 5.0 Hz, H-2_{LA} from one isomer), 3.07-3.18 (m, 0.4H, H-2 from one isomer), 3.41-3.79 (m, 10.6H, H-2 from one isomer, H-5, H-6b, H-6a, NCH_2 x 2, $C\underline{H_2}OTBDPS$, ROCH*H*), 3.82-3.91 (m, 1H, ROC*H*H), 4.36-4.51 (m, 3H, H-4, Ph-$C\underline{H_2}$), 4.66 (d, 0.4H, J 8.0 Hz, H-1 from one isomer), 4.84-4.92 (m, 4H, $(PhC\underline{H_2}O)_2P$), 5.04-5.22 (m, 3.6H, H-1 from one isomer, H-3_L x 3), 5.29 (dd, 0.6H, J 10.0, 10.0 Hz, H-3 from one isomer), 5.73 (dd, 0.4H, J 10.0, 10.0 Hz, H-3 from one isomer), 6.15 (d, 0.4H, J 8.0 Hz, NH from one isomer), 6.73 (d, 0.6H, J 8.0 Hz, NH from one isomer), 7.22-7.32 (m, 13H, Ar-H), 7.34-7.44 (m, 8H, Ar-H), 7.58-7.64 (m, 4H, Ar-H); ^{13}C NMR (125 MHz, $CDCl_3$): δ 14.15 (CH_3), 19.08 ($\underline{C}(CH_3)_3$ from one isomer), 19.15 ($\underline{C}(CH_3)_3$ from one isomer), 22.73 (CH_2), 25.06 (CH_2), 25.09 (CH_2), 25.15 (CH_2), 25.18 (CH_2), 25.25 (CH_2), 25.33 (CH_2), 25.42 (CH_2), 25.83 (CH_2), 26.85 ($C(\underline{C}H_3)_3$ from one isomer), 26.90 ($C(\underline{C}H_3)_3$ from one isomer), 29.17 (CH_2), 29.23 (CH_2), 29.27 (CH_2), 29.31 (CH_2), 29.35 (CH_2), 29.41 (CH_2), 29.43 (CH_2), 29.49 (CH_2), 29.54 (CH_2), 29.56 (CH_2), 29.61 (CH_2), 29.64 (CH_2), 29.68 (CH_2), 29.73 (CH_2), 29.76 (CH_2), 31.97 (CH_2), 34.04 (CH_2), 34.12 (CH_2), 34.33 (CH_2), 34.43 (CH_2), 34.49 (CH_2), 34.60 (CH_2), 34.700(CH_2), 38.04 (C-2_L), 38.13 (C-2_L), 39.11 (C-2_L), 39.26 (C-2_L), 40.74 (C-2_L), 41.25 (C-2_L), 45.65 ($N\underline{C}H_2$), 47.09 ($N\underline{C}H_2$), 48.29 ($N\underline{C}H_2$), 50.45 ($N\underline{C}H_2$), 54.92 (C-2 from one isomer), 56.65 (C-2 from one isomer), 61.61 ($O\underline{C}H_2$), 62.64 ($O\underline{C}H_2$), 63.42 (C-6 from one isomer), 67.22 (C-6 from one isomer), 68.21 ($O\underline{C}H_2$), 68.43 ($O\underline{C}H_2$), 69.46-69.67 (m, $(Ph\underline{C}H_2O)_2P$), 69.99 (C-3_L), 70.07 (C-3_L), 70.15 (C-3_L), 70.68 (C-3_L), 71.22 (C-3_L), 71.70 (C-3 from one isomer), 72.35 (C-3_L), 72.87 (C-3 from one isomer), 73.30 (Ph-$\underline{C}H_2$ from one isomer), 73.32 (Ph-$\underline{C}H_2$ from one isomer), 73.73 (C-5 from one isomer), 73.98 (C-5 from one isomer), 74.09 (d, J 5.5 Hz,

C-4 from one isomer), 74.49 (d, J 5.5 Hz, C-4 from one isomer), 99.43 (C-1 from one isomer), 100.77 (C-1 from one isomer), 127.56 (CH-Ar), 127.60 (CH-Ar), 127.74 (CH-Ar), 127.77 (CH-Ar), 127.87 (CH-Ar), 127.90 (CH-Ar), 127.99 (CH-Ar), 128.10 (CH-Ar), 128.12 (CH-Ar), 128.31 (CH-Ar), 128.53 (CH-Ar), 128.56 (CH-Ar), 129.74 (CH-Ar), 129.77 (CH-Ar), 129.88 (CH-Ar), 129.90 (CH-Ar), 132.94 (C-Ar), 133.36 (C-Ar), 133.45 (C-Ar), 135.51 (CH-Ar), 135.54 (CH-Ar), 138.08 (C-Ar), 169.70 (C=O), 170.03 (C=O), 170.24 (C=O), 170.41 (C=O), 170.50 (C=O), 170.74 (C=O), 173.14 (C=O), 173.29 (C=O), 173.40 (C=O), 173.45 (C=O), 173.52 (C=O), 174.18 (C=O); MALDI-MS (*m/z*) Calcd for $C_{131}H_{215}N_2O_{18}PSi$ $[M + Na]^+$: 2186.54, found: 2186.48.

2.3.18 *N*-{2-(di-*O*-benzylphosphono)-ethyl}-*N*-{2-[6-*O*-benzyl-2-deoxy-4-*O*-(di-*O*-benzylphosphono)-3-*O*-((*R*)-3-tetradecanoyloxytetradecanoyl)-2-((*R*)-3-tetradecanoyloxytetradecanamido)-β-D-glucopyranosyloxy]-ethyl}-(*R*)-3-tetradecanoyloxytetradecanamide (27):

To a solution of **10** (85 mg, 0.044 mmol) in dry CH_2Cl_2 (1.5 mL), 5-phenyltetrazole (13 mg, 0.088 mmol) and N,N-diisopropylphosphoramidite (30 µL, 0.088 mmol) were added. The mixture was stirred at room temperature for 30 min and then cooled to 0 °C before the addition of m-chloroperbenzoic acid (22 mg, 77 %, 0.099 mmol). The mixture was stirred at the reduced temperature for 30 min before being poured into a 10% sodium thiosulphate solution (10 mL) and then extracted with CH_2Cl_2 (3 x 20 mL). The combined organic phase was washed with a saturated sodium bicarbonate solution (15 mL), dried over Na_2SO_4, concentrated, and purified by repeated flash chromatography

(hexane/EtOAc, 3 : 2 → 1 : 1) to give **27** (69 mg, 71%) as a colorless syrup. Rf 0.28 (hexane/EtOAc, 3:1; ^{1}H NMR (500 MHz, $CDCl_3$): δ 0.86 (t, 18H, J 6.5 Hz, CH_3 x 6), 1.14-1.39 (br m, 114H, CH_2 x 57), 1.50-1.69 (br m, 12H, H-4_L x 6, H-$3_{L'}$ x 6), 2.18-2.57 (m, 11H, H-2_L x 5, H-$2_{L'}$ x 6), 2.68 (dd, 0.4H, J 15.5, 6.5 Hz, H-2_{LB} from one isomer), 2.78 (dd, 0.6 H, J 15.5, 5.0 Hz, H-2_{LA} from one isomer), 3.20-3.37 (m, 2.6H, H-2 from one isomer, NCH_2), 3.43-3.48 (m, 1H, H-6b), 3.51-3.70 (m, 4.4H, H-2 from one isomer, H-5, NCH_2, ROCH*H*), 3.75-3.87 (m, 2H, H-6a, ROC*H*H), 4.06-4.16 (m, 2H, $CH_2OP(O)(OBn)_2$), 4.40-4.52 (m, 3H, H-4, Ph-CH_2), 4.72 (d, 0.4H, J 8.0 Hz, H-1 from one isomer), 4.89-4.94 (m, 4H, $(PhCH_2O)_2P$), 4.97-5.04 (m, 4H, $CH_2OP(O)(OCH_2Ph)_2$), 5.07 (d, 0.6H, J 8.0 Hz, H-1 from one isomer), 5.09-5.23 (m, 3H, H-3_L x 3), 5.39 (dd, 0.4H, J 10.0, 10.0 Hz, H-3 from one isomer), 5.67 (dd, 0.6H, J 10.0, 10.0 Hz, H-3 from one isomer), 6.59 (d, 0.4H. J 8.0 Hz, NH from one isomer), 6.88 (d, 0.6H, J 8.0 Hz, NH from one isomer), 7.18-7.42 (m, 25H, Ar-H); ^{13}C NMR (125 MHz, $CDCl_3$): δ 14.15 (CH_3), 22.71 (CH_2), 25.05 (CH_2), 25.08 (CH_2), 25.15 (CH_2), 25.17 (CH_2), 25.24 (CH_2), 25.35 (CH_2), 25.43 (CH_2), 25.81 (CH_2), 24.84 (CH_2), 25.88 (CH_2), 29.15 (CH_2), 29.21 (CH_2), 29.25 (CH_2), 29.301 (CH_2), 29.33 (CH_2), 29.40 (CH_2), 29.43 (CH_2), 29.47 (CH_2), 29.52 (CH_2), 29.56 (CH_2), 29.62 (CH_2), 29.64 (CH_2), 29.68 (CH_2), 29.73 (CH_2), 29.77 (CH_2), 31.96 (CH_2), 34.02 (CH_2), 34.12 (CH_2), 34.35 (CH_2), 34.43 (CH_2), 34.49 (CH_2), 34.61 (CH_2), 34.70 (CH_2), 37.89 (C-2_L), 38.15 (C-2_L), 39.04 (C-2_L), 39.16 (C-2_L), 40.80 (C-2_L), 41.20 (C-2_L), 46.15 (NCH_2), 46.22 (NCH_2) 46.52 (NCH_2), 48.63 (NCH_2), 55.12 (C-2 from one isomer), 56.16 (C-2 from one isomer), 64.59 (d, J 5.5 Hz, $CH_2OP(O)(OBn)_2$ from one isomer), 65.87 (d, J 5.5 Hz, $CH_2OP(O)(OBn)_2$ from one isomer), 67.34 (C-6), 68.48 ($ROCH_2$), 68.52 ($ROCH_2$), 69.41-69.66 (m, $PhCH_2O)_2P$,

$CH_2OP(O)(O\underline{C}H_2Ph)_2$), 69.96 (C-$3_L$), 70.04 (C-$3_L$), 70.16 (C-$3_L$), 70.68 (C-$3_L$), 71.26 (C-$3_L$), 71.83 (C-$3_L$), 71.93 (C-3 from one isomer), 72.71 (C-3 from one isomer), 73.32 (Ph-$\underline{C}H_2$), 73.81 (C-5 from one isomer), 73.83 (C-5 from one isomer), 74.19 (d, *J* 5.5 Hz, C-4 from one isomer), 74.37 (d, *J* 5.5 Hz, C-4 from one isomer), 99.58 (C-1 from one isomer), 100.07 (C-1 from one isomer), 127.55 (CH-Ar), 127.58 (CH-Ar), 127.72 (CH-Ar), 127.75 (CH-Ar), 127.85 (CH-Ar), 127.90 (CH-Ar), 127.97 (CH-Ar), 128.11 (CH-Ar), 128.12 (CH-Ar), 128.31 (CH-Ar), 128.52 (CH-Ar), 128.54 (CH-Ar), 129.75 (CH-Ar), 129.78 (CH-Ar), 129.87 (CH-Ar), 129.90 (CH-Ar), 132.94 (C-Ar), 133.36 (C-Ar), 133.47 (C-Ar), 135.52 (CH-Ar), 135.54 (CH-Ar), 138.08 (C-Ar), 169.72 (C=O), 170.05 (C=O), 170.27 (C=O), 170.44 (C=O), 170.51 (C=O), 170.79 (C=O), 173.18 (C=O), 173.35 (C=O), 173.45 (C=O), 173.48 (C=O), 173.59 (C=O), 174.18 (C=O). Decomposition issues prevented the acquiring of optical rotation and mass spectral data.

2.3.19 *N*-{2-phosphonoethyl}-*N*-{2-[2-deoxy-4-*O*-phosphono-3-*O*-((*R*)-3-tetradecanoyloxytetradecanoyl)-2-((*R*)-3-tetradecanoyloxytetradecanamido)- β-D-glucopyranosyloxy]-ethyl}-(*R*)-3-tetradecanoyloxytetradecanamide (3):

To a solution of **27** (53 mg, 0.027 mmol) in freshly distilled THF (45 mL), palladium on charcoal (5%, 26 mg) was added and the mixture was stirred at room temperature under a hydrogen atmosphere for 24 h. The mixture was filtered, and the filtrate concentrated. The residue was purified by flash column chromatography ($CHCl_3$/MeOH, 9 : 1 and then $CHCl_3$/MeOH/H_2O, 3 : 1 : 0.2) to afford **13** (28 mg, 70%) as white fluffy solid after being freeze dried from a dioxane-$CHCl_3$ mixture (95:5). Rf 0.37

($CHCl_3$/MeOH/H_2O/NH_4OH, 3 : 2 : 0.2 : 0.2); $[\alpha]_D^{22}$ -0.1 (*c* 1.0, $CHCl_3$); ^{1}H NMR (500 MHz, $CDCl_3$): δ 0.89 (t, 18H, J 6.5 Hz, CH_3 x 6), 1.22-1.43 (br m, 114H, CH_2 x 57), 1.54-1.68 (br m, 12H, H-4_L x 6, H-$3_{L'}$ x 6), 2.20-2.82 (br m, 12 H, H-2_L x 6, H-$2_{L'}$ x 6), 3.68-4.16 (br m, 12H, H-2, H-5, H-6b, H-6a, NCH_2 x 2, OCH_2 x 2), 4.48-4.70 (br m, 2H, H-1, H-4), 5.06-5.38 (br m, 4H, H-3, H-3_L x 3); MALDI-MS (*m*/*z*) Calcd for $C_{94}H_{180}N_2O_{21}P_2$ $[M + Na]^+$: 1758.24, found: 1758.20.

2.3.20 *N*-{carboxymethyl}-*N*-{2-[6-*O*-benzyl-2-deoxy-4-*O*-(di-*O*-benzylphosphono)-3-*O*-((*R*)-3-tetradecanoyloxytetradecanoyl)-2-((*R*)-3-tetradecanoyloxytetradecanamido)- β-D-glucopyranosyloxy]-ethyl}-(*R*)-3-tetradecanoyloxytetradecanamide (20):

To a solution of **10** (80 mg, 0.042 mmol) in CH_2Cl_2 (3 mL) and water (0.5 mL), (2, 2, 6, 6-tetramethylpiperidin-1-yl)oxyl (TEMPO, 3 mg, 0.017 mmol) and bis(acetoxy)iodobenzene (54 mg, 0.168 mmol) were added. The mixture was stirred at room temperature for 2 h before being poured into a 10% sodium thiosulphate solution (10 mL), and extracted with CH_2Cl_2 (3 x 15 mL). The combined organic phases were dried over Na_2SO_4, concentrated, and purified by repeated flash chromatography (hexane/EtOAc/MeOH, 3 : 1 : 0.2) to afford **28** (67 mg, 83%) as a colorless syrup. Rf 0.35 (hexane/EtOAc, 3:1); $[\alpha]_D^{22}$ -0.9 (*c* 1.0, $CHCl_3$); ^{1}H NMR (500 MHz, $CDCl_3$): δ 0.88 (t, 18H, J 6.5 Hz, CH_3 x 6), 1.16-1.39 (br m, 114H, CH_2 x 57), 1.48-1.64 (br m, 12H, H-4_L x 6, H-$3_{L'}$ x 6), 2.19-2.52 (m, 11H, H-2_L x 5, H-$2_{L'}$ x 6), 2.63 (dd, 0.4H, J 15.5, 6.5 Hz,

H-2_{LB} from one isomer), 2.86 (dd, 0.6 H, J 15.5, 5.0 Hz, H-2_{LA} from one isomer), 3.27-3.34 (m, 0.6H, H-2 from one isomer), 3.44-3.68 (m, 5H, H-5, H-6b, $ROCH_2C\underline{H_2}N$, ROCH*H*), 3.70-3.78 (m, 1.4H, H-2 from one isomer, H-6a), 3.87-3.98 (m, 1H, ROC*H*H), 4.00-4.21 (m, 2H, $NC\underline{H_2}COOH$), 4.40-4.53 (m, 3H, H-4, Ph-$C\underline{H_2}$), 4.59 (d, 0.4H, J 8.0 Hz, H-1 from one isomer), 4.83-4.92 (m, 4H, $(PhC\underline{H_2}O)_2P$), 4.98 (d, 0.6H, J 8.0 Hz, H-1 from one isomer), 5.09-5.24 (m, 3H, H-3_L x 3), 5.28 (dd, 0.4H, J 10.0, 10.0 Hz, H-3 from one isomer), 5.61 (dd, 0.6H, J 10.0, 10.0 Hz, H-3 from one isomer), 6.32 (d, 0.4H, J 8.0 Hz, NH from one isomer), 6.67 (d, 0.6H, J 8.0 Hz, NH from one isomer), 7.21-7.34 (m, 15H, Ar-H); ^{13}C NMR (125 MHz, $CDCl_3$): δ 14.12 (CH_3), 22.71 (CH_2), 25.05 (CH_2), 25.14 (CH_2), 25.22 (CH_2), 25.32 (CH_2), 25.38 (CH_2), 25.58 (CH_2), 29.21 (CH_2), 29.24 (CH_2), 29.28 (CH_2), 29.32 (CH_2), 29.39 (CH_2), 29.40 (CH_2), 29.42 (CH_2), 29.45 (CH_2), 29.47 (CH_2), 29.49 (CH_2), 29.52 (CH_2), 29.57 (CH_2), 29.60 (CH_2), 29.62 (CH_2), 29.66 (CH_2), 29.68 (CH_2), 29.71 (CH_2), 29.73 (CH_2), 29.75 (CH_2), 31.95 (CH_2), 31.97 (CH_2), 34.27 (CH_2), 34.31 (CH_2), 34.44 (CH_2), 34.50 (CH_2), 34.54 (CH_2), 34.62 (CH_2), 37.86 (C-2_L), 37.94 (C-2_L), 39.19 (C-2_L), 39.40 (C-2_L), 40.87 (C-2_L), 41.45 (C-2_L), 47.59 ($N\underline{C}H_2$), 48.94 ($N\underline{C}H_2$), 49.20 ($N\underline{C}H_2$), 51.54 ($N\underline{C}H_2$), 55.05 (C-2 from one isomer), 55.97 (C-2 from one isomer), 67.63 ($O\underline{C}H_2$), 68.40 (C-6), 69.25 ($O\underline{C}H_2$), 69.52-69.63 (m, $Ph\underline{C}H_2O)_2P$), 70.15 (C-3_L), 70.18 (C-3_L), 70.44 (C-3_L), 70.87 (C-3_L), 71.16 (C-3_L), 71.80 (C-3_L), 72.09 (C-3 from one isomer), 72.62 (C-3_L), 73.35 (Ph-$\underline{C}H_2$ from one isomer), 73.44 (Ph-$\underline{C}H_2$ from one isomer), 73.70 (C-5 from one isomer), 73.74 (C-5 from one isomer), 74.22 (d, J 5.5 Hz, C-4 from one isomer), 74.30 (d, J 5.5 Hz, C-4 from one isomer), 99.76 (C-1 from one isomer), 100.50 (C-1 from one isomer), 127.59 ($\underline{C}$H-Ar), 127.64 ($\underline{C}$H-Ar), 127.72 ($\underline{C}$H-Ar), 127.80 ($\underline{C}$H-Ar), 127.99 ($\underline{C}$H-Ar), 128.04 ($\underline{C}$H-Ar),

128.10 (CH-Ar), 128.13 (CH-Ar), 128.33 (CH-Ar), 128.38 (CH-Ar), 128.54 (CH-Ar), 128.56 (CH-Ar), 128.59 (CH-Ar), 128.60 (CH-Ar), 128.64 (CH-Ar), 128.66 (CH-Ar), 135.55 (C-Ar), 135.61 (C-Ar), 137.67 (C-Ar), 137.98 (C-Ar), 169.90 (C=O), 170.35 (C=O), 170.79 (C=O), 170.93 (C=O), 171.00 (C=O), 171.25 (C=O), 173.23 (C=O), 173.39 (C=O), 173.75 (C=O), 173.78 (C=O), 173.91 (C=O); MALDI-MS (*m*/*z*) Calcd for $C_{115}H_{195}N_2O_{19}P$ $[M + Na]^+$: 1962.39, found: 1962.30.

2.3.21 *N*-{carboxymethyl}-*N*-{2-[2-deoxy-4-*O*-phosphono-3-*O*-((*R*)-3-tetradecanoyloxytetradecanoyl)-2-((*R*)-3-tetradecanoyloxytetradecanamido)- β-D-glucopyranosyloxy]-ethyl}-(*R*)-3-tetradecanoyloxytetradecanamide (14):

In a similar manner as described for preparation of **13**, a solution of **28** (35 mg, 0.018 mmol) and palladium on charcoal (5%, 20 mg) in freshly distilled THF (40 mL) was stirred under a hydrogen atmosphere at room temperature for 24 h. The mixture was filtered, the filtrate concentrated, and the resulting residue was purified by flash column chromatography ($CHCl_3$/MeOH, 9 : 1 and then $CHCl_3$/MeOH/H_2O, 3 : 1 : 0.1) to yield **14** (23 mg, 77%) as a white fluffy solid after being freeze-dried from a dioxane-$CHCl_3$ mixture (95:5). Rf 0.41 ($CHCl_3$/MeOH/H_2O, 3 : 1 : 0.1,); $[\alpha]_D^{22}$ -0.1 (*c* 1.0, $CHCl_3$); ^{1}H NMR (500 MHz, $CDCl_3$): δ 0.80 (t, 18H, J 6.5 Hz, CH_3 x 6), 1.12-1.33 (br m, 114H, CH_2 x 57), 1.46-1.62 (br m, 12H, H-4_L x 6, H-$3_{L'}$ x 6), 2.16-2.31 (m, 9 H, H-2_L x 3, H-$2_{L'}$ x 6), 2.33-2.65 (m, 3H, H-2_L x 3), 3.45-3.72 (br m, 7 H, H-2, H-5, H-6b, H-6a, $ROCH_2CH_2N$, ROCH*H*), 3.75-3.98 (br m, 3 H, NCH_2COOH, ROC*H*H), 4.41-4.55 (br m, 2 H, H-1, H-

4), 5.04-5.20 (br m, 4 H, H-3, H-3_L x 3); MALDI-MS (*m/z*) Calcd for $C_{94}H_{177}N_2O_{19}P$ [M + Na]$^+$: 1692.25, found: 1692.17.

2.3.22 Reagents for biological experiments

E. coli LPS 011:B4 was obtained from Sigma. Each of synthetic lipid A mimics **2**-**4** were reconstituted in 20% DMSO in phosphate buffered saline (PBS) with brief sonication, aliquoted and stored at -80 °C. A fresh aliquot was used for each individual experiment. Solution concentrations were set such that the total addition of DMSO never exceeded 0.5% to avoid toxic effects. THP-1 cells were obtained from American Type Culture Collection (ATCC). RPMI-1640 media, fetal bovine serum, and antibiotic-antimycotic 100X were obtained from Gibco BRL. Phorbol 12-myristate 13 acetate (PMA) was purchased from Sigma, dissolved in DMSO, aliquoted and stored at -80 °C. Lipid IVa was purchased from Peptide Institute, Inc., and was dissolved in DMSO.

2.3.23 Cell maintenance

THP-1 cells were maintained at 37 °C and 5% CO_2 atmosphere in RPMI-1640 media supplemented with 10% heat-inactivated fetal bovine serum and 1% antibiotic-antimycotic 100X. Cell counting was performed using a Beckman Coulter ViCell X-R instrument, with viability being determined through the trypan blue cellular exclusion method.

2.3.24 ICAM-1 induction and measurement

THP-1 cells were plated at 0.5 x 10^6 cells/well in 6-well tissue culture plates and incubated for 18 h. Cells were then incubated with different stimuli for a further 18h. Cells were centrifuged at 1000 g for 5 min, washed with phosphate buffered saline (PBS), and then resuspended in 100 μL 0.1% Bovine Serum Albumin/PBS to proceed with staining and flow cytometry analysis. The expression of ICAM-1 was determined via immunostaining with phycoerythrin-conjugated mAb to ICAM-1 (CD54) from BD Biosciences, San Jose, CA. The antibody was added and the mixture incubated at 4 °C for 20 h in the dark. After incubation, cells were washed twice with PBS, resuspended in 500 μL PBS, and subjected to flow cytometry analysis on FACSCalibur with CELLQUEST PRO software (BD Biosciences), acquiring 15,000 events. The results were presented as the mean fluorescence intensity (MFI) on the FL2 channel.

2.3.25 Cytokine induction and measurement

THP-1 pre-monocytic cells were plated at 0.5 x 10^6 cells $well^{-1}$ in 6-well tissue culture plates containing the RPMI media further supplemented with either 5 ng ml^{-1} or 25 ng ml^{-1} of PMA. After 48 h, the media was removed and the now adhered monocytic THP-1 cells were washed with PBS. The well were then refilled with serum-free RPMI media, incubated for 3 h, and then exposed to stimuli. After 24 h stimulation, culture supernatants were collected and stored frozen (-80 °C) until assayed for cytokine production.

All cytokine ELISAs were performed in 96-well MaxiSorp plates. Ready-Set-Go! ELISA kits (eBioscience) were used for cytokine quantification of human TNF-α, IL-6, and IL-1β according to the manufacturer's instructions. The absorbance was measured at 450 nm with wavelength correction set to 540 nm using a microplate reader (BMG Labtech). All cytokine values were measured in duplicate, and are presented as the mean ± SD of two separate experiments.

3 AROMATIC-BASED LIPID A MIMICS

3.1 Design

As part of an industrial partnership with the company Immunovaccine aimed at synthesizing and evaluating novel lipid A mimics as potential vaccine adjuvants, a novel molecular framework to replace the reducing glucosamine residue was envisioned in which an aromatic ring has been incorporated. As such, two novel aromatic-based lipid A mimic structures were targeted (**29** & **30**, **Figure 31**). Mimic **29** is a hexa-acylated, mono-phosphorylated lipid A structure with a terminal phenolic residue, whereas mimic **30** is identical in acylation, but contains the additional phenolic-based phosphate moiety. Both mimics **29** & **30** are likely the first examples of a lipid A mimic in which an aromatic residue has been incorporated into the structural backbone.

The rationale employed in the design of lipid A mimics **29** & **30** is based on the observations that subtle molecular changes in the structure of a lipid A molecule can have a profound impact on the overall biological activity that the molecule displays. Perhaps the most significant example of this is seen in monophosphoryl lipid A, in which the simple elimination of the anomeric phosphate group abolishes all endotoxicity, yet the molecule remains a potent immunostimulatory vaccine adjuvant candidate.[69-71] The presence of the aromatic Π system in lipid A mimics **29** & **30** can lead to favourable non-covalent interactions within the binding pocket, the likes of which include Π-stacking, Π-anion/cation interactions, and even Π-CH interactions. These non-covalent interactions involving Π-systems are pivotal in many biological events, including protein-ligand recognition.[175] It is entirely possible that the non-covalent Π-type interactions offered via

the inclusion of an aromatic ring in the lipid A mimic backbone may not only result in a greater affinity of the ligand for the TLR4/MD-2 receptor complex, thus ultimately resulting in increased potency, but may also alter the binding and subsequent receptor activation, the likes of which it is hoped will favour immunostimulation over endotoxicity.

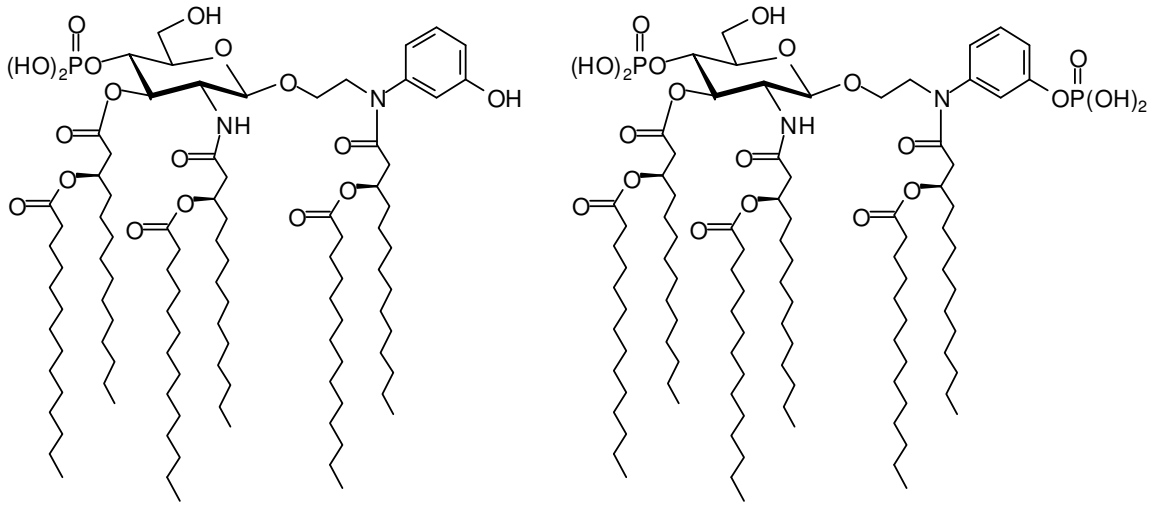

29 **30**

Figure 31. Aromatic-Based Lipid A Mimics Targeted

3.2 Retrosynthetic Analysis

Beginning with mimic **30**, elimination of the phenolic phosphate moiety yielded mimic **29**, from which the protection of the C-6 and phosphate hydroxyls as their benzyl ethers (Bn) yielded **36** (**Scheme 16**). Elimination of the primary amide bound acyl chain afforded the free amine, which was subsequently protected as the Troc-carbamate to yield **35**. Disconnection of the glycosyl bond yielded the known trichloroacetimidate glycosyl donor **4** [136], and the aromatic based glycoysl acceptor **34**. Further elimination of the

amide bound acyl chain in acceptor **34** afforded the aromatic-based framework **31**, which was further disconnected to afford commercially available 2-chloroethanol, and 3-aminophenol.

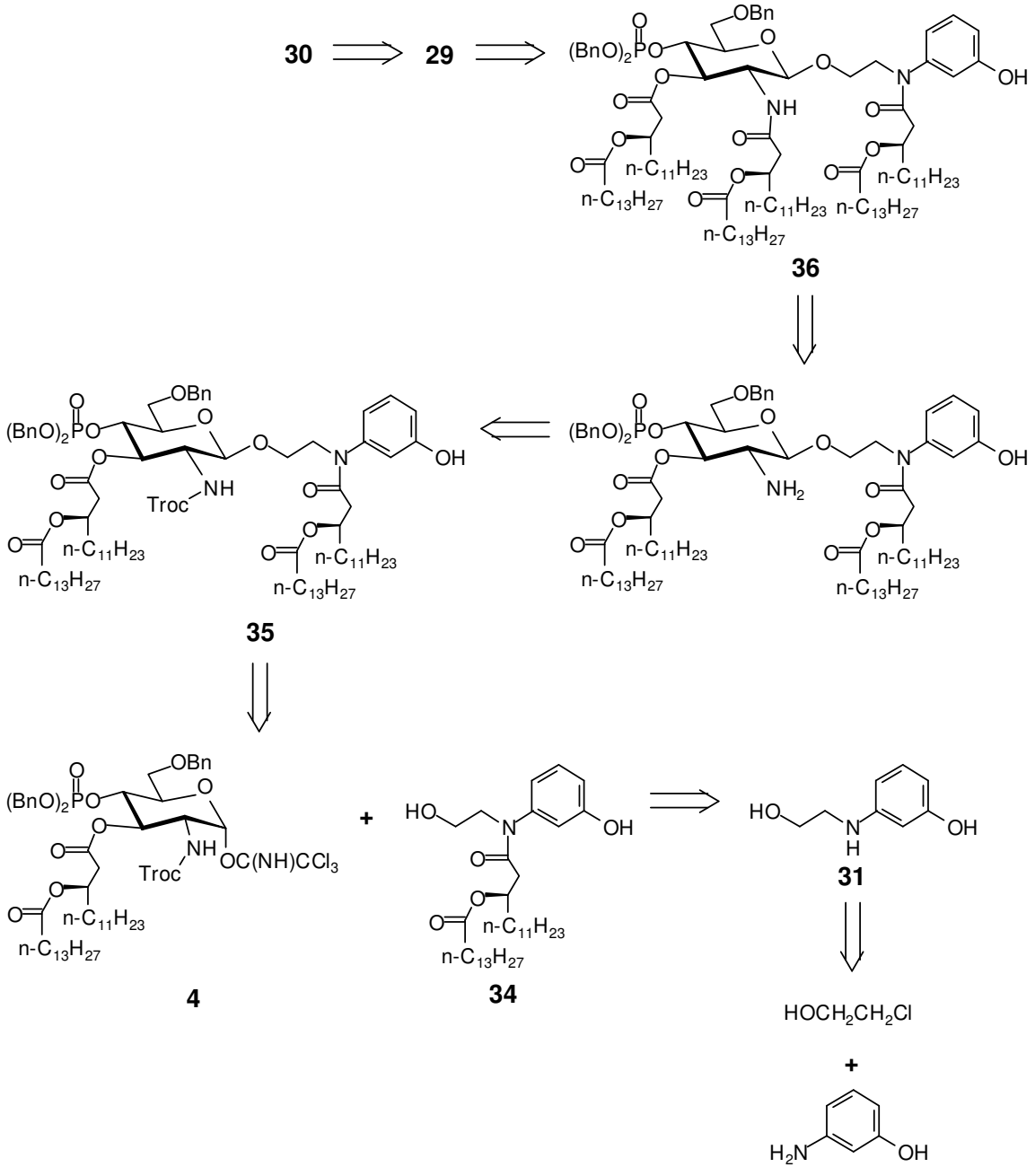

Scheme 16. Retrosynthetic Analysis of Aromatic-Based Lipid A Mimics

3.3 Synthesis

Synthesis began with formation of the aromatic-based backbone. As such, 2-chloroethanol and 3-aminophenol were reacted in water at 90 °C in the presence of sodium bicarbonate to afford **31** in a 58% yield (**Scheme 17**). The primary hydroxyl was next protected as the TBDPS ether via reaction with TBDPS-Cl and imidazole in DMF to yield **32** in 84% yield. The free amine was next acylated with dilipid acid **3** by first activating the acid as the mixed anhydride via reaction with *iso*-butyl chloroformate (IBCF) and *N*-methylmorpholine (NMM) at -20 °C, followed by the reaction with the free amine moiety in **32** to yield **33** in 80% yield. Interestingly, no rotational isomerism about the secondary amide bond was observed in **33**, as was observed with the DEA-based acylic framework. It is possible that that lone pair on the amide nitrogen is in conjugation with the aromatic ring system, thus effectively locking the framework into one conformation. However, this is only speculative. Finally, deprotection of the primary hydroxyl via treatment with tetrabutylammonium fluouride in DCM and acetic acid afforded glycosyl donor **34** in 81% yield.

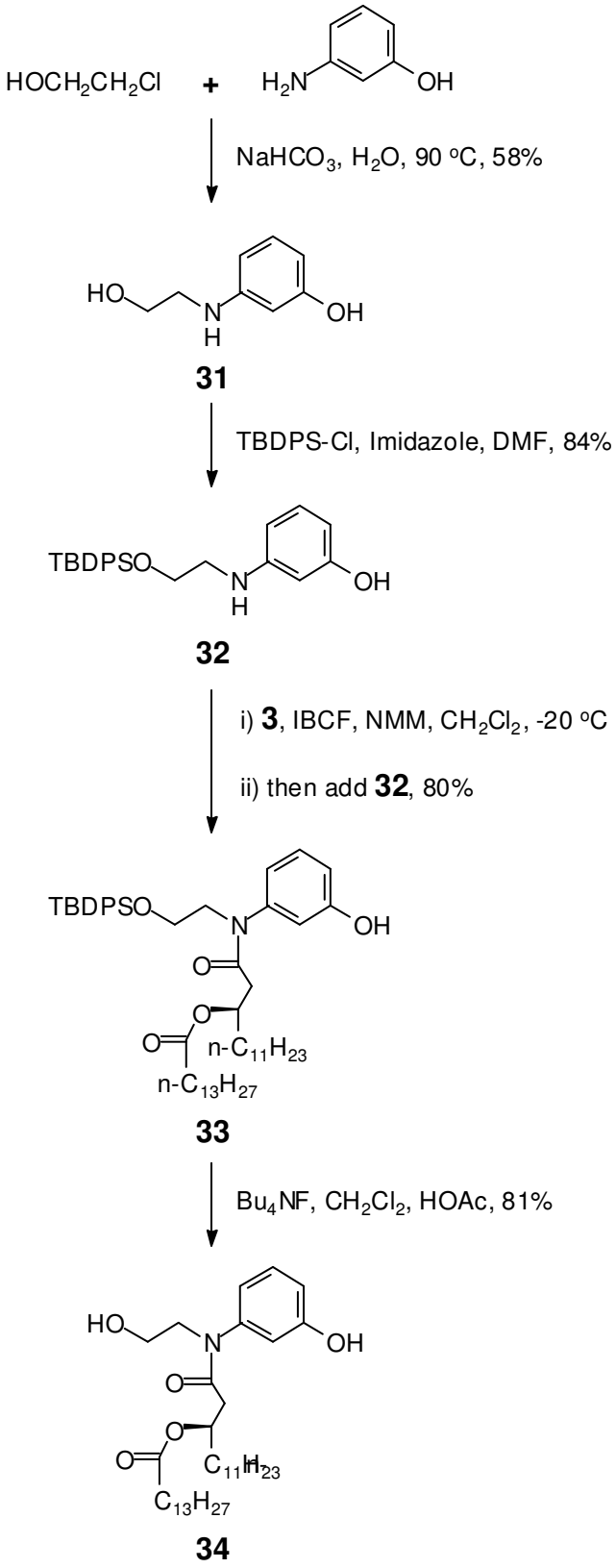

Scheme 17. Synthesis of Aromatic-Based Glycosylation Acceptor **34**

The TMSOTf promoted glycosylation between known glycosyl donor **4** [136] and aromatic-based acceptor **34** afforded glycoside **35** in 89% yield (**Scheme 18**). The desired β-glycosidic linkage in **35** was confirmed via ^{1}H NMR data δ 4.78 (d, *J* 8.5 Hz, H-1). Removal of the Troc-carbamate protecting group via treatment with zinc in acetic acid afforded the free amine, which was immediately coupled with dilipid acid **3** under diisopropylcarbodiimide (DIC) promotion to afford hexa-acylated intermediate **36**.

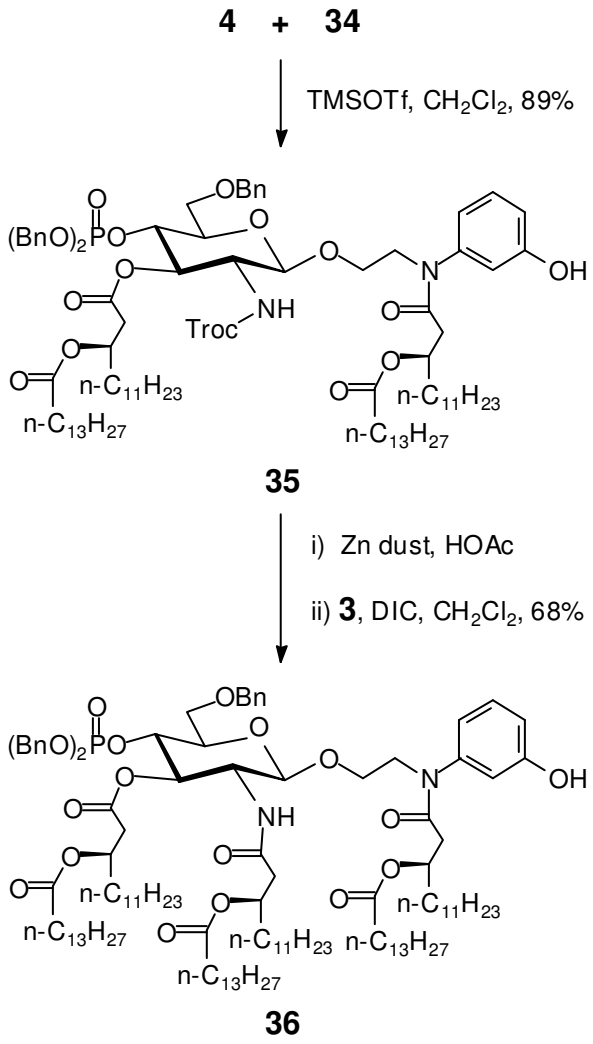

Scheme 18. Synthesis of Hexa-Acylated Intermediate **36**

To obtain targeted aromatic-based, mono-phopshorylated lipid A mimic **29**, hexa-acylated intermediate **36** was subjected to global deprotection via hydrogenolysis (**Scheme 19**) to afford **29** in 88% yield. The structure of **29** was confirmed by ^{1}H NMR and HR-MALDI MS data.

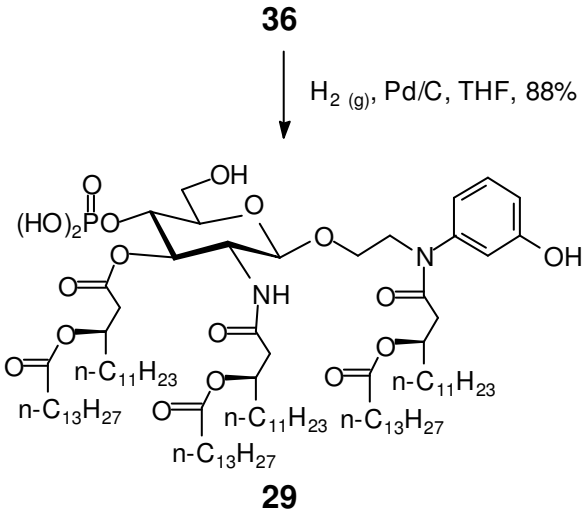

Scheme 19. Synthesis of Mono-Phosphorylated Aromatic-Based Lipid A Mimic **29**

To obtain targeted aromatic-based, di-phosphorylated lipid A mimic **30**, the phenol moiety in **36** was first converted to the corresponding phosphotriester via the typical reaction with 5-phenyl tetrazole (5-Ph-Tetrazole) and dibenzyl *N*,*N* diisopropylphosphoramidite [$(BnO)_2PN(iPr)_2$], followed by the subsequent *m*-chloroperbenzoic acid (*m*-CPBA) promoted oxidation at 0 °C to yield intermediate **37** in a 93% yield (**Scheme 20**). A similar global deprotection of **37** via hydrogenolysis afforded **30** in 88% yield. Again, the structure of **30** was confirmed via ^{1}H NMR and HR-MALDI MS data.

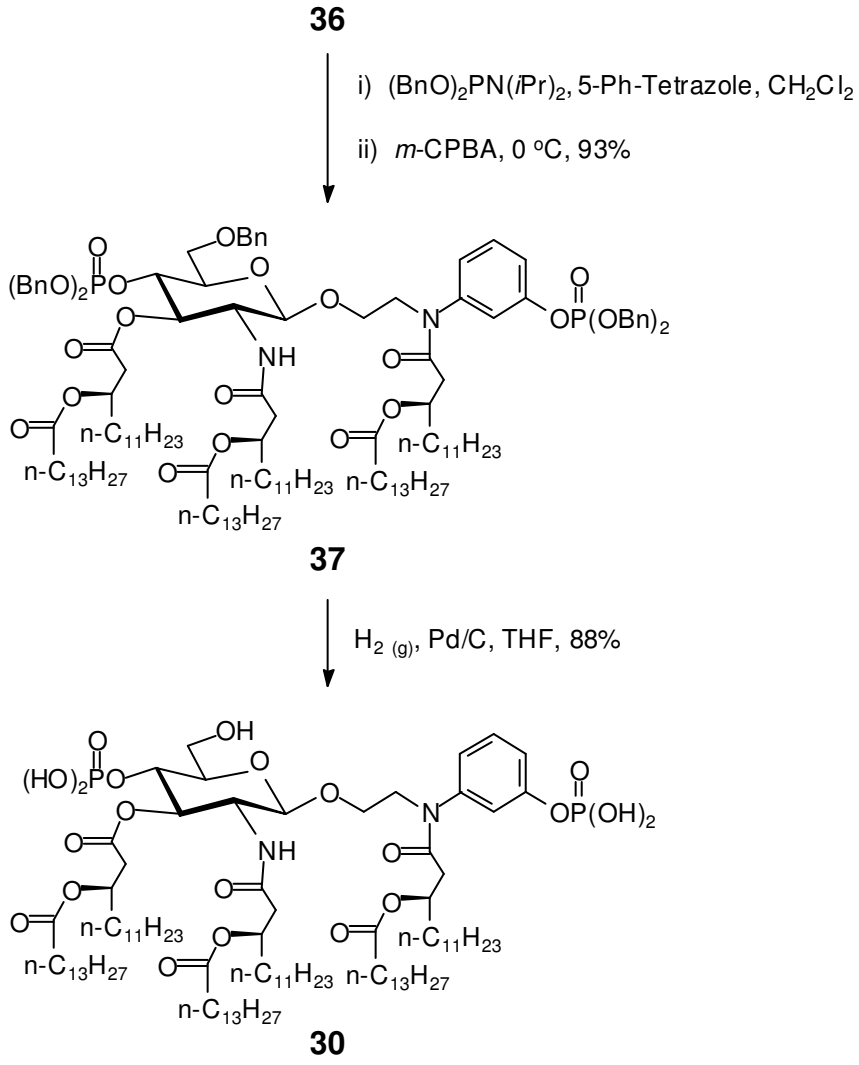

Scheme 20. Synthesis of Di-Phosphorylated Aromatic-Based Lipid A Mimic **30**

3.4 Biological Evaluation

***** Disclaimer:***** All Biological Evaluations Performed With Lipid A Mimics **29** & **30** Have Been Performed By Scientists At Immunovaccine. Specific Experimental Details Have Been Omitted For Intellectual Property Purposes.

To evaluate the potential adjuvant properties of aromatic-based lipid A mimics **29** and **30**, the compounds were first tested *in vivo* in a vaccine formulation against cervical cancer. Mice bearing tumours derived from the C3 tumor cell line were vaccinated with a liposomal-based vaccine formulation containing a HPV16E7 $_{49\text{-}57}$ (R9F) peptide with either **29** or **30** as vaccine adjuvant. The C3 tumor cell line is a well-described mouse model used for pre-clinical cervical cancer research, and develops tumors when injected subcutaneously. It has been used in cancer challenge studies to examine vaccine efficacy administered either before or after C3 tumor cell implantation.[176] After 28 days, those mice vaccinated with formulations containing either **29** or **30** as adjuvant had significantly smaller tumour volumes compared to mice vaccinated only with saline or a formulation containing no adjuvant (**Figure 32**).

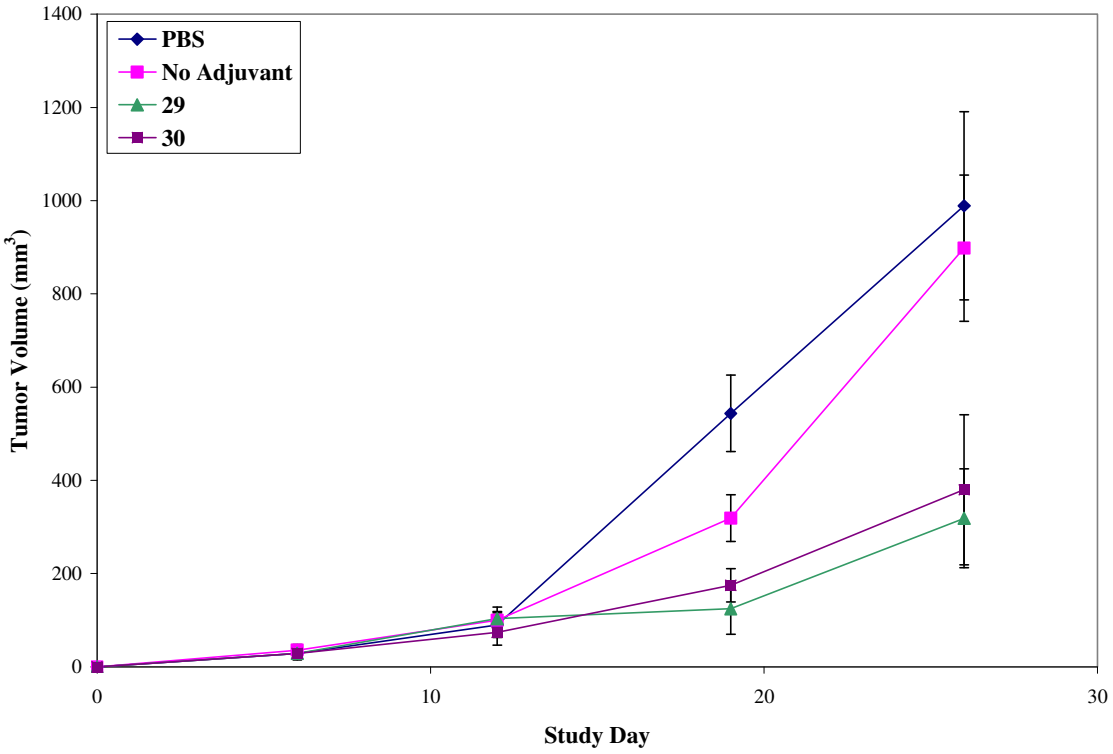

Figure 32. Tumor volumes of mice vaccinated with liposomal-based vaccine formulations containing aromatic-based lipid A mimics **29** or **30**. Mice were implanted with C3 tumors subcutaneously on day 1. On day five, groups of mice (n = 7) were vaccinated with liposomal based formulations containing the HPV16E7 $_{49\text{-}57}$ peptide construct and either no adjuvant, or **29** and **30** individually as potential adjuvants. Mice vaccinated with saline (PBS) containing no peptide or adjuvant served as a tumor growth control. Tumor size was measured weekly with calipers.

The aromatic-based lipid A mimics **29** and **30** were next evaluated in the patented DepoVax™ (DPX) vaccine platform [177]. Mice bearing tumors derived from the C3 tumor cell line were vaccinated with the DPX vaccine formulation containing the HPV16E7 $_{49\text{-}57}$ peptide with either **29** or **30** as vaccine adjuvant. After 40 days, mice vaccinated with either **29** or **30** showed significantly smaller tumor volumes than those mice vaccinated

with either saline or just the DPX vaccine platform containing no additional adjuvant (**Figure 33**).

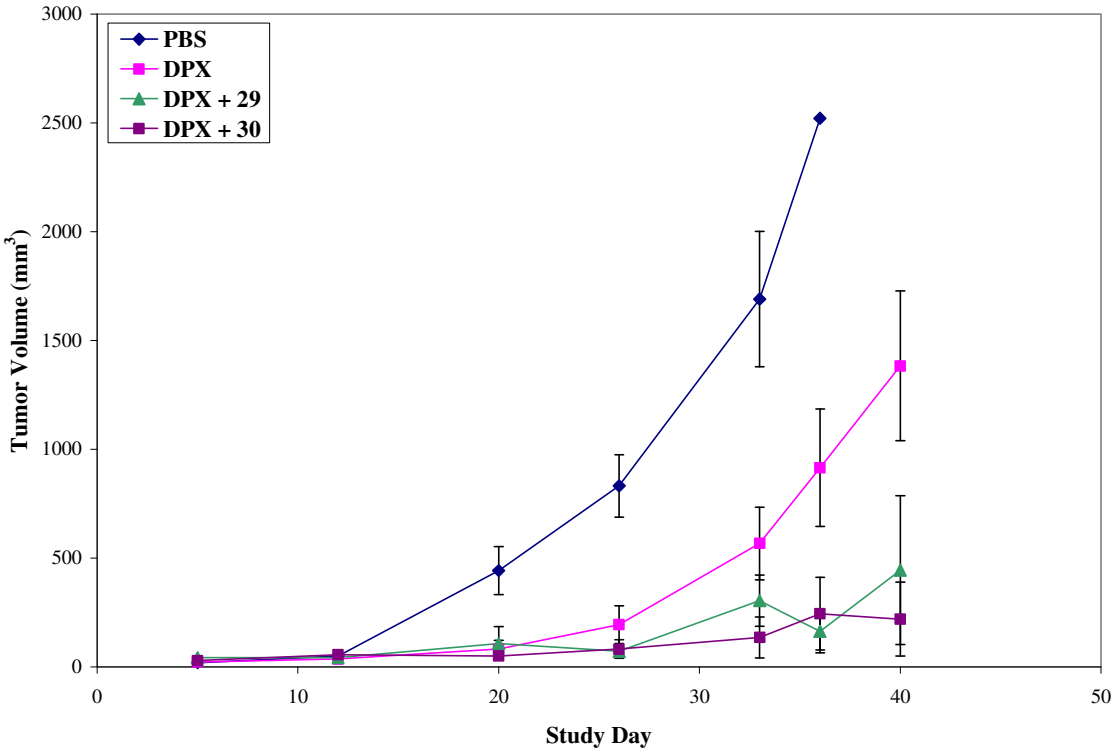

Figure 33. Tumor volumes of mice vaccinated with DPX vaccine formulations containing aromatic-based lipid A mimics **29** or **30**. Mice were implanted with C3 tumors subcutaneously on day 1. On day five, groups of mice (n = 8) were vaccinated with DPX-based formulations containing the HPV16E7 $_{49\text{-}57}$ peptide and either no adjuvant, or **29** and **30** individually as potential adjuvants. Mice vaccinated with saline (PBS) containing no peptide or adjuvant served as a tumor growth control. Tumor size was measured weekly with calipers.

The ability of aromatic-based lipid A mimics **29** and **30** to influence DC antigen presentation was also evaluated *in vivo* via the measurement of the expression levels of both CD40 and CD86. CD40 and CD86 are stimulatory proteins expressed on the surface of DCs necessary for antigen presentation and T-cell activation. DCs derived from both

C3H / HeOuJ mice, which are known to express TLR4, and C3H / HeJ mice, which are deficient in TLR4, were exposed to various stimuli including lipid A mimics **29** and **30**. Expression levels of both CD40 and CD86 were measured via immunostaining and flow cytometry (**Figures 34** & **35**). Both lipid A mimics **29** and **30** stimulate significant increases in both CD40 and CD86 expression levels over cells that were not stimulated. Moreover, said increase is not observed in DCs derived from the TLR4 deficient C3H / HeJ mice, thus confirming TLR4 as the stimulatory target of lipid A mimics **29** and **30**.

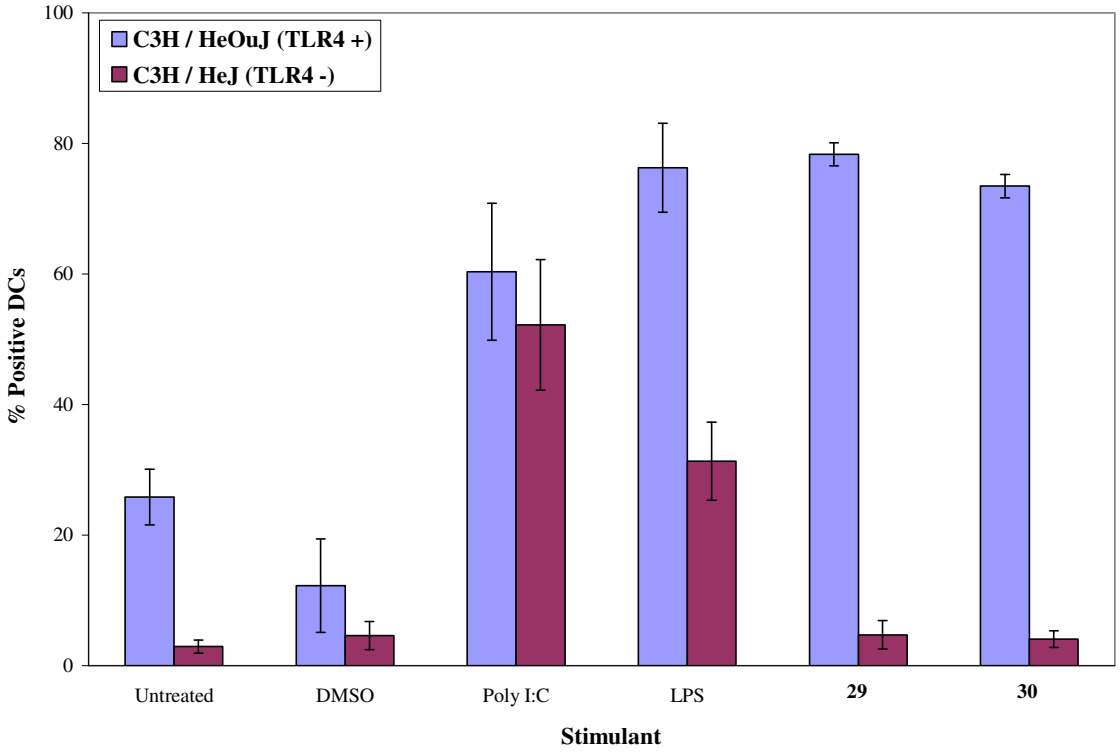

Figure 34. CD40 expression in DCs exposed to various stimuli including aromatic-based lipid A mimics **29** and **30**. DCs were isolated from either C3H / HeOuJ or C3H / HeJ mice and were stimulated overnight with various stimuli. Expression levels of CD40 was then measured via immunostaining and flow cytometry.

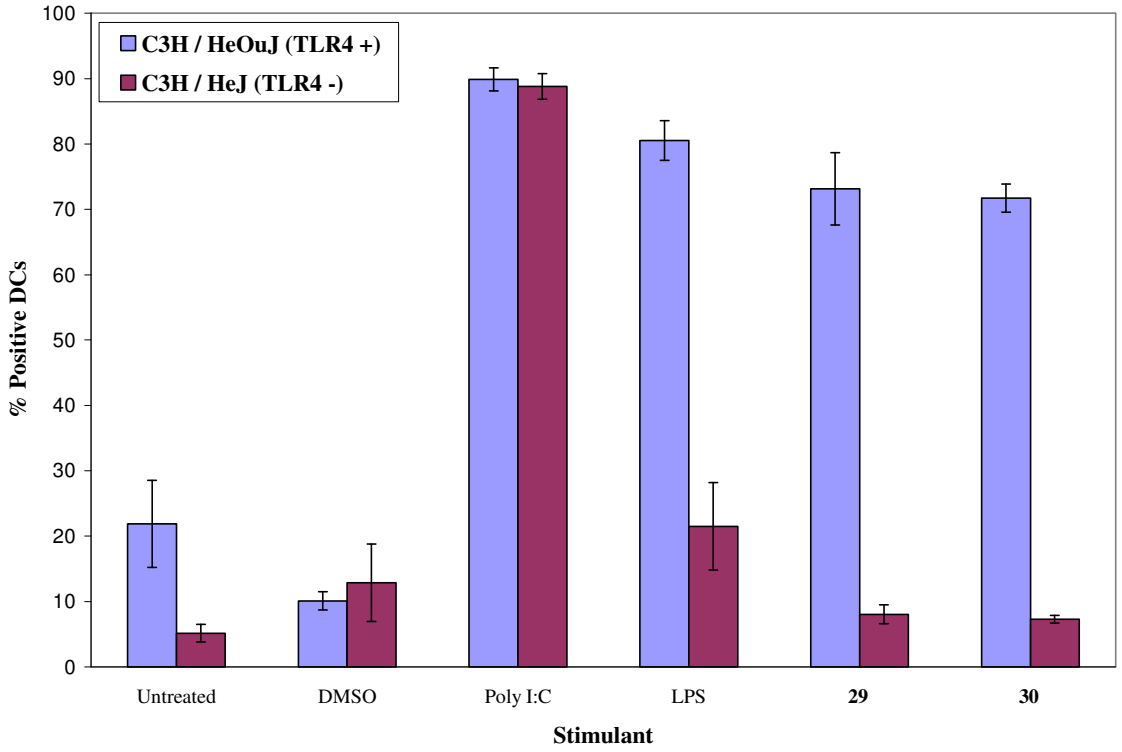

Figure 35. CD86 expression in DCs exposed to various stimuli including aromatic-based lipid A mimics **29** and **30**. DCs were isolated from either C3H / HeOuJ or C3H / HeJ mice and were stimulated overnight with various stimuli. Expression levels of CD86 was then measured via immunostaining and flow cytometry.

Finally, to test the immunogenicity of the DPX-based vaccine containing aromatic-based lipid A mimics **29** and **30**, mice were first immunized with the vaccine formulations containing a HPV16E7 $_{49\text{-}57}$ (R9F) antigen, and either mimic, or no adjuvant. After 8 days, mice were terminated, spleens were collected, and suspensions of splenocytes were prepared. The splenocytes were plated and stimulated overnight with either the R9F peptide, or an irrelevant peptide and no peptide as controls. The next day, antigen specific IFN-γ responses were measured via ELISPOT (**Figure 36**). Monophosphorylated lipid A

mimic **29** did not enhance antigen specific IFN-γ responses, whereas it appears that diphosphorylated lipid A mimic **30** did.

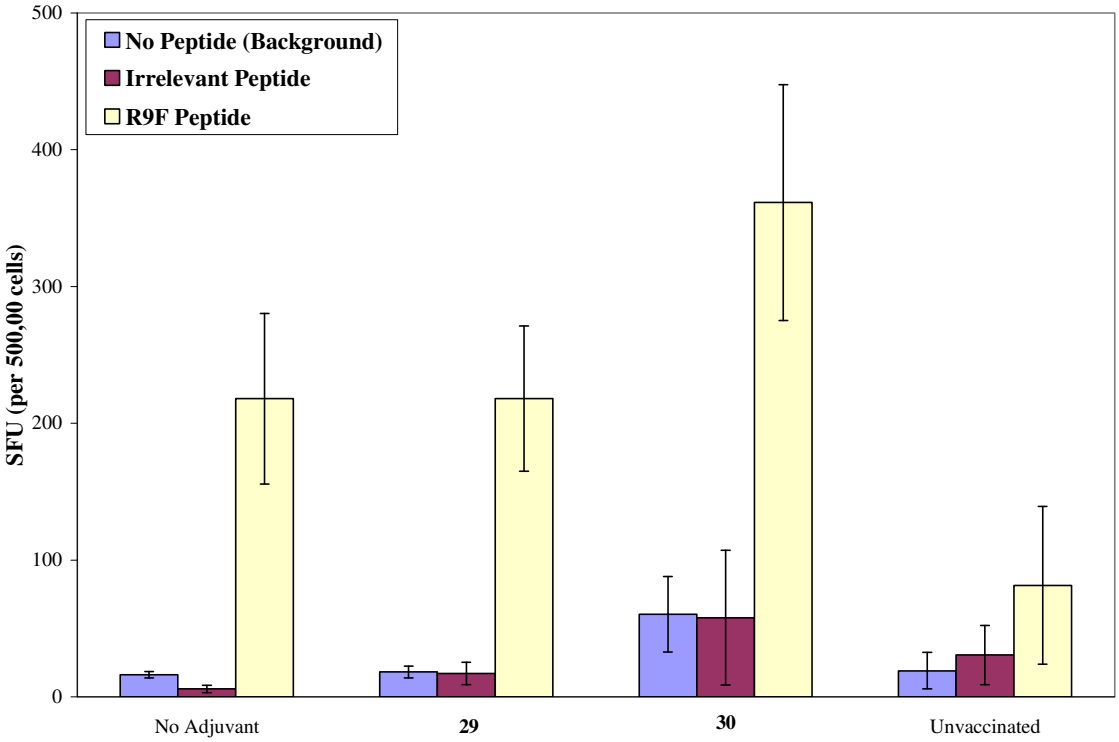

Figure 36. Antigen specific IFN-γ production after DPX-based vaccination with aromatic-based lipid A mimics 29 and 30. Mice (n = 5) were vaccinated with the DPX-based vaccine formulations containing either no adjuvant, or either lipid A mimics **29** and **30** as adjuvants. After 8 days, mice were terminated, splenocytes were obtained and then stimulated overnight. IFN-γ production was measured via ELISPOT the next day.

3.5 Experimental

3.5.1 General methods

All air and moisture sensitive reactions were performed under nitrogen atmosphere. All commercial reagents were used as supplied. Anhydrous dichloromethane was distilled over calcium hydride, whereas anhydrous *N*,*N*-dimethylformamide (DMF) was purchased from Aldrich. ACS grade solvents were purchased from Fisher Scientific and used for

chromatography without distillation. TLC plates (silica gel 60 F_{254}, thickness 0.25 mm) and silica gel 60 (40-63 μm) for flash column chromatography were purchased from SILICYCLE INC., Canada. ^{1}H and ^{13}C NMR spectra were recorded on a Varian Unity Inova 500 MHz spectrometer. Tetramethylsilane (TMS, δ 0.00 ppm) or solvent peaks were used as internal standards for ^{1}H and ^{13}C NMR spectra. The chemical shifts were given in ppm and coupling constants in Hz indicated to a resolution of ± 0.5 Hz. Multiplicity of proton signals is indicated as follows: s (singlet), d (doublet), dd (double doublet), t (triplet), q (quartet), m (multiplet), br (broad). Structural assignments were made using standard gCOSY and gHSQC methodology. NMR peaks belonging to primary lipid chains are denoted with an L subscript, whereas those belonging to secondary lipid chains are denoted with an L' subscript. ESI mass spectra were measured on the Applied Biosystems Mariner Bio-Spectrometry Workstation at the University of Alberta, Canada. MALDI mass spectra were measured on the Applied Biosystems Mariner 4700 system at the University of Western Ontario. Optical rotations were measured with Perkin Elmer 343 Polarimeter at 22°C.

3.5.2 *N*-(2-hydroxyethyl)-3-aminophenol (31):

To a solution of 3-aminophenol (5.00 g, 45.82 mmol) and sodium bicarbonate (8.85 g, 105.39 mmol) in water (7 mL) heated to 90 °C, 2-chloroethanol (3.4 mL, 50.40 mmol) was added dropwise over 5 minutes and the mixture was stirred overnight. Solids were filtered off through a celite pad, and the filtrate concentrated in vacuo. The resulting residue was washed three times with a CH_2Cl_2:MeOH solution (9 : 1, 10 mL), and the combined washes concentrated. Purification via repeated flash chromatography

(CH_2Cl_2/MeOH, 95 : 5 → 90 : 10) afforded **31** (4.10 g, 58%) as a brown solid. Rf 0.31 (CH_2Cl_2/MeOH, 95 : 5); $[\alpha]_D^{22}$ -0.7 (*c* 1.0, $CHCl_3$); ^{1}H NMR (500 MHz, $CDCl_3$): δ 3.15 (t, 2H, *J* 5.5 Hz, NCH_2), 3.68 (t, 2H, *J* 5.5 Hz, OCH_2), 4.58-4.96 (br s, 3H, NH, OH x 2), 6.15-6.19 (m, 3H, Ar-H), 6.93 (dd, 1H, *J* 8.5, 8.5 Hz, Ar-H); ^{13}C NMR (125 MHz, $CDCl_3$): δ 45.88 (N<u>C</u>H_2), 60.30 (O<u>C</u>H_2), 100.04 (<u>C</u>H-Ar), 104.58 (<u>C</u>H-Ar), 105.42 (<u>C</u>H-Ar), 129.81 (<u>C</u>H-Ar), 149.96 (<u>C</u>-Ar), 157.69 (<u>C</u>-Ar); HRESI-MS (*m*/*z*) Calcd for $C_8H_{11}NO_2$ $[M+H]^+$: 154.0868, found: 154.0858.

3.5.3 *N*-(2-(*tert*-butyldiphenylsilyloxy)ethyl)-3-aminophenol (32):

To a cooled solution (ice water bath) of **31** (864 mg, 5.62 mmol) and imidazole (573 mg, 8.43 mmol) in DMF (5.0 mL), *tert*-butyldiphenylsilyl chloride (1.60 mL, 6.18 mmol) was added dropwise over 2 minutes. The temperature was slowly allowed to rise to room temperature over 2 hours, and the mixture was stirred overnight. The mixture was concentrated, dissolved in EtOAc (60 mL), and washed with water (40 mL). The aqueous layer was further extracted with EtOAc (2 x 60 mL), with the combined organic layers dried over Na_2SO_4 and concentrated. Flash column chromatography purifaction (hexane/EtOAc, 3 : 1) afforded **32** (1.86 g, 84%) as a brown solid. Rf 0.38 (hexane/EtOAc, 3 : 1); $[\alpha]_D^{22}$ +3.4 (*c* 1.0, $CHCl_3$); ^{1}H NMR (500 MHz, $CDCl_3$): δ 1.06 (s, 9H, $C(CH_3)_3$), 3.22 (t, 2H, *J* 5.5 Hz, NCH_2), 3.85 (t, 2H, *J* 5.5 Hz, OCH_2), 4.02-4.18 (br s, 1H, NH), 4.60-4.74 (br s, 2H, OH x 2), 6.01 (s, 1H, Ar-H), 6.15-6.18 (m, 2H, Ar-H), 6.99 (dd, 1H, *J* 8.0, 8.0 Hz, Ar-H), 7.37-7.44 (m, 6H, Ar-H), 7.65-7.67 (m, 4H, Ar-H); ^{13}C NMR (125 MHz, $CDCl_3$): δ 19.27 (<u>C</u>$(CH_3)_3$), 26.92 (C(<u>C</u>$H_3)_3$), 45.90 (N<u>C</u>H_2),

62.28 (O<u>C</u>H$_2$), 100.22 (<u>C</u>H-Ar), 104.85 (<u>C</u>H-Ar), 106.48 (<u>C</u>H-Ar), 127.85 (<u>C</u>H-Ar), 129.86 (<u>C</u>H-Ar), 130.27 (<u>C</u>H-Ar), 133.39 (<u>C</u>-Ar), 135.64 (<u>C</u>H-Ar), 149.76 (<u>C</u>-Ar), 156.81 (<u>C</u>-Ar); HRESI-MS (*m*/*z*) Calcd for $C_{24}H_{29}NO_2Si$ $[M+H]^+$: 392.2047, found: 392.2033.

3.5.4 *N*-(3-hydroxyphenyl)-*N*-(2-(*tert*-butyldiphenylsilyloxy)ethyl)-(*R*)-3-tetradecanoyloxytetradecanamide (33):

To a solution of dilipid acid **3** (926 mg, 2.04 mmol) in CH_2Cl_2 (4 mL) cooled to -20 °C, *N*-methylmorpholine (336 µL, 3.06 mmol) and isobutyl chloroformate (278 µL, 2.14 mmol) were added successively. A solution of **32** (1.6 g. 4.08 mmol) in CH_2Cl_2 (4 mL) was then added dropwise over 3 minutes. The mixture was stirred at reduced temperature for 2 hours before being allowed to warm to room temperature. MeOH (2 mL) and water (2 mL) were added and the mixture concentrated. The residue was dissolved in CH_2Cl_2 (125 mL) and washed with water (35 mL). The organic layer was dried over Na_2SO_4, concentrated, and purified via flash column chromatography (hexane/acetone, 7 : 1) to afford **33** (1.35 g, 80%) as a colorless syrup. Rf 0.35 (hexane/acetone; 6 : 1); $[\alpha]_D^{22}$ +15.9 (*c* 1.0, $CHCl_3$); ^{1}H NMR (500 MHz, $CDCl_3$): δ 0.88 (t, 6H, *J* 6.5 Hz, CH_3 x 2). 1.01 (s, 9H, $C(CH_3)_3$), 1.14-1.36 (br m, 38H, CH_2 x 19), 1.50-1.62 (br m, 4H, H-4$_L$, H-3$_{L'}$), 2.20 (t, 2H, J 7.5 Hz, H-2$_{L'}$), 2.29 (dd, 1H, *J* 15.5, 6.0 Hz, H-2$_{LB}$), 2.40 (dd, 1H, *J* 15.5, 7.0 Hz, H-2$_{LA}$), 3.76-3.85 (m, 4H, NCH_2, OCH_2), 5.16-5.22 (m, 1H, H-3$_L$), 6.38-6.48 (br s, 1H, OH), 6.64 (s, 1H, Ar-H), 6.71 (d, 1H, *J* 8.0 Hz, Ar-H), 6.83 (d, 1H, *J* 8.0 Hz, Ar-H), 7.19 (dd, 1H, *J* 8.0, 8.0 Hz, Ar-H), 7.32-7.41 (m, 6H, Ar-H), 7.58-7.61 (m, 4H, Ar-H); ^{13}C

NMR (125 MHz, $CDCl_3$): δ 14.16 (CH_3), 19.19 ($\underline{C}(CH_3)_3$), 22.72 (CH_2), 25.02 (CH_2), 25.26(CH_2), 26.83 ($C(\underline{C}H_3)_3$), 29.17 (CH_2), 29.39 (CH_2), 29.40 (CH_2), 29.55 (CH_2), 29.57 (CH_2), 29.60 (CH_2), 29.67 (CH_2), 29.68 (CH_2), 29.69 (CH_2), 29.71 (CH_2), 29.73 (CH_2), 31.95 (CH_2), 34.26 (CH_2), 34.58 (CH_2), 39.08 (C-2_L), 51.37 ($N\underline{C}H_2$), 61.07 ($O\underline{C}H_2$), 71.36 (C-3_L), 115.29 ($\underline{C}$H-Ar), 115.49 ($\underline{C}$H-Ar), 120.11 ($\underline{C}$H-Ar), 127.70 ($\underline{C}$H-Ar), 129.68 ($\underline{C}$H-Ar), 130.41 ($\underline{C}$H-Ar), 133.51 ($\underline{C}$-Ar), 135.55 ($\underline{C}$H-Ar), 143.56 ($\underline{C}$-Ar), 157.17 ($\underline{C}$-Ar), 170.05 (C=O), 173.55 (C=O); HRESI-MS (*m*/*z*) Calcd for $C_{52}H_{81}NO_5Si$ $[M+H]^+$: 828.5963, found: 828.5926.

3.5.5 *N*-(3-hydroxyphenyl)-*N*-(2-hydroxyethyl)-(*R*)-3-tetradecanoyloxytetradecanamide (34):

To a solution of **33** (993 mg, 1.20 mmol) in CH_2Cl_2 (10 mL), HOAc (0.85 mL, 14.49 mmol) and Bu_4NF (1M in THF, 7.24 mL) were added successively. The mixture was stirred at room temperature overnight, and then concentrated. The residue was dissolved in CH_2Cl_2 (150 mL) and washed with a saturated sodium bicarbonate solution (40 mL). The organic layer was dried over Na_2SO_4, concentrated, and purified via flash column chromatography (hexane/EtOAc/MeOH, 2 : 1 : 0.1) to yield **34** (571 mg, 81%) as a colorless syrup. Rf 0.31 (hexane/EtOAc/MeOH, 2 : 1 : 0.1); $[\alpha]_D^{22}$ +4.5 (*c* 1.0, $CHCl_3$); ^{1}H NMR (500 MHz, $CDCl_3$): δ 0.88 (t, 6H, *J* 6.5 Hz, CH_3 x 2), 1.10-1.32 (br m, 38H, CH_2 x 19), 1.44-1.57 (br m, 4H, H-4_L, H-$3_{L'}$), 2.27 (t, 2H, J 7.5 Hz, H-$2_{L'}$), 2.34-2.45 (m, 2H, H-2_L), 3.68-3.93 (m, 6H, NCH_2, OCH_2, OH x 2), 5.15-5.24 (m, 1H, H-3_L), 6.75 (d, 1H, J 8.0 Hz, Ar-H), 6.85 (s, 1H, Ar-H), 6.89 (d, J 8.0 Hz, Ar-H), 7.27 (dd, 1H, J 8.0 Hz,

8.0 Hz, Ar-H); ^{13}C NMR (125 MHz, $CDCl_3$): δ 14.16 (CH_3), 22.72 (CH_2), 24.99 (CH_2), 25.20 (CH_2), 29.17 (CH_2), 29.33 (CH_2), 29.40 (CH_2), 29.53 (CH_2), 29.55 (CH_2), 29.59 (CH_2), 29.68 (CH_2), 29.71 (CH_2), 29.74 (CH_2), 31.95 (CH_2), 34.41 (CH_2), 34.59 (CH_2), 39.36 (C-2_L), 52.33 (N$\underline{C}H_2$), 60.54 (O$\underline{C}H_2$), 71.45 (C-3_L), 115.48 ($\underline{C}$H-Ar), 115.97 ($\underline{C}$H-Ar), 119.01($\underline{C}$H-Ar), 130.86 ($\underline{C}$H-Ar), 143.00 ($\underline{C}$-Ar), 158.02 ($\underline{C}$-Ar), 172.18 (C=O), 174.22 (C=O); HRESI-MS (*m*/*z*) Calcd for $C_{36}H_{63}NO_5$ $[M+H]^+$: 590.4785, found: 590.4752.

3.5.6 *N*-(3-hydroxyphenyl)-*N*-{2-[6-*O*-benzyl-2-deoxy-4-*O*-(di-*O*-benzylphosphono)-3-*O*-((*R*)-3-tetradecanoyloxytetradecanoyl)-2-(2,2,2-trichloroethoxycarbonylamino)-β-D-glucopyranosyloxy]-ethyl}-(*R*)-3-tetradecanoyloxytetradecanamide (35):

A solution of **34** (565 mg, 0.96 mmol) and imidate **4** (1.23 g, 0.96 mmol) in CH_2Cl_2 (8 mL) in the presence of molecular sieves (4Å, 4.0 g) was stirred under nitrogen at room temperature for 30 min. A solution of TMSOTf (0.02 M in CH_2Cl_2, 0.95 mL) was added dropwise in about 3 min. The mixture was stirred at room temperature for 1 h before a saturated sodium bicarbonate solution (15 mL) was added to quench the reaction. Solids were filtered out, and the filtrate was extracted with CH_2Cl_2 (3 x 30 mL). The combined organic phase was dried over Na_2SO_4, concentrated, and purified via flash column chromatography (hexane/EtOAC/MeOH, 3 : 1 : 0.1) to yield **35** (1.46 g, 89%) as a colorless syrup. Rf 0.36 (hexane/EtOAC/MeOH, 3 : 1 : 0.1); $[\alpha]_D^{22}$ -10.6 (*c* 1.0, $CHCl_3$); ^{1}H NMR (500 MHz, $CDCl_3$): δ 0.88 (t, 12H, *J* 6.5 Hz, CH_3 x 4), 1.15-1.38 (br m, 76H,

CH_2 x 38), 1.42-1.58 (br m, 8H, H-4_L, H-$3_{L'}$), 2.19-2.52 (m, 8H, H-2_L, H-$2_{L'}$), 3.54-3.62 (m, 4H, H-5, H-6B, NCH_2), 3.66-3.71 (m, 1H, H-2), 3.76-3.81 (m, 1H, H-6A), 3.93-4.06 (m, 2H, OCH_2), 4.42-4.53 (m, 3H, H-4, Ph-CH_2), 4.59 (d, 1H, *J* 8.5 Hz, H-1), 4.63 (d, 1H, *J* 12.0 Hz, Troc-H_B), 4.71 (d, 1H, *J* 12.0 Hz, Troc-H_A), 4.87-4.94 (m, 4H, $(PhCH_2O)_2P$), 5.11-5.22 (m, 2H, H-3_L), 5.27 (dd, 1H, *J* 10.0, 10.0 Hz, H-3), 5.82 (d, 1H, *J* 8.0 Hz, NH), 6.00 (br s, 1H, OH), 6.65 (d, 1H, *J* 7.5 Hz, Ar-H), 6.83 (d, 1H, *J* 8.0 Hz, Ar-H), 6.95 (s, 1H, Ar-H), 7.17-7.35 (m, 16H, Ar-H); ^{13}C NMR (125 MHz, $CDCl_3$): δ 14.16 (CH_3), 22.72 (CH_2), 25.01 (CH_2), 25.05 (CH_2), 25.12 (CH_2), 25.19 (CH_2), 29.19 (CH_2), 29.36 (CH_2), 29.40 (CH_2), 29.57 (CH_2), 29.60 (CH_2), 29.62 (CH_2), 29.69 (CH_2), 29.71 (CH_2), 29.73 (CH_2), 31.95 (CH_2), 34.18 (CH_2), 34.35 (CH_2), 34.45 (CH_2), 34.61 (CH_2), 39.01 (C-2_L), 39.20 (C-2_L), 49.61 (N<u>C</u>H_2), 56.38 (C-2), 66.58 (O<u>C</u>H_2), 68.28 (C-6), 69.70-69.86 (m, (Ph<u>C</u>H_2O)$_2$P), 69.90 (C-3_L), 71.33 (C-3_L), 72.80 (C-3), 73.45 (Ph-<u>C</u>H_2), 73.88 (d, *J* 5.5 Hz, C-4), 73.93 (C-5), 74.71 (Troc-<u>C</u>H_2), 95.22 (Troc-<u>C</u>Cl_3), 100.01 (C-1), 115.42 (CH-Ar), 115.87 (CH-Ar), 119.22 (CH-Ar), 127.73 (CH-Ar), 128.04 (CH-Ar), 128.14 (CH-Ar), 128.39 (CH-Ar), 128.62 (CH-Ar), 128.70 (CH-Ar), 135.41 (C-Ar), 135.44 (C-Ar), 137.74 (C-Ar), 143.52 (C-Ar), 155.09 (C=O, Troc), 157.67 (C-Ar), 170.32 (C=O), 170.38 (C=O), 173.59 (C=O); MALDI-MS (*m/z*) Calcd for $C_{94}H_{146}Cl_3N_2O_{17}P$ $[M + Na]^+$: 1733.9325, found: 1733.9720.

3.5.7 *N*-(3-hydroxyphenyl)-*N*-{2-[6-*O*-benzyl-2-deoxy-4-*O*-(di-*O*-benzylphosphono)-3-*O*-((*R*)-3-tetradecanoyloxytetradecanoyl)-2-((*R*)-3-tetradecanoyloxytetradecanamido)-β-D-glucopyranosyloxy]-ethyl}-(*R*)-3-tetradecanoyloxytetradecanamide (36):

To a solution of **35** (550 mg, 0.32 mmol) in glacial acetic acid (20 mL) and EtOAc (5 mL), zinc powder (3.0 g) was added and the mixture was stirred at room temperature for 45 min. The mixture was then filtered, the solids were washed with an acetic acid/EtOAc solution (9:1, 40 mL), and the filtrate was concentrated. The residue was dissolved in CH_2Cl_2 (100 mL), washed with a saturated sodium bicarbonate solution (40 mL) and the aqueous layer was extracted with CH_2Cl_2 (2 x 40 mL). The combined organic phase was dried over Na_2SO_4 and concentrated to give the crude amine (455 mg) as a colorless syrup.

To a solution of dilipid acid **3** (182 mg, 0.40 mmol) in CH_2Cl_2 (2 mL), DIC (125 µL, 0.80 mmol) was added and the mixture was stirred at room temperature for 10 minutes. To this mixture, a solution of the crude amine (450 mg) in CH_2Cl_2 was added, and the resulting mixture was stirred at room temperature overnight. Water (0.5 mL) was added, and the mixture was then dried over Na_2SO_4. Solids were filtered off, and the filtrate was concentrated. The residue was purified via flash column chromatography (hexane/EtOAC/MeOH, 3 : 1 : 0.1) to afford **36** (430 mg, 68%) as a colorless syrup. Rf 0.37 (hexane/EtOAC/MeOH, 2 : 1 : 0.1); $[\alpha]_D^{22}$ -3.9 (*c* 1.0, $CHCl_3$); ^{1}H NMR (500 MHz, $CDCl_3$):): δ 0.88 (t, 18H, *J* 6.5 Hz, CH_3 x 6), 1.17-1.40 (br m, 114H, CH_2 x 57), 1.40-1.63 (br m, 12H, H-4_L, H-$3_{L'}$), 2.18-2.52 (m, 12H, H-2_L, H-$2_{L'}$), 3.55-3.63 (m, 4H, H-5, H-6B, NCH_2), 3.76-3.80 (m, 3H, H-6A, OCH_2), 4.20-4.27 (m, 1H, H-2), 4.40 (d, 1H, *J* 8.0 Hz, H-1), 4.43-4.52 (m, 3H, H-4, Ph-CH_2), 4.87-4.96 (m, 5H, $(PhCH_2O)_2P$, H-3_L), 5.09-5.14 (m, 2H, H-3, H-3_L), 5.22-5.28 (m, 1H, H-3_L), 6.50 (d, 1H, *J* 9.5 Hz, NH), 6.61 (d, 1H, *J* 8.0 Hz, Ar-H), 6.82 (d, 1H, *J* 8.0 Hz, Ar-H), 7.01 (s, 1H, Ar-H), 7.16 (dd, 1H, *J*

8.0, 8.0 Hz, Ar-H), 7.23-7.32 (m, 15H, Ar-H), 8.66 (br s, 1H, OH); ^{13}C NMR (125 MHz, $CDCl_3$): δ 14.15 (CH_3), 22.72 (CH_2), 24.96 (CH_2), 25.00 (CH_2), 25.09 (CH_2), 25.12 (CH_2), 25.24 (CH_2), 29.21 (CH_2), 29.25 (CH_2), 29.40 (CH_2), 29.47 (CH_2), 29.49 (CH_2), 29.57 (CH_2), 29.61 (CH_2), 29.65 (CH_2), 29.69 (CH_2), 29.71 (CH_2), 29.73 (CH_2), 29.75 (CH_2), 31.96 (CH_2), 34.13 (CH_2), 34.25 (CH_2), 34.40 (CH_2), 34.41 (CH_2), 34.50 (CH_2), 34.61 (CH_2), 38.87 (C-2_L), 38.97 (C-2_L), 41.84 (C-2_L), 50.69 (NCH_2), 53.78 (C-2), 67.00 (OCH_2), 68.29 (C-6), 69.68-69.73 (m, (Ph$\underline{C}H_2O)_2$P), 69.79 (C-3_L), 70.88 (C-3_L), 71.45 (C-3_L), 72.85 (C-3), 73.53 (Ph-$\underline{C}H_2$), 73.84 (d, *J* 5.5 Hz, C-4), 74.31 (C-5), 100.88 (C-1), 115.25 (CH-Ar), 115.57 (CH-Ar), 118.48 (CH-Ar), 127.66 (CH-Ar), 127.69 (CH-Ar), 128.04 (CH-Ar), 128.13 (CH-Ar), 128.41 (CH-Ar), 128.60 (CH-Ar), 128.61 (CH-Ar), 128.67 (CH-Ar), 135.48 (C-Ar), 135.53 (C-Ar), 137.86 (C-Ar), 144.12 (C-Ar), 158.41 (C-Ar), 170.04 (C=O), 170.98 (C=O), 171.92 (C=O), 173.16 (C=O), 173.43 (C=O), 173.73 (C=O); MALDI-MS (*m/z*) Calcd for $C_{119}H_{197}N_2O_{18}P$ $[M + Na]^+$: 1996.4199, found: 1996.4117.

3.5.8 *N*-(3-hydroxyphenyl)-*N*-{2-deoxy-4-*O*-phosphono-3-*O*-((*R*)-3-tetradecanoyloxytetradecanoyl)-2-((*R*)-3-tetradecanoyloxytetradecanamido)-β-D-glucopyranosyloxy]-ethyl}-(*R*)-3-tetradecanoyloxytetradecanamide (29):

To a solution of **36** (146 mg, 0.074 mmol) in freshly distilled THF (70 mL), palladium on charcoal (5%, 45 mg) was added and the mixture was stirred at room temperature under a hydrogen atmosphere for 24 h. The mixture was filtered, and the filtrate concentrated. The residue was purified by flash column chromatography ($CHCl_3$/MeOH, 9 : 1 → $CHCl_3$/MeOH/H_2O, 4 : 1 : 0.1) to afford **29** (111 mg, 88%) as white fluffy solid after

being freeze dried from a dioxane-$CHCl_3$ mixture (95 : 5). Rf 0.57 ($CHCl_3$/MeOH/H_2O, 4 : 1 : 0.1); $[\alpha]_D^{22}$ -0.6 (*c* 0.5, $CHCl_3$); ^{1}H NMR (500 MHz, $CDCl_3$): δ 0.89 (t, 18H, *J* 6.5 Hz, CH_3 x 6), 1.12-1.39 (br m, 114H, CH_2 x 57), 1.43-1.66 (br m, 12H, H-4_L, H-$3_{L'}$), 2.20-2.47 (m, 10H, H-2_L x 4, H-$2_{L'}$), 2.55-2.72 (m, 2H, H-2_L x 2), 3.61-3.74 (m, 4 H, H-5, H-6B, NCH_2), 3.83-3.94 (m, 3H, H-2, OCH_2), 4.01-4.03 (m, 1H, H-6A), 4.20-4.25 (m, 1H, H-4), 4.48 (d, 1H, *J* 8.0 Hz, H-1), 5.10-5.26 (m, 4H, H-3, H-3_L), 6.65 (d. 1H, *J* 8.0 Hz, Ar-H), 6.81-6.87 (m, 2H, Ar-H), 7.25 (dd, 1H, *J* 8.0, 8.0 Hz, Ar-H); MALDI-MS (*m*/*z*) Calcd for $C_{98}H_{179}N_2O_{18}P$ $[M + Na]^+$: 1726.2790, found: 1726.2794.

3.5.9 *N*-(3-(di-*O*-benzylphosphono)-phenyl)-*N*-{2-[6-*O*-benzyl-2-deoxy-4-*O*-(di-*O*-benzylphosphono)-3-*O*-((*R*)-3-tetradecanoyloxytetradecanoyl)-2-((*R*)-3-tetradecanoyloxytetradecanamido)-β-D-glucopyranosyloxy]-ethyl}-(*R*)-3-tetradecanoyloxytetradecanamide (37):

To a solution of **36** (122 mg, 0.062 mmol) in CH_2Cl_2 (3 mL), 5-phenyltetrazole (27 mg, 0.18 mmol) and *N,N*-diisopropylphosphoramidite (42 µL, 0.124 mmol) were added. The mixture was stirred at room temperature for 1 h and then cooled to 0 °C before the addition of *m*-chloroperbenzoic acid (46 mg, 77 %, 0.186 mmol). The mixture was stirred at the reduced temperature for 1 h before being allowed to warm to room temperature. An aqueous $NaHSO_3$ (10%, 15 mL) was added and the mixture was stirred at room temperature for 20 minutes. The mixture was then extracted with CH_2Cl_2 (3 x 15 mL), and the combined organic phase was washed with a saturated sodium bicarbonate solution (15 mL). The organic phase was dried over Na_2SO_4, concentrated, and purified

by flash column chromatography (hexane/acetone, 4 : 1) to give **37** (129 mg, 93%) as a colorless syrup. Rf 0.28 (hexane/acetone, 4 : 1); $[\alpha]_D^{22}$ -2.6 (*c* 1.0, $CHCl_3$); ^1H NMR (500 MHz, $CDCl_3$): δ 0.88 (t, 18H, *J* 6.5 Hz, CH_3 x 6), 1.15-1.37 (br m, 114H, CH_2 x 57), 1.41-1.64 (br m, 12H, H-4_L, H-$3_{L'}$), 2.14-2.48 (m, 12H, H-2_L, H-$2_{L'}$), 3.47-3.53 (m, 1H, H-2), 3.56-3.69 (m, 4H, H-5, H-6B, NCH_2), 3.75-3.77 (m, 1H, H-6A), 3.82-3.91 (m, 2H, OCH_2), 4.39-4.49 (m, 3H, H-4, Ph-CH_2), 4.85-4.92 (m, 5H, H-1, $(PhCH_2O)_2P$), 5.11-5.19 (m, 7H, $(PhCH_2O)_2P$, H-3_L x 3), 5.49 (dd, 1H, *J* 10.0, 10.0 Hz, H-3), 6.70 (d, 1H, *J* 7.5 Hz, NH), 7.02-7.10 (m, 3H, Ar-H), 7.19-7.34 (m, 26H, Ar-H); ^{13}C NMR (125 MHz, $CDCl_3$): δ δ 14.16 (CH_3), 22.72 (CH_2), 25.03 (CH_2), 25.05 (CH_2), 25.14 (CH_2), 25.28 (CH_2), 25.32 (CH_2), 29.23 (CH_2), 29.31 (CH_2), 29.40 (CH_2), 29.43 (CH_2), 29.48 (CH_2), 29.60 (CH_2), 29.62 (CH_2), 29.64 (CH_2), 29.72 (CH_2), 29.74 (CH_2), 29.76 (CH_2), 31.96 (CH_2), 31.98 (CH_2), 34.26 (CH_2), 34.34 (CH_2), 34.44 (CH_2), 34.54 (CH_2), 38.99 (C-2_L), 39.18 (C-2_L), 40.98 (C-2_L), 49.12 (NCH_2), 55.43 (C-2), 66.10 (OCH_2), 68.55 (C-6), 69.45-69.64 (m, (Ph<u>C</u>$H_2O)_2P$), 69.90 (C-3_L), 70.20-70.32 (m, (Ph<u>C</u>$H_2O)_2P$), 70.49 (C-3_L), 70.98 (C-3_L), 72.71 (C-3), 73.30 (Ph-CH_2), 73.97 (d, *J* 5.5 Hz, H-4), 74.30 (C-5), 99.35 (C-1), 119.74 (CH-Ar), 120.50 (CH-Ar), 125.53 (CH-Ar), 127.50 (CH-Ar), 127.55 (CH-Ar), 127.97 (CH-Ar), 128.08 (CH-Ar), 128.12 (CH-Ar), 128.30 (CH-Ar), 128.54 (CH-Ar), 128.70 (CH-Ar), 128.73 (CH-Ar), 128.87 (CH-Ar), 130.60 (CH-Ar), 135.16 (C-Ar), 135.21 (C-Ar), 135.60 (C-Ar), 135.65 (C-Ar), 138.14 (C-Ar), 143.82 (C-Ar), 151.02 (d, *J* 5.5 Hz, C-Ar), 169.65 (C=O), 170.06 (C=O), 170.17 (C=O), 173.15 (C=O), 173.19 (C=O), 173.35 (C=O); MALDI-MS (*m*/*z*) Calcd for $C_{133}H_{210}N_2O_{21}P_2$ $[M + Na]^+$: 2256.4801, found: 2256.5198.

3.5.10 *N*-(3-phosphonoxyphenyl)-*N*-{2-deoxy-4-*O*-phosphono-3-*O*-((*R*)-3-tetradecanoyloxytetradecanoyl)-2-((*R*)-3-tetradecanoyloxytetradecanamido)-β-D-glucopyranosyloxy]-ethyl}-(*R*)-3-tetradecanoyloxytetradecanamide (30):

In a similar manner as described for the global deprotection of **36**, a solution of **37** (203 mg, 0.091 mmol) and palladium on charcoal (5%, 45 mg) in freshly distilled THF (75 mL) was stirred under a hydrogen atmosphere at room temperature for 24 h. The mixture was filtered, the filtrate concentrated, and the resulting residue was purified by flash column chromatography (CHCl3/MeOH, 9 : 1 → $CHCl_3$/MeOH/H_2O, 2 : 1 : 0.2) to yield **30** (145 mg, 89%) as a white fluffy solid after being freeze dried from a dioxane-$CHCl_3$ mixture (95 : 5). Rf 0.51 ($CHCl_3$/MeOH/H_2O/NH_4OH, 2 : 1 : 0.2 : 0.1); $[\alpha]_D^{22}$ -0.4 (*c* 0.5, $CHCl_3$); ^{1}H NMR (500 MHz, $CDCl_3$): δ 0.89 (t, 18H, *J* 6.5 Hz, CH_3 x 6), 1.18-1.39 (br m, 114H, CH_2 x 57), 1.49-1.68 (br m, 12H, H-4_L, H-$3_{L'}$), 2.20-2.47 (m, 10H, H-2_L x 4, H-$2_{L'}$), 2.55-2.72 (m, 2H, H-2_L x 2), 3.51-3.80 (br m, H-2, H-5, H-6B, NCH_2), 3.85-3.99 (br m, 3H, H-6A, OCH_2), 4.21-4.28 (br m, 1H, H-4), 4.56 (d, 1H, *J* 8.0 Hz, H-1), 5.11-5.27 (m, 4H, H-3, H-3_L), 6.88 (d, 1H, J 8.0 Hz, Ar-H), 7.20-7.28 (br m, 2H, Ar-H), 7.35 (dd, 1H, *J* 8.0, 8.0 Hz, Ar-H); MALDI-MS (*m*/*z*) Calcd for $C_{98}H_{180}N_2O_{21}P_2$ $[M + Na]^+$: 1806.2458, found: 1806.2502.

4 SYNTHESIS OF A SELF-ADJUVANTING CARBOHYDRATE ANTIGEN FOR USE IN THERAPEUTIC CANCER VACCINES

4.1 Design

In the vast world that is cancer research, one avenue for the treatment and perhaps, prevention of the disease, is the notion of cancer immunotherapy in which the power of the host immune system is employed in place of the more traditional, and invasive treatment options. Tumour associated carbohydrate antigens (TACAs), carbohydrate containing epitopes which are either unique, or over-expressed by cancer cells have emerged as viable targets of said immunotherapy. Recently, the paradigm shifting work was reported in which the TLR4 ligand MLA was chemically conjugated to a TACA to generate a fully synthetic, self-adjuvanting cancer vaccine construct capable of eliciting high titres of high affinity IgG antibodies which were shown to effectively bind to the TACA (**Figure 17**) [132, 133]. This discovery has sparked an examination into other potential adjuvant structures which can be incorporated into synthetic vaccine constructs capable of eliciting the appropriate levels of immunological responses required for not only the clearance of cancerous cells, but also the prevention of their re-emergence.

The disaccharide Thomsen-Friedenreich (T_F) antigen (Galβ1-3GalNAcα1-Ser/Thr) (**Figure 16**) is the core structure of *O*-linked mucin type glycans. In normal epithelium, the T_F structure is concealed by various functionalities, mainly other sugar chains forming complex, branched *O*-glycans [178]. In a cancerous state, free, un-substituted T_F occurs, which has been noted in 90% of all cancers, including cancers of the colon, breast, bladder, prostate, liver, kidney, ovary, and stomach [179, 180]. The increased occurrence of the T_F antigen also correlates with cancer progression and metastasis [181,

[182]. The broad expression of the T_F antigen in various cancers has resulted in it being targeted for both disease diagnosis [182-184], and immunotherapy [186, 187-191]. Vaccination using both purified and synthetic form T_F, or T_F-conjugated with immunogenic carriers have shown high titre anti-T_F antibodies, in many cases, capable of inducing complement-mediated cytotoxicity [187-192].

Given the TLR4 stimulatory nature of the DEA-containing lipid A mimic ligands synthesized herein, the adjuvant potential of these TLR4 ligands was employed to generate the potentially self-adjuvanting carbohydrate antigen **38** (**Figure 37**). As can be seen, **38** contains both the DEA-containing lipid A mimic framework, specifically terminal acid containing mimic **14** (**Figure 24**), and the T_F TACA (**Figure 16**), chemically conjugated to each other via a flexible tetraethylene glycol based linker. Chemically speaking, the adjuvant and antigen moieties of the construct are linked via amide linkages, one between the linker and the terminal acidic moiety of **14**, and the other between the linker and an amine moiety in the T_F antigen. The choice to conjugate to terminal acid of lipid mimic **14** may seem counterintuitive at first glance, given that the incorporation of this acidic group resulted in an increased TLR4 stimulatory potency. The choice to conjugate at this chemical site is based upon the fact that the MLA-TACA conjugate previously reported has the conjugation occurring at the anomeric position, and is obviously well tolerated in terms of TLR4 binding [132, 133]. It is presumed that the acidic group in **14** mimics the anomeric phosphate of the natural lipid A structure when binding to TLR4, thus linkage through this *pseudo*-anomeric position will likely also be well tolerated by TLR4 when binding the construct.

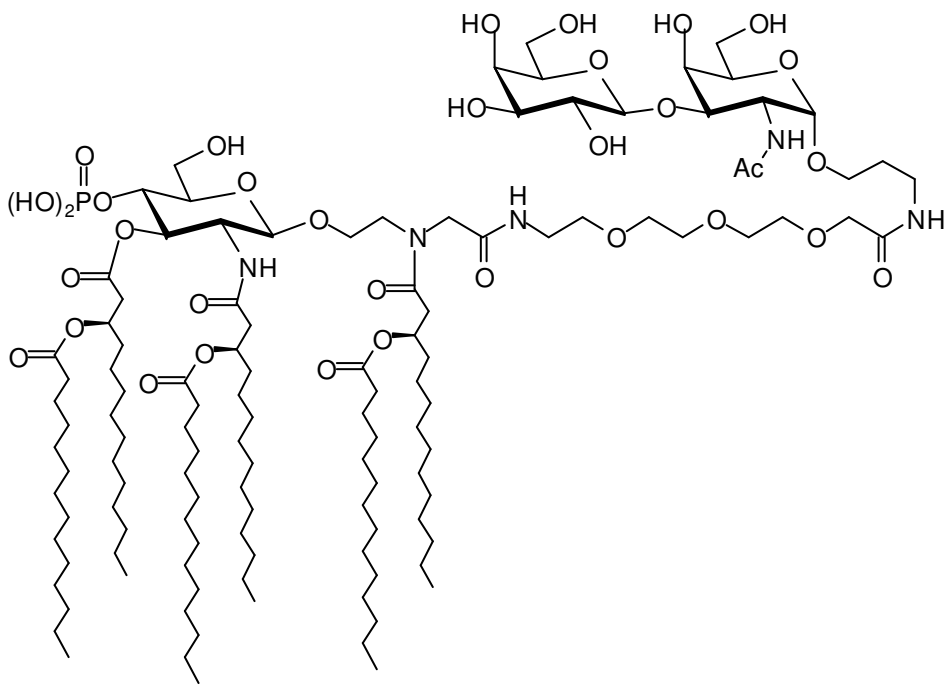

38

Figure 37. DEA-containing lipid A mimic based synthetic vaccine construct **38**

4.2 Retrosynthetic Analysis

Through a series of protections, functional group transformations, and protections, synthetic vaccine construct **38** was first deconstructed into three distinct molecular fragments: DEA-containing lipid A mimic precursor **28** (**Scheme 15**), T_F-based disaccharide **50**, and tetraethylene glycol based linker **45** (**Scheme 21**). The disaccharide **50** was further deconstructed into commercially available tetra-acetylgalactosyl bromide ($(Ac)_4$Gal-Br), known imidate derivative **46** [193], and 3-aminopropanol derivative **47** [194]. The benzylidene protecting group in **46** was chosen for its known α-glycoside directing ability, the likes of which was employed for the formation of the desired α-glycoside at the reducing end anomeric position [193].

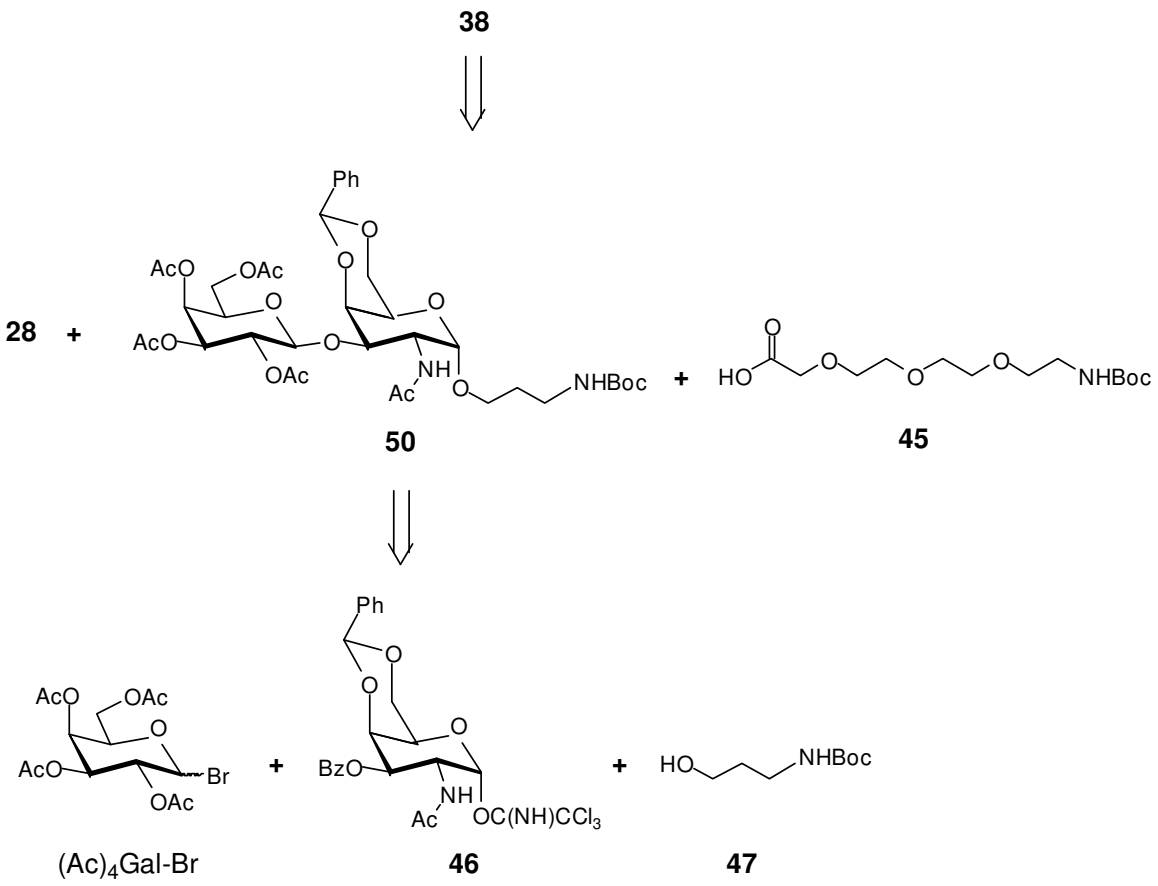

Scheme 21. Retrosynthesis of antigen conjugate **38**

4.3 Synthesis

The synthesis of antigen **38** began with the preparation of terminal acidic linker fragment **45** (**Scheme 24**). Tetraethylene glycol was first converted to the mono-tosylate **39** via reaction with tosyl-chloride in pyridine in a 75% yield. The remaining free hydroxyl was then protected as the corresponding TBDPS silyl ether via reaction with TBDPS-chloride and imidazole in DCM at 0 °C to yield intermediate **40** in 97% yield. The tosyl group was interchanged for an azide group by reaction with sodium azide in DMF at 60 °C to yield intermediate **41** in 88%. Reduction of the azide group via hydrogenation over Pd/C in ethanol furnished free amine **42** in 91% yield. Protection of the free amine as the Boc carbamate was achieved via reaction with di-*tert*-butyl dicarbonate (Boc_2O) and triethylamine in chloroform to yield intermediate **43** in 95% yield. Deprotection of the silyl ether was brought about by treatment with tetrabutylammonium fluoride in DCM to yield the free hydroxyl **44**. Finally, oxidation of the free hydroxyl to the corresponding carboxylic acid **45** was achieved in 76% yield via treatment with TEMPO and BAIB in wet DCM.

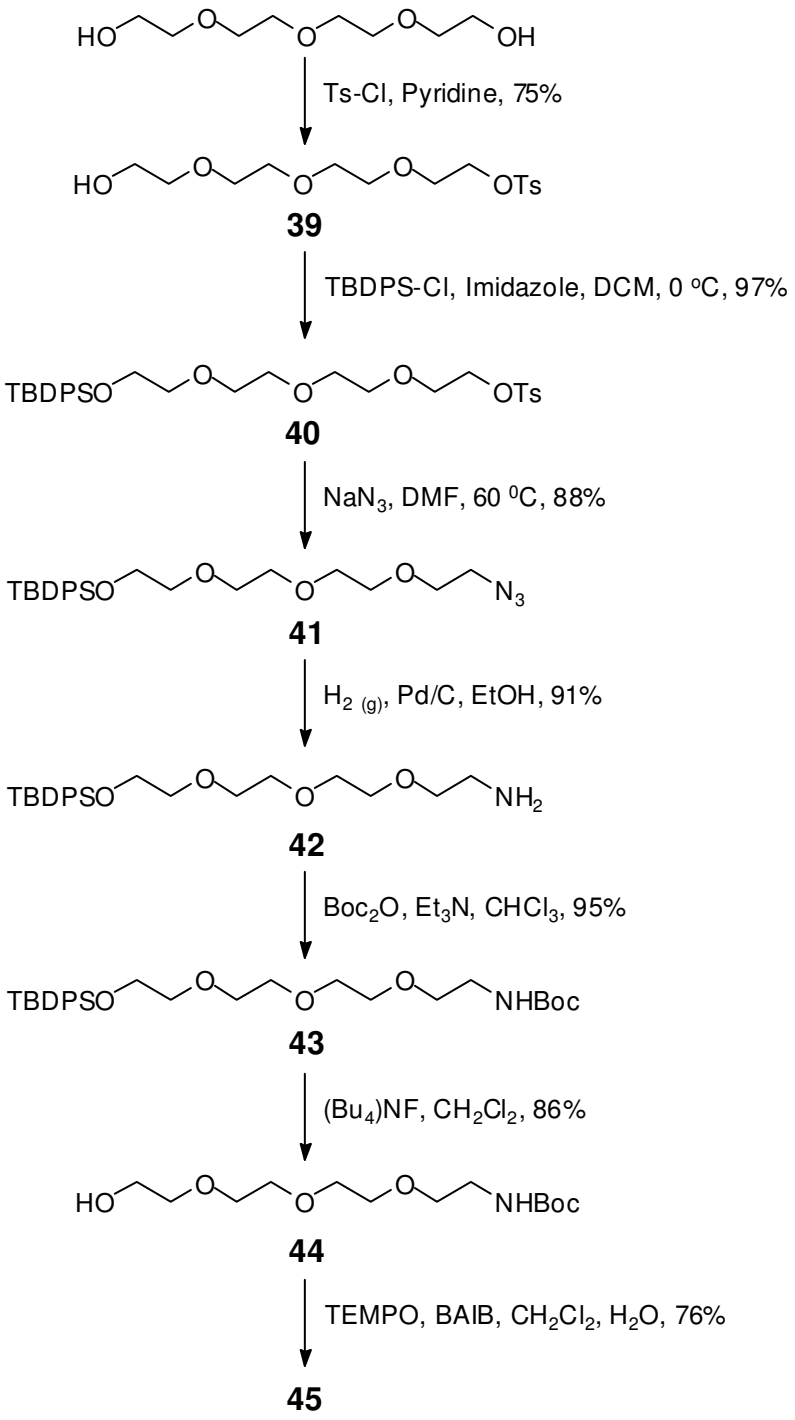

Scheme 24. Synthesis of tetraethylene glycol based linker fragment **45**

Synthesis of the T_F antigen fragment began with a boron trifluoride diethyletherate catalyzed glycosylation between imidate **46** [193] and 3-aminopropanol derivative **47** [194] in THF at -20 °C to yield glycoside **48** in 51% yield (**Scheme 25**). The desired α-glycosidic linkage was confirmed by ^{1}H NMR data (δ 5.02, d, *J* 3.5 Hz, H-1). Cleavage of the 3-*O* benzoyl (Bz) group was brought about by treatment with sodium methoxide in methanol to afford free hydroxyl **49** in 88% yield. The glycosylation of **49** with tetra-acetylgalactosyl bromide ($(Ac)_4$Gal-Br) in a 1:1 mixture of benzene and nitromethane at 40 °C was catalyzed by mercury cyanide and furnished the desired disaccharide **50** (**Scheme 21**) in 61% yield. The desired β-glycosidic linkage was again confirmed via ^{1}H NMR data (δ 4.76, d, *J* 8.0 Hz, H-1').

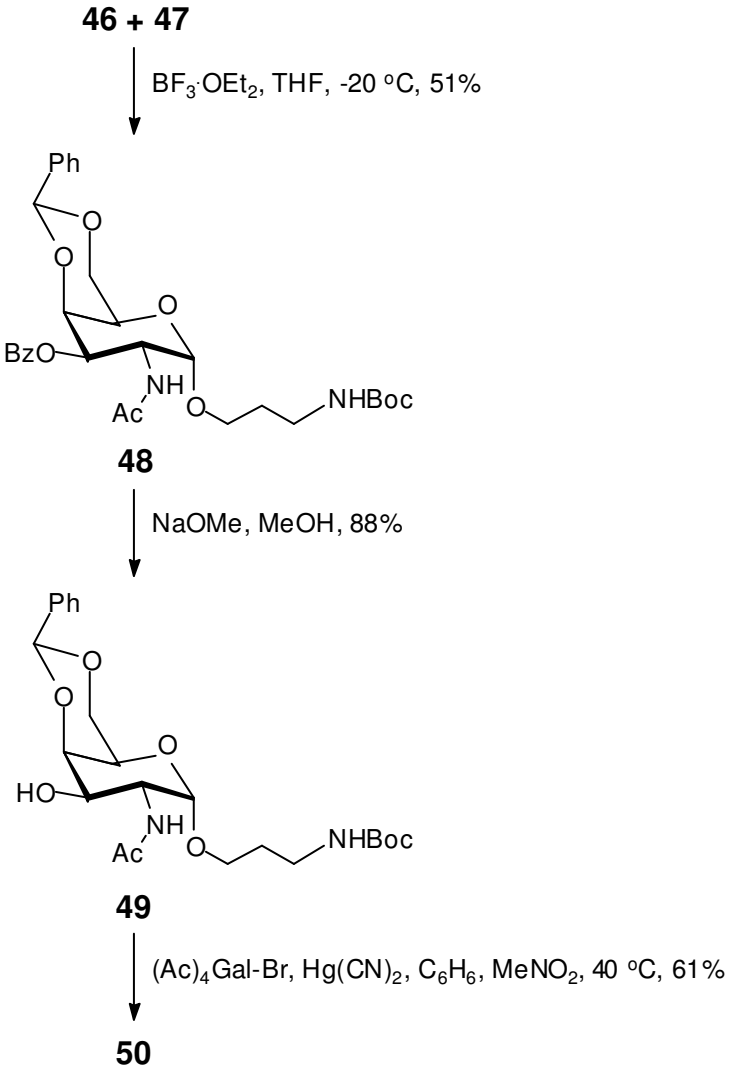

Scheme 25. Synthesis of T_F antigen based intermediate **50**

In attempting to chemically link disaccharide **50** and linker **45**, the Boc protecting group in **50** was first cleaved via treatment with trifluoroacetic acid in DCM, which also cleaved the benzylidene protecting group to yield intermediate **51** (**Scheme 26**). Multiple attempts at the conjugation of **51** with the *N*-hydroxysuccinimide (NHS) activated form of linker fragment **45** repeatedly produced a complicated mixture of product spots, as visualized by TLC. No attempts were made to isolate and characterize any of the product

spots, as this would likely have been an exercise in futility. It is believed that the free hydroxyls in **51** may have interfered with the formation of the desired amide linkage, however this is only speculative.

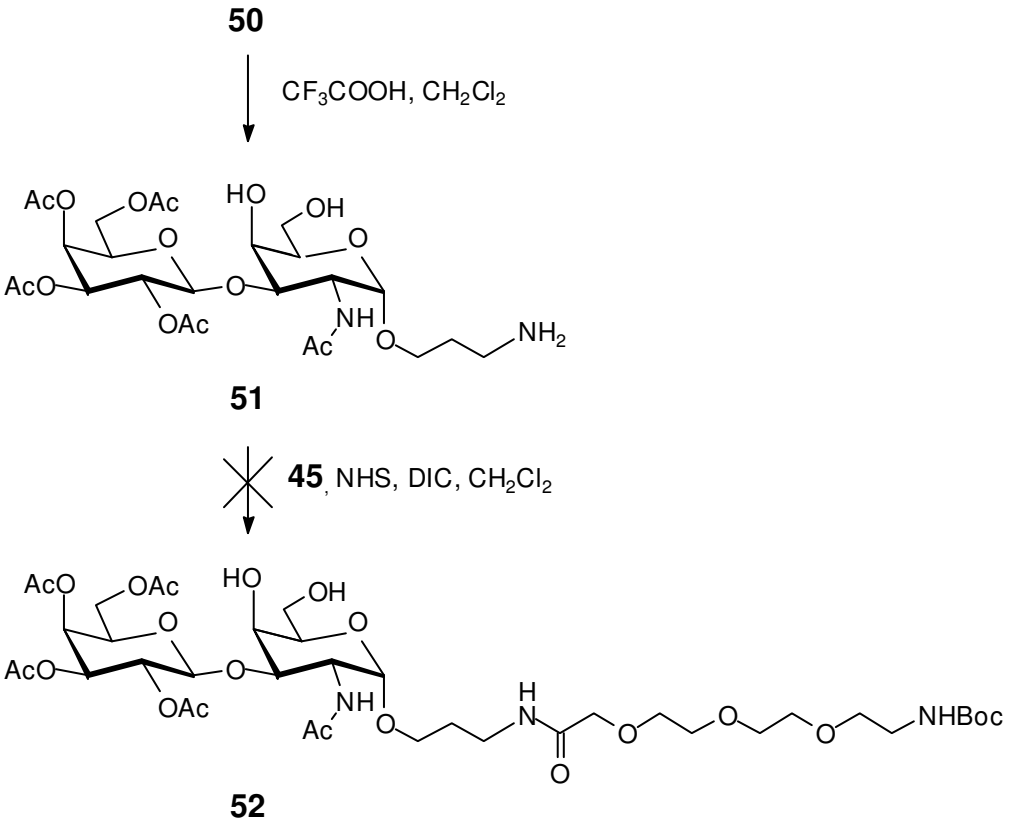

Scheme 26. Attempted synthesis of T_F antigen-linker conjugate **52**

Given the difficulties encountered in attempting to create the T_F antigen-linker conjugate **52** (**Scheme 26**), a revised synthetic strategy was adopted in which the coupling of the disaccharide and linker was to take place without the possibility of any interference from free hydroxyls. As such, disaccharide **50** was first subjected to a similar trifluoroacetic acid in DCM treatment to cleave both the Boc and benzylidene protecting groups (**Scheme 27**). The free amine in the resulting intermediate was then re-protected as the

Boc carbamate, via treatment with Boc_2O and triethylamine in a methanol and water medium. Finally, the remaining free hydroxyls were protected as their respective acetates to yield derivative **53** in an 82% overall yield via treatment with acetic anhydride and DMAP in pyridine. Deprotection of the amine was again brought about via treatment with trifluoroacetic acid in DCM, and the resulting intermediate was immediately coupled with linker fragment **45** under promotion of the peptide coupling reagents HBTU and diisopropylethylamine in DMF to yield antigen-linker conjugate **54** in 64% overall yield.

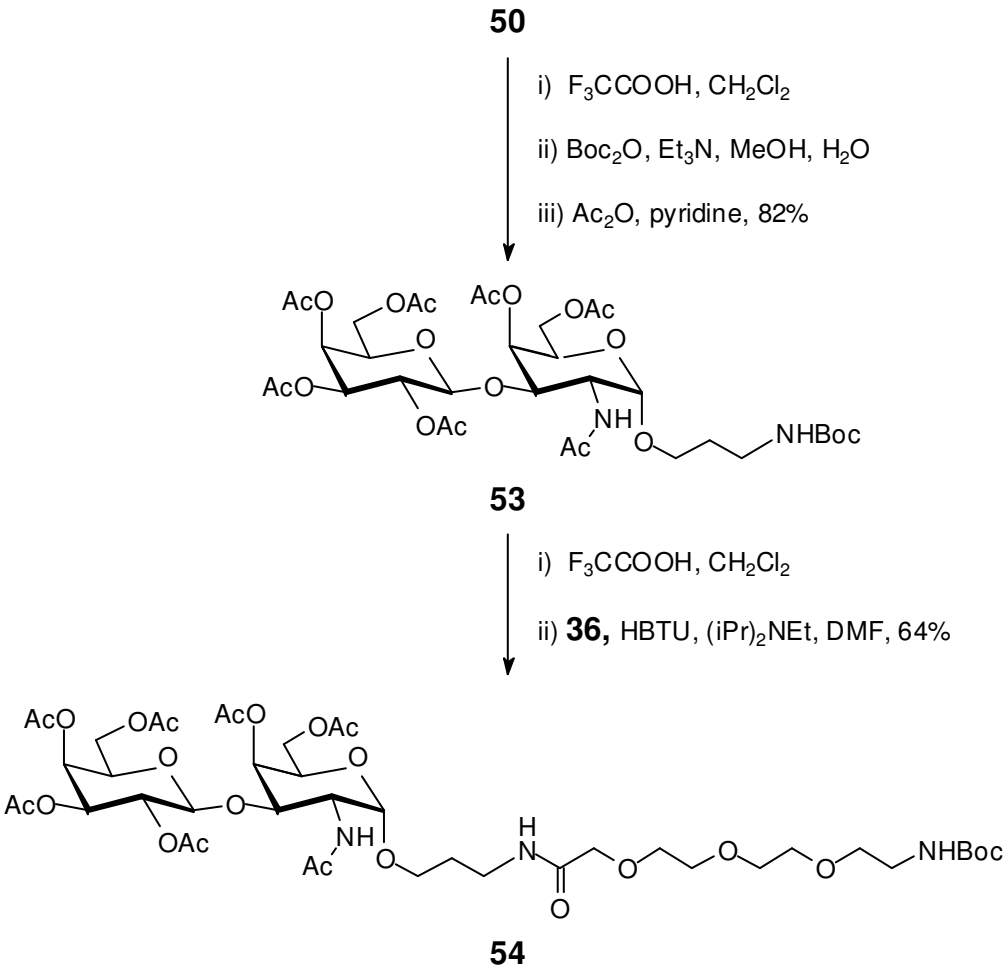

Scheme 27. Synthesis of T_F antigen-linker conjugate **54**

To couple the antigen-linker conjugate with the lipid A mimic fragment, conjugate **54** was first subjected to a sodium methoxide in methanol treatment to cleave all ester-bound acetate protecting groups. Following that, treatment with phosphoric acid in methanol cleaved the remaining Boc protecting group, and the resulting free amine was coupled with the terminal acidic moiety in lipid A mimic intermediate **28** (**Scheme 15**) under the promotion of the coupling reagent diisopropylcarbodiimide (DIC) in dimethyl sulfoxide (DMSO) to yield advanced intermediate **55** in 64% overall yield (**Scheme 28**). Deprotection of the remaining Bn protecting groups was brought about via hydrogenation over Pd/C in THF and acetic acid to yield antigen conjugate **38** in 88% yield.

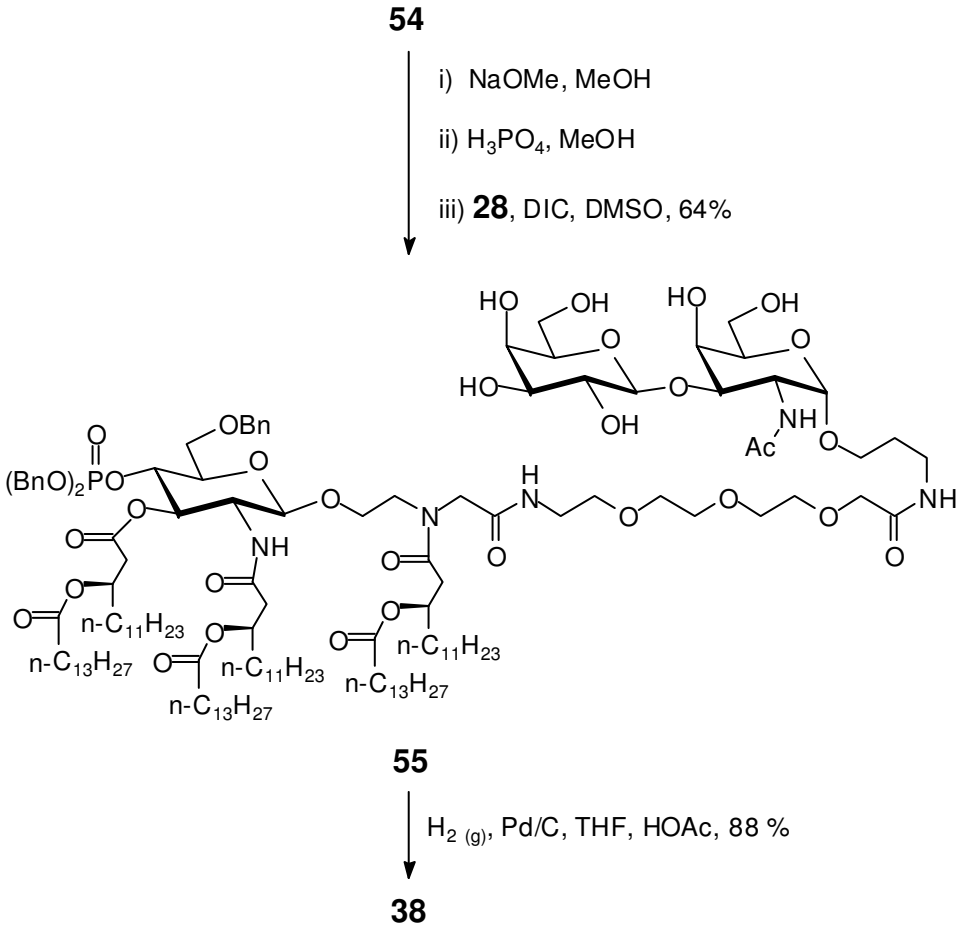

Scheme 28. Synthesis of synthetic vaccine construct **38**

4.4 Experimental

4.4.1 General methods

All air and moisture sensitive reactions were performed under nitrogen atmosphere. All commercial reagents were used as supplied. Anhydrous dichloromethane was distilled over calcium hydride, whereas anhydrous *N*,*N*-dimethylformamide (DMF) was purchased from Aldrich. ACS grade solvents were purchased from Fisher Scientific and used for chromatography without distillation. TLC plates (silica gel 60 F_{254}, thickness 0.25 mm) and silica gel 60 (40-63 μm) for flash column chromatography were purchased from SILICYCLE INC., Canada. ^{1}H and ^{13}C NMR spectra were recorded on a Varian Unity Inova 500 MHz spectrometer. Tetramethylsilane (TMS, δ 0.00 ppm) or solvent peaks were used as internal standards for ^{1}H and ^{13}C NMR spectra. The chemical shifts were given in ppm and coupling constants in Hz indicated to a resolution of ± 0.5 Hz. Multiplicity of proton signals is indicated as follows: s (singlet), d (doublet), dd (double doublet), t (triplet), q (quartet), m (multiplet), br (broad). Structural assignments were made using standard gCOSY and gHSQC methodology. NMR peaks belonging to primary lipid chains are denoted with an L subscript, whereas those belonging to secondary lipid chains are denoted with an L' subscript. MALDI mass spectra were measured on the Applied Biosystems Mariner 4700 system at the University of Western Ontario. Optical rotations were measured with Perkin Elmer 343 Polarimeter at 22°C.

4.4.2 11-tosyl-3,6,9-trioxaundecanol (39):

To a solution of tetraethylene glycol (5.00 g, 25.75 mmol) in pyridine (25 mL), tosyl chloride (6.14 g, 32.19 mmol) was added, and the resulting solution was allowed to stir at room temperature overnight. The reaction mixture was concentrated in vacuo, and purification via flash column chromatography followed (hexane/acetone, 1 : 1), and furnished **39** (6.42 g, 75%) as a colorless syrup. Rf 0.34 (hexane/acetone, 1 : 1); ^{1}H NMR (500 MHz, $CDCl_3$): δ 7.81-7.83 (m, 2H, Ar-H), 7.36-7.38 (m, 2H, Ar-H), 4.16-4.19 (m, 1H, OH), 3.61-3.74 (m, 14H, 7 x CH_2), 2.45-2.47 (m, 2H, CH_2OTs); ^{13}C NMR (125 MHz, $CDCl_3$): δ 144.86 (C-Ar), 132.95 (C-Ar), 129.86 (CH-Ar), 128.01 (CH-Ar), 72.47 (CH_2), 70.75 (CH_2), 70.67 (CH_2), 70.48 (CH_2), 70.34 (CH_2), 69.29 (CH_2), 68.72 (CH_2), 61.75 (CH_2OTs); MALDI-MS (m/z) Calcd for $C_{15}H_{24}O_6S$ $[M + K]^+$: 371.0931, found: 371.0740.

4.4.3 11-tosyl-1-*tert*-butyldiphenylsilyloxy-3,6,9-trioxaundecane (40):

To a cooled solution (ice-water bath) of **39** (1.67 g, 4.77 mmol) and imidazole (487 mg, 7.16 mmol), TBDPS-Cl (1.44 g, 5.25 mmol) was added and the reaction mixture was stirred at the reduced temperature. Upon consumption of the starting material, MeOH (1 mL) was added and the mixture was stirred for one hour before being concentrated. Purification via flash column chromatography (hexane/acetone, 3 : 1) afforded **40** (2.73 g, 97%) as a colorless syrup. Rf 0.31 (hexane/acetone, 3 : 1).

4.4.4 11-azido-1-*tert*-butyldiphenylsilyloxy-3,6,9-trioxaundecane (41):

A solution of **40** (2.5 g, 4.38 mmol) and sodium azide (427 mg, 6.57 mmol) in DMF (10 mL) was heated at 60 °C for 2 hours. The reaction mixture was concentrated, and then purified by flash column chromatography (hexane/acetone, 2 : 1 to afford **41** (1.76 g, 88%) as a colorless syrup. Rf 0.34 (hexane/acetone, 2 : 1); ^{1}H NMR (500 MHz, $CDCl_3$): δ 7.70-7.73 (m, 4H, Ar-H), 7.39-7.46 (m, 6H, Ar-H), 3.81-3.84 (m, 2H, CH_2OTBDPS), 3.61-3.70 (m, 12H, 6 x CH_2), 3.38-3.42 (m, 2H, CH2N3), 1.11 (s, 9H, $C(CH_3)_3$); ^{13}C NMR (125 MHz, $CDCl_3$): δ 135.68 (CH-Ar), 133.73 (C-Ar), 129.62 (CH-Ar), 127.66 (CH-Ar), 72.48 (CH_2), 70.81 (CH_2), 70.73 (CH_2), 70.06 (CH_2), 63.51 (CH_2OTBDPS), 50.70 (CH_2N_3), 26.82 ($C(\underline{C}H_3)_3$), 19.28 ($\underline{C}(CH_3)_3$); MALDI-MS (m/z) Calcd for $C_{24}H_{35}N_3O_4Si$ $[M + Na]^+$: 480.2295, found: 480.2538.

4.4.5 11-amino-1-*tert*-butyldiphenylsilyloxy-3,6,9-trioxaundecane (42):

A solution of **41** (1.60 g, 3.50 mmol) and Pd/C (100 mg) in EtOH (90%, 70 mL) was stirred under a hydrogen atmosphere (balloon) overnight. The Pd/C was filtered off and the remaining solution concentrated to afford **42** (1.37 g, 91%) as a colorless solid. Rf 0.38 ($CHCl_3$/MeOH/H_2O, 2 : 1 : 0.1).

4.4.6 11-*N*-(*tert*-butyloxycarbonyl)-amino-1-tert-butyldiphenylsilyloxy-3,6,9 trioxaundecane (43):

To a solution of **42** (1.3 g, 3.02 mmol) and Et_3N (1 mL) in $CHCl_3$ (20 mL), a solution of Boc_2O (987 mg, 4.53 mmol) in $CHCl_3$ (20 mL) was added drop wise over 10 minutes. The resulting solution was stirred at room temperature overnight before being concentrated. Purification via flash column chromatography (hexane/EtOAc, 2 : 1) afforded **43** (1.48 g, 95%) as a colorless syrup. Rf 0.37 (hexane/EtOAc, 2 : 1); ^{1}H NMR (500 MHz, $CDCl_3$): δ 7.67-7.70 (m, 4H, Ar-H), 7.36-7.44 (m, 6H, Ar-H), 5.01-5.04 (br m, 1H, NH), 3.80-3.82 (m, 2H, CH_2OTBDPS), 3.52-3.65 (m, 12H, 6 x CH_2), 3.28-3.31 (m, 2H, CH_2NHBoc), 1.44 (s, 9H, $C(CH_3)_3$ Boc), 1.05 ($C(CH_3)_3$ TBDPS); ^{13}C NMR (125 MHz, $CDCl_3$): δ 156.01 (C=O), 135.62 (CH-Ar), 133.69 (C-Ar), 129.64 (CH-Ar), 127.66 (CH-Ar), 79.05 ($\underline{C}(CH_3)_3$ Boc), 72.47 (CH_2), 70.81 (CH_2), 70.70 (CH_2), 70.59 (CH_2), 70.29 (CH_2), 70.21 (CH_2), 63.47 (CH_2OTBDPS), 40.38 (CH_2NHBoc), 28.46 ($C(\underline{C}H_3)_3$), 26.86 ($C(\underline{C}H_3)_3$), 19.22 ($\underline{C}(CH_3)_3$ TBDPS); MALDI-MS (m/z) Calcd for $C_{29}H_{45}NO_5Si$ $[M + Na]^+$: 554.2914, found: 554.3565.

4.4.7 11-*N*-(*tert*-butyloxycarbonyl)-amino-3,6,9-trioxaundecanol (44):

To a solution of **43** (500 mg, 0.94 mmol) in CH_2Cl_2 (4 mL), a solution of Bu_4NF in THF (1 M, 1.2 mL) was added and the resulting mixture was stirred at room temperature overnight. The mixture was then concentrated, and purified by flash column chromatography (hexane/acetone, 3 : 2) to afford **43** (224 mg, 86%) as a colorless syrup.

Rf 0.42 (hexane/acetone, 1 : 1); ^{1}H NMR (500 MHz, $CDCl_3$): δ 5.62-5.65 (br m, 1H, NH), 3.30-3.71 (m, 17H, 8 x CH_2, OH), 1.43 (s, 9H, $C(CH_3)_3$); ^{13}C NMR (125 MHz, $CDCl_3$): δ 156.19 (C=O), 78.92 ($\underline{C}(CH_3)_3$), 72.62 (CH_2), 70.59 (CH_2), 70.42 (CH_2), 70.23 (CH_2), 70.06 (CH_2), 61.60 (CH_2OH), 40.36 (CH_2NHBoc), 28.43 ($C(\underline{C}H_3)_3$); MALDI-MS (m/z) Calcd for $C_{13}H_{27}NO_5$ $[M + Na]^+$: 316.1736, found: 316.1674.

4.4.8 11-*N*-(*tert*-butyloxycarbonyl)-amino-3,6,9-trioxaundecanamide (45):

To a solution of **44** (200 mg, 0.72 mmol) in CH_2Cl_2 (2 mL) and water (0.3 mL), TEMPO (35 mg, 0.22 mmol) and BAIB (721 mg, 2.24 mmol) were added and the resulting mixture was stirred at room temperature for 1 hour. The mixture was the concentrated and purified by flash column chromatography (CH_2Cl_2/MeOH, 5 : 0.3) to afford **45** (159 mg, 76%) as a colorless syrup. Rf 0.37 (CH_2Cl_2/MeOH, 5 : 0.3); ^{1}H NMR (500 MHz, $CDCl_3$): δ 8.12-8.24 (br s, 1H, COOH), 5.20-5.22 (br m, 1H, NH), 4.15 (s. 2H, CH_2COOH), 3.53-3.76 (m, 12H, 6 x CH_2), 3.31-3.33 (m, 2H, CH_2NHBoc), 1.44 (s, 9H, $C(CH_3)_3$); ^{13}C NMR (125 MHz, $CDCl_3$): δ 173.12 (C=O), 156.24 (C=O Boc), 79.35 ($\underline{C}(CH_3)_3$), 70.95 (CH_2), 70.43 (CH_2), 70.29 (CH_2), 69.96 (CH_2), 68.98 (CH_2), 40.28 (CH_2NHBoc), 28.41 ($C(\underline{C}H_3)_3$); MALDI-MS (m/z) Calcd for $C_{13}H_{25}NO_6$ $[M + Na]^+$: 330.1529, found: 330.1417.

4.4.9 *N*-(*tert*-butyloxycarbonyl)-*N*-{3-[2-acetamido-3-*O*-benzoyl-4,6-*O*-benzylidene-2-deoxy-α-D-galactopyranosyloxy]-propyl}-amine (48):

To a solution of imidate **46** (2.58 g, 4.63 mmol) and 3-aminopropanol derivative **47** (2.03 g, 11.58 mmol) in THF (7 mL) with molecular sieves (4Å, 4.0 g) at -20 °C, a solution of BF_3•OEt_2 in THF (0.3 M, 2.3 mL) was added drop wise over 5 minutes. The mixture was allowed to stir at the reduced temperature for 1 hour before solids were filtered off. The remaining solution was diluted with CH_2Cl_2 (100 mL) and washed with a saturated sodium bicarbonate solution (30 mL), with the aqueous phase further extracted with CH_2Cl_2 (2 x 100 mL). The combined organic phase was dried over Na_2SO_4, concentrated, and purified by flash column chromatography (hexane/acetone, 2 : 1) to afford **48** (1.35 g, 51%) as a white fluffy solid. Rf 0.34 (hexane/acetone, 2 : 1); $[\alpha]_D^{22}$ +22.3 (*c* 1.0, $CHCl_3$); ^{1}H NMR (500 MHz, $CDCl_3$): δ 8.07-8.09 (m, 1H, Ar-H), 7.33-7.57 (m, 9H, Ar-H), 6.33 (d, 1H, *J* 6.5 Hz, NHAc), 5.55 (s, 1H, PHC*H*), 5.35 (dd, 1H, *J* 11.0, 3.5 Hz, H-3), 5.02 (d, 1H, *J* 3.5 Hz, H-1), 4.96-5.00 (m, 1H, H-2), 4.61-4.64 (br m, 1H, NHBoc), 4.49-4.52 (m, 1H, H-4), 4.09-4.30 (m, 2H, H-6A, H-6B), 3.80-3.84 (m, 2H, H-5, ROC*H*HCH$_2$CH$_2$NHBoc), 3.41-3.51 (m, 2H, ROCH*H*CH$_2$CH$_2$NHBoc, ROCH$_2$CH$_2$C*H*HNHBoc, 3.18-3.22 (m, 1H, ROCH$_2$CH$_2$CH*H*NHBoc), 1.95 (s, 3H, C(O)CH$_3$), 1.72-1.81 (m, 2H, ROCH$_2$C*H*$_2$CH$_2$NHBoc), 1.43 (s, 9H, C(CH$_3$)$_3$); ^{13}C NMR (125 MHz, $CDCl_3$): δ 170.59 (C=O, Ac), 166.85 (C=O, Bz), 156.22 (C=O, Boc), 137.71 (C-Ar), 133.30 (CH-Ar), 130.03 (CH-Ar), 129.59 (C-Ar), 128.48 (CH-Ar), 126.26 (CH-Ar), 100.66 (Ph<u>C</u>H), 98.34 (C-1), 79.18 (<u>C</u>(CH$_3$)$_3$), 73.62 (C-4), 70.78 (C-3), 69.33 (C-6), 64.55 (RO<u>C</u>H$_2$CH$_2$CH$_2$NHBoc), 62.73 (C-5), 47.28 (C-2), 36.87

(ROCH$_2$CH$_2$CH$_2$NHBoc), 30.04 (ROCH$_2$CH$_2$CH$_2$NHBoc), 28.39 (C(CH$_3$)$_3$), 23.22 (C(O)CH$_3$); MALDI-MS (m/z) Calcd for $C_{30}H_{38}N_2O_9$ [M + Na]$^+$: 593.2475, found: 593.3215.

4.4.10 *N*-(*tert*-butyloxycarbonyl)-*N*-{3-[2-acetamido-4,6-*O*-benzylidene-2-deoxy-α-D-galactopyranosyloxy]-propyl}-amine (49):

A solution of NaOMe in MeOH (0.5M, 0.8 mL) was added to a solution of **48** (1.3 g, 2.28 mmol) in MeOH (30 mL), and the resulting solution was stirred at room temperature for 3 hours. The reaction was then neutralized with weak acid resin IRC-64. Solids were filtered off, and the resulting solution concentrated. Purification via flash column chromatography (hexane/acetone/MeOH, 2 : 1 : 0.2) afforded **49** (936 mg, 88%) as a white fluffy solid. Rf 0.24 (hexane/acetone, 2 : 1); $[\alpha]_D^{22}$ + 18.7 (*c* 1.0, $CHCl_3$); ^{1}H NMR (500 MHz, $CDCl_3$): δ 7.52-7.54 (m, 2H, Ar-H), 7.34-7.38 (m, 3H, Ar-H; 7.05 (d, 1H, *J* 6.5 Hz, NHAc), 5.58 (s, 1H, PhC*H*), 4.87 (d, 1H, *J* 3.0 Hz, H-1), 4.60-4.62 (br m, 1H, NHBoc), 4.45-4.50 (m, 1H, H-2), 4.20-4.27 (m, 2H, H-4, H-6A), 4.07 (dd, 1H, *J* 12.5, 1.5 Hz, H-6B), 3.92-3.96 (m, 1H, H-3), 3.77-3.81 (m, 1H, H-5), 3.55-3.69 (m, 3H, ROC*H*HCH$_2$CH$_2$NHBoc, ROCH$_2$CH$_2$C*H*HNHBoc, OH), 3.36-3.40 (m, 1H, ROCH*H*CH$_2$CH$_2$NHBoc), 3.06-3.11 (m, 1H, ROCH$_2$CH$_2$CH*H*NHBoc), 2.11 (s, 3H, C(O)CH$_3$), 1.68-1.77 (m, 2H, ROCH$_2$C*H*$_2$CH$_2$NHBoc), 1.43 (s, 9H, C(CH$_3$)$_3$); ^{13}C NMR (125 MHz, $CDCl_3$): δ 173.12 (C=O, Ac), 156.45 (C=O, Boc), 137.82 (C-Ar), 128.96 (CH-Ar), 128.12 (CH-Ar), 126.39 (CH-Ar), 101.06 (PhCH), 98.19 (C-1), 79.20

($\underline{C}(CH_3)_3$), 75.64 (C-4), 69.72 (C-3), 69.34 (C-6), 63.90 ($RO\underline{C}H_2CH_2CH_2NHBoc$), 62.95 (C-5), 50.88 (C-2), 36.32 ($ROCH_2CH_2\underline{C}H_2NHBoc$), 30.05($ROCH_2\underline{C}H_2CH_2NHBoc$), 28.36 ($C(\underline{C}H_3)_3$), 22.88 ($C(O)CH_3$); MALDI-MS (m/z) Calcd for $C_{23}H_{34}N_2O_5$ $[M + Na]^+$: 489.2213, found: 489.2520.

4.4.11 *N*-(*tert*-butyloxycarbonyl)-*N*-{3-[2-acetamido-4,6-*O*-benzylidene-2-deoxy-3-*O*-(2,3,4,6-tetra-aceto-β-D-galactopyranosyl)-α-D-galactopyranosyloxy]-propyl}-amine (50):

A solution of **49** (850 mg, 1.82 mmol), tetra-acetylgalactosyl bromide (900 mg, 2.20 mmol), and mercury cyanide (504 mg, 2.00 mmol) in benzene (6 mL) and nitromethane (6 mL) was heated at 40 °C for 2 hours. The reaction mixture was then concentrated and purified by flash column chromatography (hexane/acetone, 1 : 1) to afford **50** (884 mg, 61%) as a white fluffy solid. Rf 0.33 (hexane/acetone, 1 : 1); $[\alpha]_D^{22}$ +35.5 (*c* 1.0, $CHCl_3$); ^1H NMR (500 MHz, $CDCl_3$): δ 7.52-7.56 (m, 2H, Ar-H), 7.31-7.40 (m, 3H, Ar-H), 6.21 (d, 1H, *J* 8.5 Hz, NHAc), 5.56 (s, 1H, PhC*H*), 5.37-5.39 (m, 1H, H-4'), 5.20-5.24 (m, 1H, H-2'), 4.98-5.01 (m, 1H, H-3'), 4.93-4.95 (br m, 1H, NHBoc), 4.90 (d, 1H, *J* 3.5Hz, H-1), 4.76 (d, 1H, *J* 8.0 Hz, H-1'), 4.66-4.72 (m, 1H, H-2), 4.04-4.30 (m, 5H, H-4, H-6A, H-6B, H-6A', H-6B'), 3.91-3.96 (m, 2H, H-3, H-5'), 3.68-3.84 (m, 2H, H-5, ROC*H*HCH_2CH_2NHBoc), 3.44-3.48 (m, 1H, ROCH*H*CH_2CH_2NHBoc), 3.18-3.32 ($ROCH_2CH_2CH_2NHBoc$), 1.98-2.17 (m, 15H, 5 x $C(O)CH_3$), 1.58-1.76 (m, 2H, $ROCH_2CH_2CH_2NHBoc$), 1.45 (s, 9H, $C(CH_3)_3$); ^{13}C NMR (125 MHz, $CDCl_3$): δ 170.35 (C=O, Ac), 170.33 (C=O, Ac), 170.27 (C=O, Ac), 170.21 (C=O, Ac), 170.09 (C=O, Ac),

170.03 (C=O, Ac), 169.49 (C=O, Ac), 156.17 (C=O, Boc), 137.76 (C-Ar), 128.78 (CH-Ar), 128.12 (CH-Ar), 126.26 (CH-Ar), 101.53 (C-1'), 100.69 (Ph<u>C</u>H), 98.19 (C-1), 79.31 (<u>C</u>$(CH_3)_3$), 75.71 (C-4), 74.92 (C-5), 70.95 (C-3'), 70.80 (C-3), 69.34 (C-6), 68.76 (C-2'), 66.97 (C-4'), 64.38 (RO<u>C</u>$H_2CH_2CH_2$NHBoc), 63.12 (C-5), 61.32 (C-6'), 48.16 (C-2), 36.93 (ROCH$_2$CH$_2$<u>C</u>H_2NHBoc), 29.98 (ROCH$_2$<u>C</u>H_2CH$_2$NHBoc), 28.41 (C(<u>C</u>$H_3)_3$), 23.36 (NHC(O)CH_3), 20.77 (C(O)CH_3), 20.73 (C(O)CH_3), 20.71 (C(O)CH_3), 20.58 (C(O)CH_3); MALDI-MS (m/z) Calcd for $C_{37}H_{52}N_2O_{17}$ $[M + Na]^+$: 819.3164, found: 819.4091.

4.4.12 *N*-(*tert*-butyloxycarbonyl)-*N*-{3-[2-acetamido-4,6-diaceto-2-deoxy-3-*O*-(2,3,4,6-tetra-aceto-β-D-galactopyranosyl)-α-D-galactopyranosyloxy]-propyl}-amine (53):

To a solution of **50** (500 mg, 0.63 mmol) in CH_2Cl_2 (4 mL), trifluoroacetic acid (2 mL) was added and the mixture was stirred at room temperature for 1 hr before being concentrated. The resulting residue was dissolved in MeOH (3 mL) and water (0.5 mL), and Et_3N (1 mL), and a solution of Boc_2O (205 mg, 0.94 mmol) in MeOH (3 mL) was added drop wise over 3 minutes. The resulting solution was allowed to stir at room temperature for 2 hours before being concentrated. The resulting residue was dissolved in pyridine (4 mL) and acetic anhydride (4 mL) was added. The solution was stirred overnight, concentrated, and purified by flash column chromatography (CH_2Cl_2/hexane/EtOAc/MeOH, 1 : 1 : 1 : 0.2) to afford **53** (388 mg, 82%) as a white fluffy solid. Rf 0.38 (CH_2Cl_2/hexane/EtOAc/MeOH, 1 : 1 : 1 : 0.2); $[\alpha]_D^{22}$ +33.4 (*c* 1.0,

$CHCl_3$); ^1H NMR (500 MHz, $CDCl_3$): δ 6.43 (d, 1H, *J* 8.5 Hz, NHAc), 5.33-5.37 (m, 1H, H-4'), 5.10-5.14 (m, 1H, H-4), 4.94-4.97 (m, 1H, H-2'), 4.81-4.85 (m, 1H, H-3'), 4.70-4.76 (br m, 2H, H-1, NHBoc), 4.60 (d, 1H, *J* 8.0 Hz, H-1'), 4.54-4.58 (m, 1H, H-2), 4.09-4.26 (m, 6H, H-5, H-6A, H-6B, H-6A', H-6B'), 3.87-3.96 (m, 2H, H-3, H-5'), 3.68-3.73 (m, 1H, ROC*H*HCH$_2$CH$_2$NHBoc), 3.44-3.48 (m, 1H, ROCH*H*CH$_2$CH$_2$NHBoc), 3.31-3.37 (m, 1H, ROCH$_2$CH$_2$C*H*HNHBoc), 3.19-3.23 (m, 1H, ROCH$_2$CH$_2$CH*H*NHBoc), 1.97-2.17 (m, 21H, NHC(O)CH$_3$, 6 x C(O)CH$_3$), 1.74-1.77 (m, 2H, ROCH$_2$C*H*$_2$CH$_2$NHBoc), 1.44 (s, 9H, C(CH$_3$)$_3$); ^{13}C NMR (125 MHz, $CDCl_3$): δ 171.25 (C=O, Ac), 170.68 (C=O, Ac), 170.45 (C=O, Ac), 170.34 (C=O, Ac), 170.25 (C=O, Ac), 169.69 (C=O, Ac), 156.31 (C=O, Boc), 100.88 (C-1'), 97.51 (C-1), 79.48 (C(CH$_3$)$_3$), 73.28 (C-5'), 70.78 (C-3'), 70.60 (C-3), 69.09 (C-4'), 68.56 (C-2'), 67.29 (C-5), 66.76 (C-4), 64.09 (ROCH$_2$CH$_2$CH$_2$NHBoc), 62.85 (C-6), 61.04 (C-6'), 48.80 (C-2), 36.77 (ROCH$_2$CH$_2$CH$_2$NHBoc), 29.78 (ROCH$_2$CH$_2$CH$_2$NHBoc), 28.34 (C(CH$_3$)$_3$), 23.12 (NHC(O)CH$_3$), 21.02 (C(O)CH$_3$), 20.88 (C(O)CH$_3$), 20.77 (C(O)CH$_3$), 20.74 (C(O)CH$_3$), 20.67 (C(O)CH$_3$), 20.65 (C(O)CH$_3$); MALDI-MS (m/z) Calcd for $C_{34}H_{52}N_2O_{19}$ [M + Na]$^+$: 815.3062, found: 815.4035.

4.4.13 *N*-(*tert*-butyloxycarbonyl)-*N*-{3-[2-acetamido-4,6-diaceto-2-deoxy-3-*O*-(2,3,4,6-tetra-aceto-β-D-galactopyranosyl)-α-D-galactopyranosyloxy]- propyl}-3,6,9-trioxaundecanamide (54):

To a solution of **53** (140 mg, 0.19 mmol) in CH_2Cl_2 (2 mL), trifluoroacetic acid (1 mL) was added and the resulting solution was stirred at room temperature for 1 hour before

being concentrated. The remaining residue was dissolved in DMF (1 mL) and added to a solution of **36** (75 mg, 0.24 mmol), HBTU (138 mg, 0.36 mmol), and (iPr)$_2$NEt (0.1 mL, 0.36 mmol) in DMF (2 mL). The resulting solution was stirred at room temperature overnight and then concentrated. Purification via flash column chromatography ($CHCl_3$/hexane/acetone/MeOH, 1 : 1 : 1 : 0.2) afforded **54** (117 mg, 64%) as a white fluffy solid. Rf 0.36 ($CHCl_3$/hexane/acetone/MeOH, 1 : 1 : 1 : 0.2); $[\alpha]_D^{22}$ +9.2 (*c* 1.0, $CHCl_3$); ^{1}H NMR (500 MHz, $CDCl_3$): δ 7.22-7.24 (br m, 1H, $ROCH_2CH_2CH_2NHC(O)R'$), 7.11 (d, 1H *J* 8.5 Hz, NHAc), 5.23-5.28 (m, 2H, H-4, H-4'), 5.09-5.13 (br m, 1H, NHBoc), 4.98-5.02 (m, 1H, H-2', 4.84-4.87 (m, 1H, H-3'), 4.67 (d, 1H, *J* 3.5 Hz, H-1), 4.60 (d, 1H, *J* 8.0 Hz, H-1'), 4.44-4.49 (m, 1H, H-2), 3.98-4.09 (m, 5H, H-5', H-6A, H-6B, H-6A', H-6B'), 3.78-3.94 (m, 4H, H-3, H-5, $ROCH_2CH_2CH_2NHC(O)CH_2R'$), 3.52-3.63 (m, 9H, $ROCHCH_2CH_2NHC(O)R'$, OCH_2 x 4), 3.42-3.44 (m, 3H, $ROCH_2CH_2CHNHC(O)R'$, $ROCH_2CH_2NHBoc$), 3.31-3.35 (m, 1H, $ROCHCH_2CH_2NHC(O)R'$), 3.17-3.23 (m, 3H, $ROCHCH_2CH_2NHC(O)R'$, $ROCH_2CH_2NHBoc$), 1.85-2.04 (m, 21H, $NHC(O)CH_3$, 6 x $C(O)CH_3$), 1.63-1.68 (m, 2H, $ROCH_2CH_2CH_2NHC(O)R'$), 1.32 (s, 9H, $C(CH_3)_3$); ^{13}C NMR (125 MHz, $CDCl_3$): δ 170.61 (C=O), 170.48 (C=O), 170.44 (C=O), 170.41 (C=O), 170.35 (C=O), 170.23 (C=O), 170.11 (C=O), 169.68 (C=O), 155.97 (C=O, Boc), 100.99 (C-1'), 97.65 (C-1), 79.38 ($\underline{C}(CH_3)_3$), 73.18 (C-5'), 70.97 ($ROCH_2CH_2CH_2NHC(O)\underline{C}H_2R'$), 70.81 (C-3'), 70.50 (C-3), 70.31 (OCH_2), 70.14 (OCH_2), 70.06 (OCH_2), 70.03 (OCH_2), 69.18 (C-4'), 68.51 (C-2'), 67.42 (C-5), 66.78 (C-4), 63.96 ($RO\underline{C}H_2CH_2CH_2NHC(O)R'$), 62.82 (C-6), 60.92 (C-6'), 48.68 (C-2), 40.27 ($ROCH_2\underline{C}H_2NHBoc$), 34.67 ($ROCH_2CH_2\underline{C}H_2NHC(O)R'$), 29.06 ($ROCH_2\underline{C}H_2CH_2NHC(O)R'$), 28.39 ($C(\underline{C}H_3)_3$), 23.07

(NHC(O)CH_3), 20.80 (C(O)CH_3), 20.71 (C(O)CH_3), 20.68 (C(O)CH_3), 20.57 (C(O)CH_3); MALDI-MS (m/z) Calcd for $C_{42}H_{67}N_3O_{22}$ $[M + K]^+$: 1004.3853, found: 1004.5851.

4.4.14 *N*-{*N*-3-(2-acetamido-2-deoxy-3-*O*-(β-D-galactopyranosyl)-α-D-galactopyranosyloxy]-propyl)-3,6,9-trioxaundecan-11-amide}-*N*-{2-[6-*O*benzyl-2-deoxy-4-*O*-(di-*O*-benzylphosphono)-3-*O*-((*R*)-3-tetradecanoyloxytetradecanoyl)-2-((*R*)-3-tetradecanoyloxytetradecanamido)-β-D-glucopyranosyloxy]-ethyl}-(*R*)-3-tetradecanoyloxytetradecanamide (55):

A solution of NaOMe in MeOH (0.5M, 0.1 mL) was added to a solution of **54** (124 mg, 0.128 mmol) in MeOH (5 mL), and the resulting solution was stirred at room temperature for 3 hours. The reaction was then neutralized with weak acid resin IRC-64. Solids were filtered off, and the resulting solution concentrated. The remaining residue was then dissolved in a solution of H_3PO_4 in MeOH (0.15 M, 2.0 mL) and allowed to stir at room temperature for a further 3 hours, upon which it was neutralized with Et_3N (0.2 mL) and concentrated. The resulting amine was combined with **28** (210 mg, 0.128 mmol) and dissolved in DMSO (2 mL). To the resulting solution, DIC (25 mg, 0.192 mmol) was added and the mixture allowed to stir overnight at room temperature. The mixture was then concentrated and purified via flash column chromatography (hexane/EtOAc/MeOH, 3 : 1 : 0.1) to afford **55** (209 mg, 64%) as a colorless syrup. Rf 0.33 (hexane/EtOAc/MeOH, 3 : 1 : 0.1); $[\alpha]_D^{22}$ +8.4(*c* 1.0, $CHCl_3$); ^{1}H NMR (500 MHz, $CDCl_3$): δ 7.87 (d, 1H *J* 8.5 Hz, N*H*Ac), 7.22-7.45 (m, 17H, C(O)N*H* x 2, Ar-H), 6.49-

6.54 (m, 1H, NH from lipid A mimic), 5.55 (dd, 1/3 H, *J* 9.5, 9.5 Hz, H-3 from one isomer of lipid A mimic), 5.43 (dd, 2/3 H, *J* 9.5, 9.5 Hz, H-3 from one isomer of lipid A mimic), 5.14-5.19 (m, 3H, H-3_L x 3), 4.85-4.92 (m, 5H, H-1 from lipid A mimic, $(PhCH_2O)_2P(O)$), 4.39-4.54 (m, 6H, $PhCH_2$, H-4 from lipid A mimic, H-1, H-1', H-2), 3.93-4.16 (m, 19H, OCH2 from lipid A mimic, $NCH_2C(O)NHR$ from lipid A mimic, H-2', H-3, H-3', H-4, H-4', H-5, H-5', H-6A, H-6B, H-6A', H-6B', H-5, $CH_2C(O)NHR$ x 2), 3.44-3.79 (m, 26H, H-2 from lipid A mimic, H-5 from lipid A mimic, H-6A from lipid A mimic, H-6B from lipid A mimic, CH_2N from lipid A mimic, 5 x OCH_2, OH x 6, ROC*H*$_2$$CH_2$C*H*$_2$NHC(O)R'), 2.14-2.72 (m, 12H, H-2_L x 6, H-$2_{L'}$ x 6), 1.47-1.61 (br m, 17H, H-4_L x 6, H-$3_{L'}$ x 6, $ROCH_2CH_2CH_2NHC(O)R'$, NHC(O)C*H*$_3$, 1.17-1.36 (br m, 114H, 57 x CH_2), 0.88 (t, 18H, J 6.5 Hz, 6 x CH_3); ^{13}C NMR (125 MHz, $CDCl_3$): δ 173.56 (C=O), 173.32 (C=O), 173.22 (C=O), 171.47 (C=O), 170.40 (C=O), 170.18 (C=O), 168.29 (C=O), 153.60 ($NHC(O)CH_3$), 138.02 (C-Ar), 135.58 (C-Ar), 135.53 (C-Ar), 128.56 (CH-Ar), 128.54 (CH-Ar), 128.31 (CH-Ar), 128.11 (CH-Ar), 128.07 (CH-Ar), 127.98 (CH-Ar), 127.58 (CH-Ar), 100.61 (CH), 99.91 (CH), 74.08 (CH), 73.35 (CH_2), 72.78 (CH), 72.28 (CH), 72.19 (CH), 71.74 (CH), 74.39 (CH),70.63 (CH), 70.32 (CH), 70.09 (CH), 69.91 (CH), 69.67 (CH_2), 69.63 (CH_2), 69.54 (CH_2), 69.50 (CH_2), 68.48 (CH_2), 68.21 (CH_2), 67.74 (CH_2), 67.61 (CH_2), 60.38 (CH_2), 55.19 (CH), 52.05 (CH), 50.04 (CH_2), 49.52 (CH_2), 47.30 (CH), 42.99 (CH), 41.43 (CH_2), 40.88 (CH_2), 39.25 (CH_2), 39.09 (CH_2), 37.86 (CH_2), 34.55 (CH_2), 34.45 (CH_2), 34.42 (CH_2), 34.29 (CH_2), 31.95 (CH_2), 29.73 (CH_2), 29.71 (CH_2), 29.65 (CH_2), 29.59 (CH_2), 29.53 (CH_2), 29.49 (CH_2), 29.42 (CH_2), 29.39 (CH_2), 29.32 (CH_2), 29.24 (CH_2), 29.21 (CH_2), 25.49 (CH_2), 25.25 (CH_2), 25.13 (CH_2), 25.05 (CH_2), 25.02 (CH_2), 22.71 (CH_2), 22.32

(NHC(O)$\underline{C}H_3$), 14.14 (CH_3); MALDI-MS (m/z) Calcd for $C_{140}H_{240}N_5O_{33}P$ $[M + Na]^+$: 2573.6891, found: 2573.6724.

4.4.15 *N*-{*N*-3-(2-acetamido-2-deoxy-3-*O*-(β-D-galactopyranosyl)-α-D-galactopyranosyloxy]-propyl)-3,6,9-trioxaundecan-11-amide}-*N*-{2-[2-deoxy- 4-*O*-phosphono-3-*O*-((*R*)-3-tetradecanoyloxytetradecanoyl)-2-((*R*)- 3-tetradecanoyloxytetradecanamido)-β-D-glucopyranosyloxy]-ethyl}-(*R*)-3-tetradecanoyloxytetradecanamide (38):

A solution of **55** (35 mg, 0.013 mmol) and palladium on charcoal (5% , 20 mg) in freshly distilled THF (45 mL) and acetic acid (5 mL) was stirred under a hydrogen atmosphere for 24 h. The solution was then filtered, concentrated, and purified by flash column chromatography ($CHCl_3$/MeOH, 8 : 1) to afford **38** (27 mg, 88%) as a white fluffy solid after being freeze dried from dioxane. Rf 0.41 ($CHCl_3$/MeOH, 8 : 1); $[\alpha]_D^{22}$ +6.3 (*c* 0.5, $CHCl_3$); ^{1}H NMR (500 MHz, $CDCl_3$): 5.32-5.45 (br m, 4H, H-3 from lipid A mimic, H-3_L x 3), 4.41-4.92 (br m, 5H, H-1 from lipid A mimic,H-4 from lipid A mimic, H-1, H-1', H-2), 3.93-4.28 (br m, 19H, OCH2 from lipid A mimic, $NCH_2C(O)$ from lipid A mimic, H-2', H-3, H-3', H-4, H-4', H-5, H-5', H-6A, H-6B, H-6A', H-6B', H-5, $CH_2C(O)R$ x 2), 3.36-3.84 (br m, 26H, H-2 from lipid A mimic, H-5 from lipid A mimic, H-6A from lipid A mimic, H-6B from lipid A mimic, CH_2N from lipid A mimic, 5 x OCH_2, OH x 6, ROC*H*$_2$CH$_2$C*H*$_2$NDC(O)R'), 2.09-2.73 (br m, 12H, H-2_L x 6, H-$2_{L'}$ x 6), 1.49-1.61 (br m, 17H, H-4_L x 6, H-$3_{L'}$ x 6, $ROCH_2C$*H*$_2$CH$_2$NDC(O)R', NDC(O)C*H*$_3$, 1.19-1.35 (br m,

114H, 57 x CH_2), 0.87 (t, 18H, J 6.5 Hz, 6 x CH_3) δ ; MALDI-MS (m/z) Calcd for $C_{119}H_{222}N_5O_{33}P$ $[M + Na]^+$: 2303.5483, found: 2303.5316.

5 SUMMARY

In relation to the primary goal of the current study, which was the design and synthesis of novel molecular frameworks to mimic the disaccharide structure of natural lipid A in the activation of the TLR4 receptor complex, significant strides have been made. Two novel lipid A mimic families were investigated, namely diethanolamine-containing and aromatic based lipid A mimics. In terms of the diethanolamine-containing lipid A mimic family, several structural variants were obtained and evaluated *in vitro* as immunostimulatory ligands of the TLR4 receptor complex. A direct correlation between the functionalization of the terminal ethanol hydroxyl and immunostimulatory potency was observed, with maximal potency noted with a terminal carboxylic acid as a phosphate bioisostere. The two members of the aromatic-based lipid A mimic family obtained were evaluated *in vivo* and display TLR4 stimulatory based adjuvant properties. Future studies will aim at generating further structural variants of these family of lipid A mimics, and ultimately examine their therapeutic potential.

In relation to the secondary goal of the current study, which was the construction of synthetic self-adjuvanting carbohydrate antigens, the adjuvant properties of the diethanolmine-containing lipid A mimic family were employed and a synthetic construct containing the T_F-carbohydrate and a diethanolamine-containing lipid A mimic was obtained. Future studies will examine the ability of the antigen to induce an immunological response and its potential use in therapeutic cancer vaccines.

6 REFERENCES

1) Schijns, V.E.J.C. *Crit. Rev. Immunol*. **2001**, *21*, 75.

2) Akira, S.; Uematsu, S.; Takeuchi, O. *Cell* **2006**, *124*, 783.

3) Martinon, F.; Burns, K.; Tschopp, *J. Mol. Cell*. **2002**, *10*, 417.

4) Shi, Y.; Evans, J.E.; Rock, K.L. *Nature* **2003**, *425*, 516.

5) Stuart, L.M.; Ezekowitz, R.A. *Immunity* **2005**, *22*, 539.

6) Luster, A.D.; Alon, R.; von Andrian, U.H. *Nat. Immunol*. **2005**, *6*, 1182.

7) Bowie, A.G.; Unterholzner, L. *Nat. Rev. Immunol*. **2008**, *8*, 911.

8) Burnet, A. *Aust. J. Sci*. **1957**, *20*, 67.

9) Hodgkin, P.D.; Heath, W.R.; Baxter, A.G.; *Nat. Immunol*. **2007**, *8*, 1019.

10) Loureiro, J.; Ploegh, H.L.; *Adv. Immunol*. **2006**, *92*, 225.

11) Chowdhury, D.; Lieberman, J. *Ann. Rev. Immunol*. **2008**, *26*, 389.

12) Bartee, E.; Mohamed, M.R.; McFadden, G. *Curr. Opin. Microbiol*. **2008**, *11*, 378.

13) Gourley, T.S.; Wherry, E.J.; Masopust, D.; Ahmed, R. *Semin. Immunol*. **2004**, *16*, 323.

14) Liu, Y.; Zhang, J.; Lane, P.J.; Chan, E.Y.; MacLennan, I.C. *Eur. J. Immunol.* **1991**, *21*, 2951.

15) Macpherson, A.J.; Gatto, D.; Sainsbury, E.; Harriman, G.R.; Hengartner, H.; Zinkernagel, R.M. *Science*, **2000**, *288*, 2222.

16) Sun, J.C.; Williams, M.A.; Bevan, M.J. *Nat. Immunol*. **2004**, *5*, 927.

17) Steinman, R.M.; Cohn, Z.A. *J. Exp. Med*. **1973**, *137*, 1142.

18) Joffre, O.; Nolte, M.A.; Sporri, R.; Reis e Sousa, C. *Immunol. Rev*. **2009**, *227*, 234.

19) O'Quinn, D.B.; Palmer, M.T.; Lee, Y.K.; Weaver, C.T. *Adv. Immunol*. **2008**, *99*, 115.

20) Vos, Q.; Lees, A.; Wu, Z.Q.; Snapper, C.M.; Mond, J. *Immunol. Rev*. **2000**, *176*, 154.

21) Fazilleau, N.; McHeyzer-Williams, L.J.; McHeyzer-Williams, M.G. *Curr. Opin. Immunol*. **2007**, *19*, 259.

22) Geeraedts, F.: Goutagny, N. Hornung, V.; Severa, M.; de Haan, A.; Pool, J. *PLos Pathog*. **2008**, *4*, 18.

23) Lambrecht, B.N.; Kool, M.; Willart, M.A.; Hammad, H. *Curr. Opin. Immunol*. **2009**, *21*, 23.

24) Lemaitre, B.; Nicolas, E.; Michauf, L.; Reichart, J.M.; Hoffman, J.A. *Cell* **1996**, *86*, 973.

25) Akira, S.; Takeda, K. *Nat. Rev. Immunol*. **2004**, *4*, 499.

26) Rock, F.L.; Hardiman, G.; Timas, J.C.; Kastelein, R.A.; Bazan, J.F. *Proc. Natl. Acad.* Sci. U.S.A. **1998**, *95*, 588.

27) Iwasaki, A.; Medzhitov, R. *Nat. Immunol*. **2004**, *5*, 987.

28) Meylan, E.; Tschopp, J.; Karin M. *Nature* **2006**, *442*, 39.

29) Leroux-Roels, G. *Vaccine* **2010**, *28*, 25.

30) Raetz, C.R.H.; Whitfield, C. *Ann. Rev. Biochem.* **2002**, *71*, 635.

31) Morrison, D.; Ryan J.; Bacterial Endotoxic Lipopolysaccharide, Molecular Biochemical and Cellular Biology, Vol. I; CRC Press: Boca Raton, FL, **1992**.

32) Janeway, C.A.; Medzhitov, R. *Ann. Rev. Immunol.* **2002**, *20*. 197.

33) Pffeifer, R. *Hygiene* **1892**, *11*, 393.

34) Westphal, U.; Lüderitz, O. *Z. Naturforsch*. **1952**, *7*, 548.

35) Hase, S.; Rietschel, E.T. *Eur. J. Biochem*. **1976**, *63*, 101.

36) Gmainer, J.; Westphal, U.; Lüderitz, O. *Eur. J. Biochem*. **1969**, *7*, 270.

37) Imoto, M.; Kusumoto, S.; Shiba, T.; Naoki, H.; Iwashita, T.; Rietschel, E.T.; Wollenweber, H.W.Z.; Galanos, C.; Lüderitz, O. *Tetrahedron Lett*. **1983**, *24*, 4017.

38) Imoto, M.; Yoshimura, H.; Sakaguchi, N.; Kusumoto, S.; Shiba, T. *Tetrahedron Lett*. **1985**, *26*, 1545.

39) Imoto, M.; Yoshimura, H.; Sakaguchi, N.; Kusumoto, S.; Shiba, T.; Shimamoto, T. *Bull. Chem. Soc. Jpn.* **1987**, *60*, 2205.

40) Galanos, C.; Lüderitz, O.; Rietschel, E.T.; Westphal, O.; Brade, L.; Freudenberg, M.; Schade, U.; Imoto, M.; Yoshimura, H.; Kusumoto, S.; Shiba, T. *Eur. J. Biochem.* **1985**, *148*, 1.

41) Yu, B.; Wright, S.D. *J. Biol. Chem*. **1996**, *271*, 4100.

42) Pugin, J.; Ulevitch, R.J.; Tobia, P.S. *J. Exp. Med*. **1993**, *178*, 2193.

43) Poltorak, A.; He, X.L.; Smirnova, I.; Liu, M.Y.; Van Huffel, C.; Du, X.; Birdwell, D.; Alejos, E.; Silva, M.; Galanos, C.; Freudenberg, M.; Ricciardi-Castagnoli, P.; Layton B.; Beutler, B. *Science* **1998**, *282*, 2085.

44) Shimazu, R.; Akashi, S.; Ogata, Y.; Nagai, Y.; Fukudome, K.; Miyake, K.; Kimoto, M. *J. Exp. Med.* **1999**, *189*, 1777.

45) O'Neill, L.A.J.; Bowie, A.G. *Nat. Rev. Immunol*. **2007**, *7*, 353.

46) Imoto, M.; Yoshimura, H.; Yamamoto, M.; Shimamotu, T.; Kusumoto, S.; Shiba, T. *Tetrahedron Lett.* **1984**, *25*, 2667.

47) Imoto, M.; Yoshimura, H.; Yamamoto, M.; Shimamotu, T.; Kusumoto, S.; Shiba, T. *Bull. Chem. Soc. Jpn*. **1983**, *60*, 2197.

48) Galanos, C.; Lehmann, V.; Lüderitz, O.; Rietschel, E.T.; Westphal, O.; Brade, H.; Brade, L.; Freudenberg, M.A.; Hansen-Hagge, T.; Lüderitz, T.; McKenzie, G.; Schade, U.; Stritmatter, W.; Tanamoto, K.; Zähringer, U.; Imoto, M.; Yoshimura, H.; Yamamoto, M.; Shimamtoto, T.; Kusumoto, S.; Shiba T. *Eur. J. Biochem*. **1984**, *140*, 221.

49) Loppnow, H.; Brade, L.; Brade, H.; Reitschel, E.T.; Kusumoto, S.; Shiba, T.; Flad, H.D. *Eur. J. Immunol.* **1986**, *16*, 1263.

50) Saitoh, S.; Akashi, S.; Yamada, T.; Tanimura, N.; Kobayashi, M.; Konno, K.; Fukase, K.; Kusumoto, S.; Nagai, Y.; Kusumoto, Y.; Kosugi, A.; Miyake, K.. *Int. Immunol*. **2004**, *16*, 961.

51) Visintin, A.; Halmen, K.A.; Latz, E.; Monks, B.G.; Golenbock, D.T. *J. Immunol*. **2005**, *175*, 6465.

52) Jiang, Z.-H.; Koganty, R.R. *Curr. Top. Med. Chem*. **2003**, *10*, 1423.

53) Wiemann, B.; Starnes, C.O. *Pharmacol. Ther*. **1994**, *64*, 529.

54) Shear, M.J.; Turner, F.C. *J. Natl. Cancer Inst*. **1943**, *4*, 81.

55) Garay, R.P.; Patrice, V.; Bauer, J.; Normier, G.; Bardou, M.; Jeannin, J.-F.; Chiavaroli, C. *Eur. J. Pharm*. **2007**, *563*, 1.

56) Umansky, V.; Schirrmacher, V. *Adv. Cancer Res*. **2001**, *82*, 107.

57) Lechner, M.; Lirk, P.; Rieder, J. *Semin. Cancer Biol*. **2005**, *15*, 277.

58) Dobrovolskaia, M.A.; Vogel, S.N. *Microbes Infect*. **2002**, *4*, 903.

59) Persing, D.H; Coler, R.N.; Lacy, M.J.; Johnson, D.A.; Baldridge, J.R.; Hershberg, R.M.; Reed, S.G. *Trends in Microbiology*. **2002**, *10*, 32.

60) Hajjar, A.M.; Ernst, R.K.; Tsai, J.H.; Wilson, C.B.; Miller, S.I. *Nat Immunol*. **2002**, *3*, 354.

61) Kusumoto, S.; Fukase, K.; Fukase, Y.; Kataoka, M.; Yoshizaki, H.; Sato, K.; Oikawa, M.; Suda, Y. *J. Endotoxin Res*. **2003**, *9*, 361.

62) Johnson, D.A.; Keegan, D.S.; Sowell, C.G.; Livesay, M.T.; Johnson, C.L.; Taubner, L.M.; Harris. A.; Myers, K.R.; Thompson, J.D.; Gustafson, G.L.; Rhodes, M.J.; Ulrich, J.T.; Ward, J.R.; Yorgenson, Y.M.; Cantrell, J.L.; Brookshire, V.G. *J. Med. Chem.* **1992**, *42*, 4640.

63) Stover, A.G.; Da Silva Correia, J.; Evans, J.T.; Cluff, C.W.; Elliott, M.W; Jeffrey E.W.; Johnson, D.A.; Lacy, M.J.; Baldridge, J.R.; Probst, P.; Ulevitch, R.J.; Persing D.H.; Hershberg, R.M. *J. Biol. Chem*. **2004**, *279*, 4440.

64) Rietshcel, E.T.; Kirikae, T.; Schade, F.U.; Mamat, U.; Schmidt, G.; Loppnow, H.; Ulmer, A.J.; Zähringer, U.; Seydel, U.; Di Padora, F. *FASEB J*, **1994**, *8*. 217.

65) Seydel, U.; Schromm, A.B.; Brade, L.; Gronow, S.; Andra, J.; Muller, M.; Koch, M.H.; Fukase, K.; Kataoka, M.; Hashimoto, M., Kusumoto, S.; Brandenburg, K. *FEBS J* **2005**, *272*, 327.

66) Ulmer, A.J.; Heine, H.; Feist, W.; Kusumoto, S. Kusama, T.; Brade, H.; Schade, U.; Rietschel, E.T. Flad, H.D. *Infect. Immun.* **1992**, *60*, 3309.

67) Ohto, U.; Fukase, K.; Miyake, K.; Satow, Y. *Science* **2007**, *316*, 1632.

68) Park, B.S.; Song, D.H.; Kim, H.M.; Choi, B.-S.; Lee, H.; Lee, J.-O. *Nature* **2009**, *458*, 1191.

69) Kobayashi, M.; Saitoh, S.; Tanimura, N.; Takahashi, K.; Kawasaki, K.; Nishijima, M.; Fujimoto, Y.; Fukase, K.; Akashi-Takamura, S.; Miyake. K. *J. Immunol*. **2006**, *176*, 621.

70) Jiang, Z.-H.; Budzynski, W.A.; Qiu, D; Yalamati, D; Koganty, R.R. *Carbohydr. Res*. **2007**, *342*, 784.

71) Evans, J.T.; Cluff, C.W.; Johnson, D.A.; Lacy, M.J.; Persing, D.H.; Baldridge, J.R. *Expert Rev. Vaccines*. **2003**, *2,* 219.

72) Mata-Haro, V; Cekic, C; Martin, M; Chilton, P.M.; Casella, C.R.; Mitchell, T.C. *Science*. **2007**, *316*, 1628.

73) Salkowski, C.A.; Detore, G.R.; Vogel, S.N. *Infect. Immun*. **1997**, *65*, 3239.

74) Okemoto, K.; Kawasaki, K.; Hanada, K.; Miura, M.; Nishijima, M. *J. Immunol*. **2006**, *176*, 1203.

75) Christ, W.J.; Asano, O; Robidoux, A.L.C.; Perez, M; Wang, Y.A.; Dubuc, G.R.; Gavin, W.E.; Hawkins, L.D.; Mcguiness, P.D.; Mullarkey, M.A.; Lewis, M.D.; Kishi, Y; Kawata, T; Bristol, J.R.; Rose, J.R.; Rossignol, D.P.; Kobayashi, S; Hishinuma, L; Kimura, A; Askawa, N; Katayama, K; Yamatsu, I. *Science*. **1995**, 268, 80.

76) Christ, W.J.; Asano, O; Robidoux, A.L.C.; Perez, M; Wang, Y.A.; Dubuc, G.R.; Gavin, W.E.; Hawkins, L.D.; Mcguiness, P.D.; Mullarkey, M.A.; Lewis, M.D.; Kishi, Y; Kawata, T; Bristol, J.R.; Rose, J.R.; Rossignol, D.P.; Kobayashi, S; Hishinuma, L; Kimura, A; Askawa, N; Katayama, K; Yamatsu, I. *Prog. Clin. Biol. Res*. **1995**, *392*, 499.

77) Kawata, T; Bristol, J.R.; Rossignol, D.P.; Rose, J.R.; Kobayashi, S; Yokohama, H; Ishibashi, A; Christ, W.J.; Katayama, K; Yamatsu, I; Kishi, Y. *Br. J. Pharmacol*. **1999**, *127*, 853.

78) Bunnel, E; Lynn, M; Habet, K; Neumann, A; Perdomo, C.A.; Friedhoff, L.T.; Rogers, S.L.; Parillo, J.E. *Crit. Care Med*. **2000**, *28*, 2713.

79) Qureshi, N; Honovich, J.P.; Hara, H; Cotter, R.J.; Takayama, K. *J. Biol. Chem*. **1998**, *263*, 5502.

80) Salimath, P.V.; Weckesser, J; Strittmatter, W; Mayer, H. *Eur. J. Biochem*. **1983**, *136*, 195.

81) Kalatshov, I.A.; Doroshenko, V; Cotter, R.J.; Takayama, K; Qureshi, N. *Anal. Chem*. **1997**, *69*, 2317.

82) Kim, H.M.; Park, B.S.; Kim, J.I.; Kim, S.E.; Lee, J; Oh, S.C.; Enkhbayar, P; Matsushima, N; Lee, H; Yoo, O.J.; Lee, J.O. *Cell*. **2007**, *130*, 906.

83) Brandenburg, K; Lindner, B.B.; Schromm, A; Koch, M.H.J.; Bauer, J; Merkli, A; Zbaeren, C; Davies, J.G.; Seydel, U. *Eur. J. Biochem*. **2000**, *267*, 3370.

84) Johnson, D.A. *Curr. Top. Med. Chem*. **2008**, *8*, 64.

85) Matsuura, M; Kiso, M; Hasegawa, A. *Infect. Immun*. **1999**, *67*, 6286.

86) Brandenburg, K; Matsuura, M; Kiso, M; Hasegawa, A; Nishimura, C; De Clercq, E. *J. Gen. Virol.* **1992**, *74*, 1399.

87) Bowen, S.W.; Minns, L.A.; Johnson, D.A.; Mitchell, T.C.; Hutton, M.M, Evans, J.T. *Science Signaling* **2012**, *5*, 1.

88) Jiang, Z.-H; Budzynski, W.A.; Skeels, L.N.; Krantz, M.J.; Koganty, R.R. *Tetrahedron* **2002**, *58*, 8833.

89) Ishizaka, S.T.; Hawkins, L.D. *Exp. Rev. Vaccines* **2007**, *6*, 773.

90) Morefield, G.L.; Hawkins, L.D.; Ishizaka, S.T.; Kissner, T.L.; Ulrich, R.G. *Clin Vaccine Immunol.* **2007**, *14*, 1499.

91) Martin, O.R.; Zhou, W.; Wu, X.; Front-Deschamps, S.; Moutel, S.; Schindl, K.; Jeandet, P.; Zbaeren, C.; Bauer, J.A. *J. Med. Chem*. **2006**, *49*, 6000.

92) Coley, W. Am. *J. Med. Sci*. **1893**, *105*, 487.

93) Finn, O.J. *Nat. Rev. Immunol*. **2003**, *3*, 630.

94) Ragupathi, C. *Cancer Immunol*. **1996**, *43*, 152.

95) Livingston, P.O.; Ragupathi, G. *Cancer Immunol. Immunother*. **1997**, *45*, 10.

96) Jones, P.C.; Sze, L.L.; Liu, P.Y.; Morton, D.L.; Irie, R.F. *J. Natl. Cancer Inst*. **1981**, *66*, 249.

97) Sinkovics, J.G.; Horvath, J.C. *Int. J. Oncol*. **2000**, *16*, 81.

98) Kruger, C.; Greten, T.F.; Korangy, F. *Histol. Histopathol*. **2007**, *22*, 687.

99) Ward, S.; Casey, D.; Labarthe, M.C.; Whelan, M.; Dalgleish, A.; Pandha, H.; Todryk, S. *Cancer Immunol. Immunother*. **2002**, *51*, 351.

100) Springer, G.F. *J. Mol. Med*. **1997**, *75*, 594.

101) Kim, Y.J.; Varki, A. *Glycoconjugate J*. **1997**, *14*, 569.

102) Hakomori, S. *Acta Anat*. **1998**, *161*, 79.

103) Brooks, S.A.; Carter, T.M.; Royle, L.; Harvey, D.J.; Fry, S.A.; Kinch, C.; Dwek, R.A.; Rudd P.M. *Anticancer Agents Med. Chem*. **2008**, *8*, 2.

104) Sewell, R.; Backstrom, M.; Dalziel, M.; Gschmeissner, S.; Karlsson H.; Noll, T.; Gatgens J.; Clausen, H.; Hansson G.C.; Burchell, J.; Taylor-Papadimitrou, J. *J. Biol. Chem*. **2006**, *281*, 3586.

105) Escrevente, C.; Machado, E.; Brito, C.; Reis, C.A.; Stoeck, A.; Runz, S.; Marme, A.; Altevogt, P.; Costa, J. *Int. J. Oncol*. **2006**, *29*, 557.

106) Serpa, J.; Mesquita, P.; Mendes, N.; Oliveira, C.; Almeida, R.; Santos-Silva, F.; Reis, C.A.; LePendu, J.; David, L. *Cancer Lett*. **2006**, *242*, 191.

107) Dwek, R.A. *Chem. Rev*. **1996**, *96*, 683.

108) Rudd, P.M.; Elliott, T.; Cresswell. P.; Wilson, I.A.; Dwek, R.A. *Science* **2001**, *291*, 2370.

109) Ohtsubo, K.; Marh, J.D. *Cell* **2006**, *126*, 855.

110) Flovin, S.F.; Kleding, S.J.; Ragupathi, G. *Immunol. Cell. Biol*. **2005**, *83*, 418.

111) Zhang, S.; Cordon-Cardo, C.; Zhang, H.S.; Reuter, V.E.; Adluri, S.; Hamilton, W.B.; Lloyd, K.O.; Livingston, P.O. *Int. J. Cancer* **1997**, *73*, 42.

112) Kobayashi, H.; Boelte, K.C.; Lin, P.C. *Curr. Med. Chem*. **2007**, *14*, 377.

113) Nudelman, E.; Levery, S.B.; Kaizu, T.; Hakomori, S. *J. Biol. Chem*. **1986**, *261*, 11247.

114) Kaizu, T.; Levery, S.B.; Nudelman, E.; Stenkamp, R.E.; Hakamori, S. *J. Biol. Chem*. **1986**, *261*, 11254.

115) Kim, Y.S.; Yuan, M.; Itzkowitz, S.H.; Sun, Q.; Kaizu, T.; Palekar, A., Trump, B.F.; Hakamori, S. *Cancer Res*. **1986**, *46*, 5985.

116) Hattrup, C.L.; Gendler, S.J.; *Annu. Rev. Physiol*. **2008**, *70*, 431.

117) Seeberger, P.H. *Chem. Soc. Rev*. **2008**, *37*, 19.

118) Bundle, D.R. *Nat. Chem. Biol*. **2007**, *3*, 604.

119) Cipolla, L.; Peri, F.; Airoldi, C.; *Anticancer Agents Med. Chem*. **2008**, *8*, 92.

120) Ragupathi, G.; Howard, L.; Cappello, S.; Koganty, R.R.; Qiu, D.; Longenecker, B.M.; Reddish, M.A.; Lloyd, K.O.; Livingston, P.O. *Cancer Immunol. Immunother*. **1999**, *48*, 1.

121) Kudryashov, V.; Glunz, P.W.; Williams, L.J.; Hintermann, S.; Danishefky, S.J.; Lloyd, K.O. *Proc. Natl. Acad. Sci. U.S.A.* **2001**. *98*. 3264.

122) Buskas, T.; Li. Y.H.; Boons, G.J. *Chem. Eur. J*. **2004**, 10, 3517.

123) Kagan, E.; Ragupathi, G.; Yi. S.; Reis, C.A.; Gildersleeve, J.; Kahne, D.; Clausen, H.; Danishefsky, S.J.; Livinsgton, P.O. *Cancer Immunol. Immunther*. **2005**, *54*, 424.

124) Helling, F.; Shang, Y.; Calves, M.; Ren. S.; Yu, R.K., Oettgen, H.F.; Livingston, P.O. *Cancer. Res*. **1994**, *54*, 197.

125) Toyukuni, T.; Dean, B.; Cai, S.P.; Boivin, D.; Hakomori, S.; Singhal, A.K. *J. Am. Chem. Soc*. **1994**, *116*, 395.

126) Toyukuni, T.; Hakomori, S.; Singhal, A.K. *Bioog. Med. Chem*. **1994**, *2*, 1119.

127) Glunz, P.W.; Hintermann, S.; Williams, L.J.; Schwarz, J.B.; Kuduk, S.D.; Kudryahsov, V.; Lloyd, K.O.; Danishefsky, S.J. *J. Am. Chem. Soc.* **2000**, *122*, 7273.

128) Glunz, P.W.; Hintermann, S.; Williams, L.J.; Schwarz, J.B.; Kuduk, S.D.; Chen, X.T.; Sames, D.; Kudryahsov, V.; Lloyd, K.O.; Danishefsky, S.J. *J. Am. Chem. Soc.* **1999**, *121*, 10636.

129) Reichel, F.; Ashton, P.R.; Boons, G.J. *Chem. Commun*. **1997**, 2087.

130) Buskas, T.; Ingale, S.; Boons, G.J. *Angew. Chem. Int. Ed*. **2005**, *44*, 5985.

131) Krikorian, D.; Panou-Pomonis, E.; Voitharou, C.; Sakarellos, C.; Sakarellos-Daitsiotis, M. *Bioconjugate Chem*. **2005**, *16*, 812.

132) Wang, Q.; Xue, J.; Guo, Z. *Chem. Commun*. **2009**, 5536.

133) Wang, Q; Zhou, Z.; Tang, S.; Guo, Z. *ACS Chem. Biol*. **2012**, *7*, 235.

134) Stöver, A.G.; Correia, J.D.S. Evans, J.T.; Cluff, C.W.; Elliott, M.W.; Jeffrey, E.W.; Johnson, D.A.; Lacy, M.J.; Baldridge, J.R.; Probst, P.; Ulevitch, R.J.; Persing, D.H.; Hershberg, R.M. *J. Biol. Chem*. **2004**, *6*, 4440.

135) Martin, O.R.; Zhou, W.; Wu, X.; Font-Deschamps, S.; Moutel, S.; Schindl, K.; Jeandet, P.; Zbaeren, C.; Bauer, J.A. *J. Med. Chem*. **2006**, *49*, 6000.

136) Jiang, Z.-H.; Budzynski, W.A.; Skeels, L.N.; Krants, M.J.; Koganty, R.R. *Tetrahedron* **2002**, *58*, 8833.

137) Lien, E.; Chow, J.C.; Hawkins, L.D.; McGuinness, P.D.; Miyake, K.; Espevik, T.; Susovsky, F.; Golenbock, D.D. *J.Biol. Chem.* **2001**, *276*, 1873.

138) Eustache, J.; Grob, A.; Retscher, H. *Carbohydr. Res*. **1994**, *251*, 251.

139) Bulusu, M.A.; Waldstatten, P.; Hildebrandt, J., Schutze, E.; Schulz, G. *J. Med. Chem.* **1992**, *35*, 3463.

140) Ikeda, K.; Asahara, T.; Achiwa, K. *Chem. Pharm. Bull*. **1993**, *41*, 1879.

141) Johnson, D.A.; Sowell, C.G.; Johnson, C.L.; Livesay, M.T.; Keegan, D.S.; Rhodes, M.J.; Ulrich, J.T.; Ward. J.R.; Cantrell, J.L.; Brookshire, V.G. *Bioorg. Med. Chem. Lett*. **1999**, *9*, 2273.

142) Kusumoto, S.; Fukase, K.; Fukase, Y.; Kataoka, M.; Yoshizaki, H.; Sato, K,; Oikawa, M.; Suda, U. *J. Endotoxin Res*. **2003**, *9*, 361.

143) Kiso, M.; Tanaka, S.; Fujita, M.; Fujishima, Y.; Ogawa, Y.; Hasagawa, A. *Carbohydr. Res*. **1987**, *162*, 247.

144) Lewicky, J.D.; Ulanova, M.; Jiang, Z.-H. *Carbohydr. Res*. **2011**, *346*, 1705.

145) Matsuo, Y.; Iwashita, A.; Oyama, H.; Nakamura, E. *Tetrahedron Lett*. **2009**, *50*, 3411.

146) Olah, G.A.; Wang, Q.; Li, X.; Rasul, G.; Prakash, G.K.S. *Macromolecules* **1996**, *29*, 1857.

147) Akhrem, I.S.; Avetisvan, D.V.; Vitt, S.V.; Petrovskii, P.V. *Mendeleev Commun.* **2005**, *15*, 185.

148) van Renterghem, L.M.; Goethals, E.J.; Du Prez, F.E. *Macromolecules*, **2006**, *39*, 528.

149) Stanssens, D.; Hermanns, R.; Wories, H. *Prog. Org. Coat*. **1993**, *22*, 379.

150) van Benthem, R.A.T.M.; Neijerink, N.; Gelade, E.; de Koster C.G.; Muscat, D.; Froehling, P.E.; Hendriks, P.H.M.; Vermsulen C.J.A.A.; Zwartkruis, T.J.G. *Macromolecules* **2001**, *34*, 3559.

151) Wicks, Z.W. Jr.; Chiang, N.C.J. *Coat. Technol*. **1982**, *54*, 27.

152) Lomax, J.; Swift, G.J. *Coat. Technol*. **1982**, *50*, 49.

153) Jiang, Z.-H.; Budzynski, W.A.; Skeels, L.N.; Krantz, M.J.; Koganty, R.R. *Tetrahedron* **2002**, *58*, 8833.

154) Jiang, Z.-H., Budzynski, Bach, M.V.; Budzynski, W.A.; Krantz, M.J.; Koganty, R.R.; Longenecker, B.M. *Bioorg. Med. Chem. Lett*. **2002**, *12*, 2193.

155) Jiang, Z.-H.; Xu, R.; Wilson, C.; Brenk, A. *Tetrahedron Lett*. **2007**, *48*, 2915.

156) Kalluri, M.D.; Datla, P.; Bellary, A.; Basha, K.; Sharma, A.; Singh, S.; Upadhyay, S.; Rajagopal V. *FEBS J.* **2010**, *277*, 1639.

157) Lee, S.H.; Jun, H.K.; Lee, H.R.; Chung, C.P.; Choi, B.K. *Int. J. Antimicrob. Agents*. **2010**, *35*, 138.

158) Luk, J.M.; Lai, W.; Tam P.; Koo M.W. *Life Sci*. **2000**, *67*, 155.

159) Roebuck, K.A.; Finnegan A. *J. Leukocyte Biol*. **1999**, *66*, 876.

160) Jahnke, A. van de Stolpe, A.; Caldenhoven, E.; Johnson, J.P. *Eur. J. Biochem*. **1995**, *228*, 439.

161) Takashiba, S.; van Dyke, T.E.; Amar, S.; Murayama, Y.; Soskolne, A.W.; Shapira, L. *Infect. Immun*. **1999**, *67*, 5573.

162) Park, E.K, Jung, H.S.; Yang, H.I.; Yoo, M.C.; Kim, C.; Kim, K.S. *Inflammation Res.* **2007**, *56*, 45.

163) van de Veerdonk, F.L.; Netea, M.G.; Dinarello, C.A.; Joosten, L.A. *Trends Immunol.* **2011**, *32*, 110.

164) Dinarello, C.A. *Blood* **1996**, *97*, 2095.

165) Latz, E. *Curr. Opin. Immunol*. **2010**, *22*, 28.

166) Rietschel, E.T.; Kirikae, T.; Schade, F.U,; Mamat, U.; Schmidt, G.; Loppnow, H.; Ulmer, A.J.; Zahringer, U.; Seydel, U.; Di Padova, F.; Schreier, M.; Brade, H. *FASEB J*. **1994**, *8*, 217.

167) Ulmer, A.J.; Heine, H.; Feist, W.; Kusumoto, S.; Kusama, T.; Brade, H.; Schade, U.; Rietschel, E.T.; Flad, H.D. *Infect. Immun*. **1992**, *60*, 3309.

168) Kataoka, M.; Hashimoto, M.; Suda, Y.; Kusumoto, S.; Fukase, S. *Heterocycles* **2006**, *69*, 395.

169) Dullenkopf, W.; Castro-Palomino, J.C.; Manzoni, L.; Schmidt, R.R. *Carbohydr. Res.* **1996**, *296*, 135.

170) Ellervik, U.; Magnusson, G. *Tetrahedron Lett*. **1997**, *38*, 1627.

171) O'Sullivan, M.C.; Dalrymple, D.M. *Tetrahedrom Lett*. **1995**, *36*, 3451.

172) Kim, T.H.; Yang, G.-Y. *Tetrahedron Lett*. **2002**, *43*, 9553.

173) Chen, F.; Kuhn, D.C.; Gaydos, L.J.; Demers, L.M. *APMIS* **1996**, *104*, 176.

174) Golenbock, D.T.; Hampton, R.Y.; Qureshi, N.; Takayama, K.; Raetz, C.R. *J. Biol. Chem.* **1991**, *266*, 19490.

175) Meyer, E.A.; Castellano, P.K. *Angewandte Chemie* **2003**, *42*, 1210.

176) Feltkamp, M.C.; Smits, H.L.; Vierboom, M.P.; Minnaar, R.P.; de J.B.M; Drifjhout, J.W.; ter Schegget, J.; Melief, C.J.; Kast, W.M. *Eur. J. Immunol*. **1993**, *23*, 2242.

177) Karkada, M.; Quinton, T.; Weir, G.; Debay, D.; Leblanc, S.; Bowen, C.; Monsour, M. *J. Immunother*. **2011**, *33*, 883.

178) Campbell, B.J.; Finnie, I.A.; Hounsell, E.F.; Rhodes. J.M. *J. Clin. Invest.* **1995**, *95*, 571.

179) Springer, G.F. *Science* **1984**, *224*, 1198.

180) Hanisch, F.G.; Baldus, S.E. *Histol. Histopathol*. **1997**, *12*, 263.

181) Moriyama, H.; Nakano, H.; Iqawa, M.; Nihira, H. *Urol. Int*. **1987**, *42*, 120.

182) Wolf, M.F.; Ludwig, A.; Fritz, P.; Schumacher, K. *Tumour Biol*. **1988**, *9*, 190.

183) Samuel, J.; Longenecker, B.M. *Pharm. Biotechnol*. **1995**, *6*, 875.

184) Adluri, S.; Helling, F.; Ogata, S.; Zhang, S.; Itzkowitz, S.H.; Lloyd, K.O.; Livingston, P.O. *Cancer Immunol. Immunother*. **1995**, *41*, 185.

185) MacLean, G.D.; Bowen-Yacyshyn, M.B.; Samuel, J.; Meikle, A.; Stuart, G.; Nation, J.; Poppenma, S.; Jerry, M.; Koganty, R.; Wong, T. *J. Immunol*. **1992**, *11*, 292.

186) Yacyshyn, M.B.; Poppema, S.; Berg, A.; MacLean, G.D.; Reddish, M.A.; Meikle A.; Longenecker, B.M. *Int. J. Cancer* **1995**, *61*, 470.

187) Slovin, S.F.; Ragupathi, G.; Mussselli, C.; Fernandez, C.; Diani, M.; Verbel, D.; Danishefsky, S.; Livingston, P.; Scher, H.I. *Cancer Immunol. Immunother*. **2005**, *54*, 694.

188) Ragupathi, G. *Cancer Immunol. Immunother*. **1996**, *43*, 152.

189) Springer, G.F. *J. Mol. Med*. **1997**, *75*, 594.

190) Desai, P.R.; Ujjainwala, L.H.; Carlstedt, S.C.; Springer, G.F. *J. Immunol. Methods* **1995**, *188*, 75.

191) Xu. Y.; Gendler, S.J.; Franco, A. *J. Exp. Med*. **2004**, *99*, 707.

192) Kurtenkov, O.; Klaamas, K.; Rittenhouse-Olson, K.; Vahter, L.; Sergejev, B.; Miljukhina, L.; Shljapnikova, L. *Exp. Oncol*. **2005**, *27*, 136.

193) Yule, J.E.; Wong, T.C.; Gandhi, S.S.; Qiu, D.; Riopel, M.A.; Koganty, R.R. *Tetrahedron Lett*. **1995**, *36*, 6839.

194) Ju, M.; Gong, F.; Chang, S.; Gua, Y. *Int. J. Polymer Sci*. **2011**, 16, *198*.

7 Appendix: Spectral Analyses

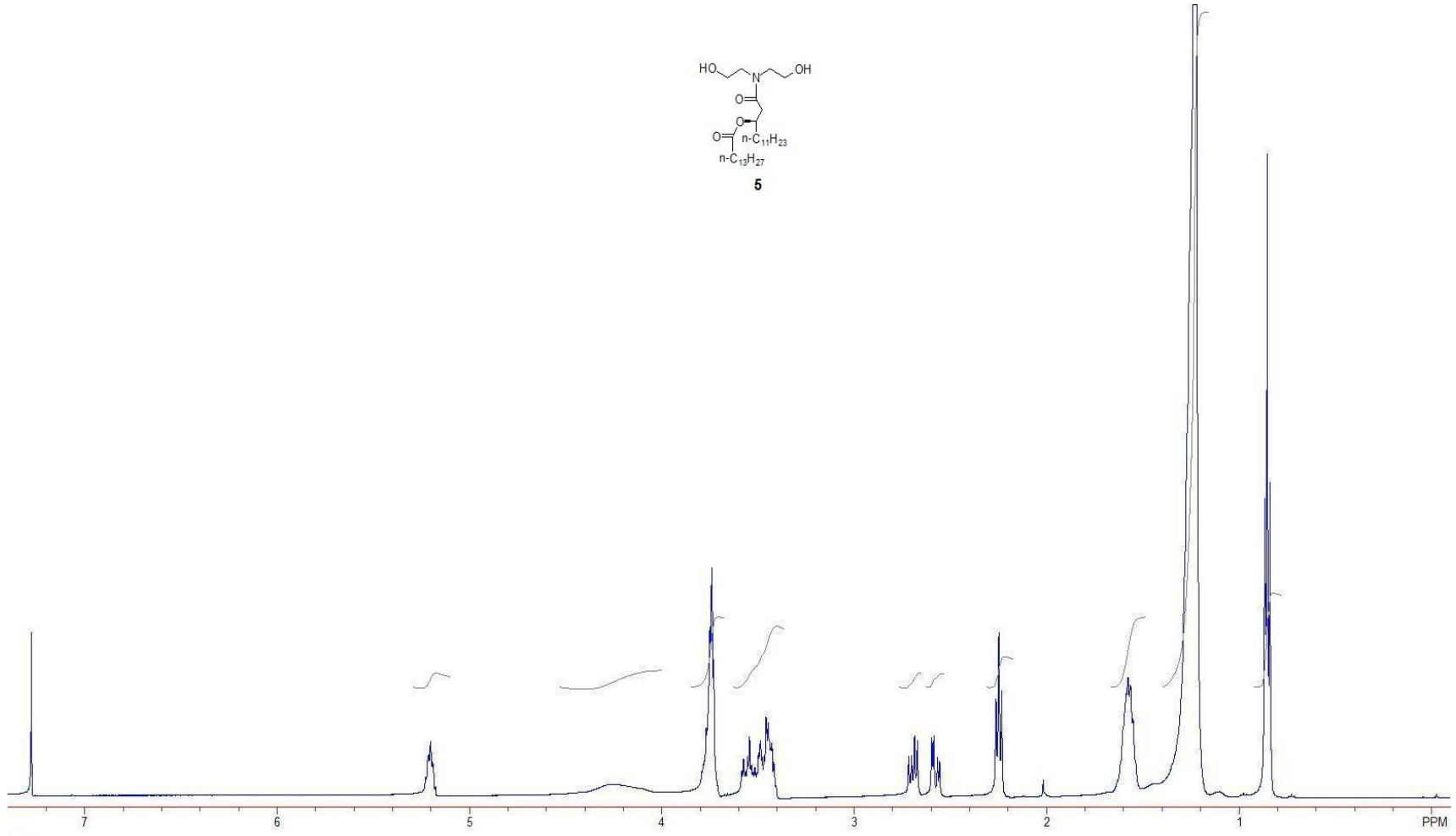
HO
N
OH
O
O
O
n-C11H23
n-C13H27
5
7
6
5
4
3
2
1
PPM

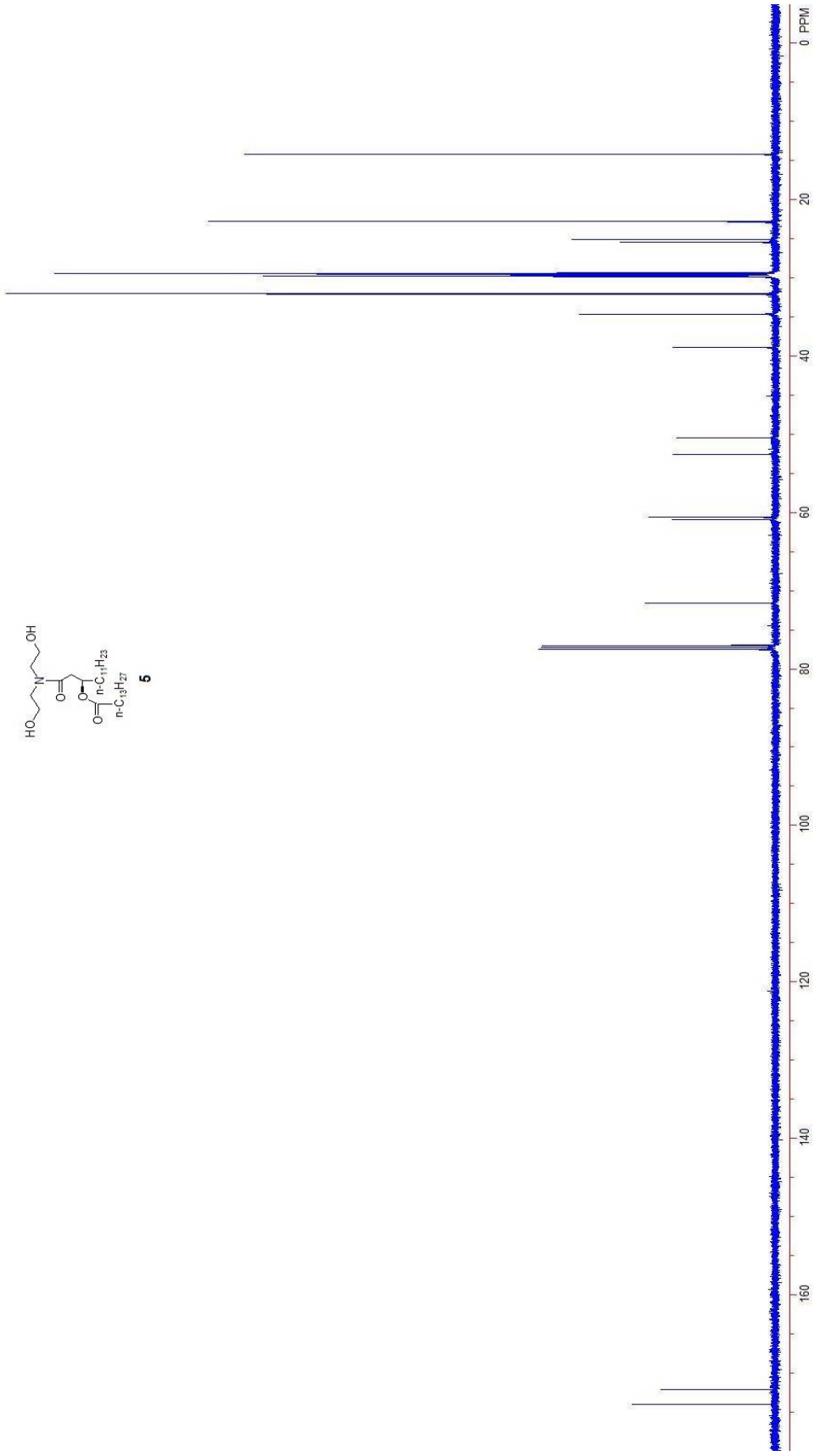
HO
OH
N
O
O
O
n-C11H23
n-C13H27
5
0 PPM
20
40
60
80
100
120
140
160

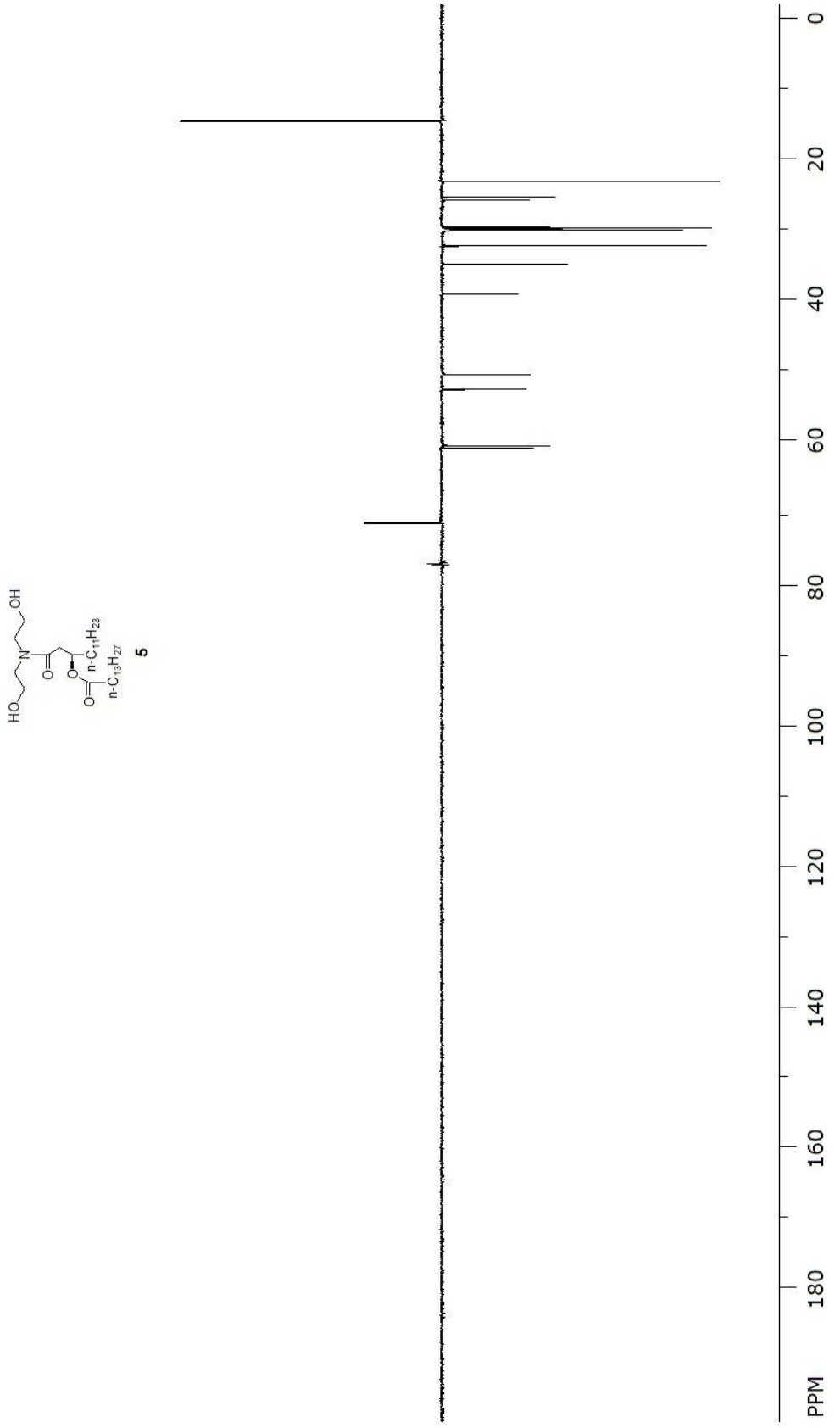
HO
OH
N
O
O
O
n-C11H23
n-C13H27
5
PPM
0
20
40
60
80
100
120
140
160
180

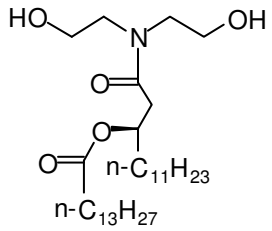

5

HRESI-MS (*m*/*z*) Calcd for $C_{32}H_{63}NO_5Na$ $[M+Na]^+$: 564.4587, found: 564.4588.

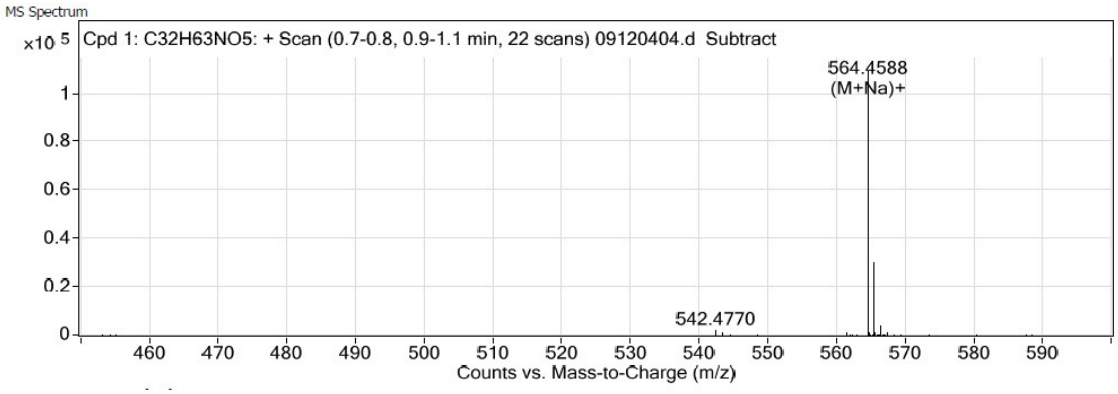

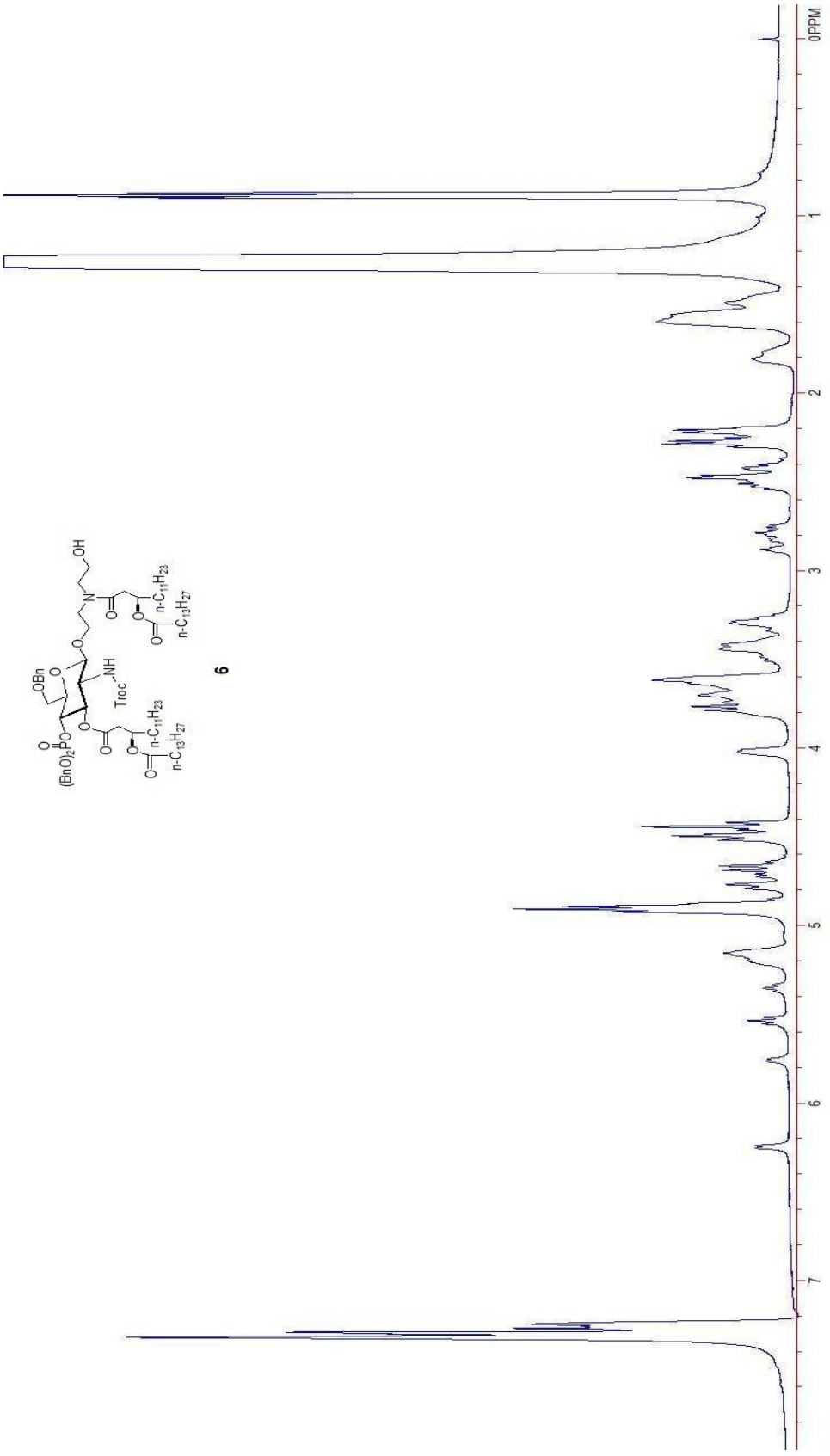
OBn
O
(BnO)2P
O
O
O
NH
Troc
O
O
O
N
OH
O
O
n-C11H23
n-C13H27
O
O
n-C11H23
n-C13H27
6
0PPM
1
2
3
4
5
6
7

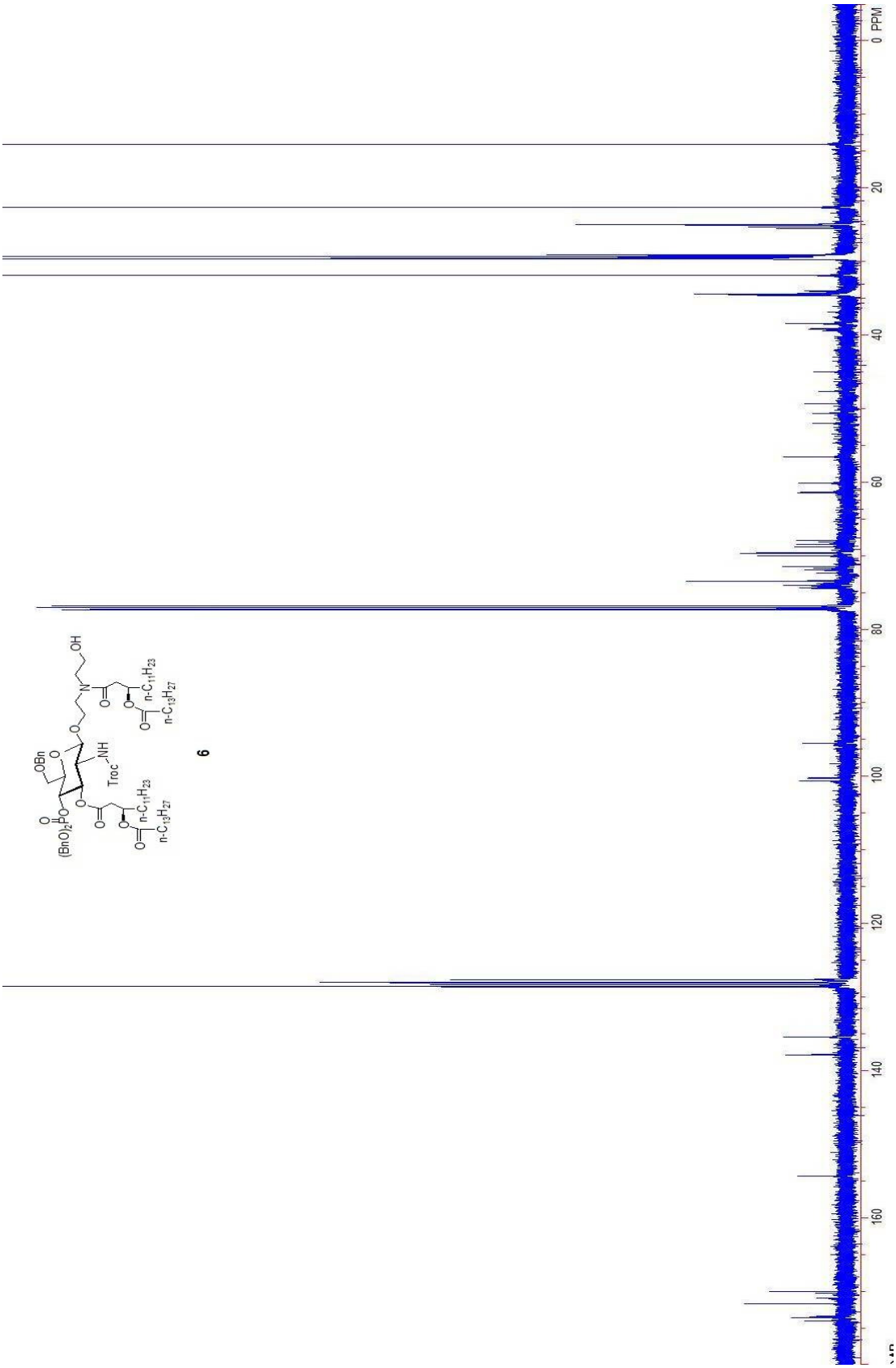
OBn
Troc
NH
OH
n-C11H23
n-C13H27
6
0 PPM
20
40
60
80
100
120
140
160

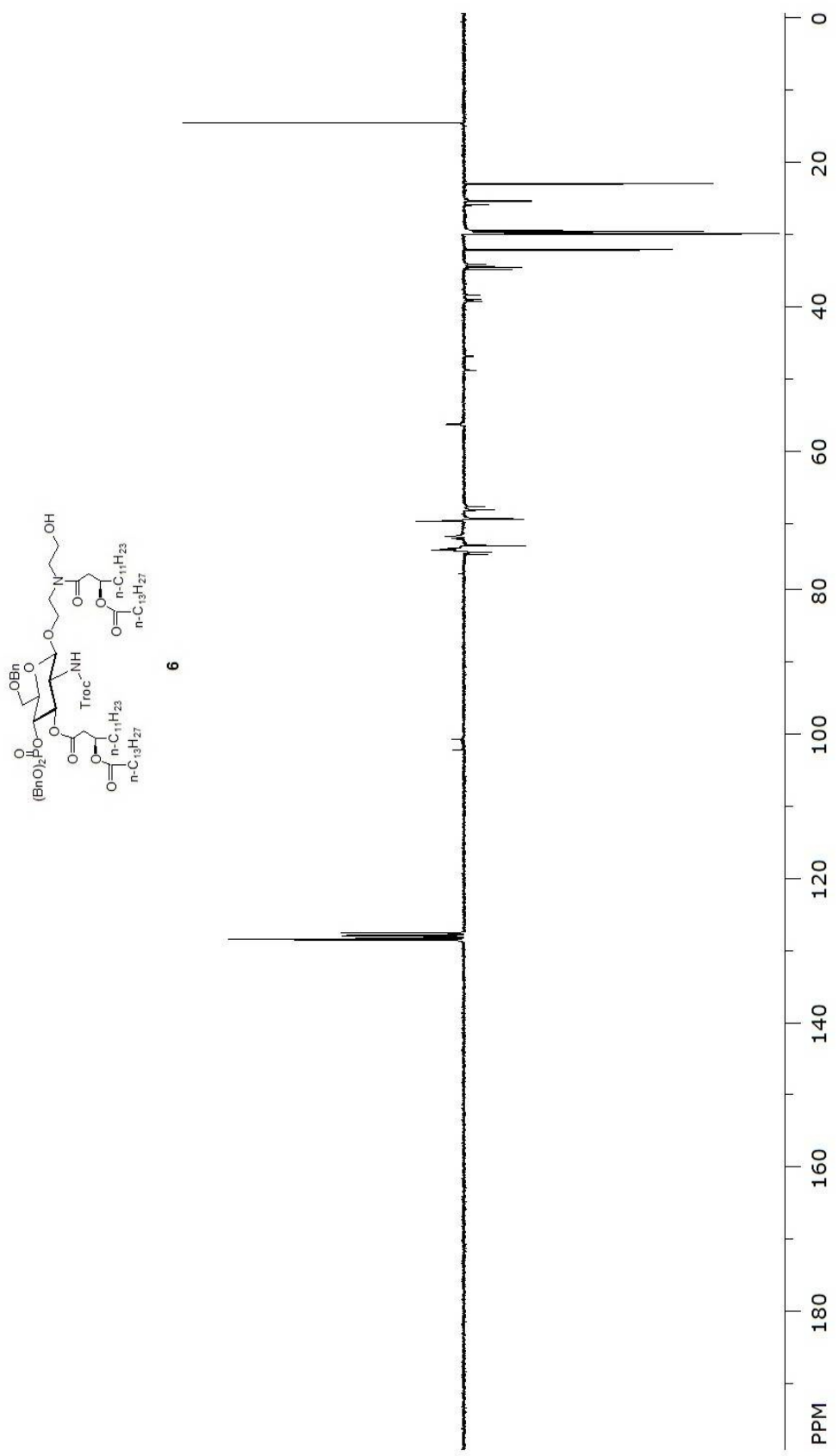
6
PPM
0
20
40
60
80
100
120
140
160
180

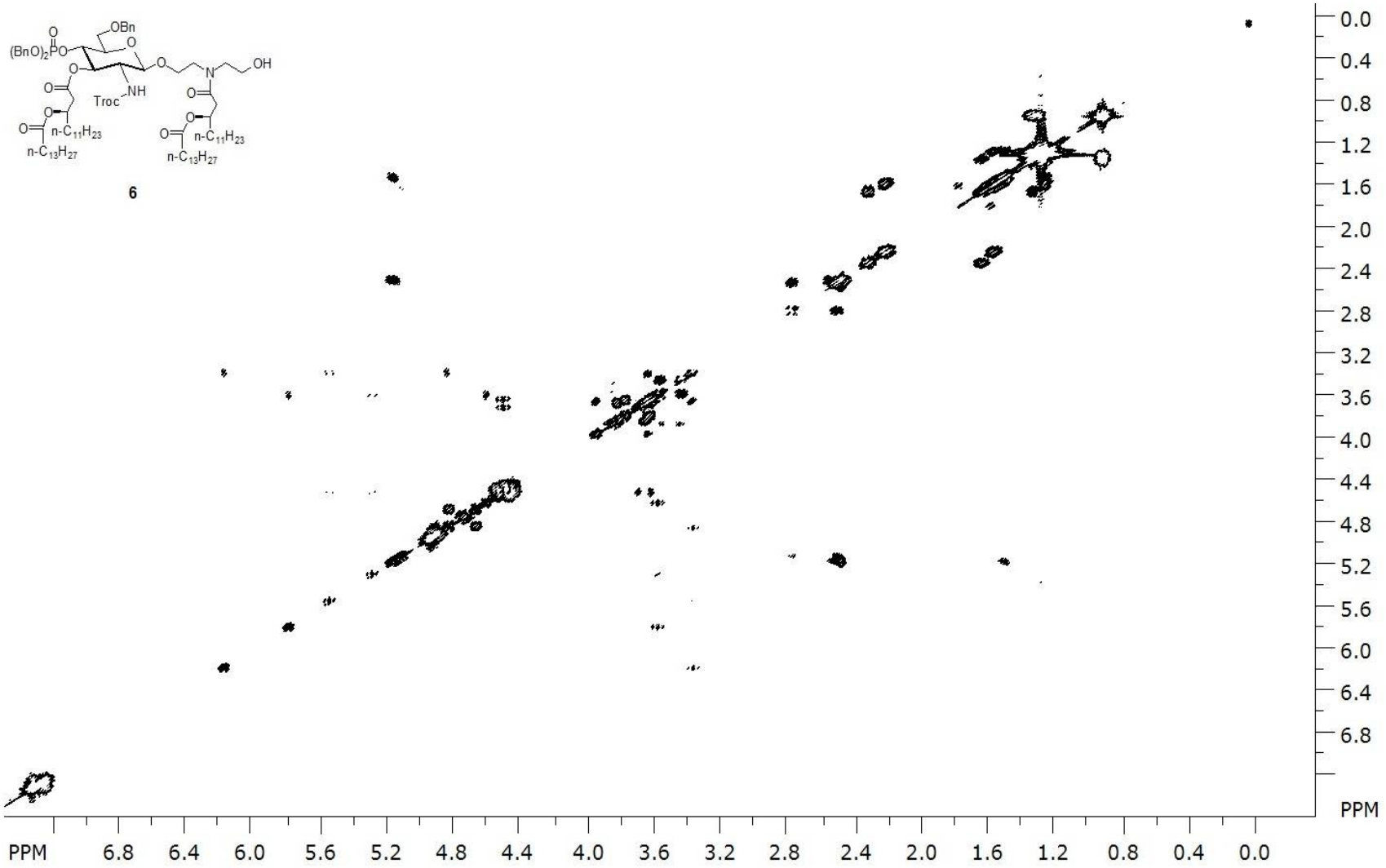
OBn
(BnO)2PO
O
NH
Troc
OH
n-C11H23
n-C13H27
6
0.0
0.4
0.8
1.2
1.6
2.0
2.4
2.8
3.2
3.6
4.0
4.4
4.8
5.2
5.6
6.0
6.4
6.8
PPM
PPM
6.8
6.4
6.0
5.6
5.2
4.8
4.4
4.0
3.6
3.2
2.8
2.4
2.0
1.6
1.2
0.8
0.4
0.0

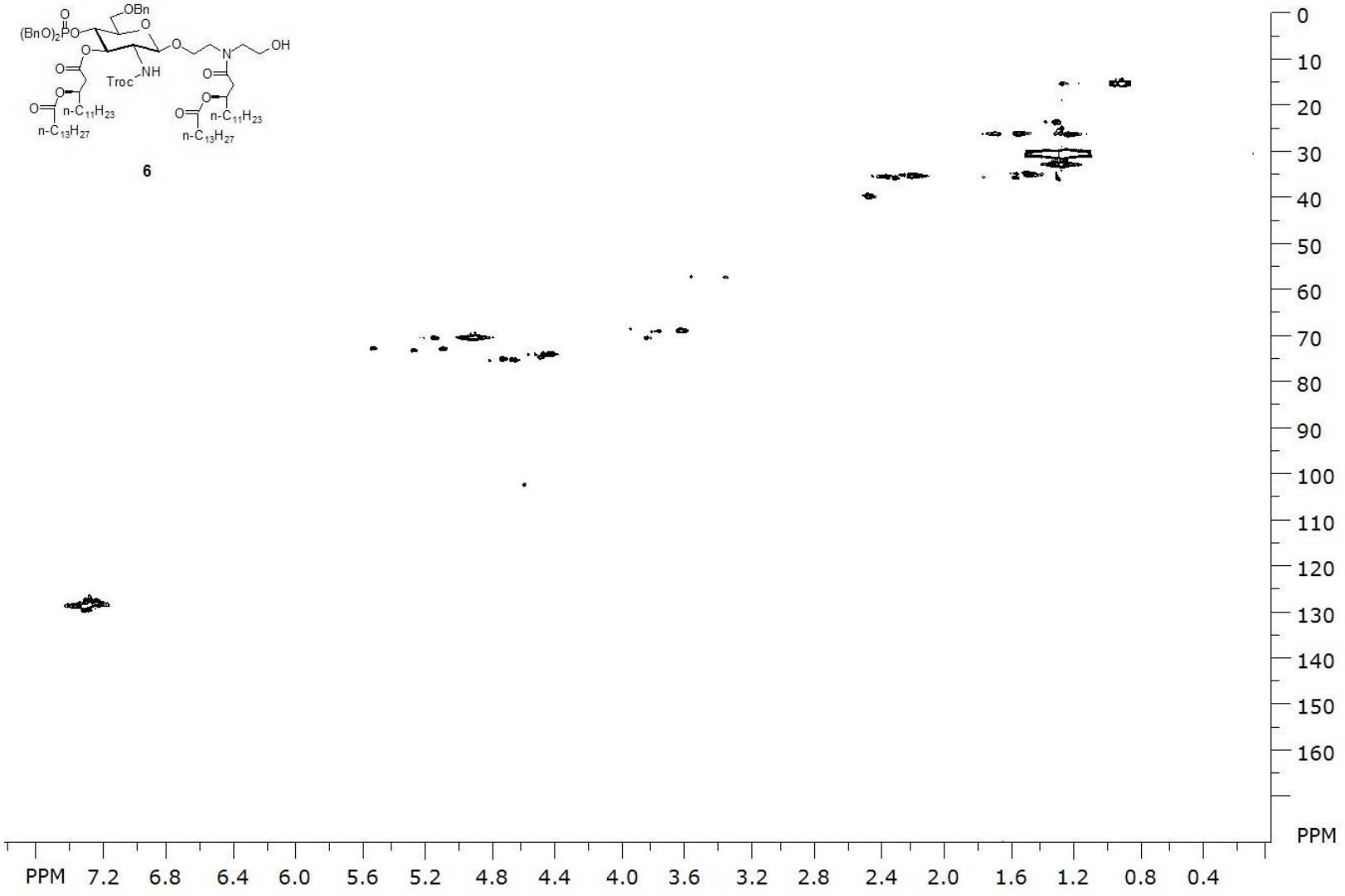
OBn
(BnO)2PO
O
Troc
NH
OH
n-C11H23
n-C13H27
6
0
10
20
30
40
50
60
70
80
90
100
110
120
130
140
150
160
PPM
PPM 7.2 6.8 6.4 6.0 5.6 5.2 4.8 4.4 4.0 3.6 3.2 2.8 2.4 2.0 1.6 1.2 0.8 0.4

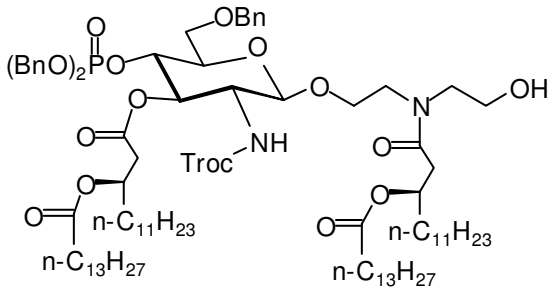

6

HRESI-MS (*m/z*) Calcd for $C_{90}H_{146}Cl_3N_2O_{17}P$ $[M+Na]^+$: 1685.9282, found: 1685.9339.

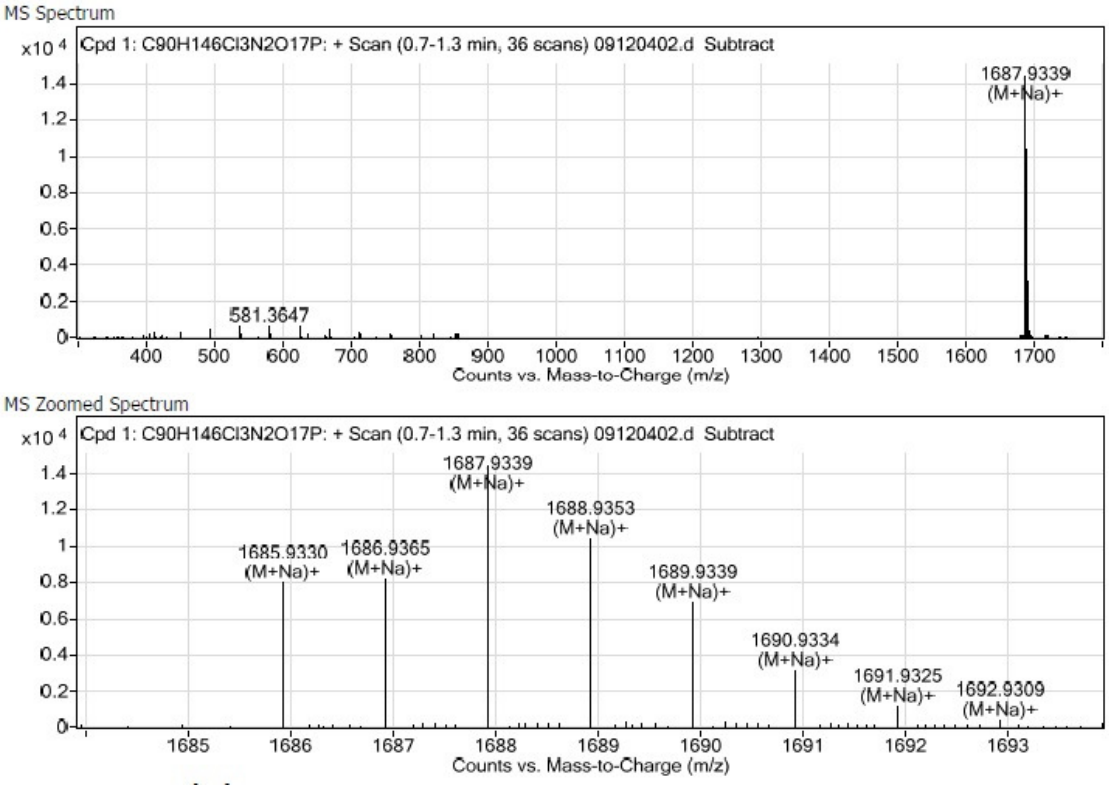

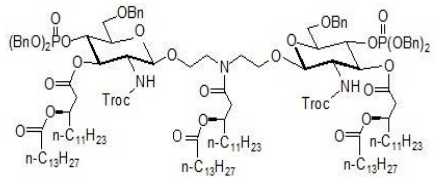

7

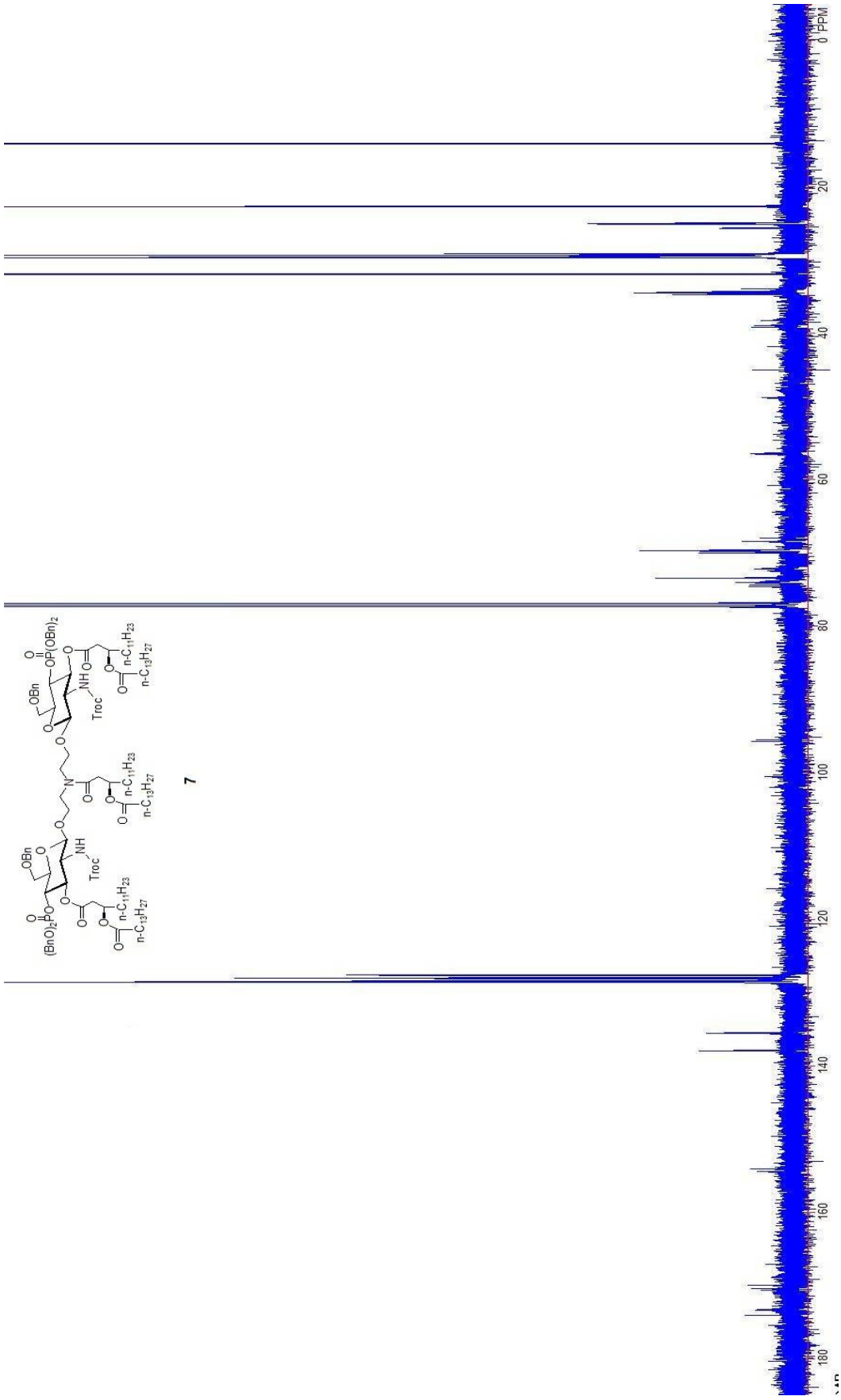
7
0 PPM
20
40
60
80
100
120
140
160
180

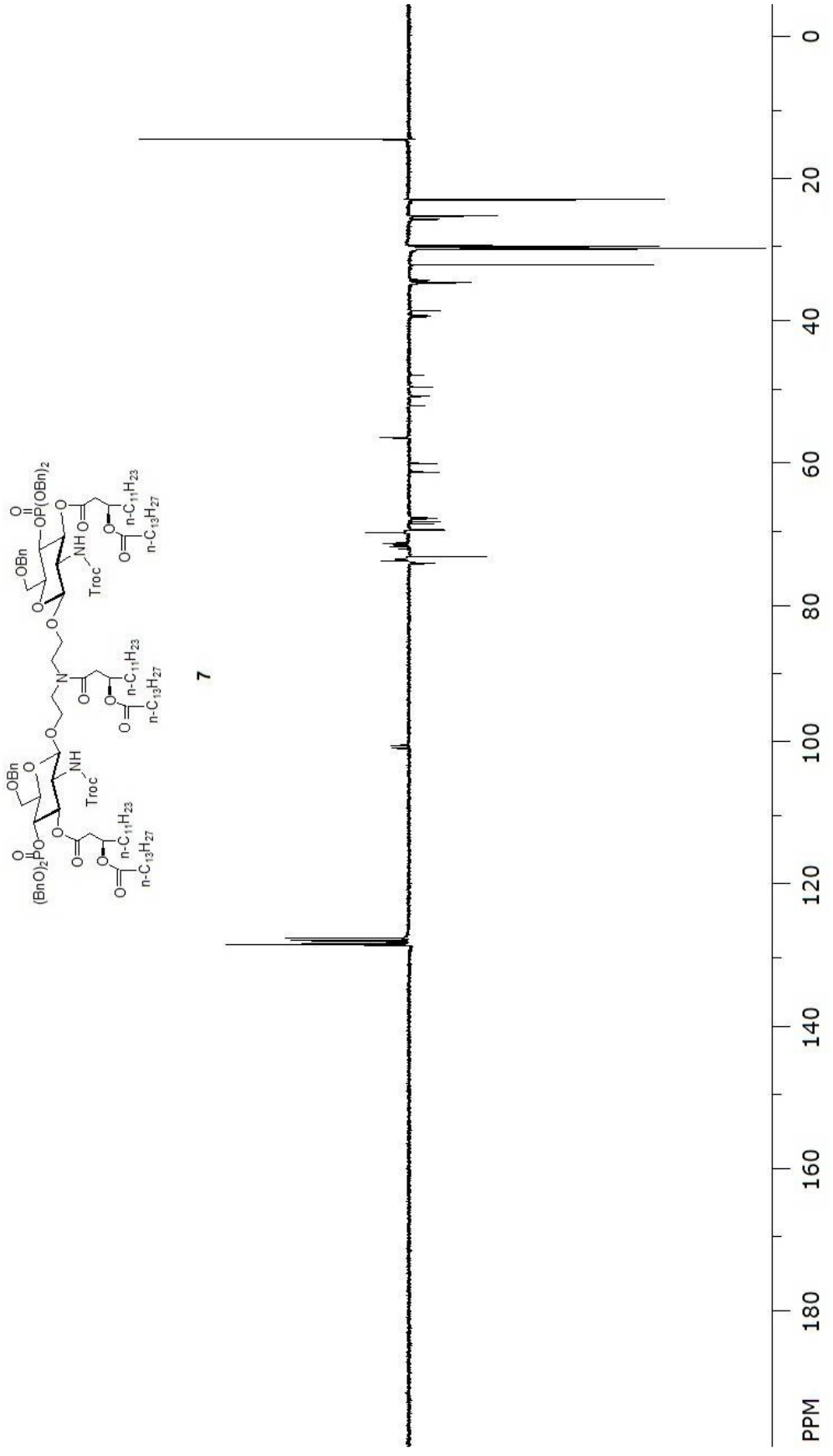
7
PPM
0
20
40
60
80
100
120
140
160
180

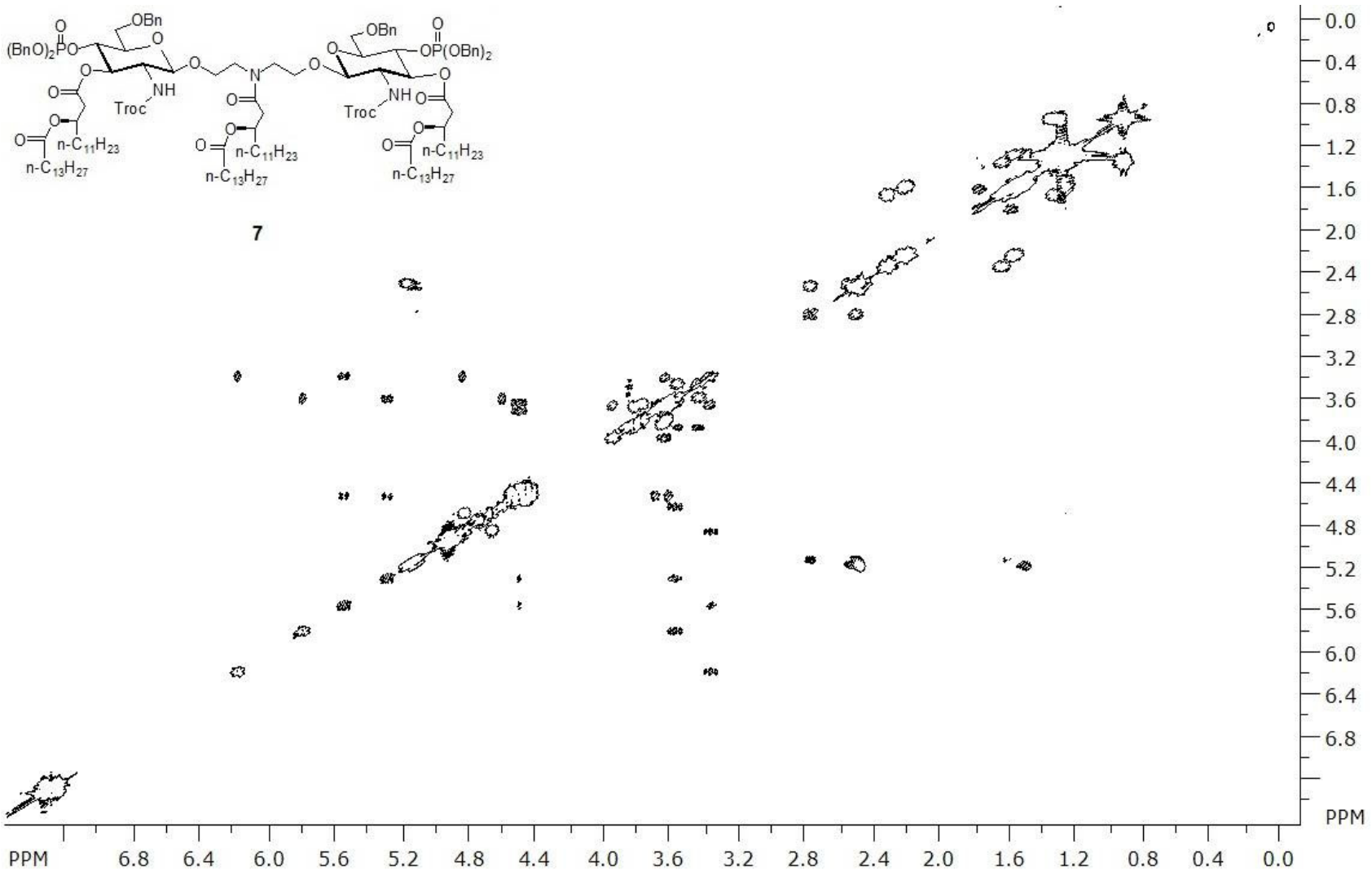
OBn
(BnO)2PO
NH
Troc
n-C11H23
n-C13H27
OP(OBn)2
7
PPM
6.8
6.4
6.0
5.6
5.2
4.8
4.4
4.0
3.6
3.2
2.8
2.4
2.0
1.6
1.2
0.8
0.4
0.0

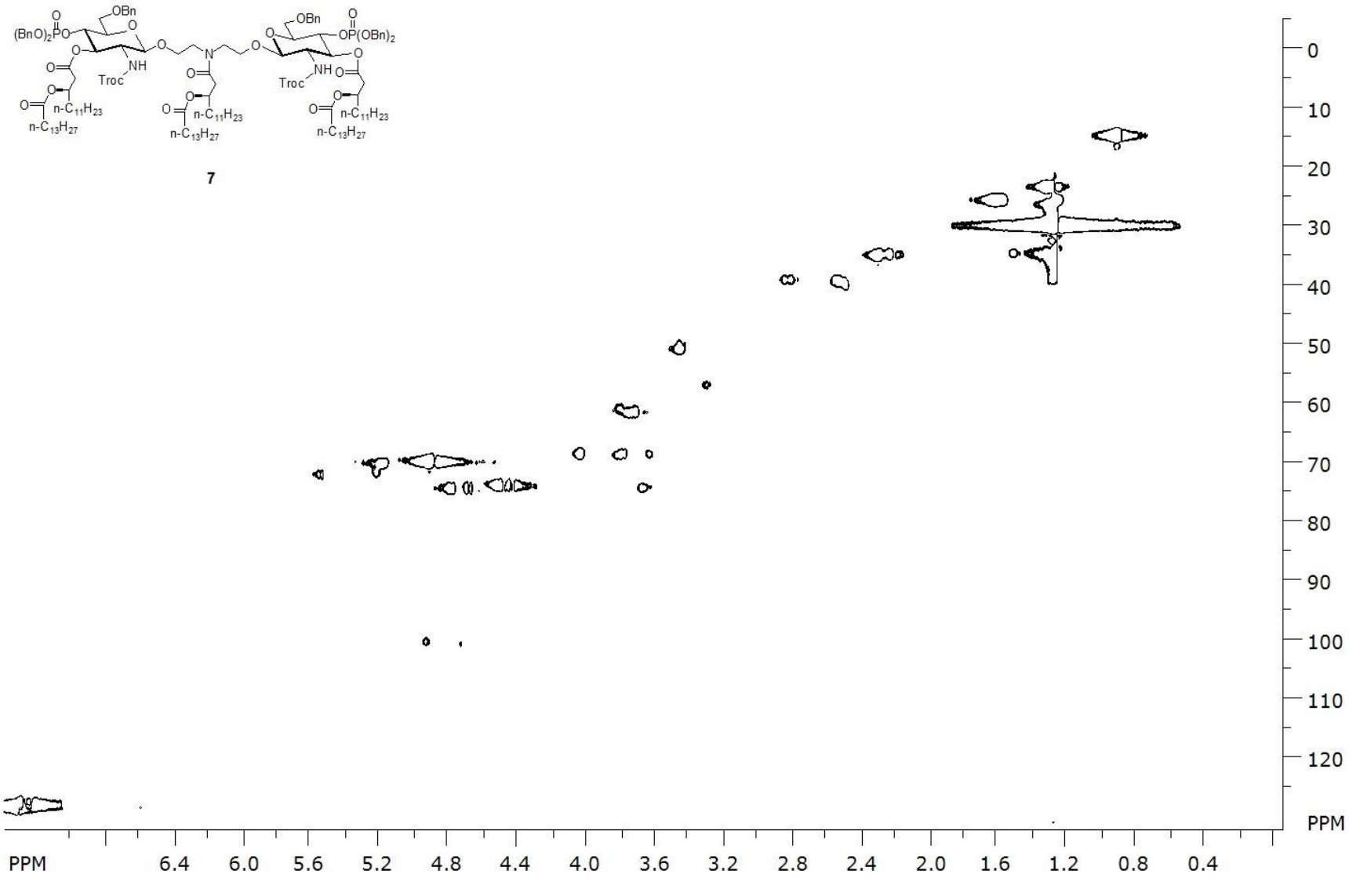
OBn
(BnO)2PO
OP(OBn)2
NH
Troc
n-C11H23
n-C13H27
7
0
10
20
30
40
50
60
70
80
90
100
110
120
PPM
PPM
6.4
6.0
5.6
5.2
4.8
4.4
4.0
3.6
3.2
2.8
2.4
2.0
1.6
1.2
0.8
0.4

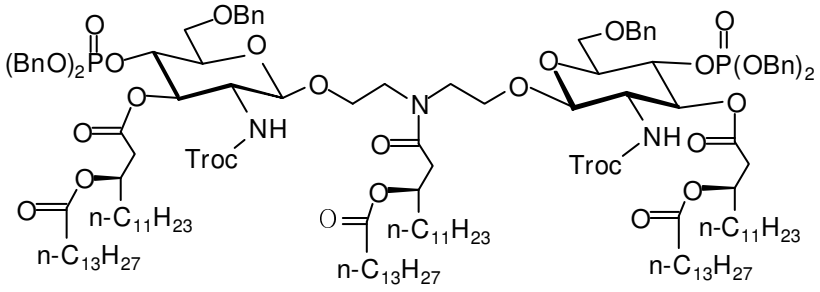

7

HRESI-MS (*m*/*z*) Calcd for $C_{148}H_{229}Cl_6N_3O_{29}P_2$ $[M+Na]^+$: 2807.3979, found: 2807.4086.

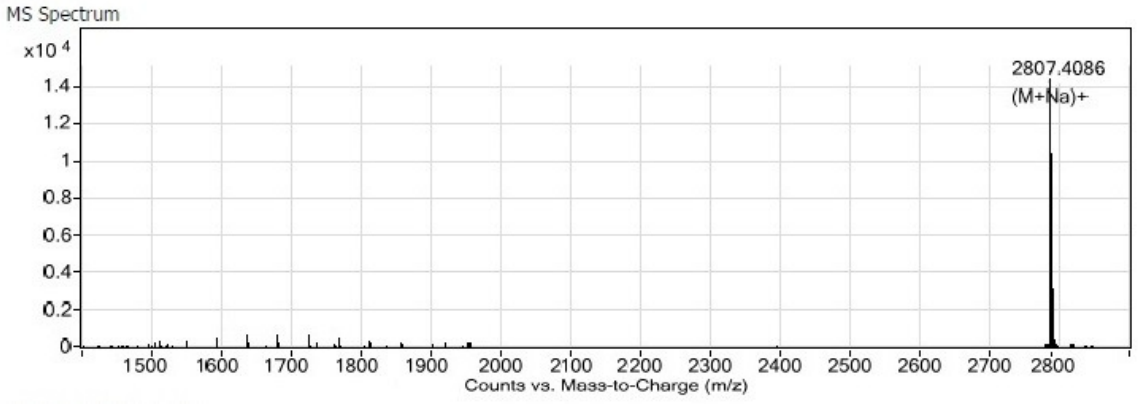

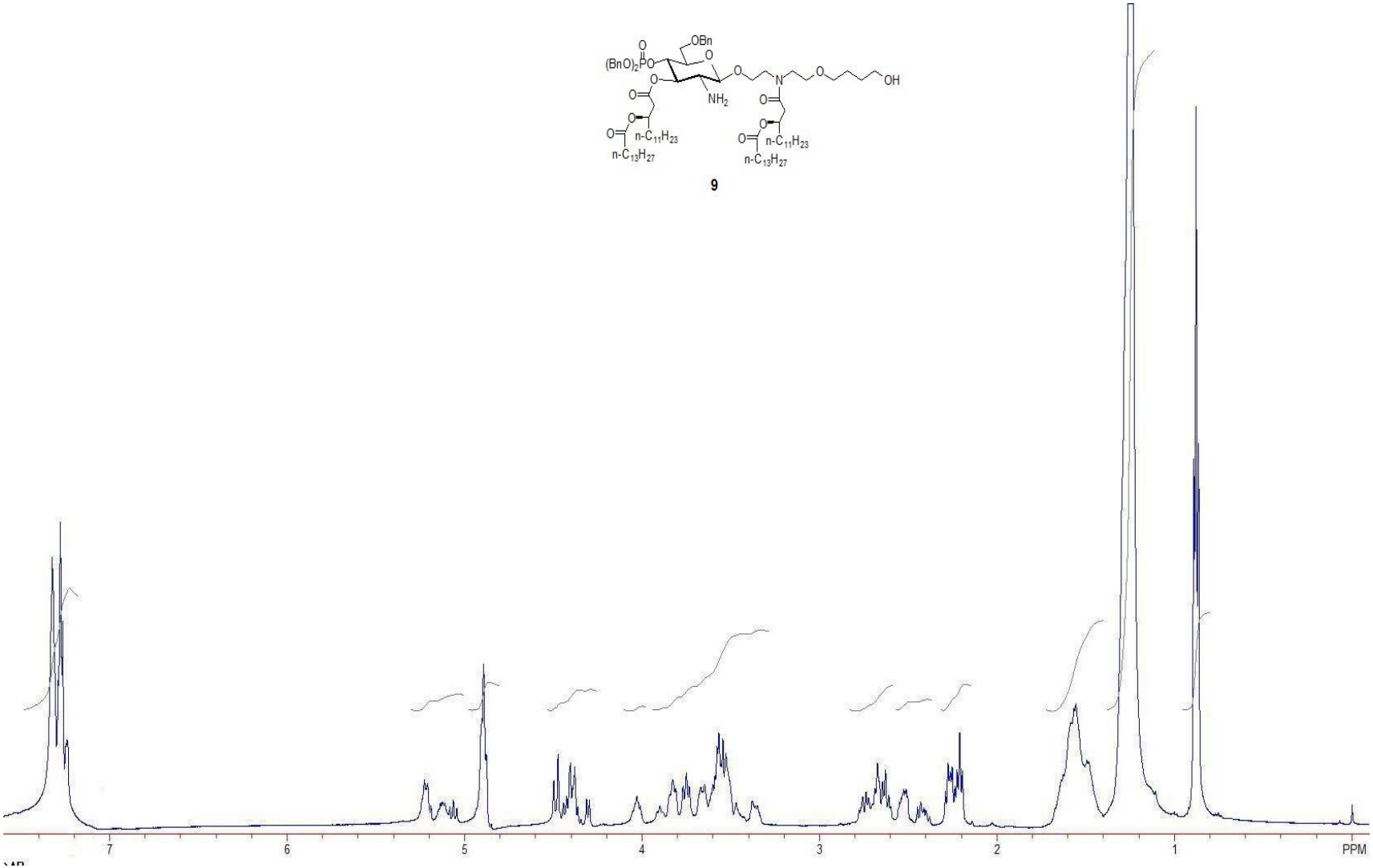
OBn
O
(BnO)2PO
O
O
NH2
O
N
O
OH
O
n-C11H23
n-C13H27
O
n-C11H23
n-C13H27
9
7
6
5
4
3
2
1
PPM

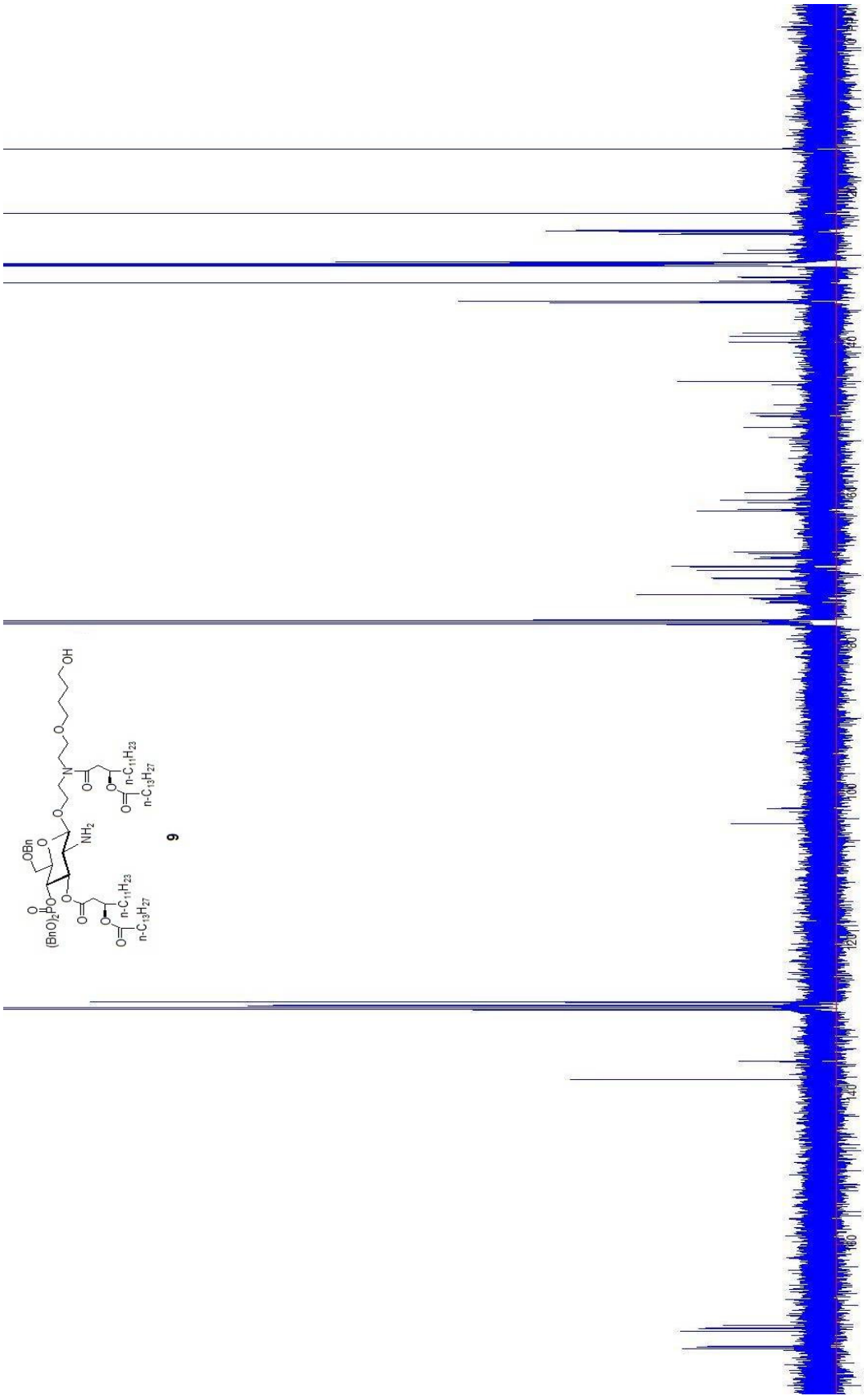
OBn
NH2
OH
n-C11H23
n-C13H27
(BnO)2P
O
9

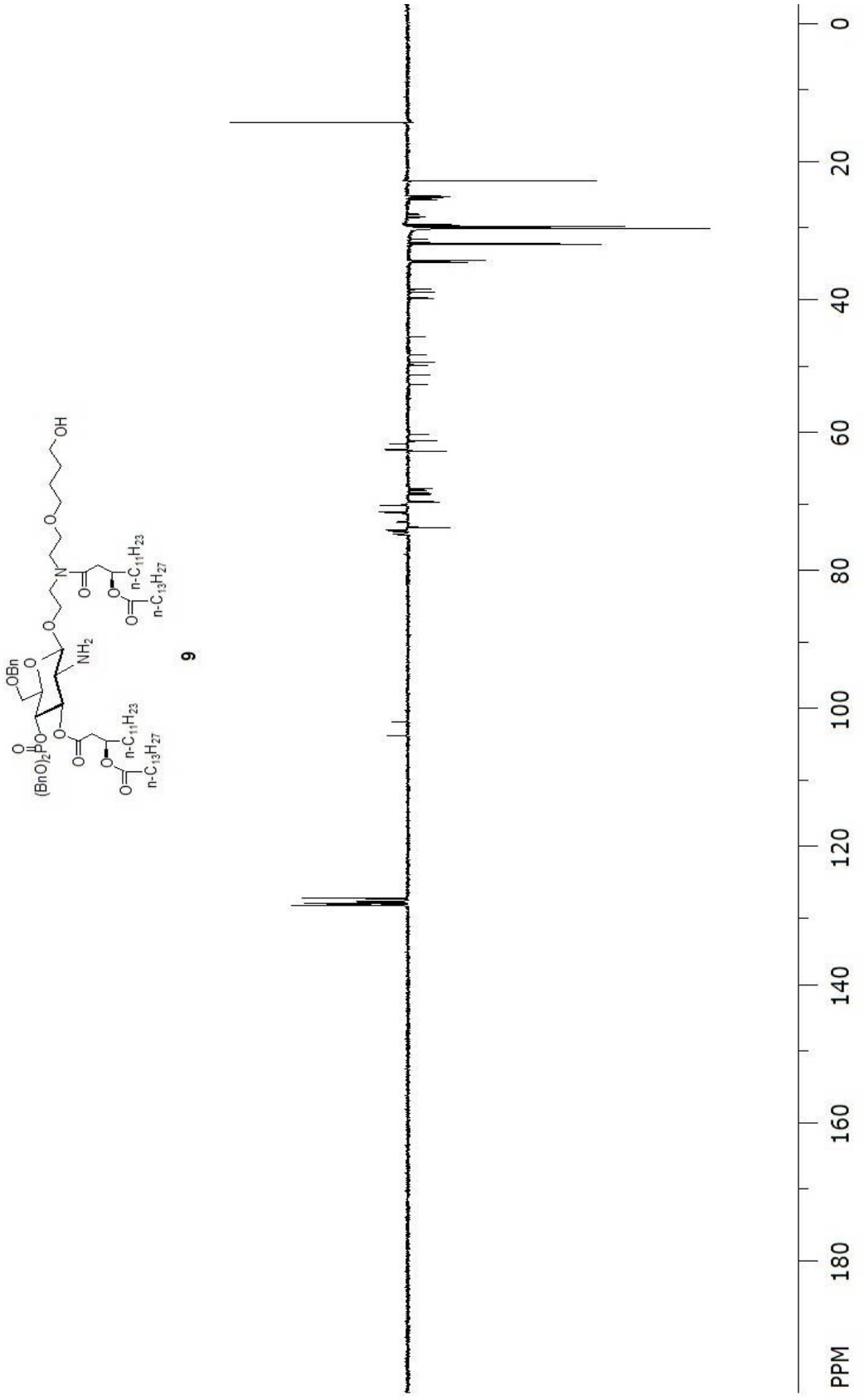
OH
OBn
NH2
n-C11H23
n-C13H27
(BnO)2P
9
PPM
0
20
40
60
80
100
120
140
160
180

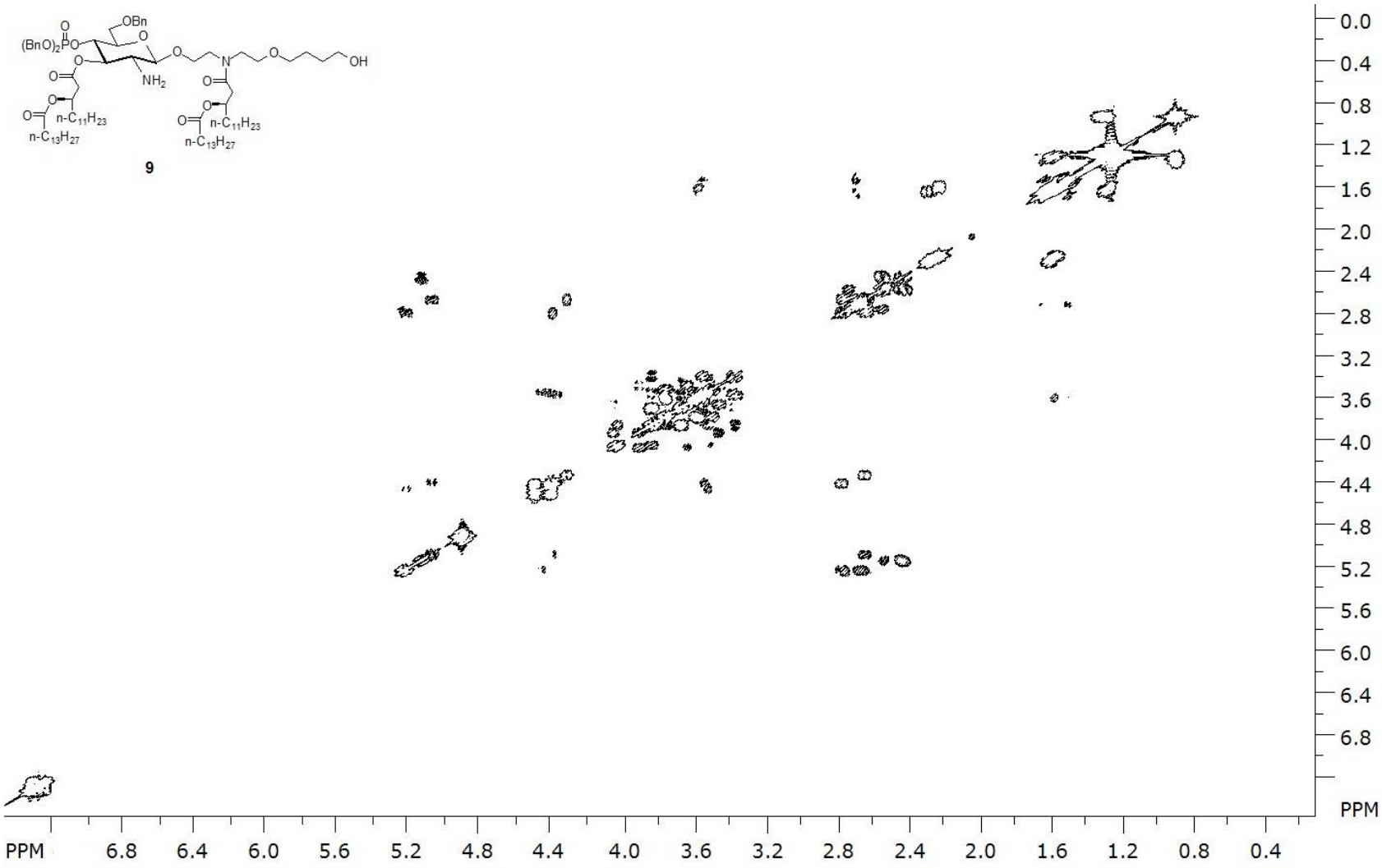
OBn
(BnO)2PO
NH2
n-C11H23
n-C13H27
OH
9
0.0
0.4
0.8
1.2
1.6
2.0
2.4
2.8
3.2
3.6
4.0
4.4
4.8
5.2
5.6
6.0
6.4
6.8
PPM
PPM
6.8
6.4
6.0
5.6
5.2
4.8
4.4
4.0
3.6
3.2
2.8
2.4
2.0
1.6
1.2
0.8
0.4

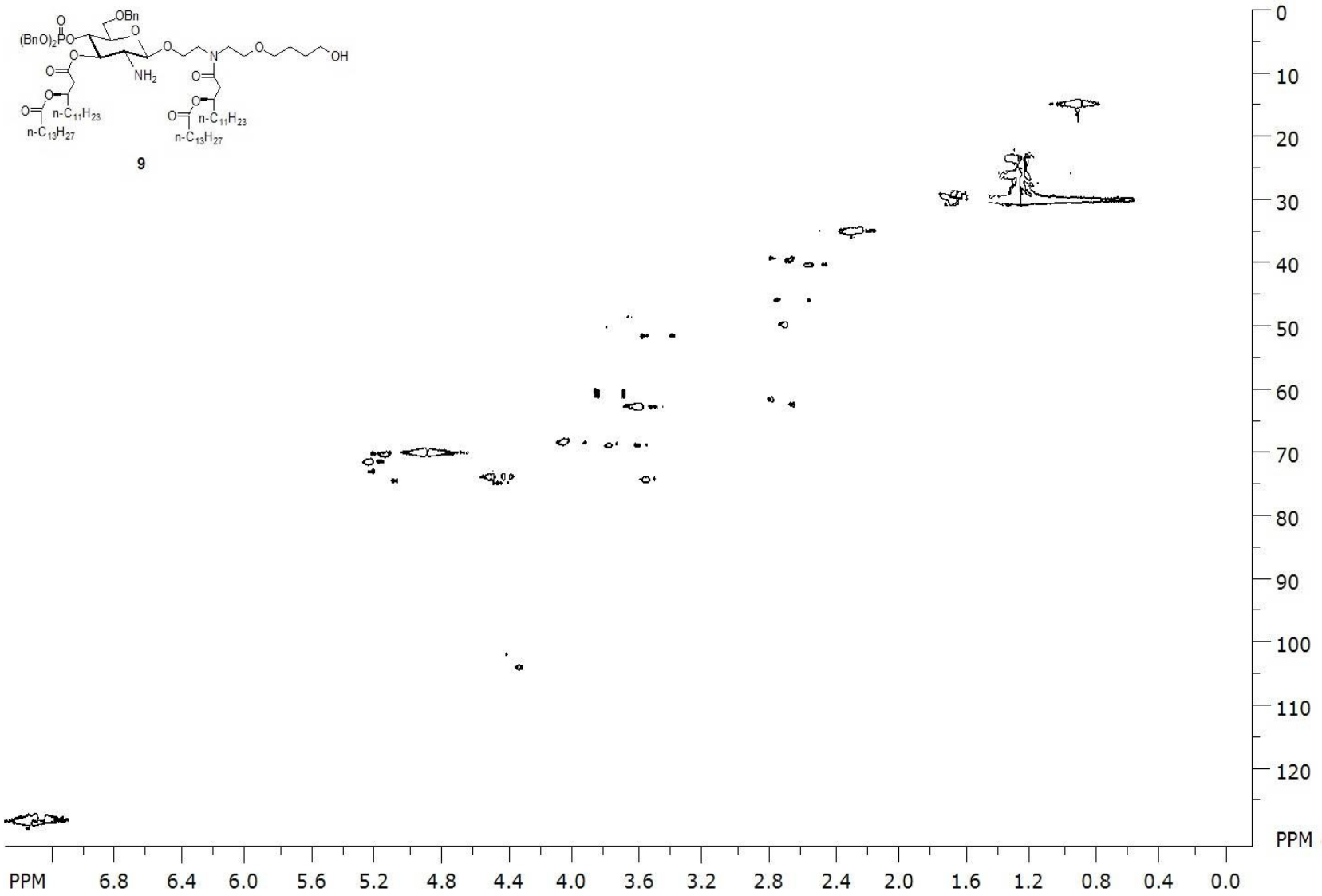
OBn
O
(BnO)2P
O
O
NH2
O
N
O
OH
O
O
n-C11H23
n-C13H27
O
O
n-C11H23
n-C13H27
9
0
10
20
30
40
50
60
70
80
90
100
110
120
PPM
PPM
6.8
6.4
6.0
5.6
5.2
4.8
4.4
4.0
3.6
3.2
2.8
2.4
2.0
1.6
1.2
0.8
0.4
0.0

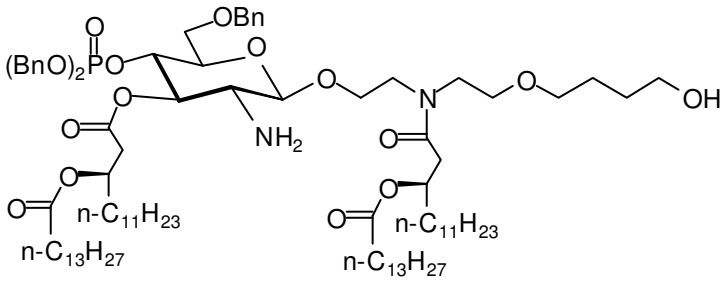

9

ESI-MS (*m/z*) Calcd for $C_{91}H_{154}N_2O_{16}P$ $[M+H]^+$: 1563.1, found: 1563.1.

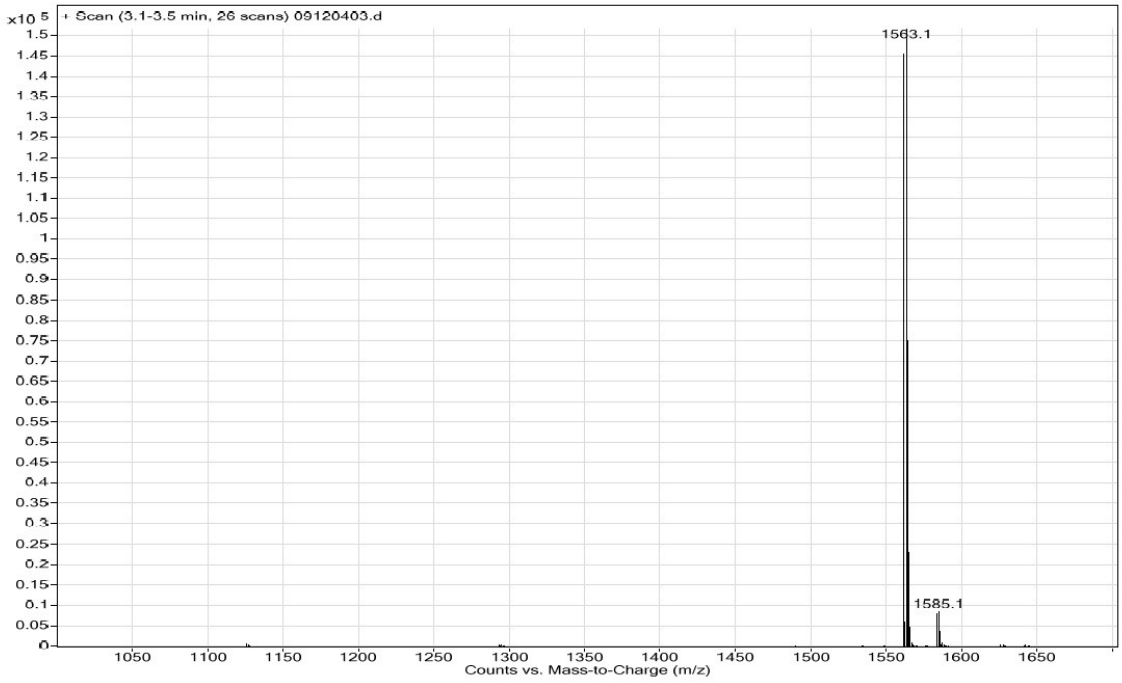

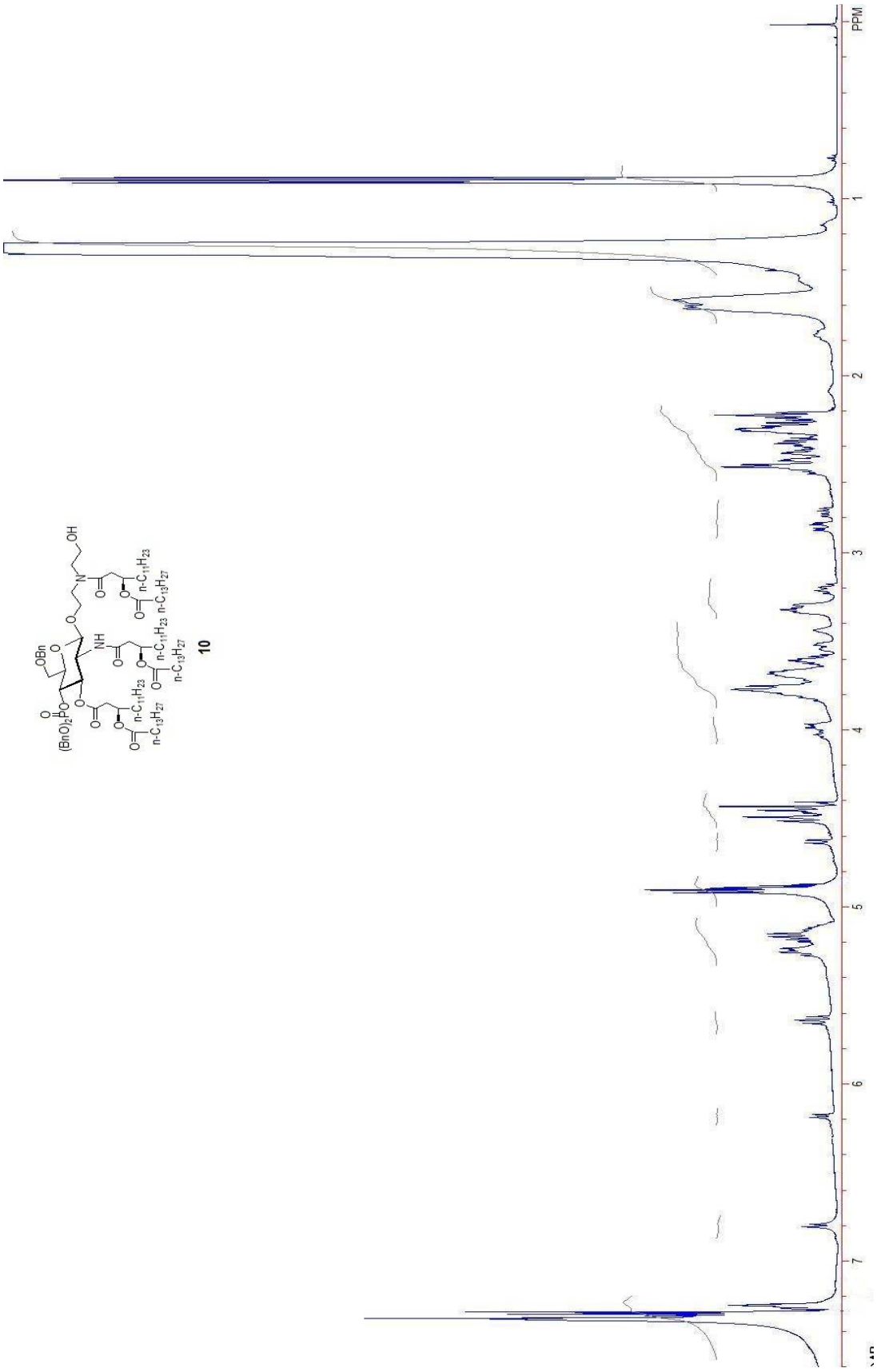
10
PPM

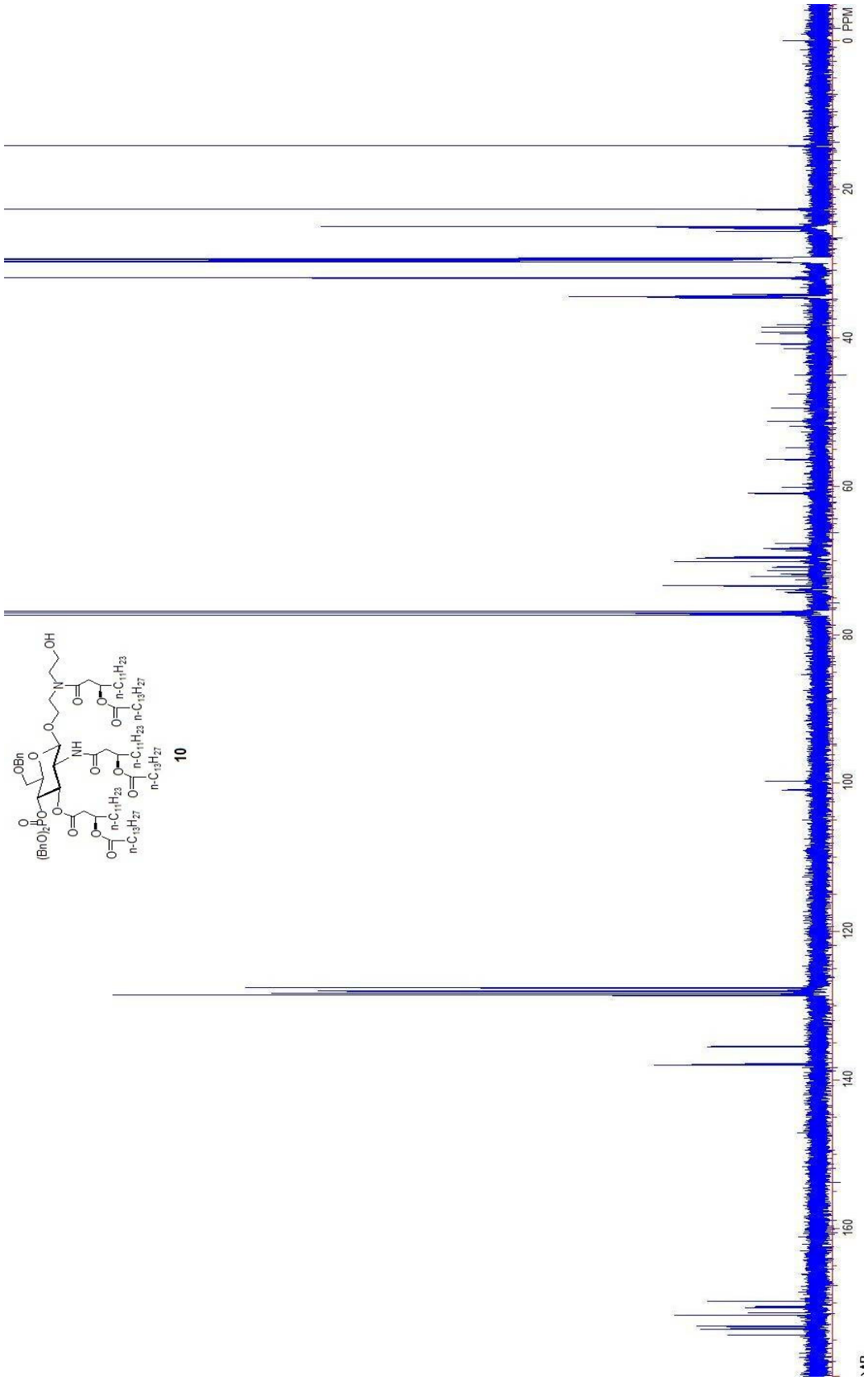
OBn
NH
OH
(BnO)2P
n-C11H23
n-C13H27
10
0 PPM
20
40
60
80
100
120
140
160

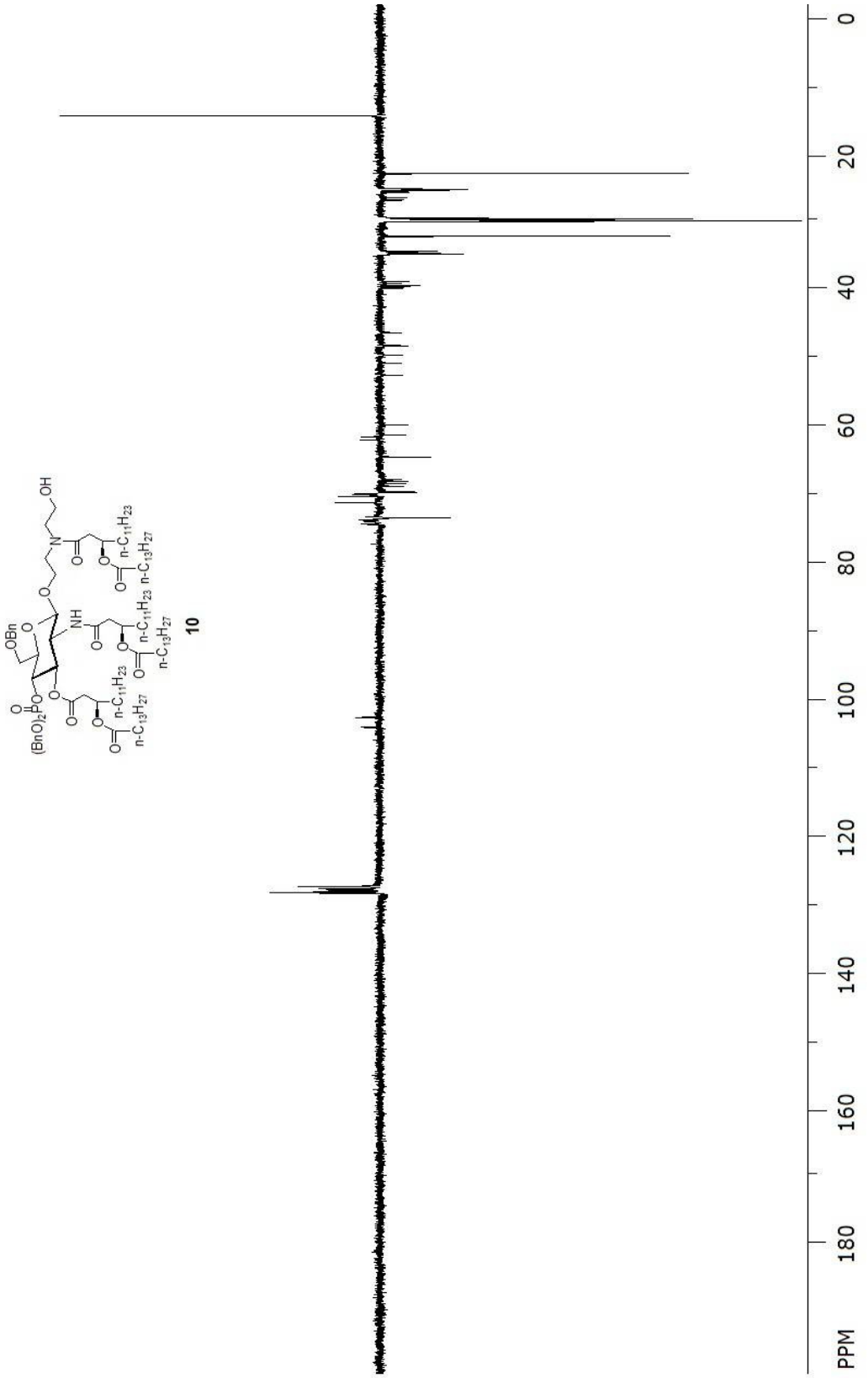
OBn
O
NH
OH
N
O
O
O

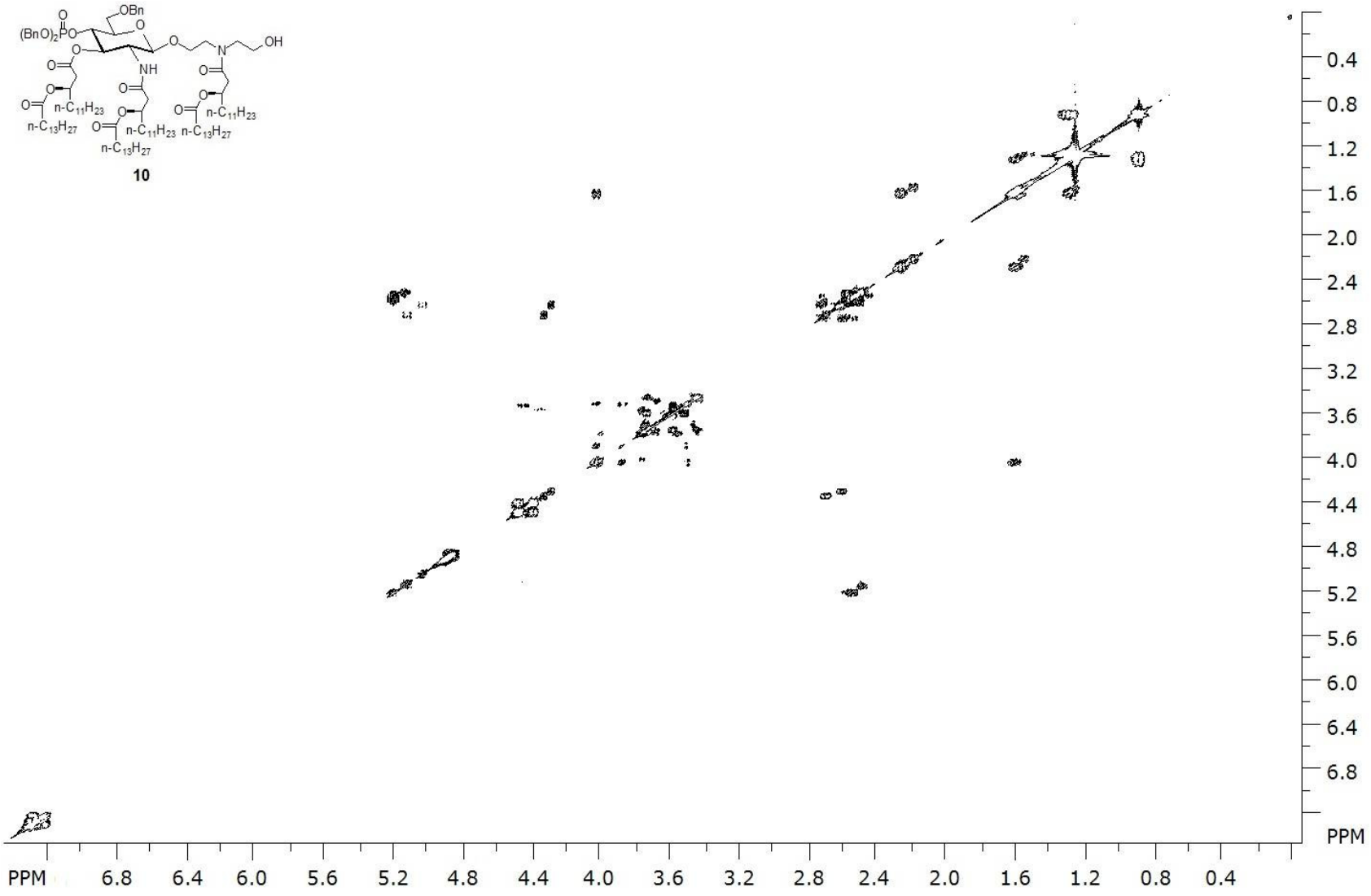
OBn
(BnO)2PO
O
NH
N
OH
n-C11H23
n-C13H27
10
0.4
0.8
1.2
1.6
2.0
2.4
2.8
3.2
3.6
4.0
4.4
4.8
5.2
5.6
6.0
6.4
6.8
PPM
PPM
6.8
6.4
6.0
5.6
5.2
4.8
4.4
4.0
3.6
3.2
2.8
2.4
2.0
1.6
1.2
0.8
0.4

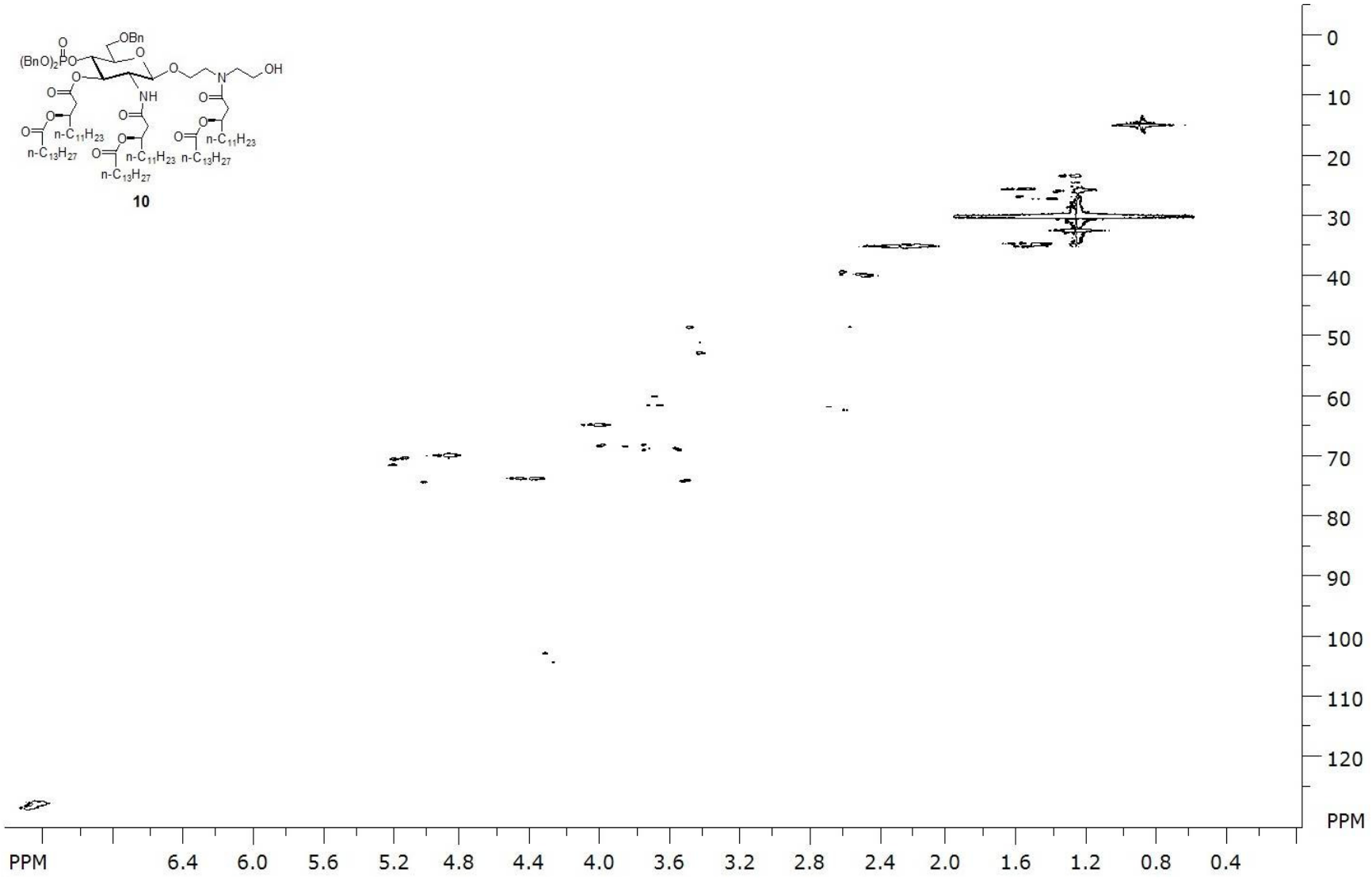
OBn
(BnO)2PO
O
NH
OH
n-C11H23
n-C13H27
10
0
10
20
30
40
50
60
70
80
90
100
110
120
PPM
PPM
6.4
6.0
5.6
5.2
4.8
4.4
4.0
3.6
3.2
2.8
2.4
2.0
1.6
1.2
0.8
0.4

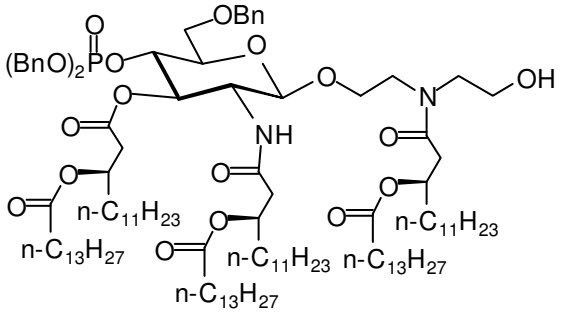

10

HRESI-MS (*m/z*) Calcd for $C_{115}H1_{97}N_2O_{18}P$ $[M+Na]^+$: 1948.4144, found: 1948.4183.

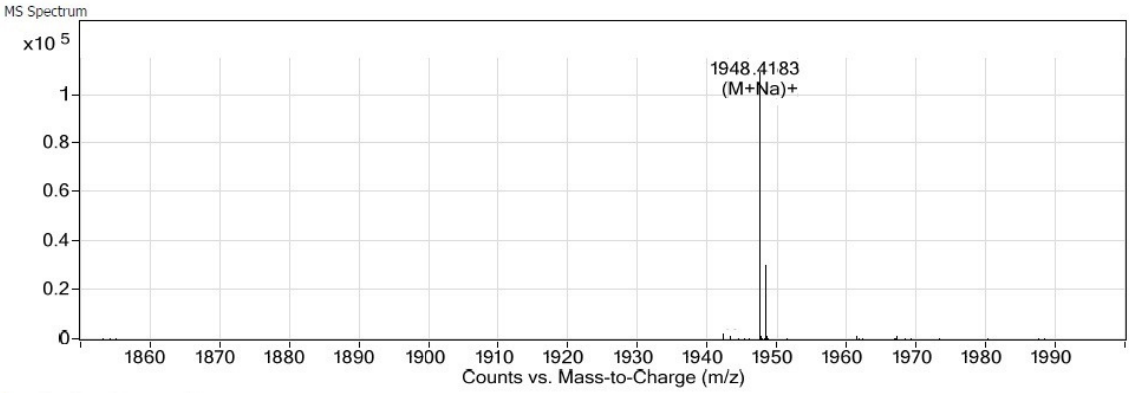

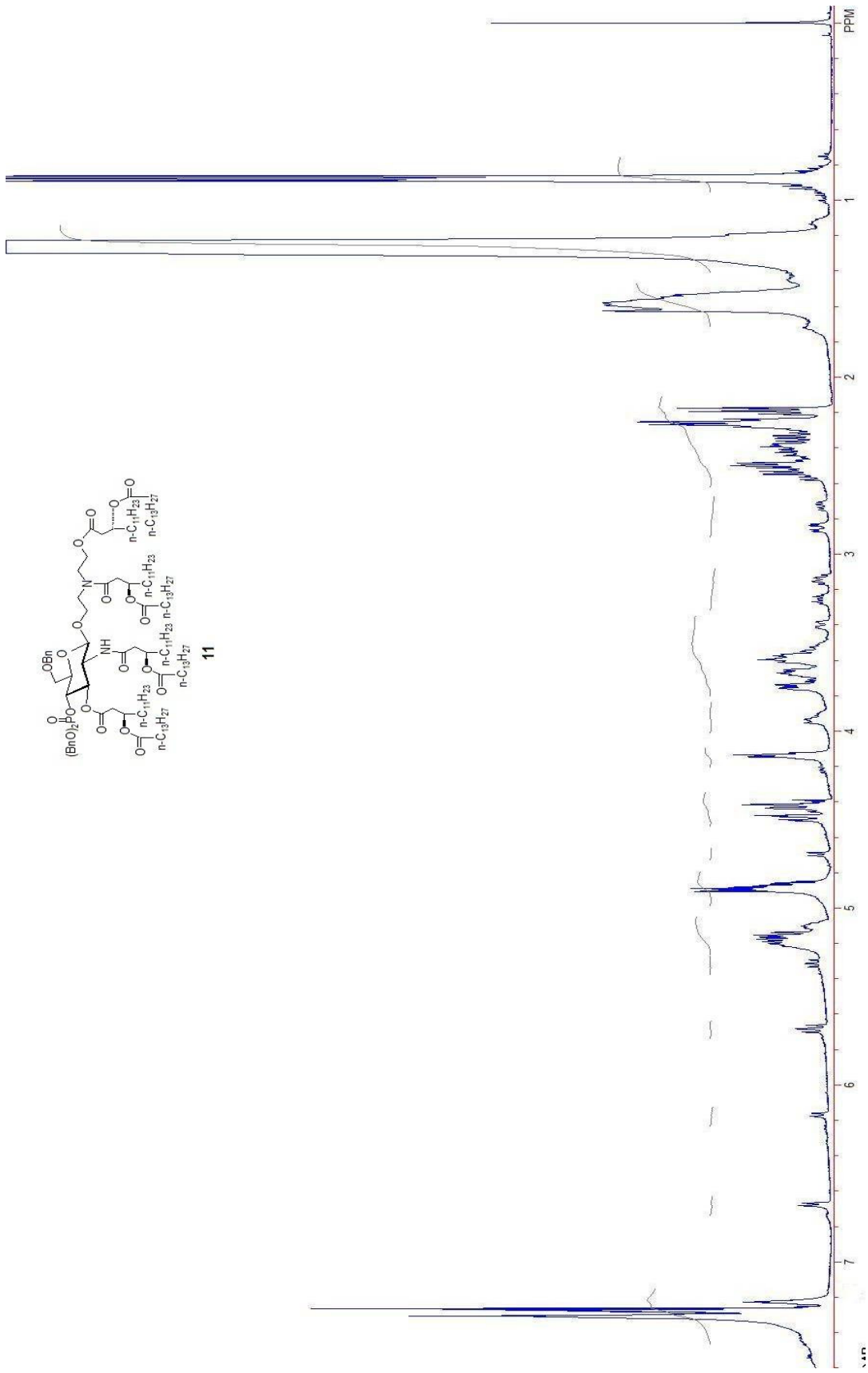

11

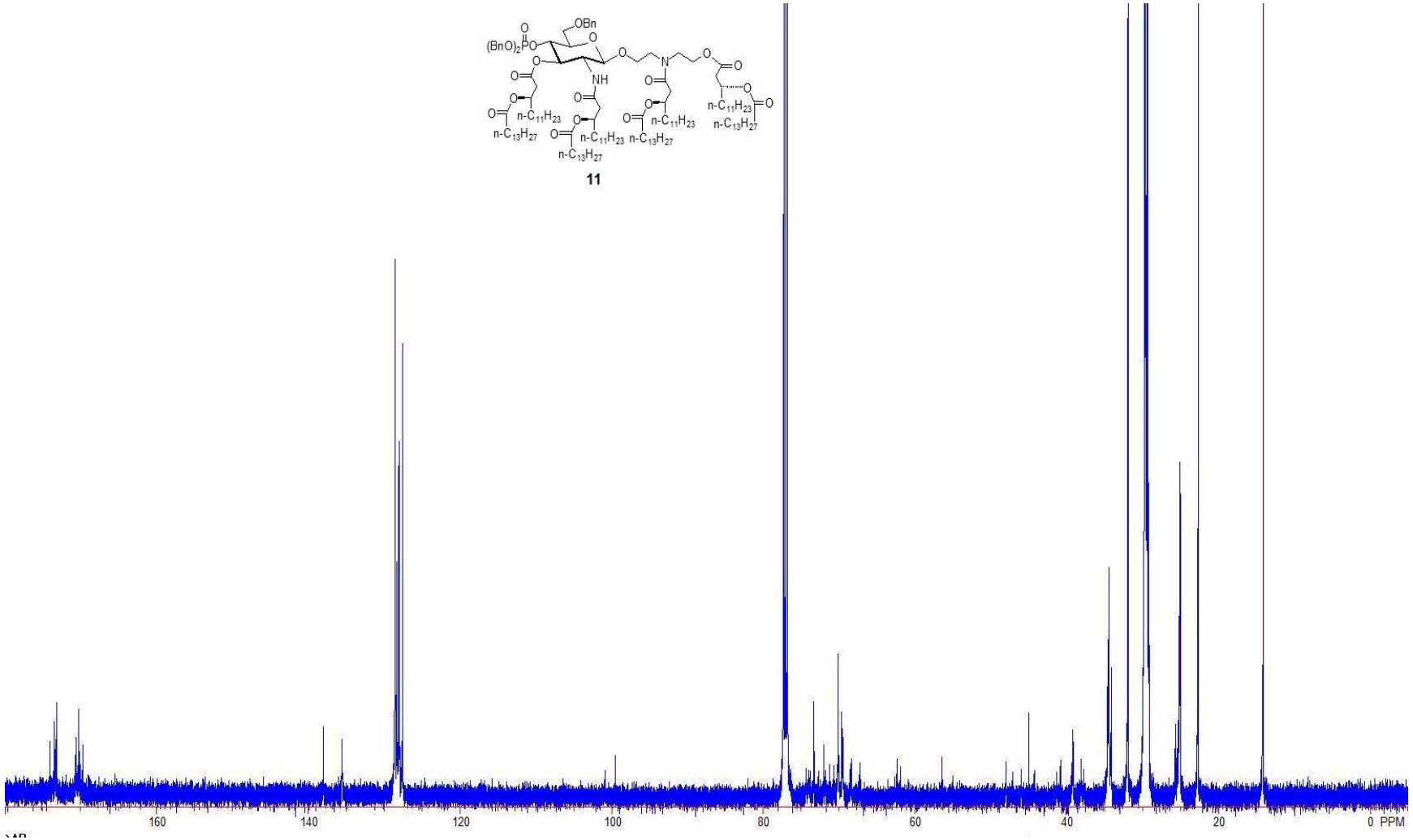
OBn
(BnO)2PO
NH
n-C11H23
n-C13H27
11
160
140
120
100
80
60
40
20
0 PPM

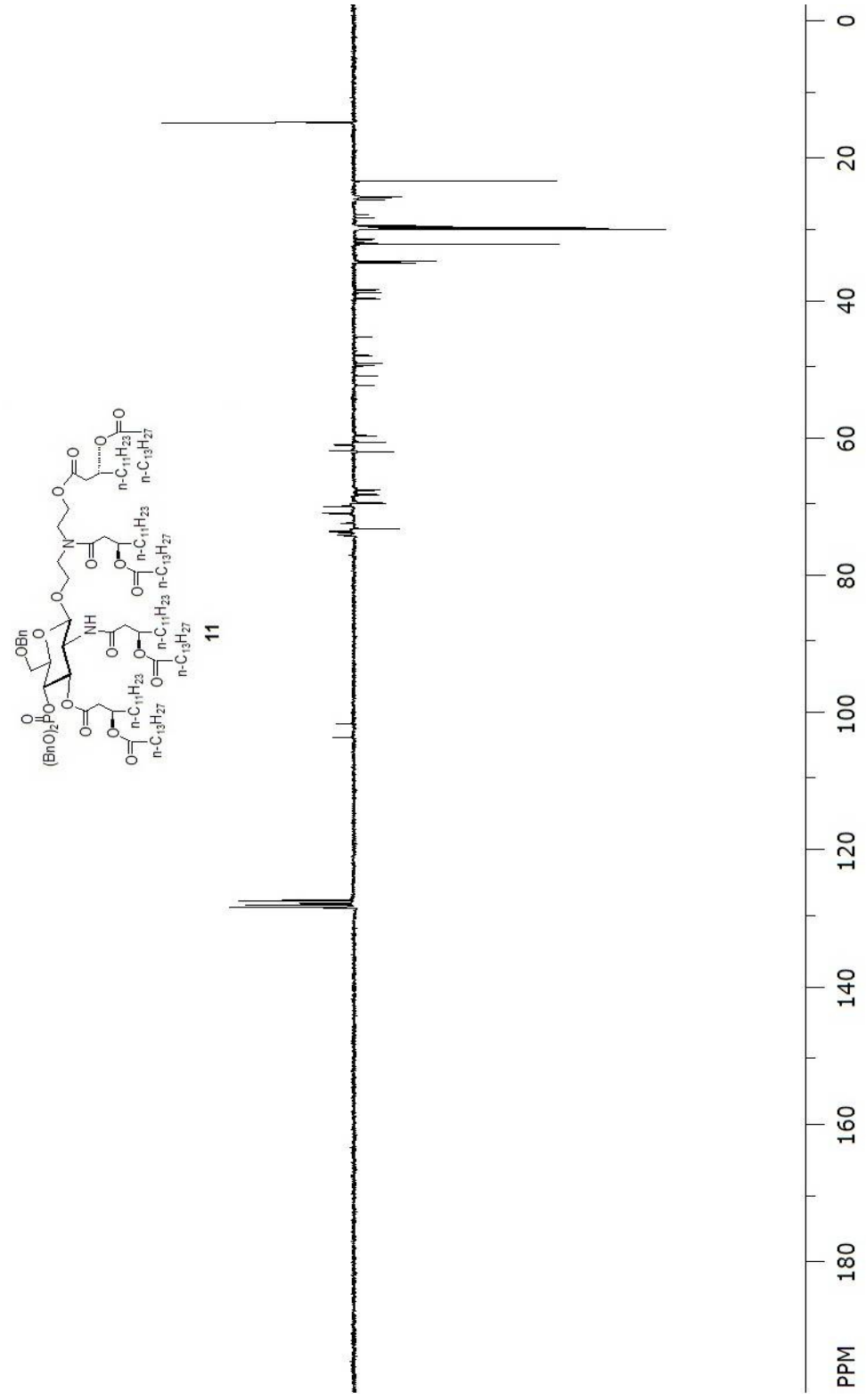
11
PPM
0
20
40
60
80
100
120
140
160
180

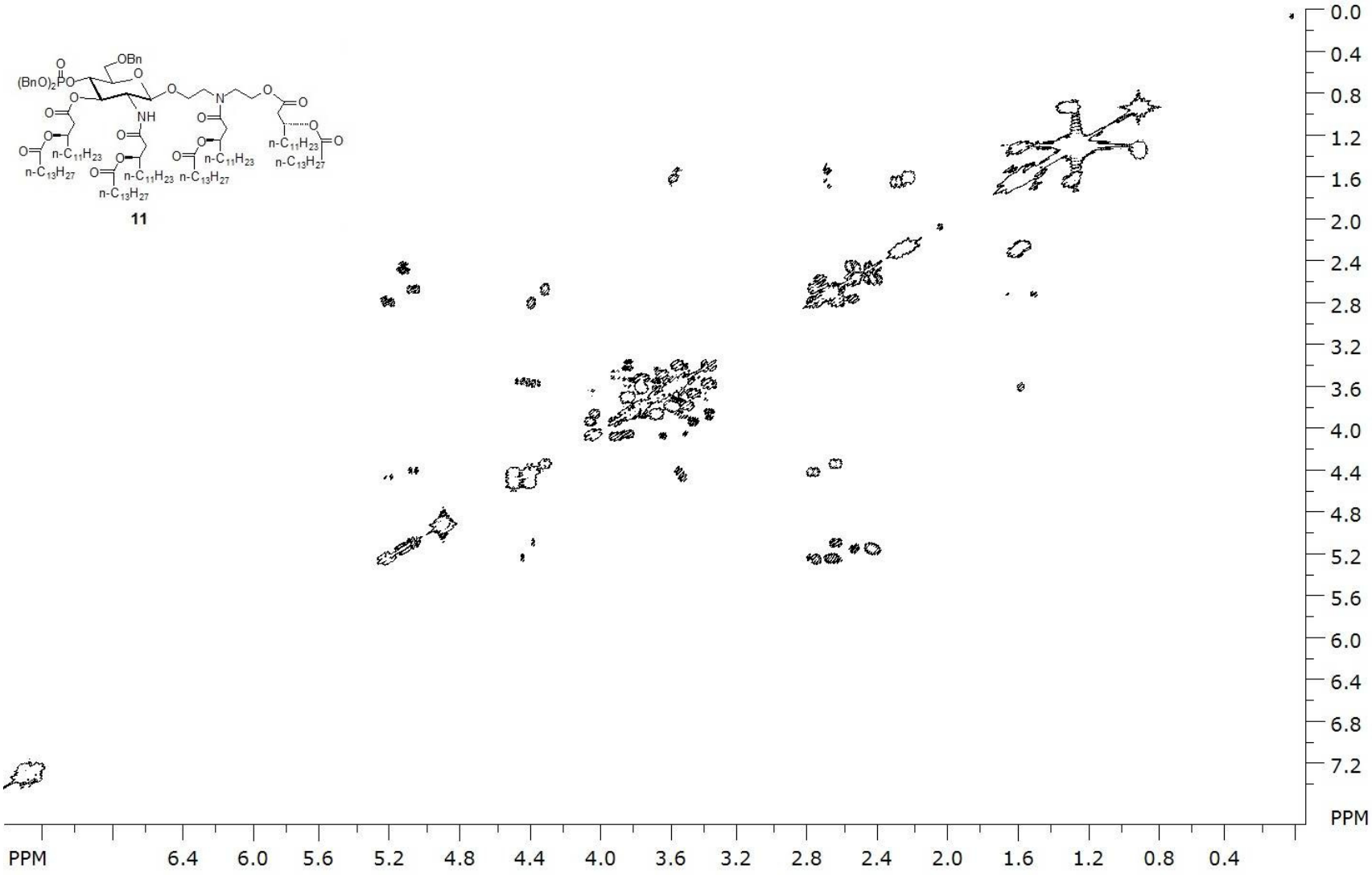
OBn
(BnO)2PO
NH
n-C11H23
n-C13H27
11
0.0
0.4
0.8
1.2
1.6
2.0
2.4
2.8
3.2
3.6
4.0
4.4
4.8
5.2
5.6
6.0
6.4
6.8
7.2
PPM
PPM
6.4
6.0
5.6
5.2
4.8
4.4
4.0
3.6
3.2
2.8
2.4
2.0
1.6
1.2
0.8
0.4

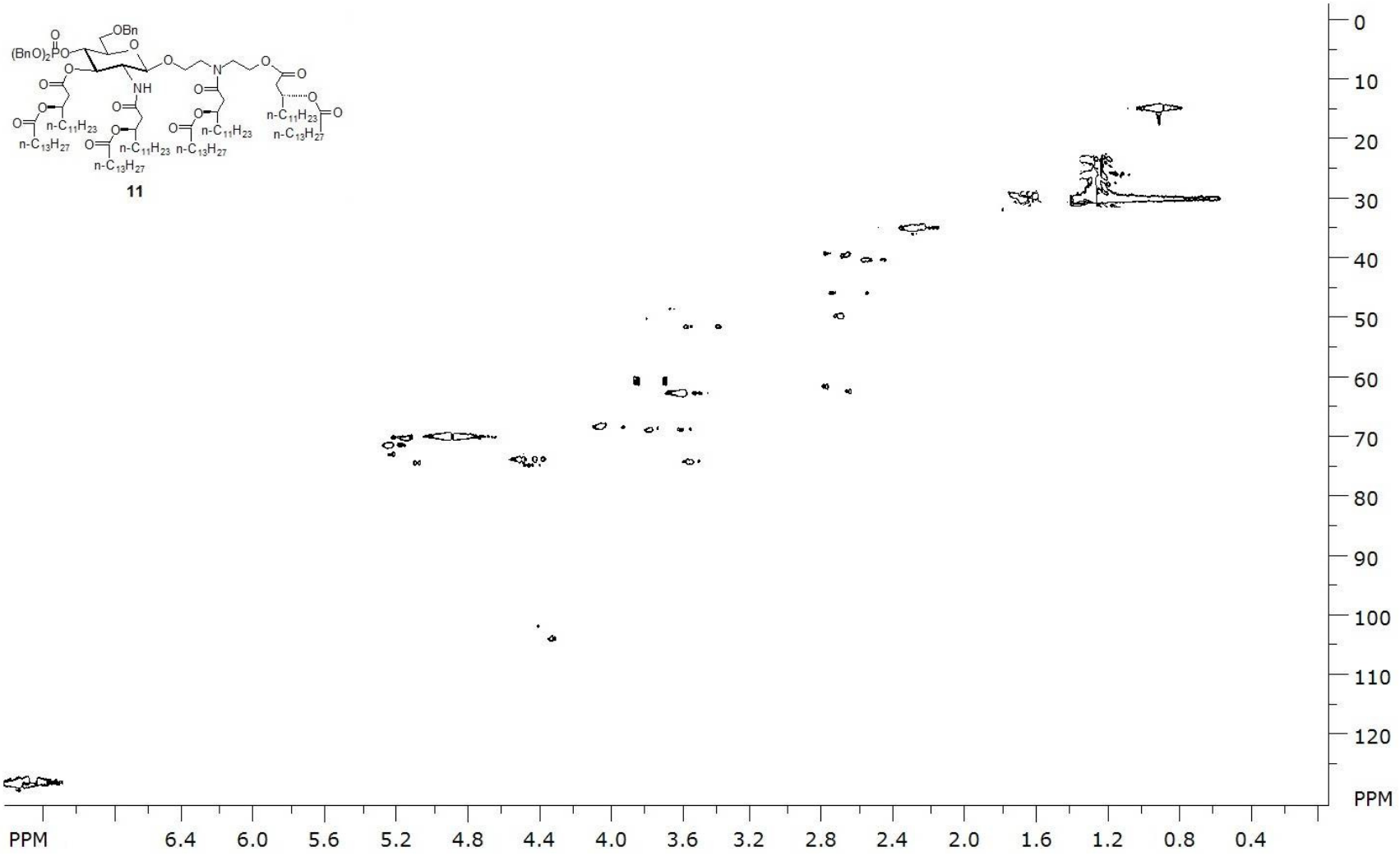
11
PPM
6.4
6.0
5.6
5.2
4.8
4.4
4.0
3.6
3.2
2.8
2.4
2.0
1.6
1.2
0.8
0.4
0
10
20
30
40
50
60
70
80
90
100
110
120
PPM

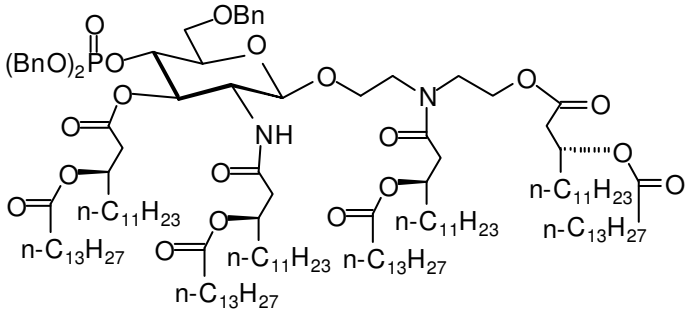

11

HRESI-MS (*m*/*z*) Calcd for $C_{143}H_{249}N_2O_{21}P$ $[M+Na]^+$: 2384.8047, found: 2384.8032.

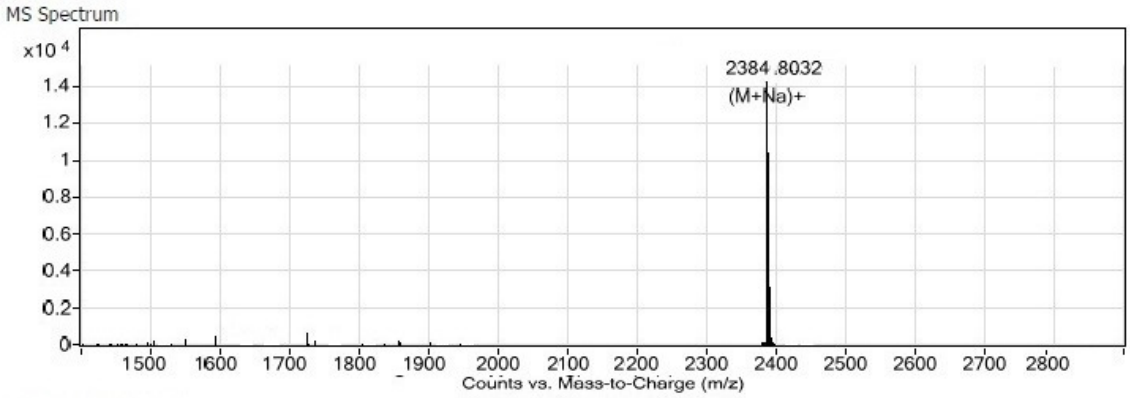

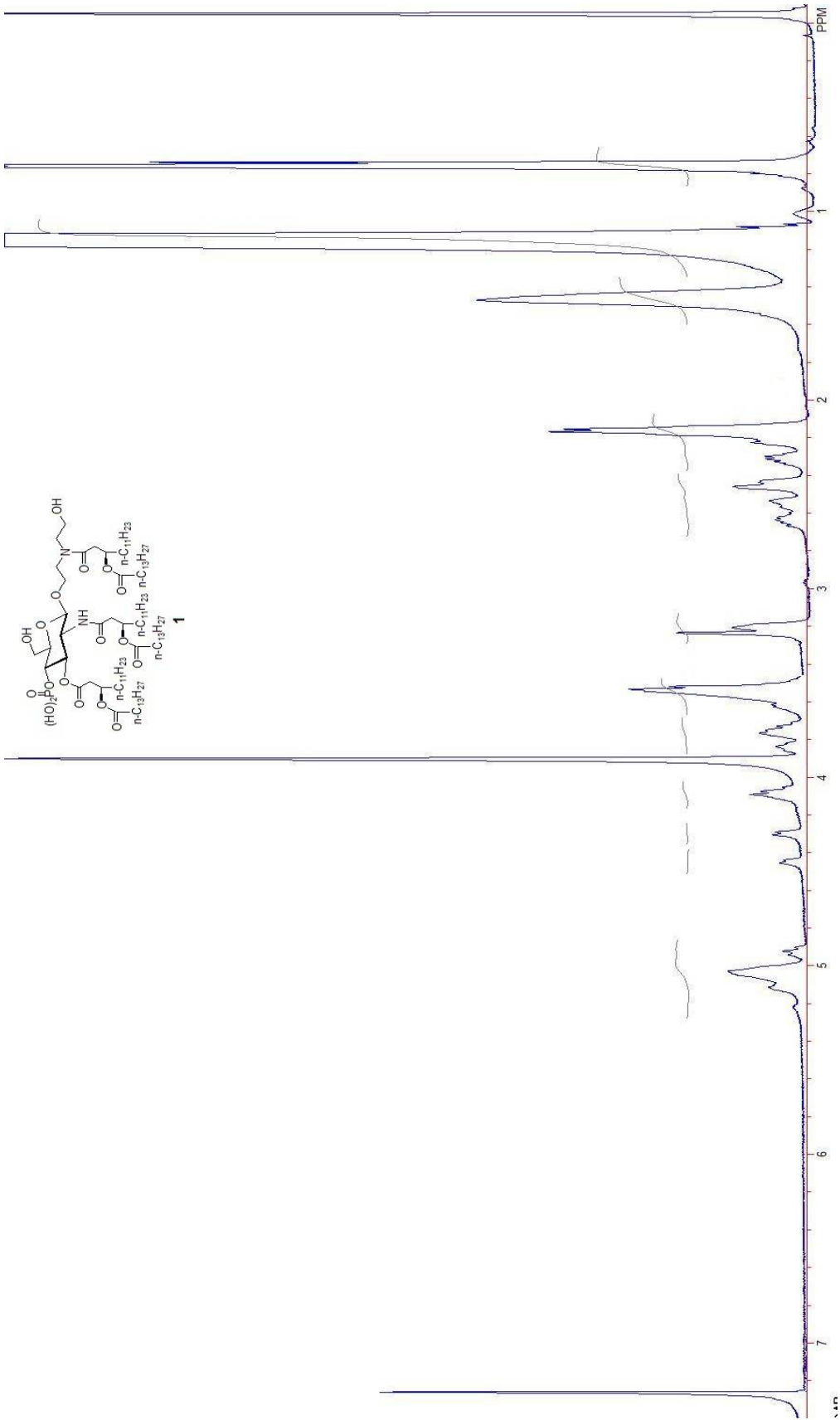
PPM
1
2
3
4
5
6
7
1

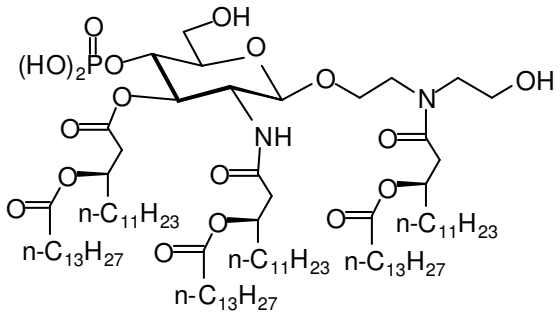

1

HRESI-MS (*m*/*z*) Calcd for $C_{94}H_{178}N_2O_{18}P$ $[M-H]^-$ 1654.2843, found: 1654.2837.

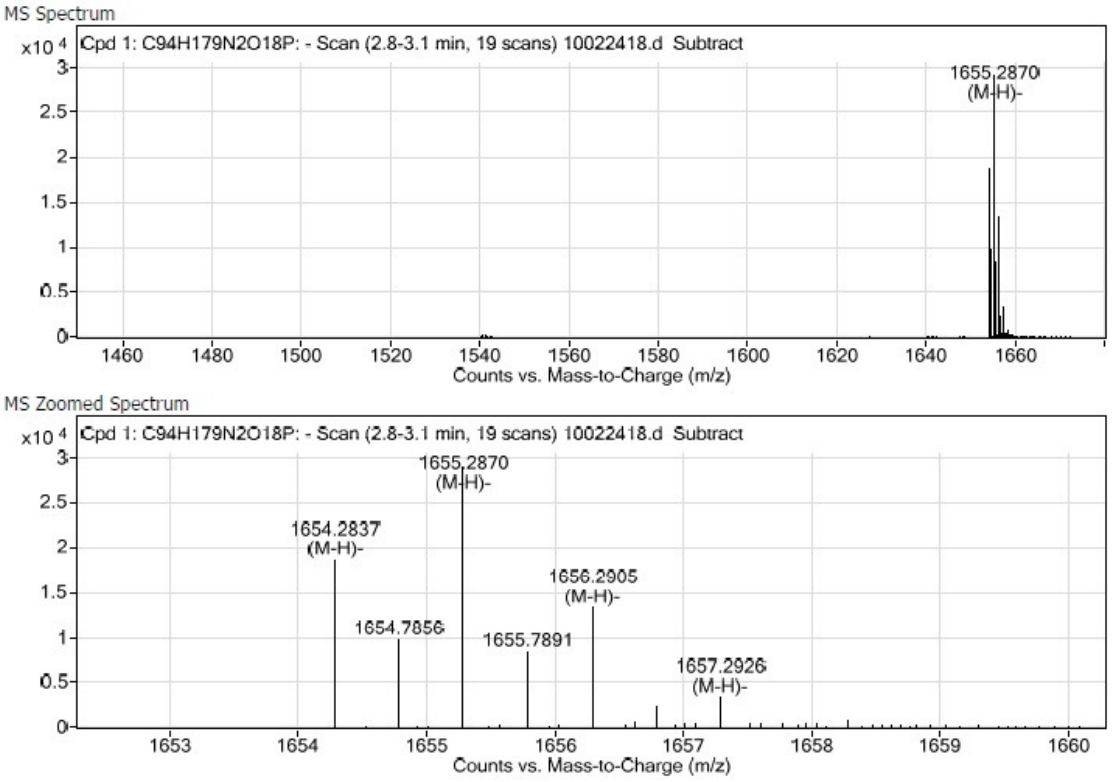

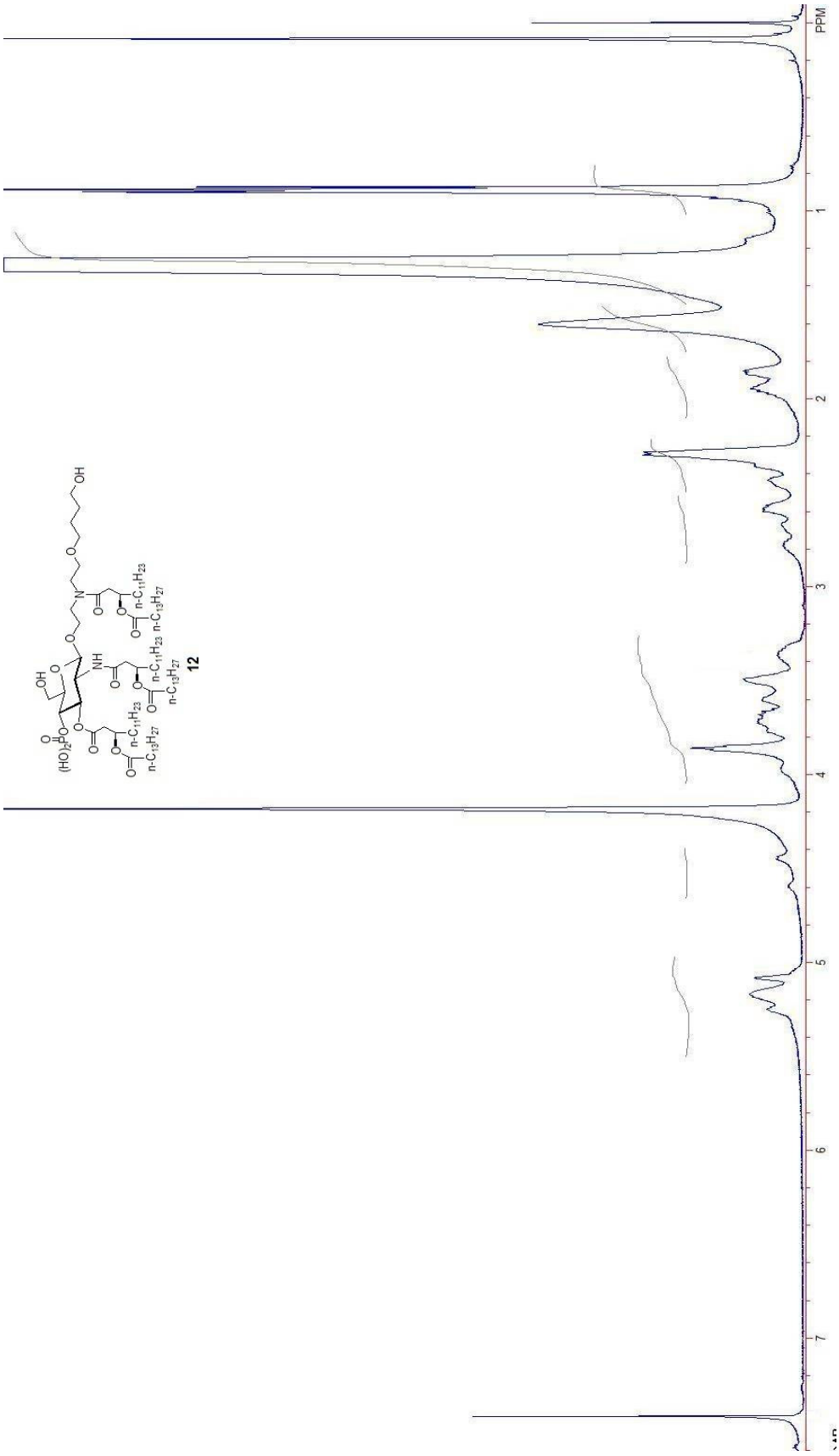
PPM
12

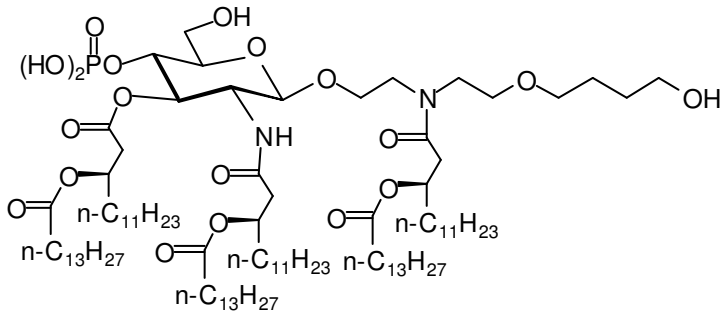

12

ESI-MS (*m/z*) Calcd for $C_{98}H_{186}N_2O_{19}P$ $[M-H]^-$ 1726.3, found: 1726.3.

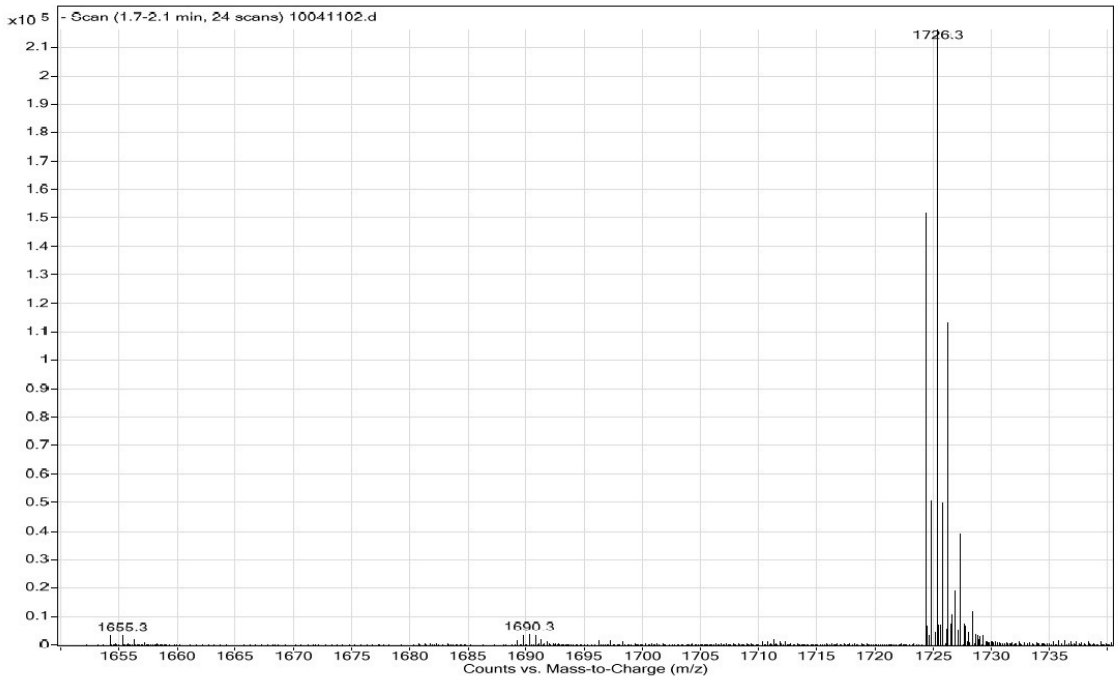

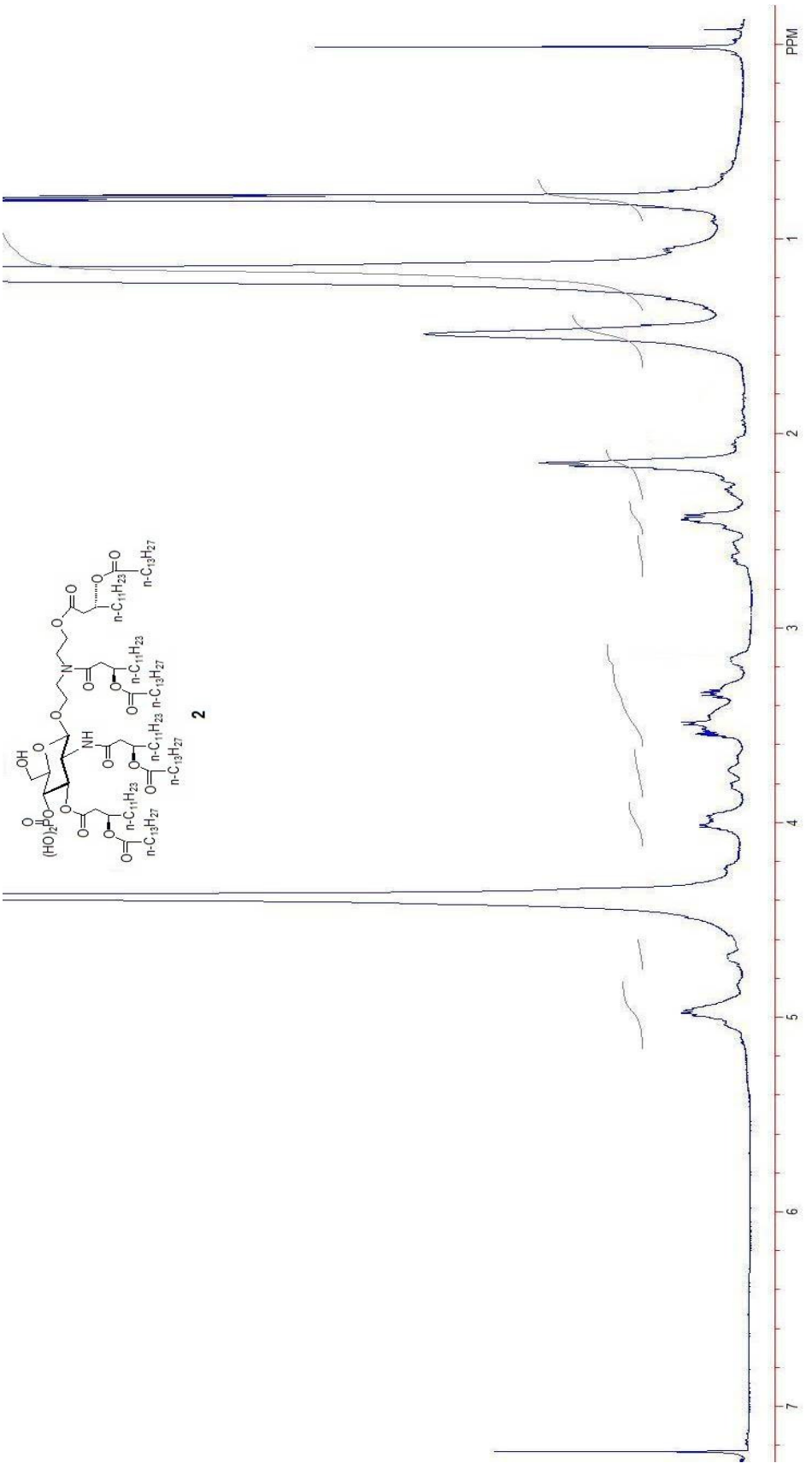
PPM
1
2
3
4
5
6
7
2

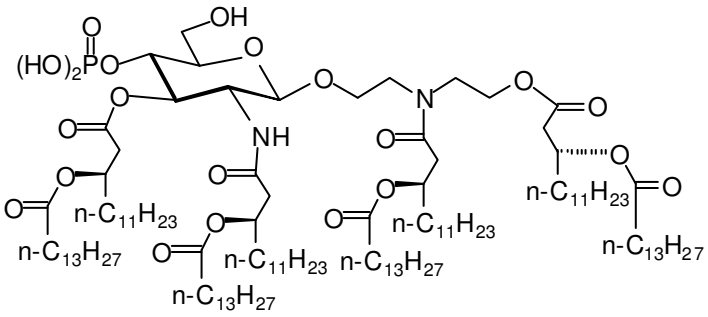

2

HRESI-MS (*m*/*z*) Calcd for $C_{122}H_{230}N_2O_{21}P$ $[M-H]^-$: 2090.6746, found: 2090.6758.

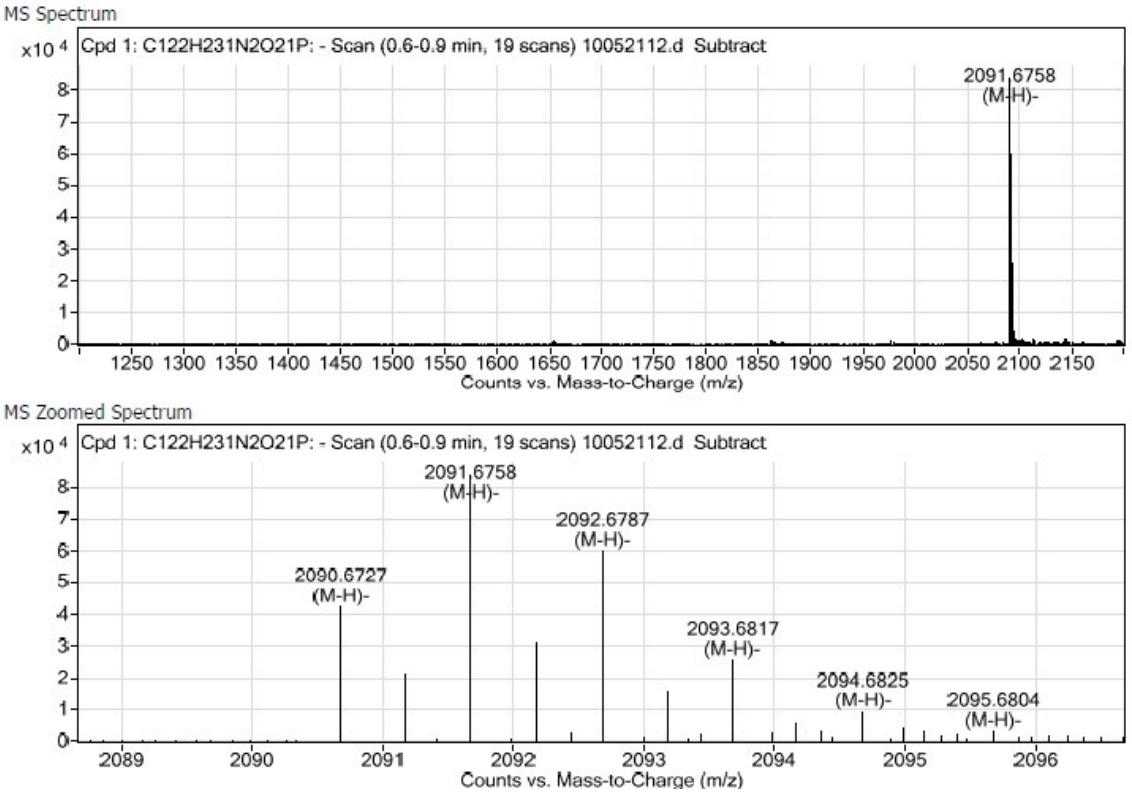

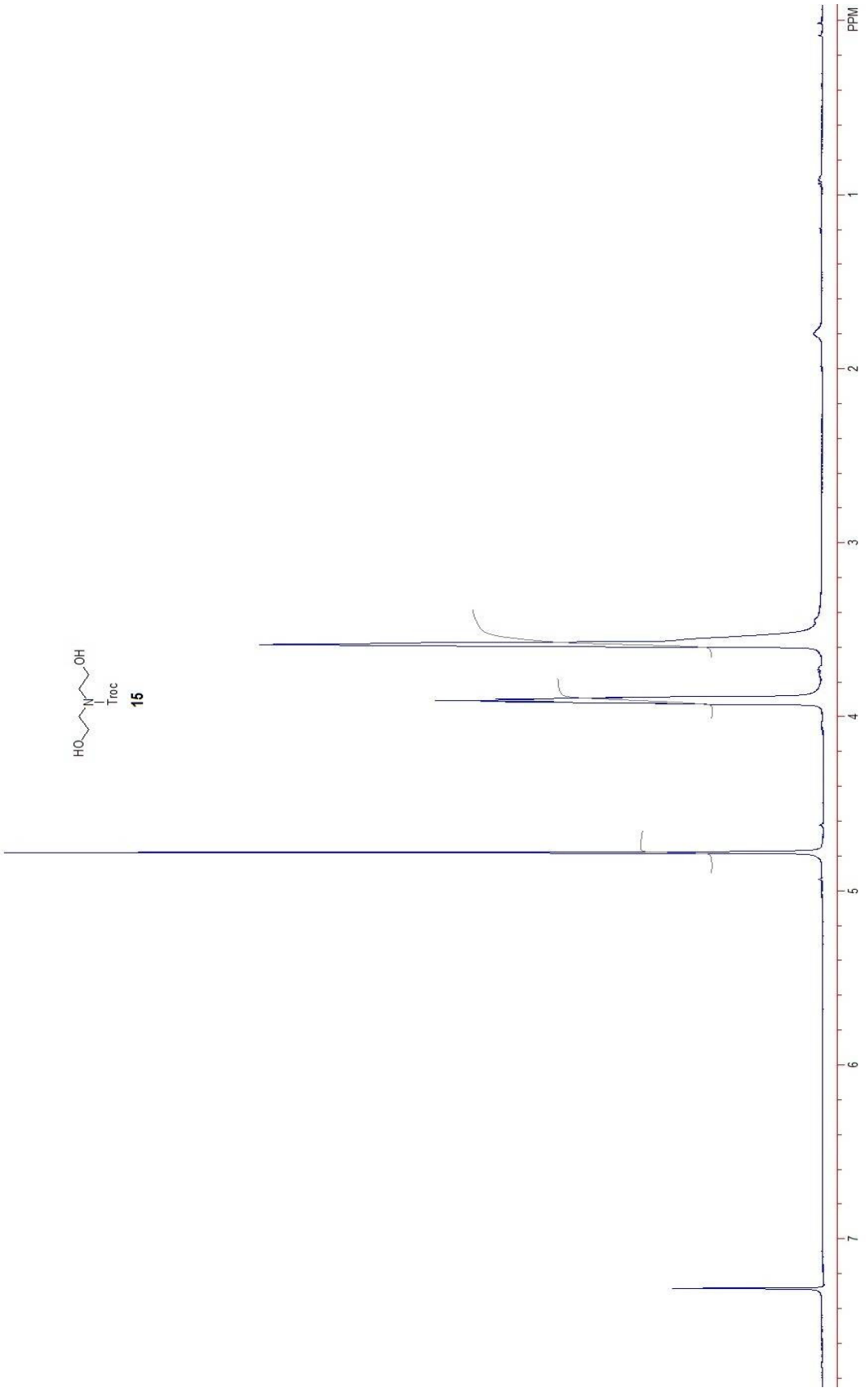
HO
N
Troc
OH
15
PPM
1
2
3
4
5
6
7

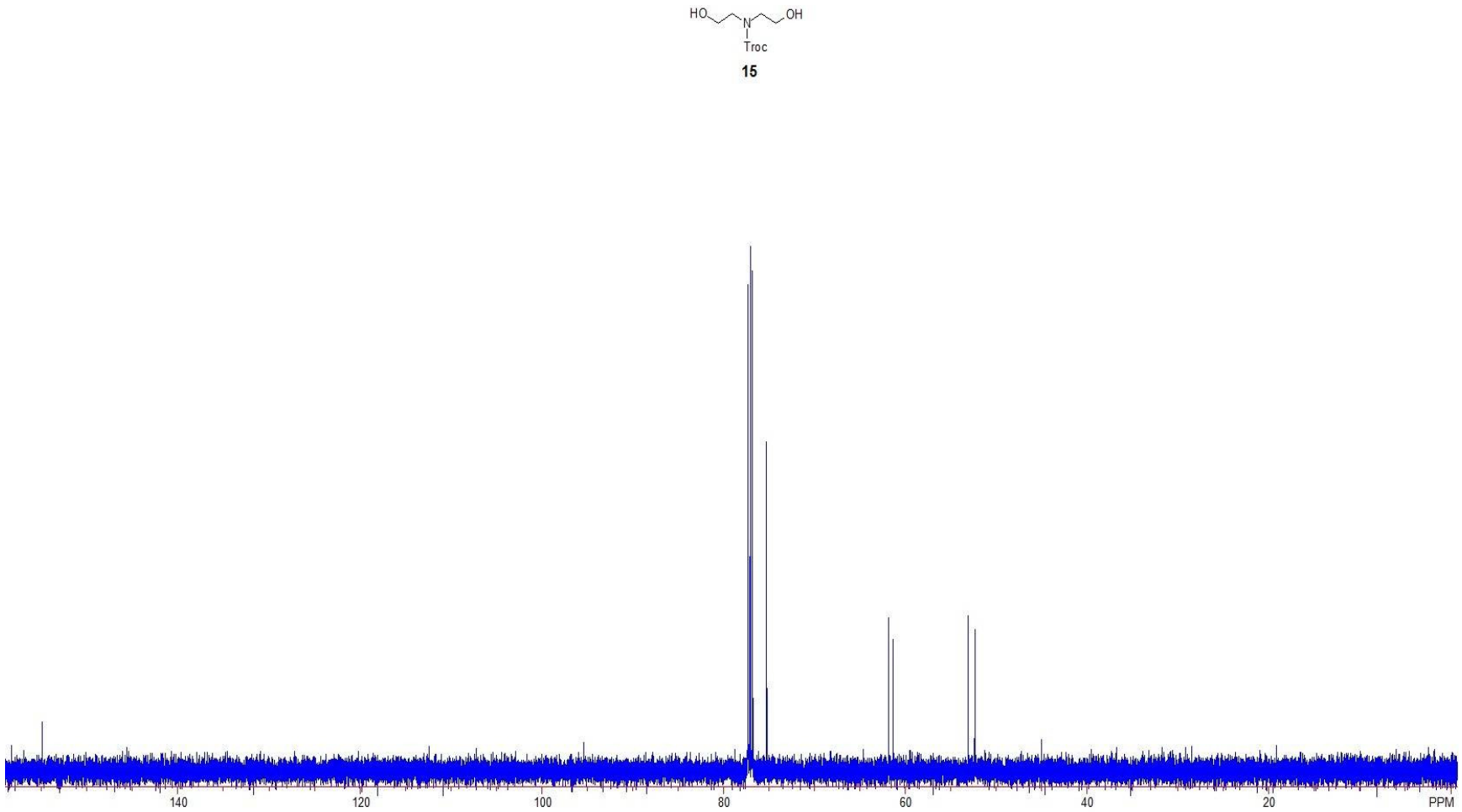

15

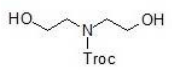

15

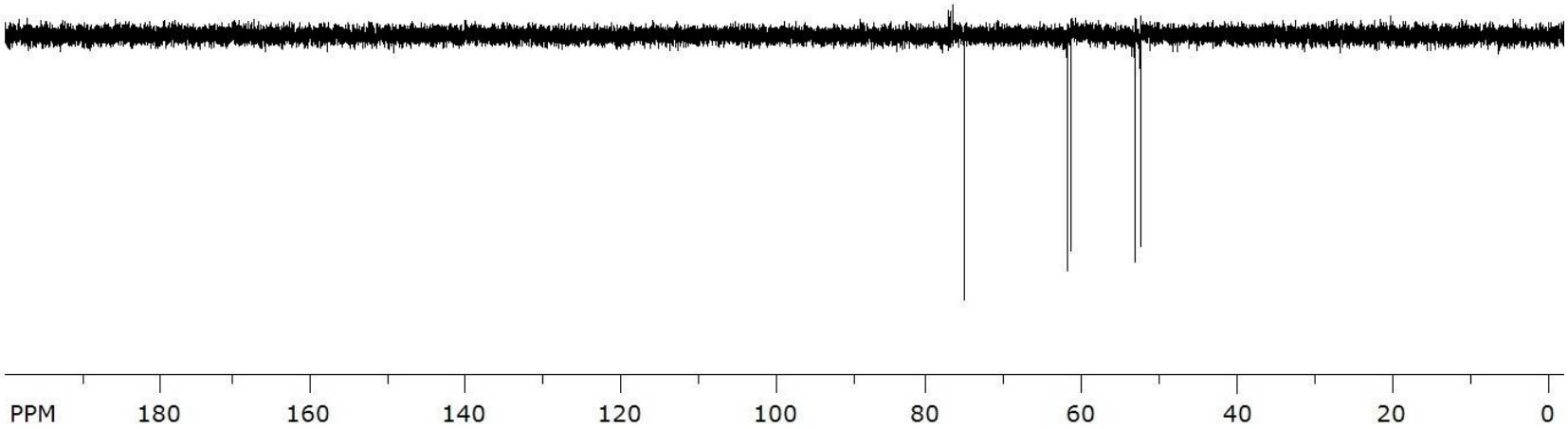

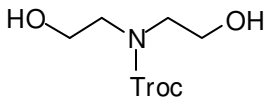

15

ESI-MS (*m*/*z*) Calcd for $C_7H_{12}Cl_3NO_4$ $[M + Na]^+$: 301.9, found: 302.0.

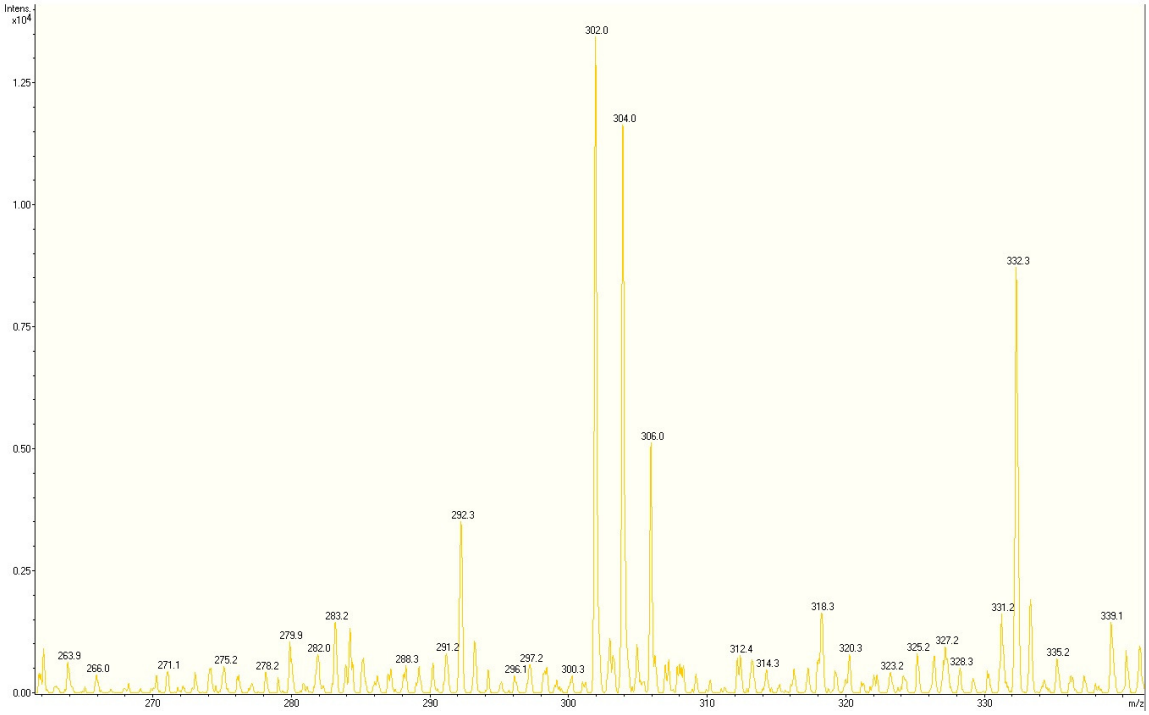

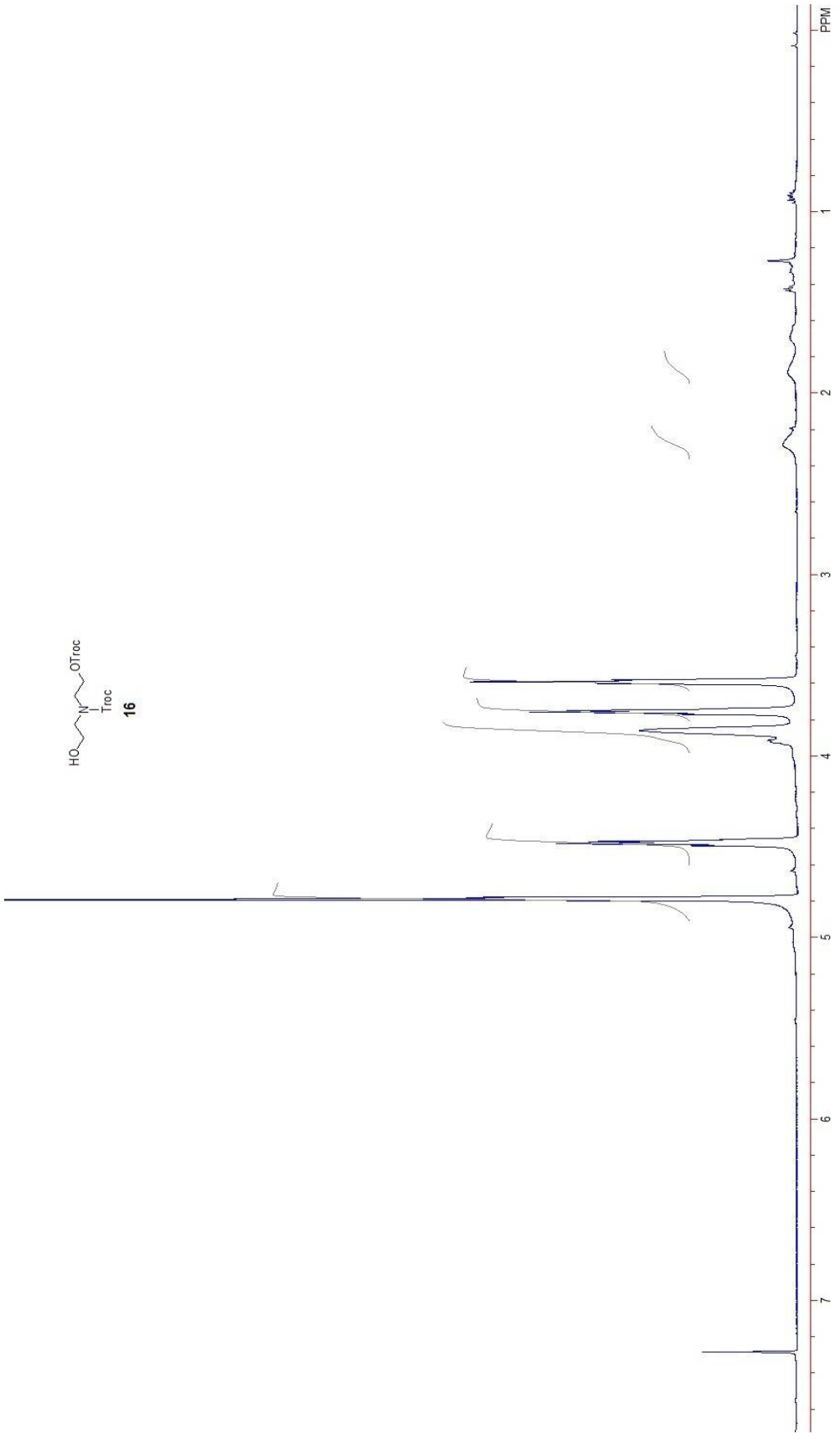
HO
OTroc
N
Troc
Troc
16
PPM
1
2
3
4
5
6
7

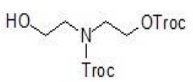

16

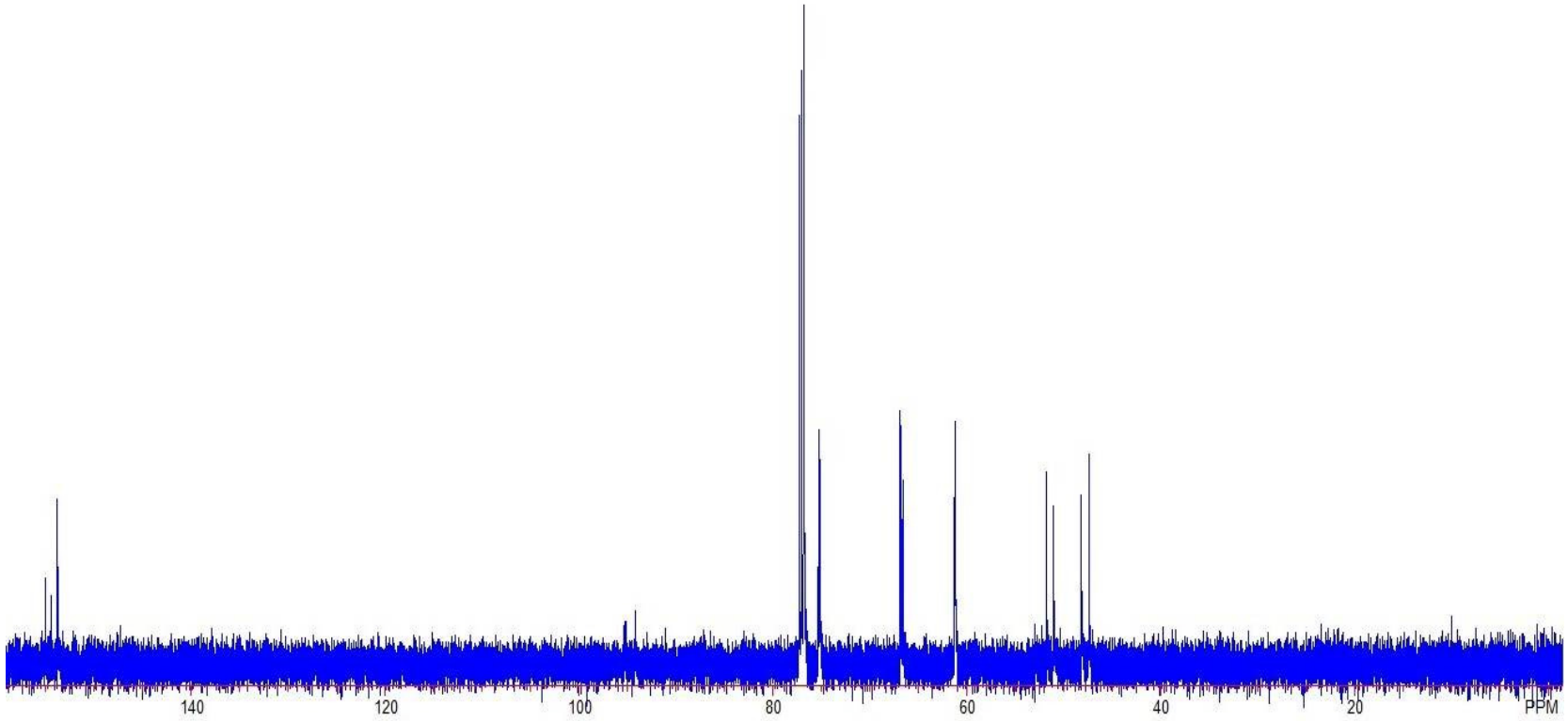

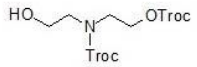

16

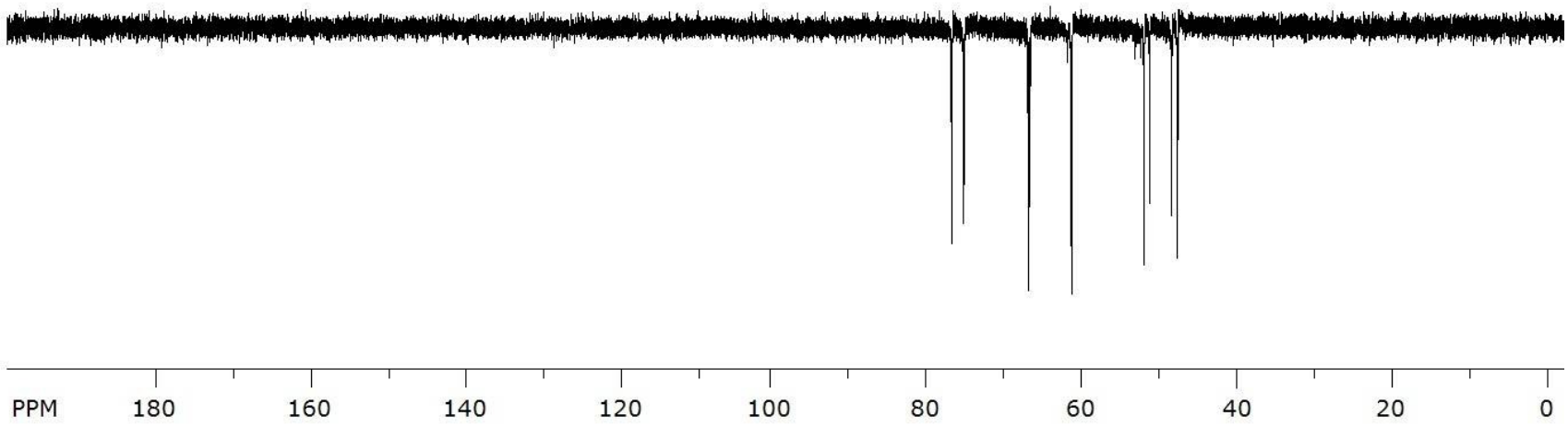

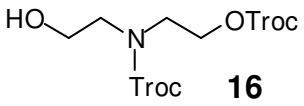

16

ESI-MS (*m*/*z*) Calcd for $C_{10}H_{13}Cl_6NO_6$ $[M + Na]^+$: 475.9, found: 475.9.

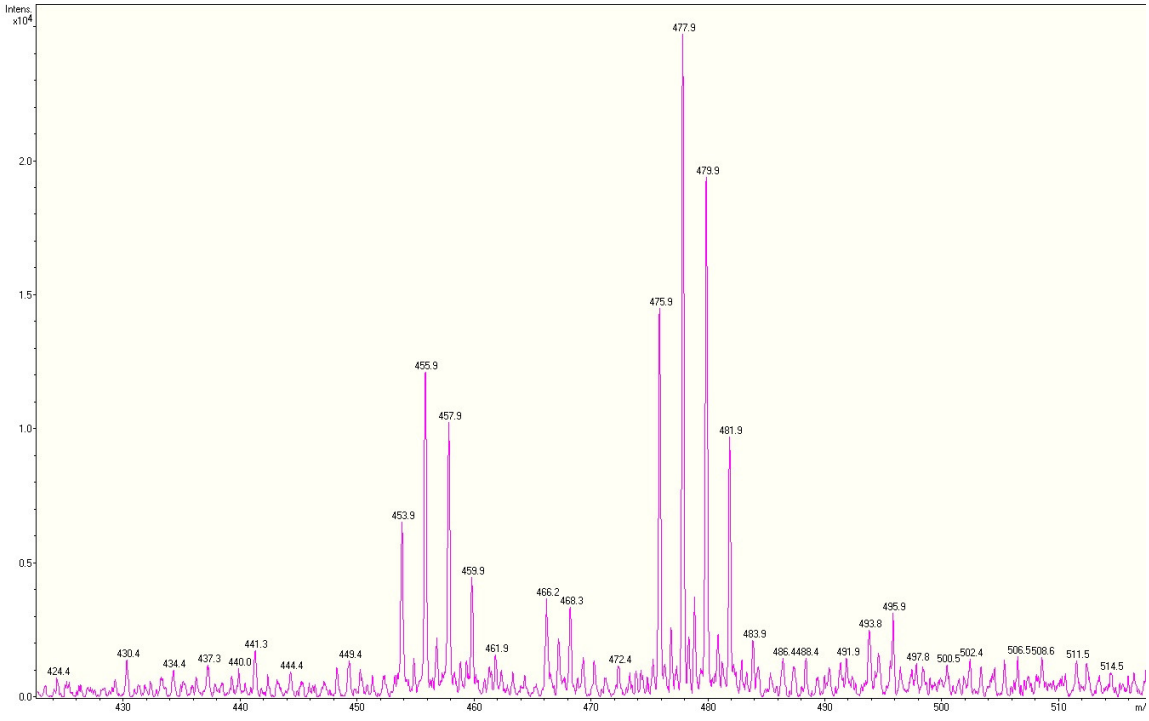

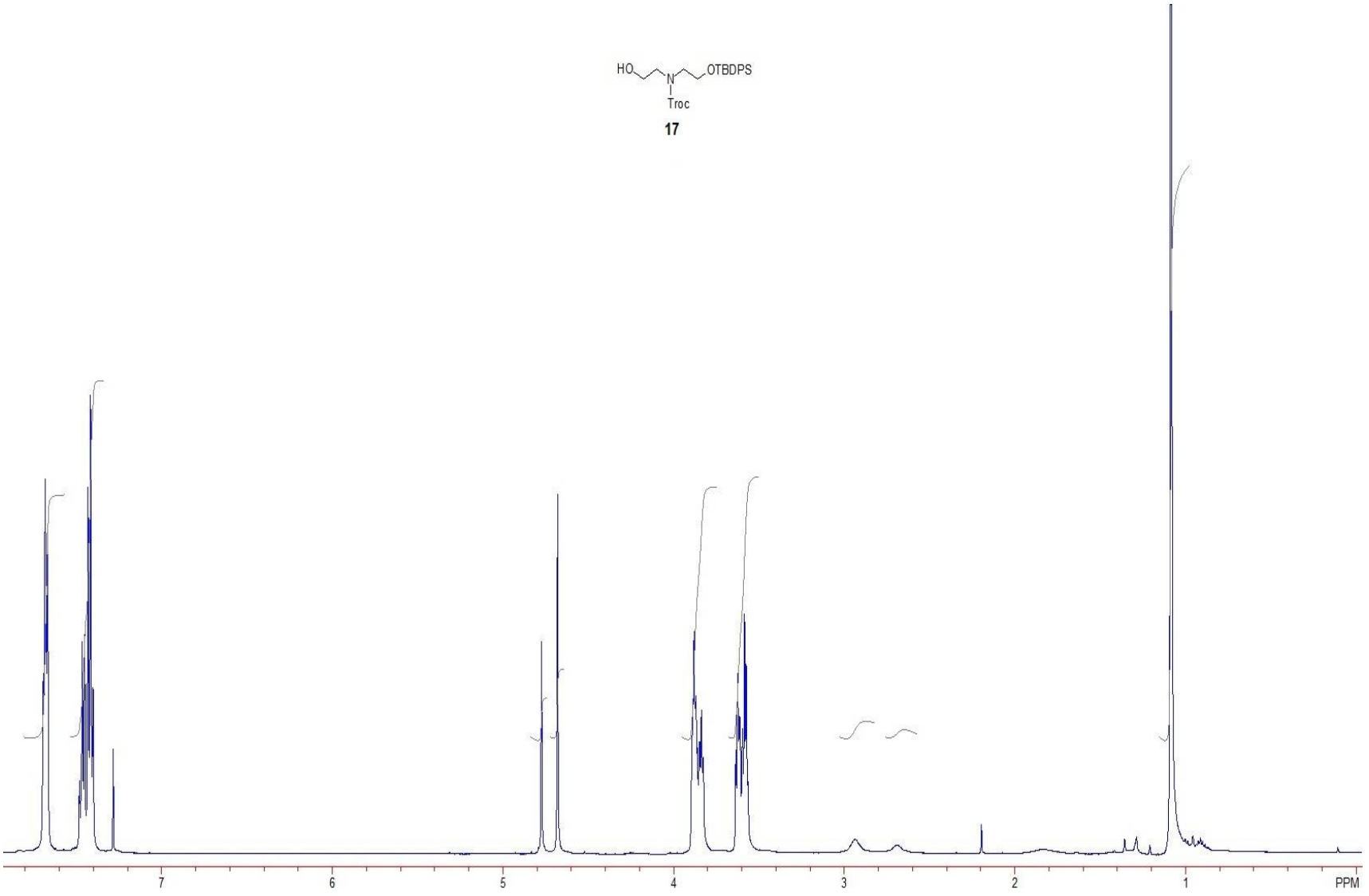
HO
OTBDPS
N
Troc
17
7
6
5
4
3
2
1
PPM

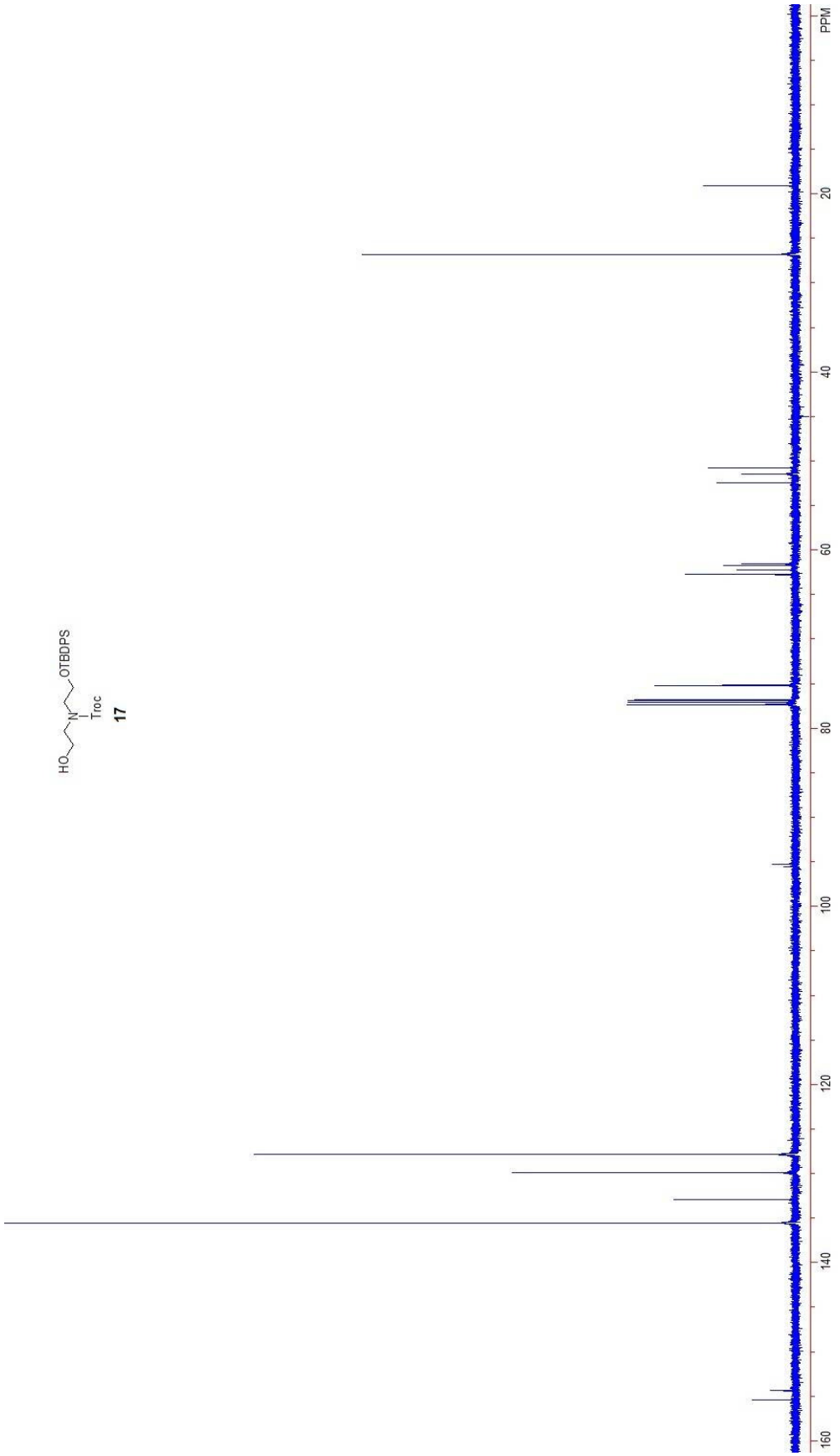
HO
N
Troc
OTBDPS
17
PPM
20
40
60
80
100
120
140
160

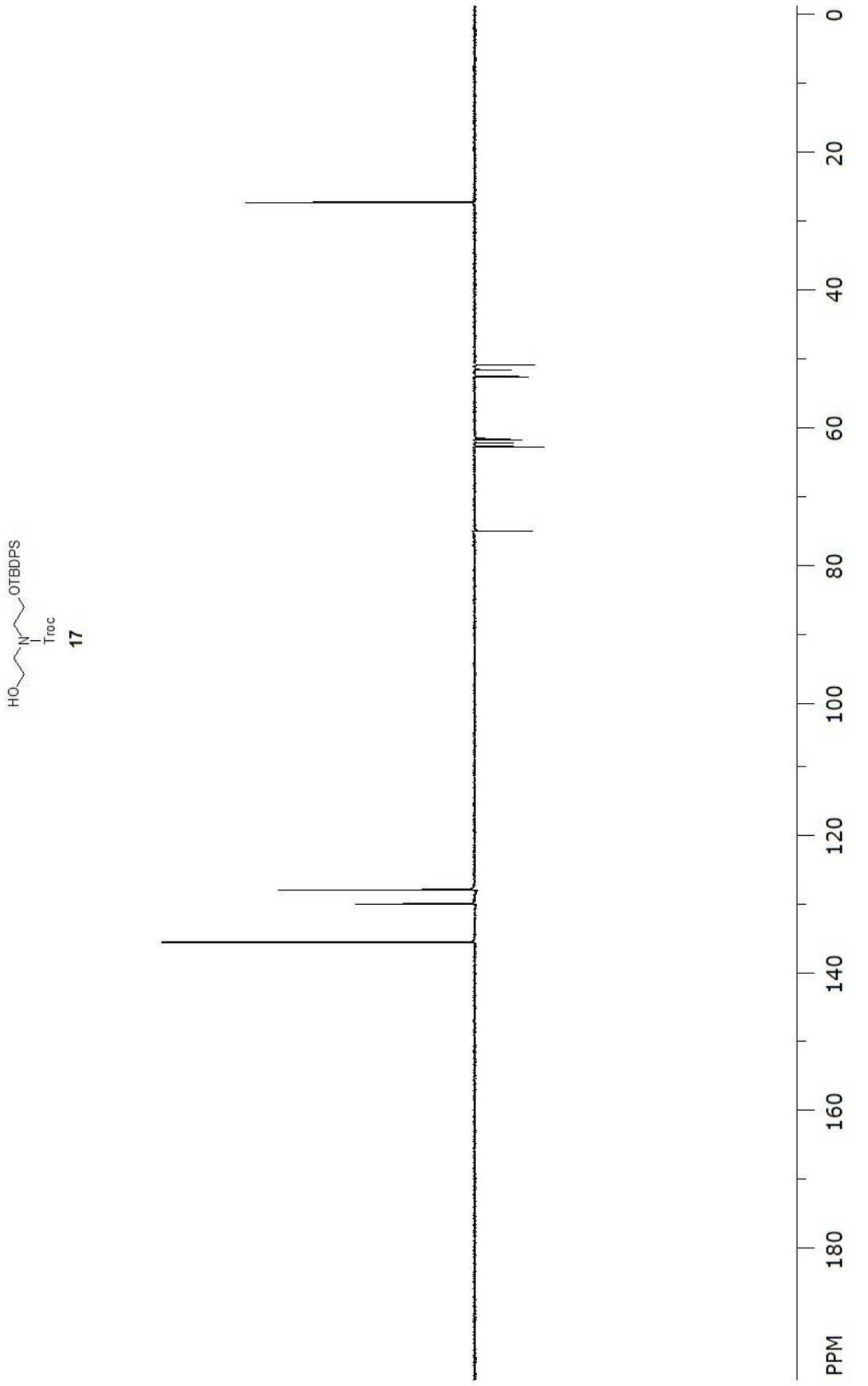
OTBDPS
N
Troc
HO
17
0
20
40
60
80
100
120
140
160
180
PPM

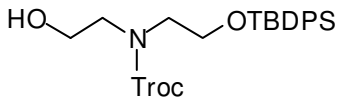

17

ESI-MS (*m*/*z*) Calcd for $C_{23}H_{30}Cl_3NO_4Si$ $[M - C_4H_9]^+$: 460.0, found: 460.4.

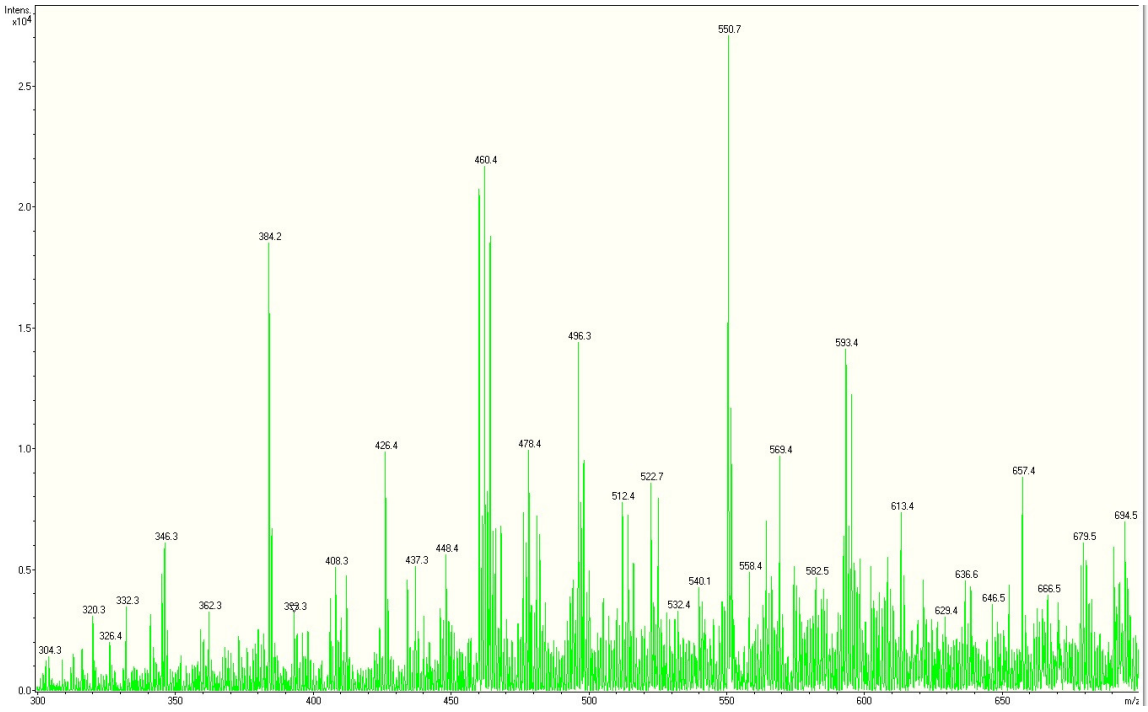

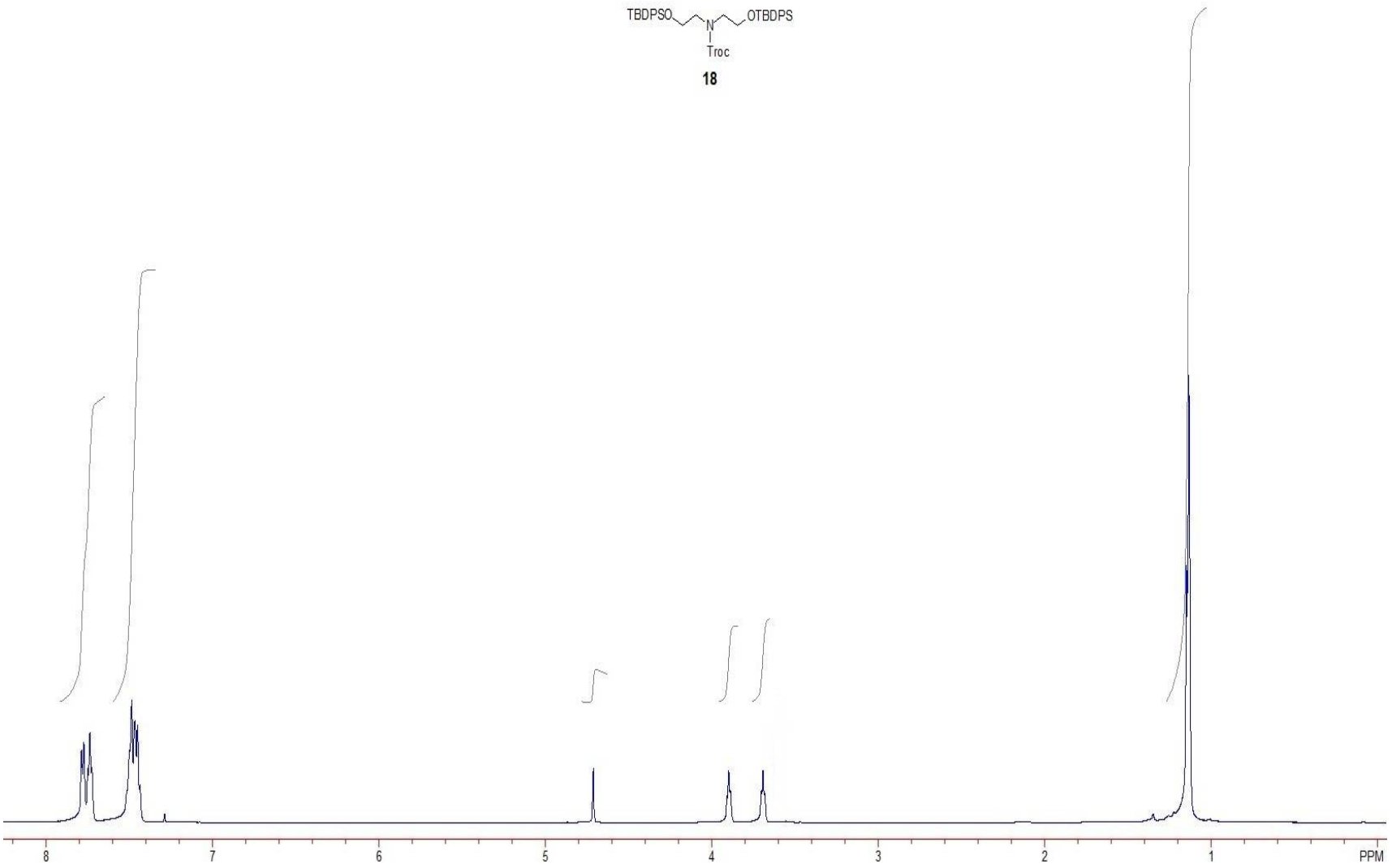
TBDPSO
N
OTBDPS
Troc
18
8
7
6
5
4
3
2
1
PPM

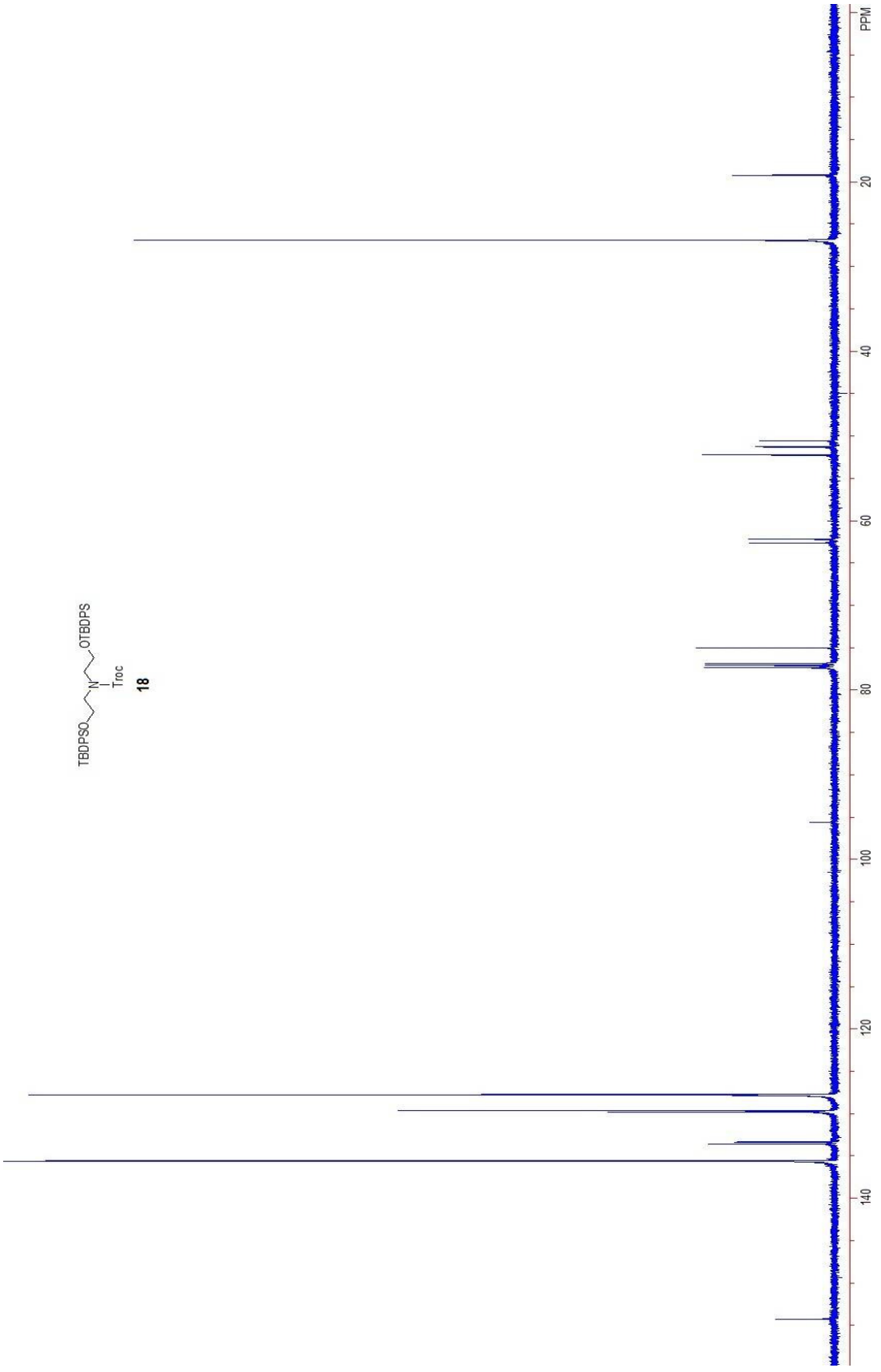
TBDPSO
OTBDPS
N
Troc
18
PPM
20
40
60
80
100
120
140

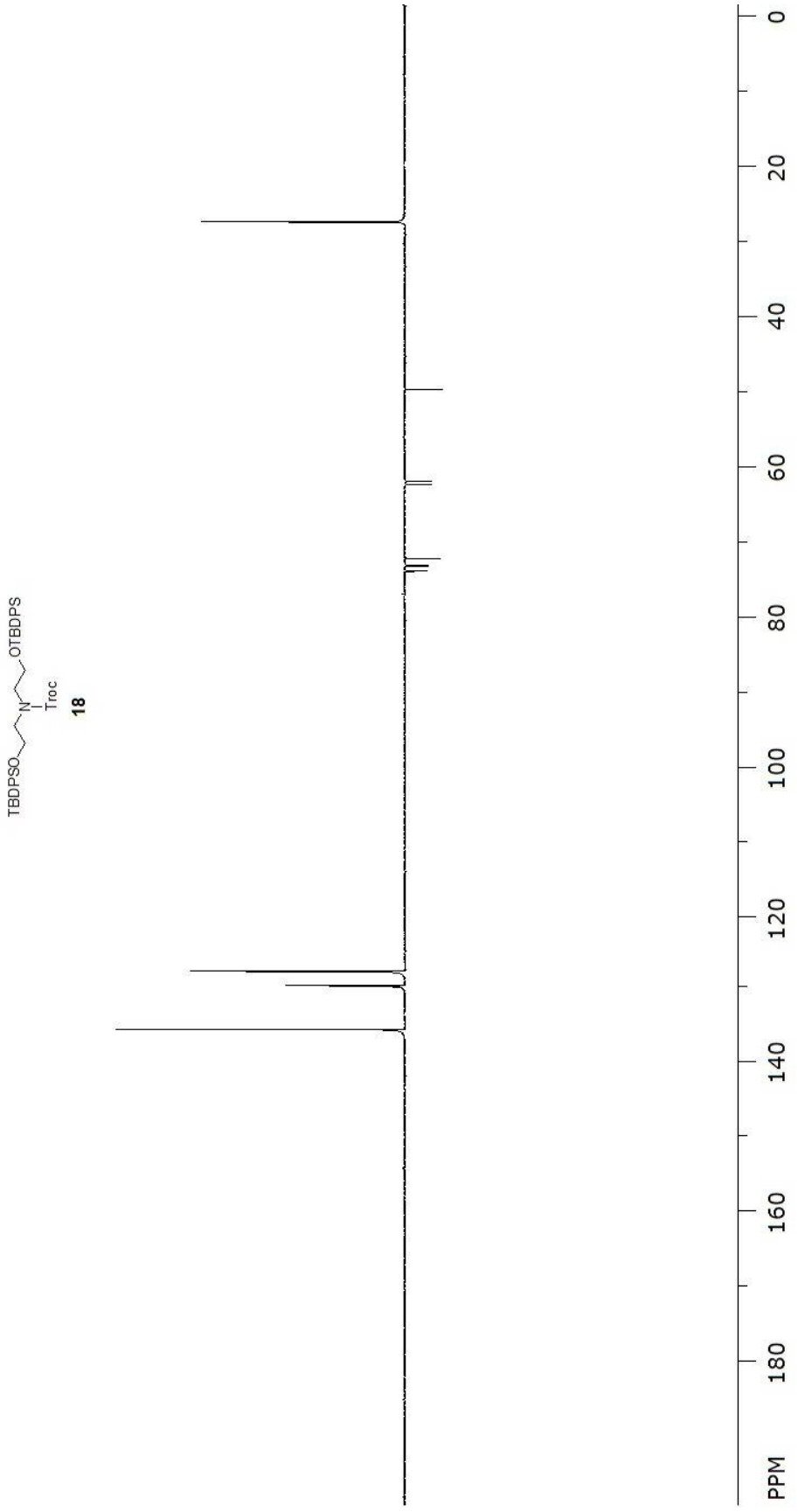
TBDPSO
N
Troc
OTBDPS
18
PPM
180
160
140
120
100
80
60
40
20
0

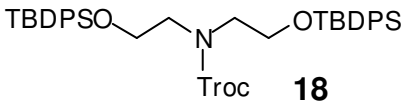

18

ESI-MS (*m*/*z*) Calcd for $C_{39}H_{48}Cl_3NO_4Si_2$ $[M - C_4H_9]^+$: 698.2, found: 698.5.

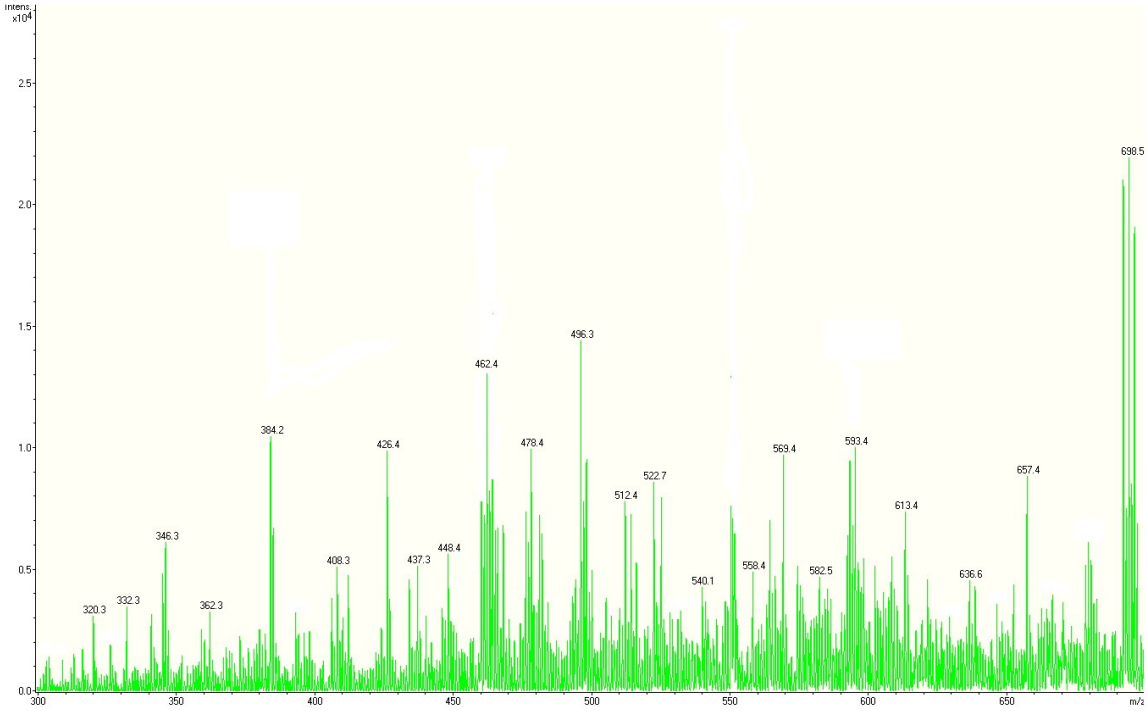

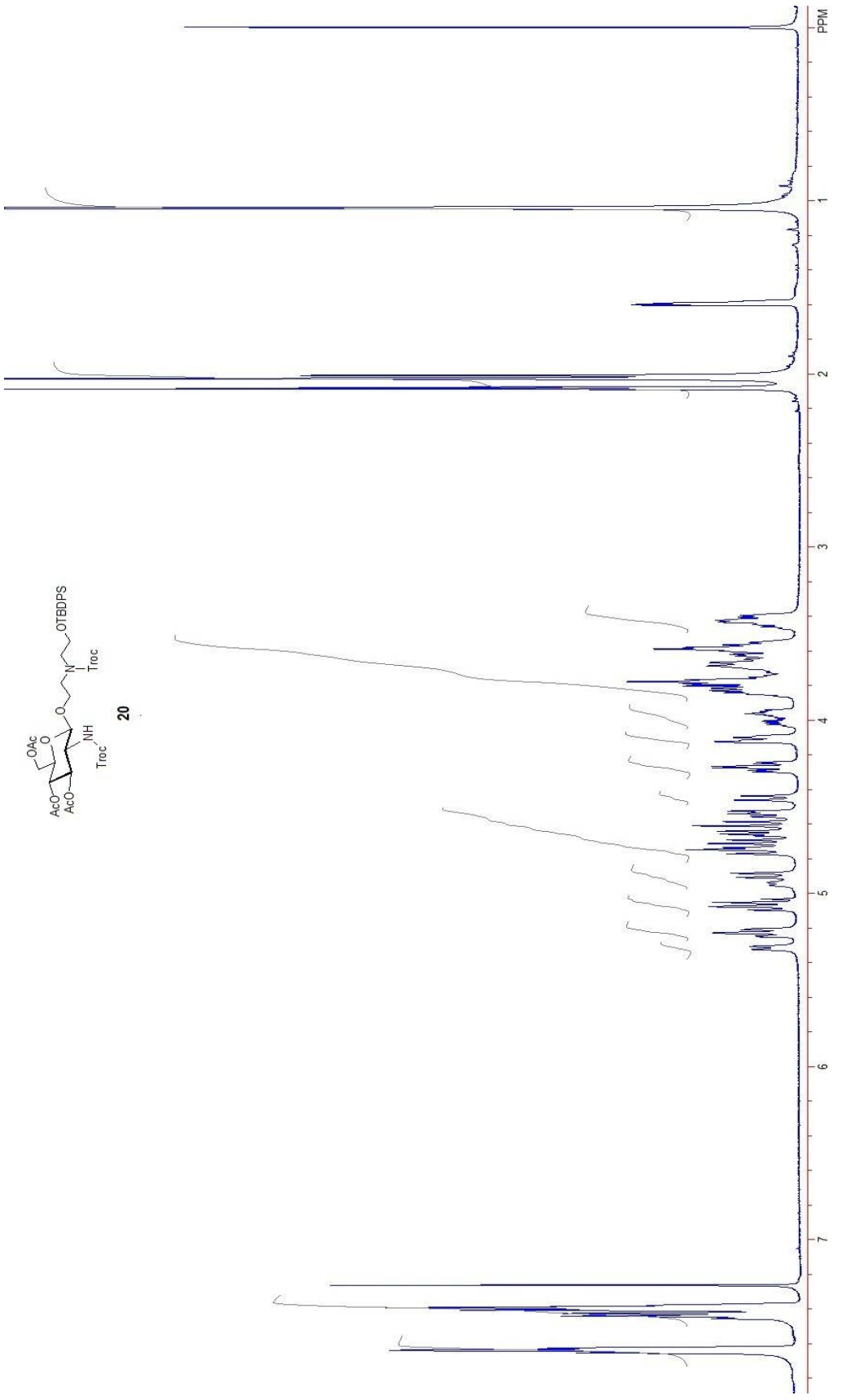
OTBDPS
Troc
O
NH
Troc
OAc
O
AcO
AcO
20
PPM
1
2
3
4
5
6
7

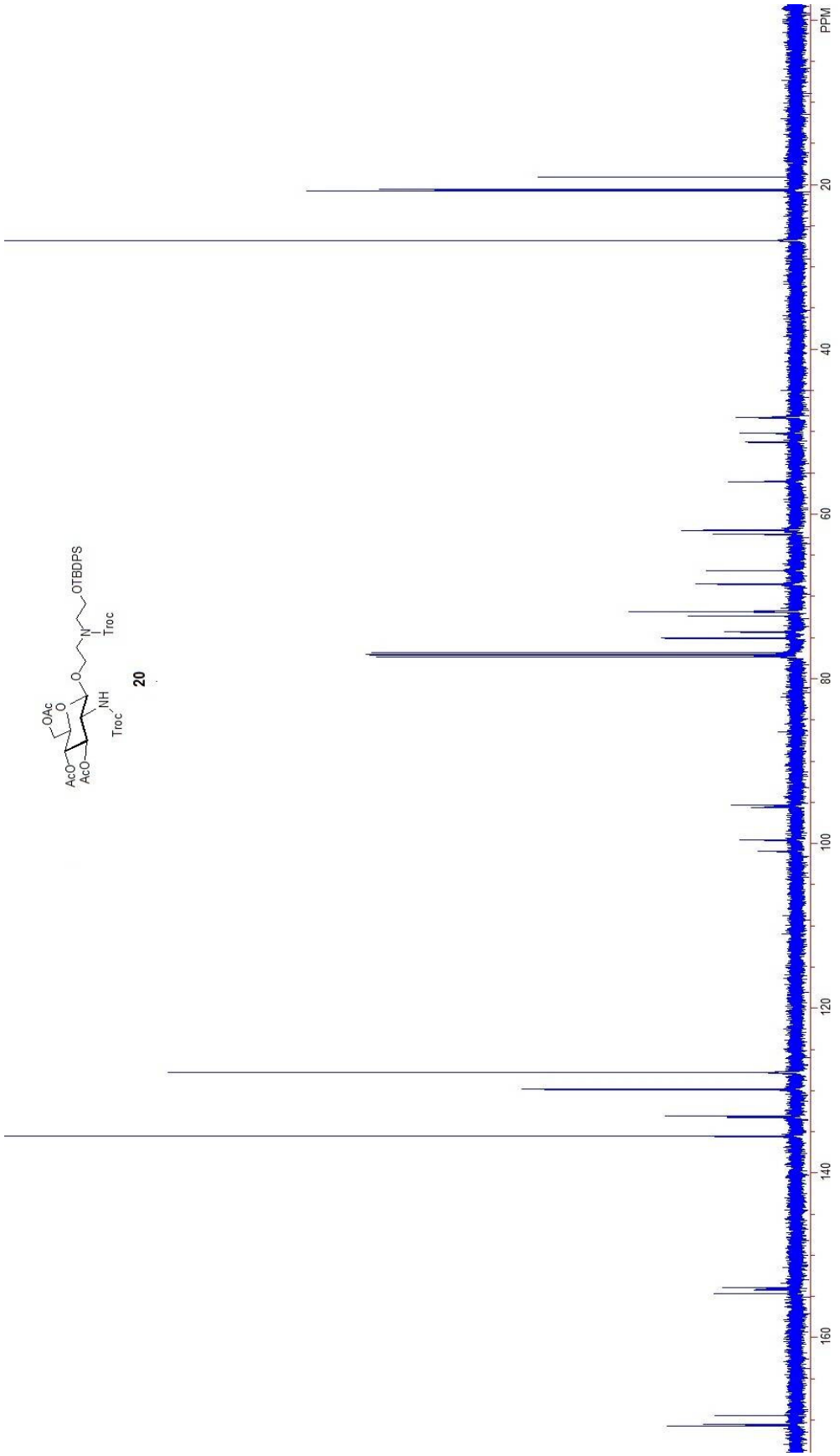
OTBDPS
N
Troc
O
NH
Troc
OAc
O
AcO
AcO
20
PPM
20
40
60
80
100
120
140
160

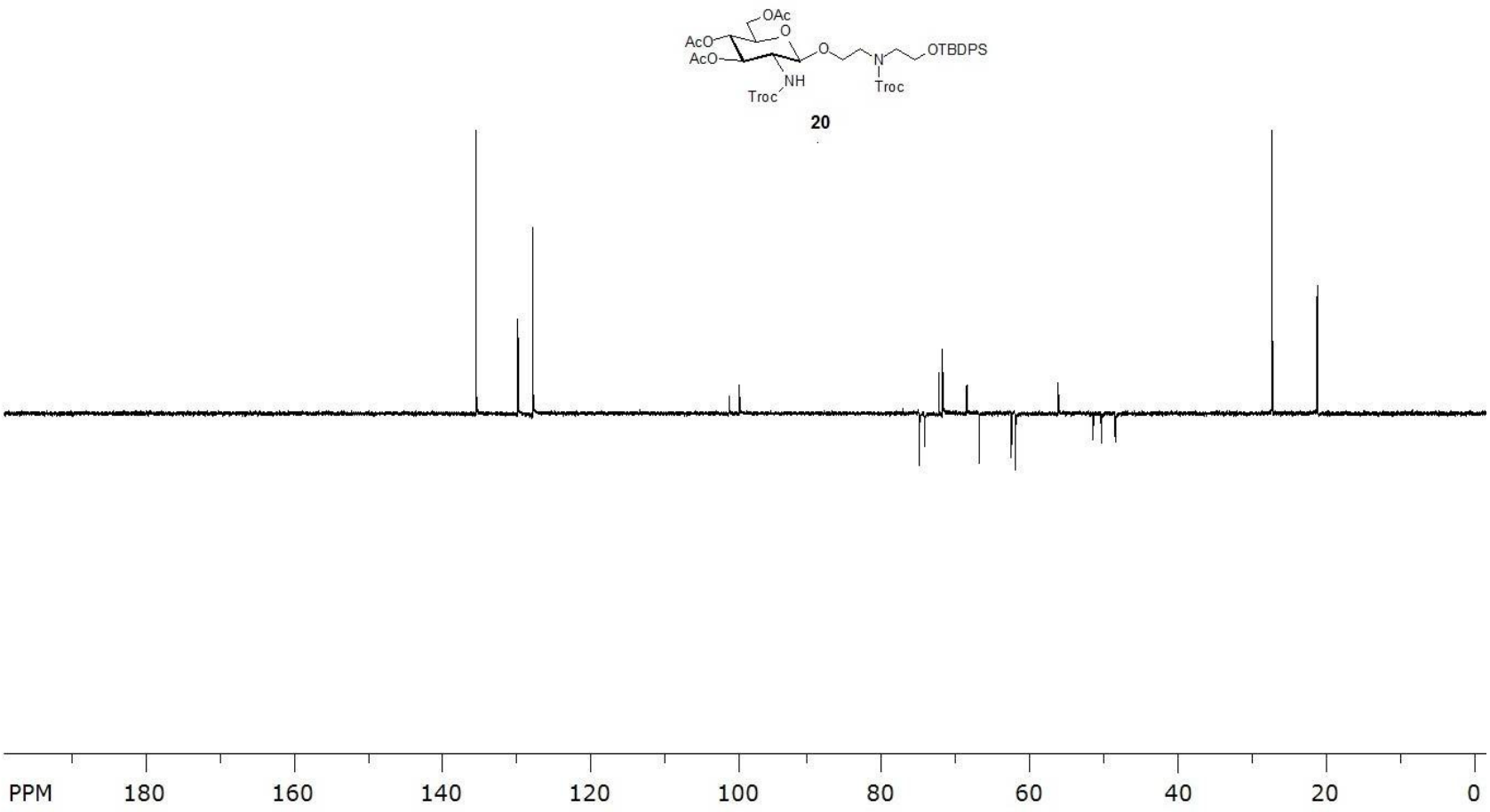
OAc
O
AcO
AcO
O
N
OTBDPS
NH
Troc
Troc
20
PPM
180
160
140
120
100
80
60
40
20
0

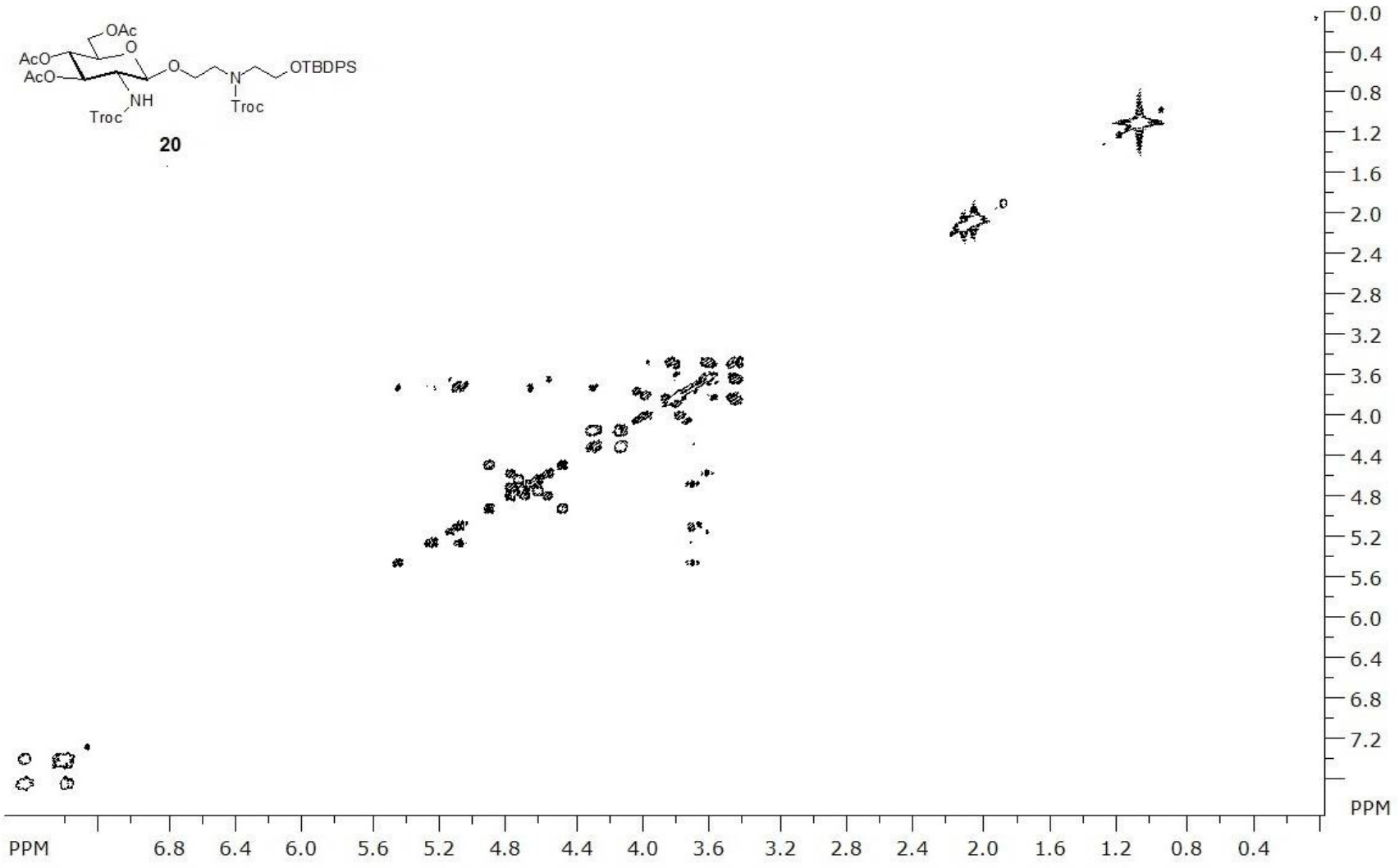
OAc
AcO
AcO
O
O
N
OTBDPS
NH
Troc
Troc
20
0.0
0.4
0.8
1.2
1.6
2.0
2.4
2.8
3.2
3.6
4.0
4.4
4.8
5.2
5.6
6.0
6.4
6.8
7.2
PPM
PPM
6.8
6.4
6.0
5.6
5.2
4.8
4.4
4.0
3.6
3.2
2.8
2.4
2.0
1.6
1.2
0.8
0.4

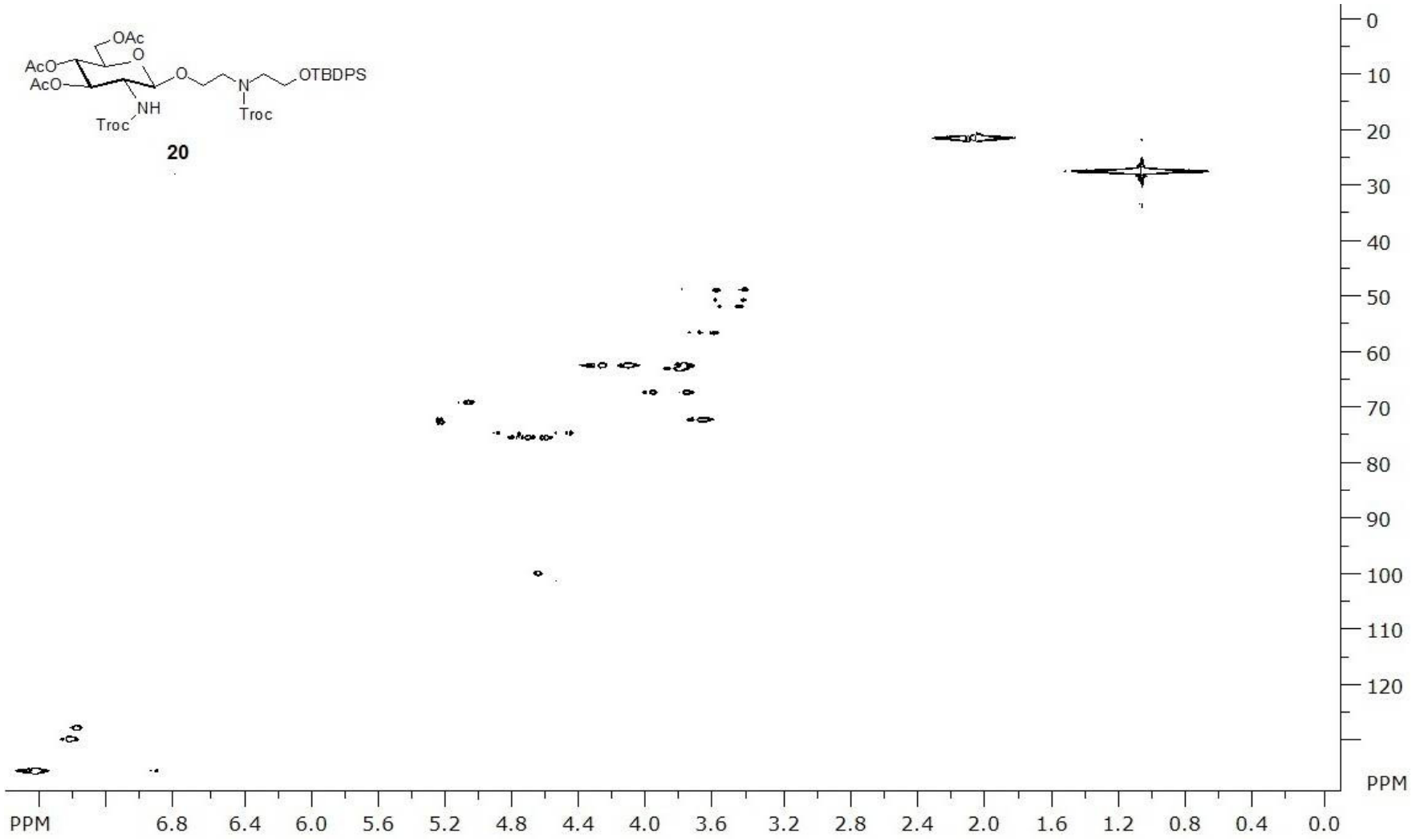
OAc
O
AcO
AcO
O
N
OTBDPS
NH
Troc
Troc
20
0
10
20
30
40
50
60
70
80
90
100
110
120
PPM
PPM
6.8
6.4
6.0
5.6
5.2
4.8
4.4
4.0
3.6
3.2
2.8
2.4
2.0
1.6
1.2
0.8
0.4
0.0

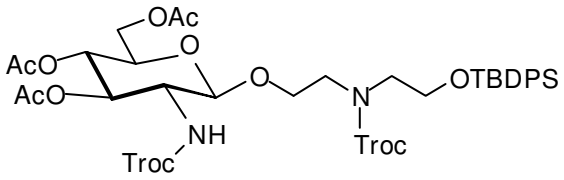

20

MALDI-MS (*m/z*) Calcd for $C_{38}H_{48}Cl_6N_2O_{13}Si$ $[M + Na]^+$: 1001.09, found: 1001.08.

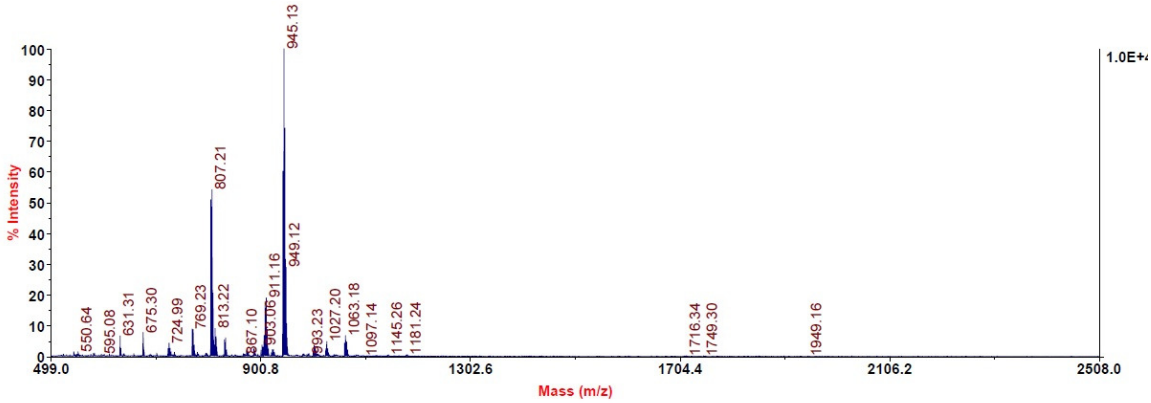

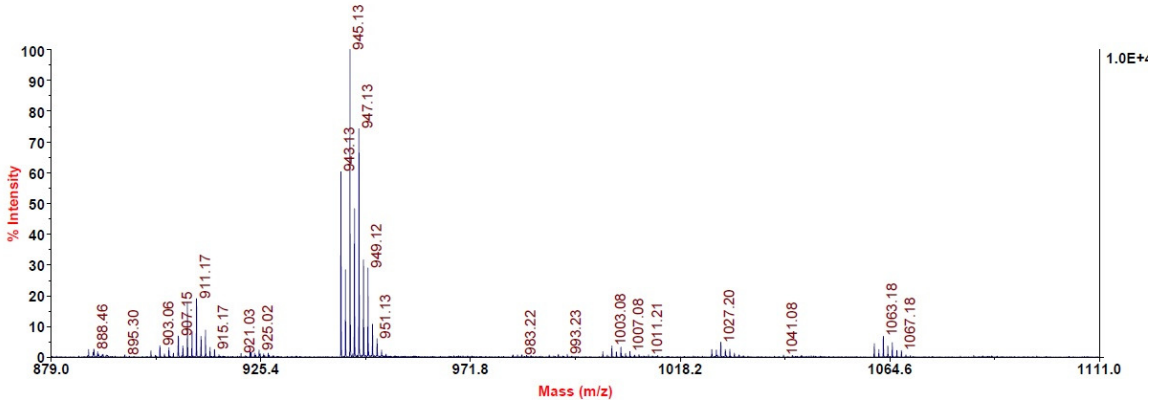

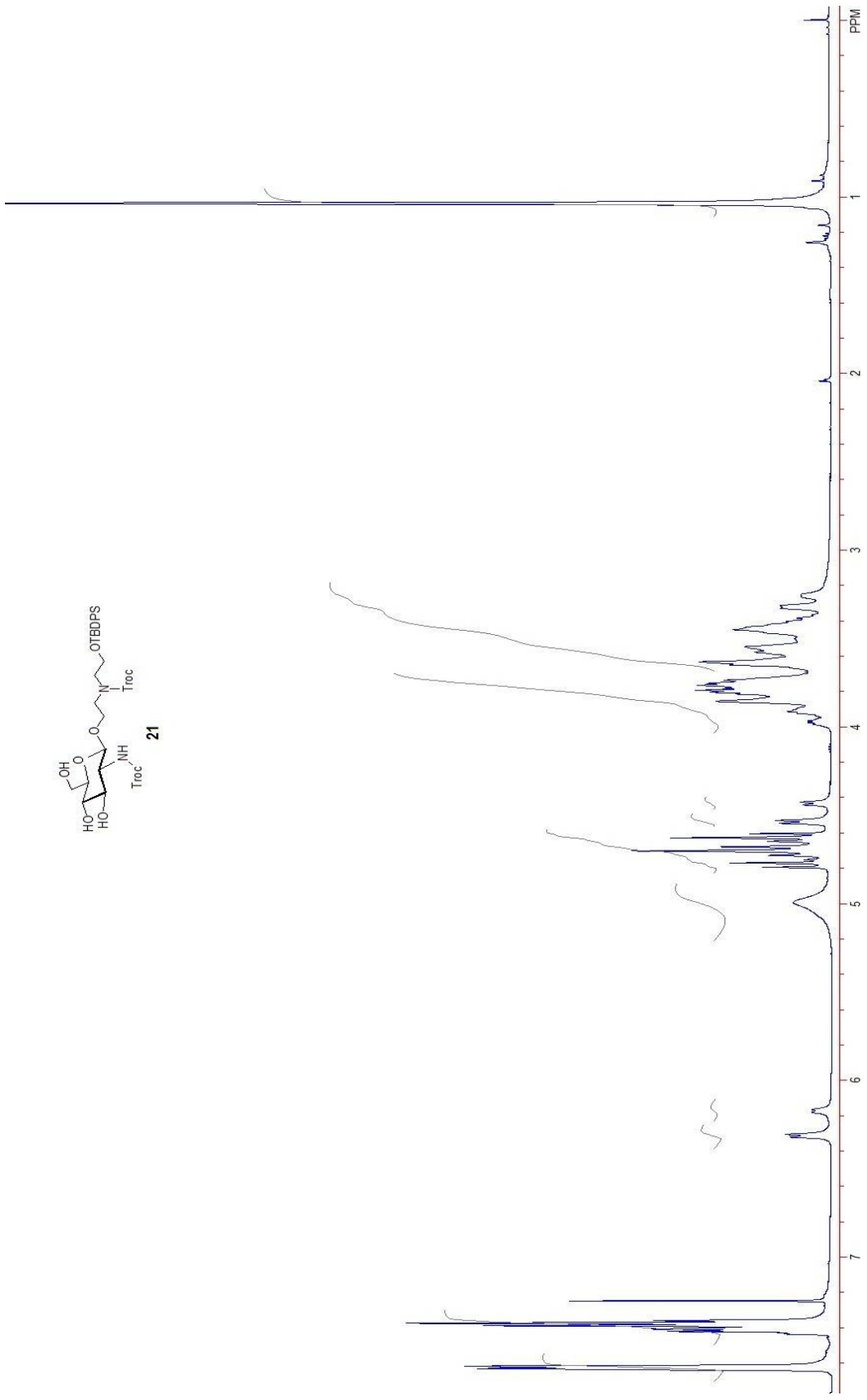
OTBDPS
Troc
N
O
NH
Troc
OH
O
HO
HO
21
PPM
1
2
3
4
5
6
7

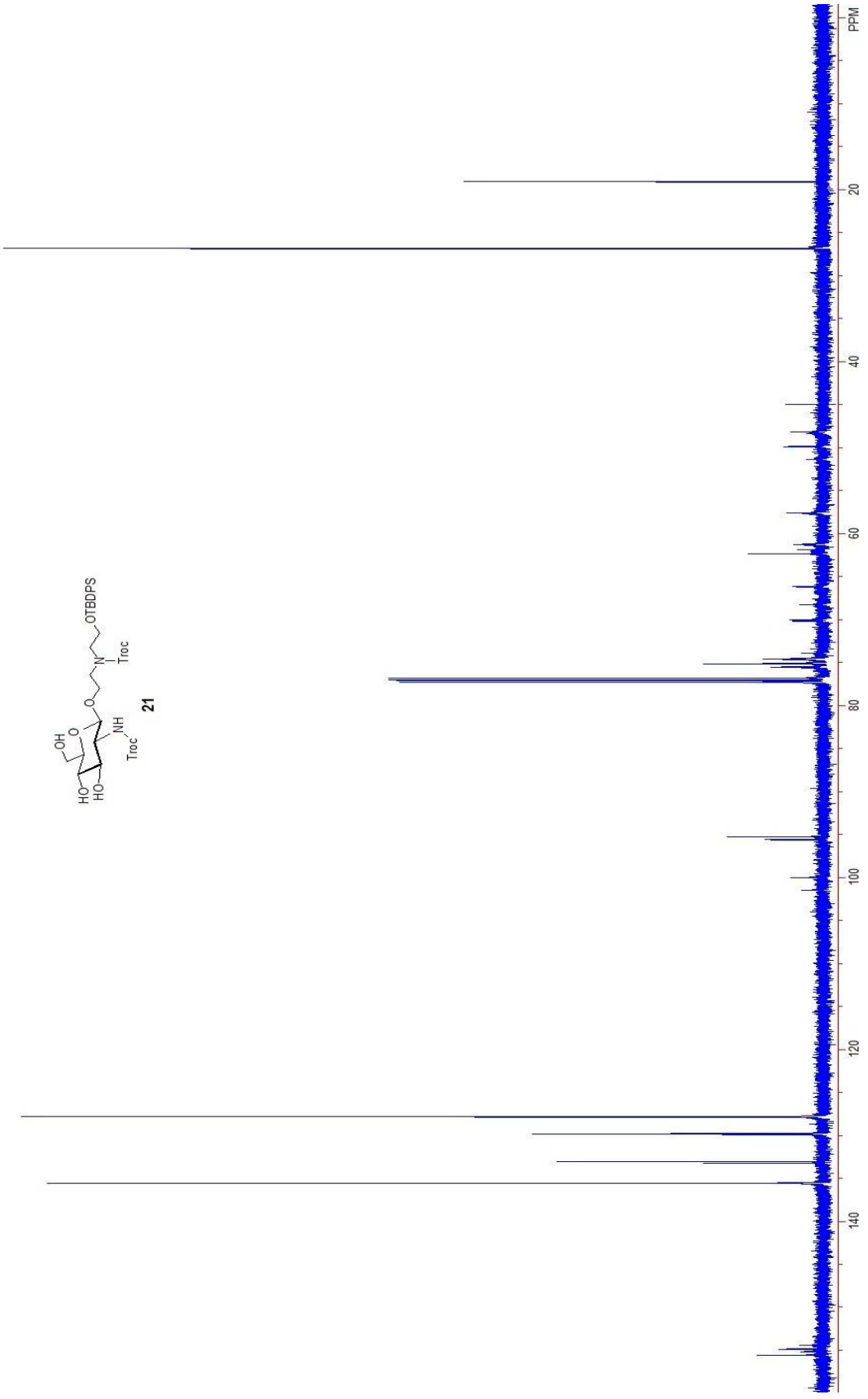
OTBDPS
Troc
N
O
NH
Troc
OH
O
HO
HO
21
PPM
20
40
60
80
100
120
140

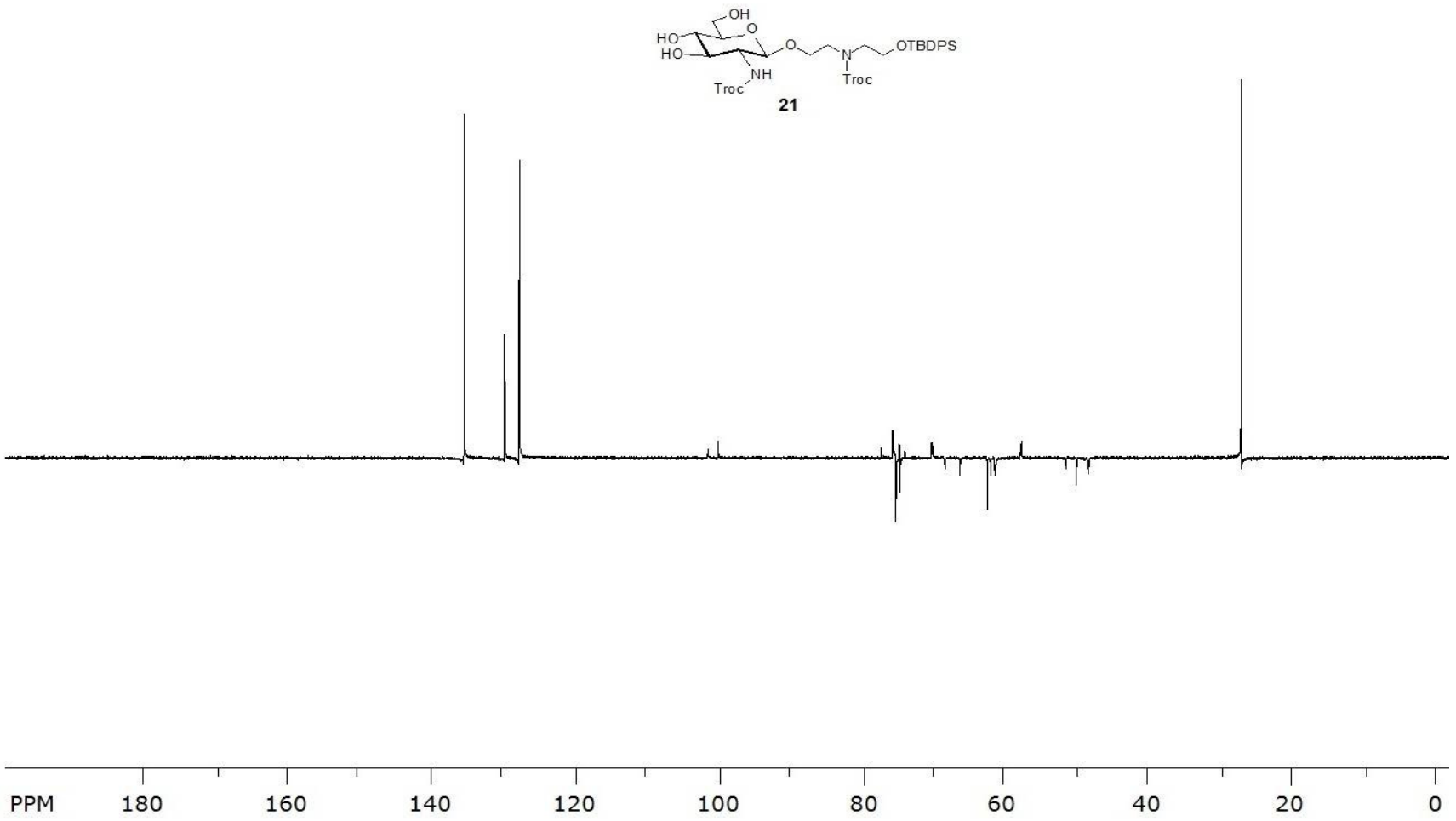
OH
O
HO
HO
O
N
OTBDPS
Troc
NH
Troc
Troc
21
PPM
180
160
140
120
100
80
60
40
20
0

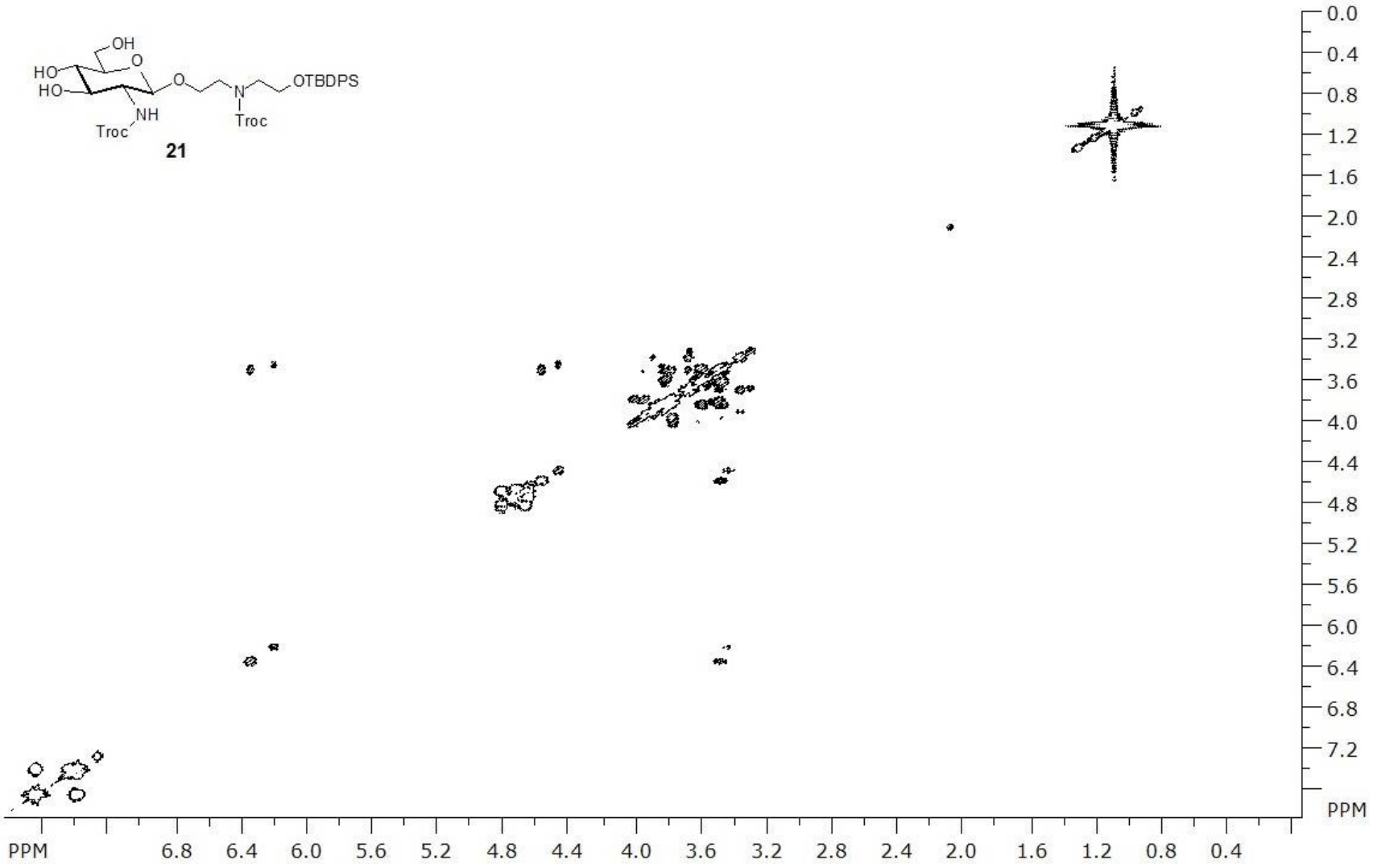
OH
O
HO
HO
O
N
OTBDPS
NH
Troc
Troc
21
0.0
0.4
0.8
1.2
1.6
2.0
2.4
2.8
3.2
3.6
4.0
4.4
4.8
5.2
5.6
6.0
6.4
6.8
7.2
PPM
PPM
6.8
6.4
6.0
5.6
5.2
4.8
4.4
4.0
3.6
3.2
2.8
2.4
2.0
1.6
1.2
0.8
0.4

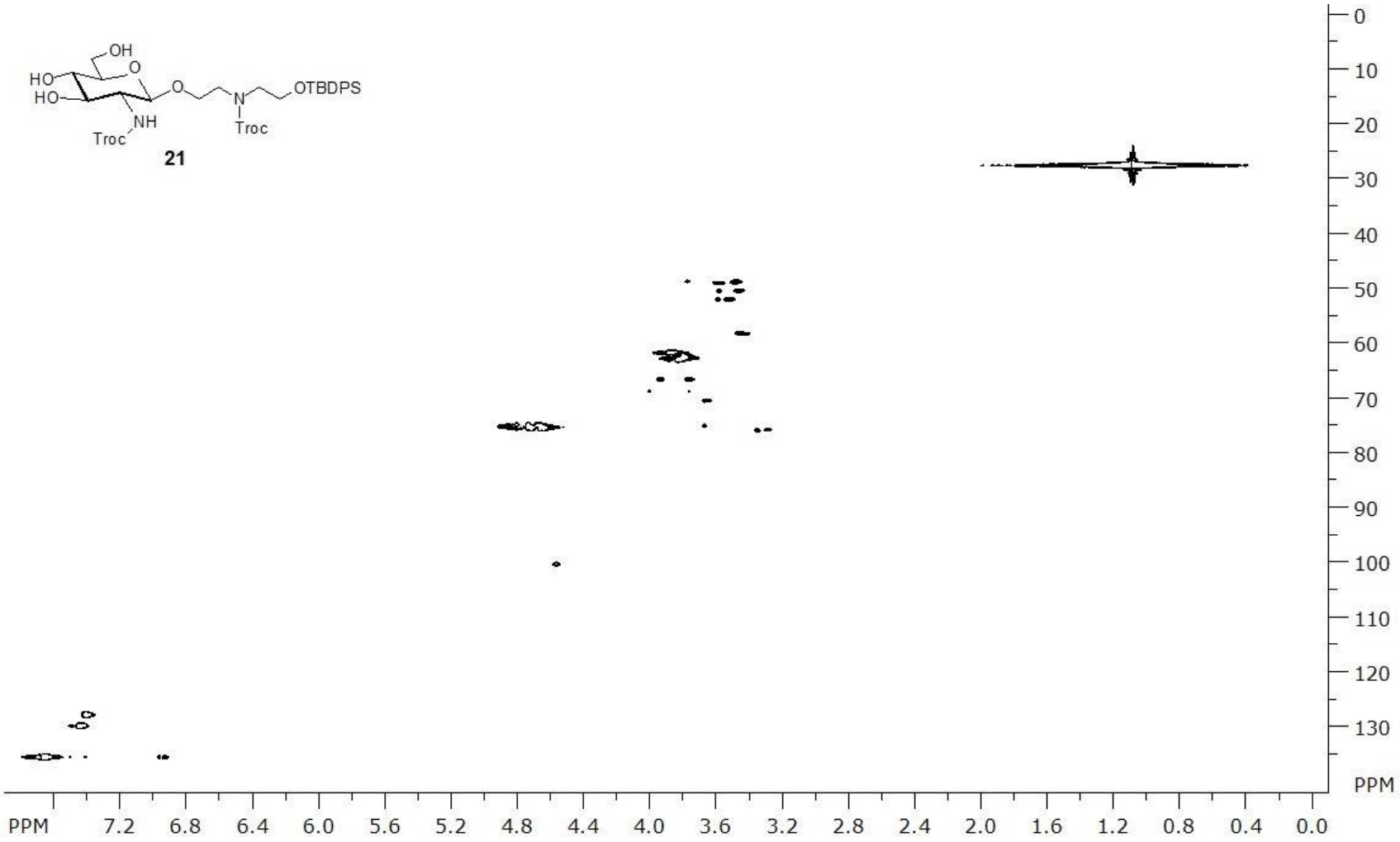
OH
O
HO
HO
O
N
OTBDPS
NH
Troc
Troc
21
0
10
20
30
40
50
60
70
80
90
100
110
120
130
PPM
PPM
7.2
6.8
6.4
6.0
5.6
5.2
4.8
4.4
4.0
3.6
3.2
2.8
2.4
2.0
1.6
1.2
0.8
0.4
0.0

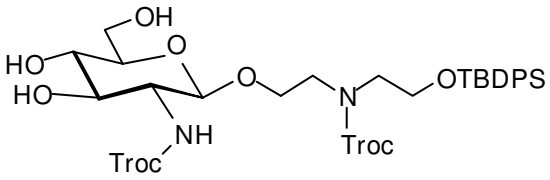

21

MALDI-MS (*m*/*z*) Calcd for $C_{32}H_{42}Cl_6N_2O_{10}Si$ $[M + Na]^+$: 875.06, found: 875.05.

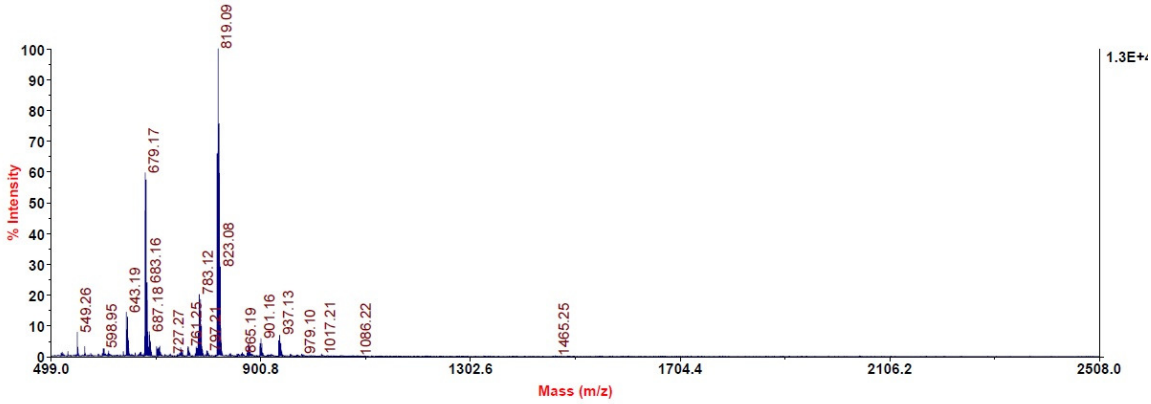

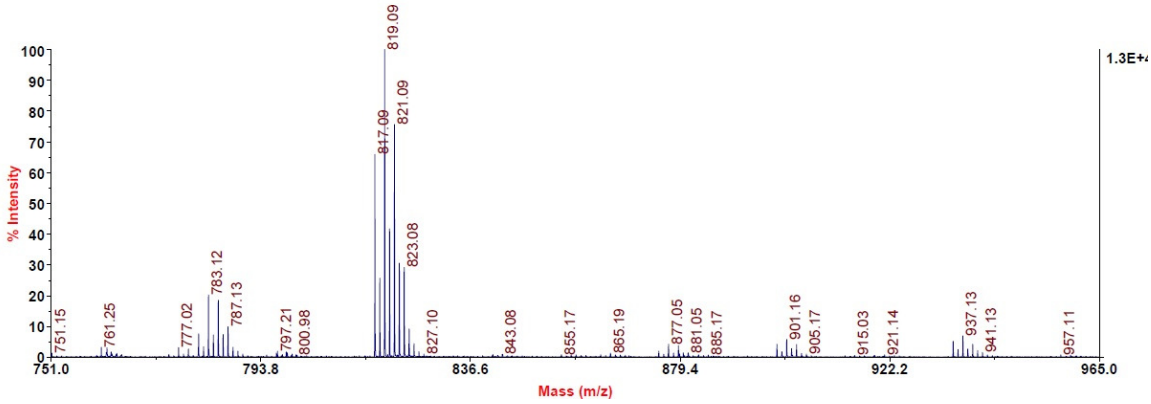

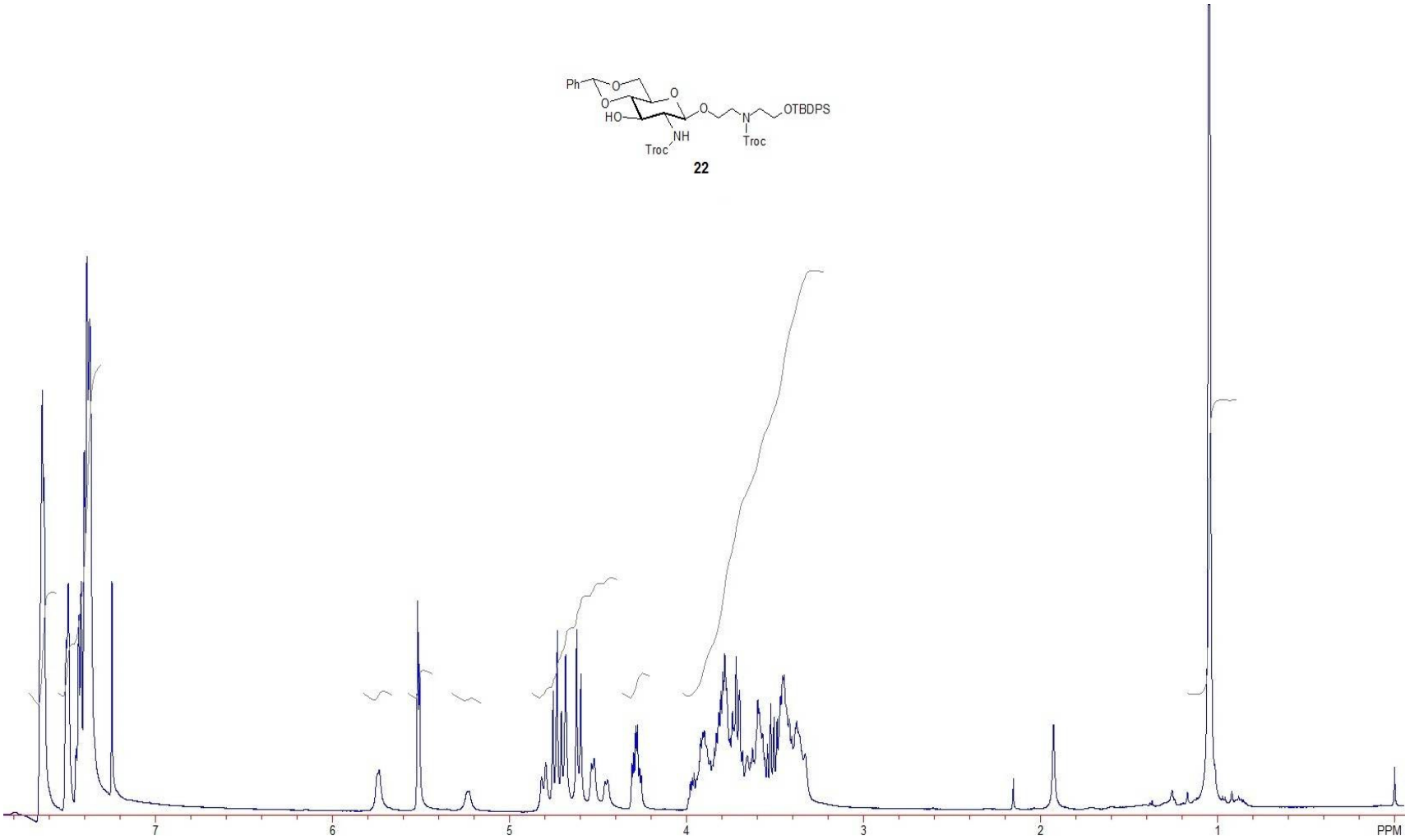
Ph
O
O
O
HO
O
N
OTBDPS
NH
Troc
Troc
Troc
22
7
6
5
4
3
2
1
PPM

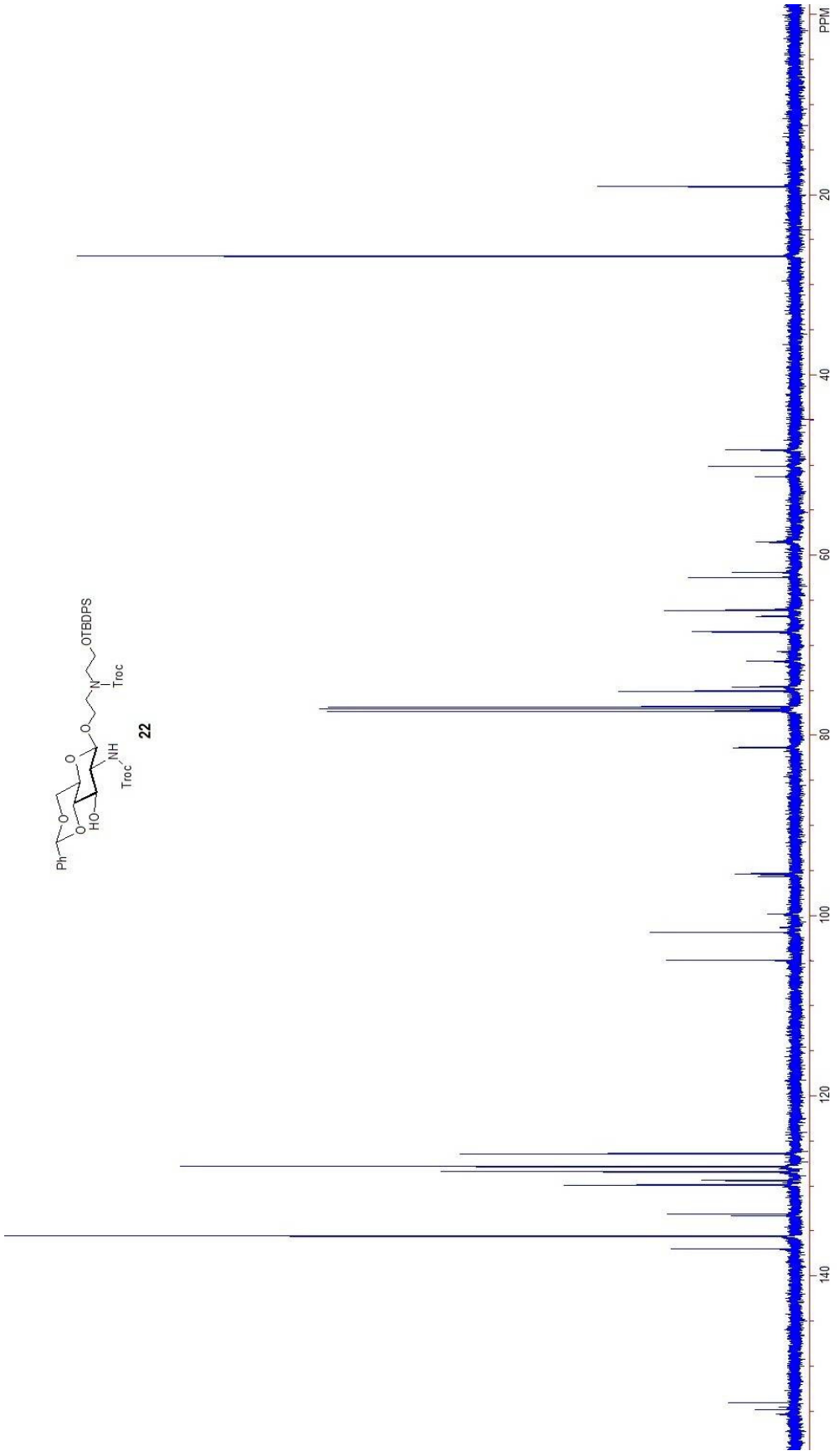
OTBDPS
N
Troc
O
O
NH
Troc
HO
O
O
Ph
22
PPM
20
40
60
80
100
120
140

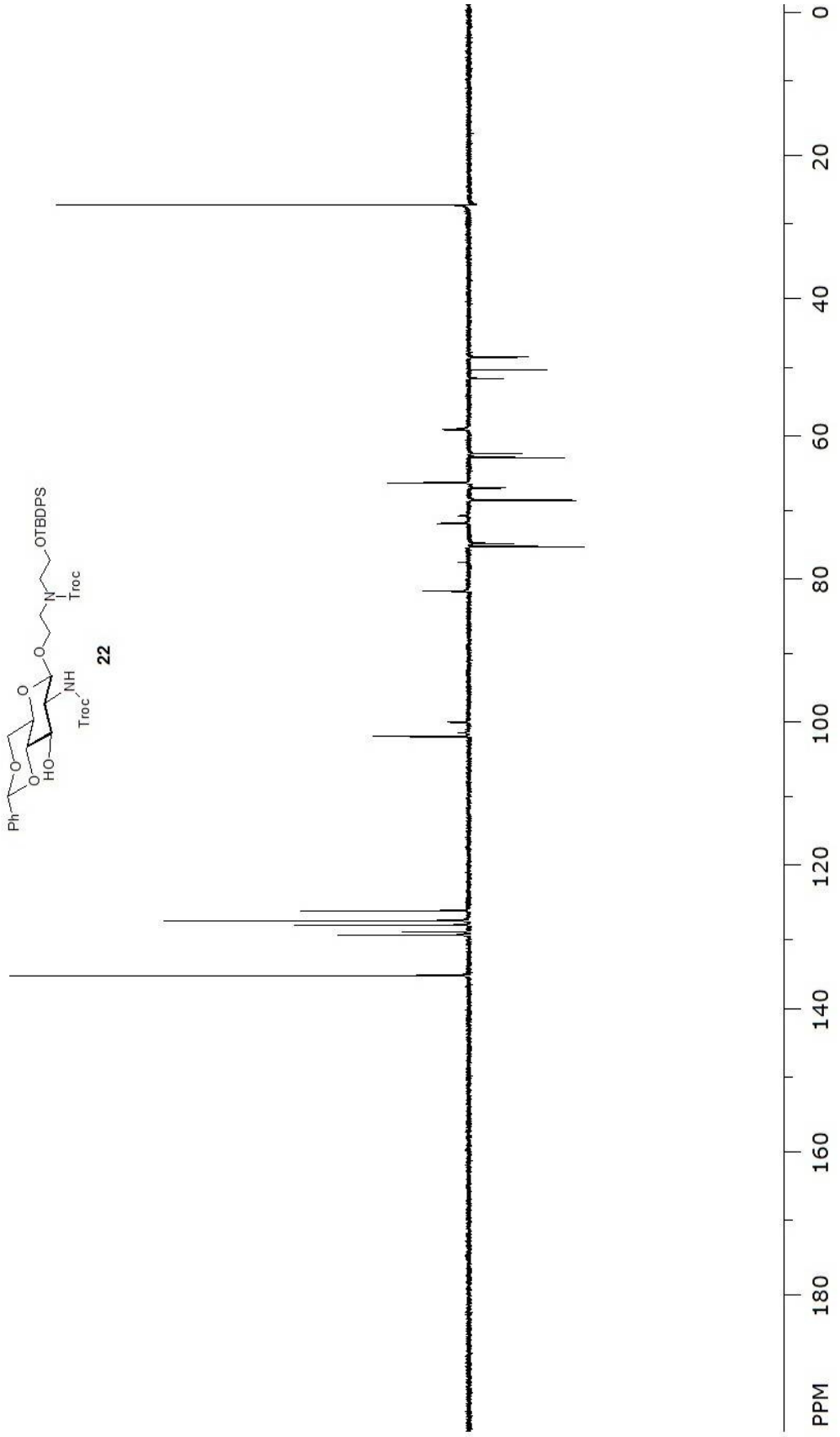
OTBDPS
Troc
N
O
NH
Troc
22
O
O
O
HO
Ph
PPM
0
20
40
60
80
100
120
140
160
180

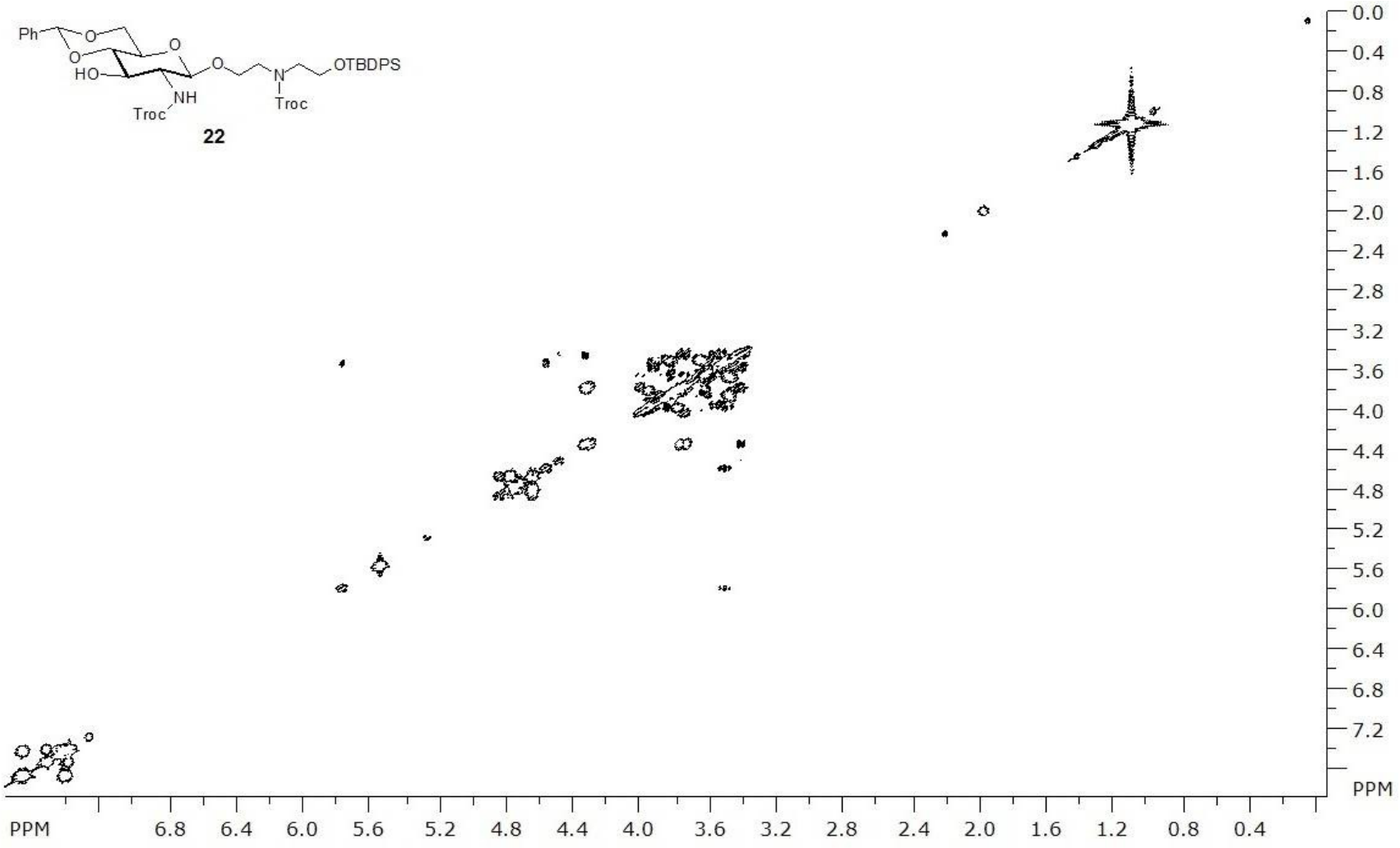
Ph
O
O
O
HO
O
N
OTBDPS
NH
Troc
Troc
22
0.0
0.4
0.8
1.2
1.6
2.0
2.4
2.8
3.2
3.6
4.0
4.4
4.8
5.2
5.6
6.0
6.4
6.8
7.2
PPM
PPM
6.8
6.4
6.0
5.6
5.2
4.8
4.4
4.0
3.6
3.2
2.8
2.4
2.0
1.6
1.2
0.8
0.4

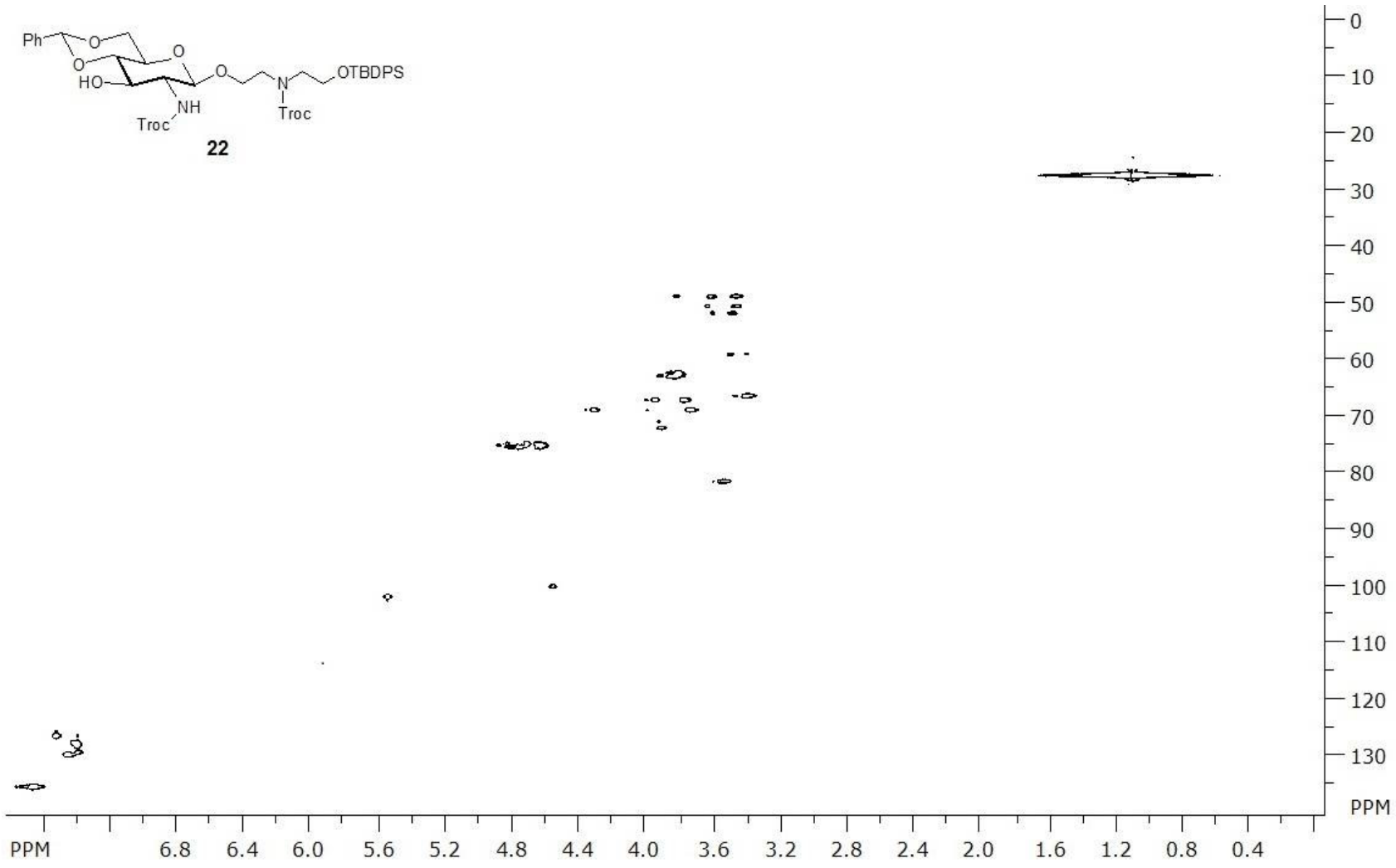
Ph
O
O
O
HO
NH
Troc
O
N
Troc
OTBDPS
22
0
10
20
30
40
50
60
70
80
90
100
110
120
130
PPM
PPM
6.8
6.4
6.0
5.6
5.2
4.8
4.4
4.0
3.6
3.2
2.8
2.4
2.0
1.6
1.2
0.8
0.4

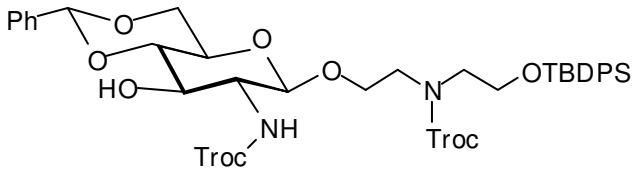

22

MALDI-MS (*m*/*z*) Calcd for $C_{39}H_{46}Cl_6N_2O_{10}Si$ [M + Na - C_4H_9]$^+$: 906.06, found: 906.12.

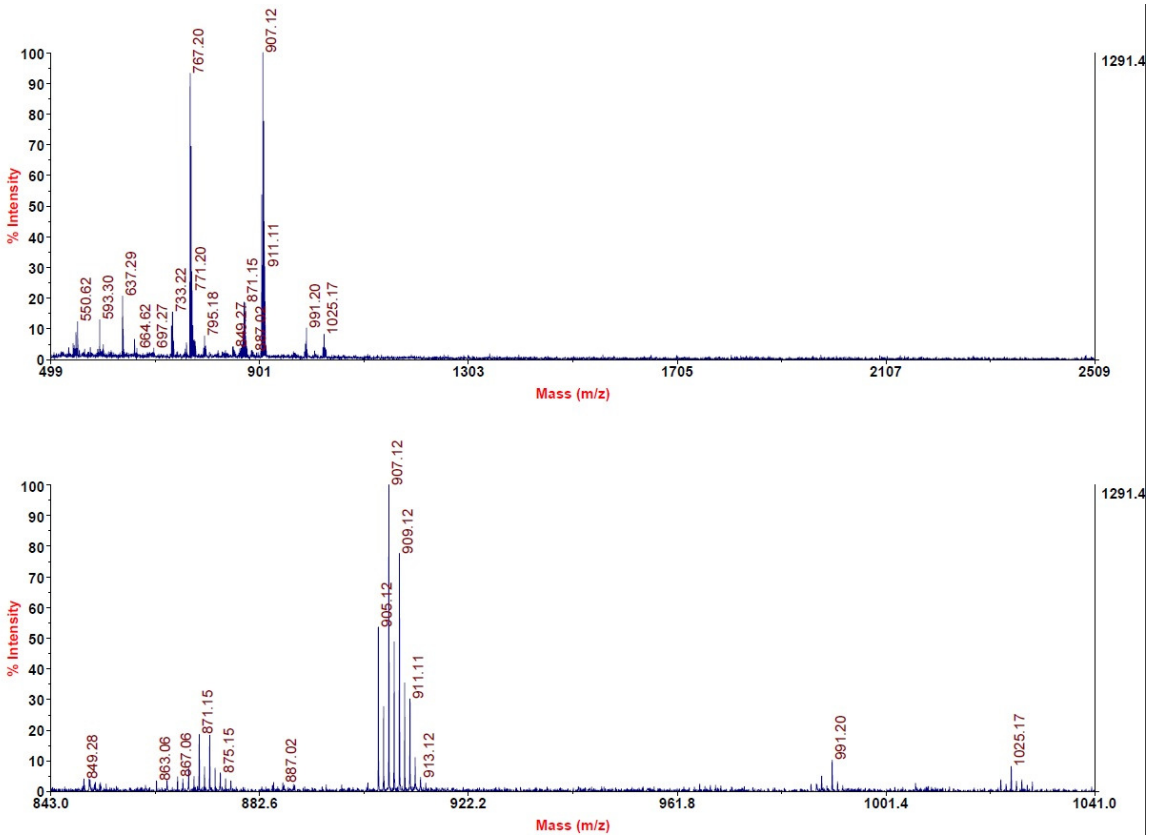

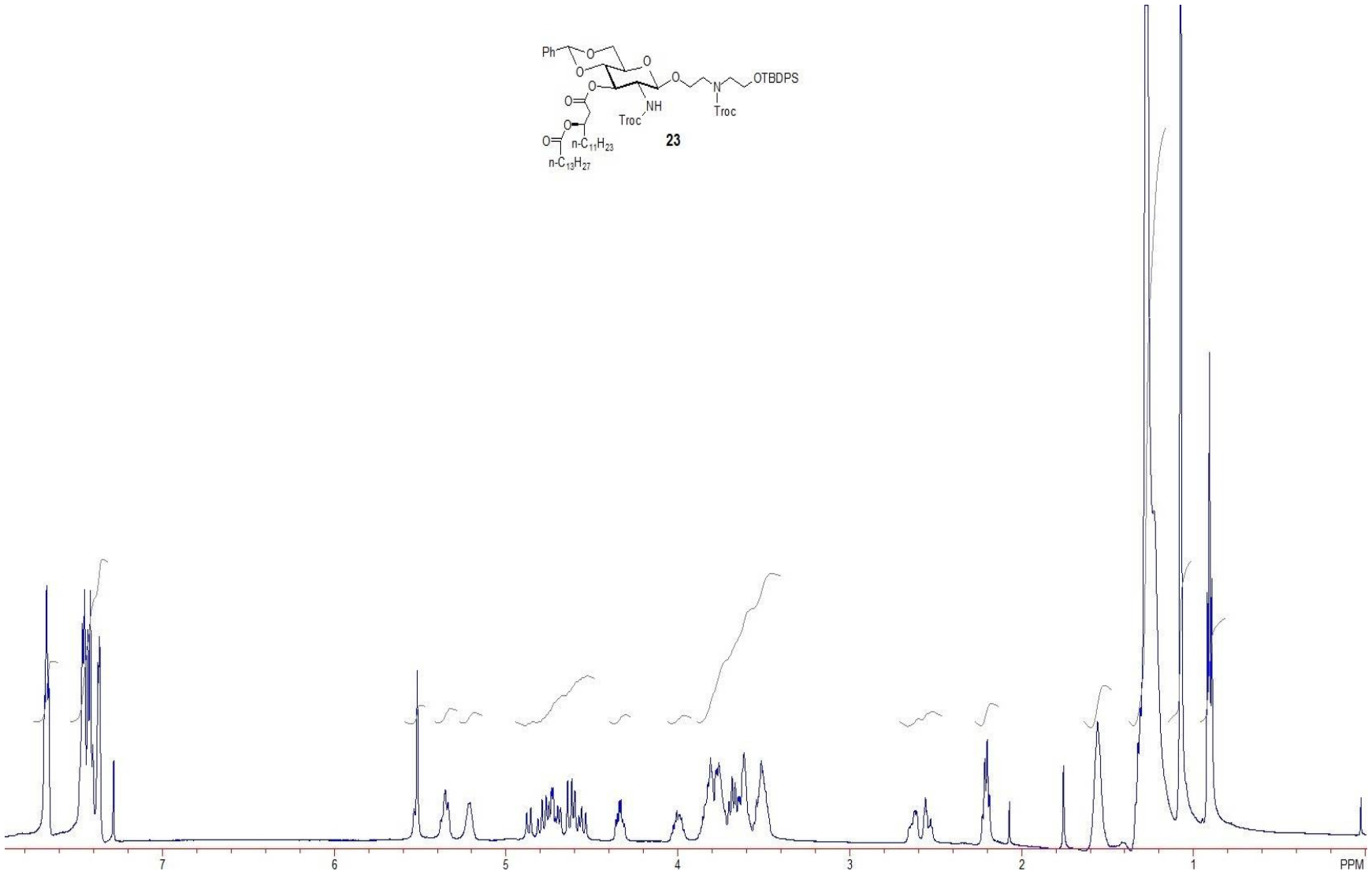
Ph
O
O
O
O
O
O
OTBDPS
N
Troc
NH
Troc
O
O
n-C11H23
O
n-C13H27
23
7
6
5
4
3
2
1
PPM

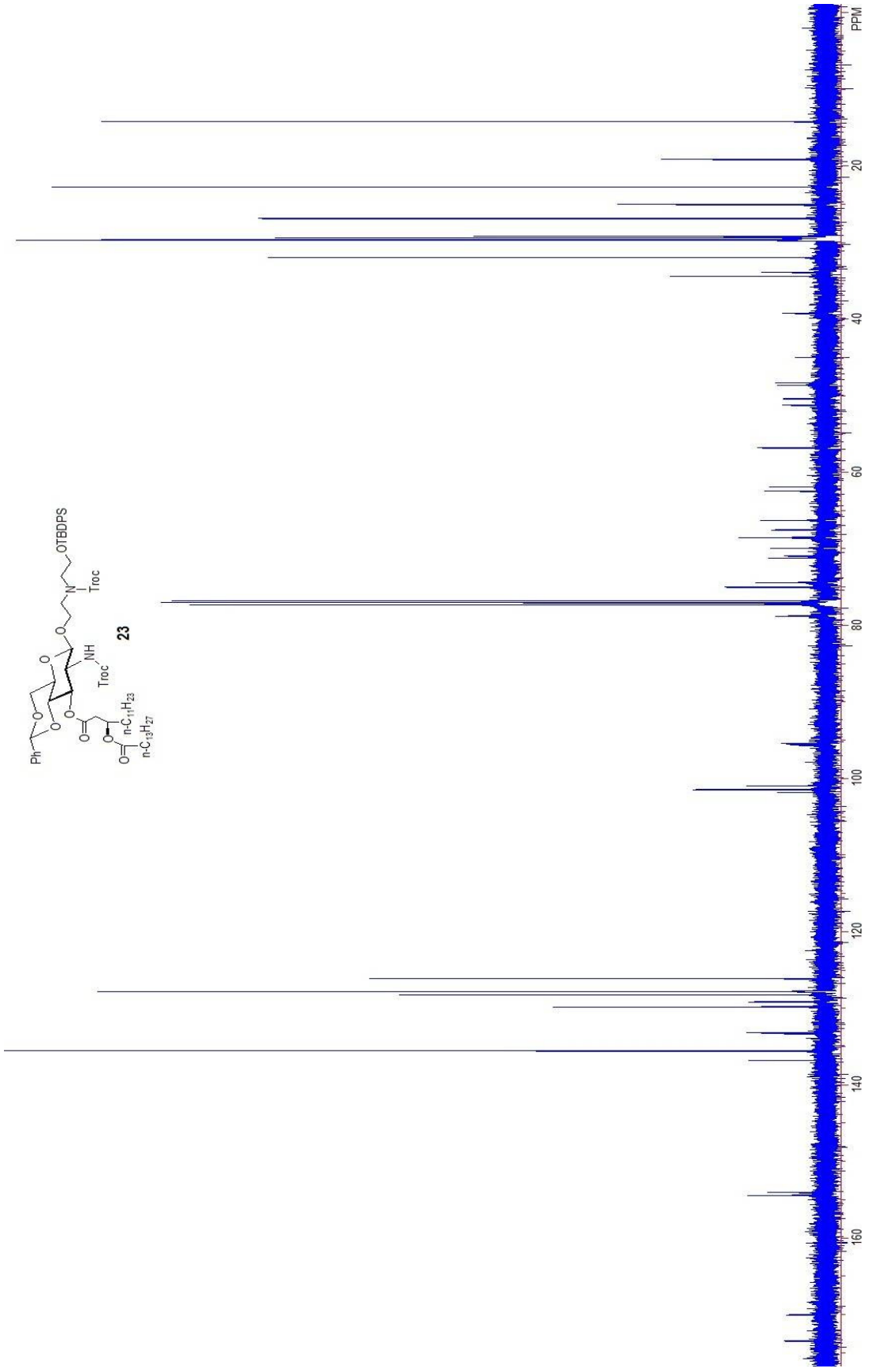
OTBDPS
Troc
NH
Troc
23
Ph
n-C11H23
n-C13H27
PPM
20
40
60
80
100
120
140
160

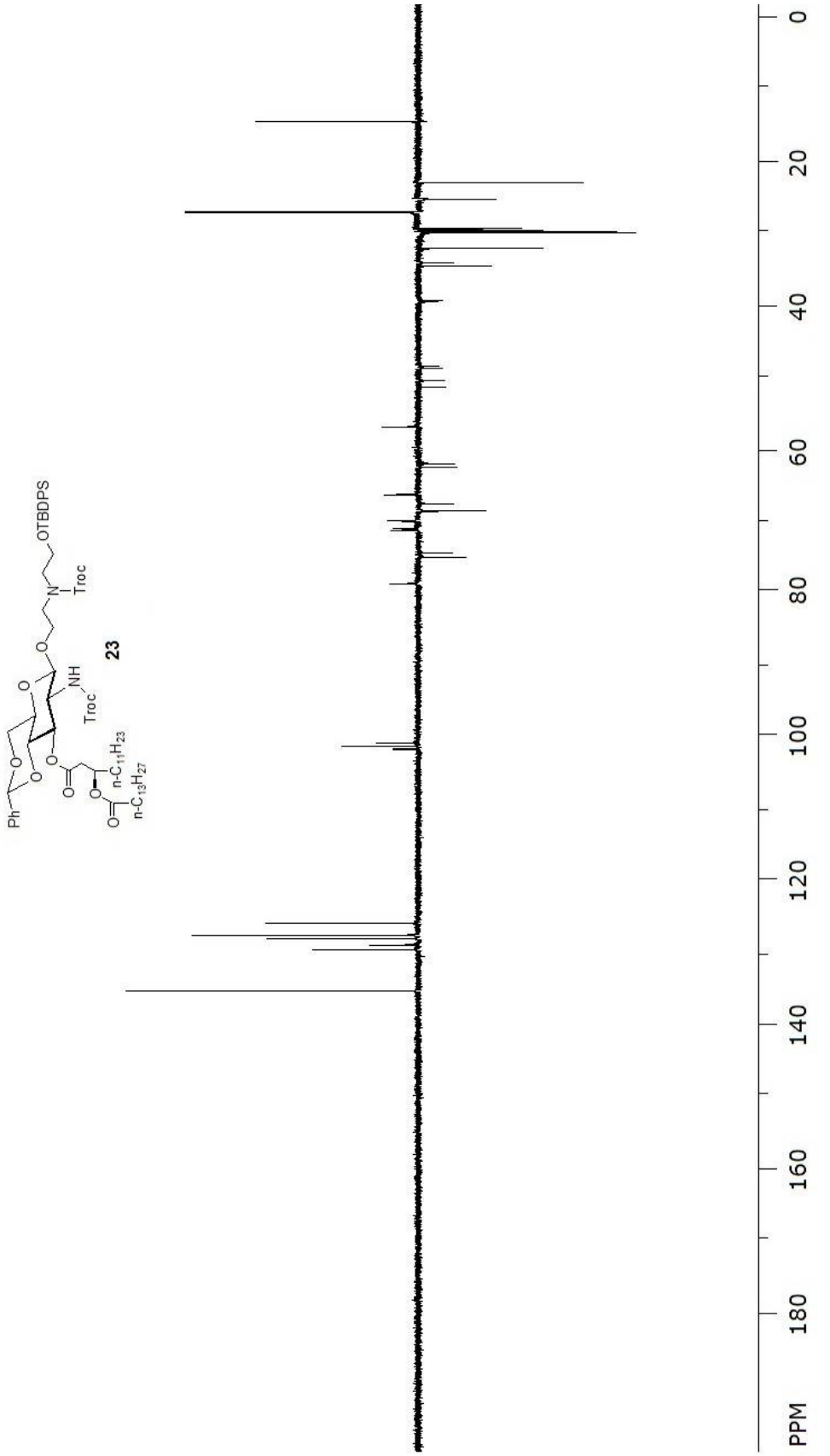
OTBDPS
N
Troc
O
NH
Troc
23
Ph
n-C11H23
n-C13H27
0
20
40
60
80
100
120
140
160
180
PPM

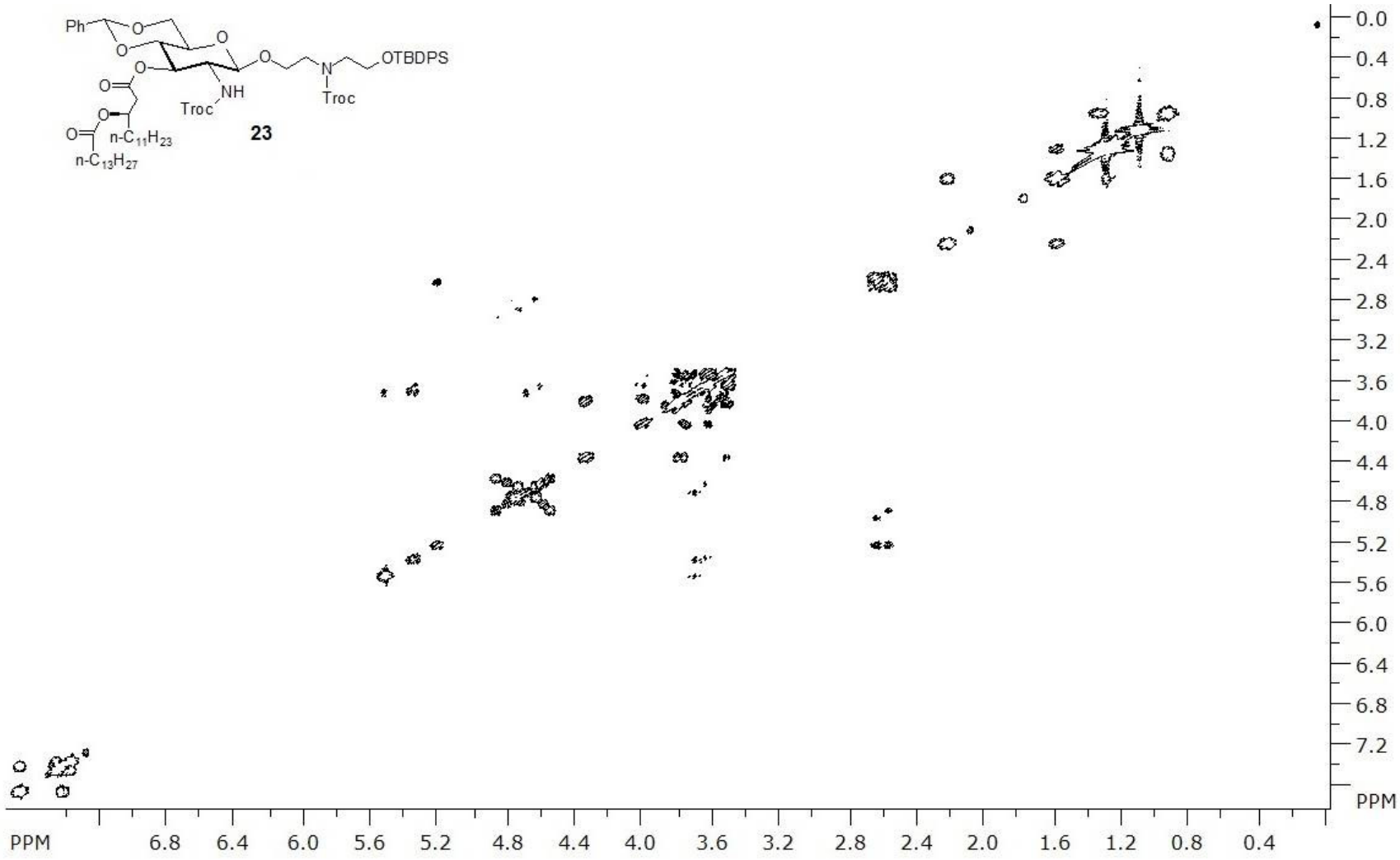
Ph
O
O
O
O
O
O
NH
Troc
N
Troc
OTBDPS
O
O
n-C11H23
n-C13H27
23
0.0
0.4
0.8
1.2
1.6
2.0
2.4
2.8
3.2
3.6
4.0
4.4
4.8
5.2
5.6
6.0
6.4
6.8
7.2
PPM
PPM
6.8
6.4
6.0
5.6
5.2
4.8
4.4
4.0
3.6
3.2
2.8
2.4
2.0
1.6
1.2
0.8
0.4

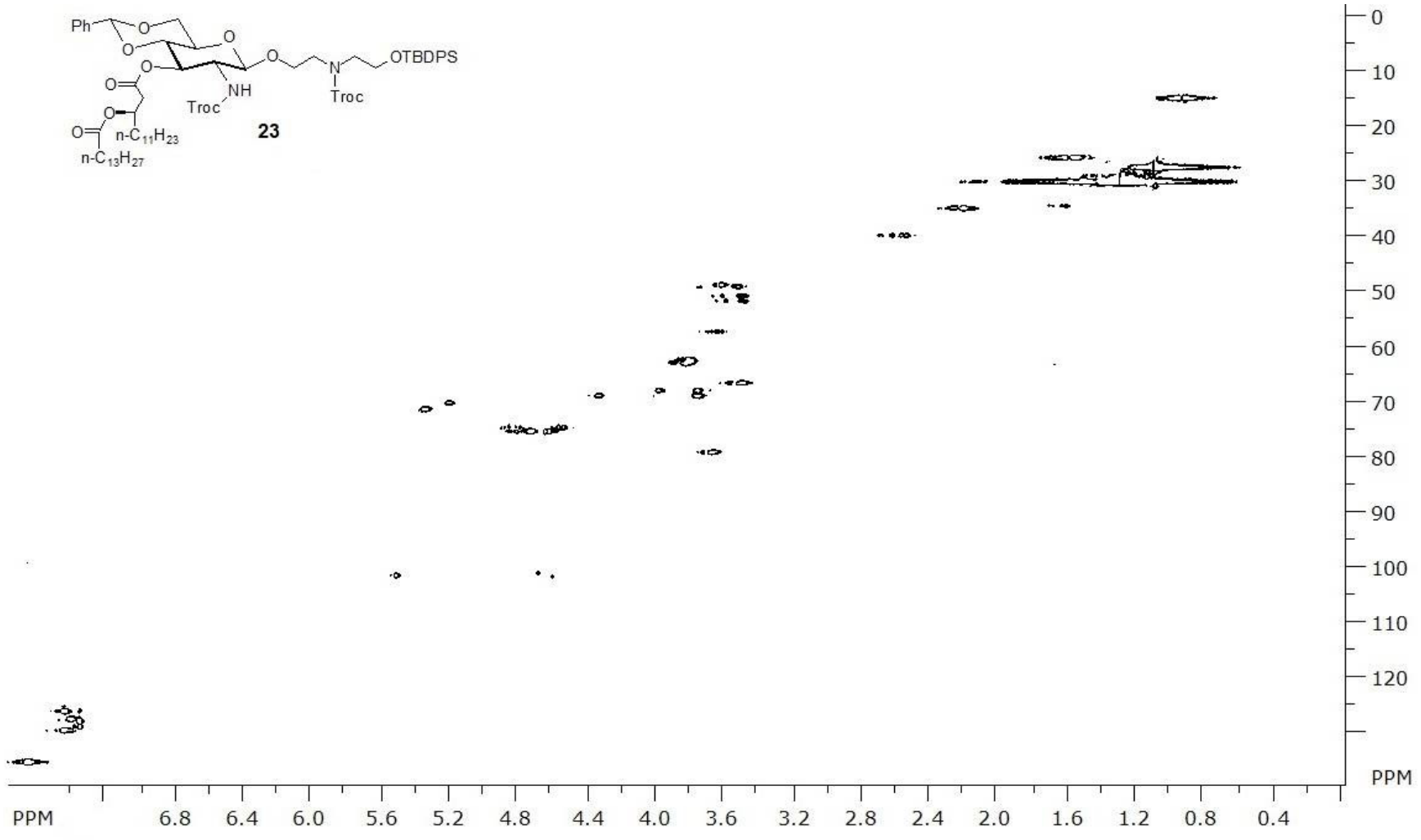
Ph
O
O
O
O
O
O
NH
Troc
N
Troc
OTBDPS
O
O
n-C11H23
O
n-C13H27
23
0
10
20
30
40
50
60
70
80
90
100
110
120
PPM
PPM
6.8
6.4
6.0
5.6
5.2
4.8
4.4
4.0
3.6
3.2
2.8
2.4
2.0
1.6
1.2
0.8
0.4

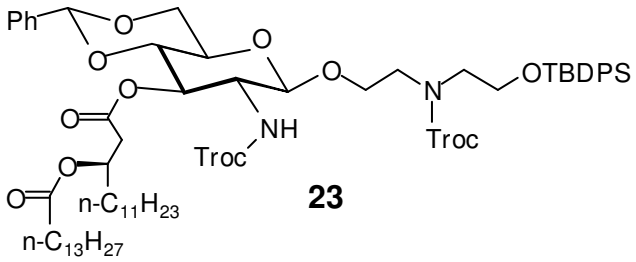

23

MALDI-MS (*m*/*z*) Calcd for $C_{67}H_{98}Cl_6N_2O_{13}Si$ $[M + Na]^+$: 1399.49, found: 1399.50.

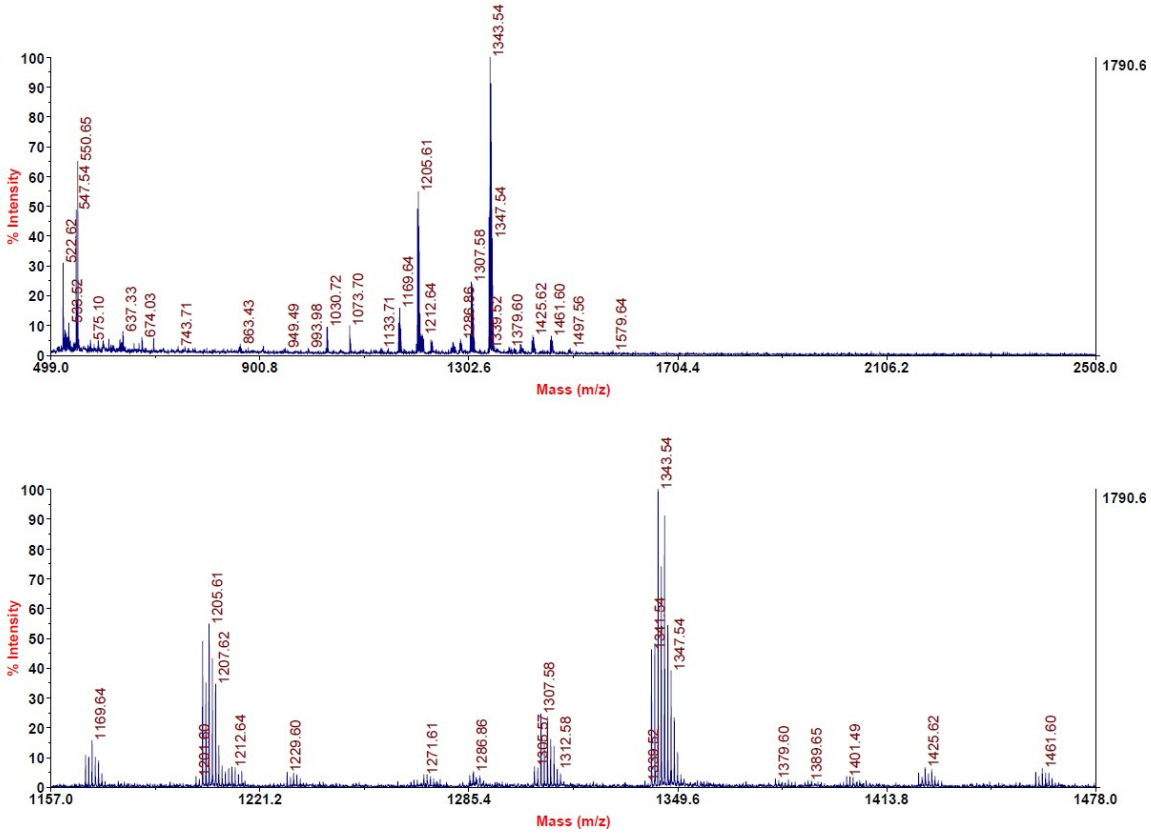

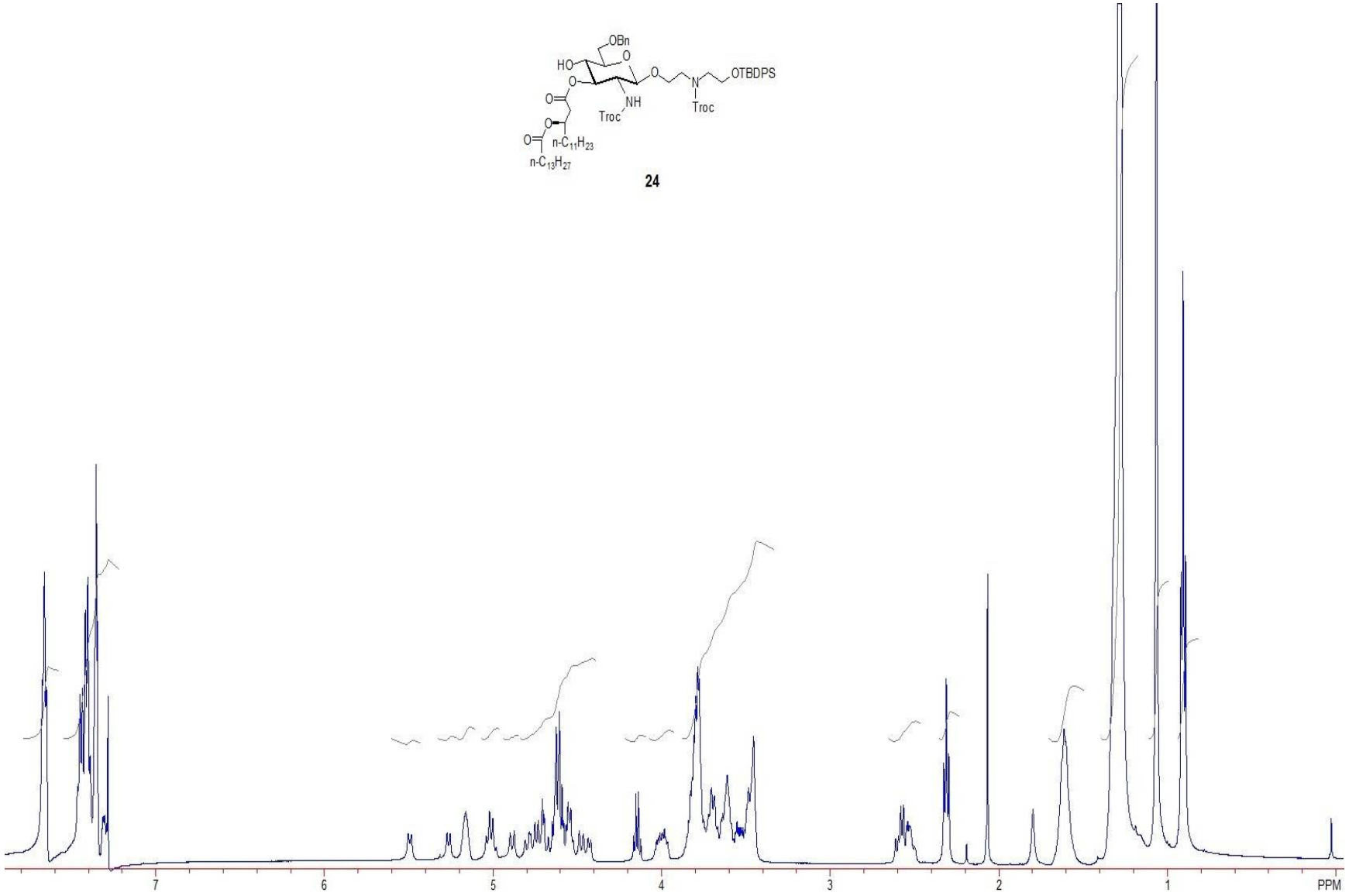
OBn
HO
O
O
O
O
NH
Troc
N
Troc
OTBDPS
O
O
n-C11H23
n-C13H27
7
6
5
4
3
2
1
PPM

24

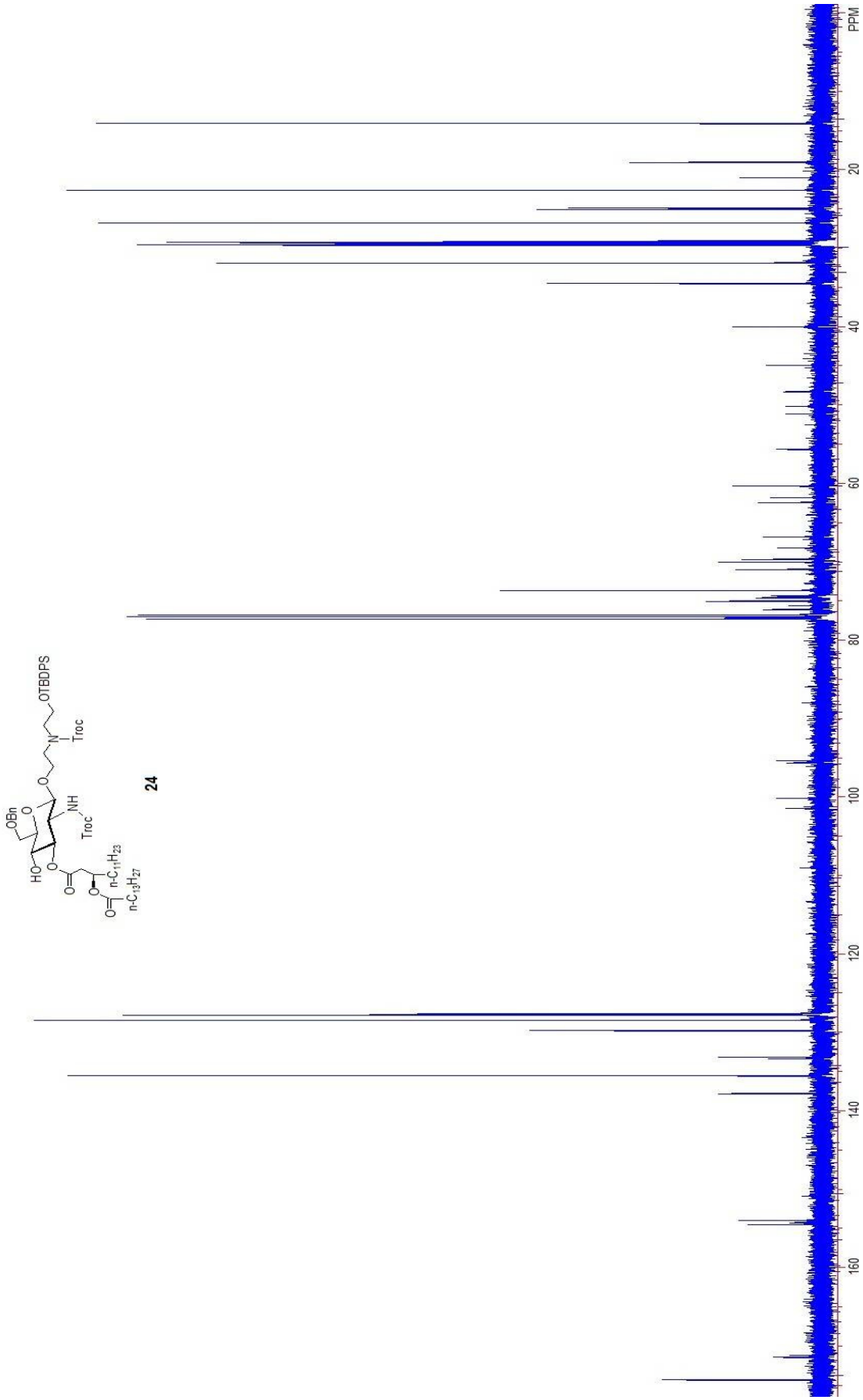
OTBDPS
Troc
N
O
NH
Troc
OBn
O
HO
O
O
O
O
n-C11H23
n-C13H27
24
PPM
20
40
60
80
100
120
140
160

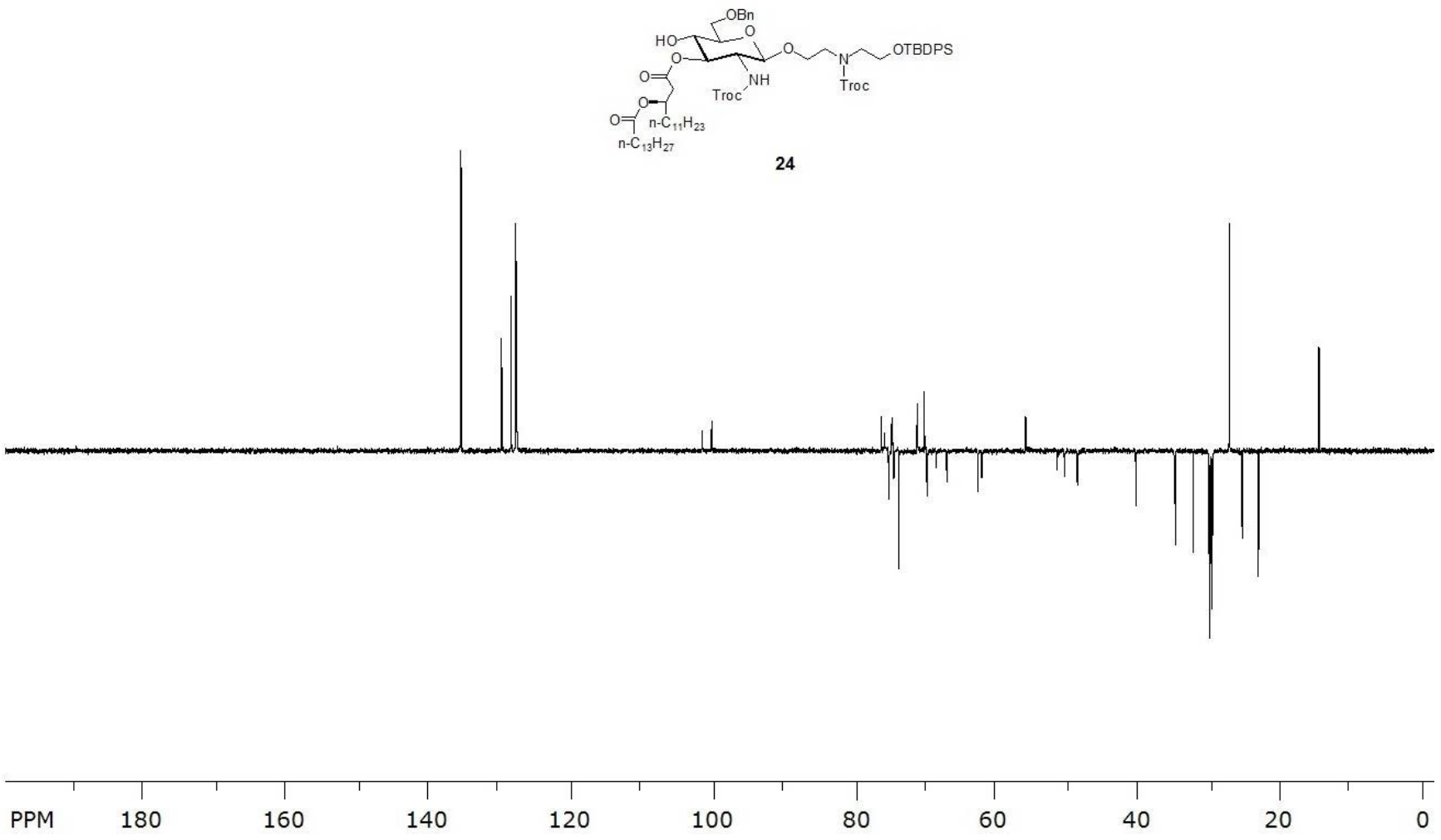
OBn
HO
O
O
O
O
NH
Troc
N
Troc
OTBDPS
O
O
n-C11H23
n-C13H27
24
PPM
180
160
140
120
100
80
60
40
20
0

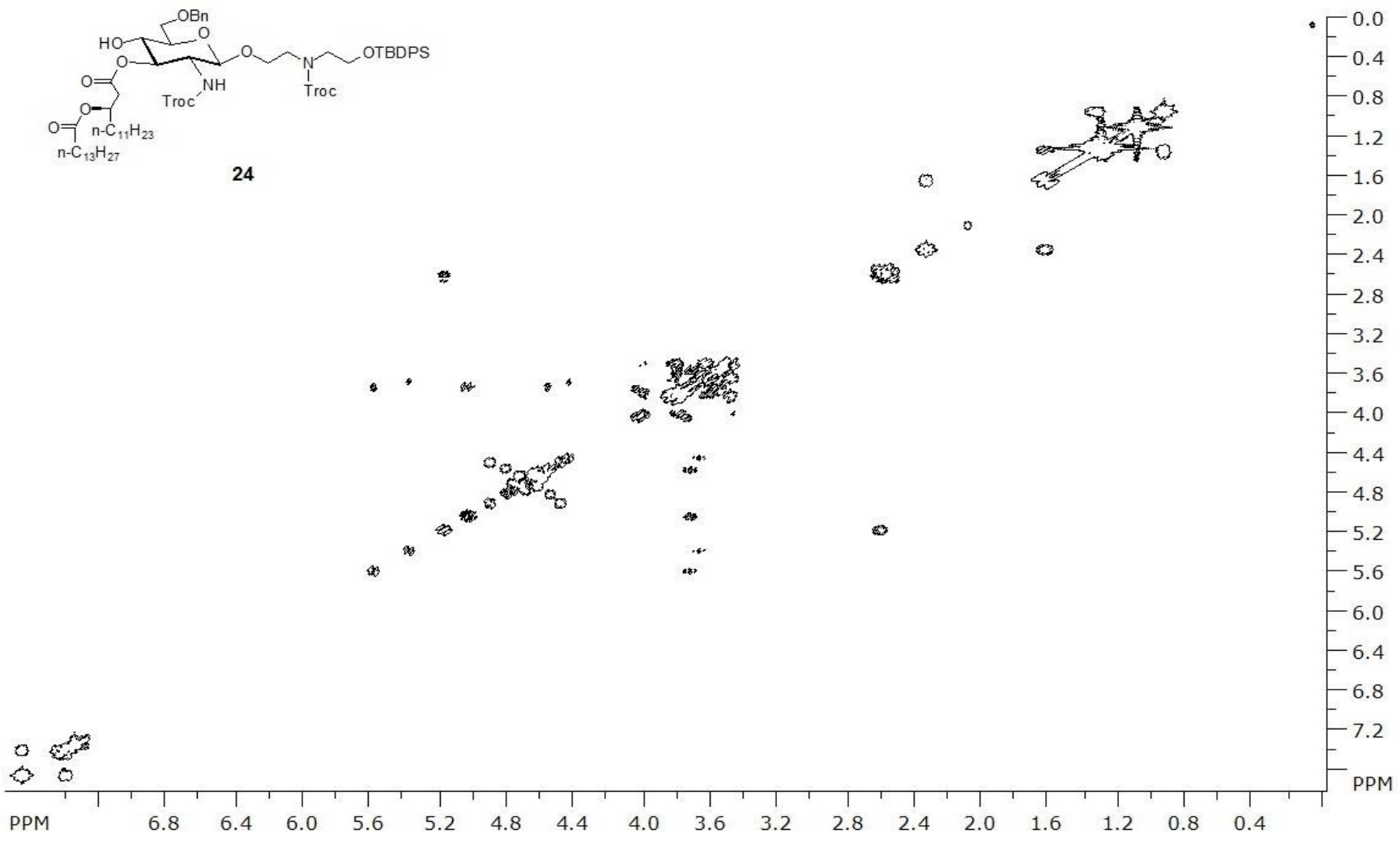
OBn
HO
O
O
O
NH
Troc
O
N
Troc
OTBDPS
O
O
n-C11H23
n-C13H27
24
0.0
0.4
0.8
1.2
1.6
2.0
2.4
2.8
3.2
3.6
4.0
4.4
4.8
5.2
5.6
6.0
6.4
6.8
7.2
PPM
PPM
6.8
6.4
6.0
5.6
5.2
4.8
4.4
4.0
3.6
3.2
2.8
2.4
2.0
1.6
1.2
0.8
0.4

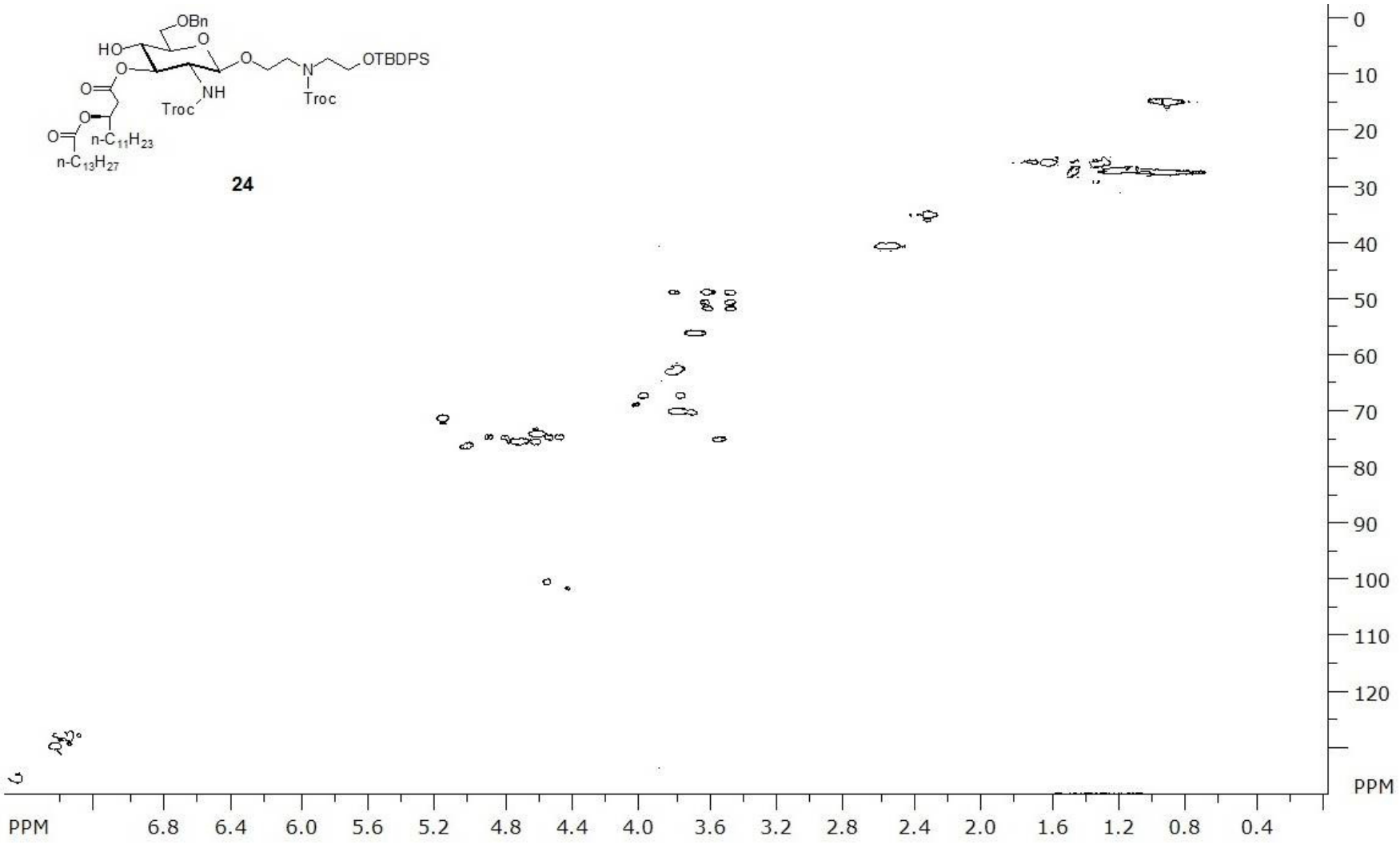
OBn
HO
O
O
O
O
NH
Troc
N
Troc
OTBDPS
O
O
n-C11H23
n-C13H27
24
0
10
20
30
40
50
60
70
80
90
100
110
120
PPM
PPM
6.8
6.4
6.0
5.6
5.2
4.8
4.4
4.0
3.6
3.2
2.8
2.4
2.0
1.6
1.2
0.8
0.4

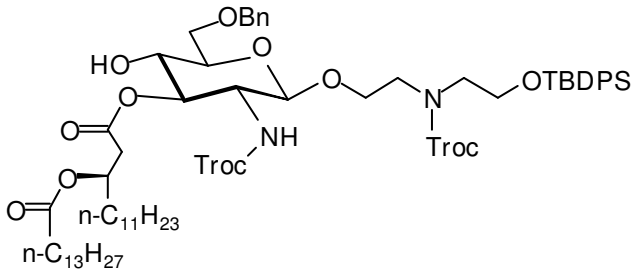

24

MALDI-MS (*m*/*z*) Calcd for $C_{67}H_{100}Cl_6N_2O_{13}Si$ $[M + Na]^+$: 1401.50, found: 1401.45.

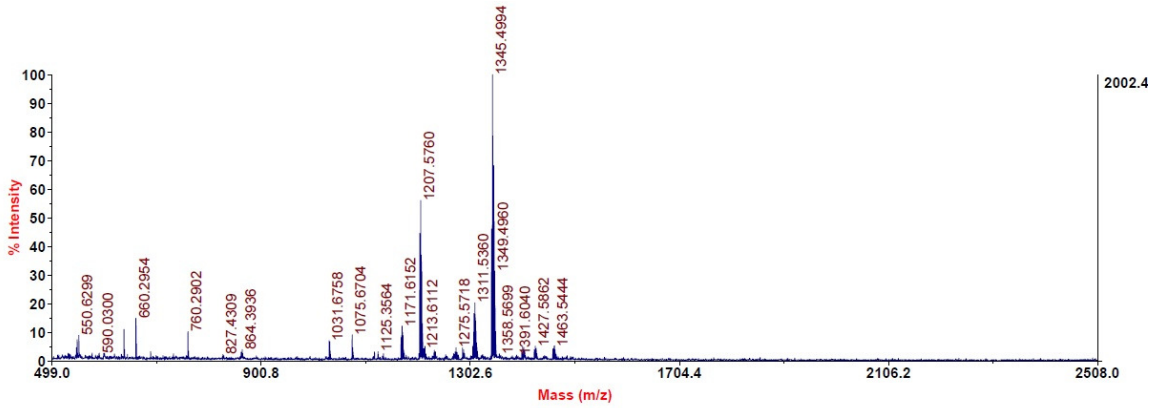

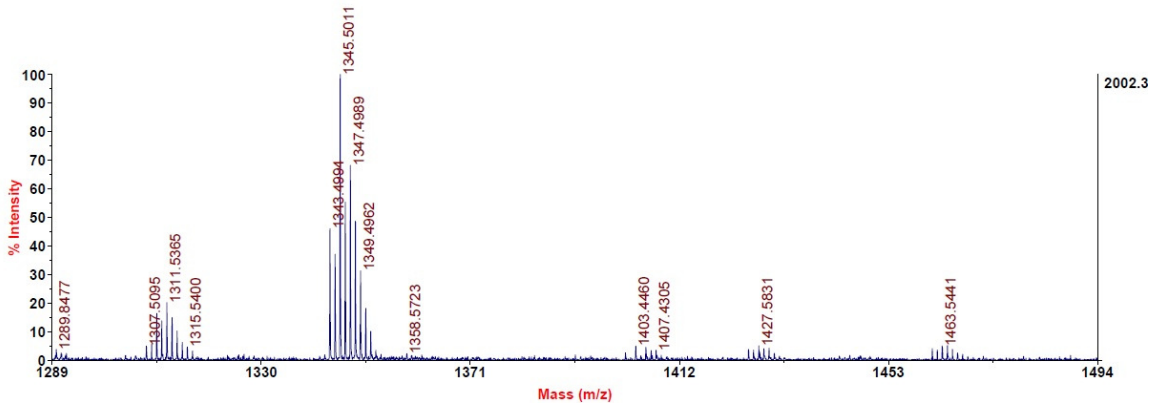

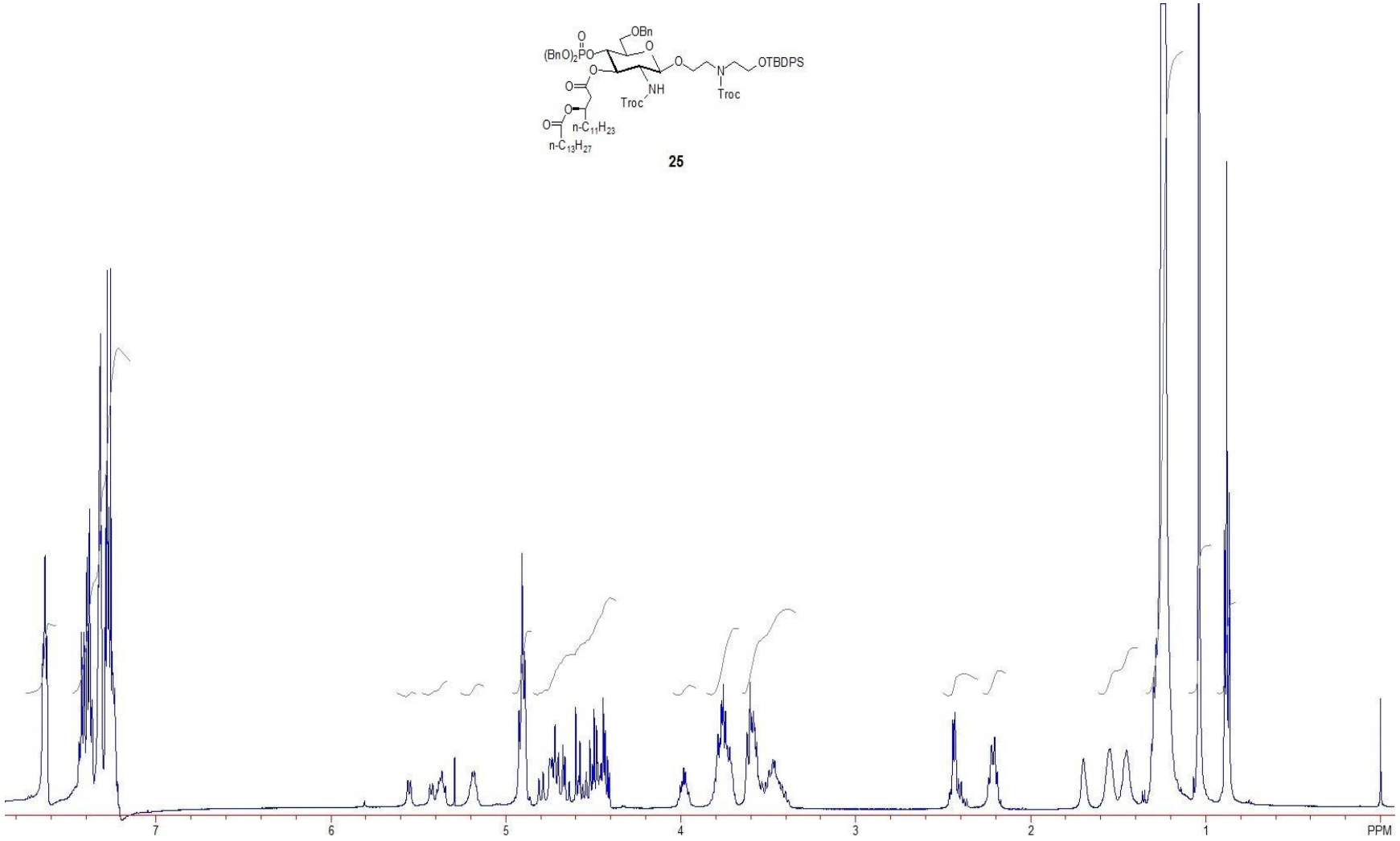
OBn
(BnO)2PO
O
O
NH
Troc
N
Troc
OTBDPS
n-C11H23
n-C13H27
25
7
6
5
4
3
2
1
PPM

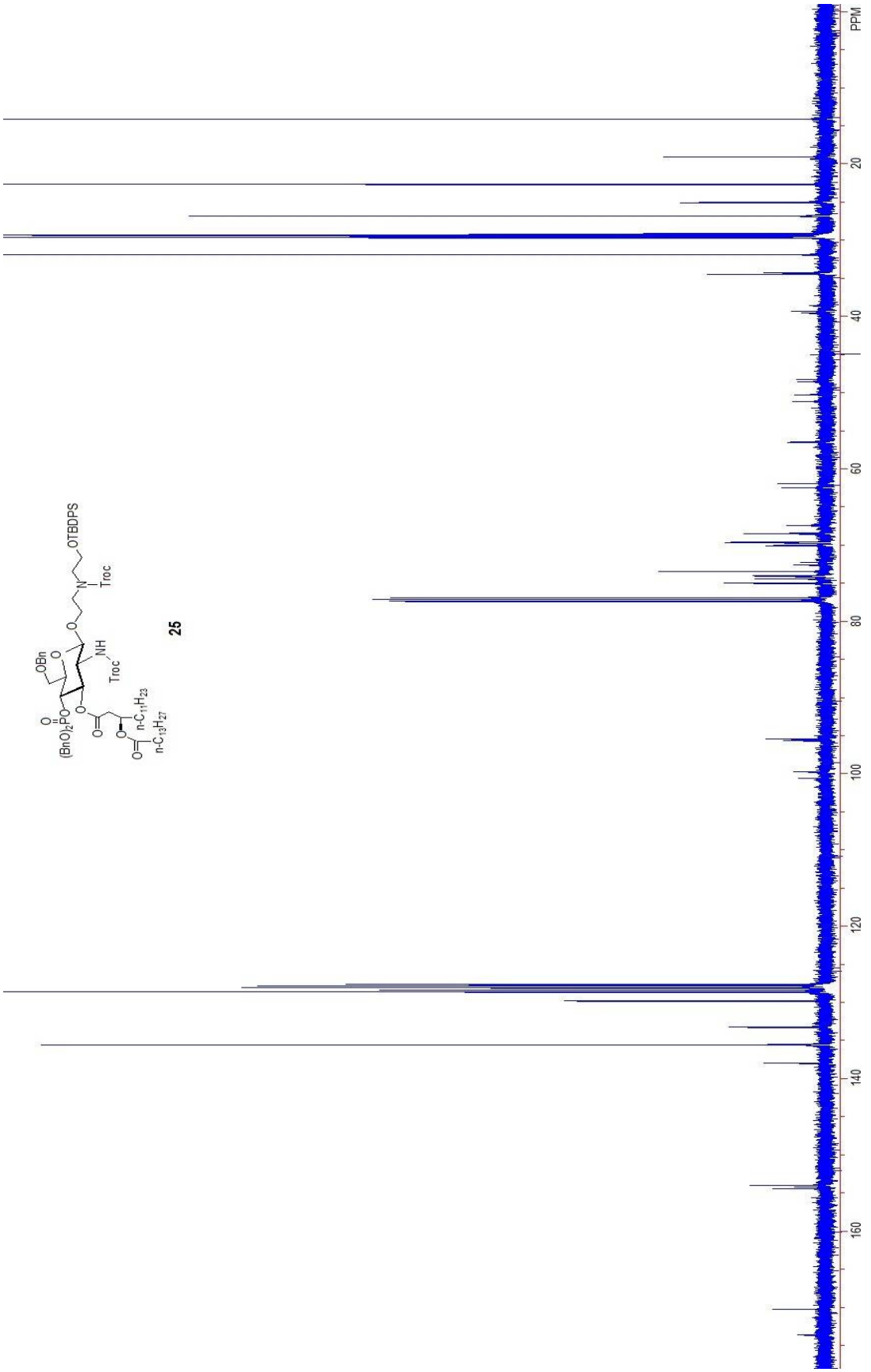
OTBDPS
Troc
N
O
NH
Troc
OBn
O
O
O
O
O
O
O
O
P
(BnO)2PO
n-C11H23
n-C13H27
25
PPM
20
40
60
80
100
120
140
160

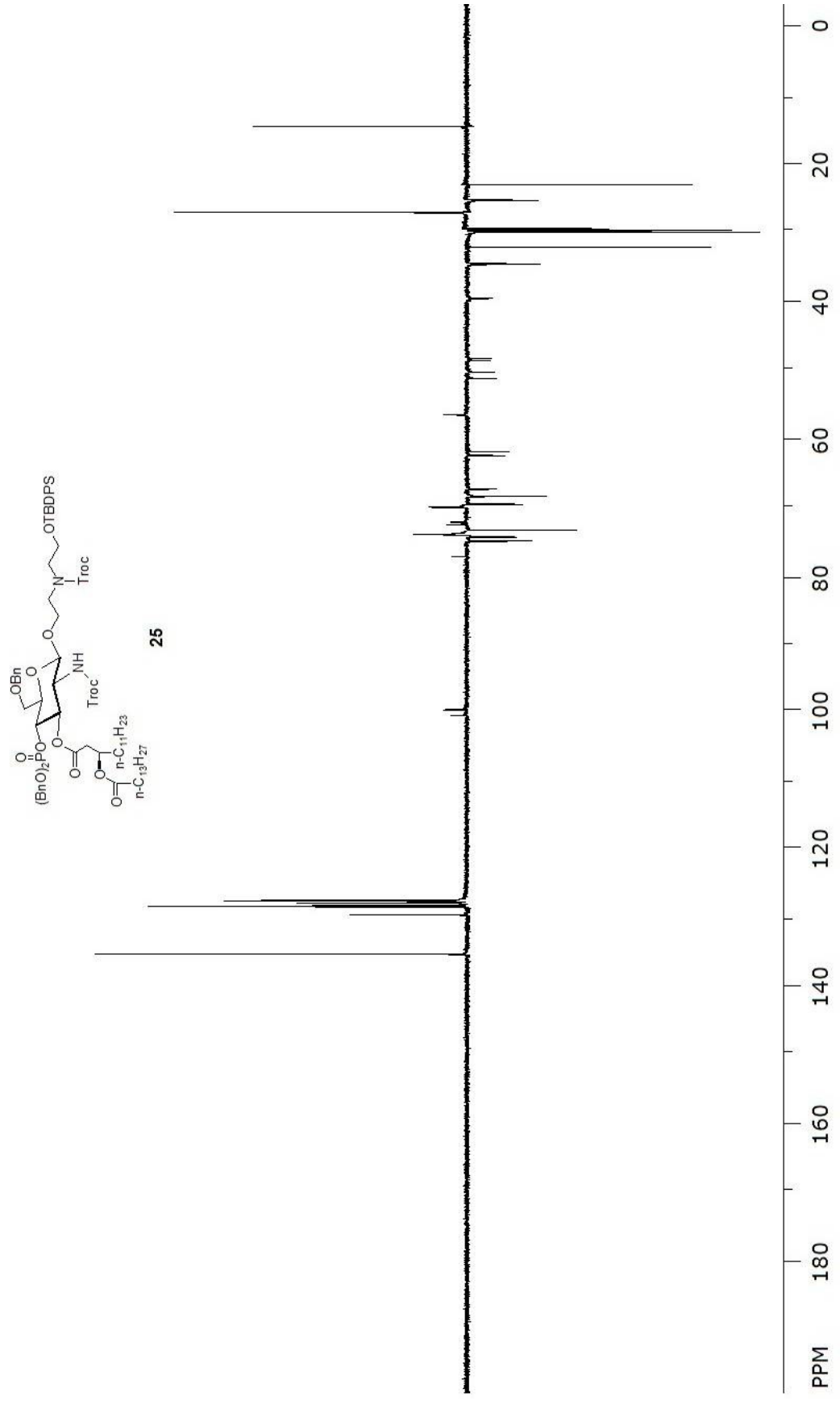
OTBDPS
Troc
N
O
NH
Troc
OBn
O
O
O
(BnO)2PO
O
O
n-C11H23
n-C13H27
25
PPM
0
20
40
60
80
100
120
140
160
180

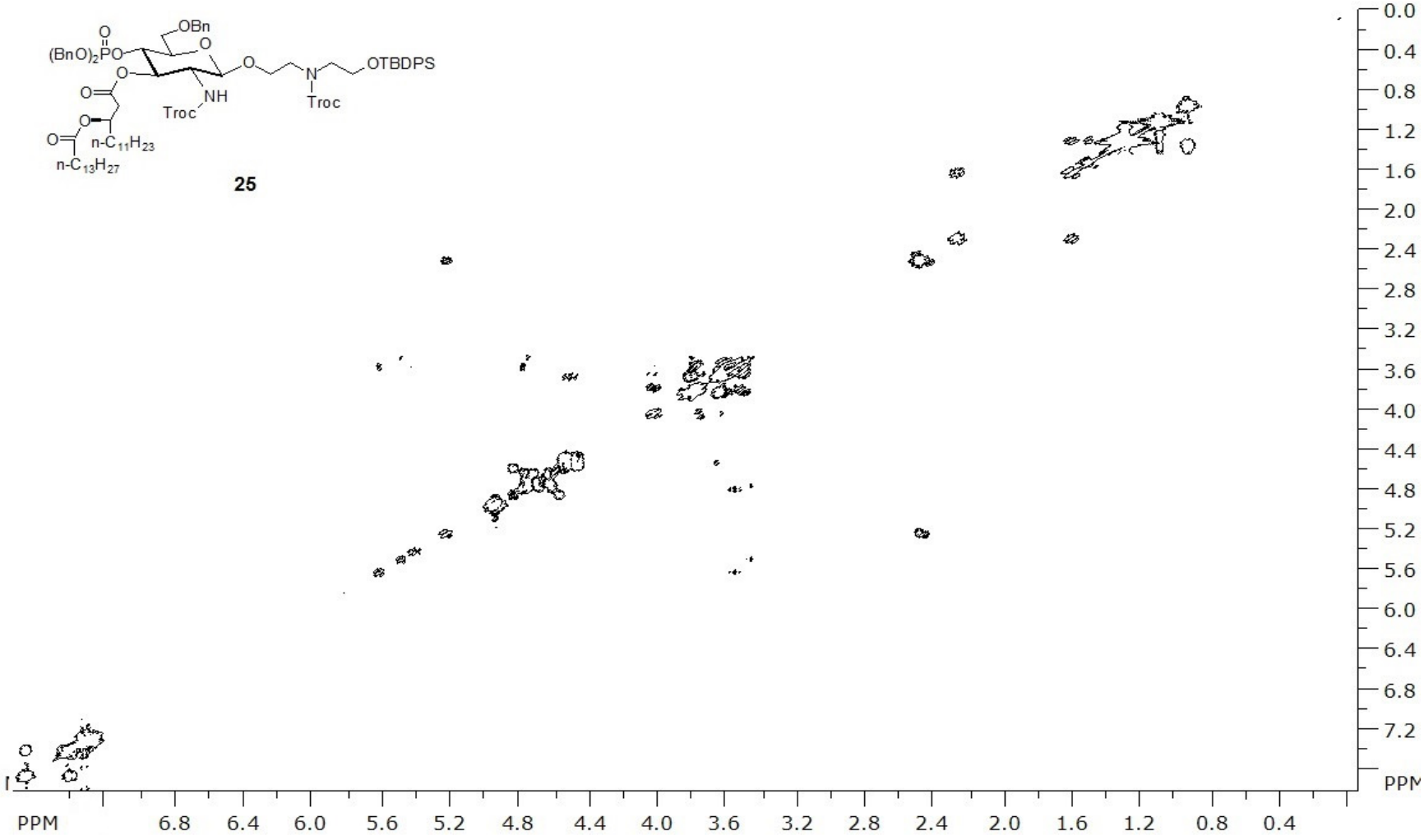
OBn
O
(BnO)2PO
O
O
O
NH
Troc
N
Troc
OTBDPS
O
O
n-C11H23
n-C13H27
25
0.0
0.4
0.8
1.2
1.6
2.0
2.4
2.8
3.2
3.6
4.0
4.4
4.8
5.2
5.6
6.0
6.4
6.8
7.2
PPM
PPM
6.8
6.4
6.0
5.6
5.2
4.8
4.4
4.0
3.6
3.2
2.8
2.4
2.0
1.6
1.2
0.8
0.4

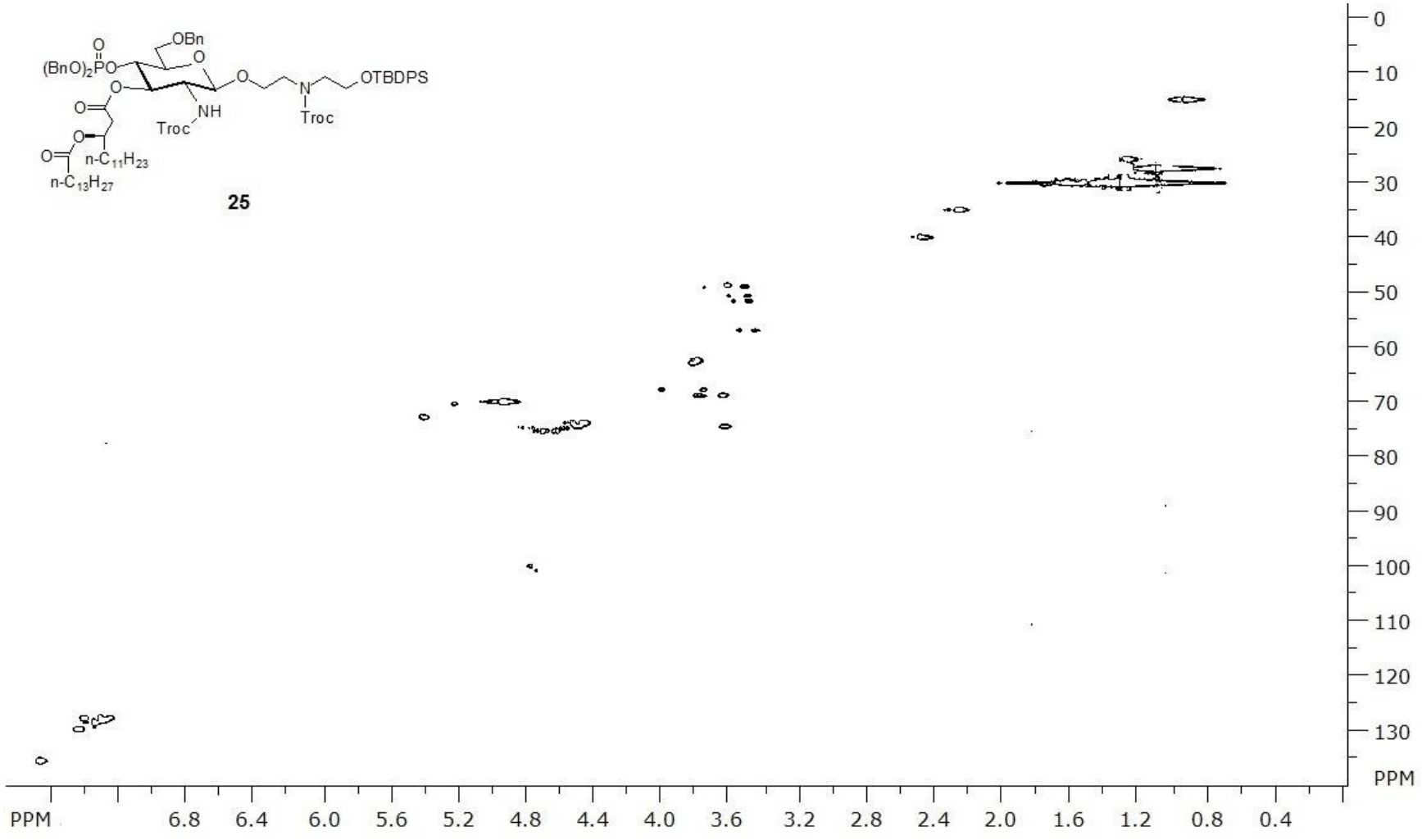
OBn
O
(BnO)2PO
O
O
NH
Troc
N
Troc
OTBDPS
O
O
n-C11H23
n-C13H27
25
0
10
20
30
40
50
60
70
80
90
100
110
120
130
PPM
PPM
6.8
6.4
6.0
5.6
5.2
4.8
4.4
4.0
3.6
3.2
2.8
2.4
2.0
1.6
1.2
0.8
0.4

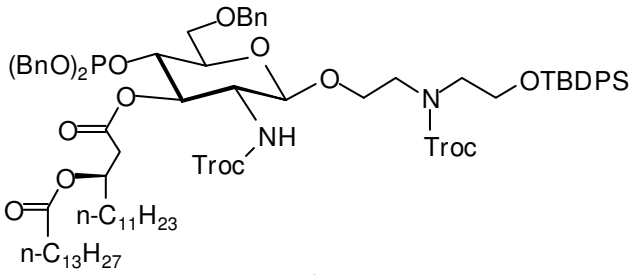

25

MALDI-MS (*m*/*z*) Calcd for $C_{81}H_{113}Cl_6N_2O_{16}PSi$ $[M + Na]^+$: 1661.56, found: 1661.48.

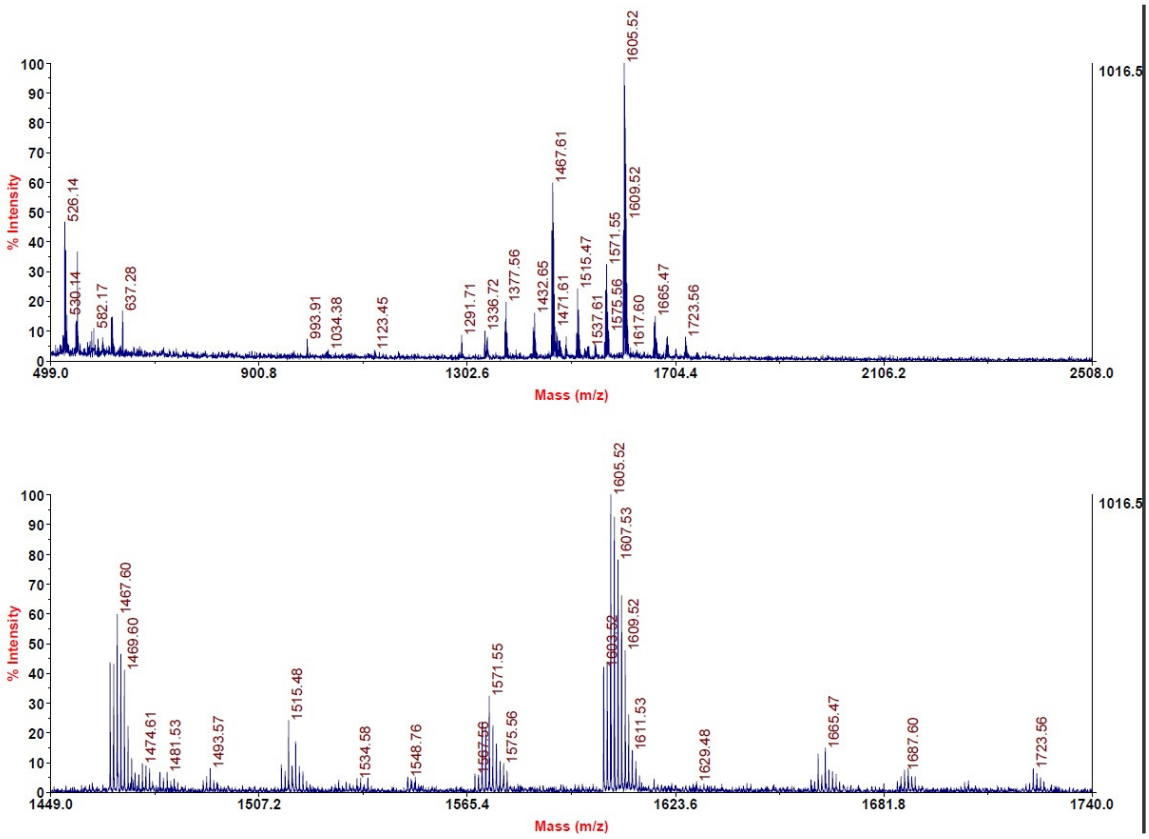

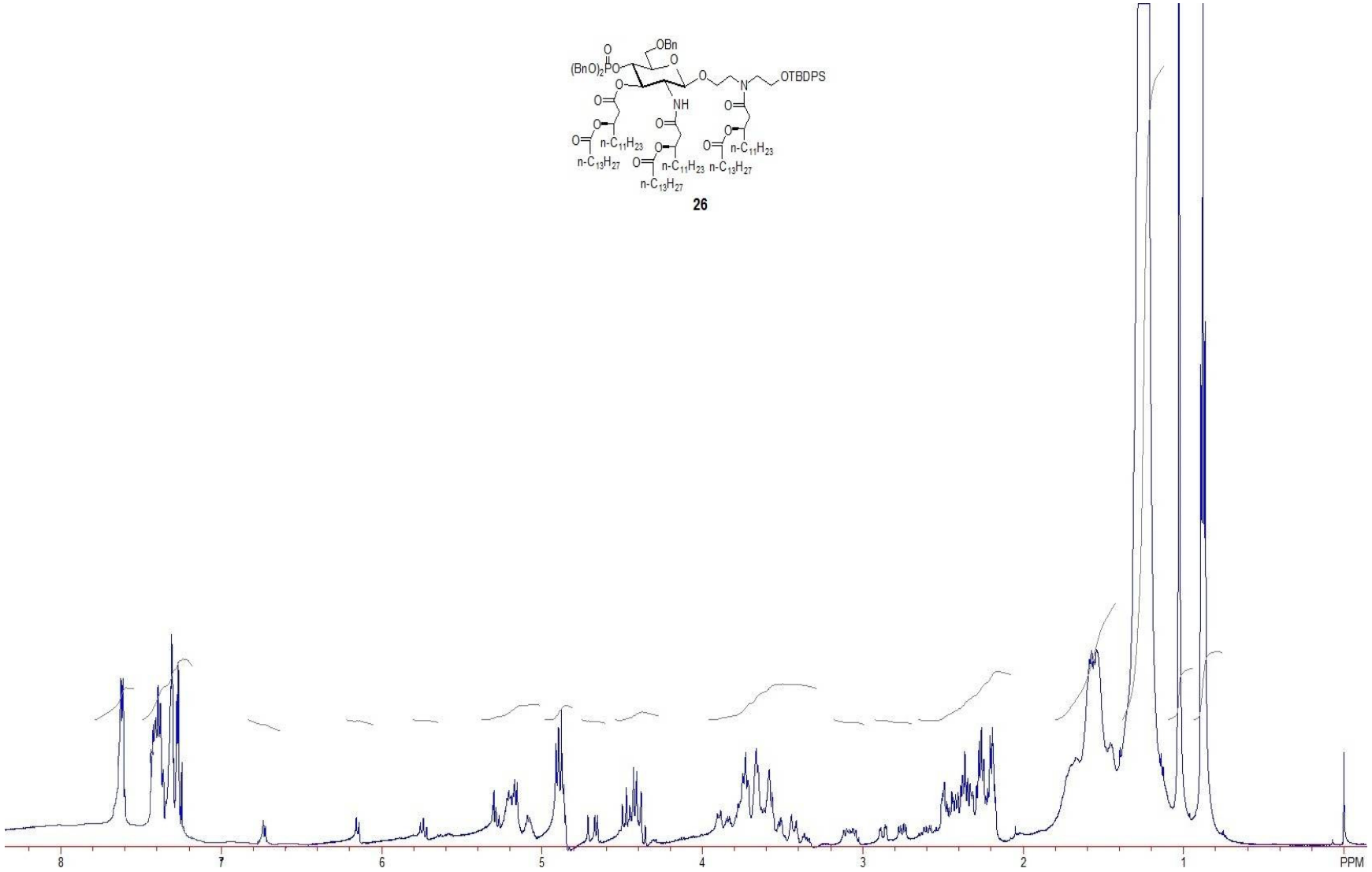

26

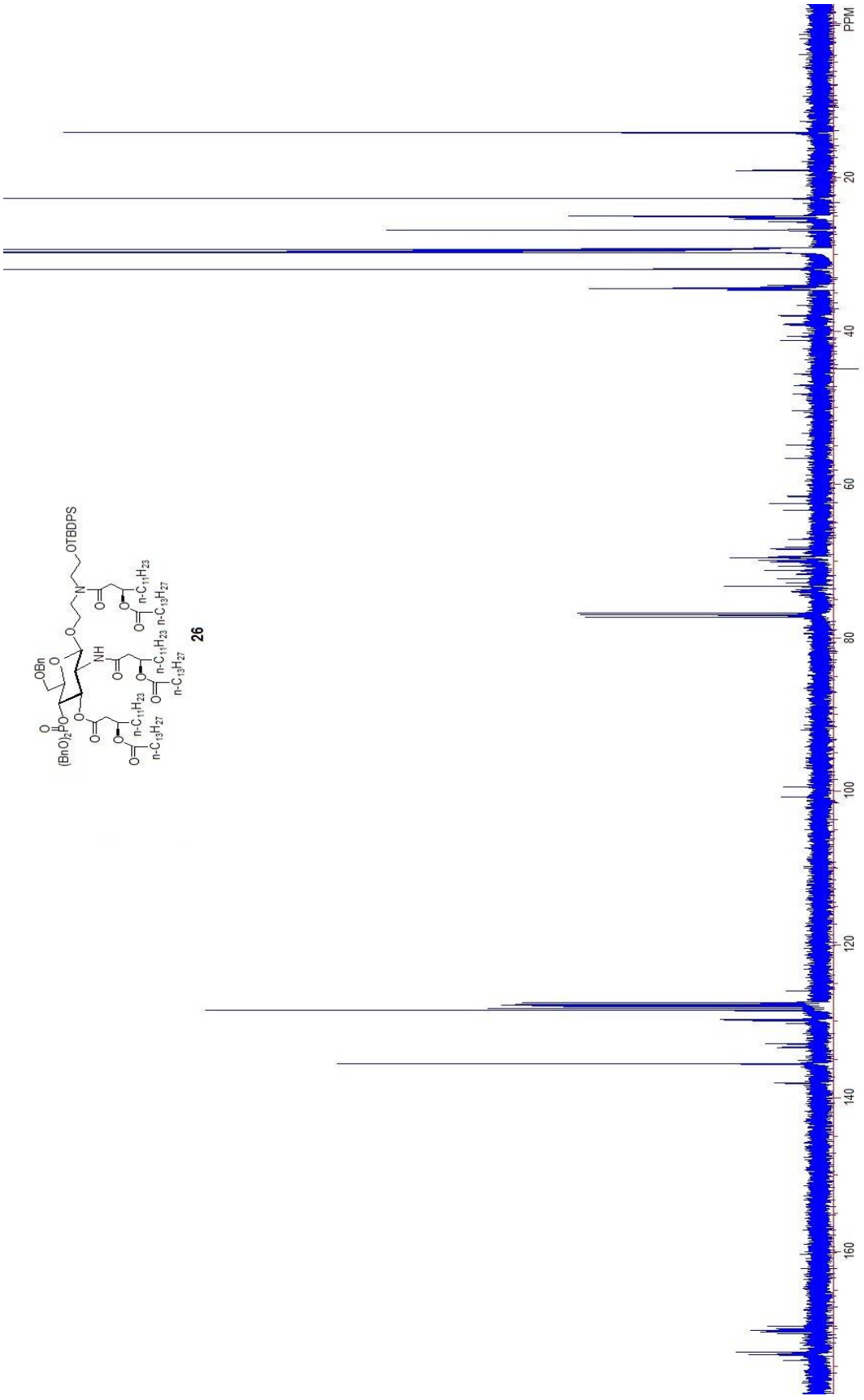
OTBDPS
OBn
NH
(BnO)2PO
n-C11H23
n-C13H27
26
PPM
20
40
60
80
100
120
140
160

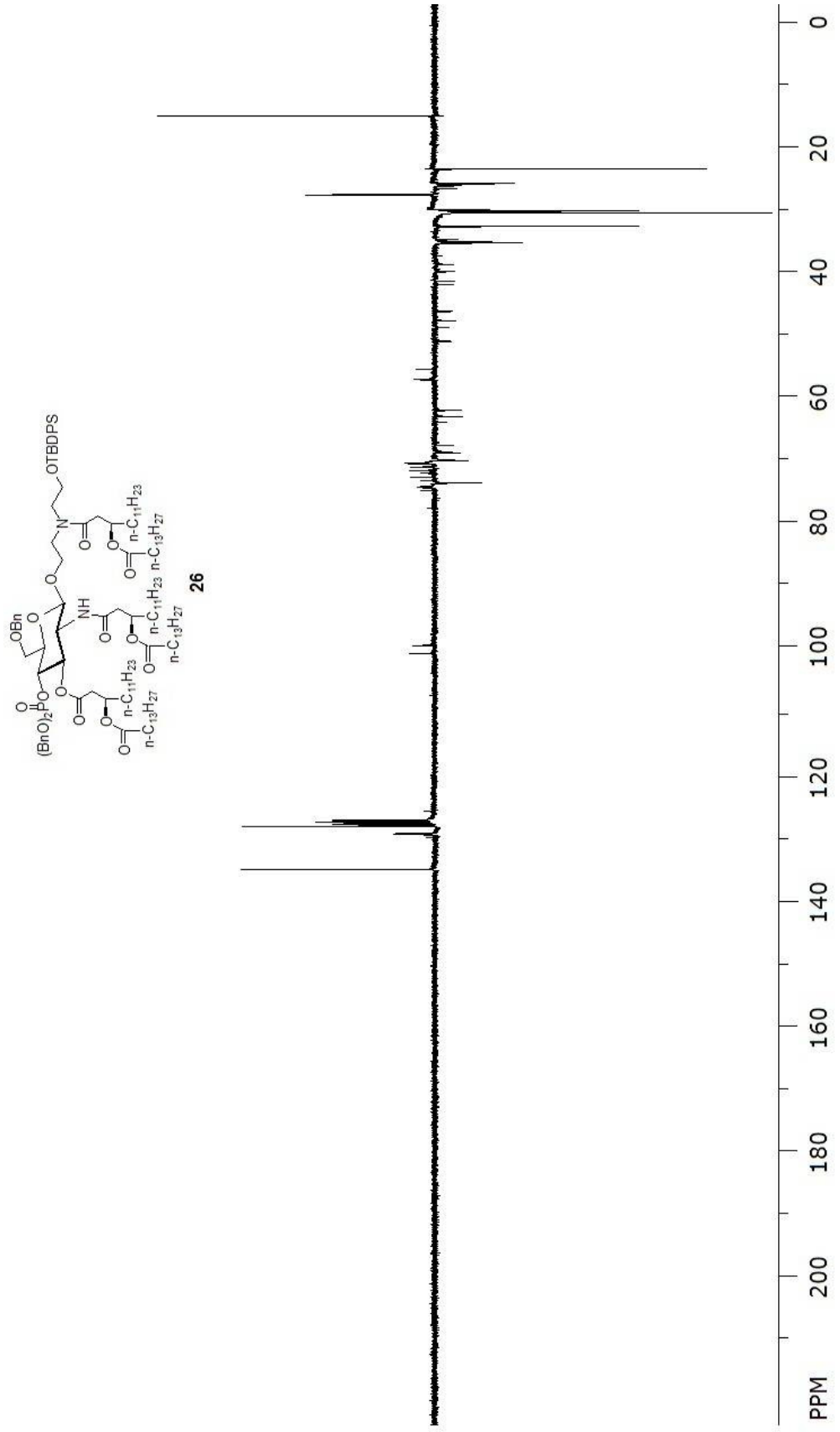
OTBDPS
OBn
NH
n-C11H23
n-C13H27
(BnO)2P
26
PPM
0
20
40
60
80
100
120
140
160
180
200

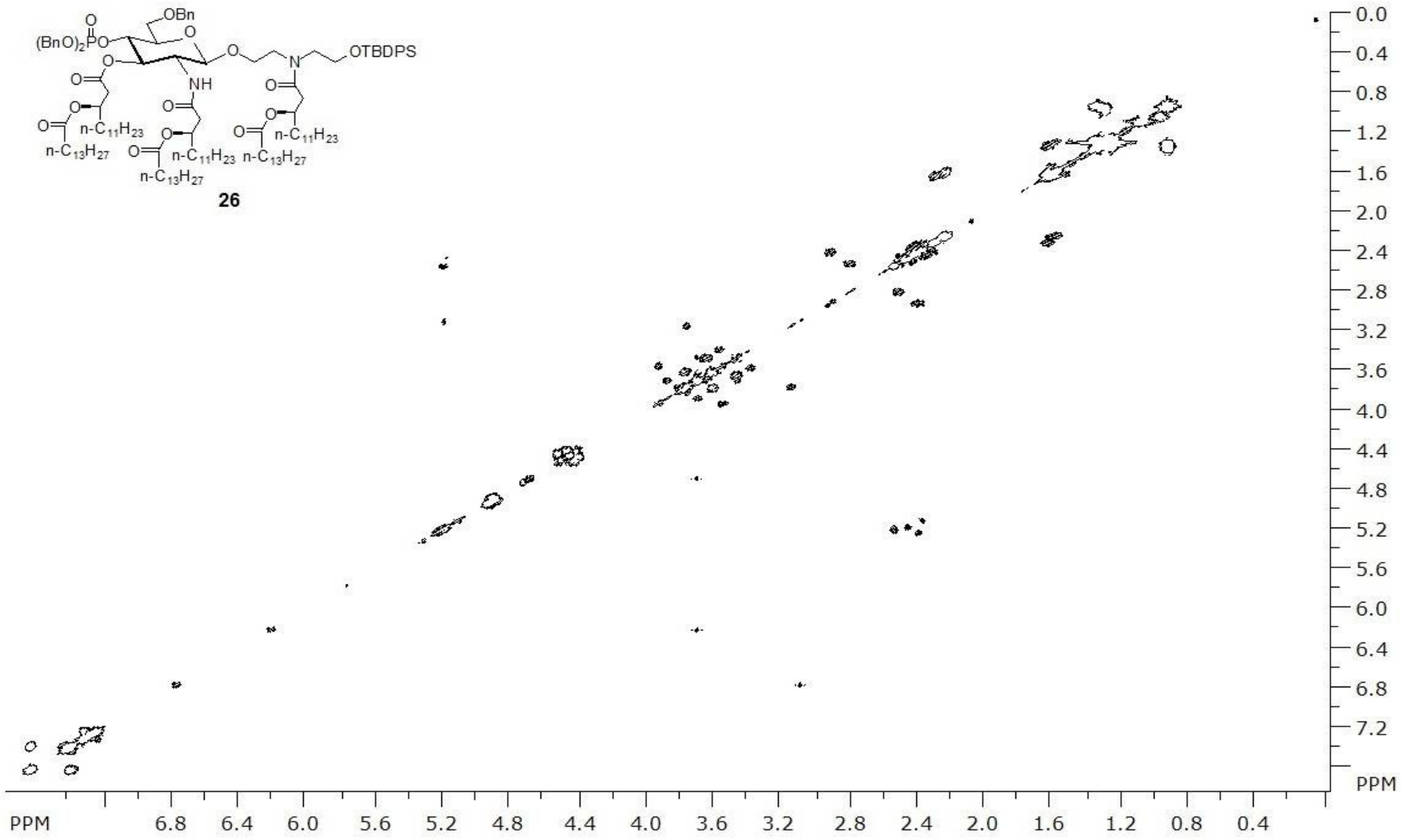
OBn
O
(BnO)2P
O
O
NH
O
N
OTBDPS
n-C11H23
n-C13H27
n-C11H23
n-C13H27
n-C11H23
n-C13H27
26
0.0
0.4
0.8
1.2
1.6
2.0
2.4
2.8
3.2
3.6
4.0
4.4
4.8
5.2
5.6
6.0
6.4
6.8
7.2
PPM
PPM
6.8
6.4
6.0
5.6
5.2
4.8
4.4
4.0
3.6
3.2
2.8
2.4
2.0
1.6
1.2
0.8
0.4

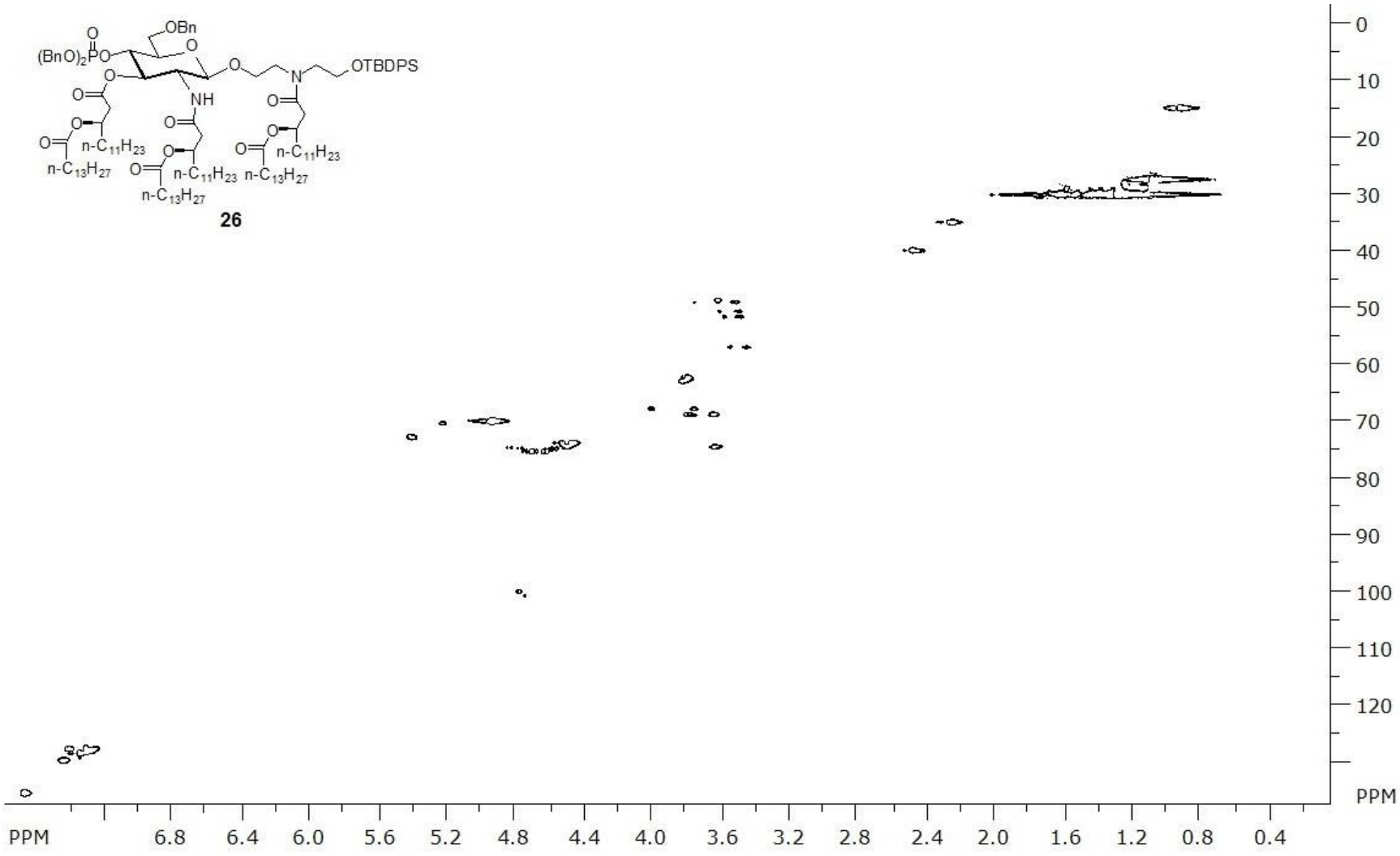
OBn
O
(BnO)2PO
O
O
NH
N
OTBDPS
n-C11H23
n-C13H27
26
0
10
20
30
40
50
60
70
80
90
100
110
120
PPM
PPM
6.8
6.4
6.0
5.6
5.2
4.8
4.4
4.0
3.6
3.2
2.8
2.4
2.0
1.6
1.2
0.8
0.4

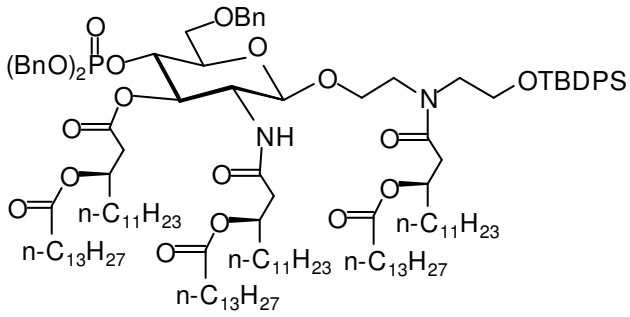

26

MALDI-MS (*m/z*) Calcd for $C_{131}H_{215}N_2O_{18}PSi$ $[M + Na]^+$: 2186.54, found: 2186.48.

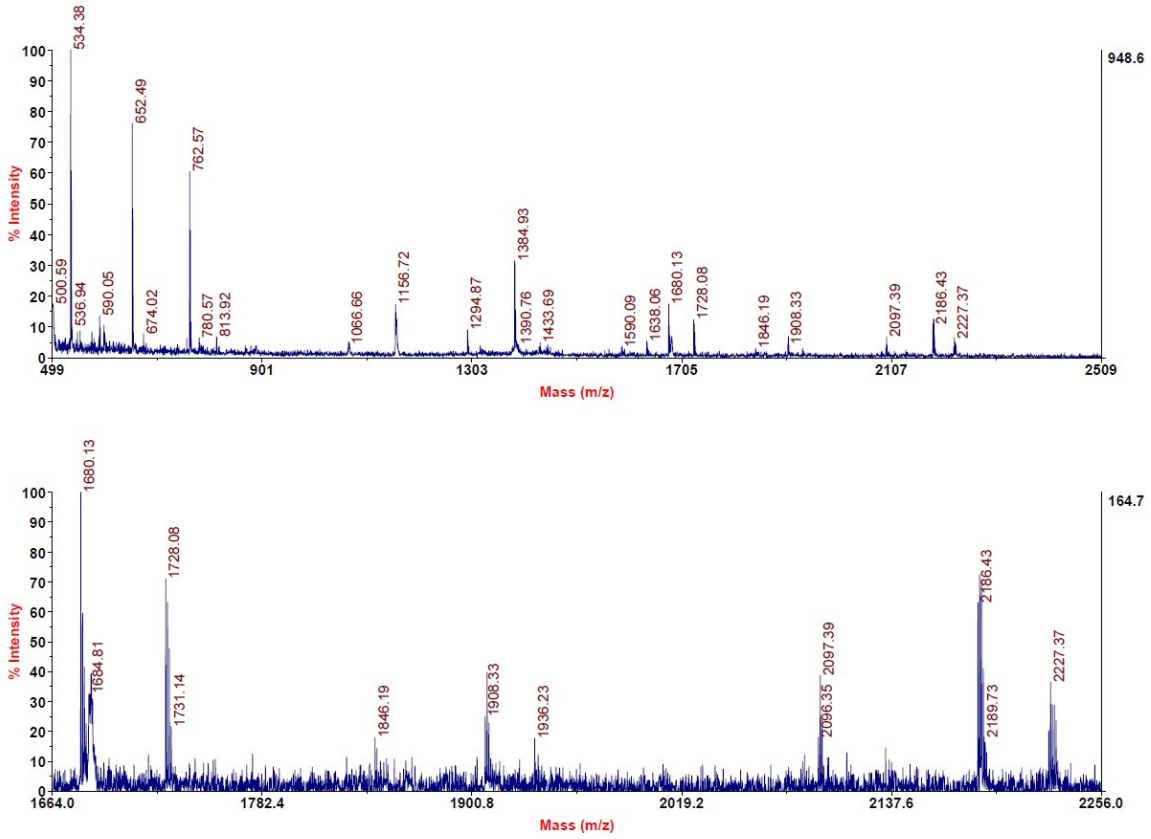

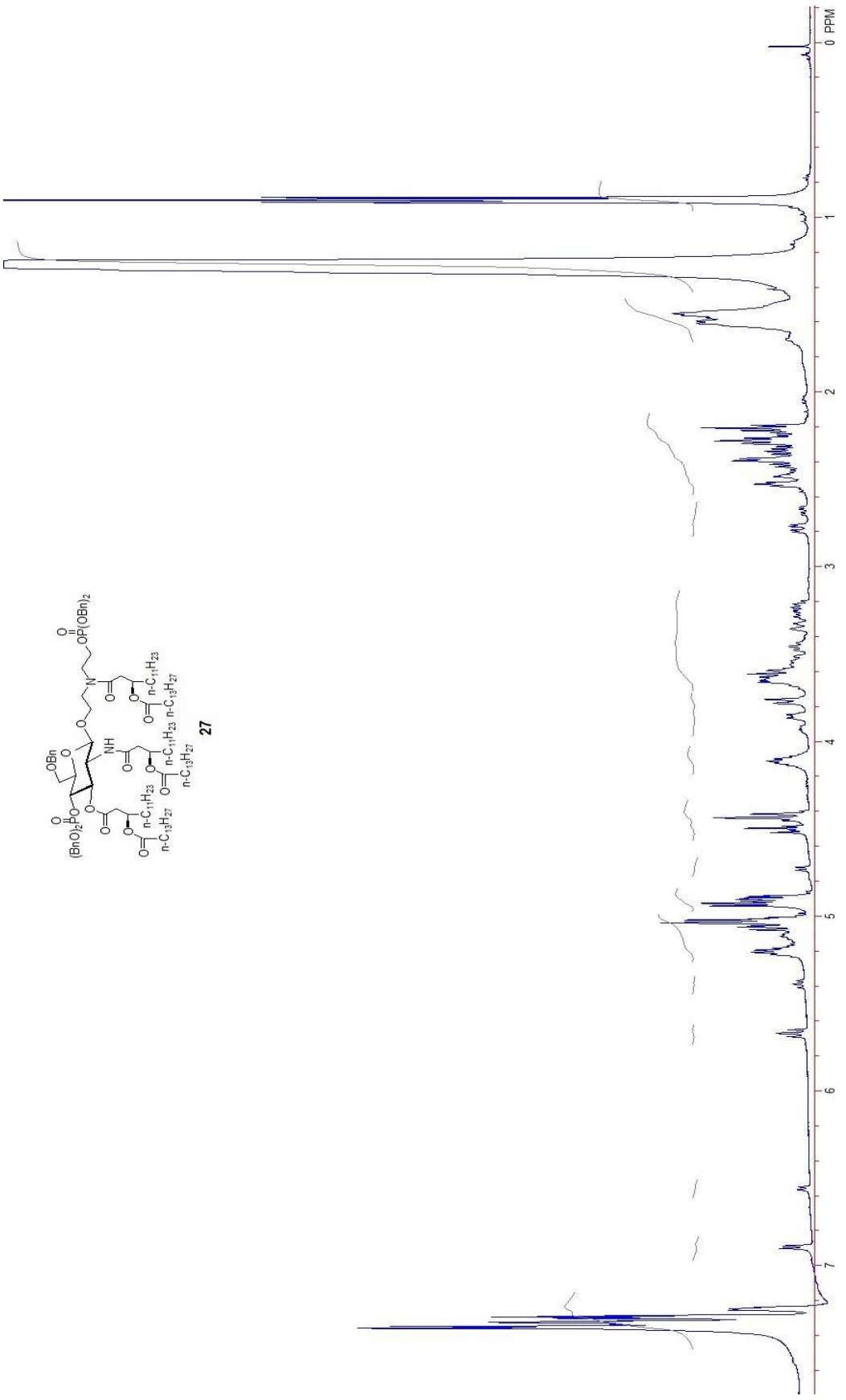
27
0 PPM

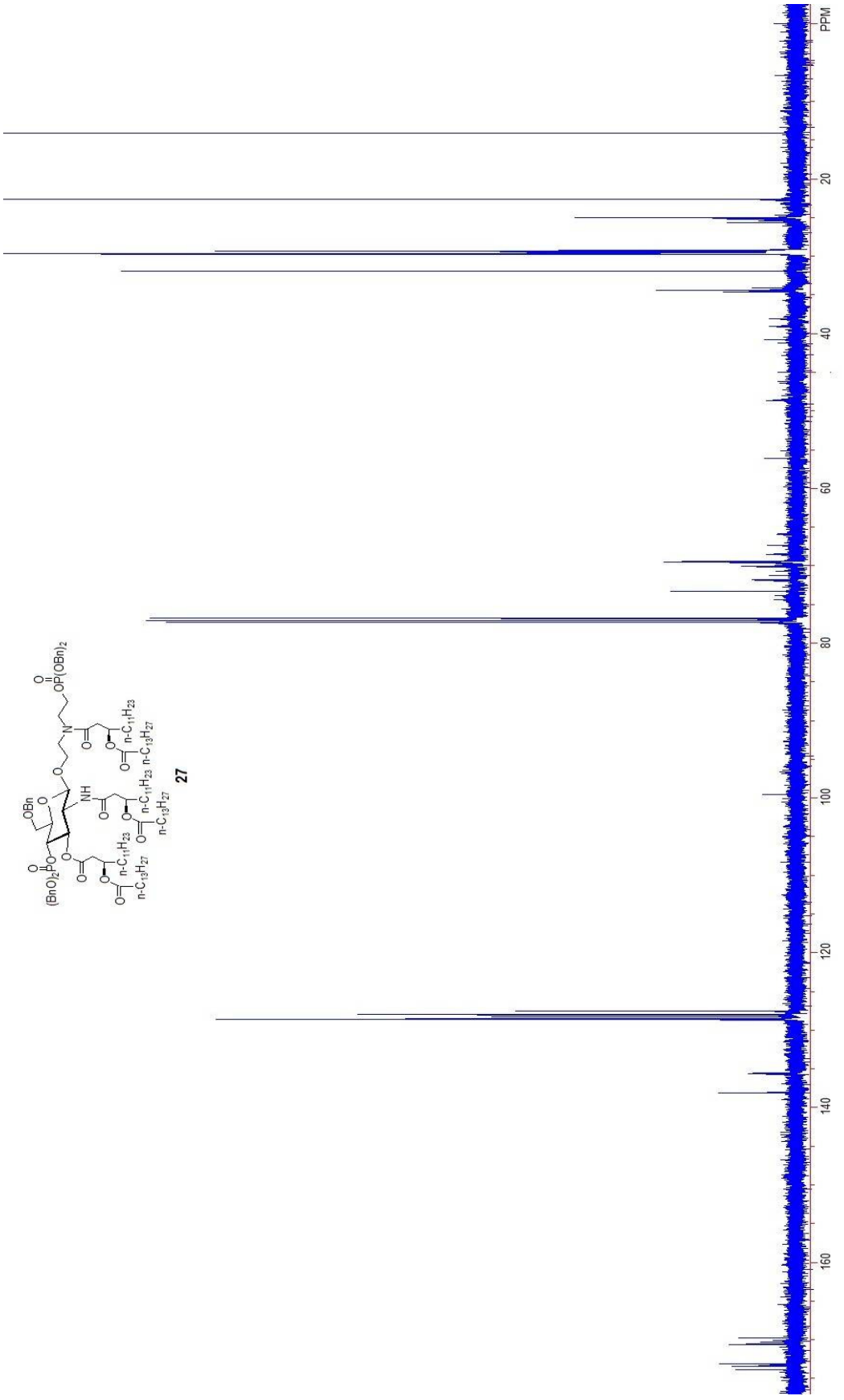
PPM
20
40
60
80
100
120
140
160
OBn
NH
OP(OBn)2
(BnO)2PO
n-C11H23
n-C13H27
27

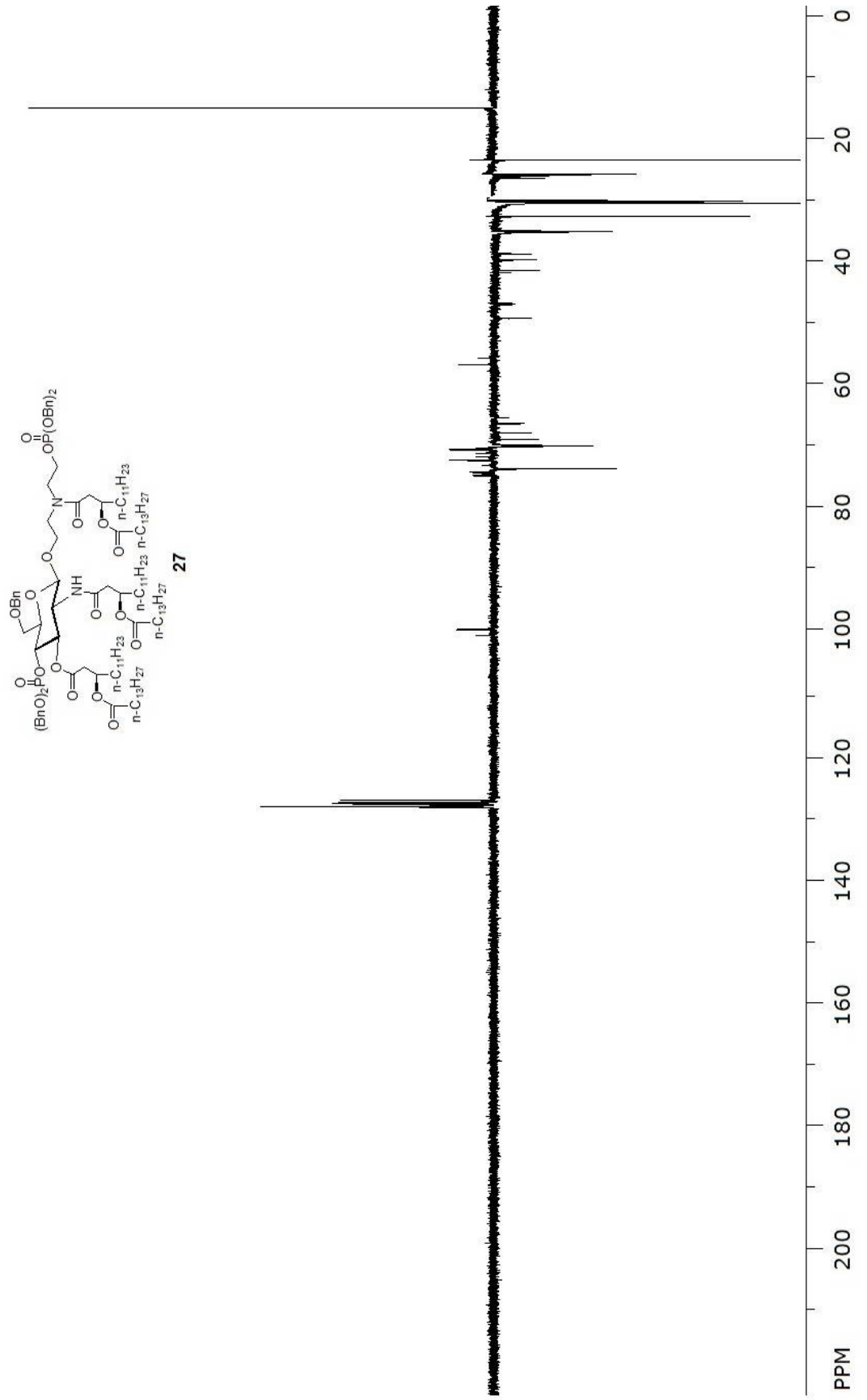
27
PPM
0
20
40
60
80
100
120
140
160
180
200

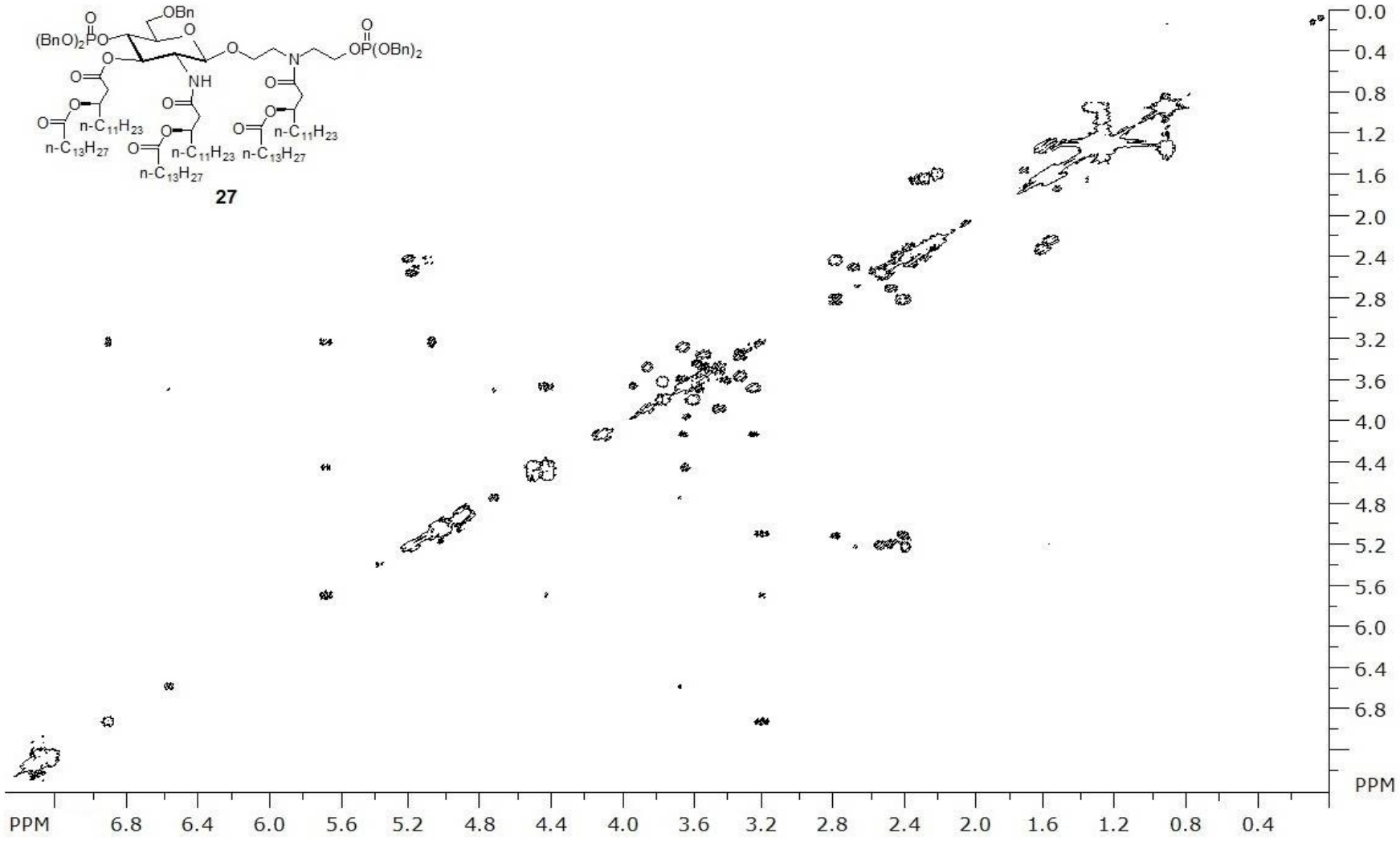
OBn
O
(BnO)2P
O
O
O
NH
N
O
OP(OBn)2
n-C11H23
n-C13H27
n-C11H23
n-C13H27
n-C11H23
n-C13H27
n-C11H23
n-C13H27
27
0.0
0.4
0.8
1.2
1.6
2.0
2.4
2.8
3.2
3.6
4.0
4.4
4.8
5.2
5.6
6.0
6.4
6.8
PPM
PPM
6.8
6.4
6.0
5.6
5.2
4.8
4.4
4.0
3.6
3.2
2.8
2.4
2.0
1.6
1.2
0.8
0.4

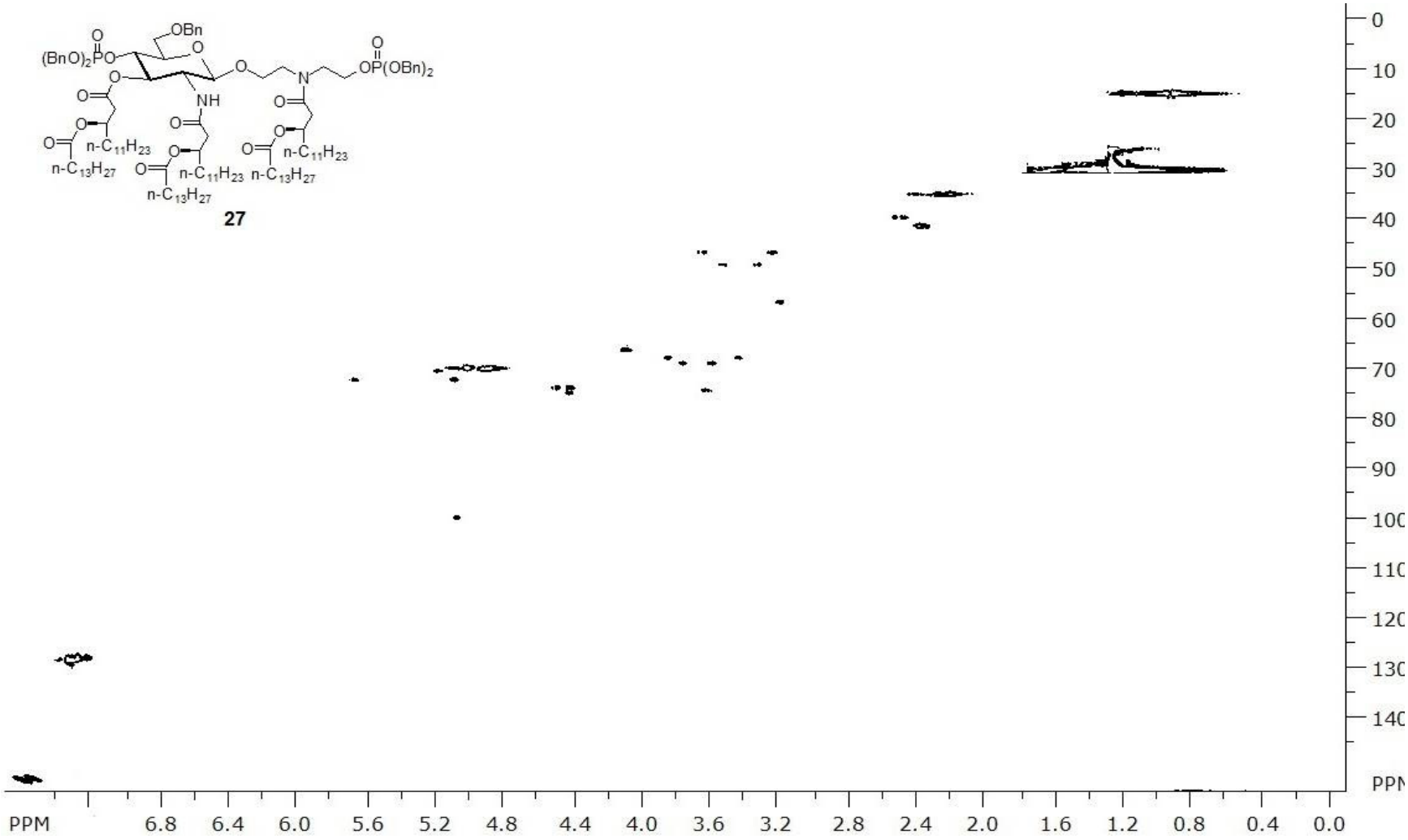
OBn
O
(BnO)2PO
O
O
NH
O
n-C11H23
n-C13H27
O
n-C11H23
n-C13H27
O
n-C13H27
O
N
O
OP(OBn)2
O
n-C11H23
n-C13H27
27
0
10
20
30
40
50
60
70
80
90
100
110
120
130
140
PPM
PPM
6.8
6.4
6.0
5.6
5.2
4.8
4.4
4.0
3.6
3.2
2.8
2.4
2.0
1.6
1.2
0.8
0.4
0.0

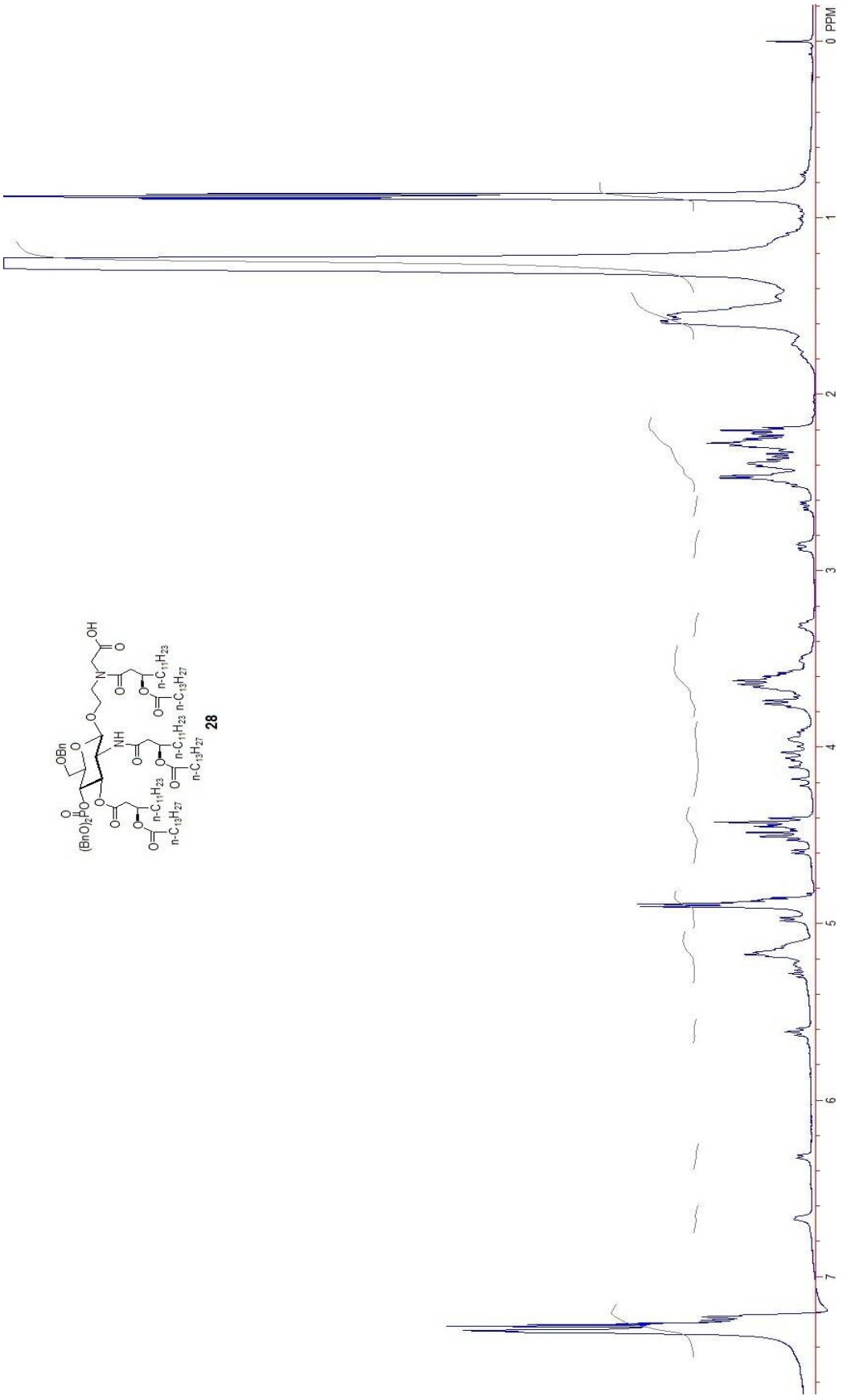
28
0 PPM

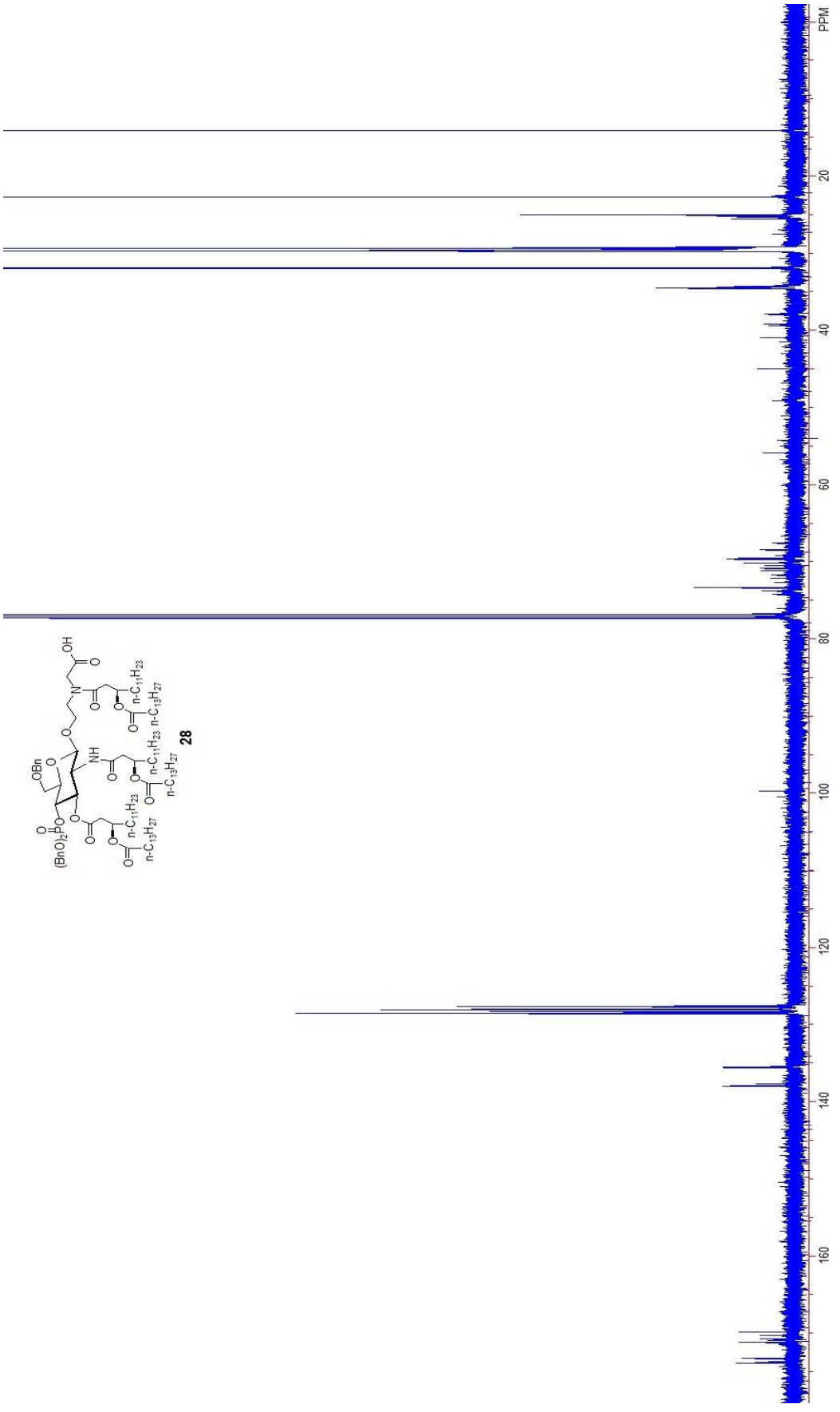
PPM
20
40
60
80
100
120
140
160
28

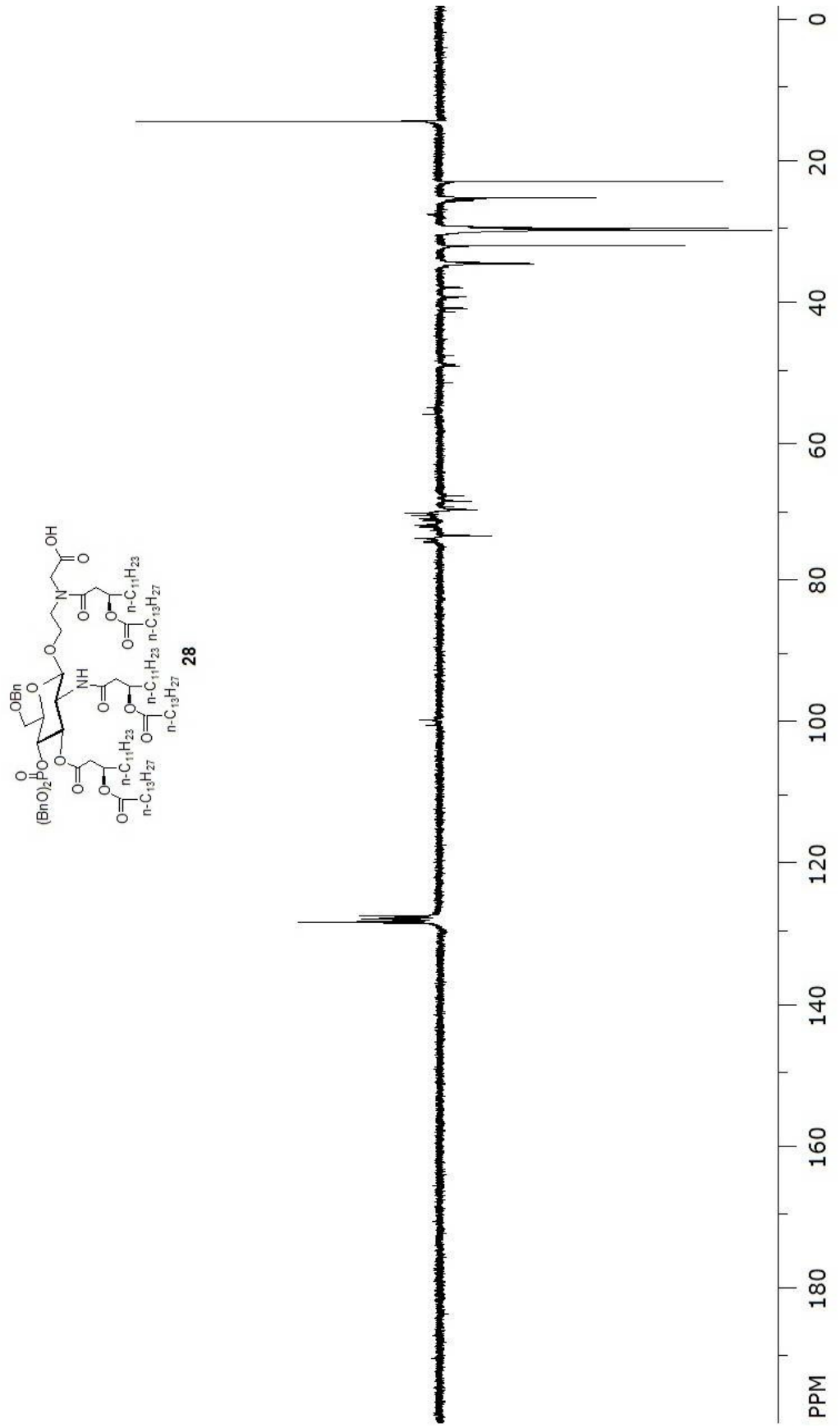
OBn
OH
NH
$(BnO)_2P$
$n\text{-}C_{11}H_{23}$
$n\text{-}C_{13}H_{27}$
28
PPM
0
20
40
60
80
100
120
140
160
180

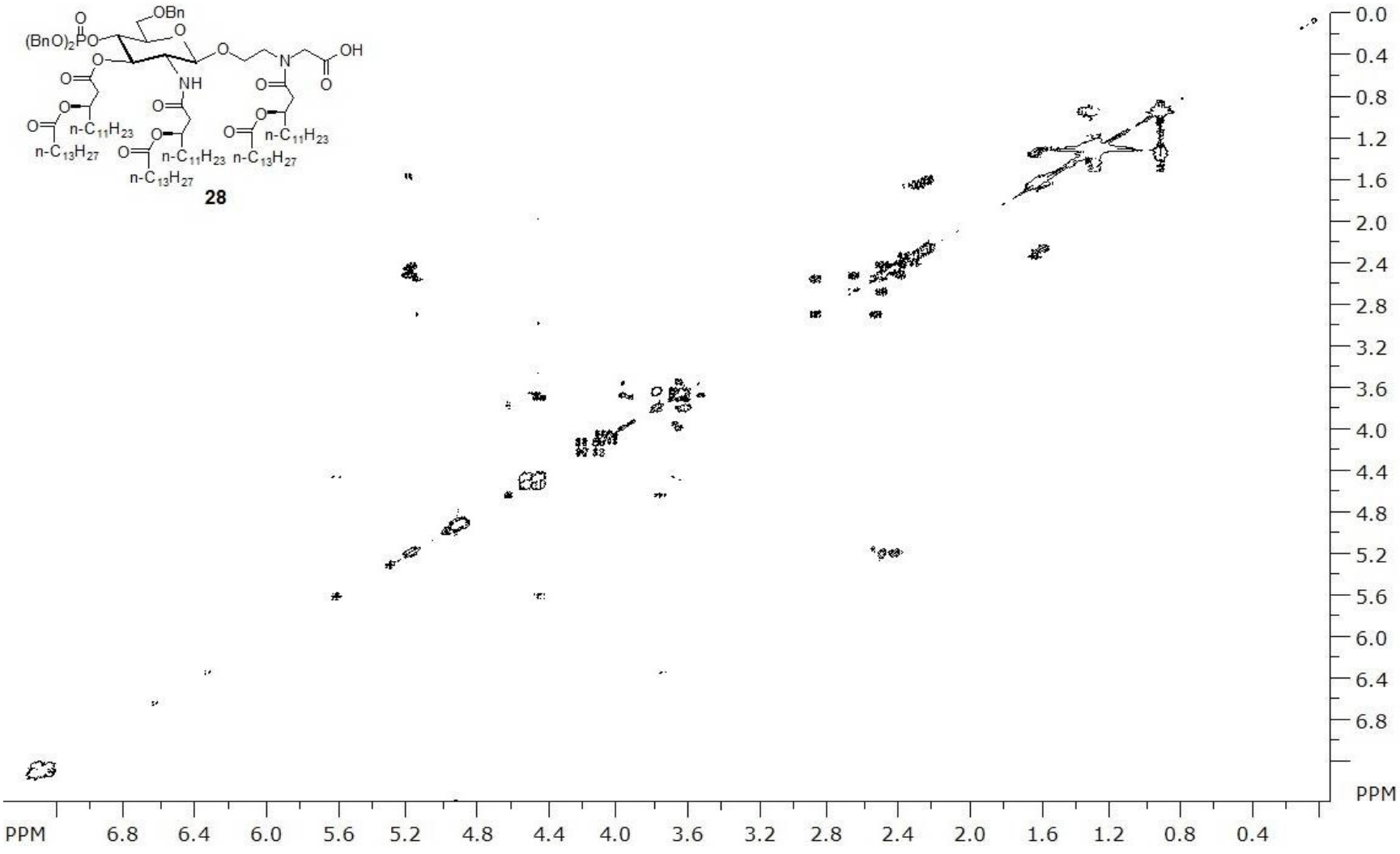
OBn
(BnO)2PO
O
NH
N
OH
n-C11H23
n-C13H27
28
0.0
0.4
0.8
1.2
1.6
2.0
2.4
2.8
3.2
3.6
4.0
4.4
4.8
5.2
5.6
6.0
6.4
6.8
PPM
PPM
6.8
6.4
6.0
5.6
5.2
4.8
4.4
4.0
3.6
3.2
2.8
2.4
2.0
1.6
1.2
0.8
0.4

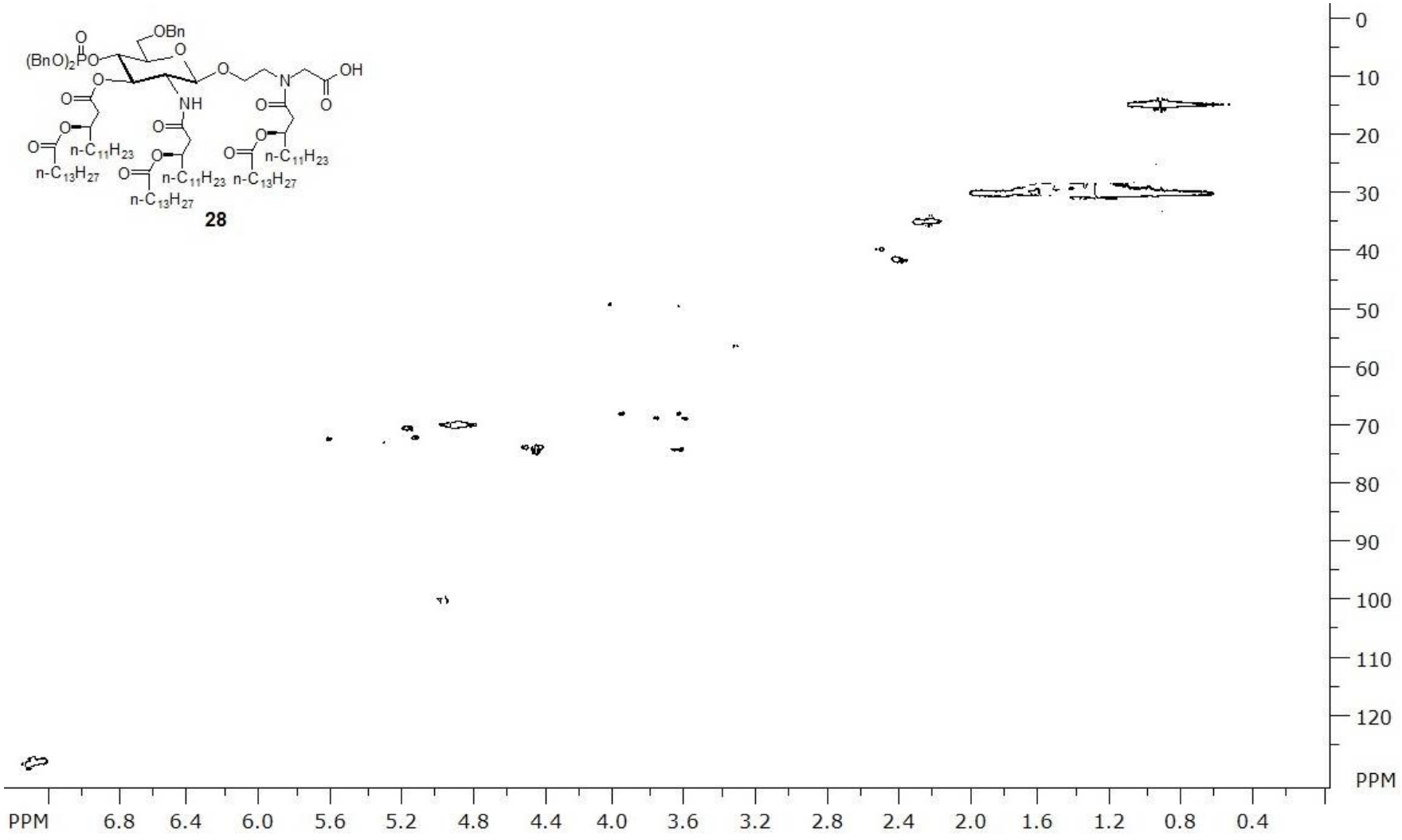
OBn
(BnO)2PO
O
O
NH
N
OH
n-C11H23
n-C13H27
28
0
10
20
30
40
50
60
70
80
90
100
110
120
PPM
PPM
6.8
6.4
6.0
5.6
5.2
4.8
4.4
4.0
3.6
3.2
2.8
2.4
2.0
1.6
1.2
0.8
0.4

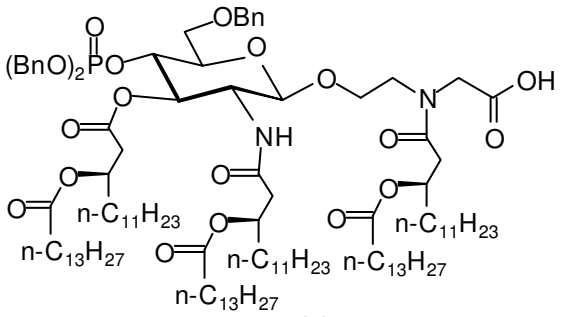

28

MALDI-MS (*m/z*) Calcd for $C_{115}H_{195}N_2O_{19}P$ $[M + Na]^+$: 1962.39, found: 1962.30.

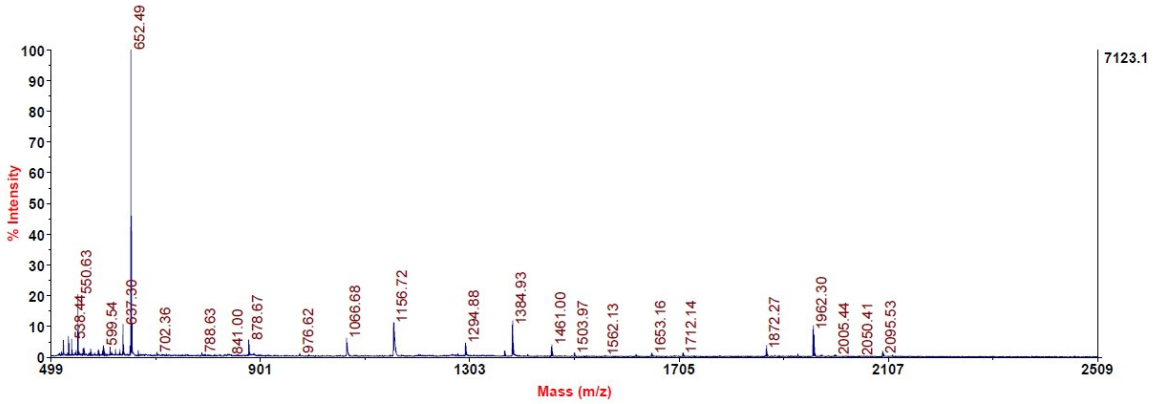

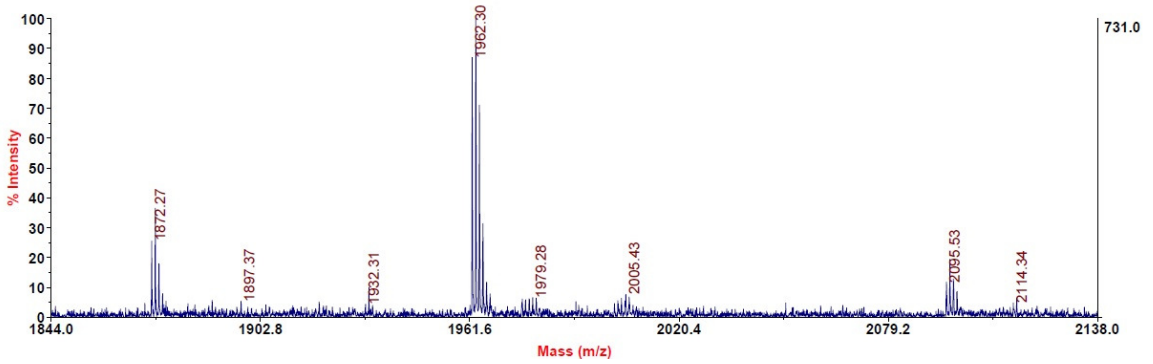

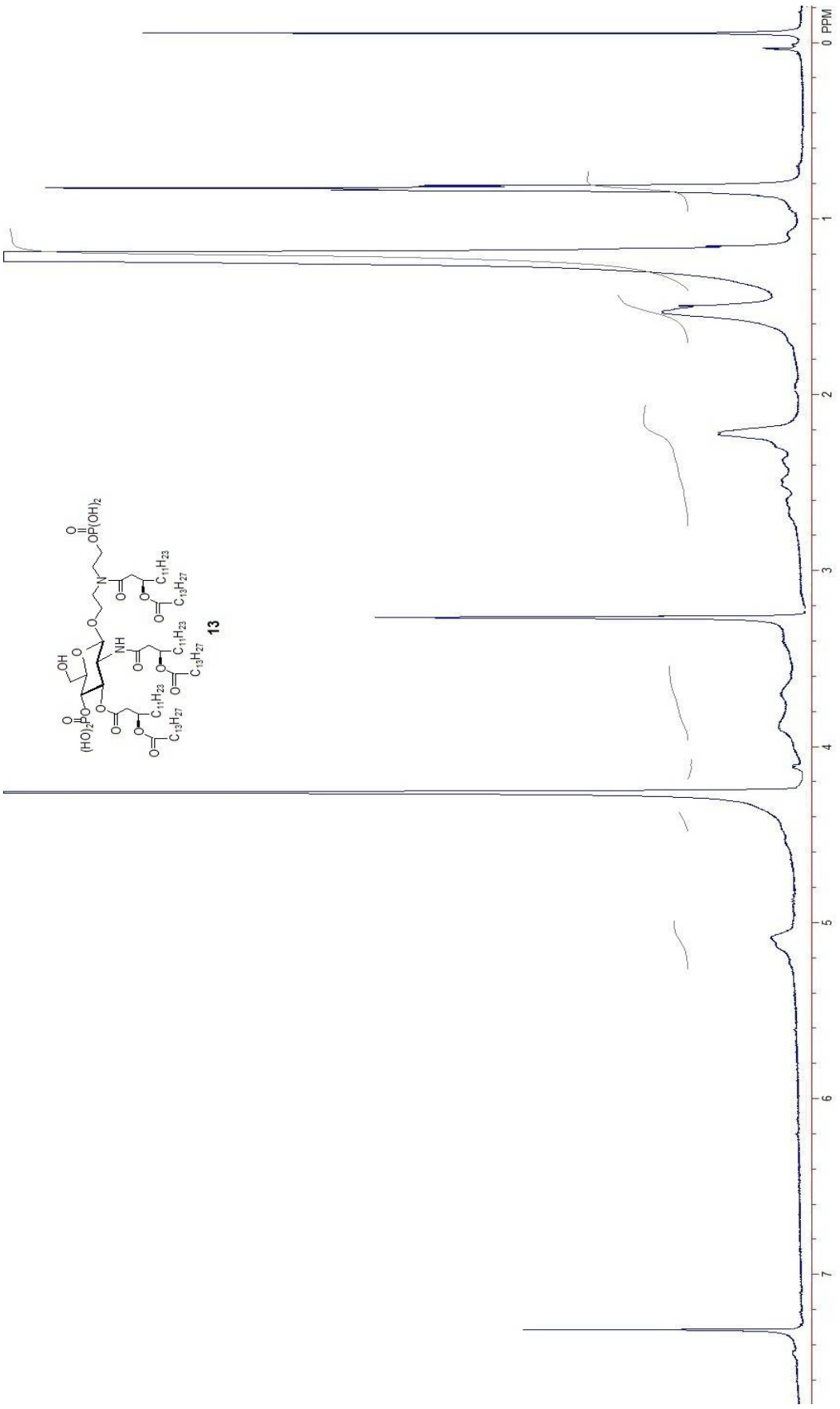
13
0 PPM

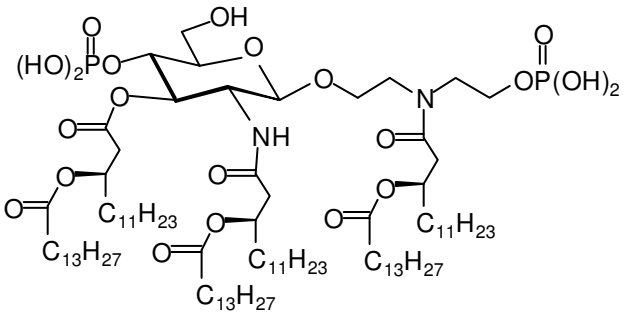

13

MALDI-MS (*m/z*) Calcd for $C_{94}H_{180}N_2O_{21}P_2$ $[M + Na]^+$: 1758.24, found: 1758.20.

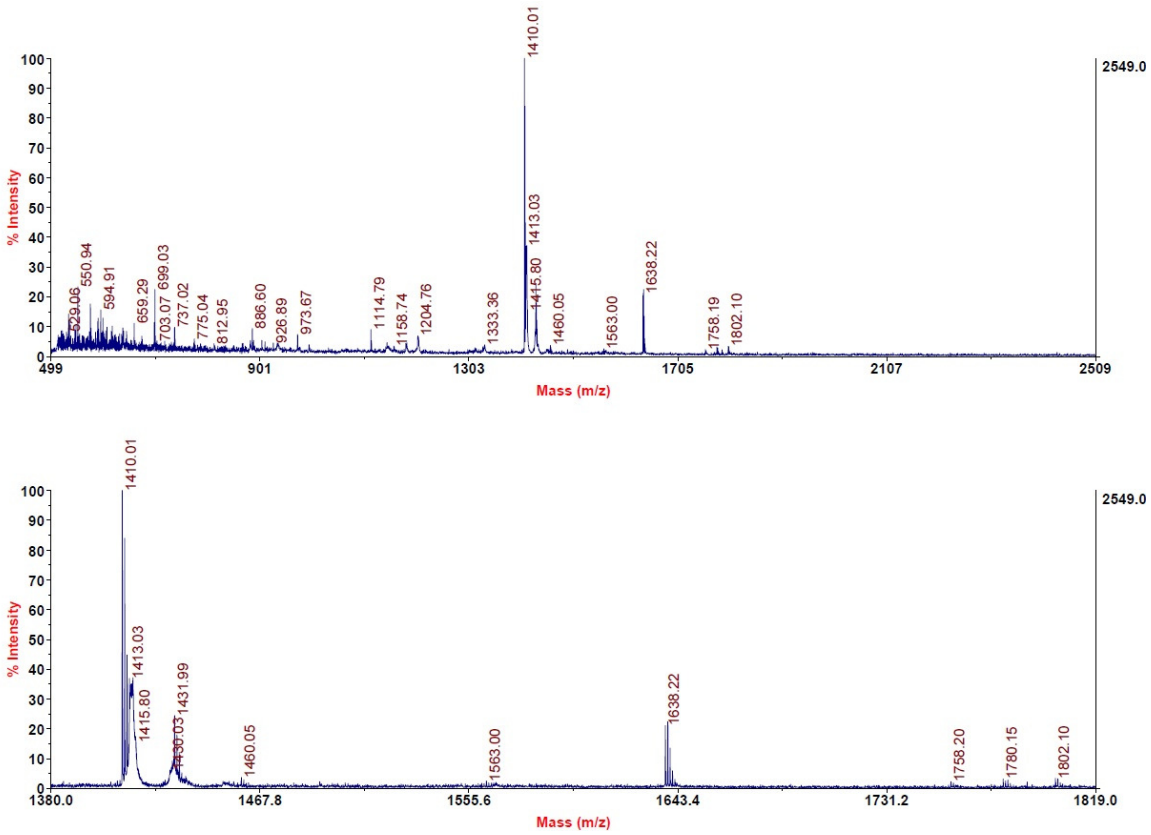

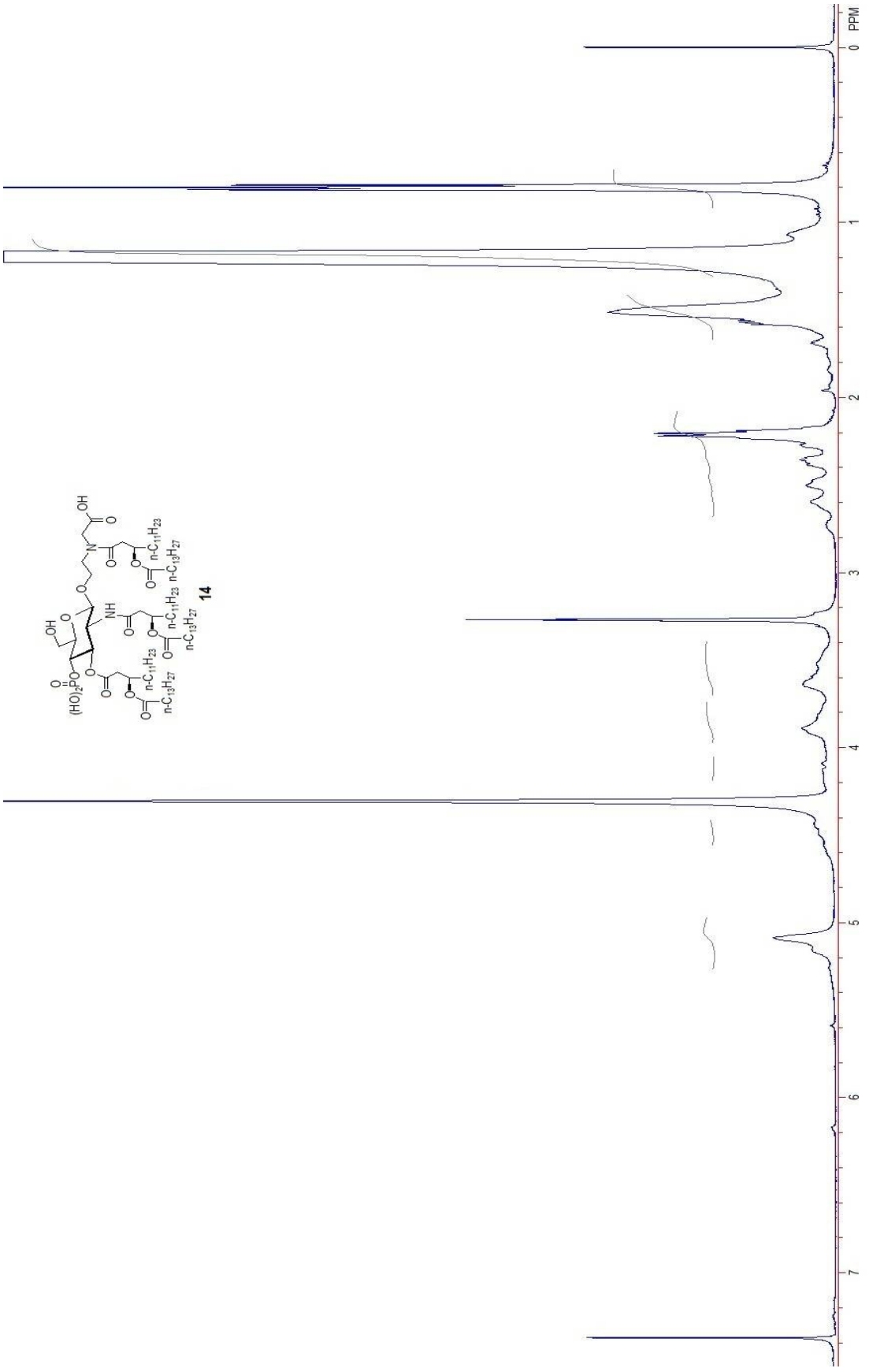
14
PPM
0
1
2
3
4
5
6
7

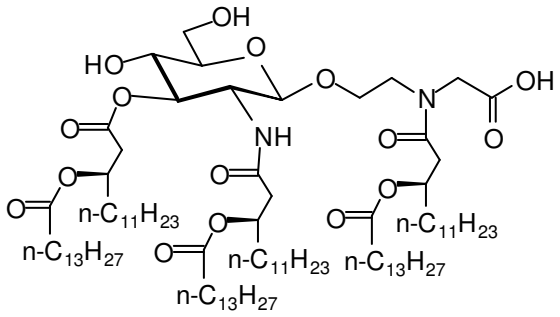

14

MALDI-MS (*m*/*z*) Calcd for $C_{94}H_{177}N_2O_{19}P$ $[M + Na]^+$: 1692.25, found: 1692.17.

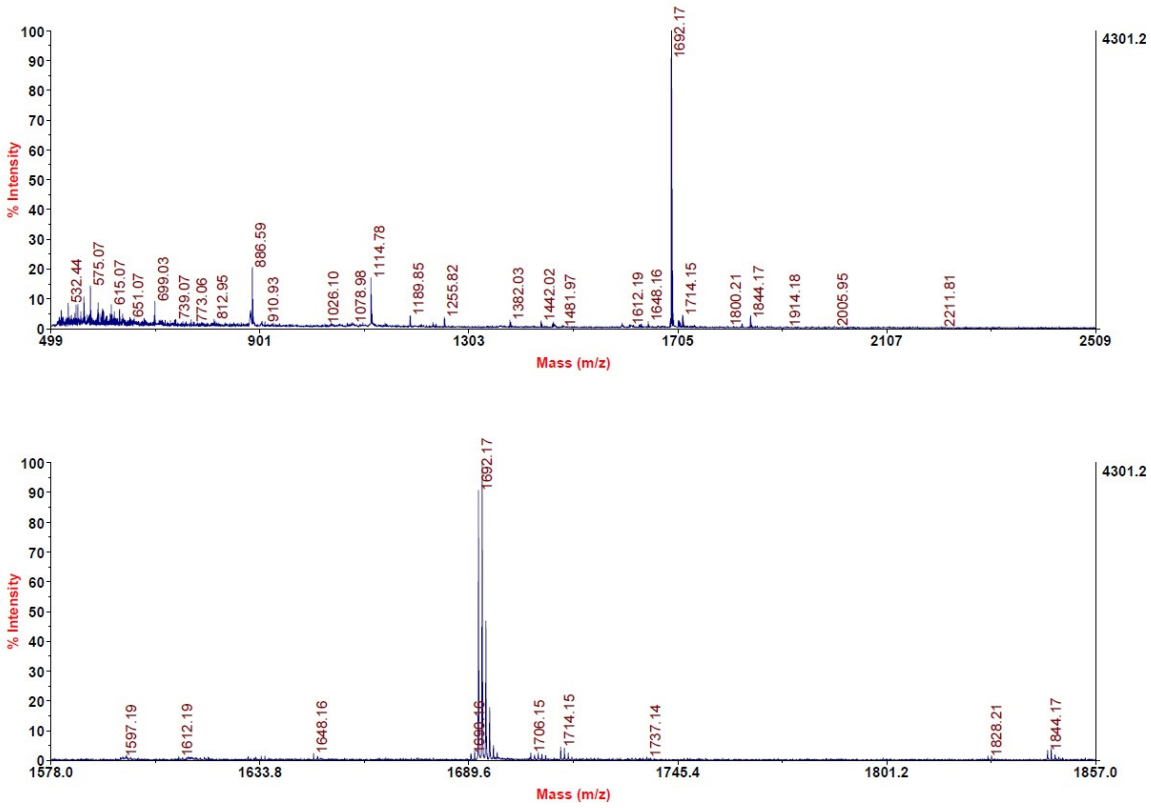

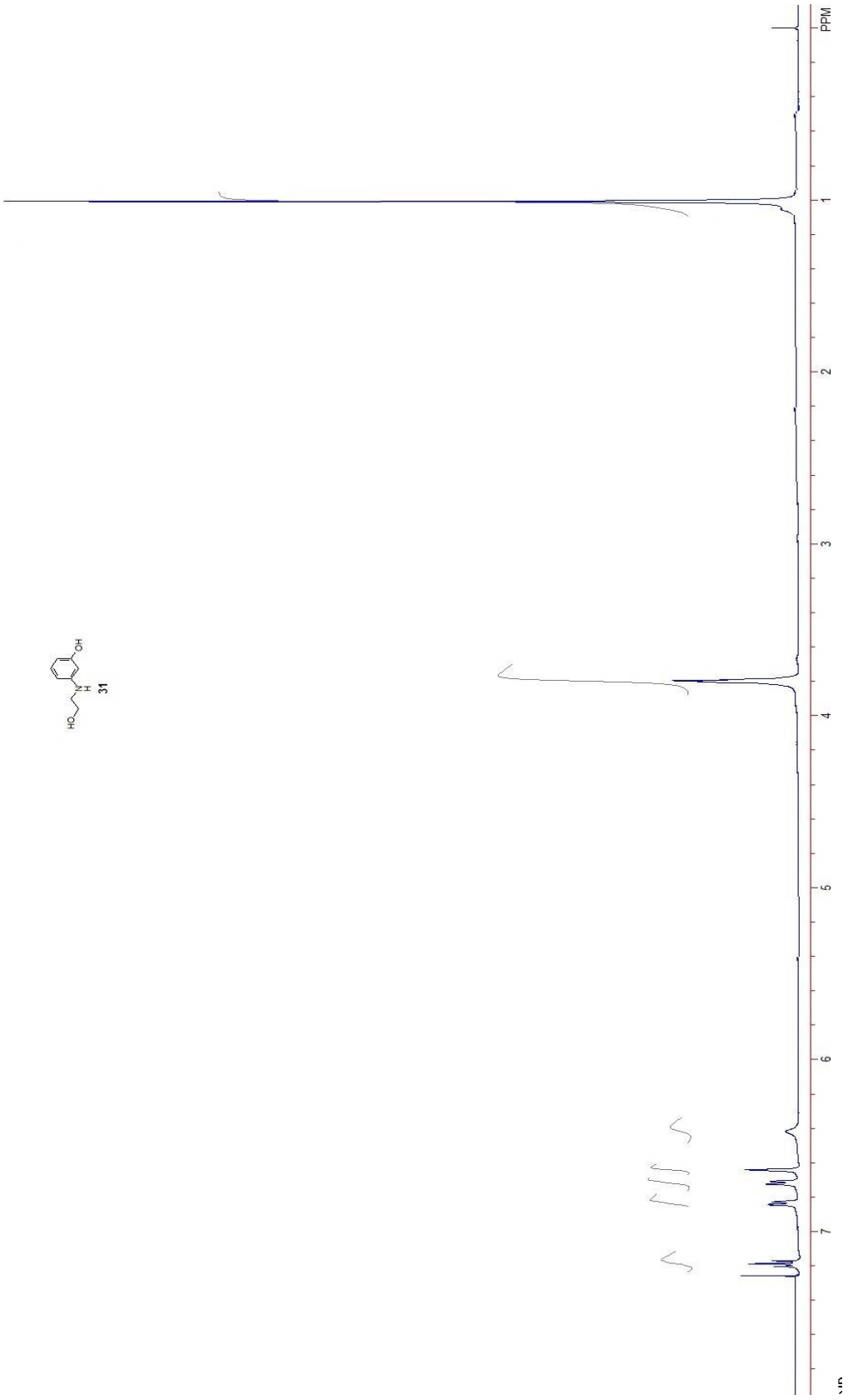
OH
N
H
HO
31
PPM
1
2
3
4
5
6
7

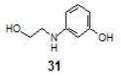

31

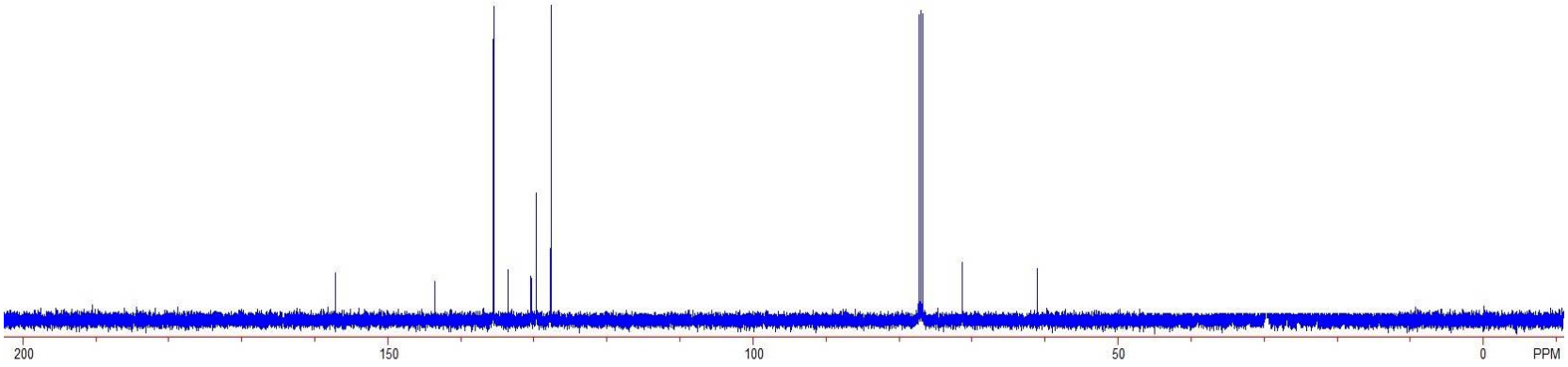

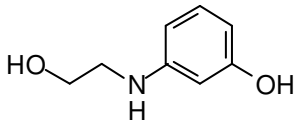

31

HRESI-MS (*m*/*z*) Calcd for $C_8H_{11}NO_2$ $[M+H]^+$: 154.0868, found: 154.0858.

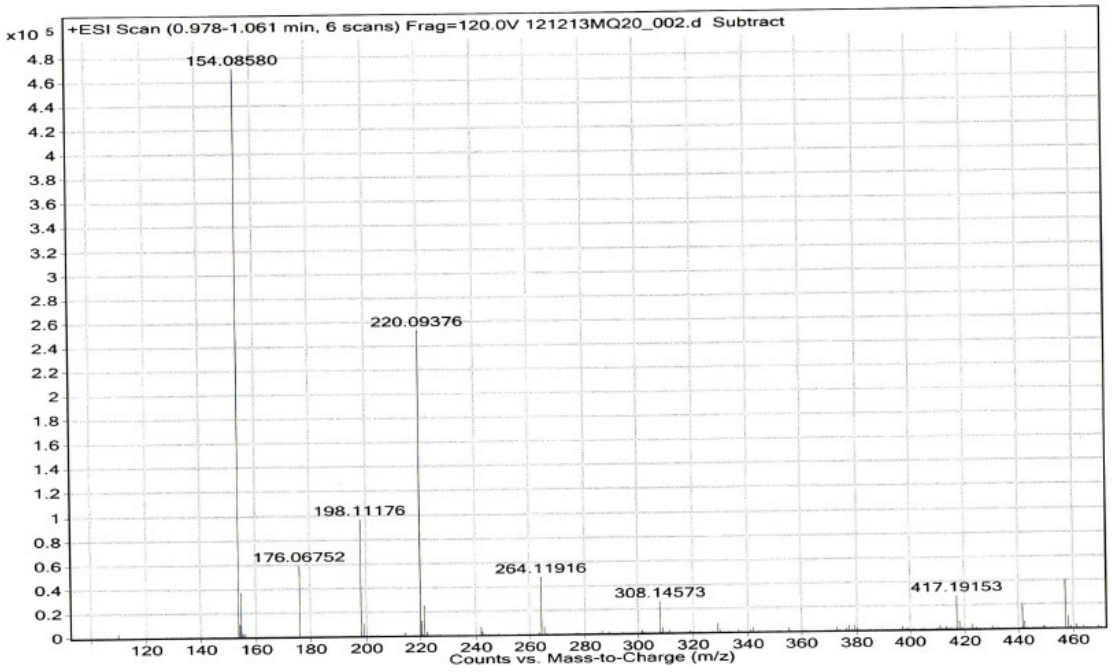

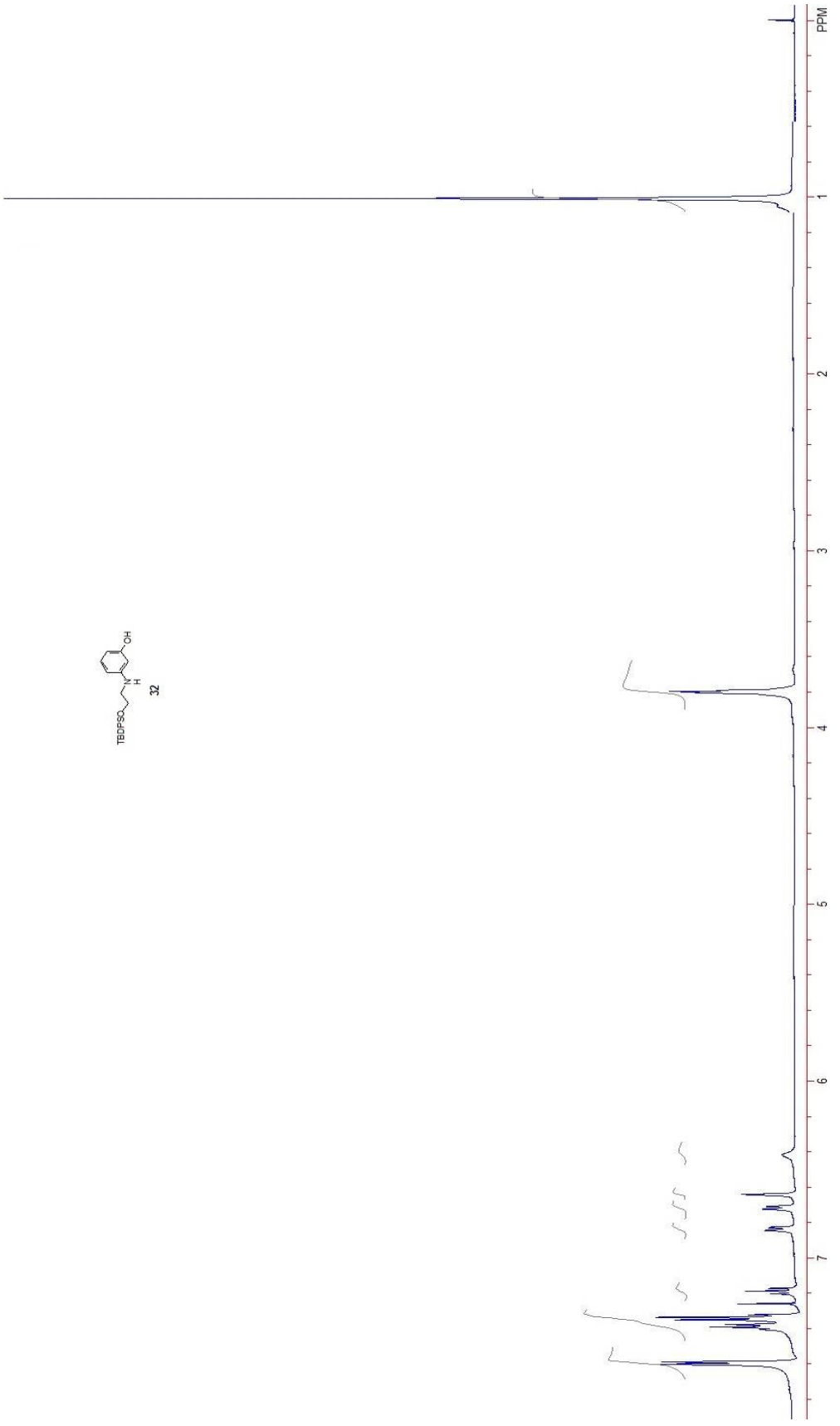
TBDPSO
OH
N
H
32
PPM
1
2
3
4
5
6
7

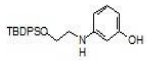

32

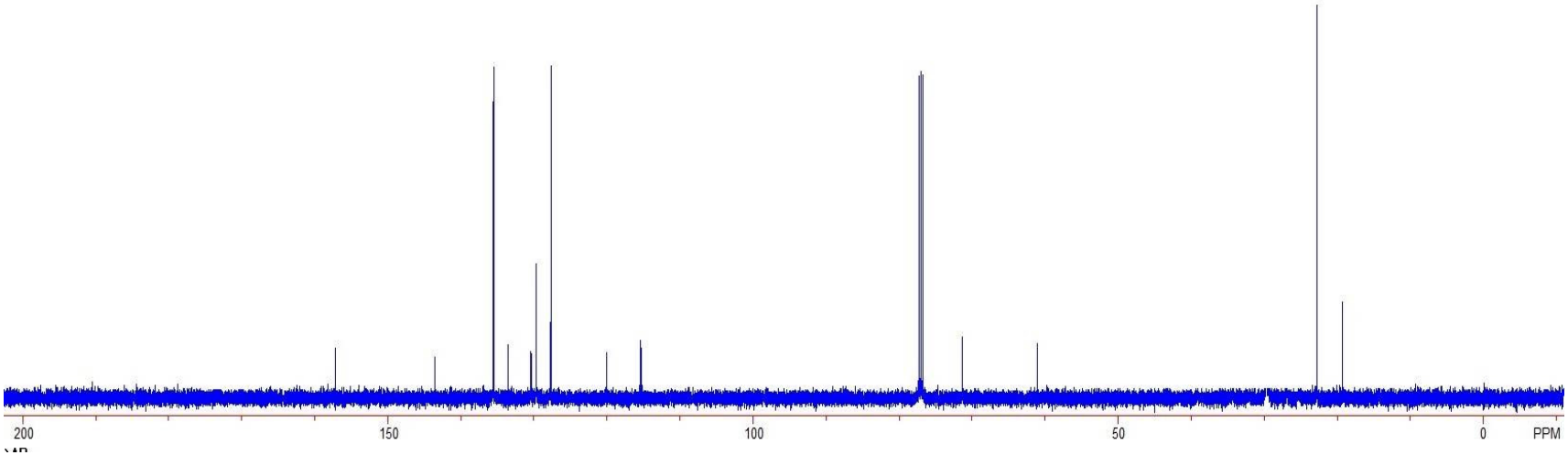

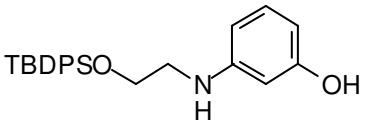

32

HRESI-MS (*m*/*z*) Calcd for $C_{24}H_{29}NO_2Si$ $[M+H]^+$: 392.2047, found: 392.2033.

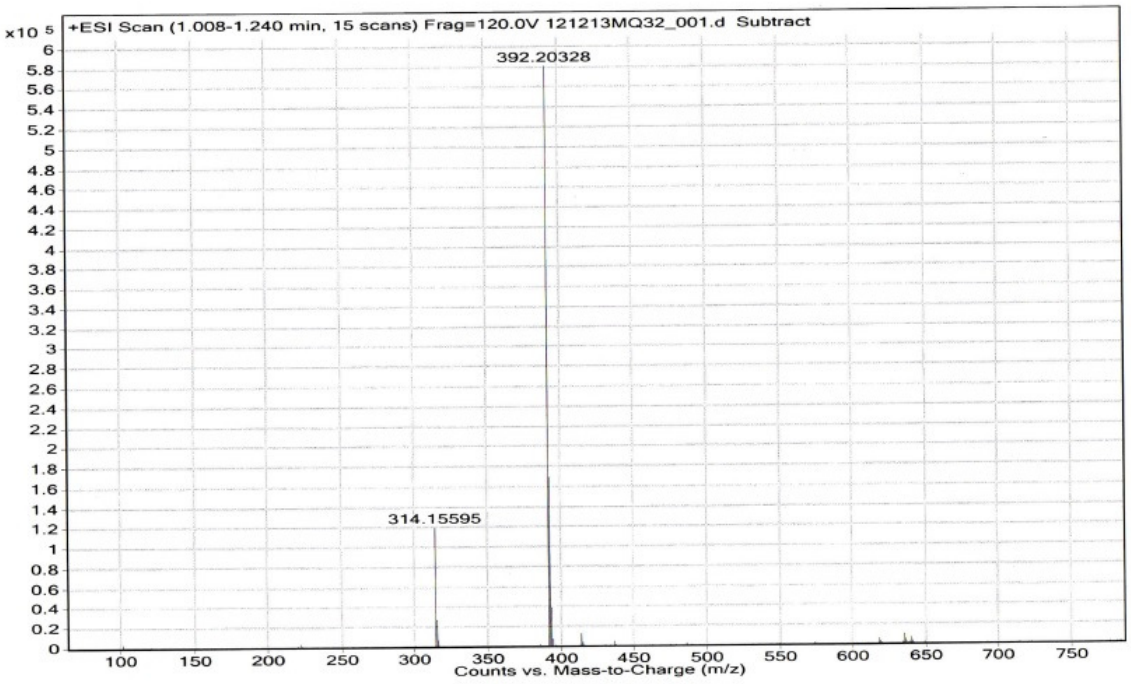

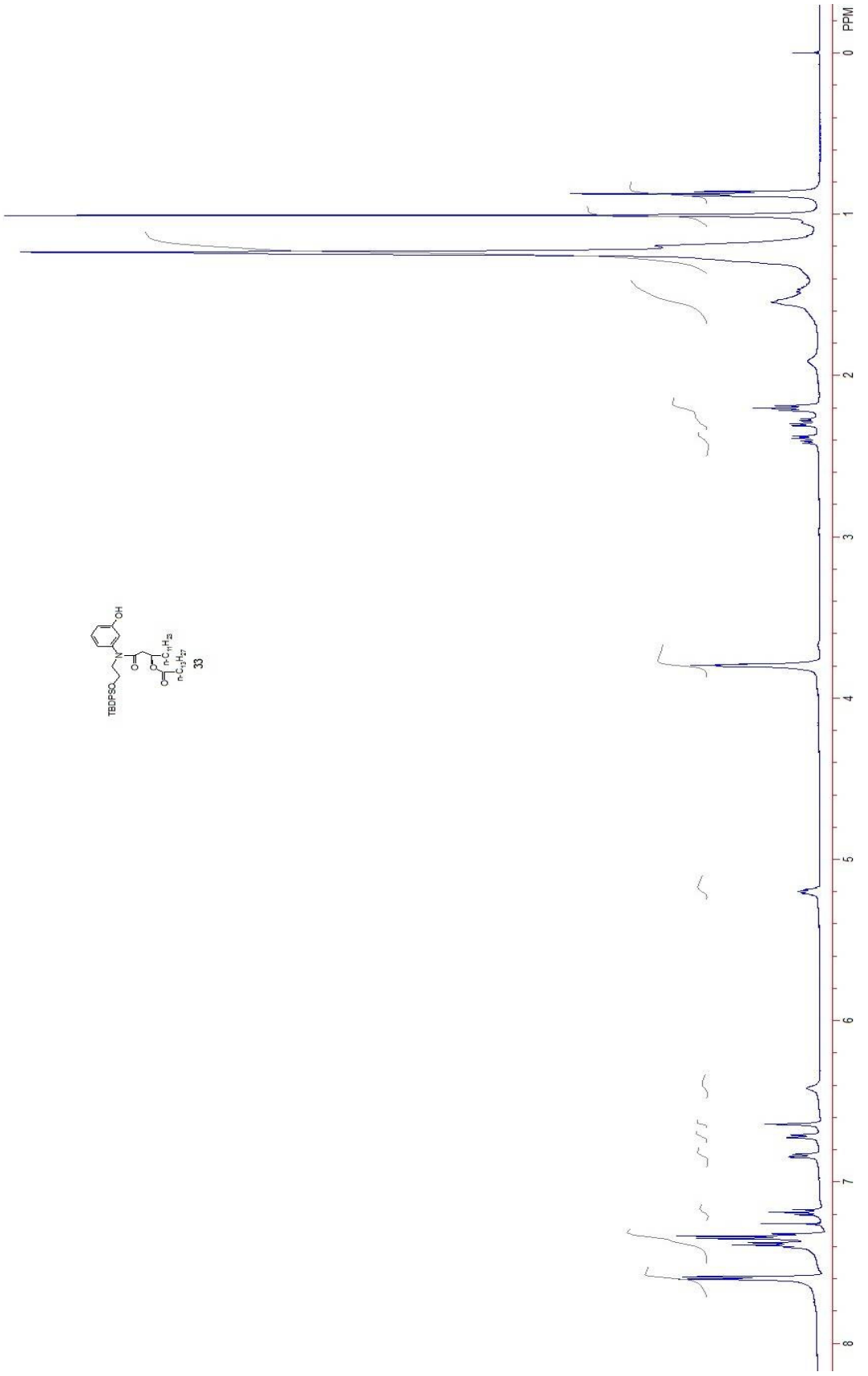
TBDPSO
OH
n-C11H23
n-C13H27
33
PPM
0
1
2
3
4
5
6
7
8

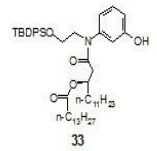

33

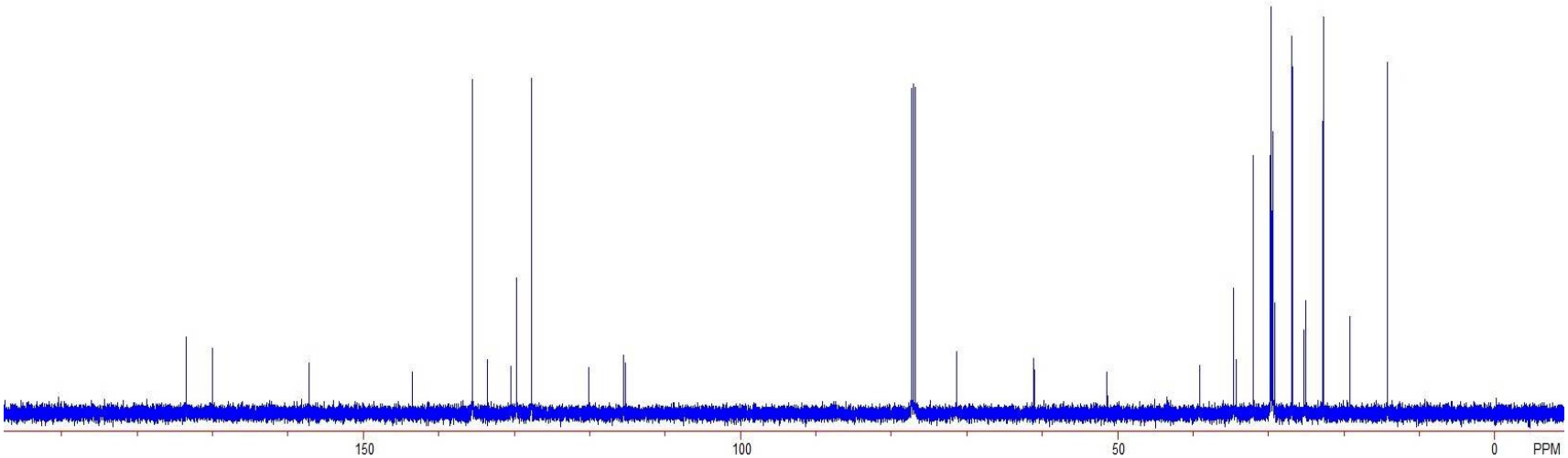

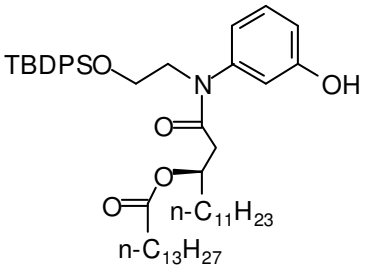

33

HRESI-MS (*m*/*z*) Calcd for $C_{52}H_{81}NO_5Si$ $[M+H]^+$: 828.5963, found: 828.5926.

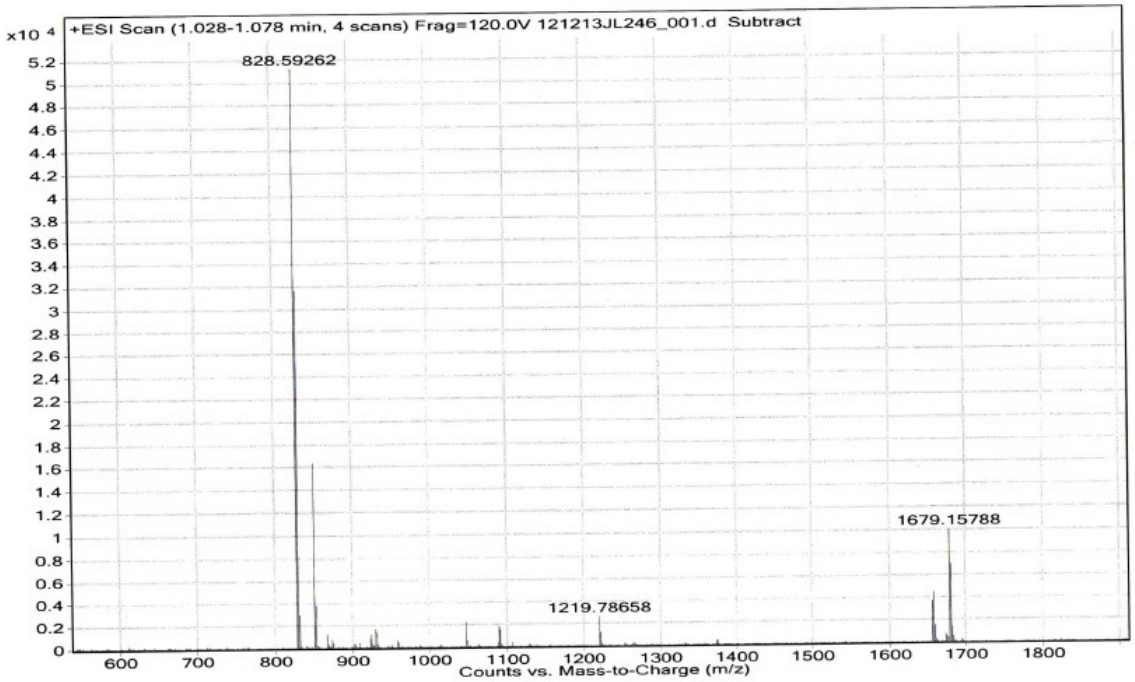

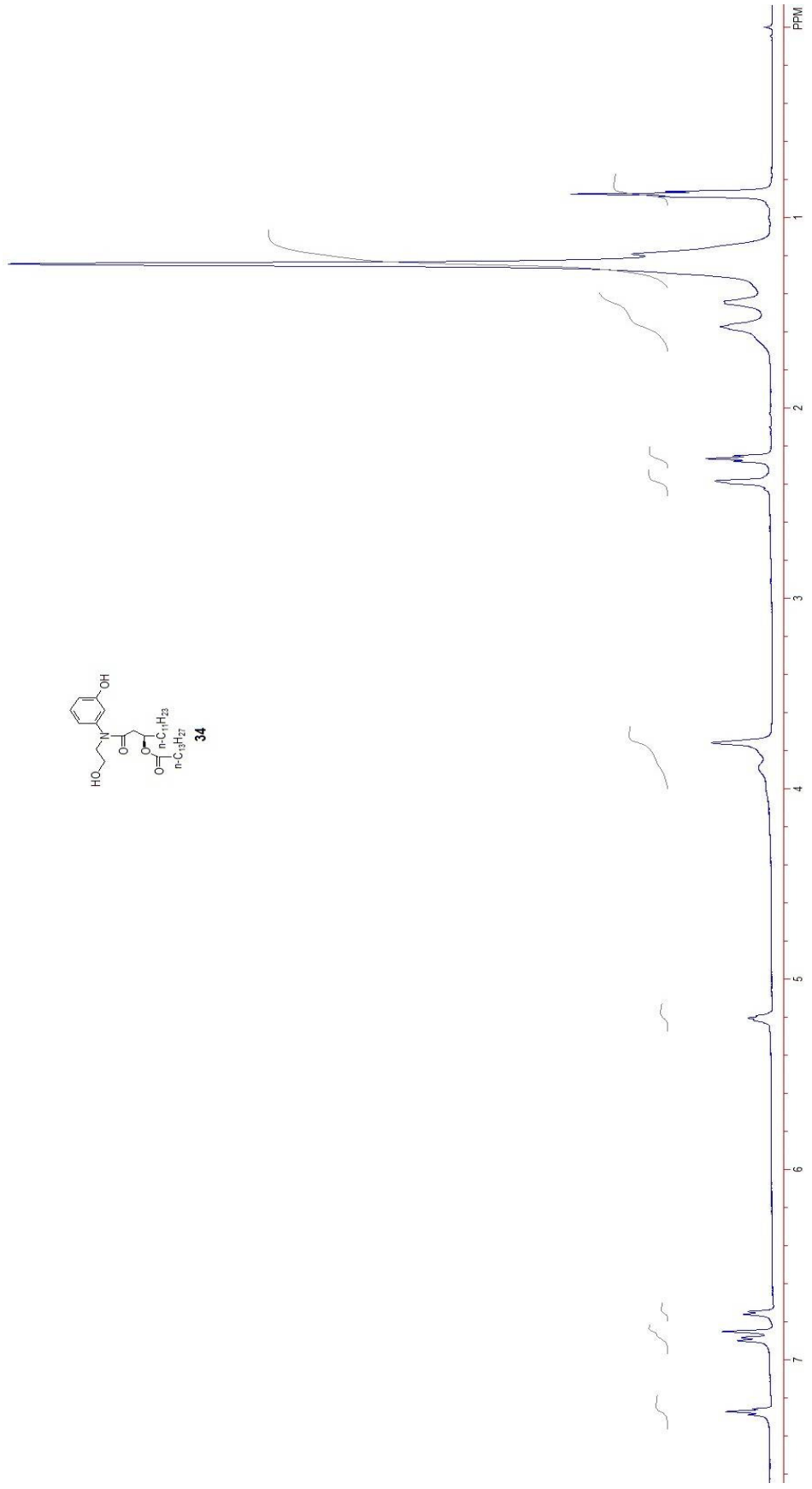
OH
N
HO
O
O
O
n-C11H23
n-C13H27
34
PPM
1
2
3
4
5
6
7

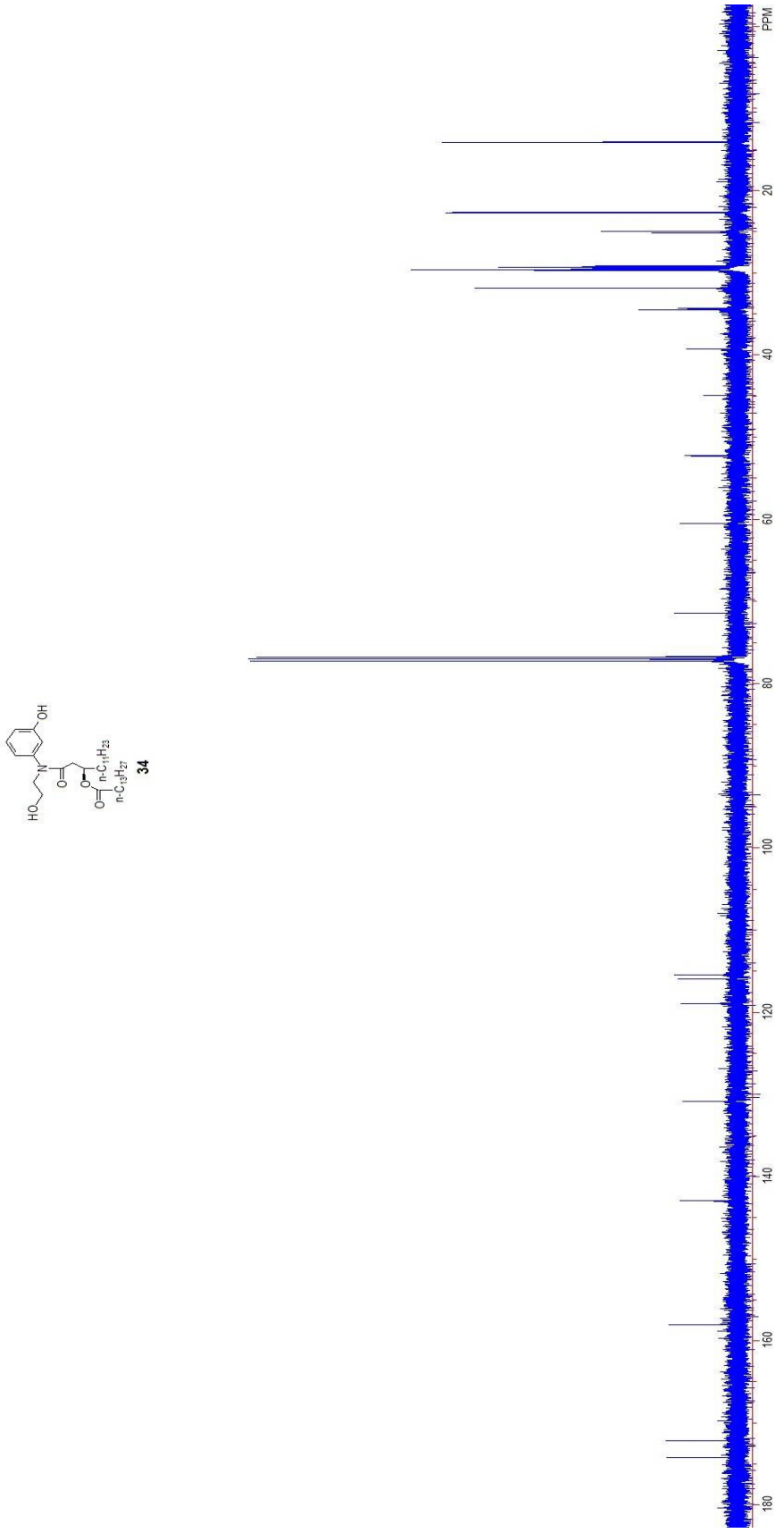
OH
N
O
O
O
n-C11H23
n-C13H27
HO
34
PPM
20
40
60
80
100
120
140
160
180

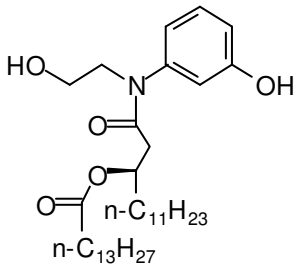

34

HRESI-MS (*m*/*z*) Calcd for $C_{36}H_{63}NO_5$ $[M+H]^+$: 590.4785, found: 590.4752.

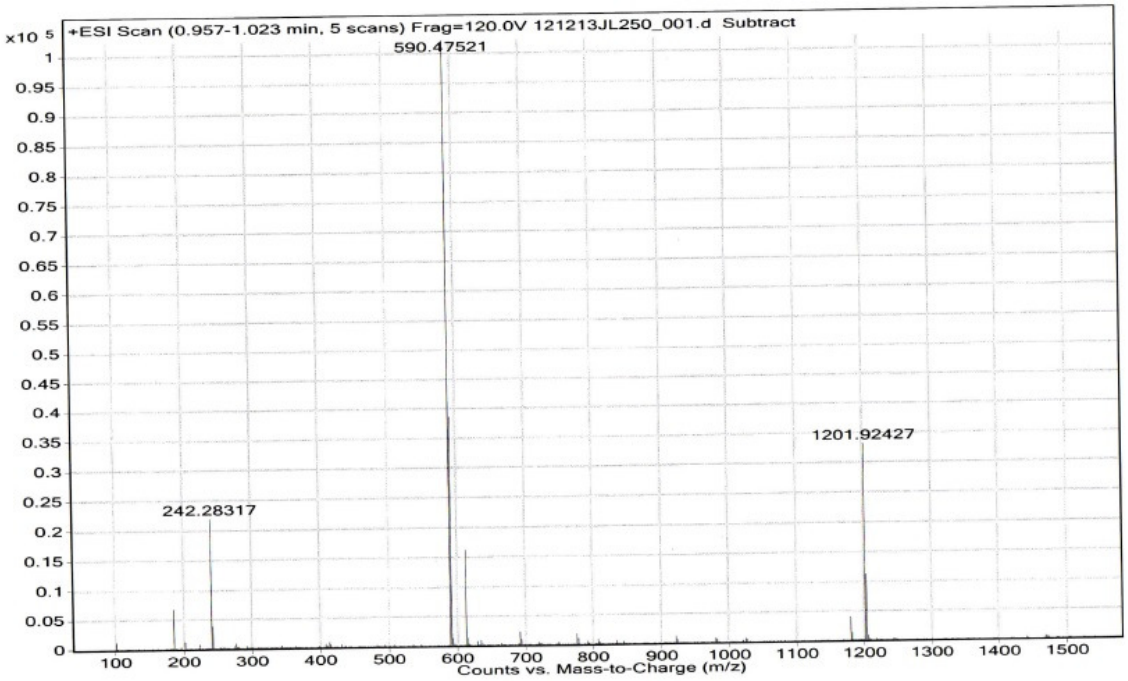

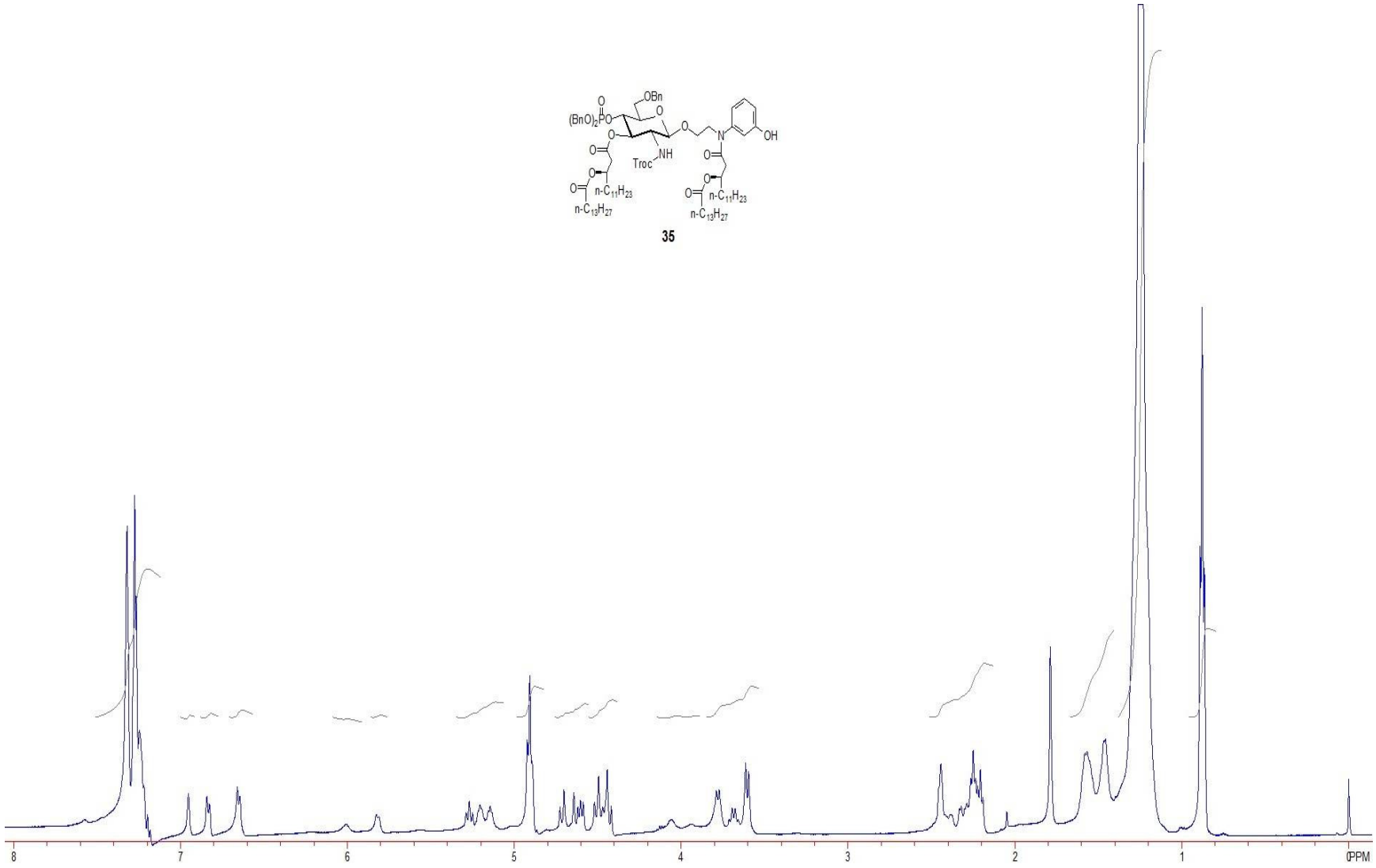
OBn
(BnO)2PO
O
O
O
N
OH
Troc
NH
n-C11H23
n-C13H27
n-C11H23
n-C13H27
35
8
7
6
5
4
3
2
1
0
PPM

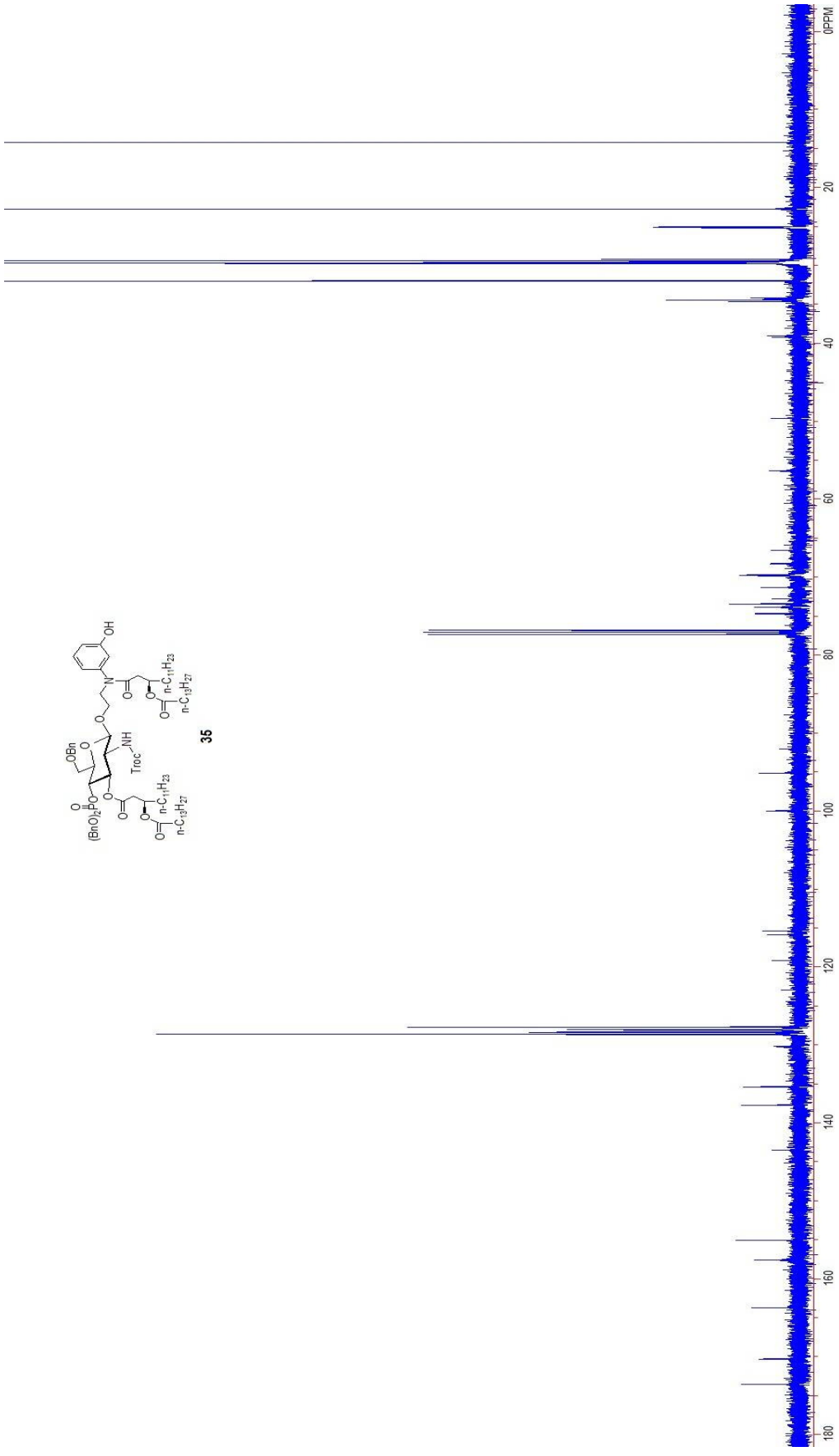
OH
N
O
n-C11H23
n-C13H27
OBn
O
NH
Troc
(BnO)2P
35
0PPM
20
40
60
80
100
120
140
160
180

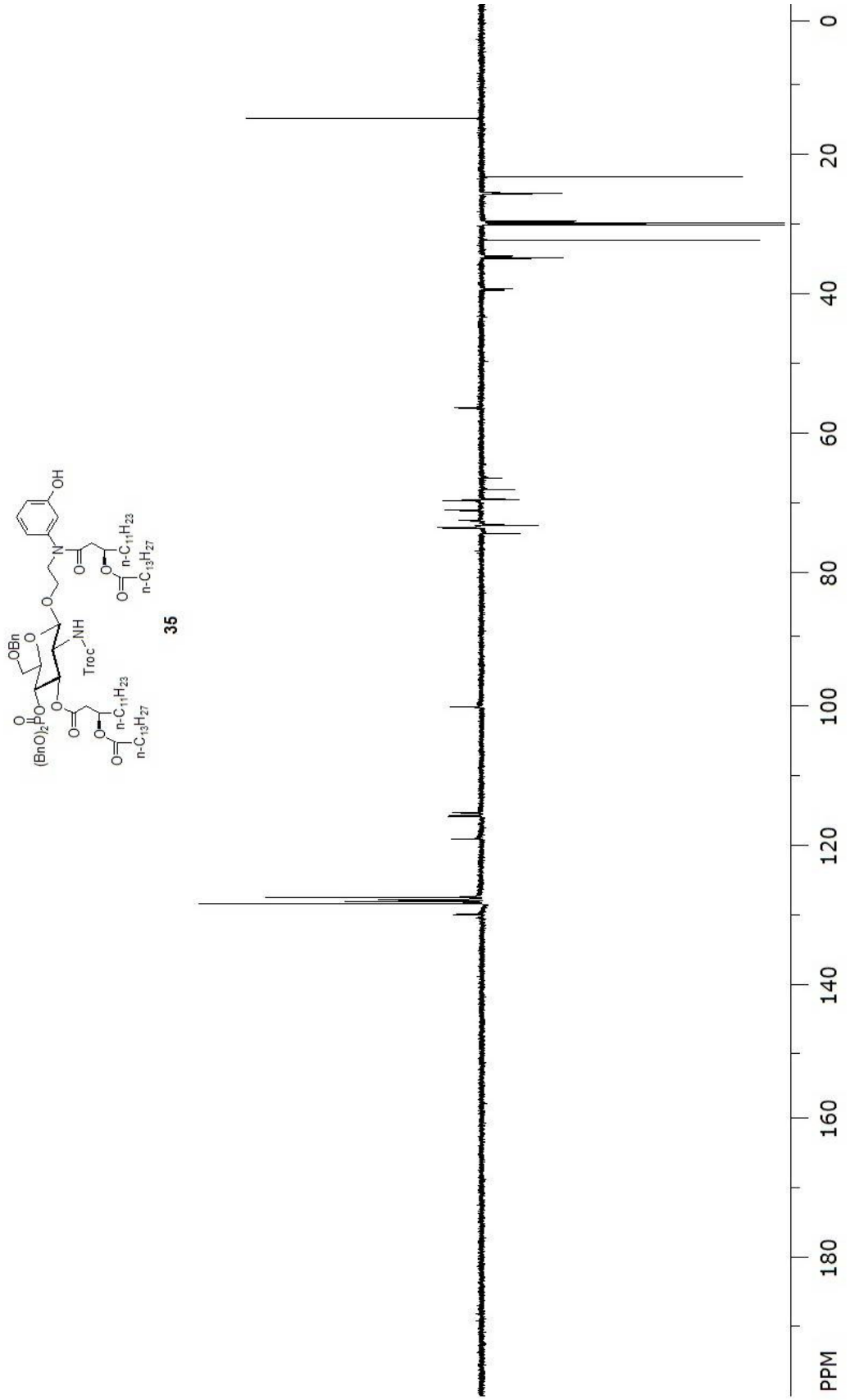
OH
N
O
n-C11H23
n-C13H27
OBn
NH
Troc
(BnO)2P
35
PPM
0
20
40
60
80
100
120
140
160
180

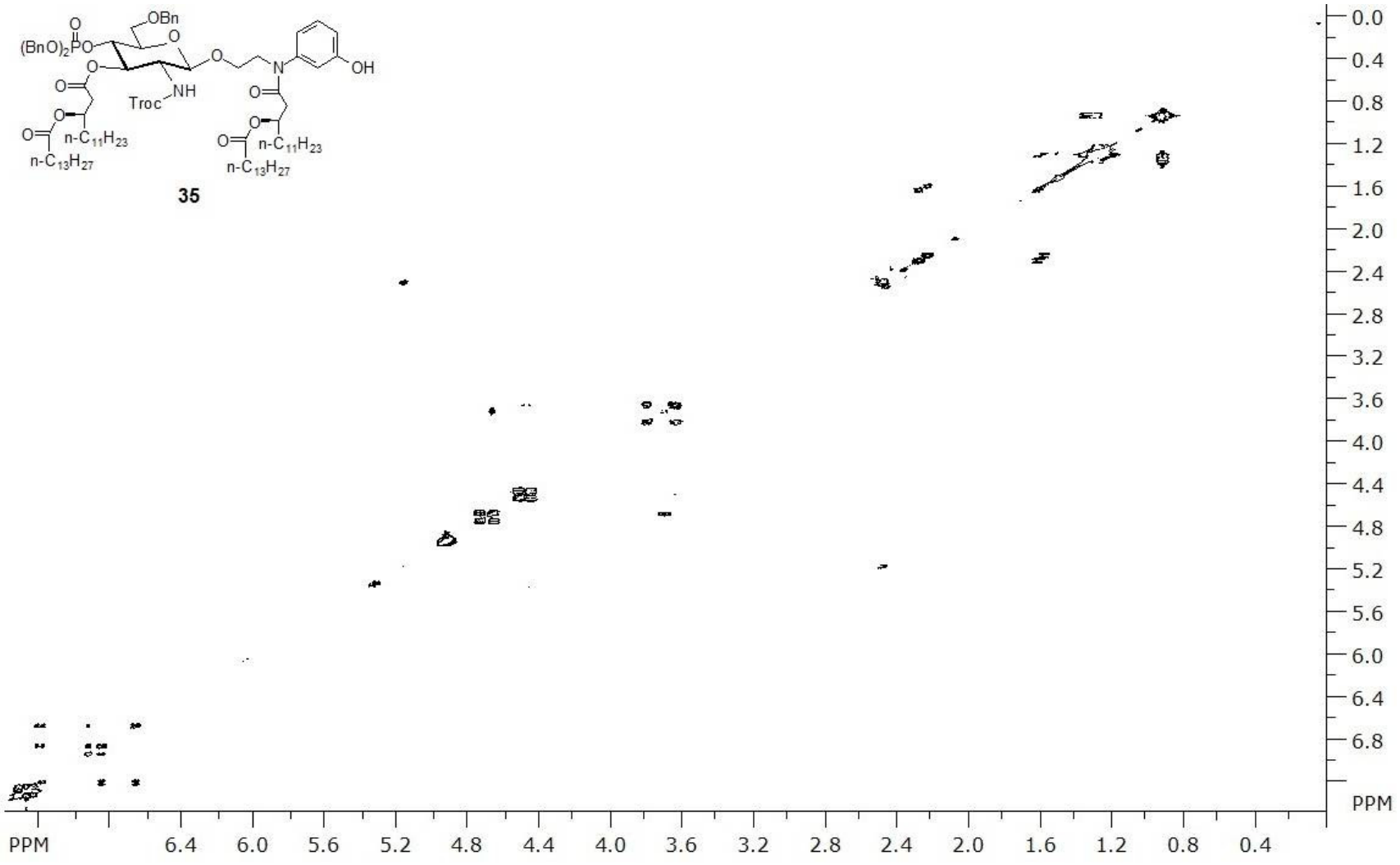
OBn
(BnO)2PO
O
Troc
NH
OH
n-C11H23
n-C13H27
35
0.0
0.4
0.8
1.2
1.6
2.0
2.4
2.8
3.2
3.6
4.0
4.4
4.8
5.2
5.6
6.0
6.4
6.8
PPM
6.4
6.0
5.6
5.2
4.8
4.4
4.0
3.6
3.2
2.8
2.4
2.0
1.6
1.2
0.8
0.4

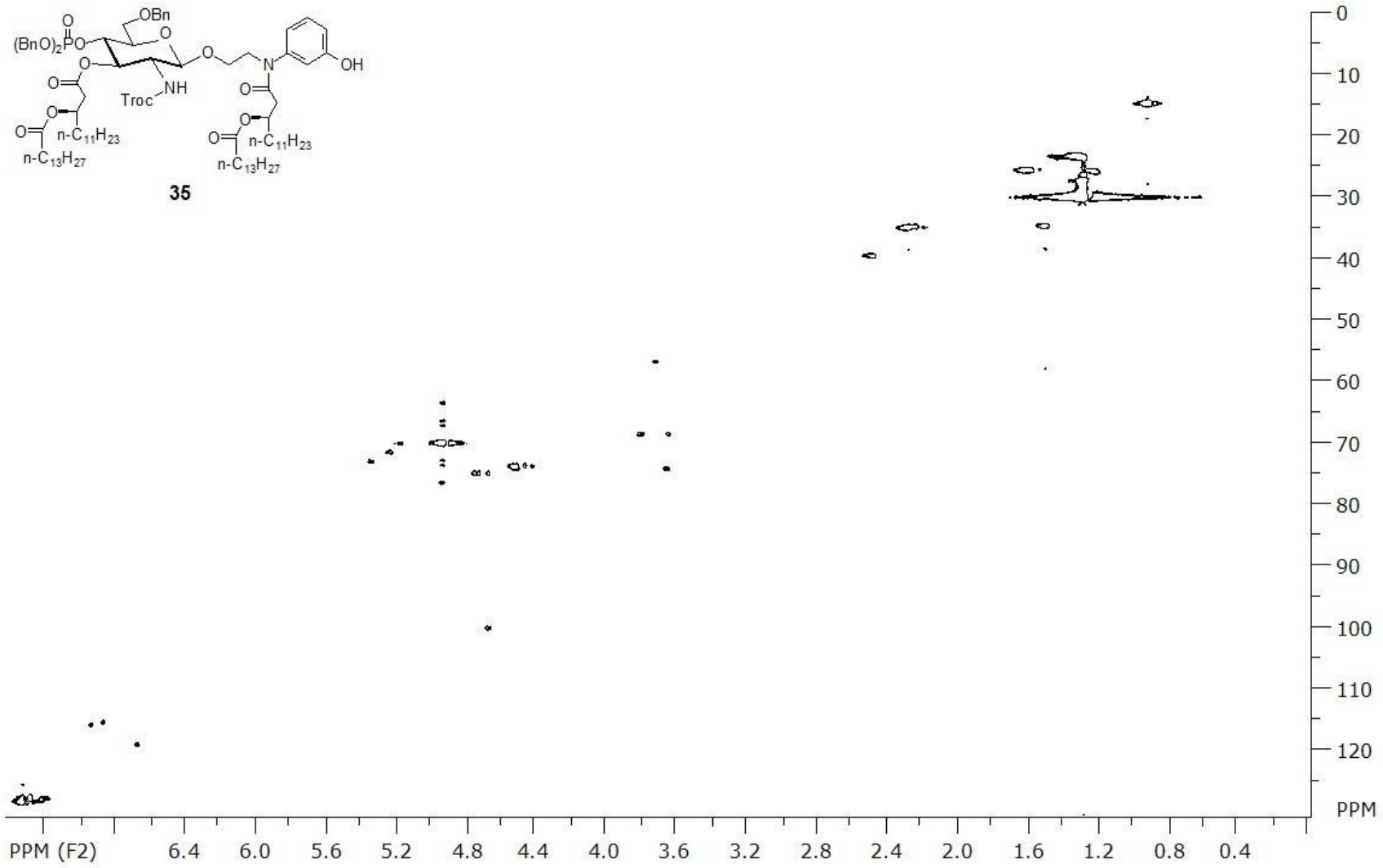
OBn
(BnO)2PO
O
O
NH
Troc
N
OH
n-C11H23
n-C13H27
n-C11H23
n-C13H27
35
0
10
20
30
40
50
60
70
80
90
100
110
120
PPM
PPM (F2)
6.4
6.0
5.6
5.2
4.8
4.4
4.0
3.6
3.2
2.8
2.4
2.0
1.6
1.2
0.8
0.4

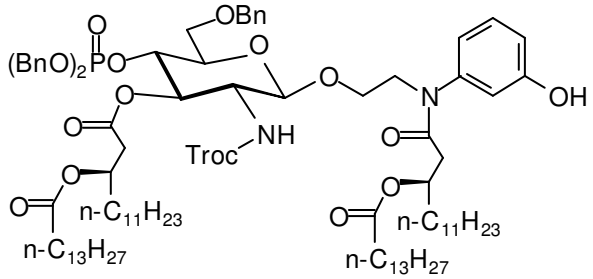

35

MALDI-MS (*m*/*z*) Calcd for $C_{94}H_{146}Cl_3N_2O_{17}P$ $[M + Na]^+$: 1733.9325, found: 1733.9720.

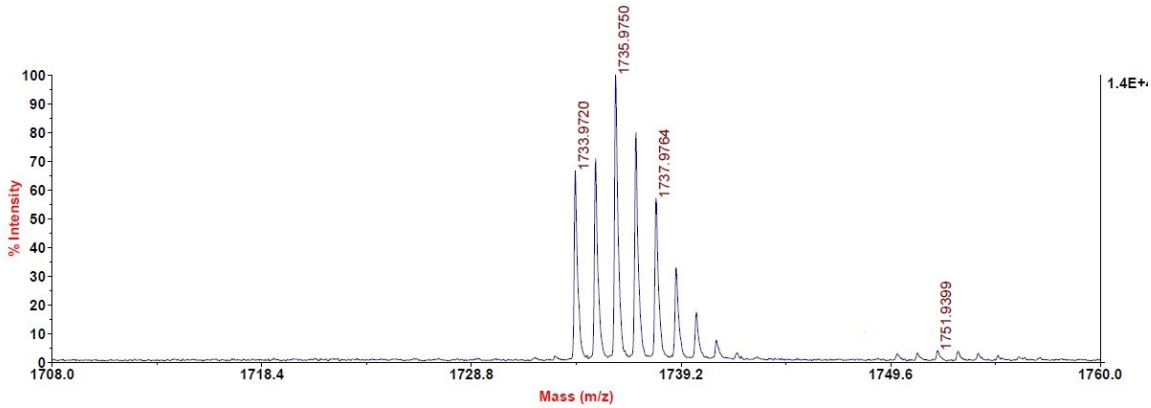

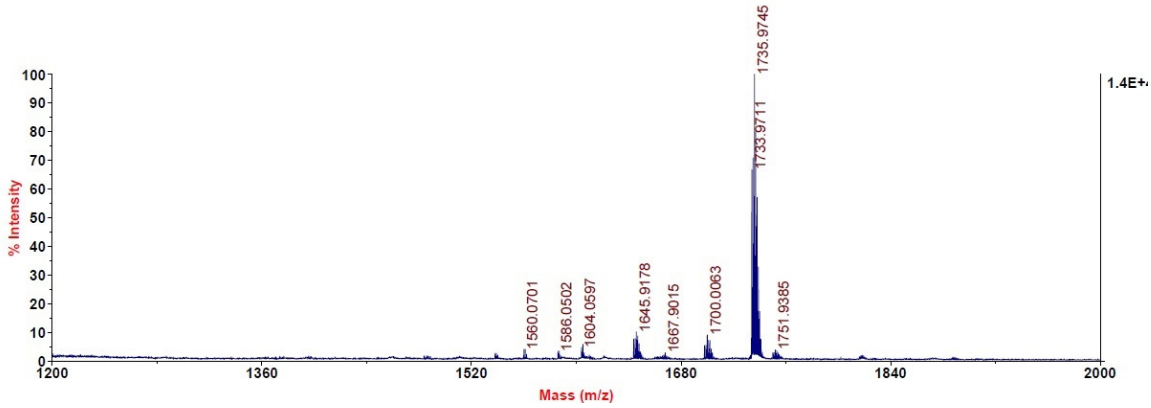

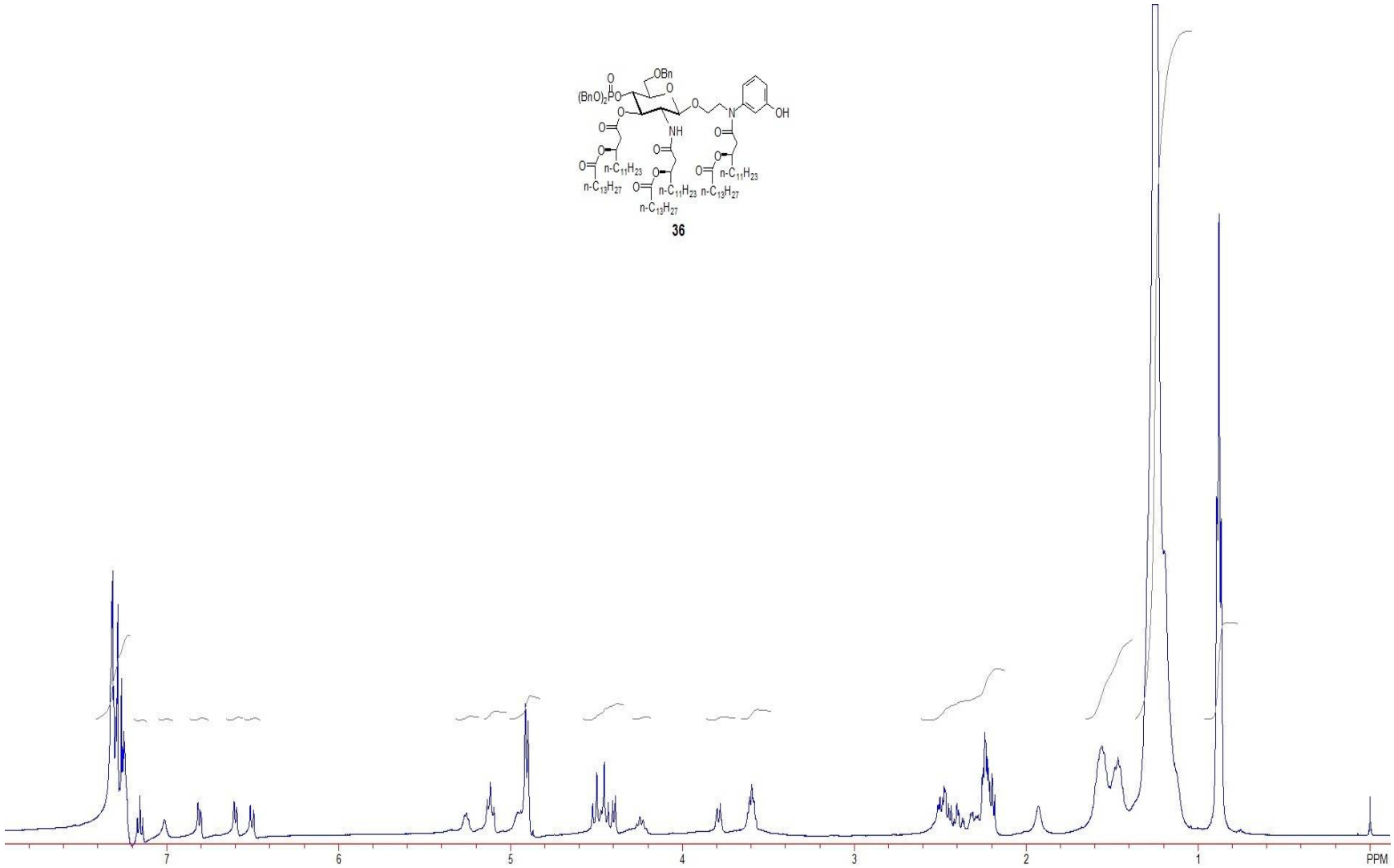

36

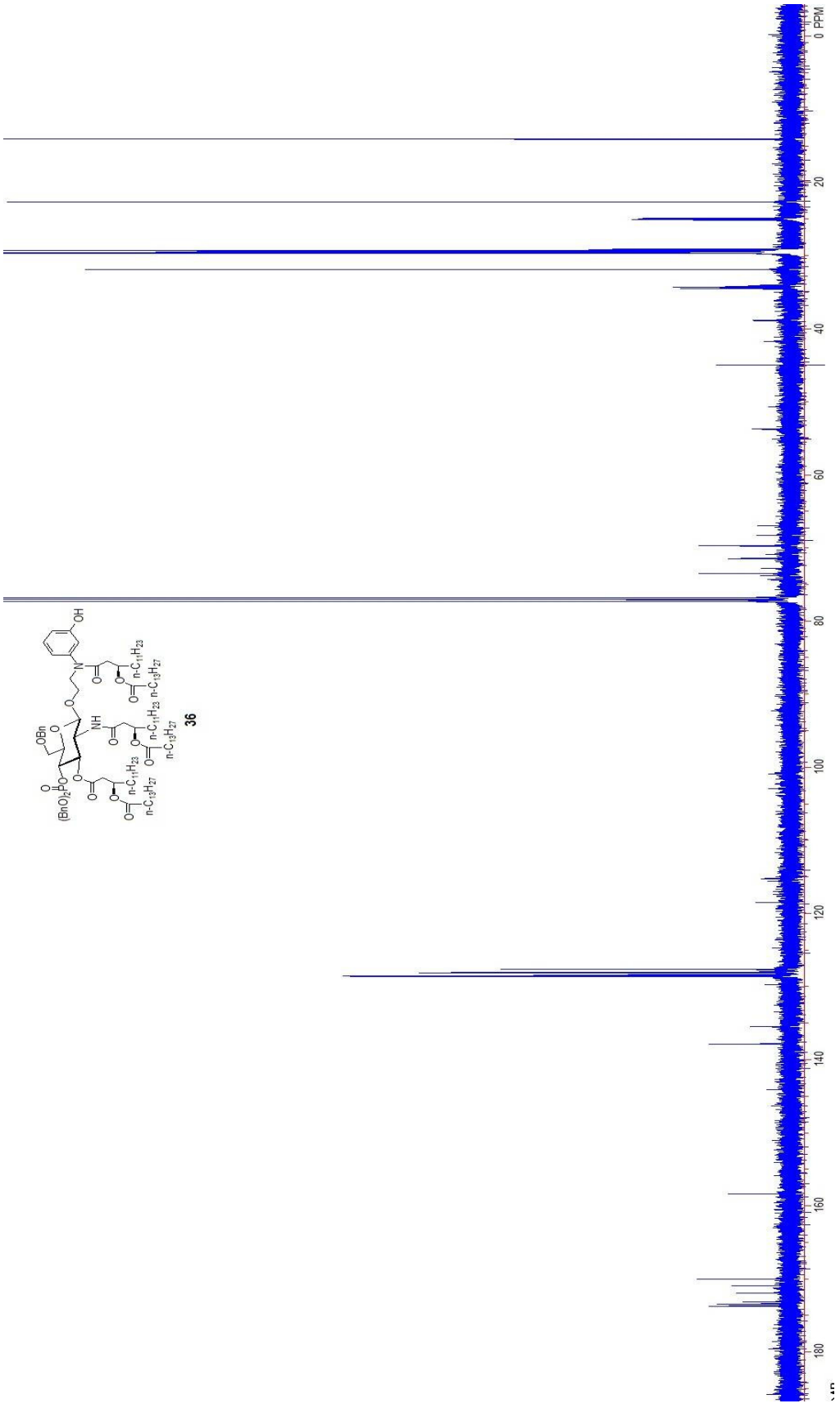
OH
NH
OBn
(BnO)2PO
n-C11H23
n-C13H27
36
0 PPM
20
40
60
80
100
120
140
160
180

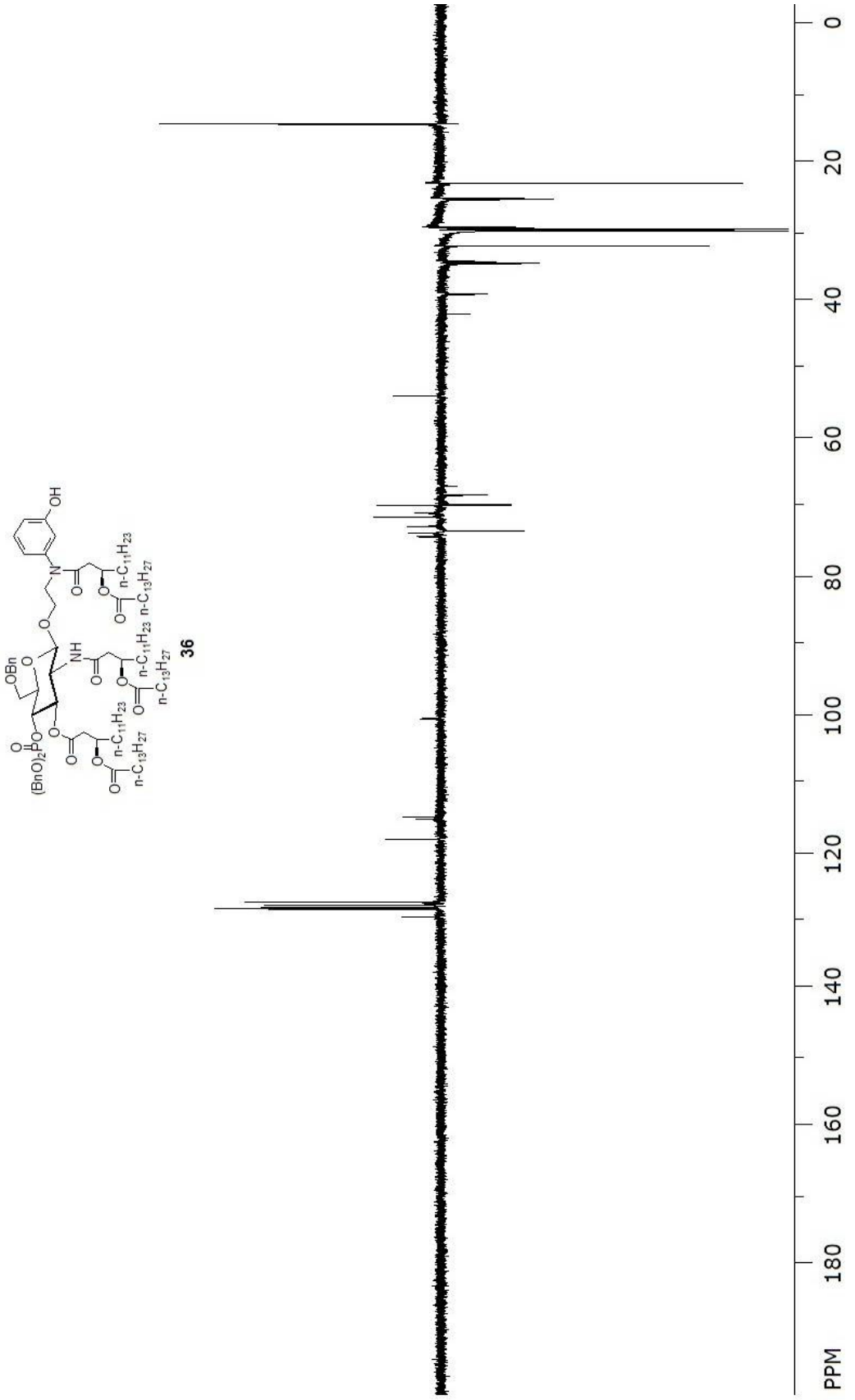
OH
OBn
NH
$(BnO)_2P$
$n\text{-}C_{11}H_{23}$
$n\text{-}C_{13}H_{27}$
36
PPM
0
20
40
60
80
100
120
140
160
180

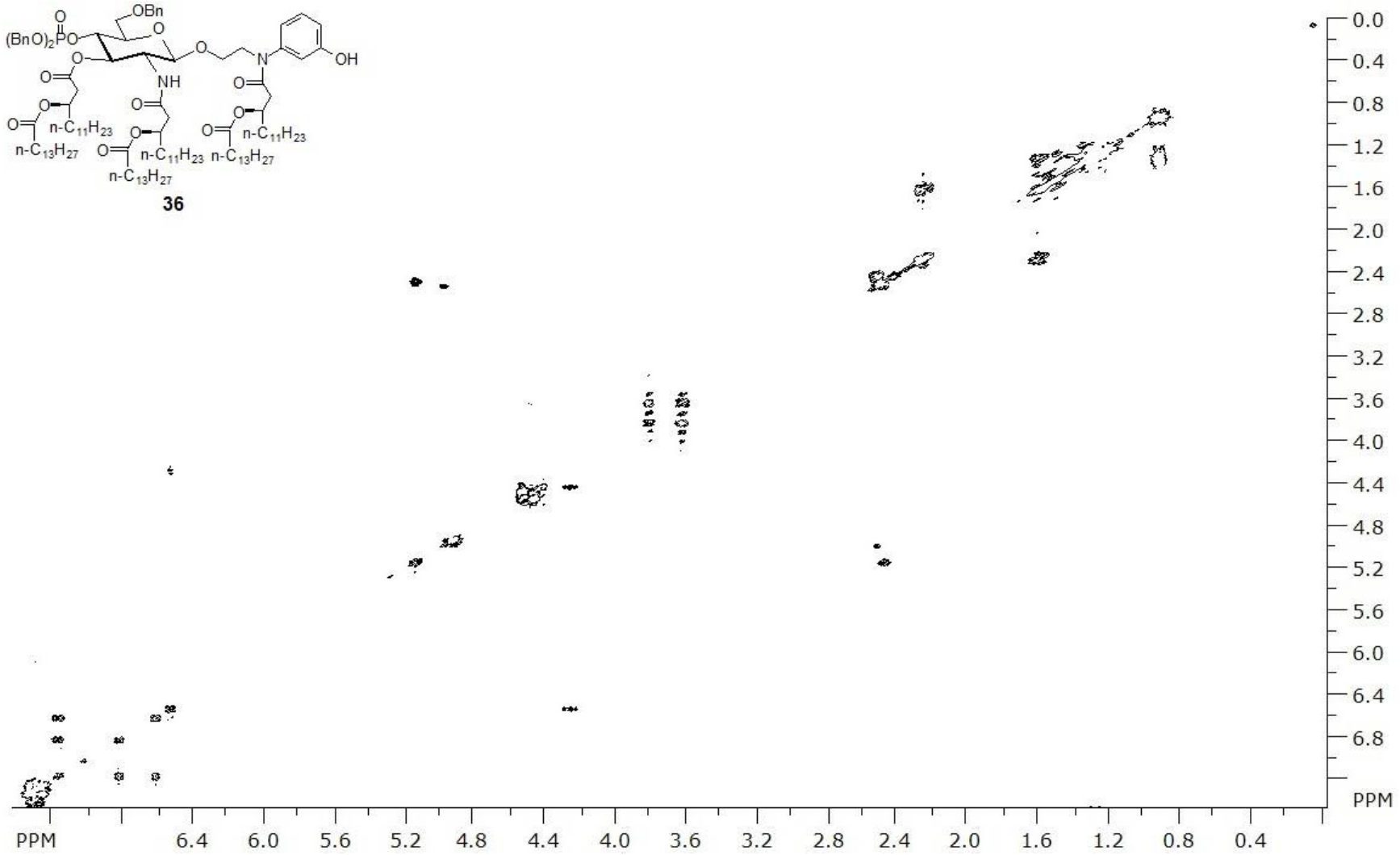
OBn
(BnO)2P
O
NH
N
OH
n-C11H23
n-C13H27
36
0.0
0.4
0.8
1.2
1.6
2.0
2.4
2.8
3.2
3.6
4.0
4.4
4.8
5.2
5.6
6.0
6.4
6.8
PPM
PPM
6.4
6.0
5.6
5.2
4.8
4.4
4.0
3.6
3.2
2.8
2.4
2.0
1.6
1.2
0.8
0.4

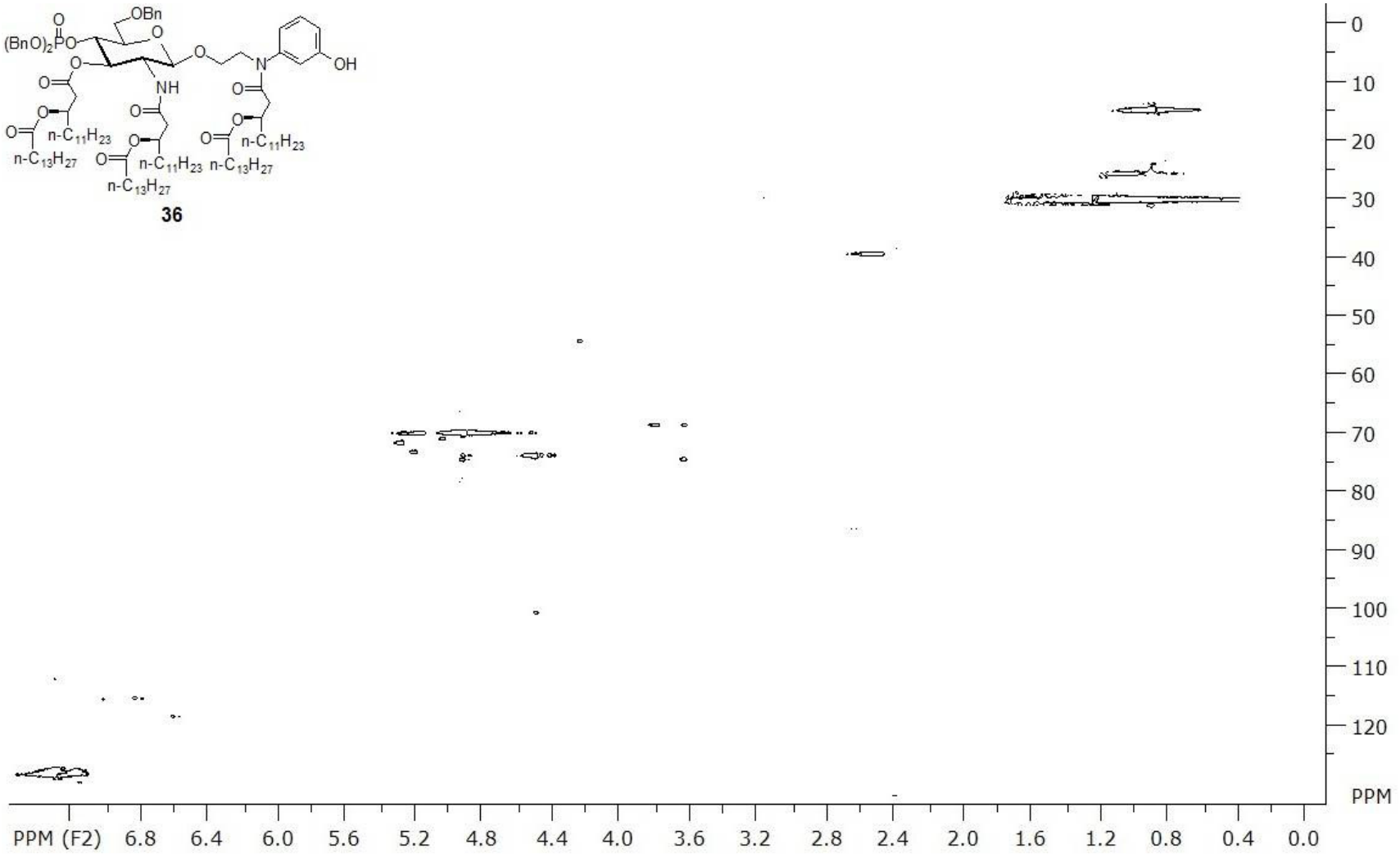
OBn
O
(BnO)2PO
O
O
NH
O
N
OH
n-C11H23
n-C13H27
n-C11H23
n-C13H27
n-C11H23
n-C13H27
n-C11H23
n-C13H27
36
0
10
20
30
40
50
60
70
80
90
100
110
120
PPM
PPM (F2) 6.8 6.4 6.0 5.6 5.2 4.8 4.4 4.0 3.6 3.2 2.8 2.4 2.0 1.6 1.2 0.8 0.4 0.0

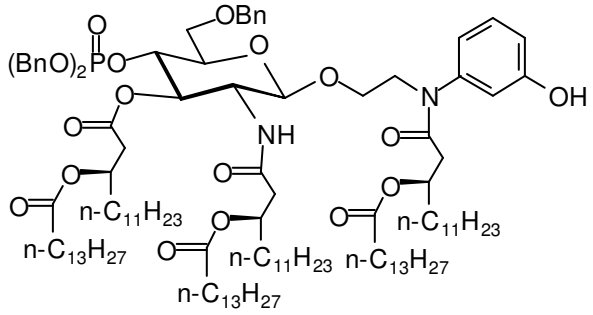

36

MALDI-MS (*m*/*z*) Calcd for $C_{119}H_{197}N_2O_{18}P$ $[M + Na]^+$: 1996.4199, found: 1996.4117.

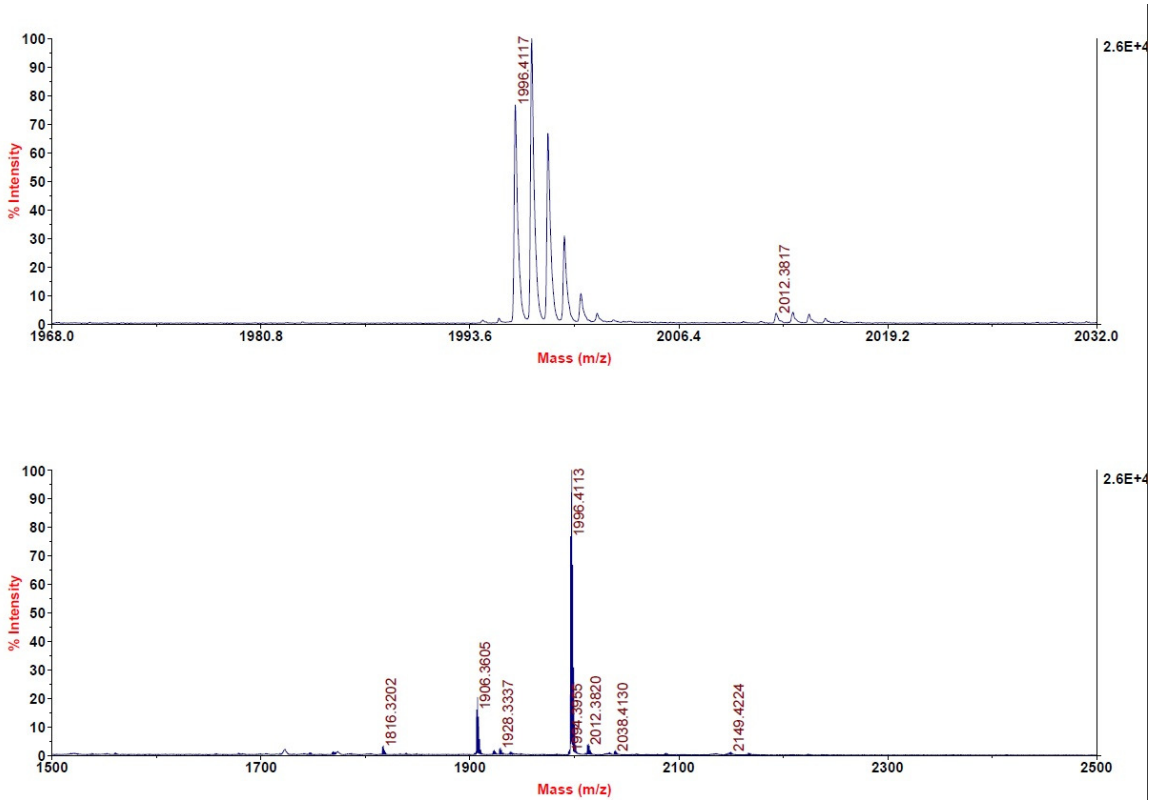

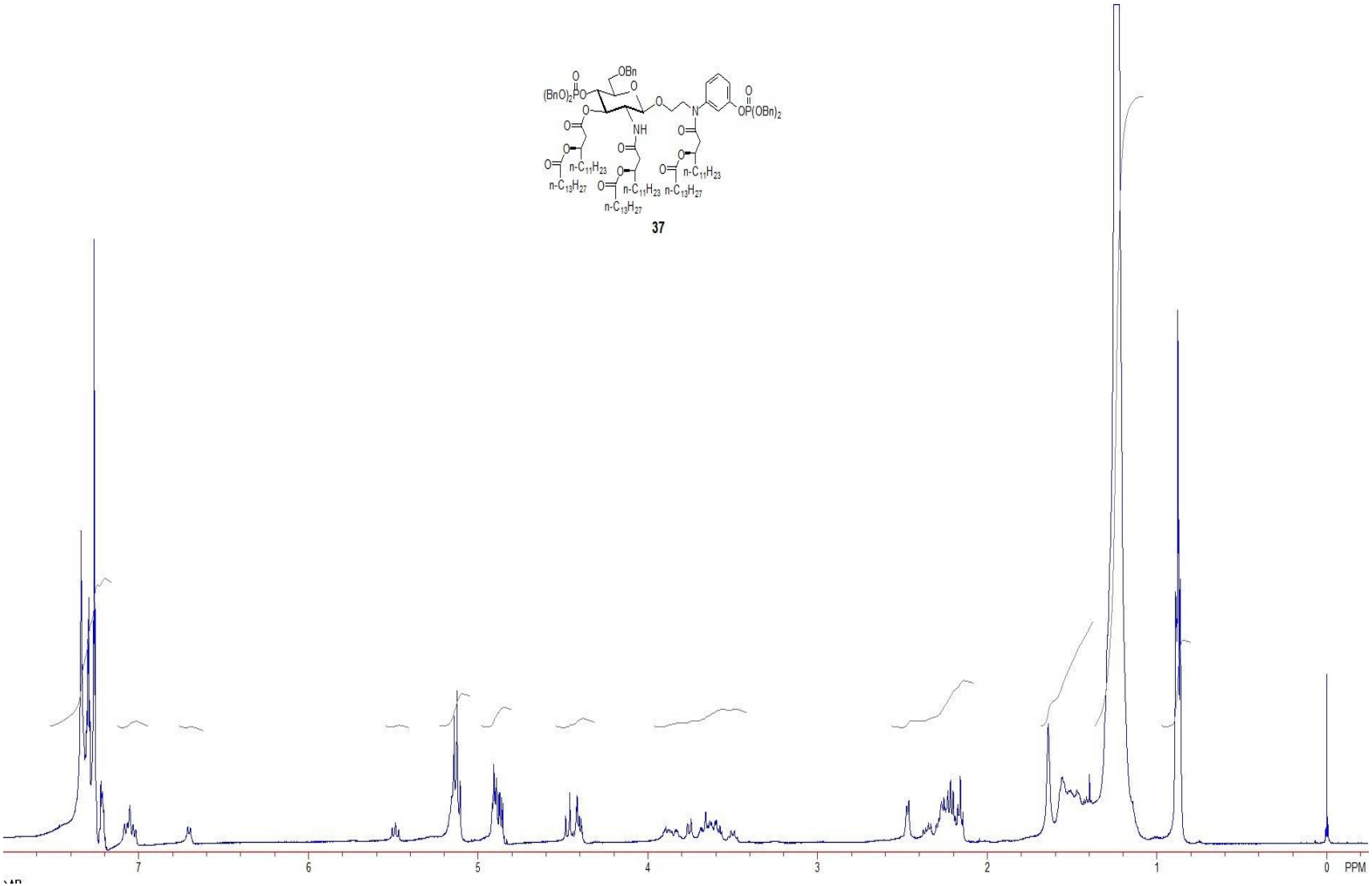

37

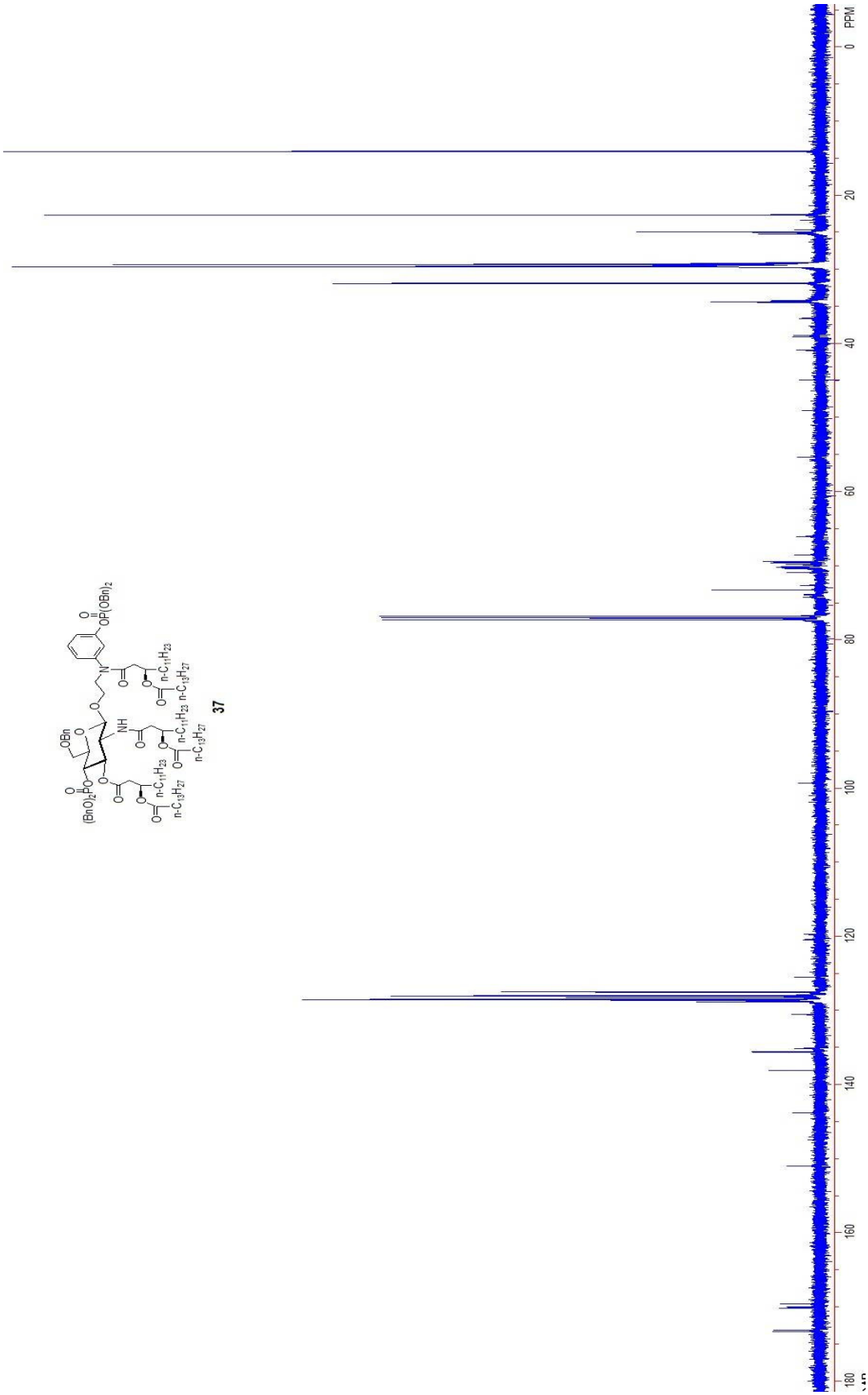
PPM
0
20
40
60
80
100
120
140
160
180
OBn
NH
OP(OBn)2
(BnO)2PO
n-C11H23
n-C13H27
37

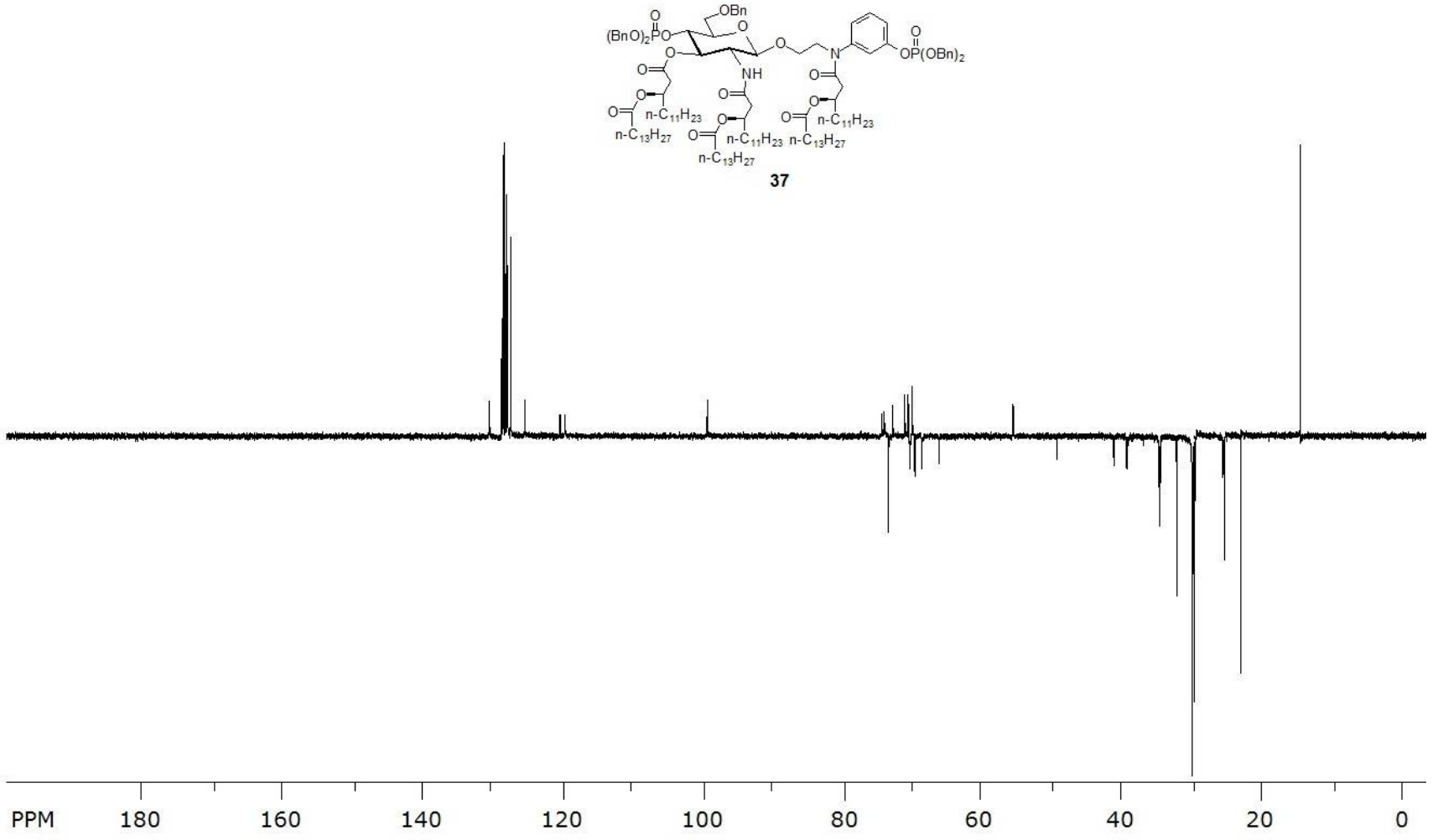
OBn
O
(BnO)2P
O
O
NH
N
OP(OBn)2
n-C11H23
n-C13H27
37
PPM
180
160
140
120
100
80
60
40
20
0

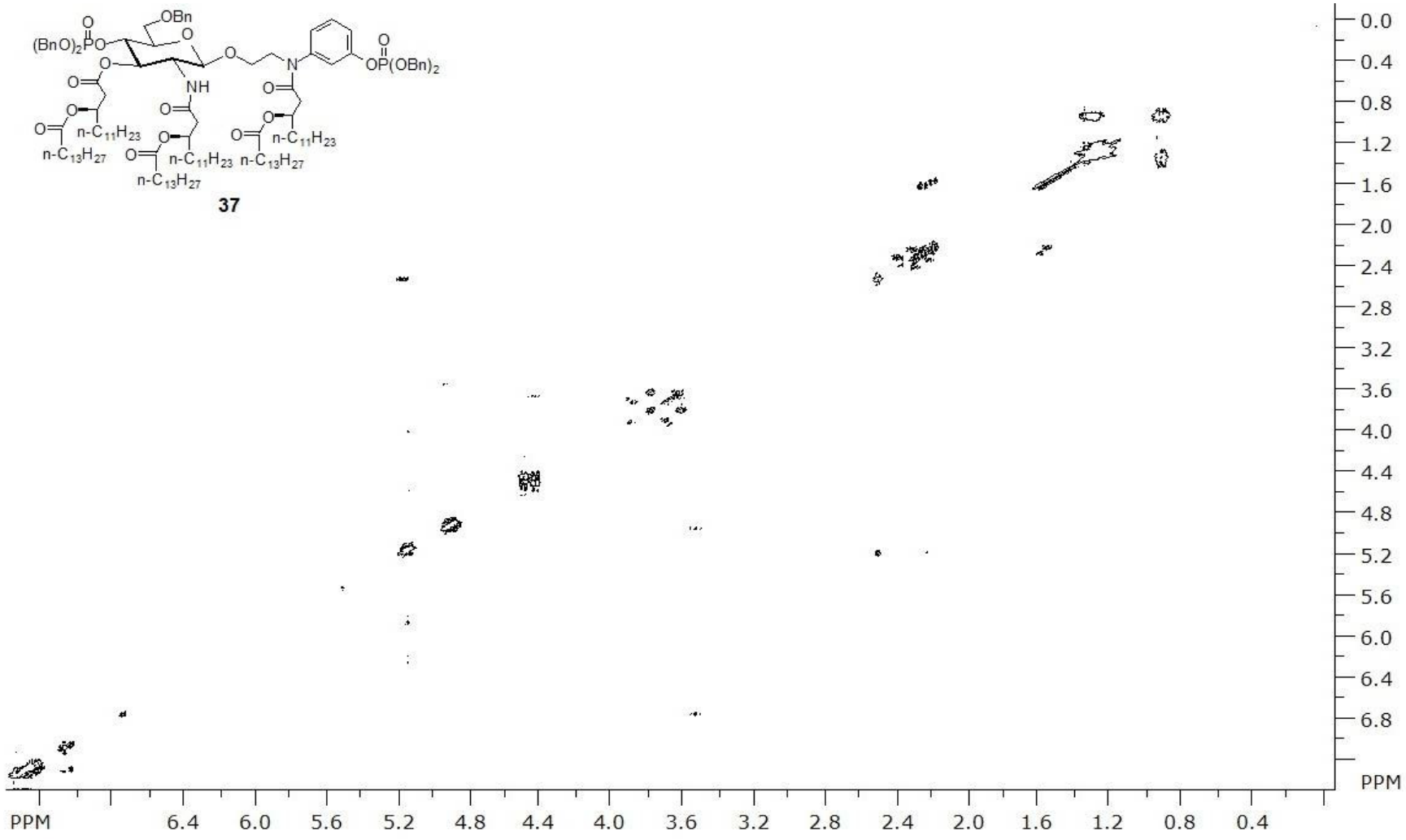
OBn
(BnO)2P
OP(OBn)2
NH
n-C11H23
n-C13H27
37
0.0
0.4
0.8
1.2
1.6
2.0
2.4
2.8
3.2
3.6
4.0
4.4
4.8
5.2
5.6
6.0
6.4
6.8
PPM
6.4
6.0
5.6
5.2
4.8
4.4
4.0
3.6
3.2
2.8
2.4
2.0
1.6
1.2
0.8
0.4

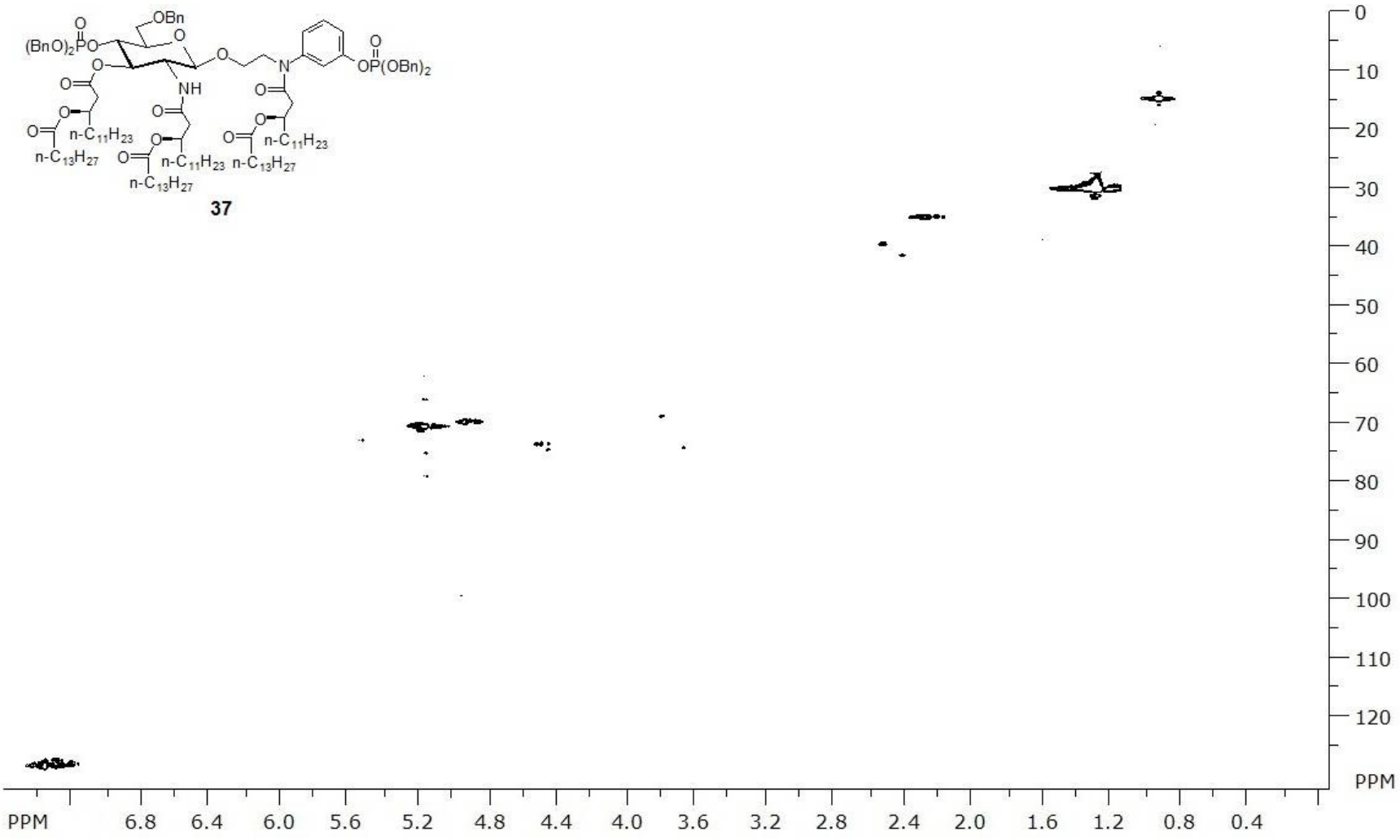
OBn
(BnO)2PO
OP(OBn)2
NH
n-C11H23
n-C13H27
37
0
10
20
30
40
50
60
70
80
90
100
110
120
PPM
PPM
6.8
6.4
6.0
5.6
5.2
4.8
4.4
4.0
3.6
3.2
2.8
2.4
2.0
1.6
1.2
0.8
0.4

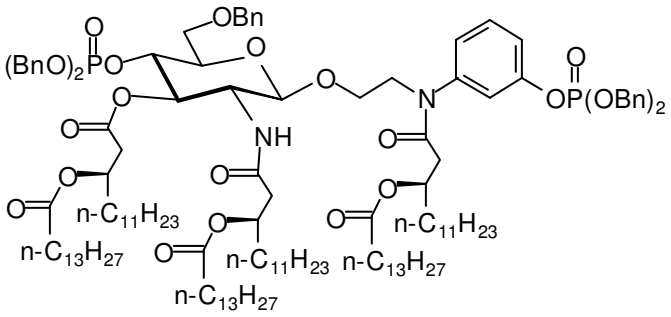

37

MALDI-MS (*m*/*z*) Calcd for $C_{133}H_{210}N_2O_{21}P_2$ $[M + Na]^+$: 2256.4801, found: 2256.5198..

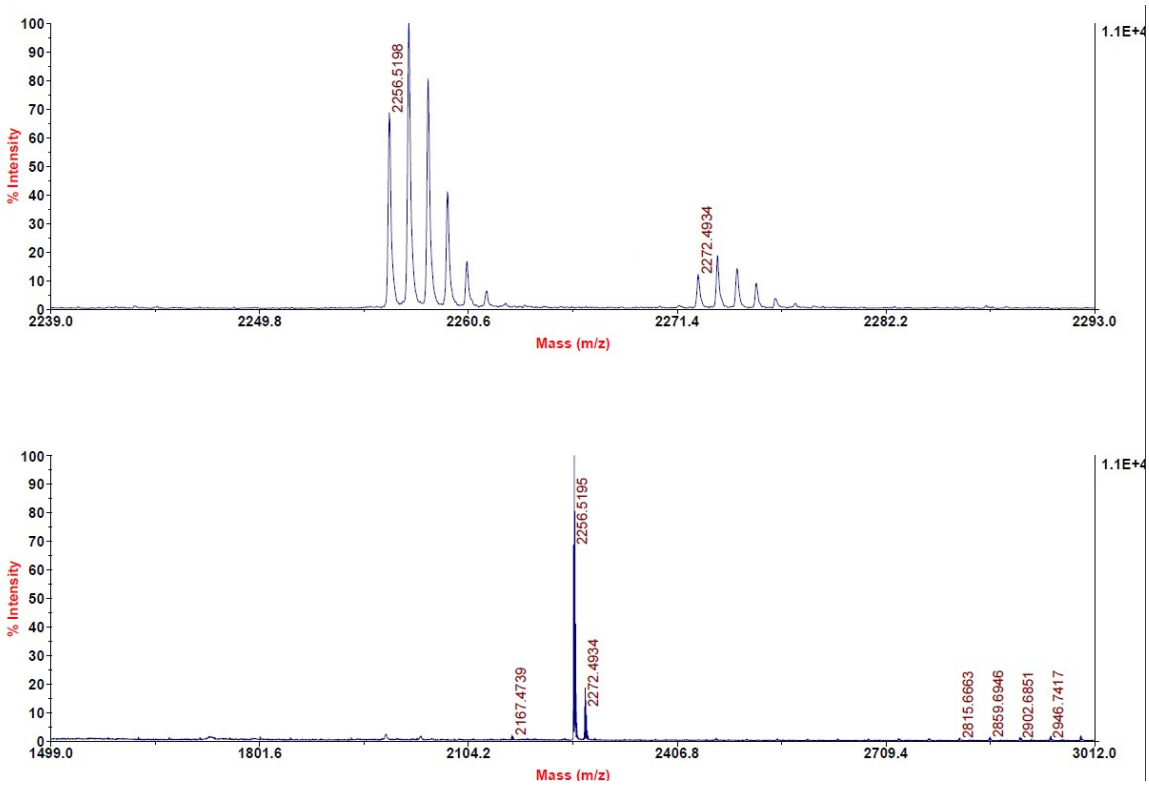

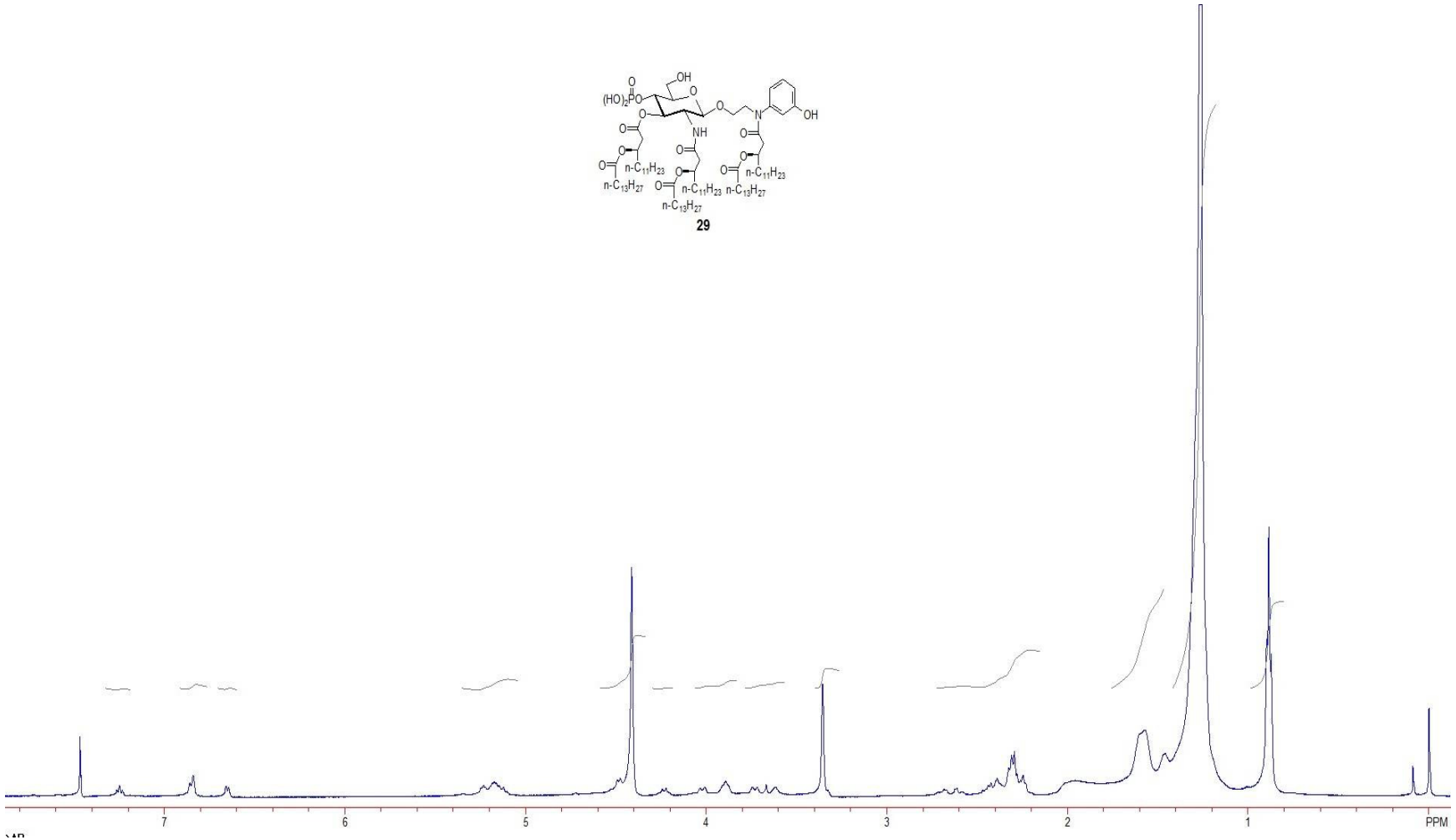
29
7
6
5
4
3
2
1
PPM

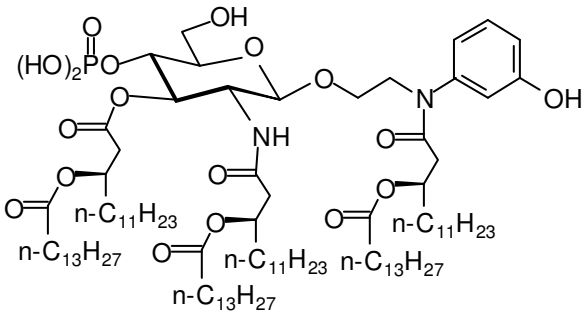

29

MALDI-MS (*m/z*) Calcd for $C_{98}H_{179}N_2O_{18}P$ $[M + Na]^+$: 1726.2790, found: 1726.2794.

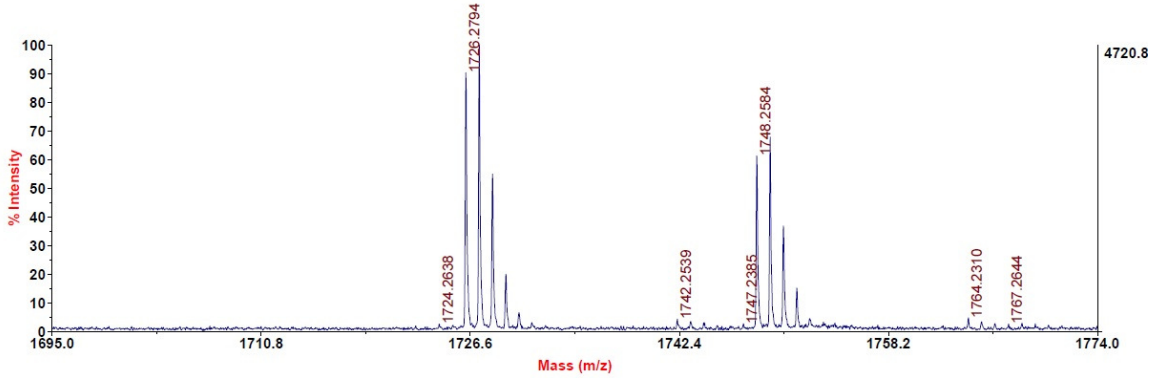

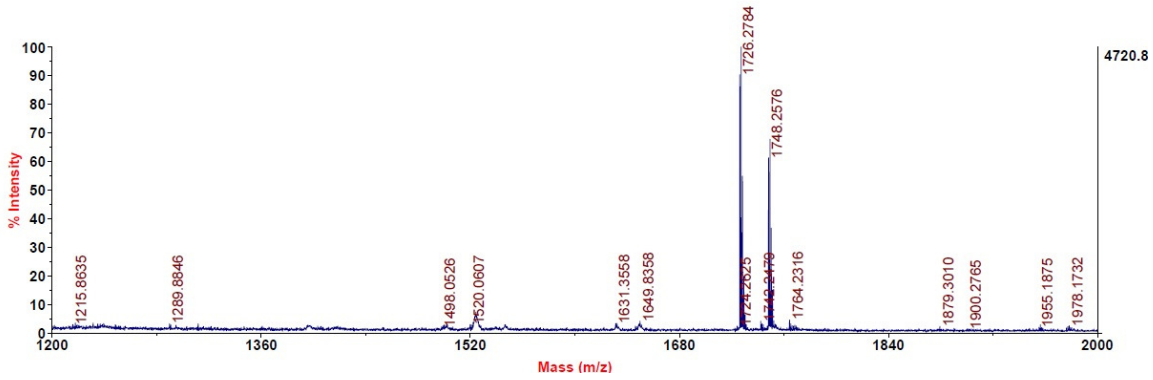

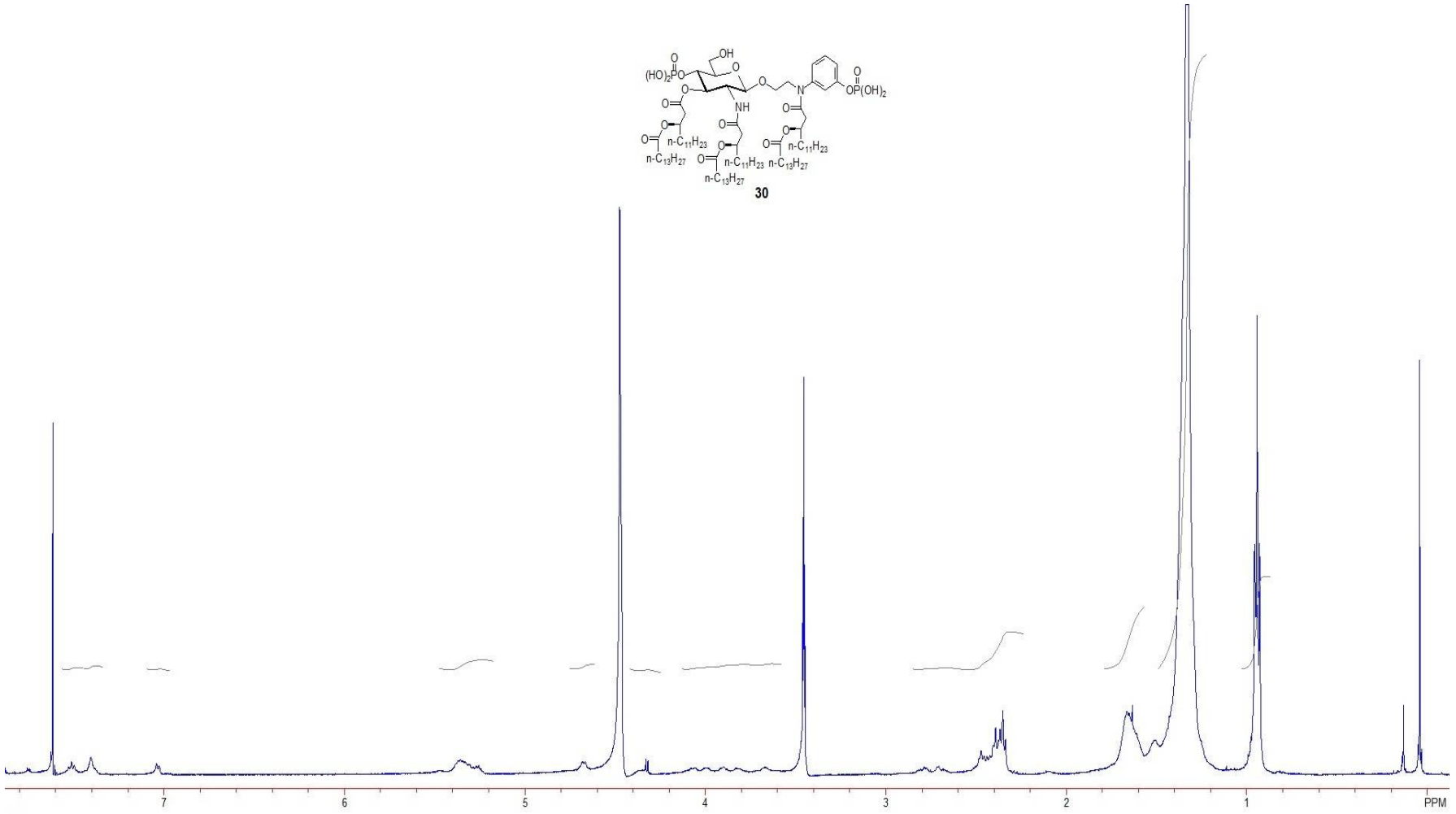
30
7
6
5
4
3
2
1
PPM

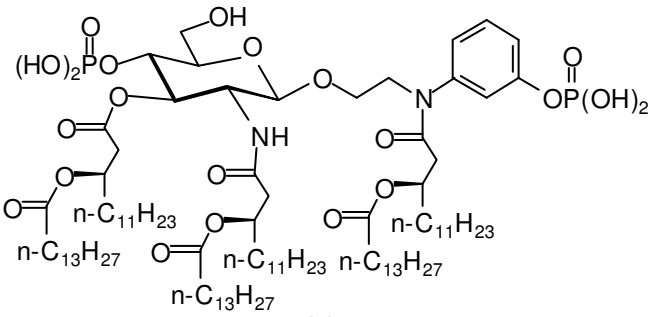

30

MALDI-MS (*m*/*z*) Calcd for $C_{98}H_{180}N_2O_{21}P_2$ $[M + Na]^+$: 1806.2458, found: 1806.2502.

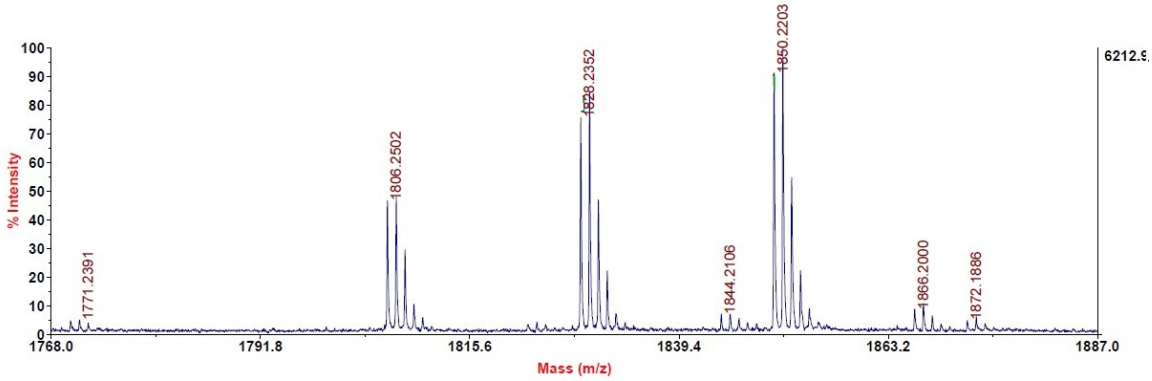

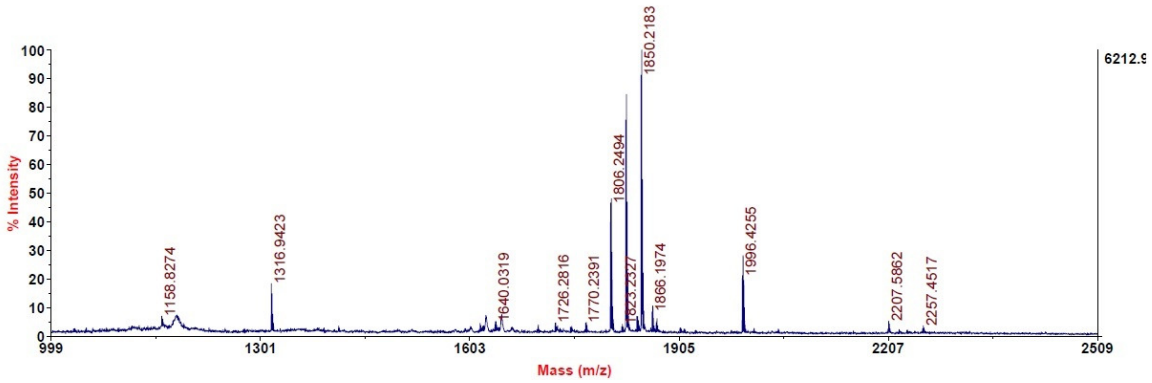

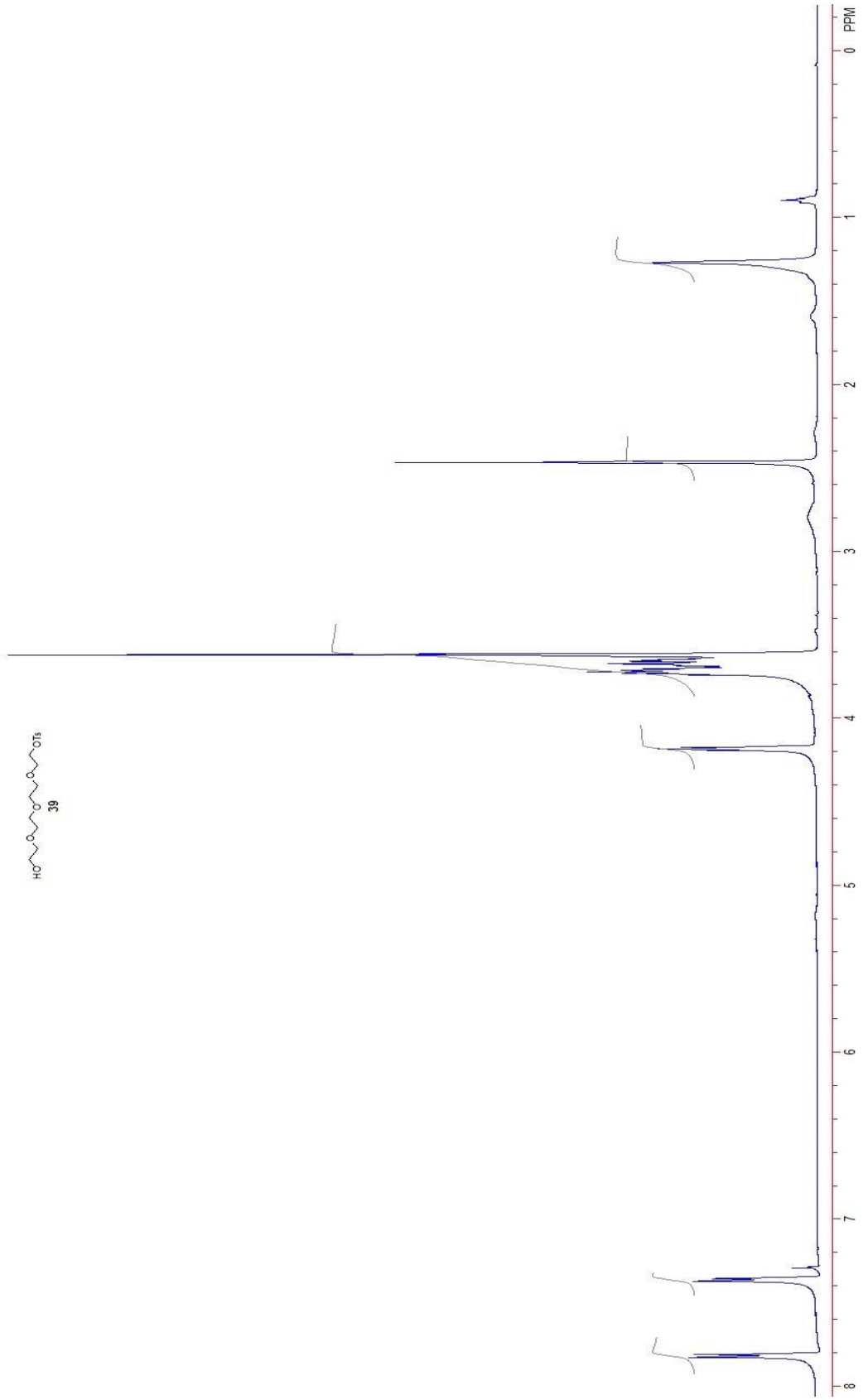
HO
O
O
O
OTs
39
8
7
6
5
4
3
2
1
0
PPM

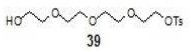

39

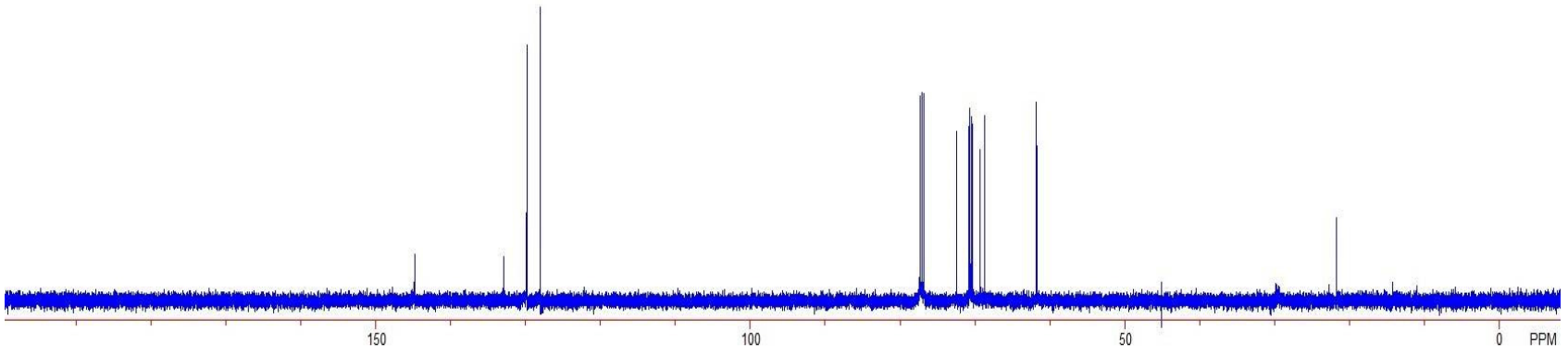

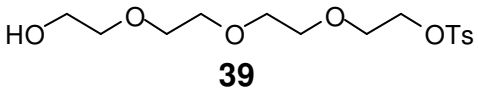

39

MALDI-MS (m/z) Calcd for $C_{15}H_{24}O_6S$ $[M + K]^+$: 371.0931, found: 371.0740.

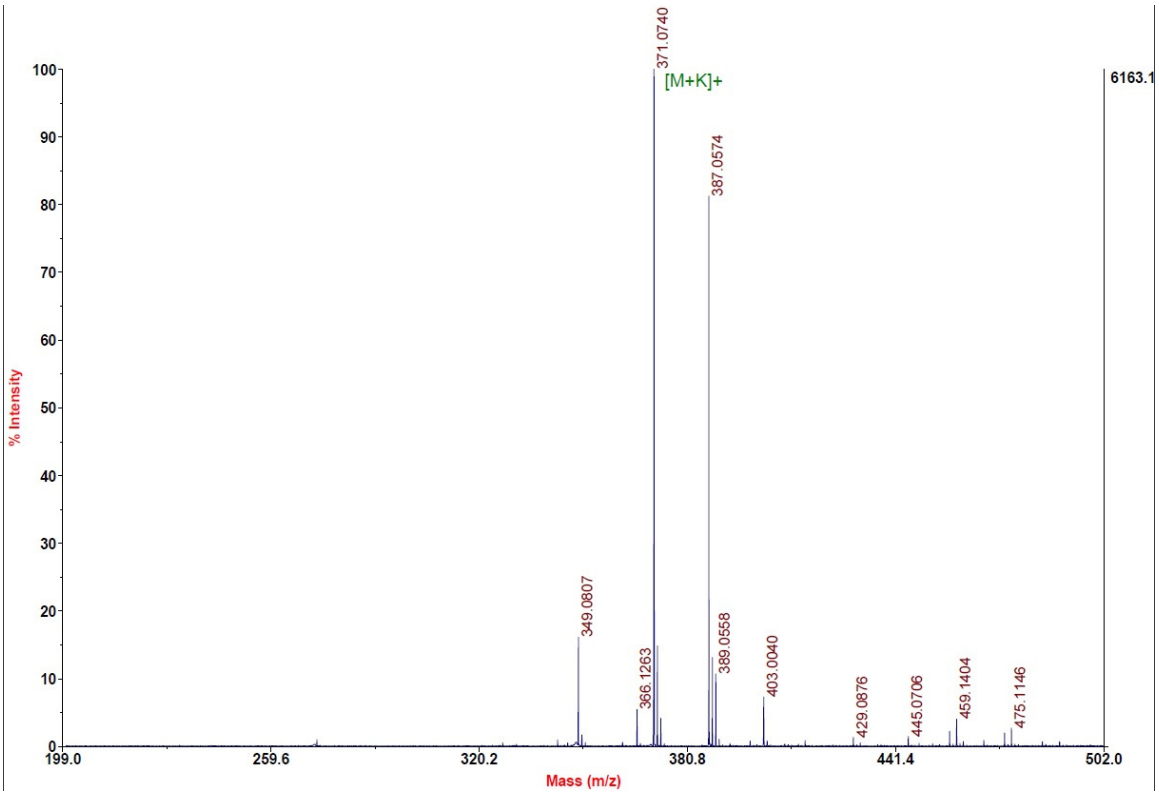

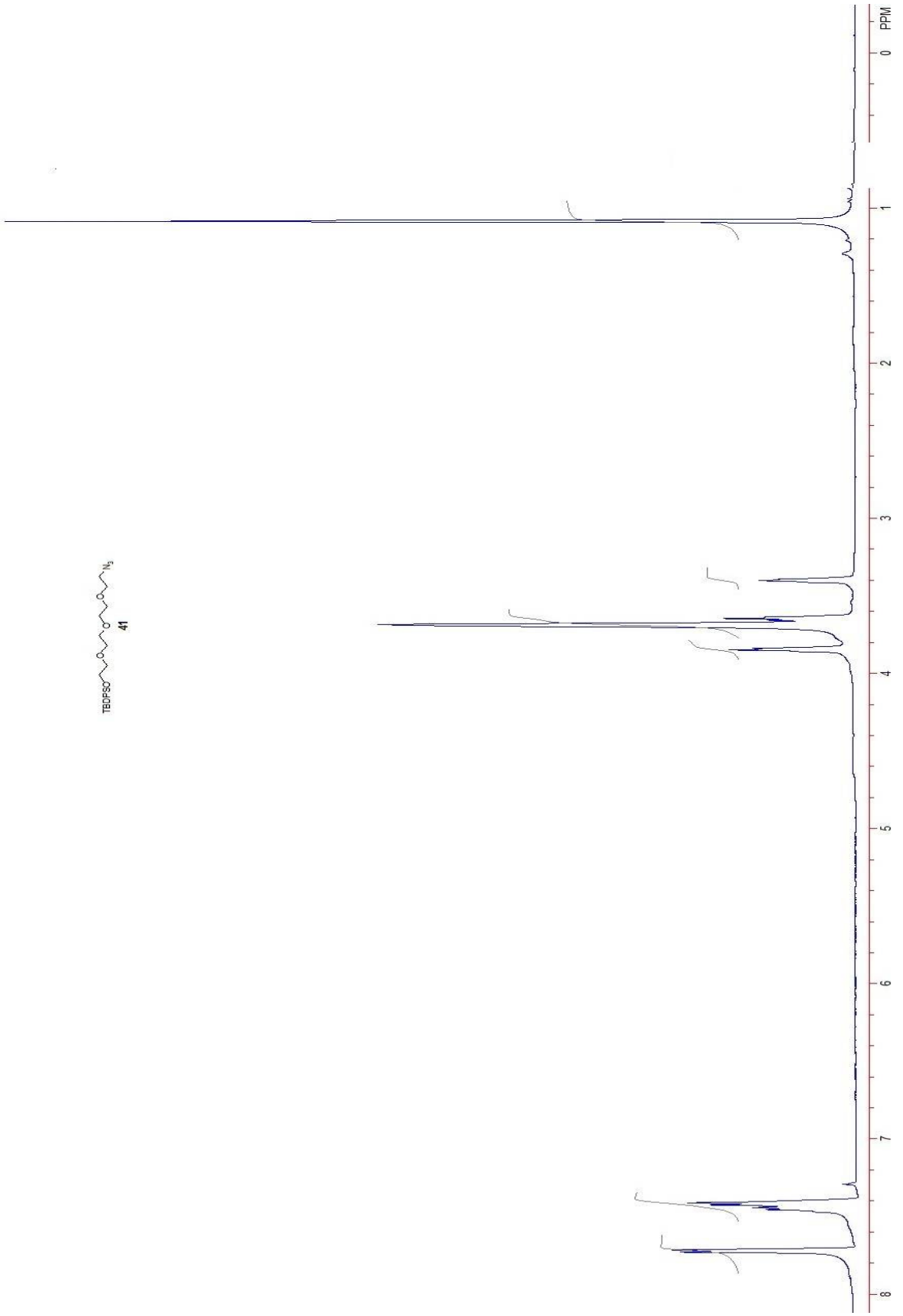
TBDPSO
O
O
O
N3
41
PPM
0
1
2
3
4
5
6
7
8

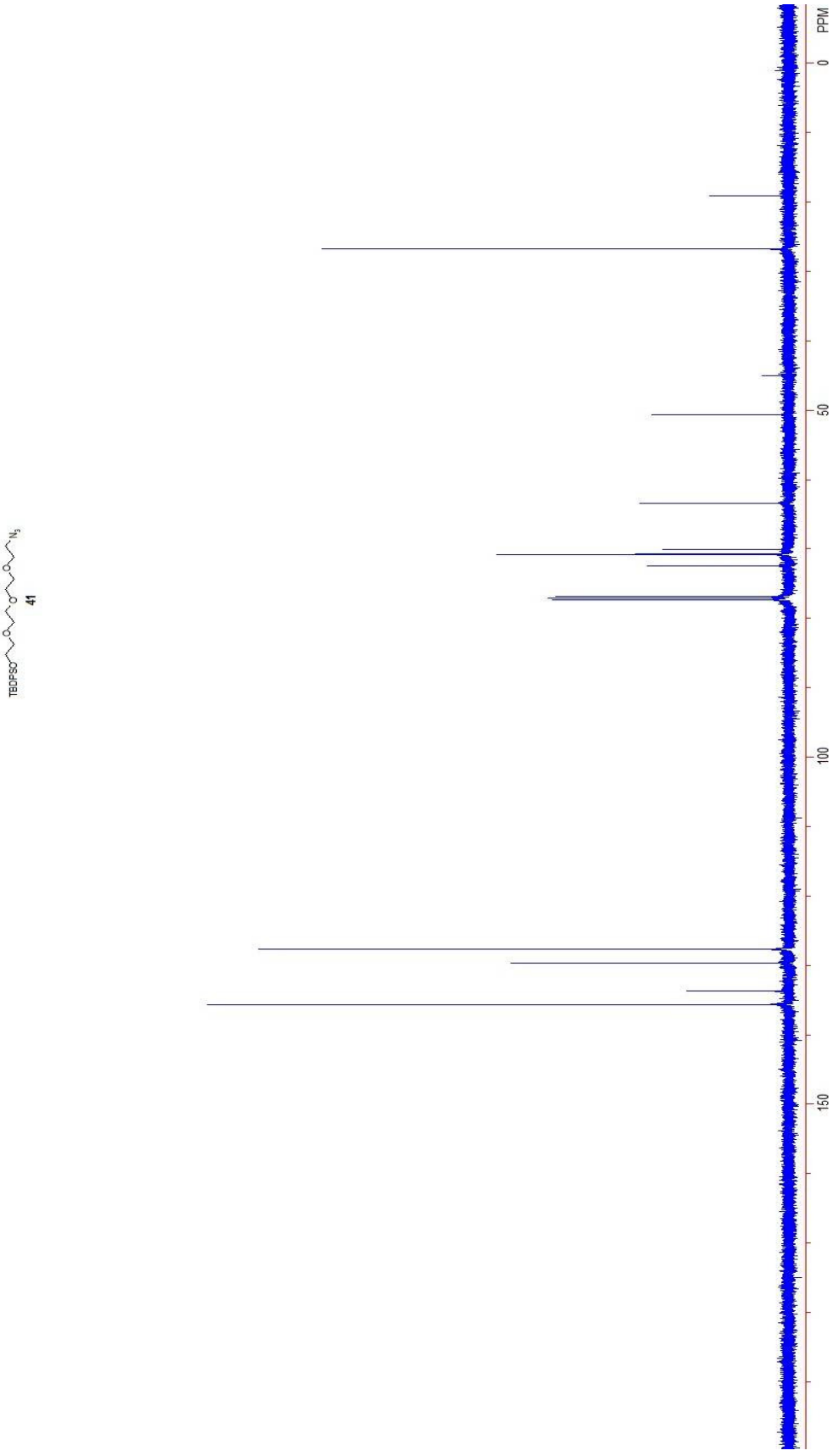
TBDPSO
O
O
O
N3
41
PPM
0
50
100
150

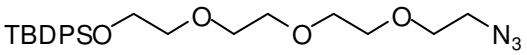

41

MALDI-MS (m/z) Calcd for $C_{24}H_{35}N_3O_4Si$ $[M + Na]^+$: 480.2295, found: 480.2538.

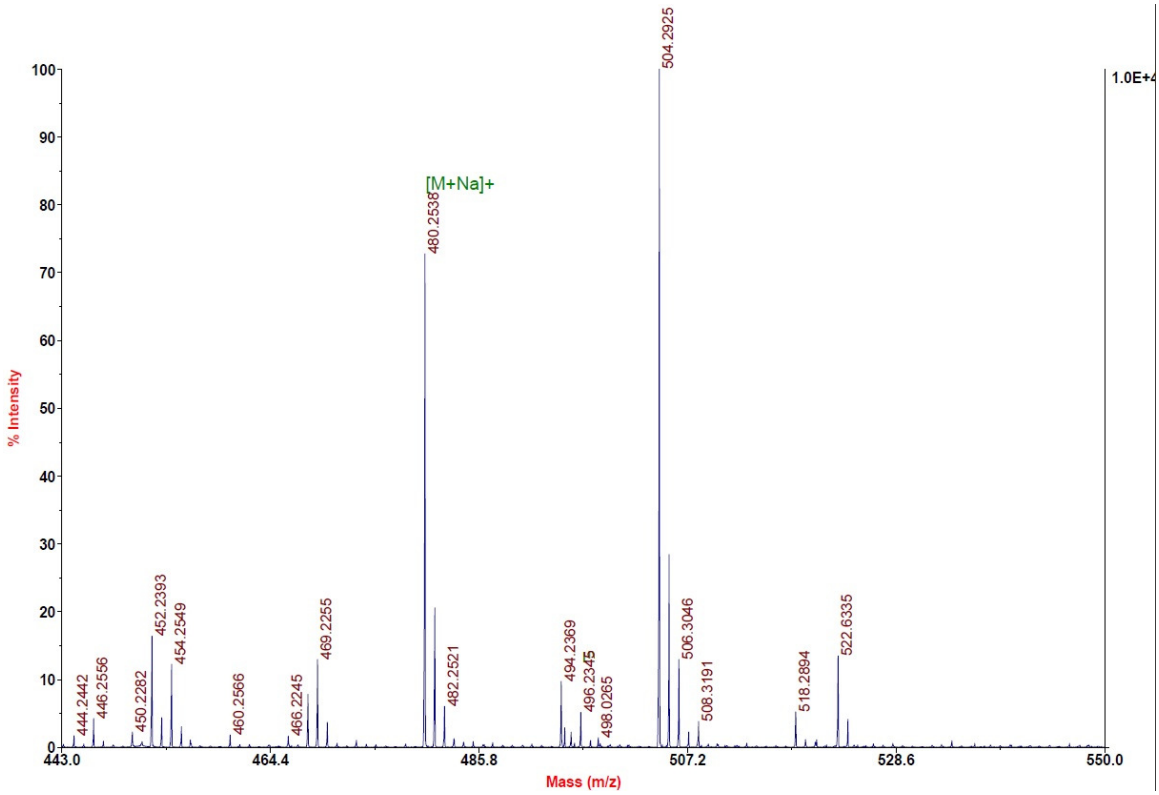

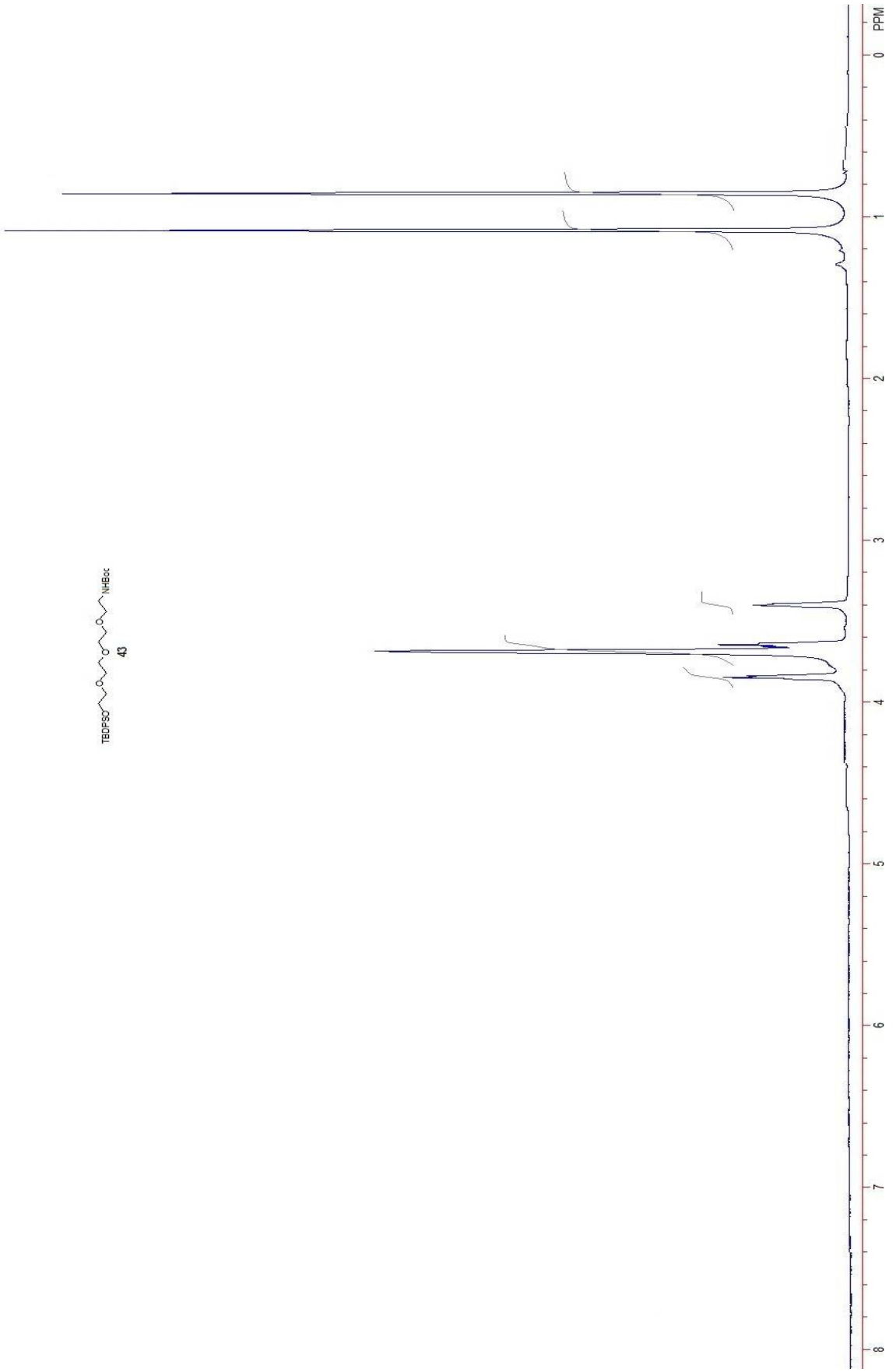
TBDPSO
O
O
O
NHBoc
43
PPM
0
1
2
3
4
5
6
7
8

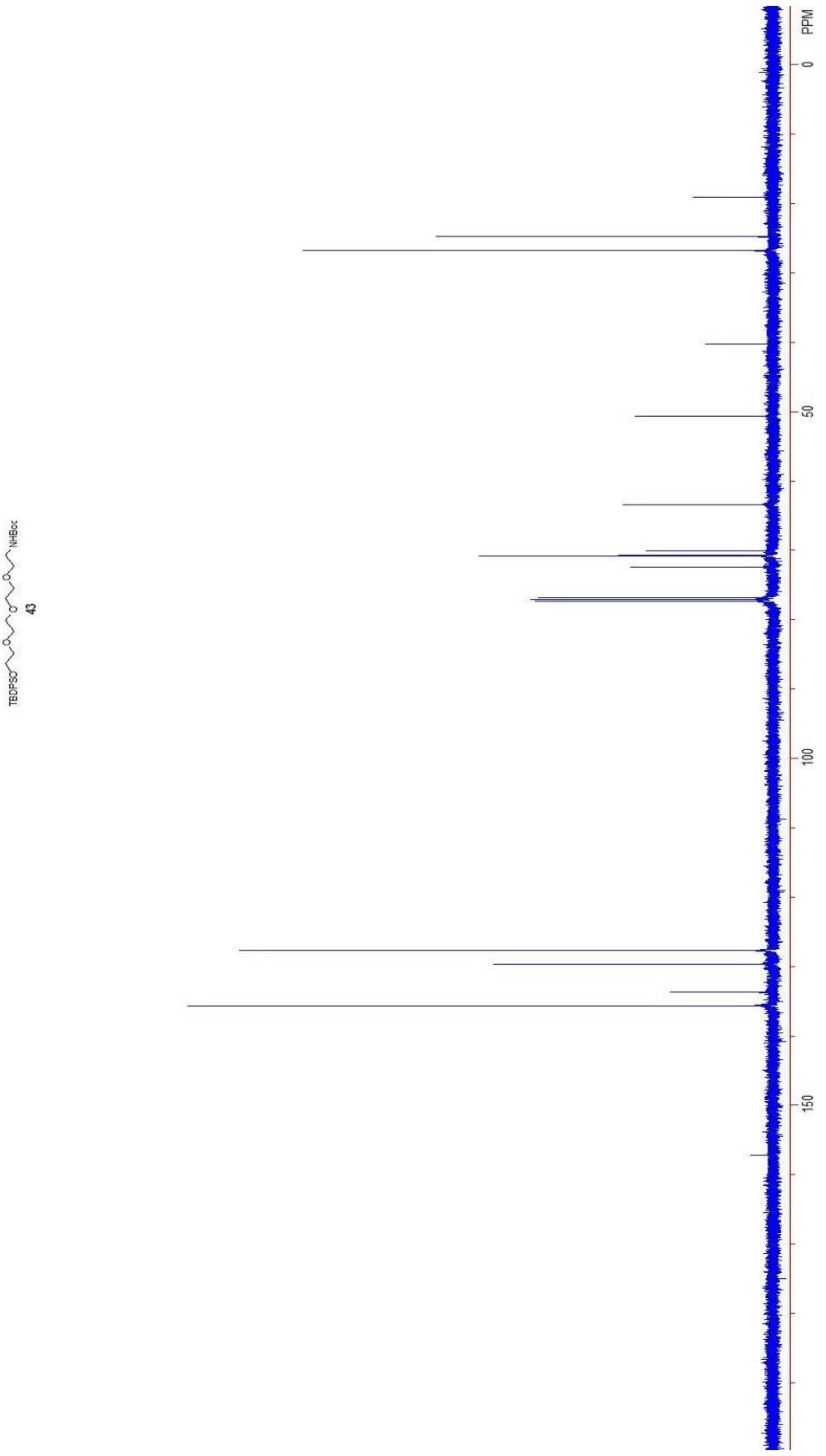
TBDPSO
NHBoc
43
PPM
0
50
100
150

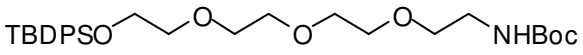

43

MALDI-MS (m/z) Calcd for $C_{29}H_{45}NO_5Si$ $[M + Na]^+$: 554.2914, found: 554.3565.

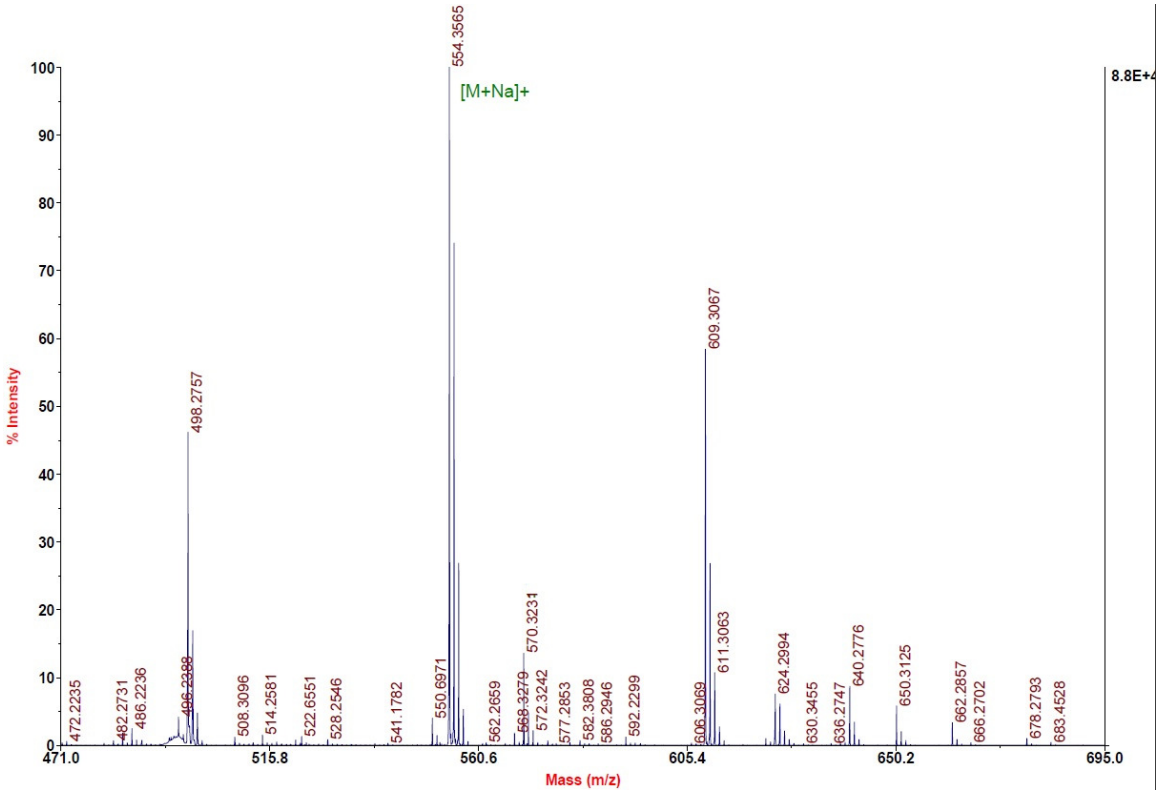

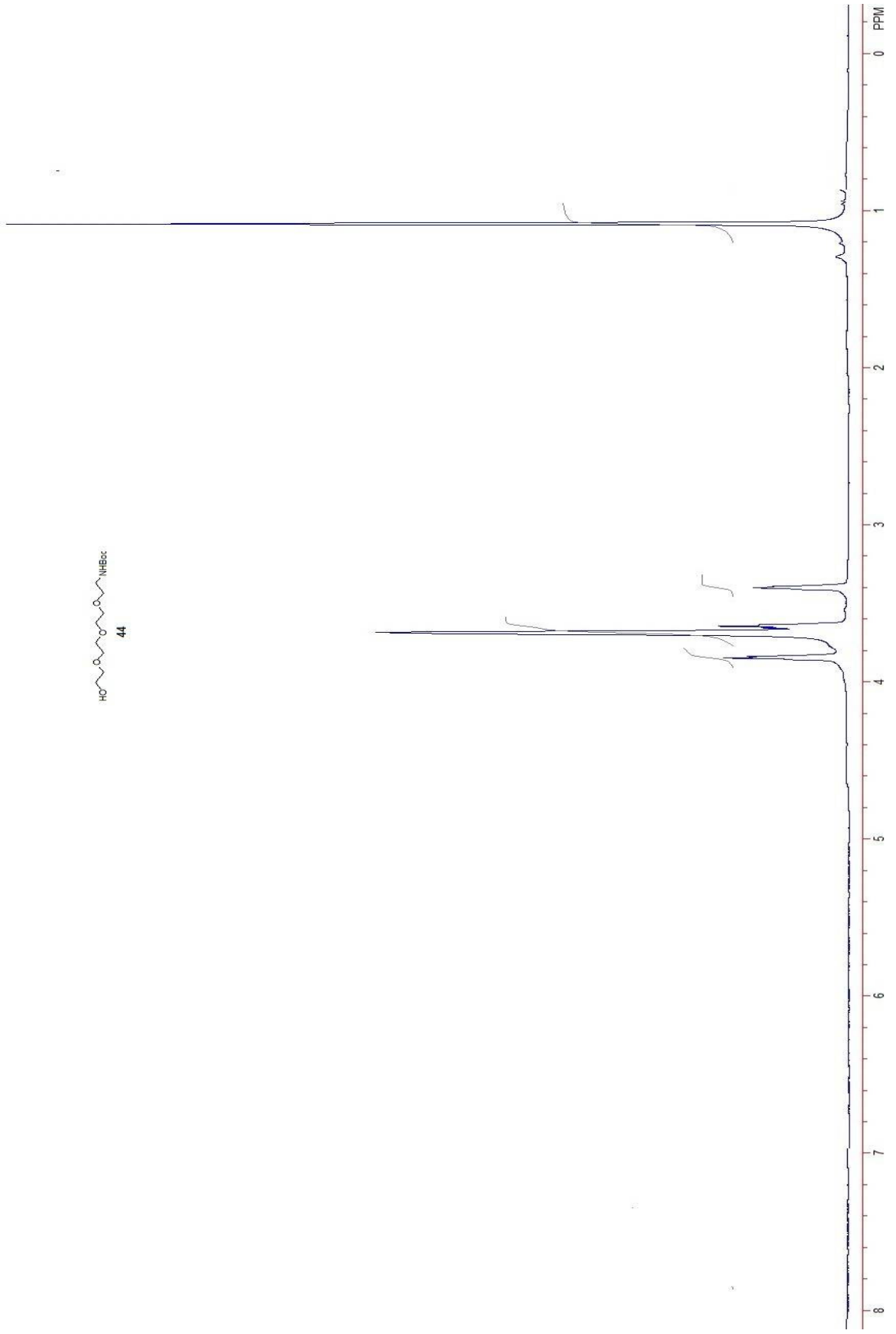
HO
NHBoc
44
PPM
0
1
2
3
4
5
6
7
8

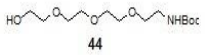

44

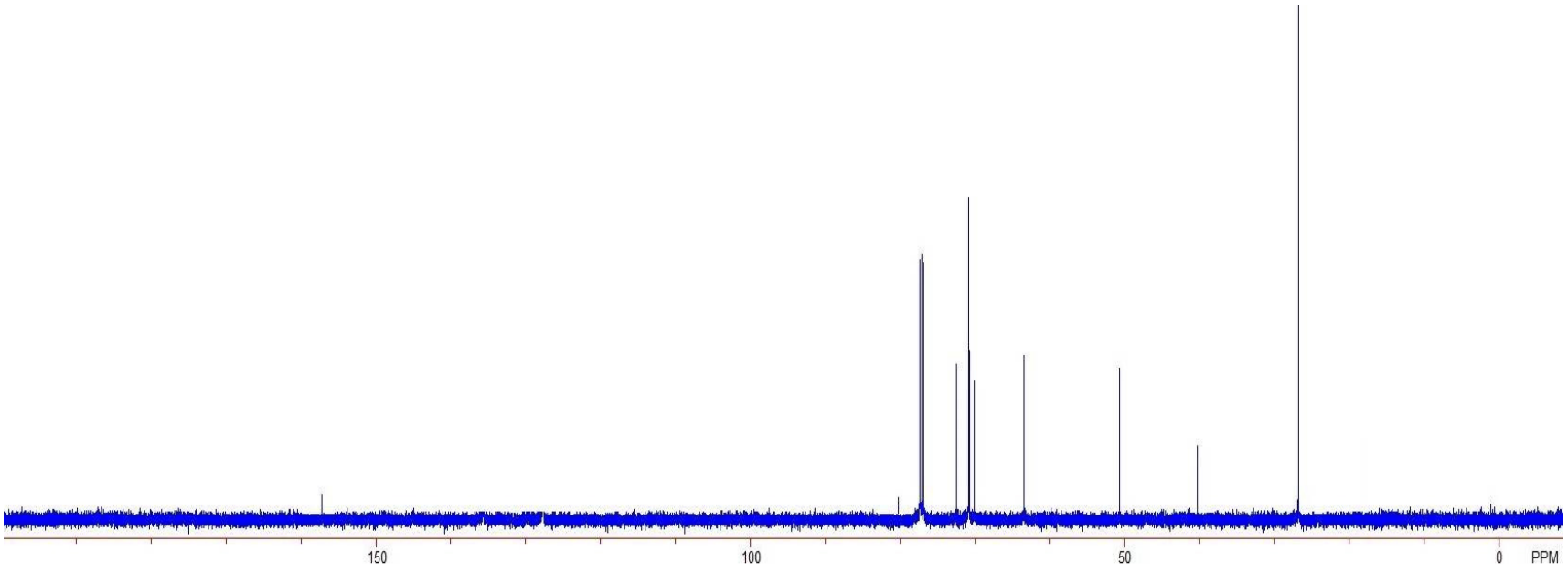

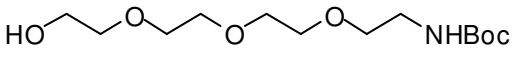

44

MALDI-MS (m/z) Calcd for $C_{13}H_{27}NO_5$ [M + Na]$^+$: 316.1736, found: 316.1674.

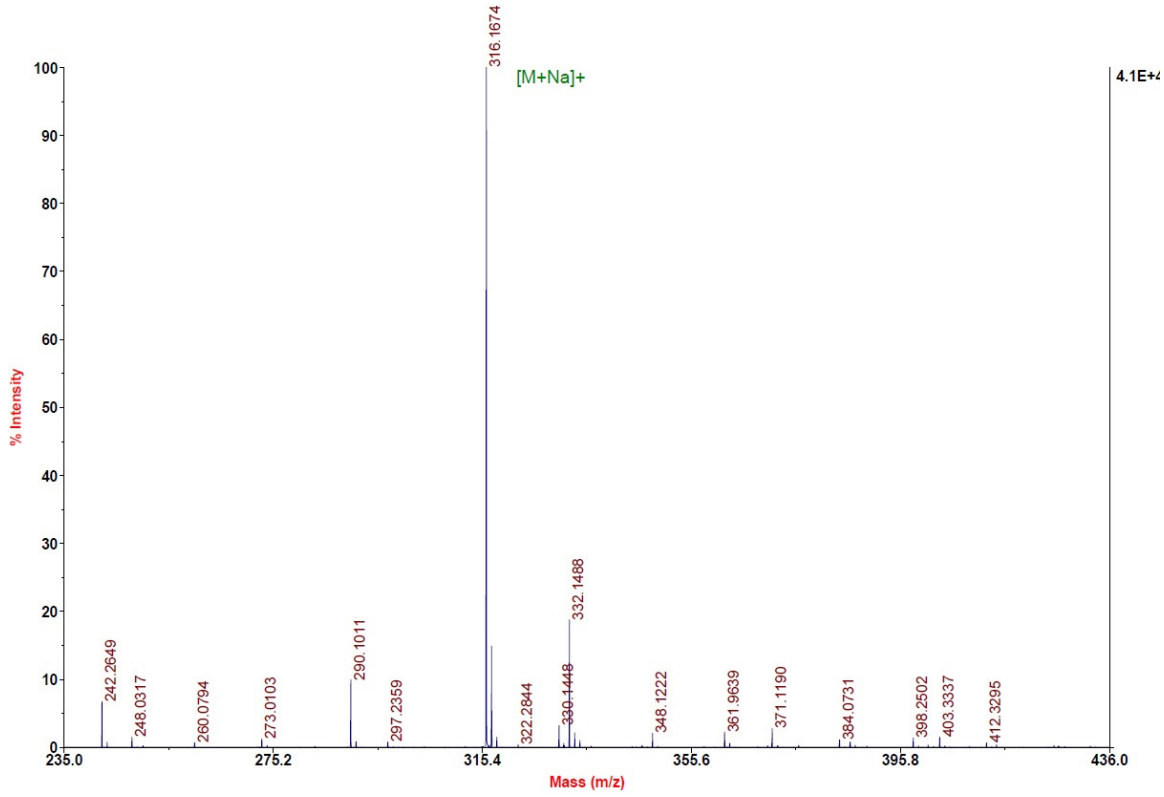

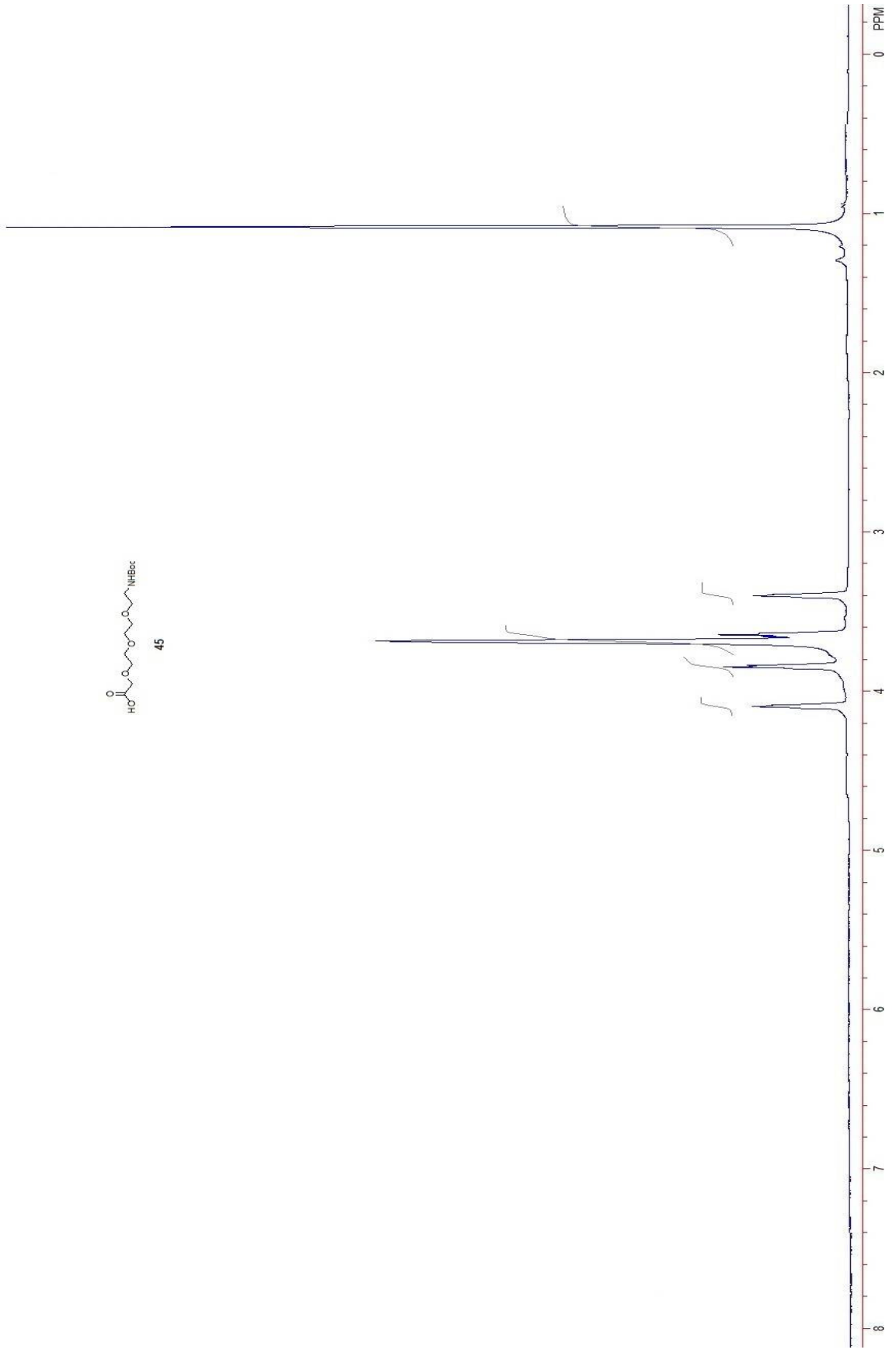
HO
NHBoc
45
PPM
0
1
2
3
4
5
6
7
8

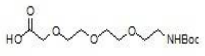

45

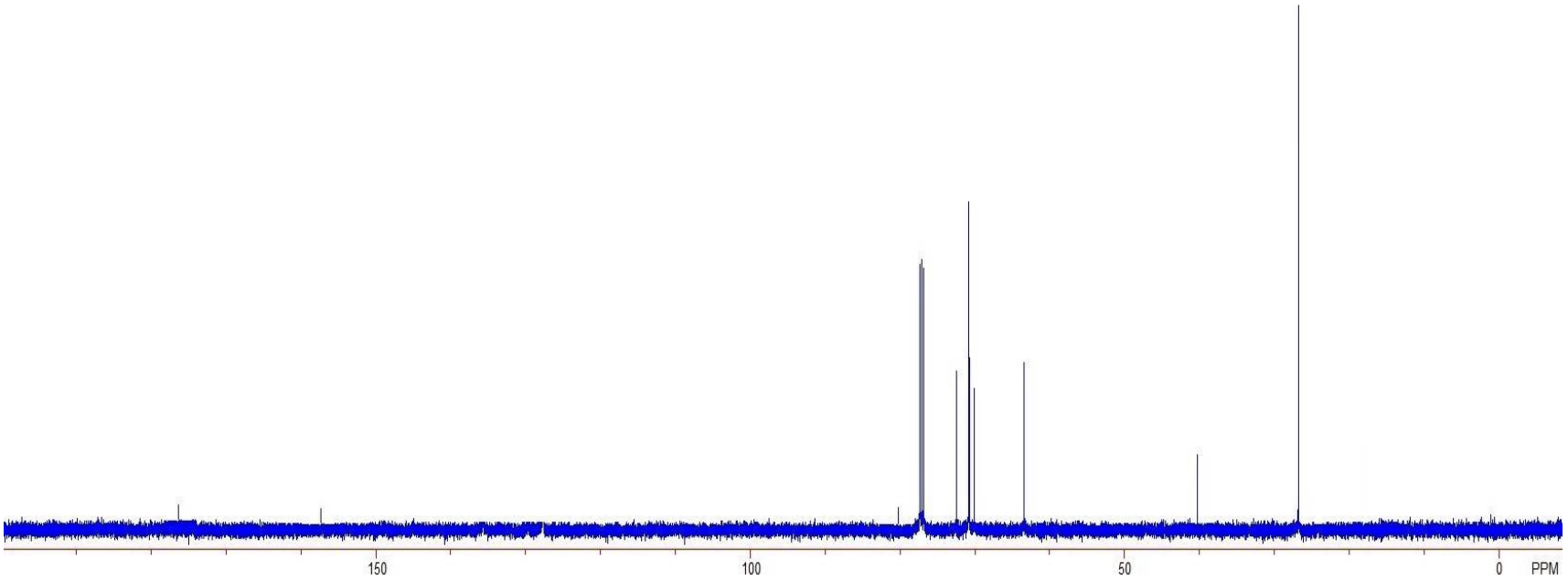

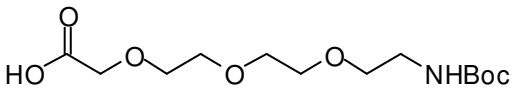

45

MALDI-MS (m/z) Calcd for $C_{13}H_{25}NO_6$ $[M + Na]^+$: 330.1529, found: 330.1417.

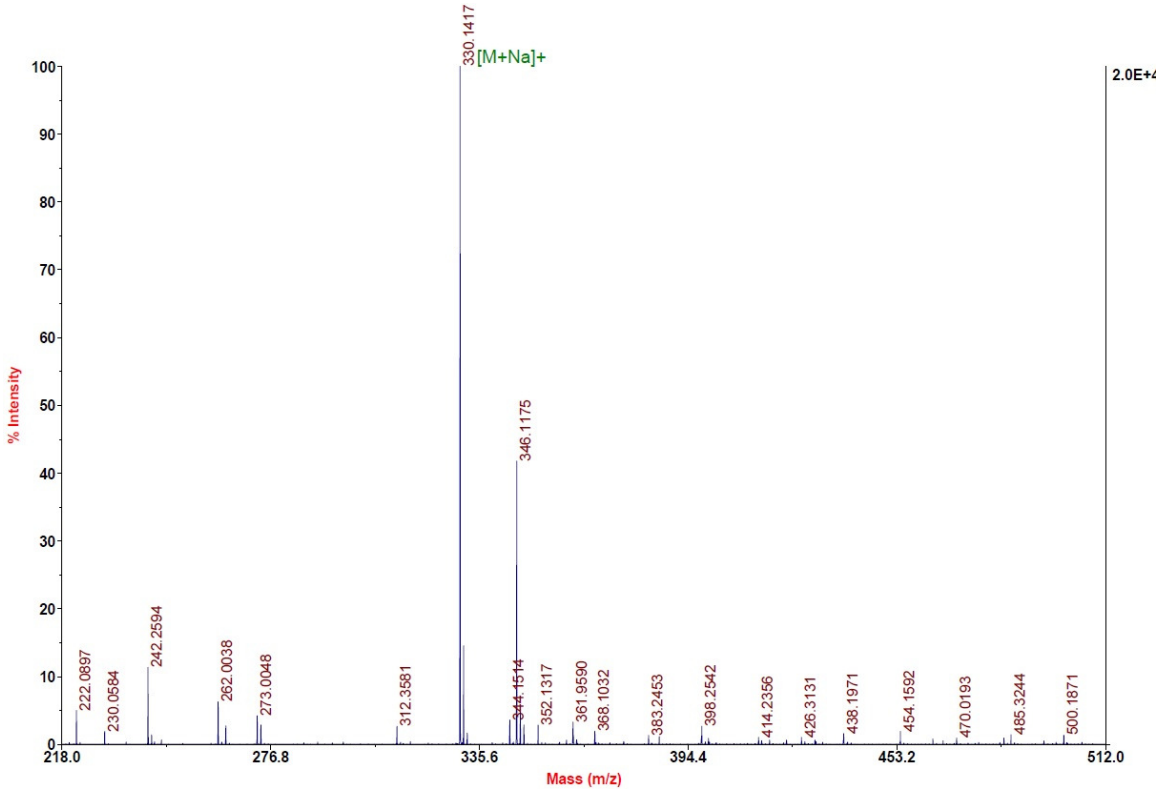

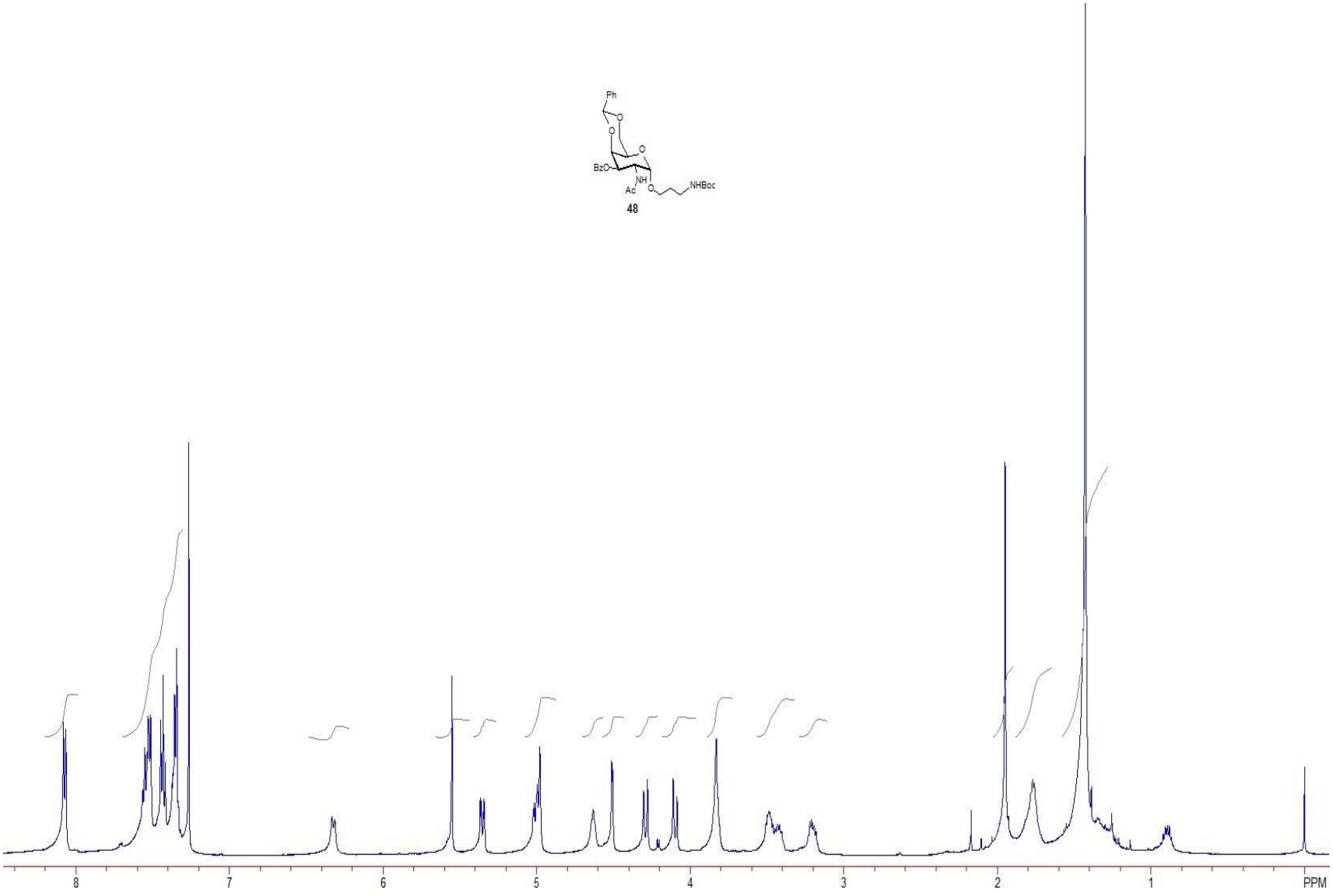
Ph
O
O
O
BzO
NH
Ac
O
NHBoc
48
8
7
6
5
4
3
2
1
PPM

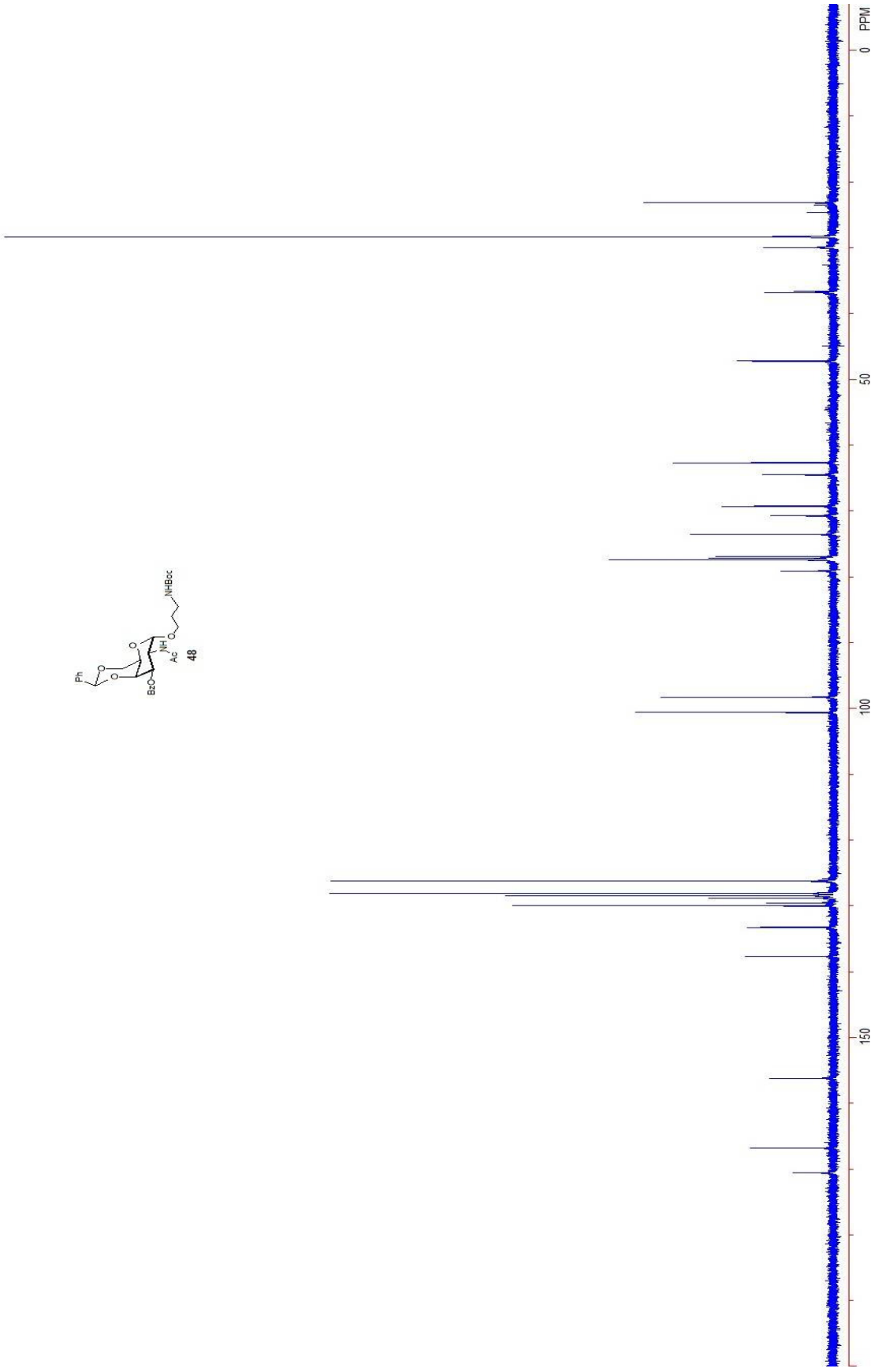
PPM
0
50
100
150
NHBoc
NH
Ac
BzO
Ph
O
O
O
O
48

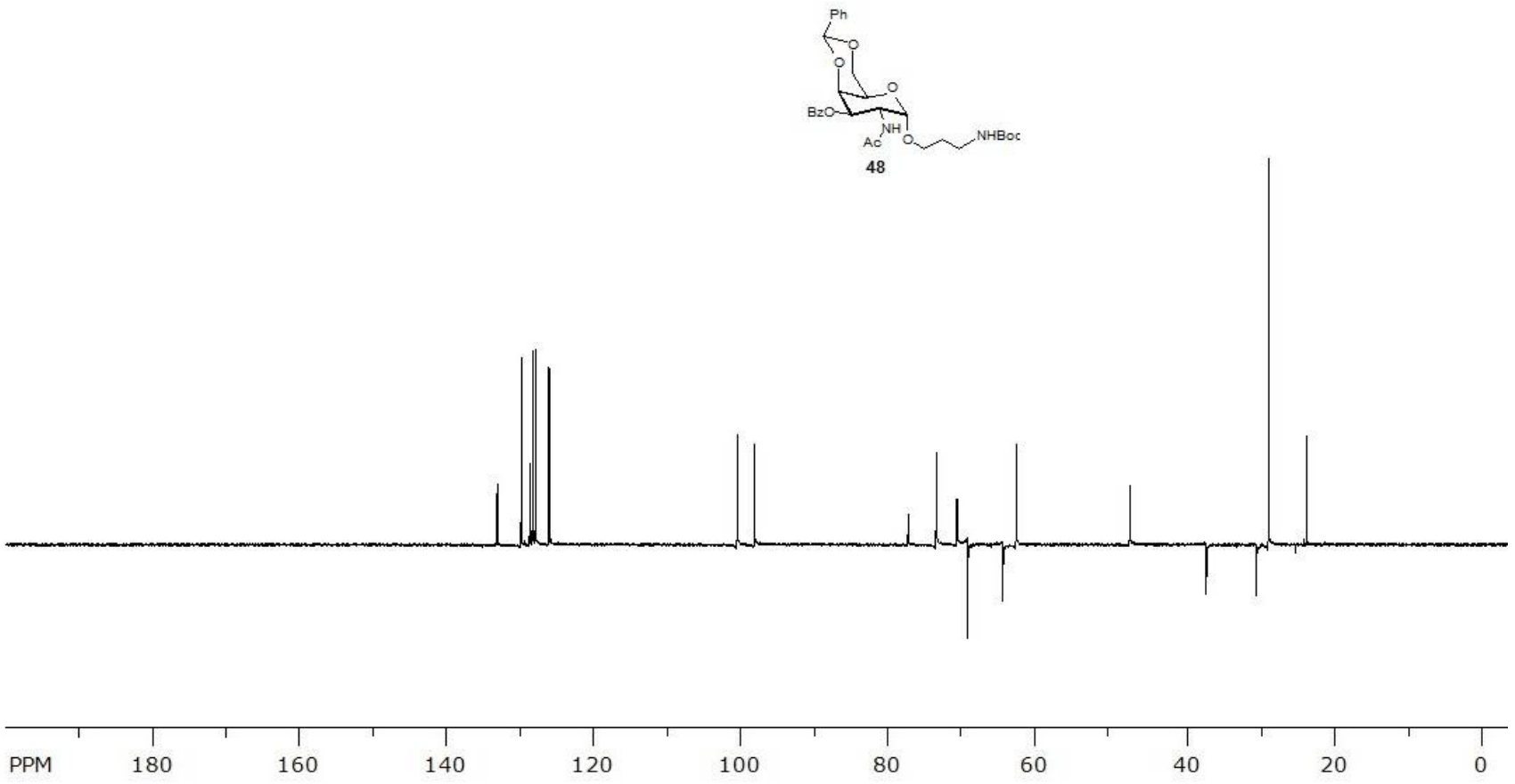
Ph
O
O
O
BzO
NH
Ac
O
NHBoc
48
PPM
180
160
140
120
100
80
60
40
20
0

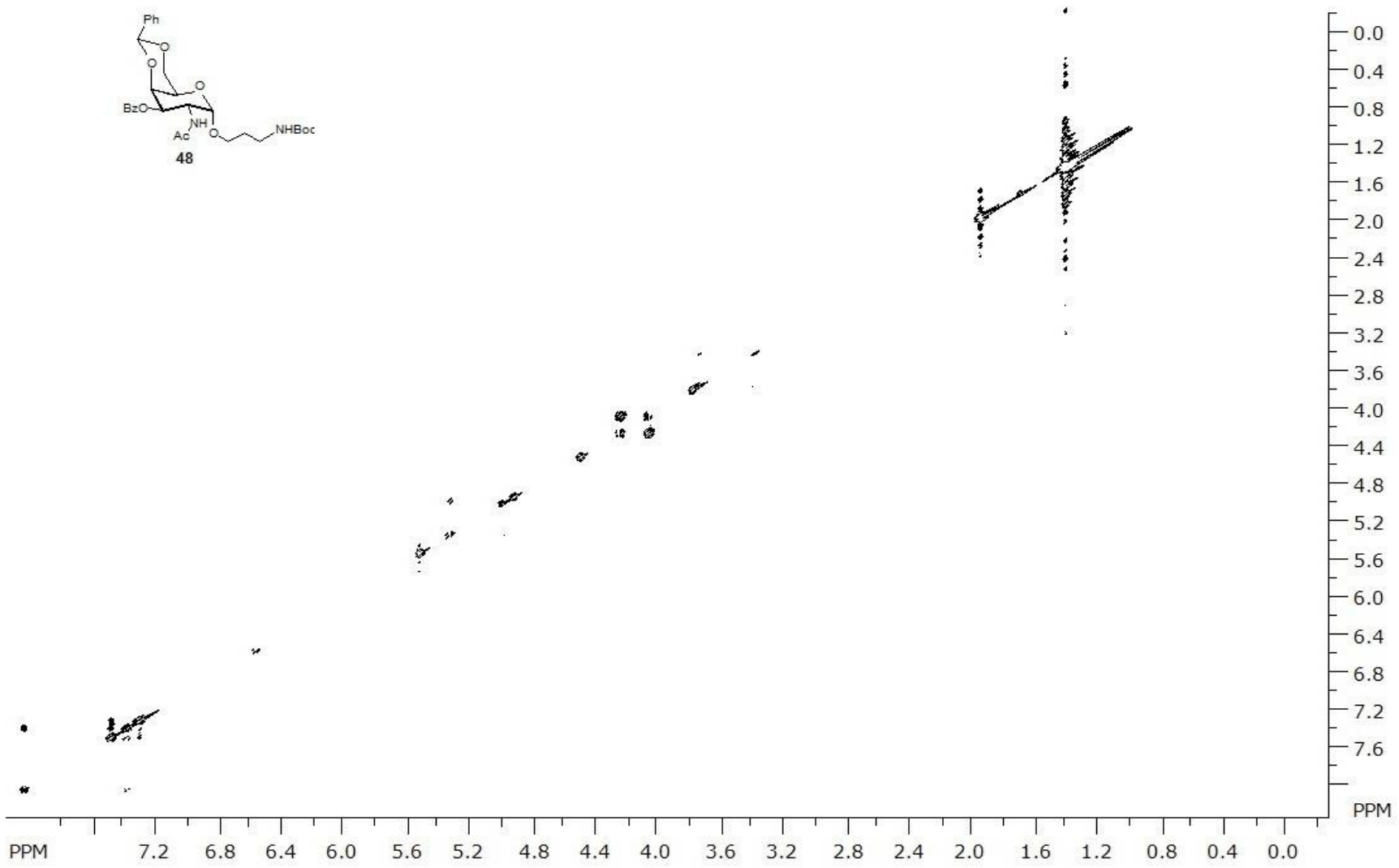
Ph
O
O
O
BzO
NH
Ac
O
NHBoc
48
0.0
0.4
0.8
1.2
1.6
2.0
2.4
2.8
3.2
3.6
4.0
4.4
4.8
5.2
5.6
6.0
6.4
6.8
7.2
7.6
PPM
PPM
7.2
6.8
6.4
6.0
5.6
5.2
4.8
4.4
4.0
3.6
3.2
2.8
2.4
2.0
1.6
1.2
0.8
0.4
0.0

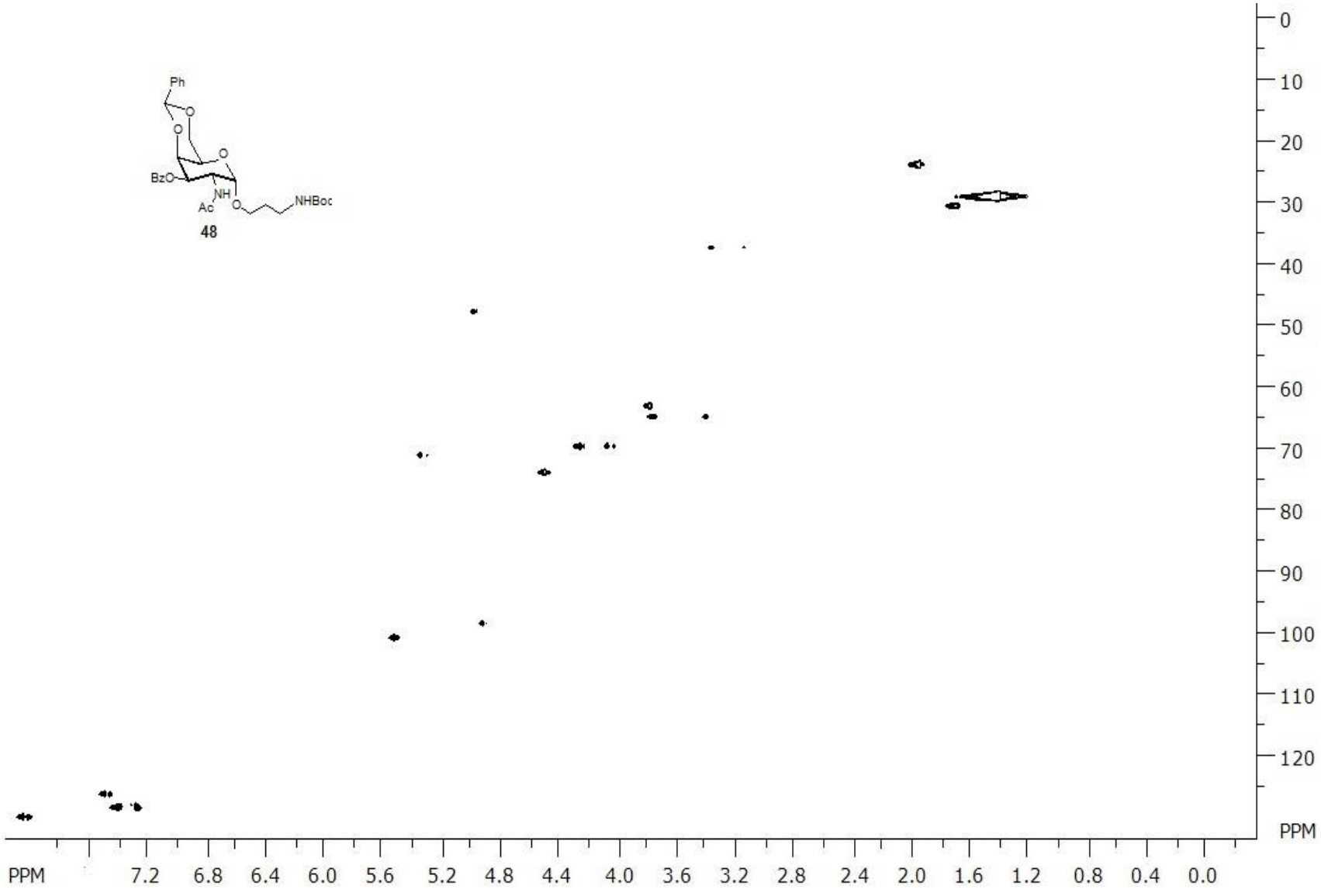
Ph
O
O
O
BzO
NH
Ac
O
NHBoc
48
0
10
20
30
40
50
60
70
80
90
100
110
120
PPM
PPM
7.2
6.8
6.4
6.0
5.6
5.2
4.8
4.4
4.0
3.6
3.2
2.8
2.4
2.0
1.6
1.2
0.8
0.4
0.0

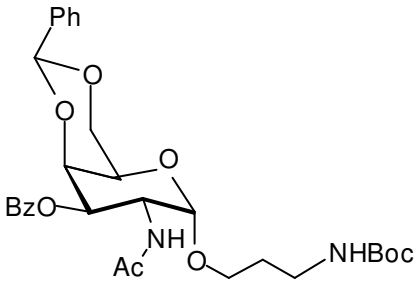

48

MALDI-MS (m/z) Calcd for $C_{30}H_{38}N_2O_9$ $[M + Na]^+$: 593.2475, found: 593.3215.

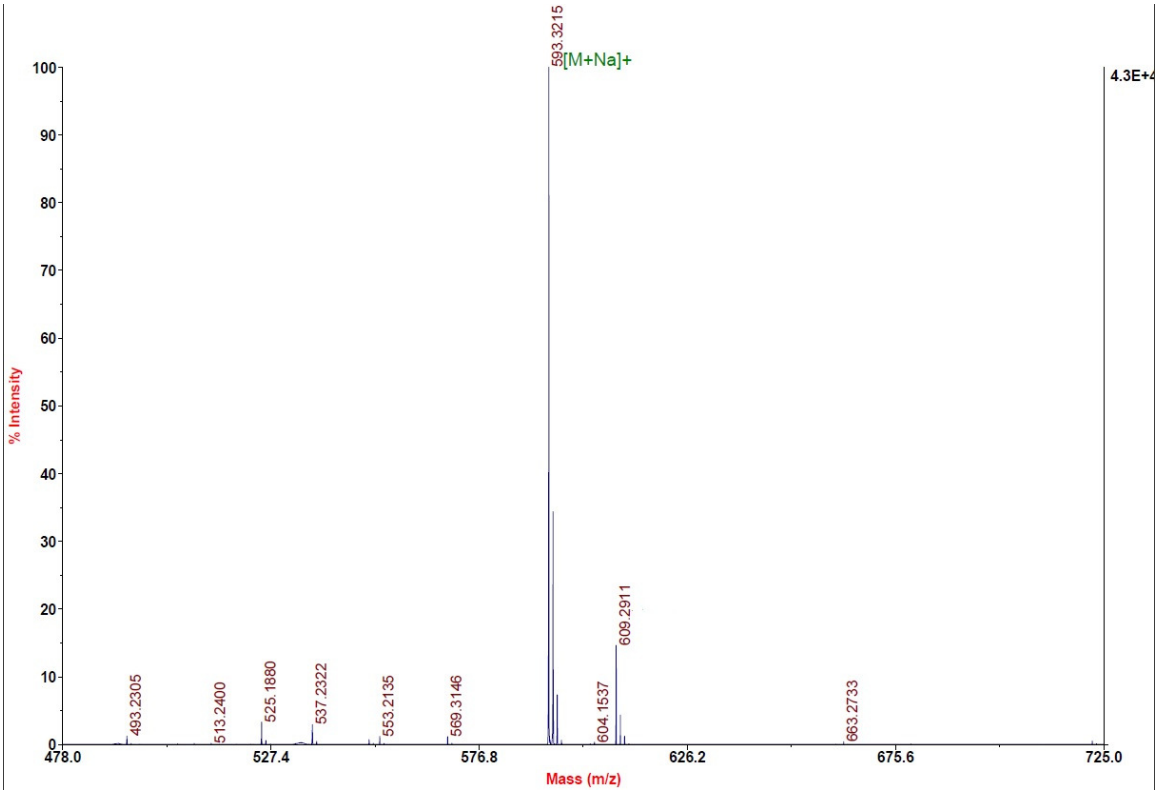

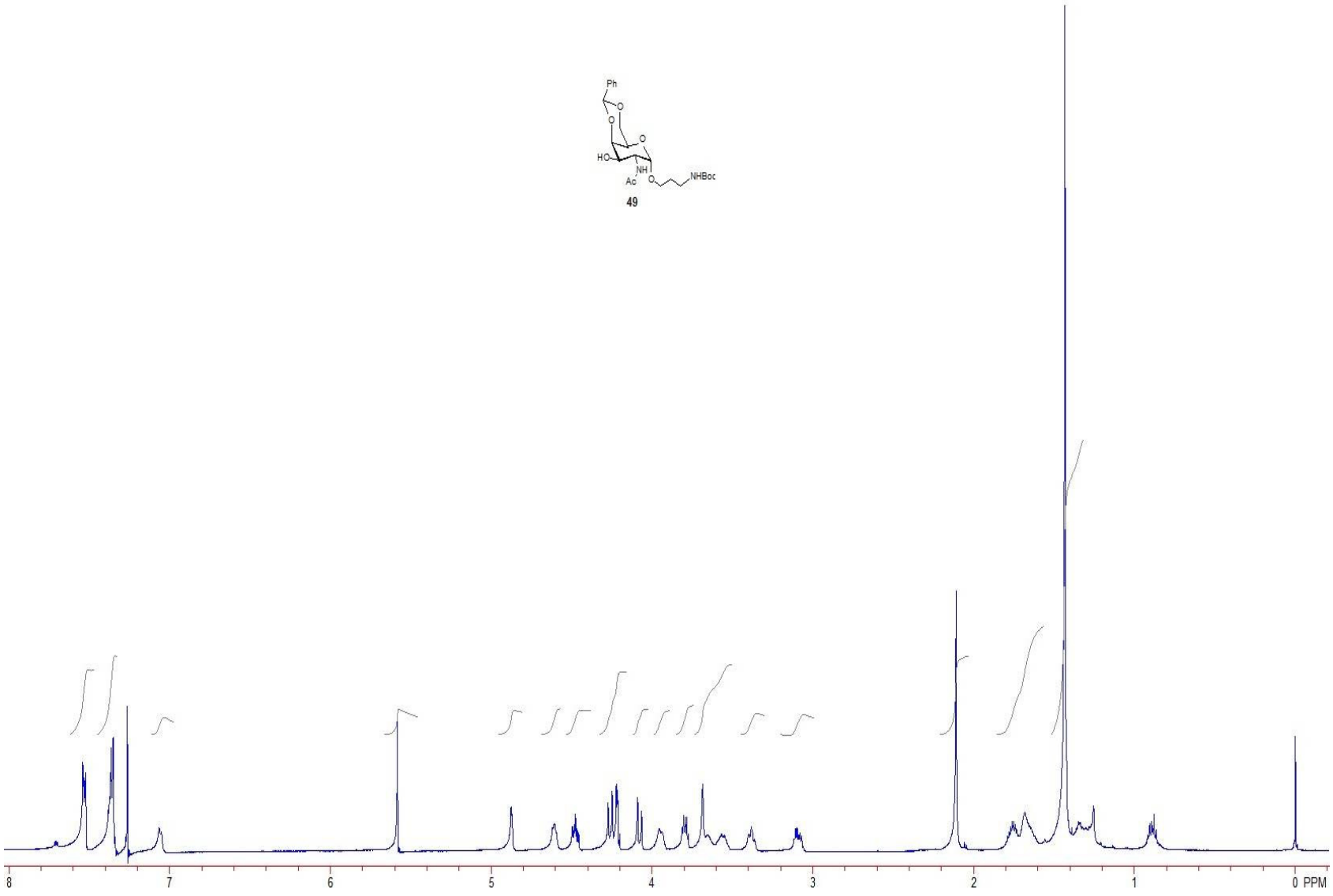
Ph
O
O
O
HO
NH
Ac
O
NHBoc
49
8
7
6
5
4
3
2
1
0 PPM

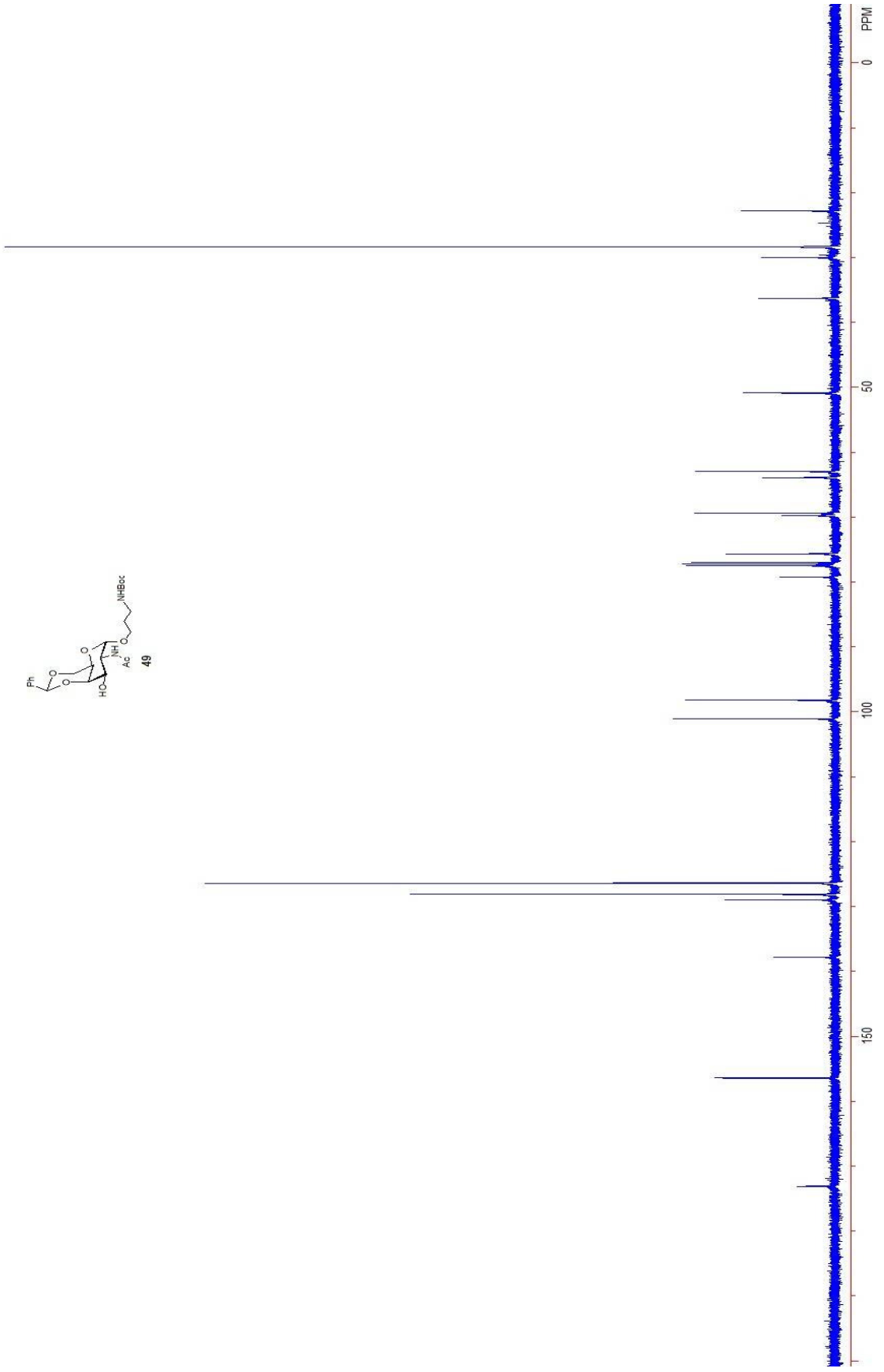
PPM
0
50
100
150
Ph
O
O
O
HO
O
NH
Ac
O
NHBoc
49

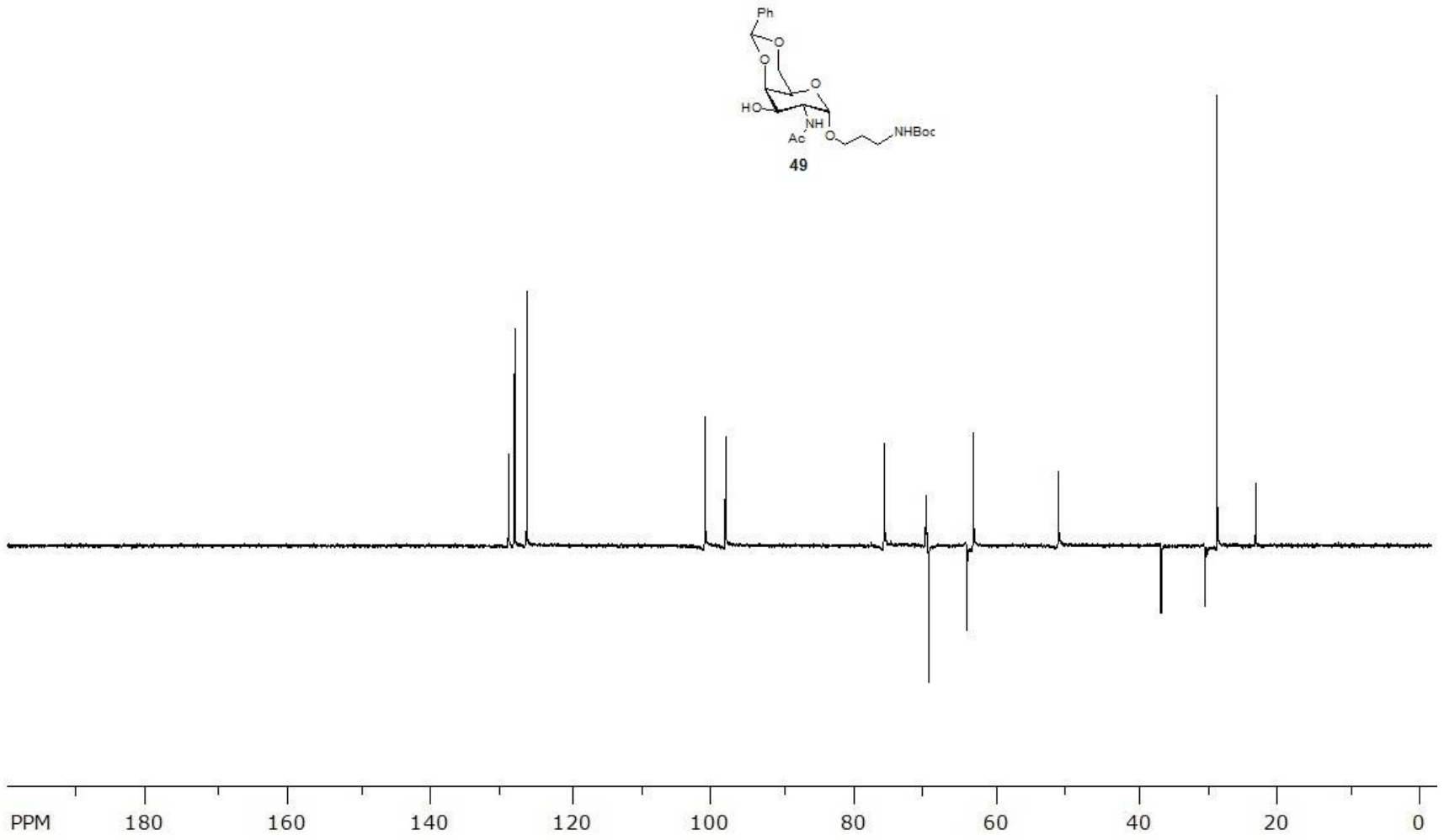
Ph
O
O
O
HO
NH
Ac
O
NHBoc
49
PPM
180
160
140
120
100
80
60
40
20
0

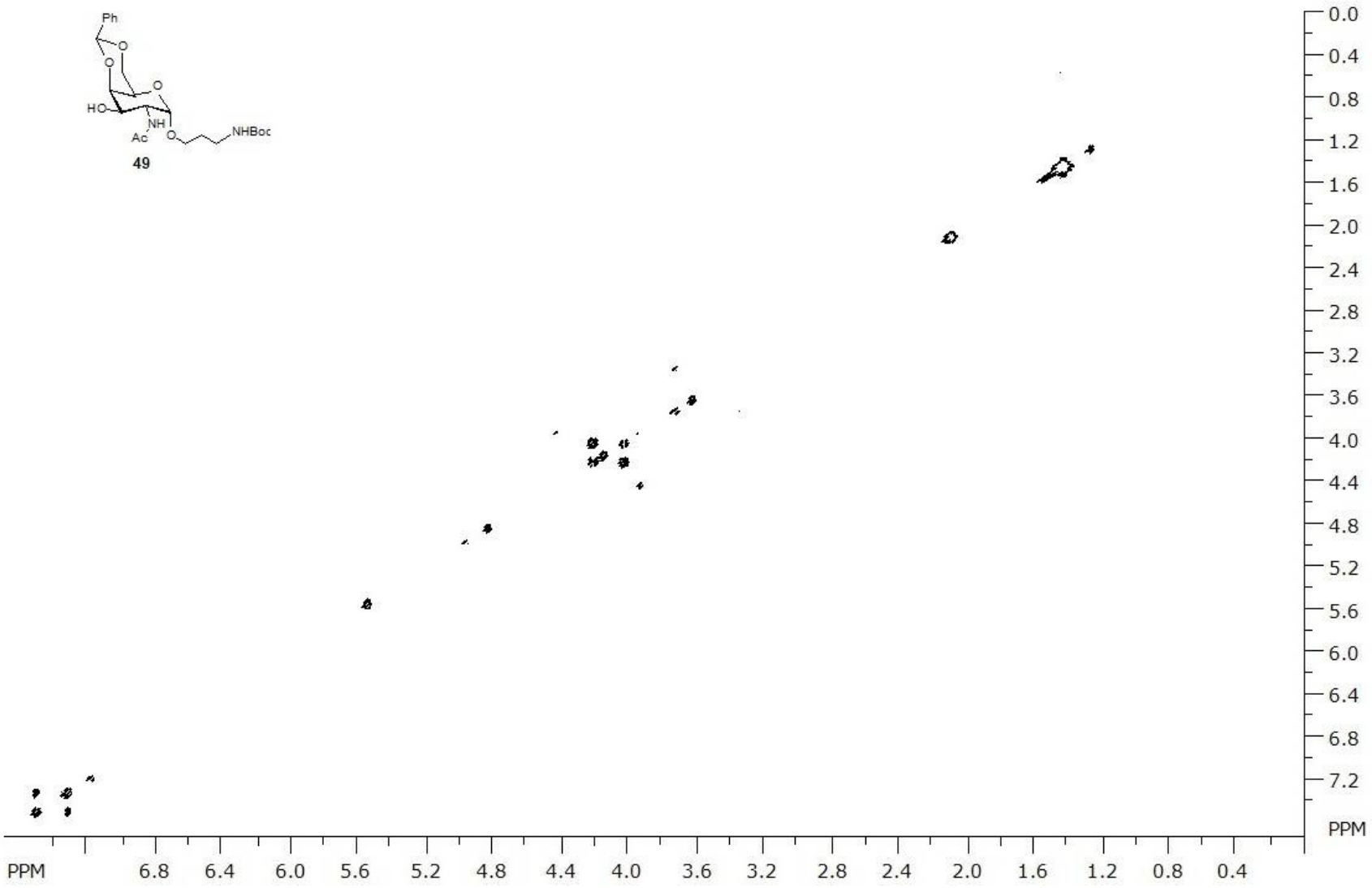
Ph
O
O
O
HO
NH
Ac
O
NHBoc
49
0.0
0.4
0.8
1.2
1.6
2.0
2.4
2.8
3.2
3.6
4.0
4.4
4.8
5.2
5.6
6.0
6.4
6.8
7.2
PPM
PPM
6.8
6.4
6.0
5.6
5.2
4.8
4.4
4.0
3.6
3.2
2.8
2.4
2.0
1.6
1.2
0.8
0.4

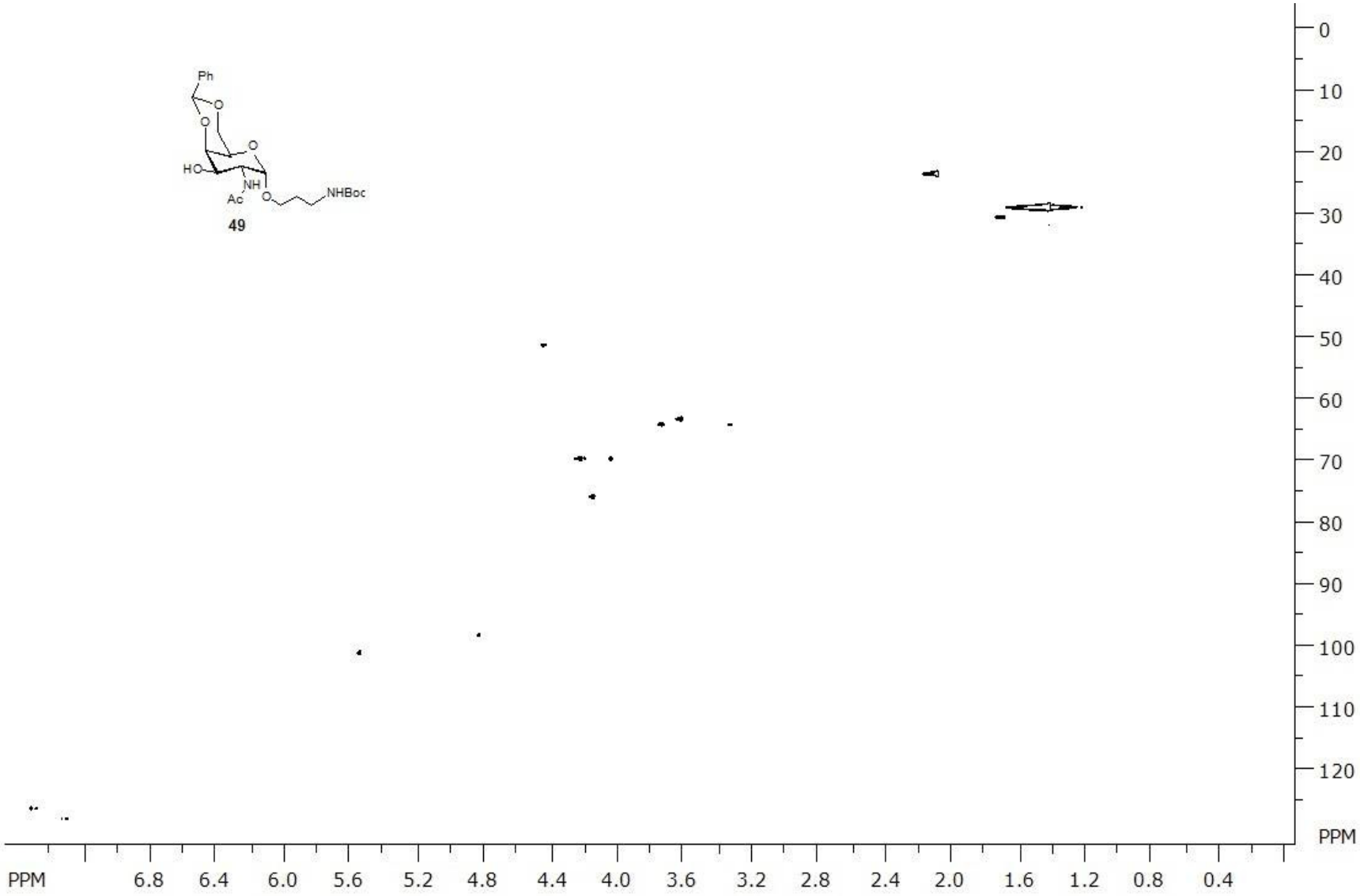
Ph
O
O
O
HO
NH
Ac
O
NHBoc
49
0
10
20
30
40
50
60
70
80
90
100
110
120
PPM
PPM
6.8
6.4
6.0
5.6
5.2
4.8
4.4
4.0
3.6
3.2
2.8
2.4
2.0
1.6
1.2
0.8
0.4

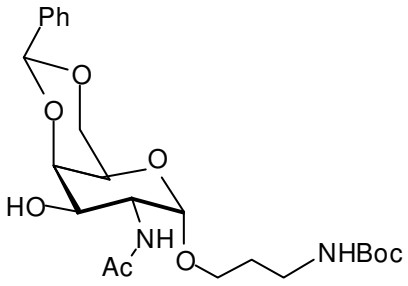

49

MALDI-MS (m/z) Calcd for $C_{23}H_{34}N_2O_5$ $[M + Na]^+$: 489.2213, found: 489.2520.

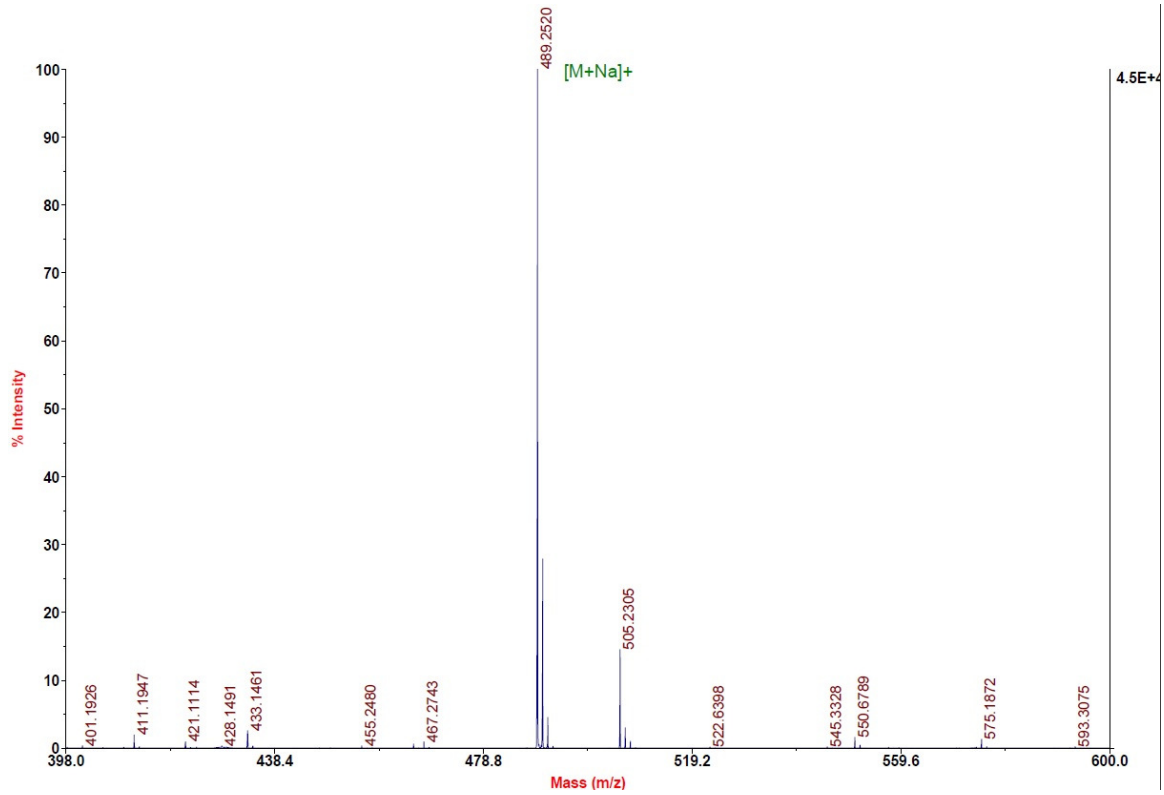

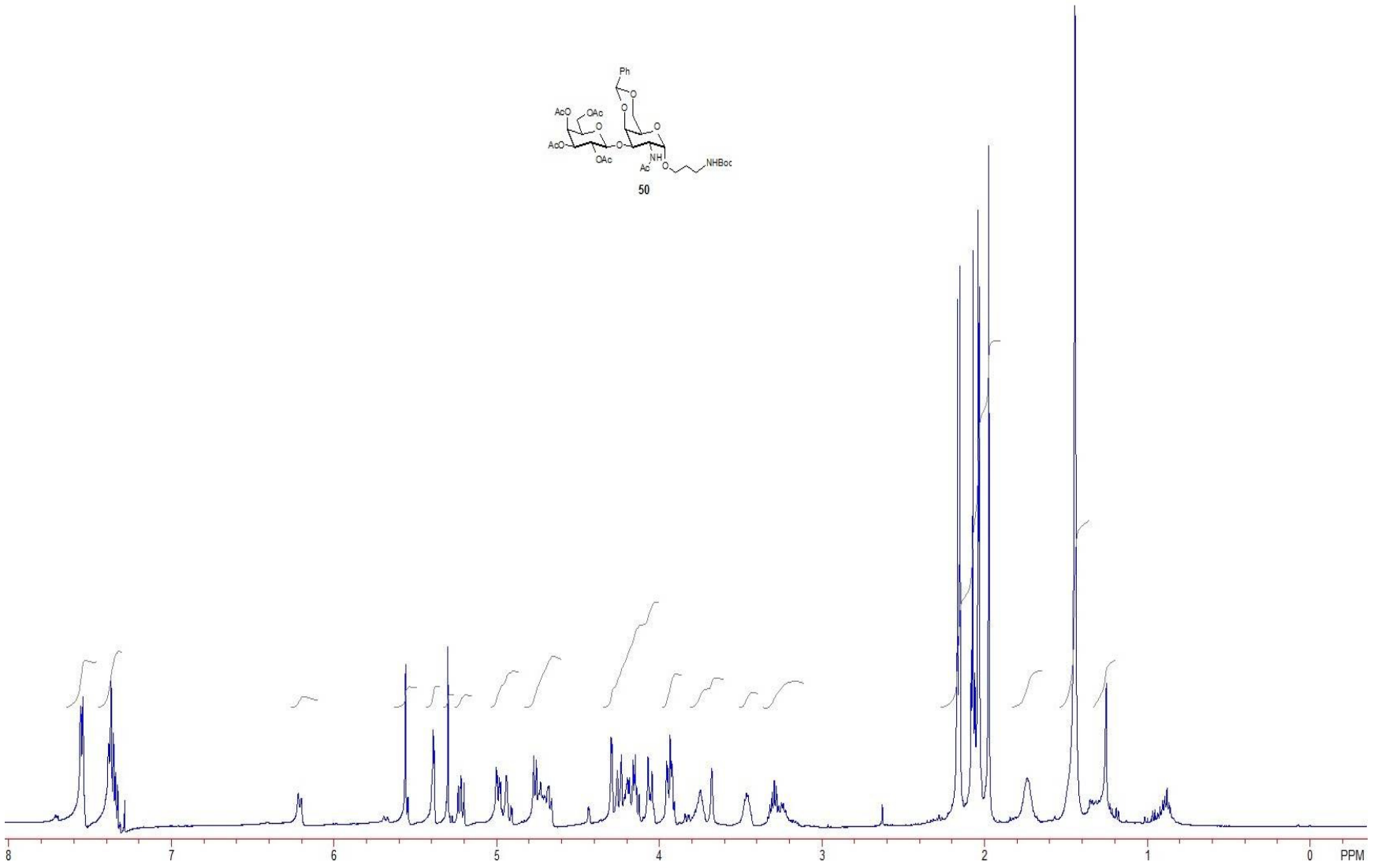
Ph
O
AcO
OAc
O
O
AcO
O
NH
Ac
O
NHBoc
OAc
50
8
7
6
5
4
3
2
1
0
PPM

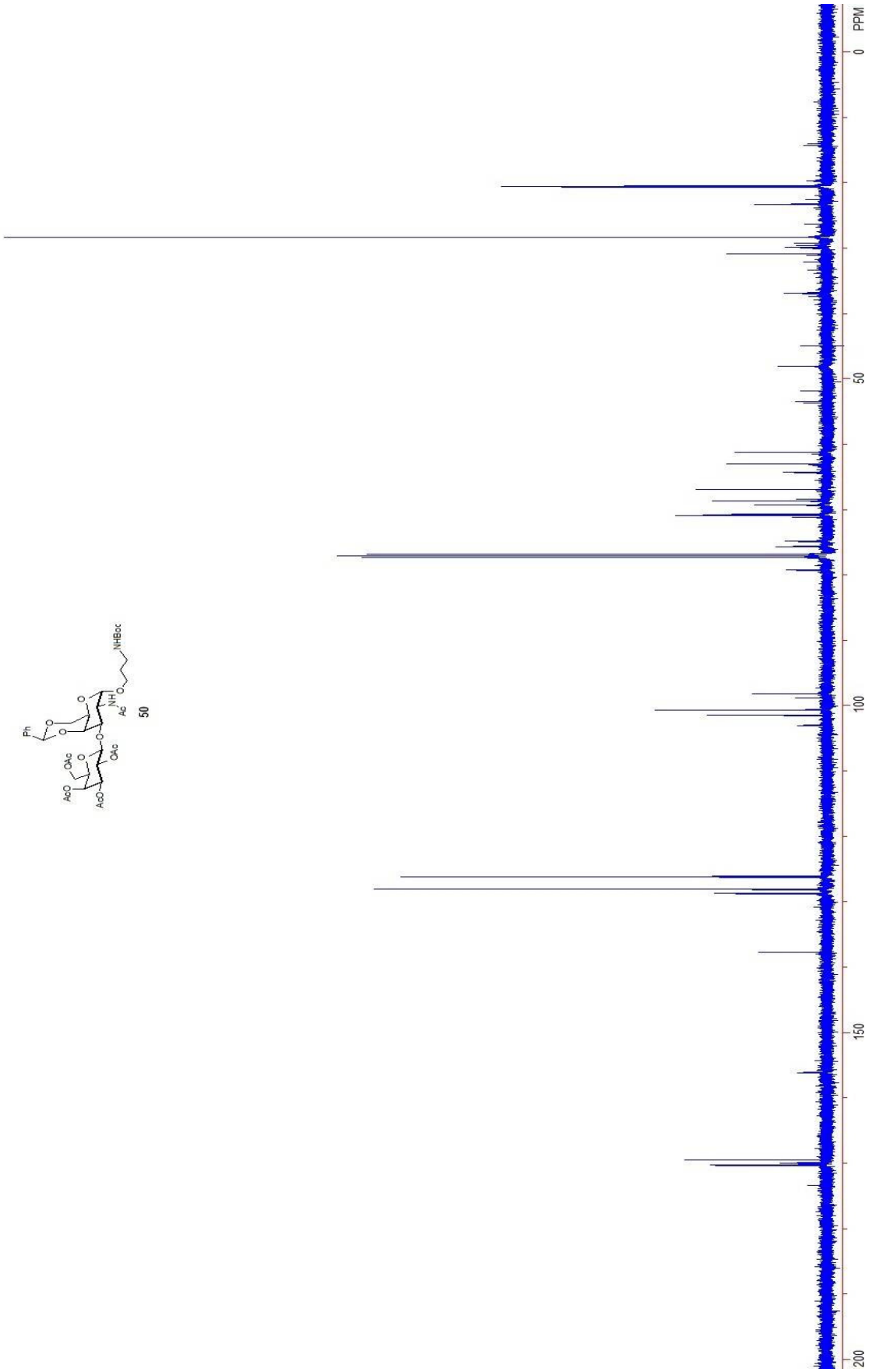
Ph
O
O
O
O
NH
Ac
O
NHBoc
AcO
AcO
OAc
OAc
O
50
0
50
100
150
200
PPM

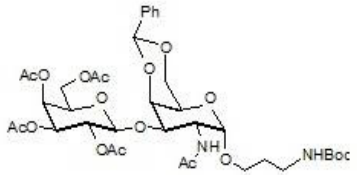
Ph
O
O
AcO
OAc
O
O
AcO
O
O
OAc
NH
Ac
O
NHBoc

50

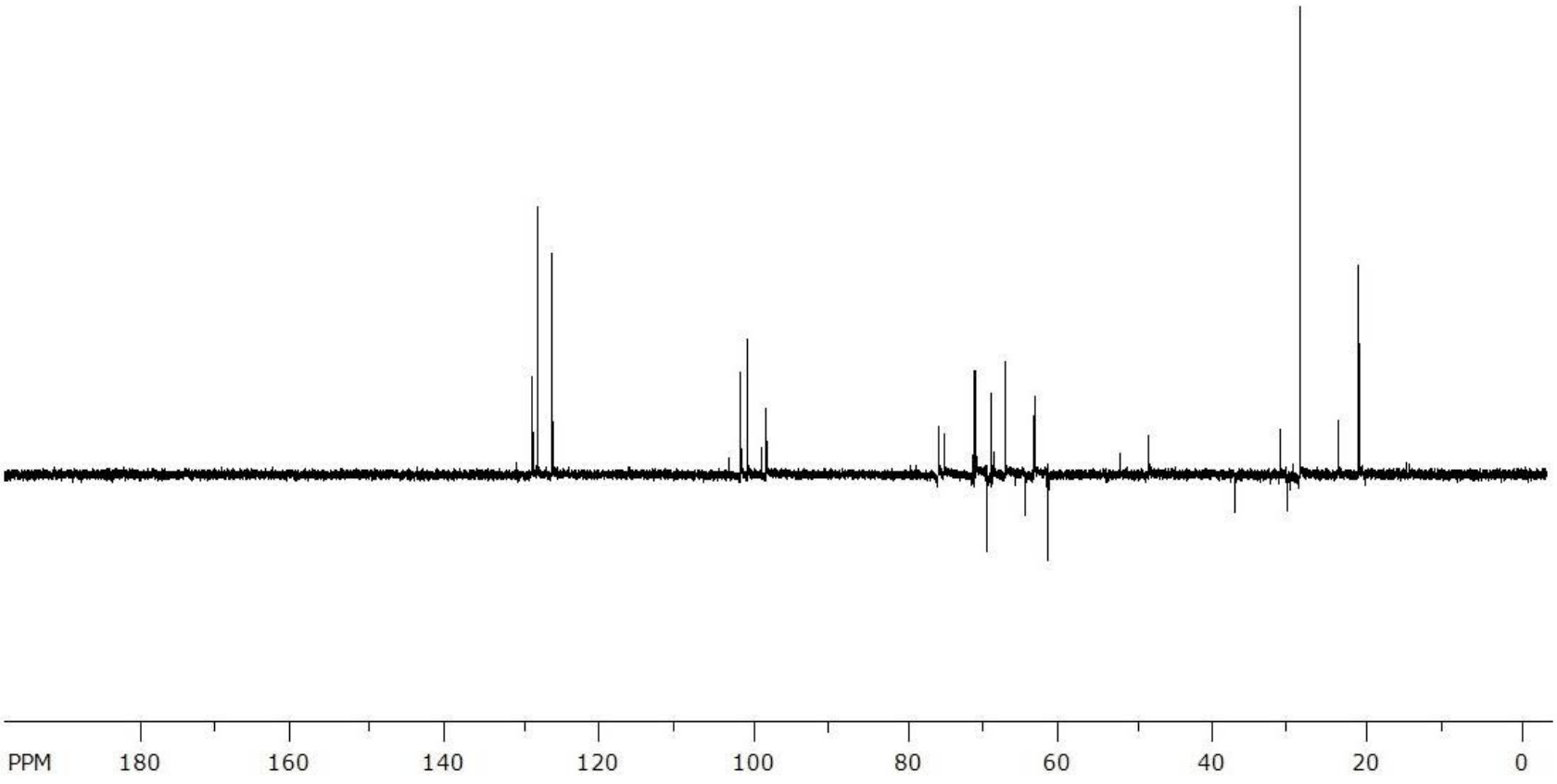
PPM
180
160
140
120
100
80
60
40
20
0

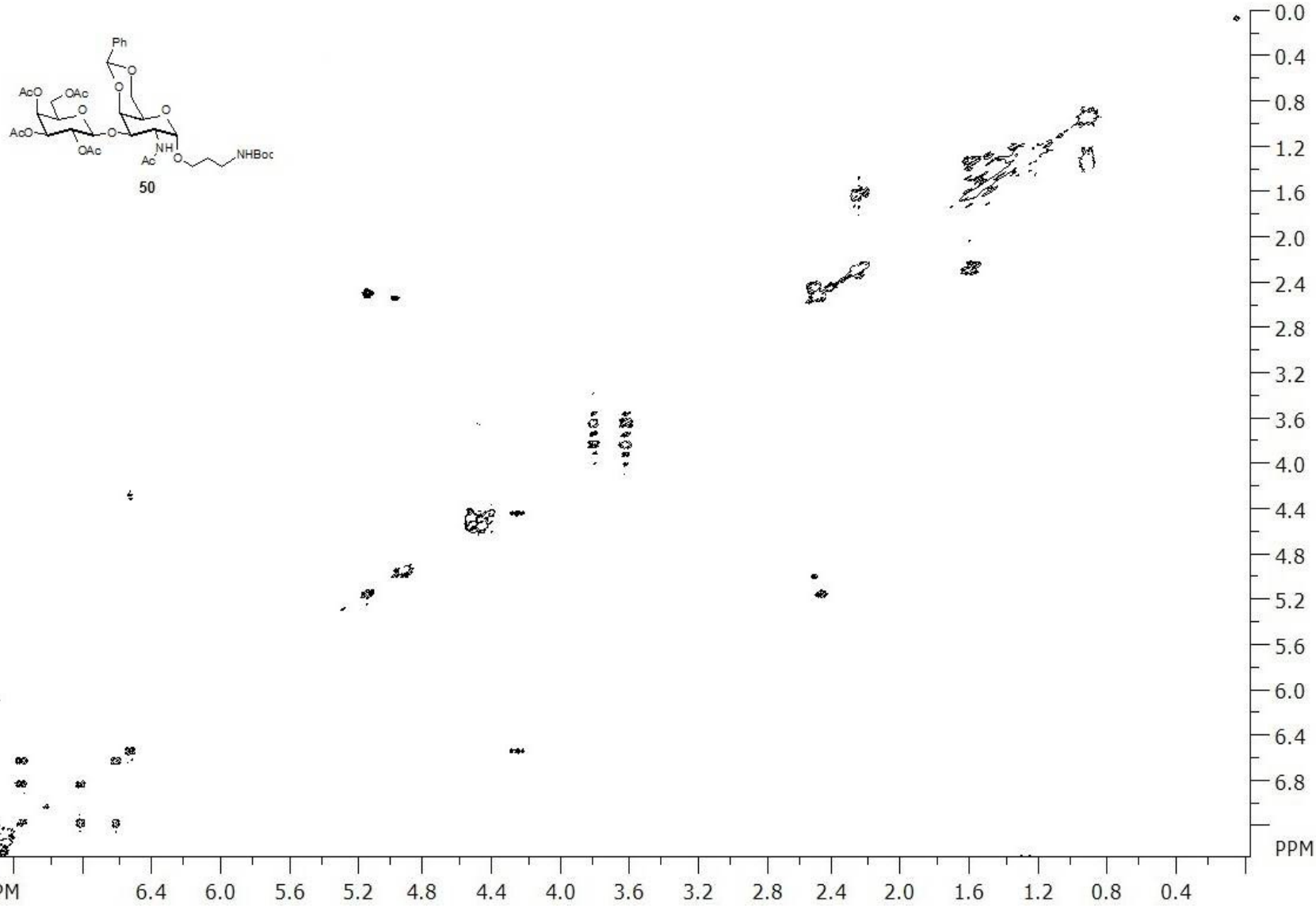
Ph
AcO
OAc
AcO
OAc
NH
Ac
NHBoc
50
0.0
0.4
0.8
1.2
1.6
2.0
2.4
2.8
3.2
3.6
4.0
4.4
4.8
5.2
5.6
6.0
6.4
6.8
PPM
PPM
6.4
6.0
5.6
5.2
4.8
4.4
4.0
3.6
3.2
2.8
2.4
2.0
1.6
1.2
0.8
0.4

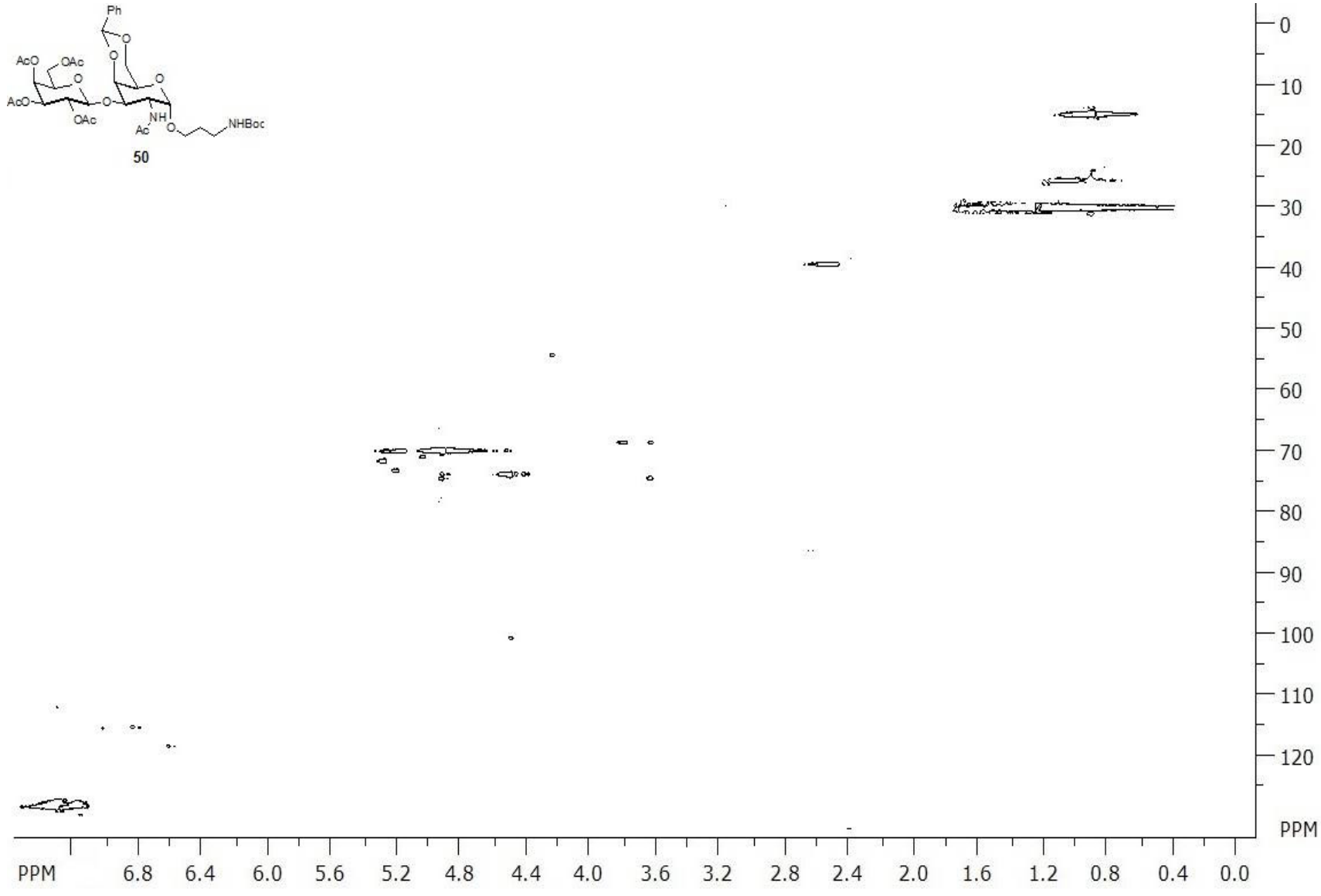
Ph
AcO
OAc
AcO
OAc
NH
Ac
NHBoc
50
0
10
20
30
40
50
60
70
80
90
100
110
120
PPM
PPM
6.8
6.4
6.0
5.6
5.2
4.8
4.4
4.0
3.6
3.2
2.8
2.4
2.0
1.6
1.2
0.8
0.4
0.0

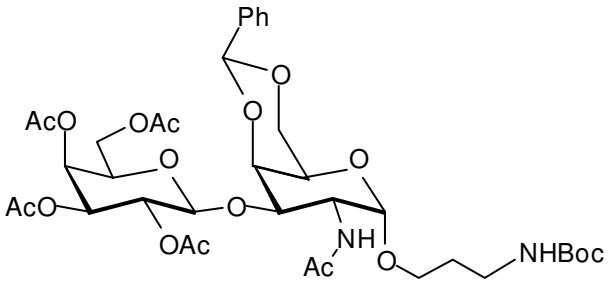

50

MALDI-MS (m/z) Calcd for $C_{37}H_{52}N_2O_{17}$ $[M + Na]^+$: 819.3164, found: 819.4091.

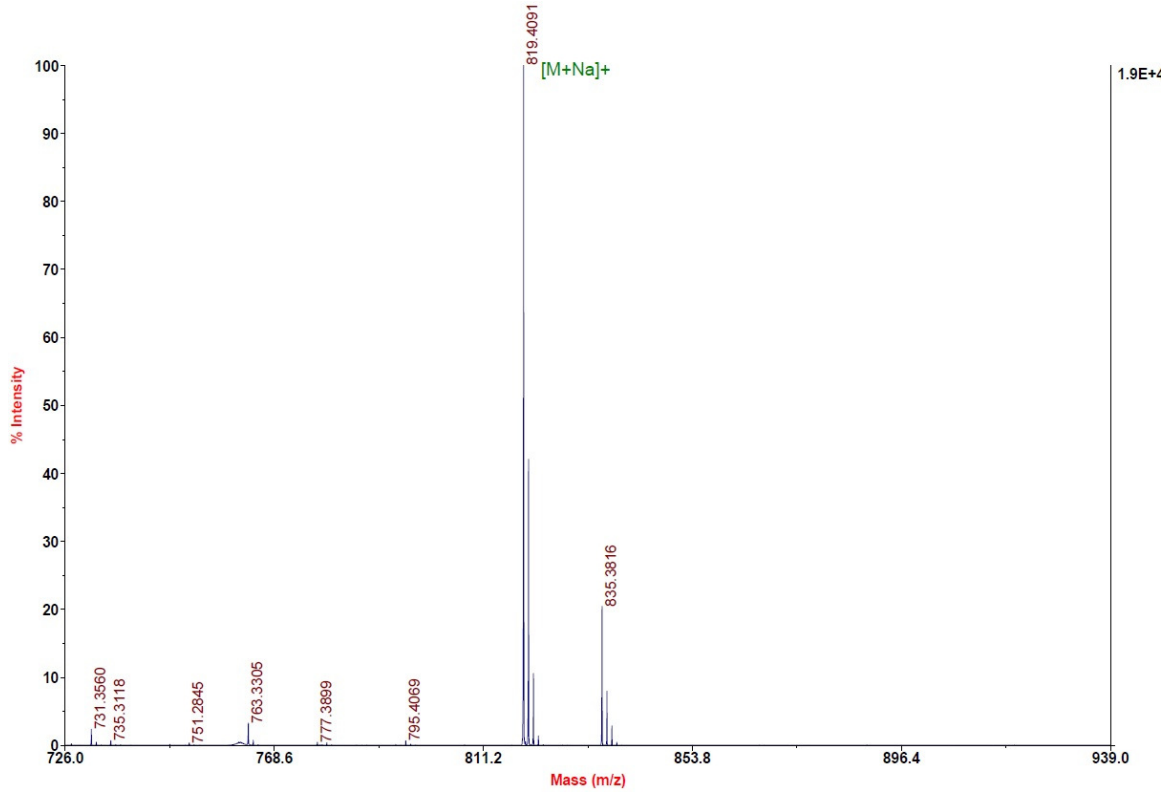

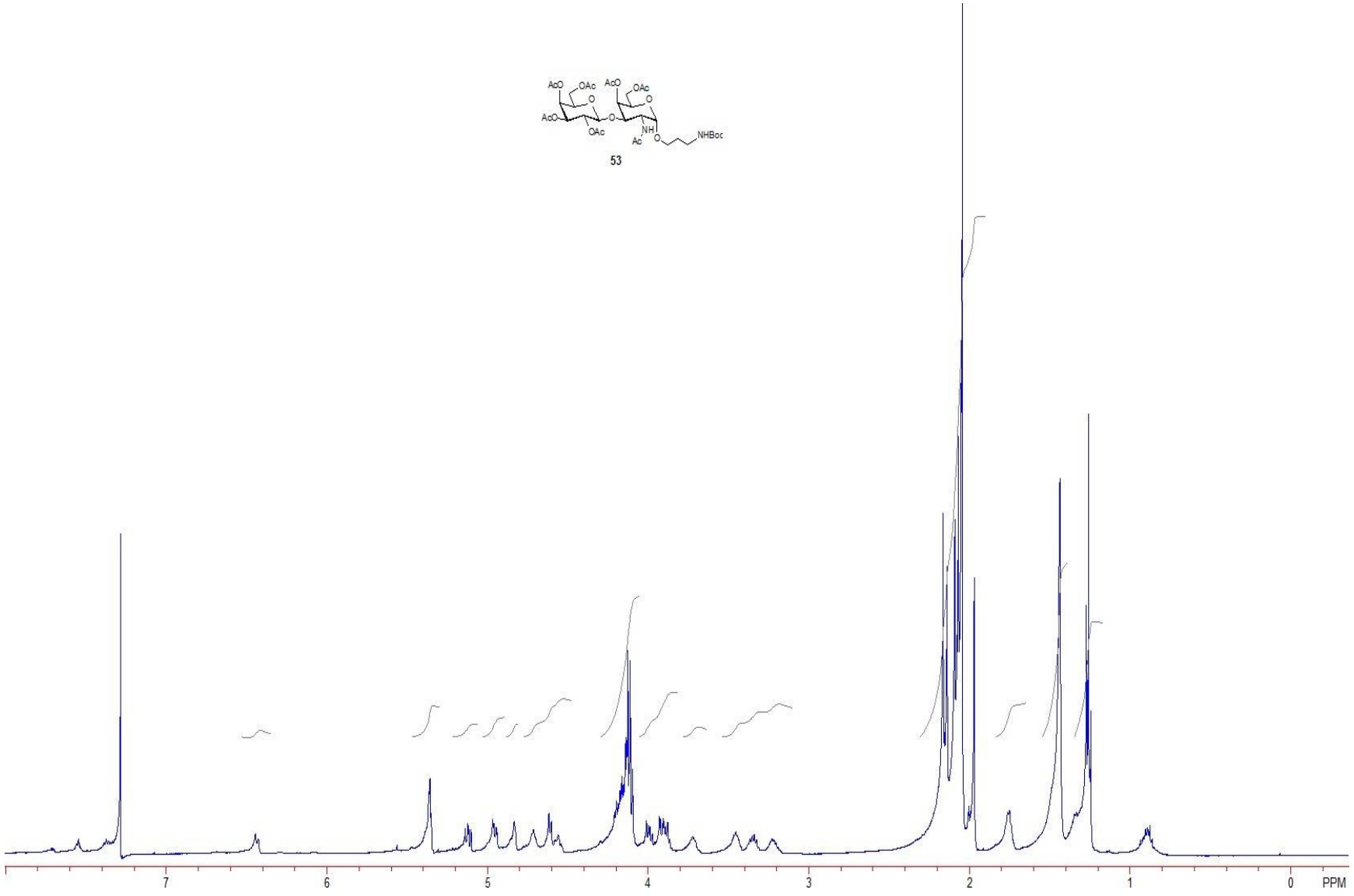
AcO
OAc
AcO
OAc
O
AcO
O
OAc
NH
Ac
O
NHBoc
53
7
6
5
4
3
2
1
0
PPM

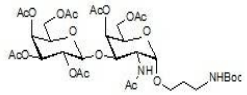

53

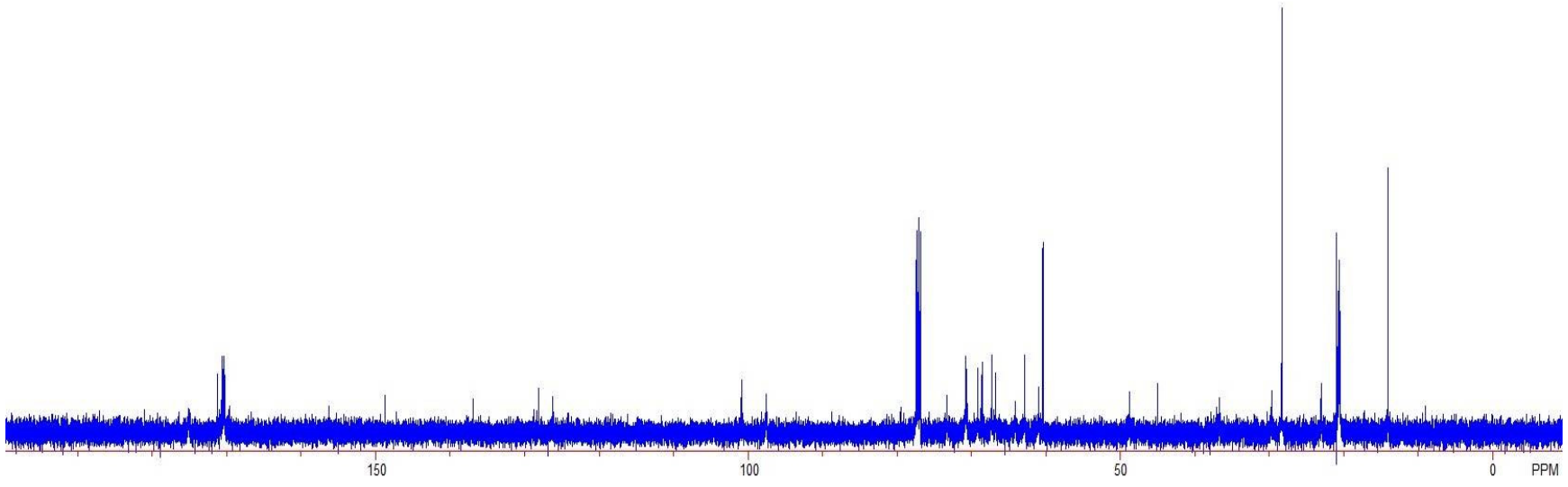

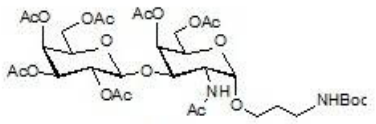
AcO
OAc
AcO
OAc
O
O
AcO
O
OAc
NH
Ac
O
NHBoc

53

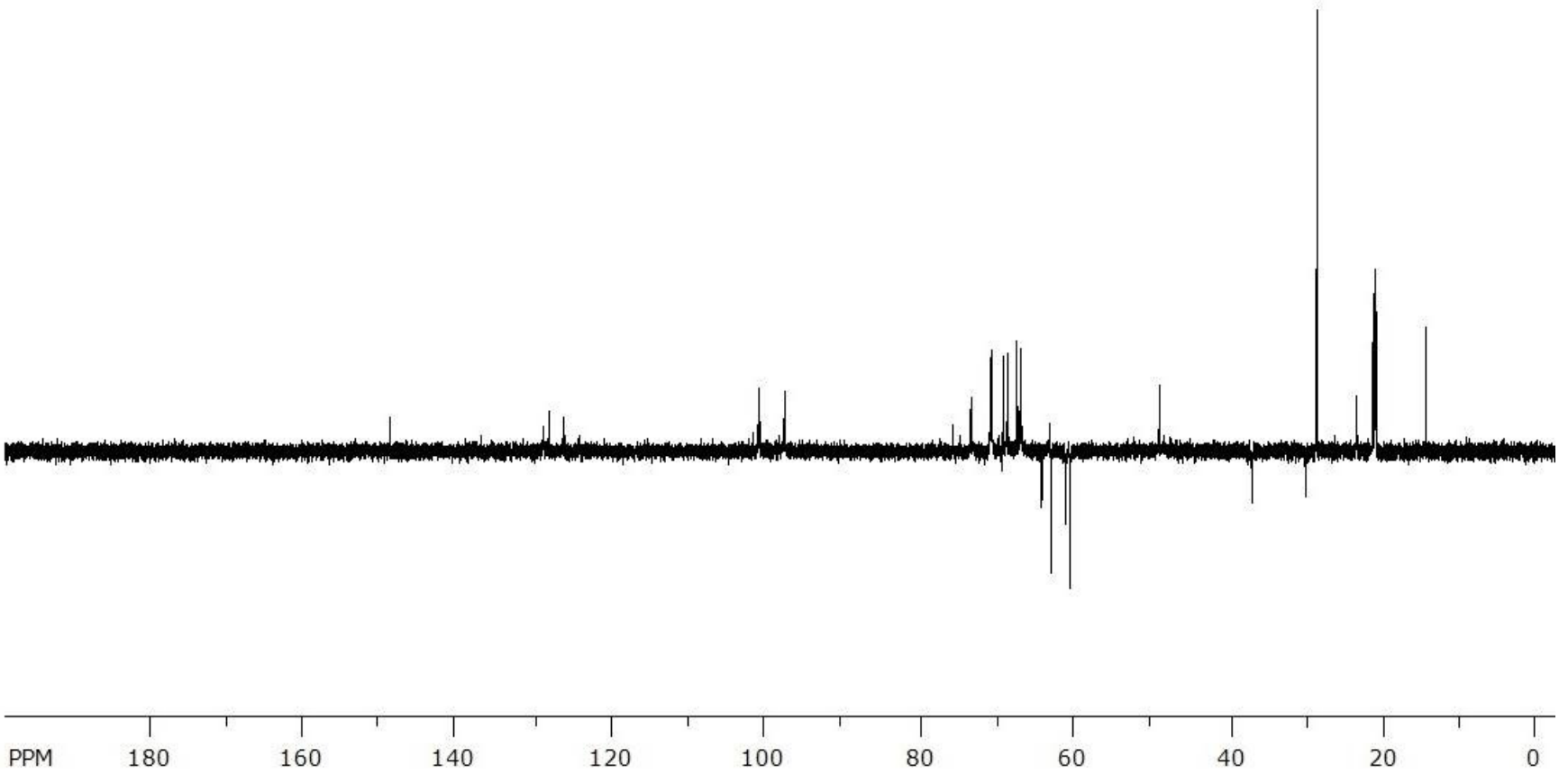
PPM
180
160
140
120
100
80
60
40
20
0

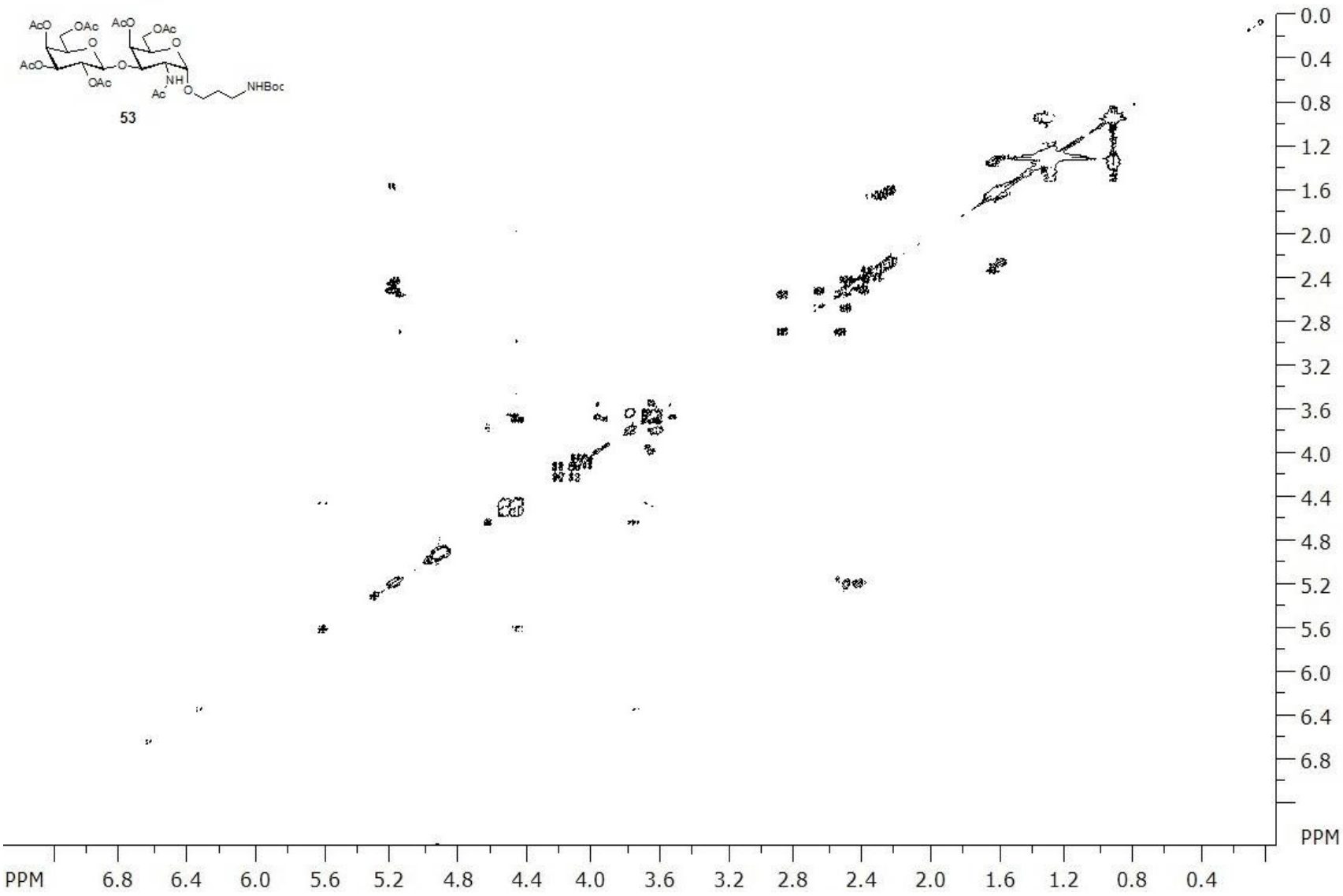
AcO
OAc
AcO
OAc
O
AcO
O
OAc
NH
Ac
O
NHBoc
53
0.0
0.4
0.8
1.2
1.6
2.0
2.4
2.8
3.2
3.6
4.0
4.4
4.8
5.2
5.6
6.0
6.4
6.8
PPM
PPM
6.8
6.4
6.0
5.6
5.2
4.8
4.4
4.0
3.6
3.2
2.8
2.4
2.0
1.6
1.2
0.8
0.4

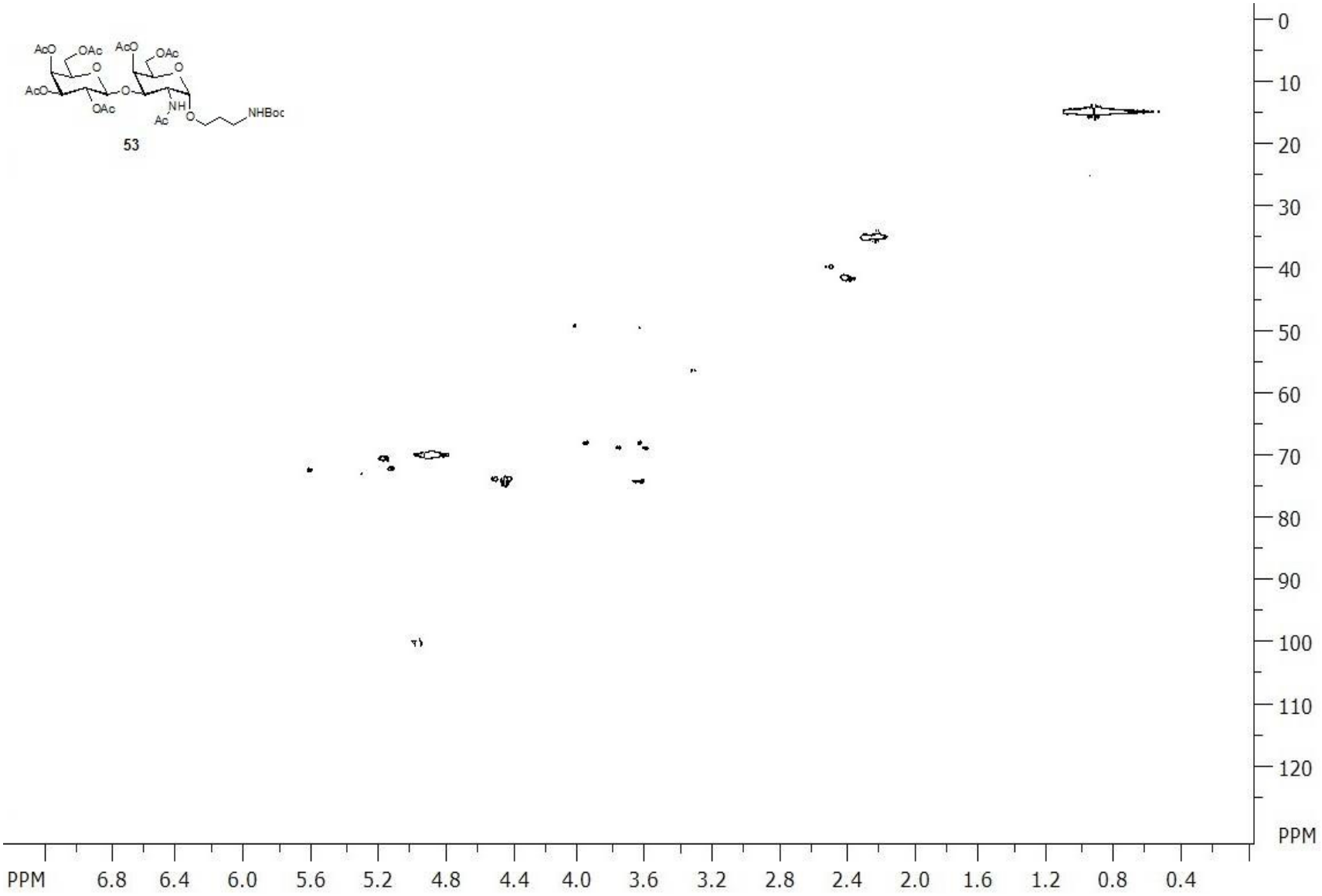
AcO
OAc
AcO
OAc
O
AcO
O
OAc
NH
Ac
O
NHBoc
53
0
10
20
30
40
50
60
70
80
90
100
110
120
PPM
PPM
6.8
6.4
6.0
5.6
5.2
4.8
4.4
4.0
3.6
3.2
2.8
2.4
2.0
1.6
1.2
0.8
0.4

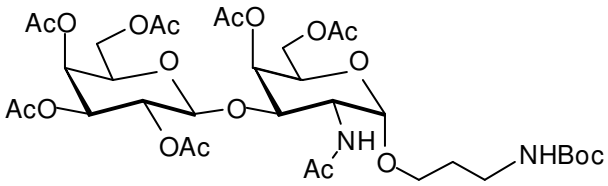

53

MALDI-MS (m/z) Calcd for $C_{34}H_{52}N_2O_{19}$ $[M + Na]^+$: 815.3062, found: 815.4035.

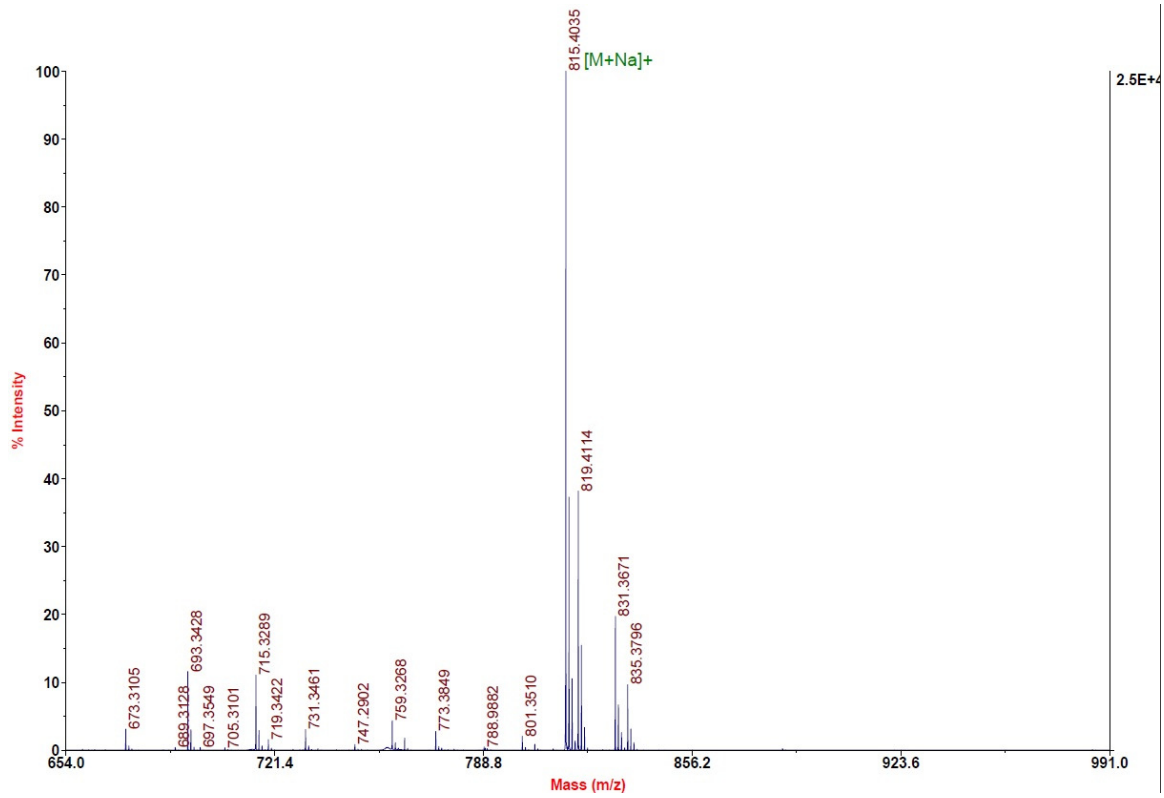

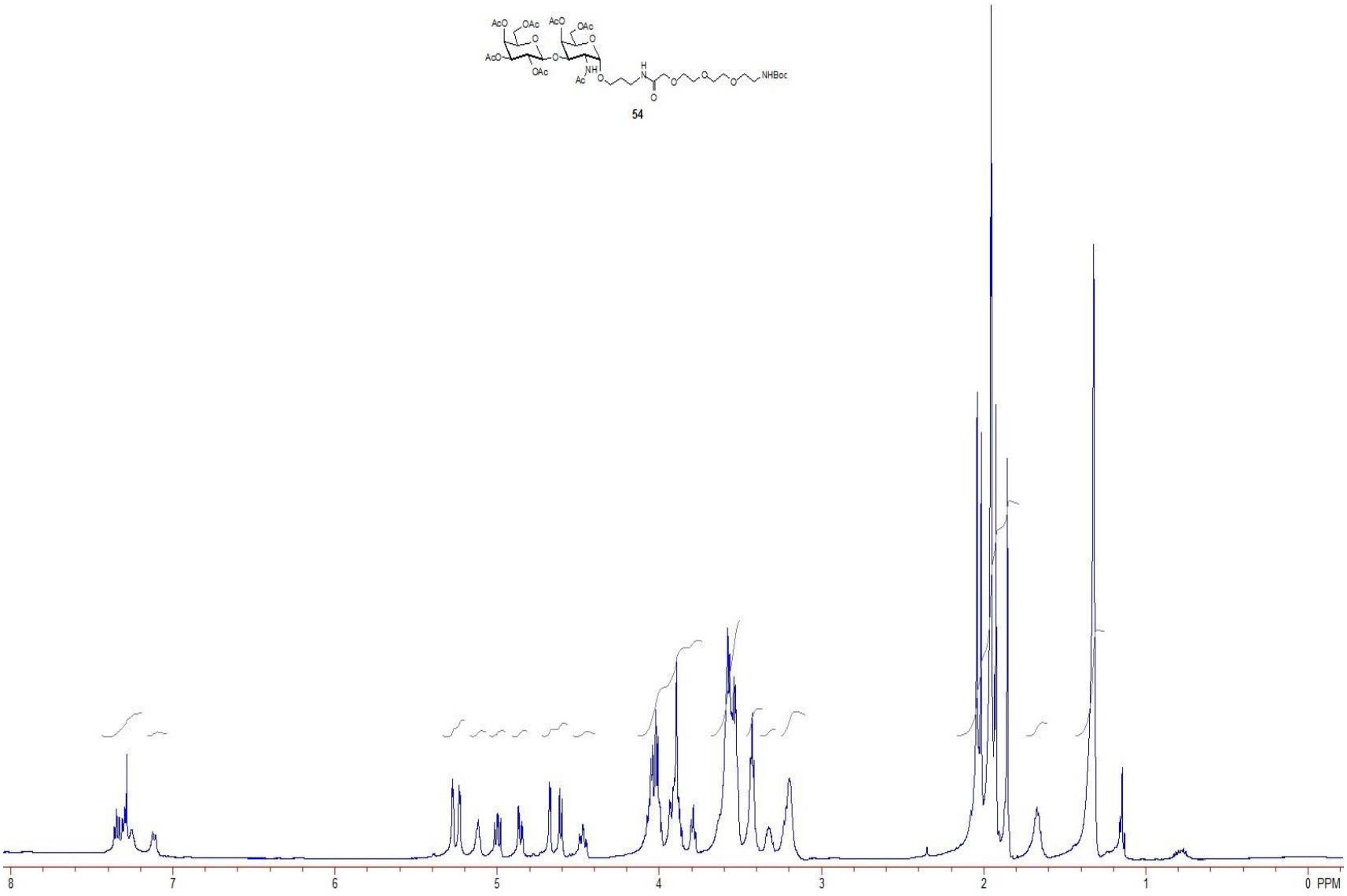
AcO
OAc
AcO
OAc
AcO
OAc
NH
Ac
H
N
O
O
O
O
O
NHBoc
54
8
7
6
5
4
3
2
1
0 PPM

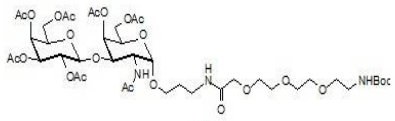

54

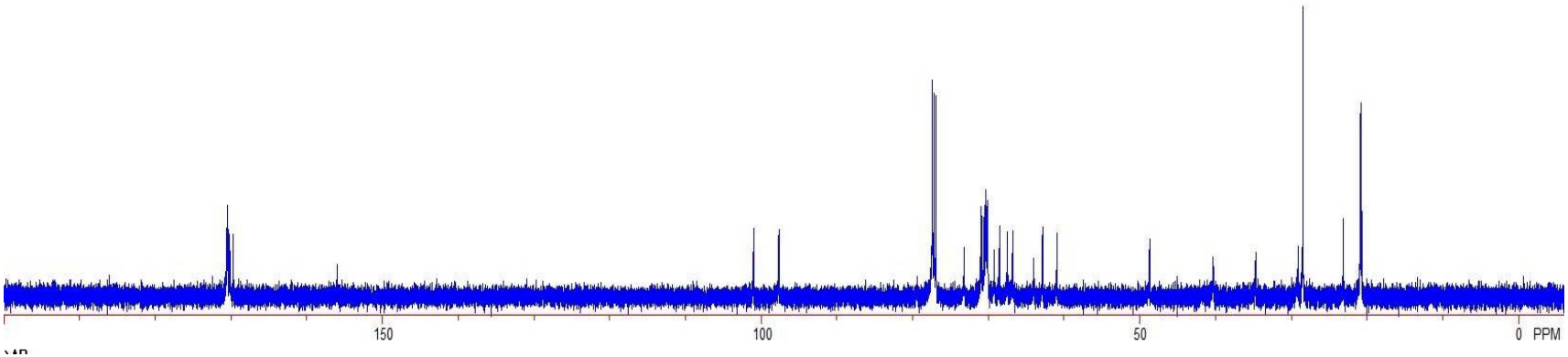

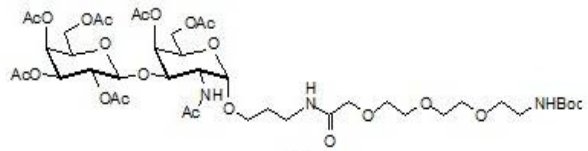
AcO
OAc
AcO
OAc
O
AcO
OAc
NH
Ac
O
H
N
O
O
O
O
NHBoc

54

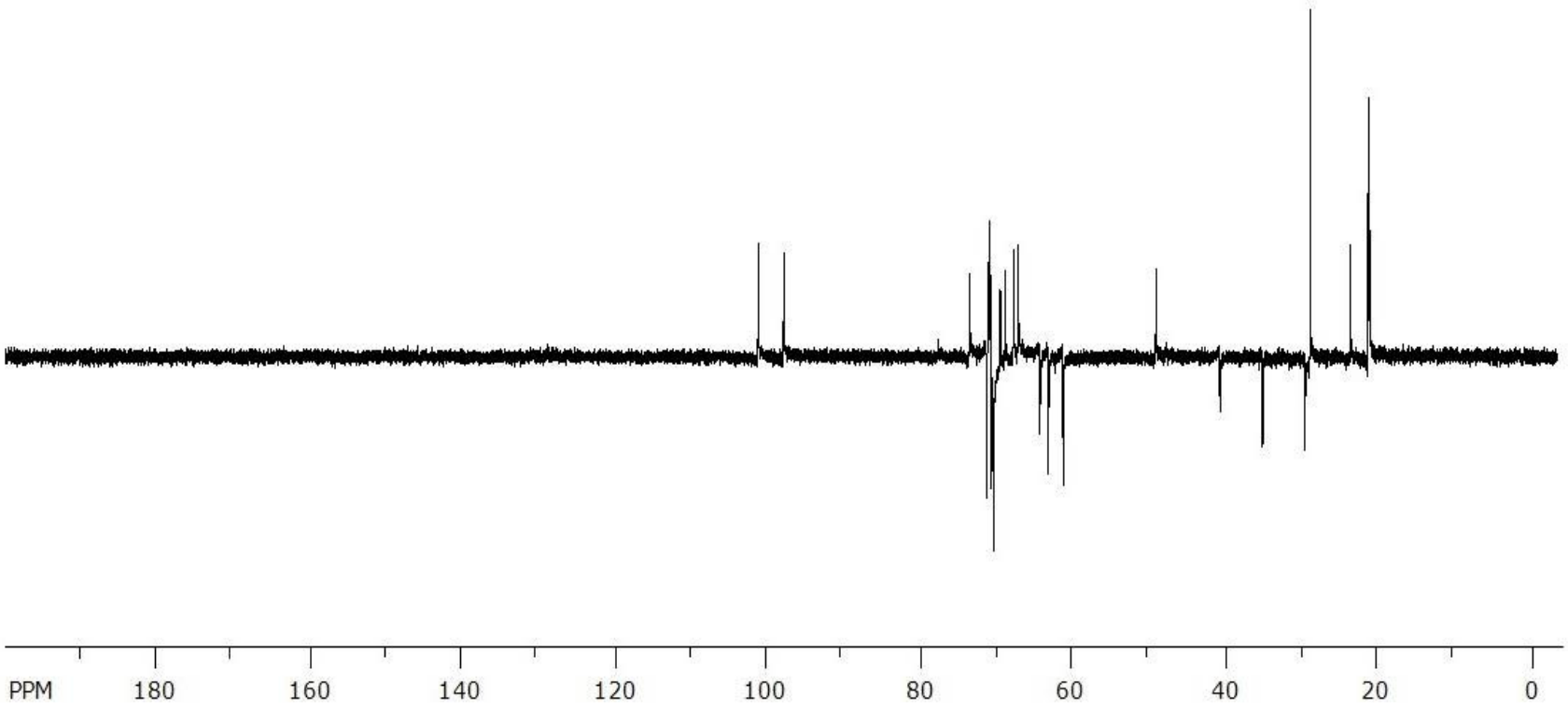
PPM
180
160
140
120
100
80
60
40
20
0

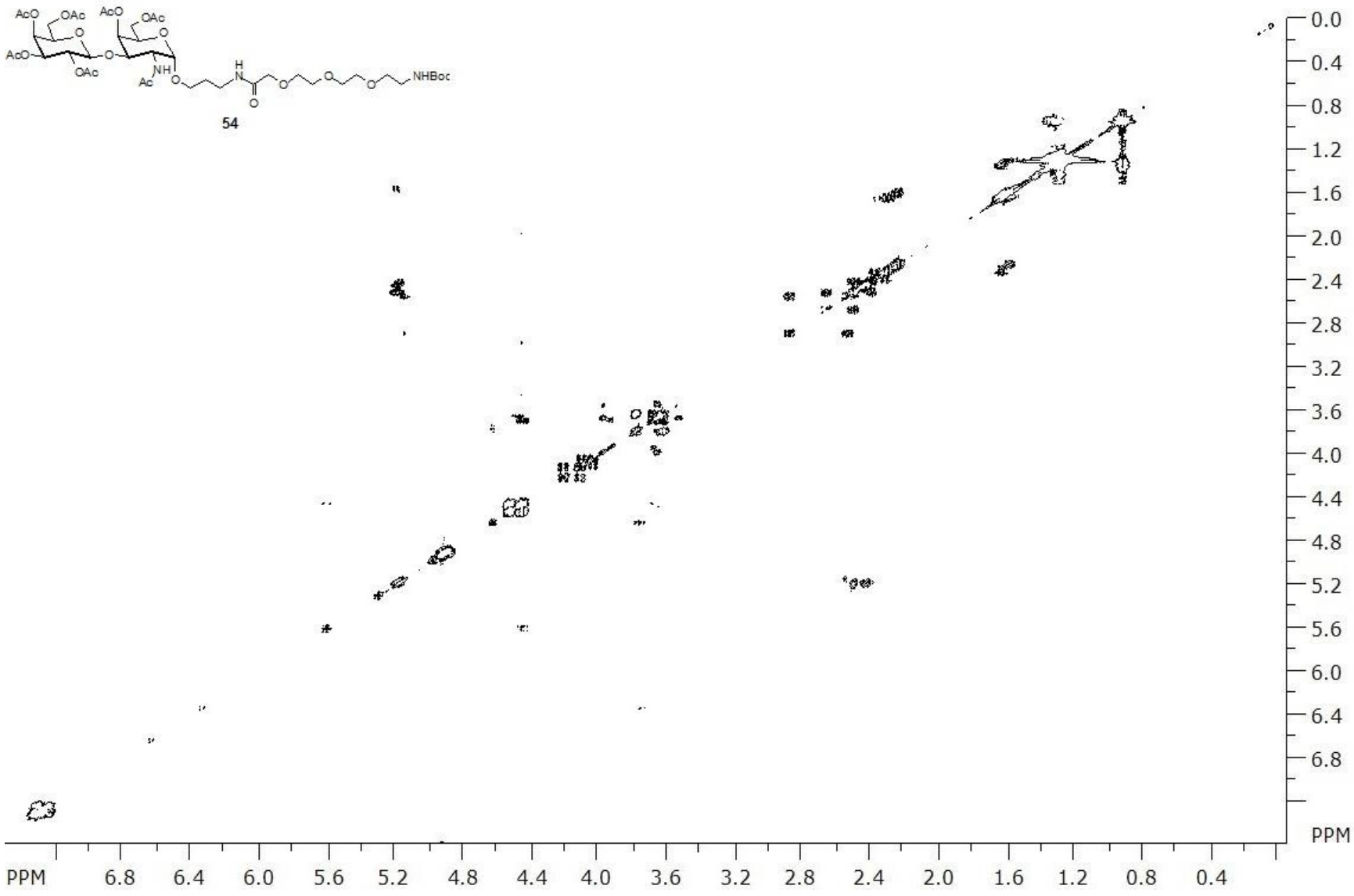
AcO
OAc
AcO
OAc
AcO
OAc
NH
Ac
H
N
O
O
O
O
O
NHBoc
54
0.0
0.4
0.8
1.2
1.6
2.0
2.4
2.8
3.2
3.6
4.0
4.4
4.8
5.2
5.6
6.0
6.4
6.8
PPM
PPM
6.8
6.4
6.0
5.6
5.2
4.8
4.4
4.0
3.6
3.2
2.8
2.4
2.0
1.6
1.2
0.8
0.4

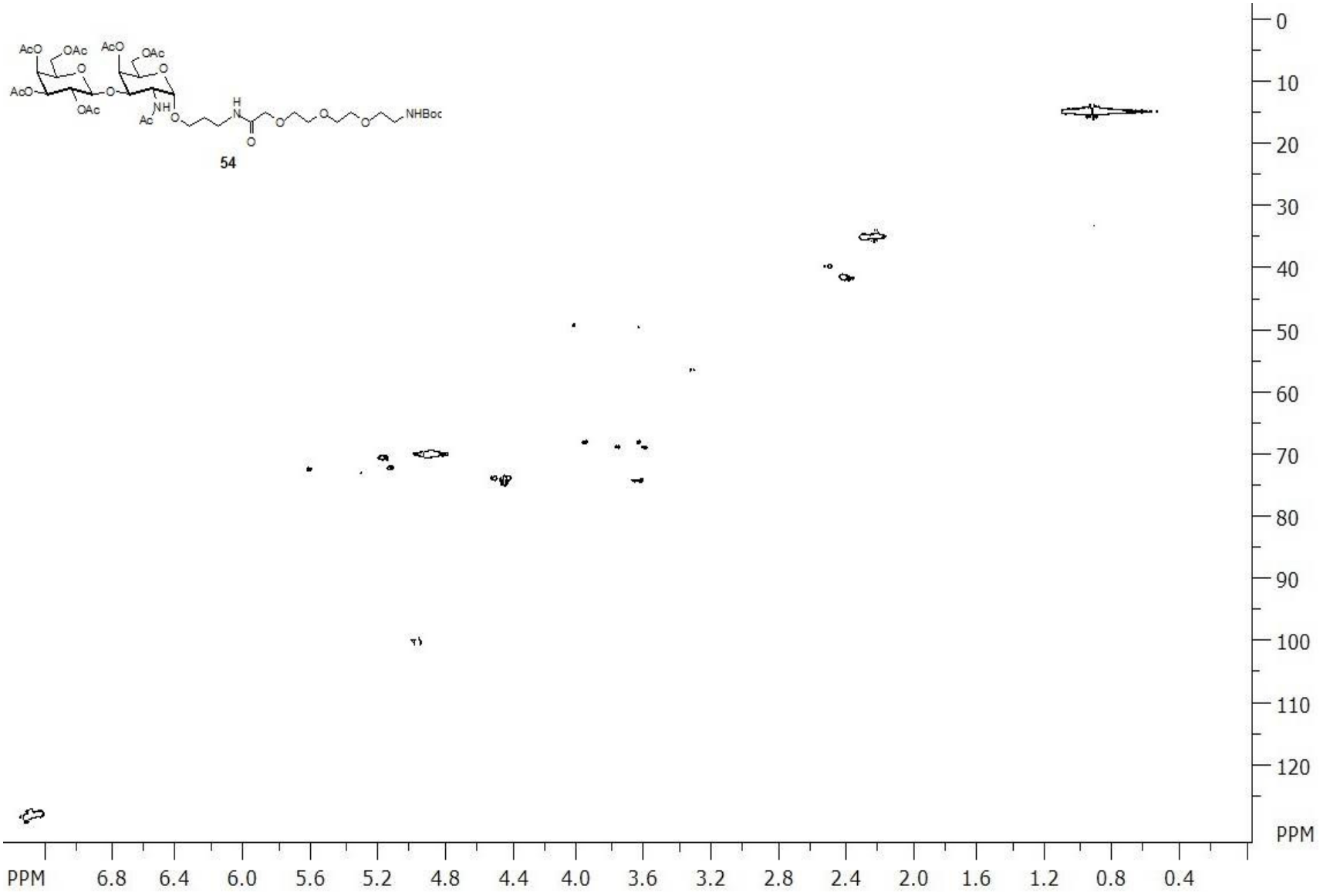
AcO
OAc
AcO
OAc
AcO
OAc
NH
Ac
H
N
O
O
O
O
O
NHBoc
54
0
10
20
30
40
50
60
70
80
90
100
110
120
PPM
PPM
6.8
6.4
6.0
5.6
5.2
4.8
4.4
4.0
3.6
3.2
2.8
2.4
2.0
1.6
1.2
0.8
0.4

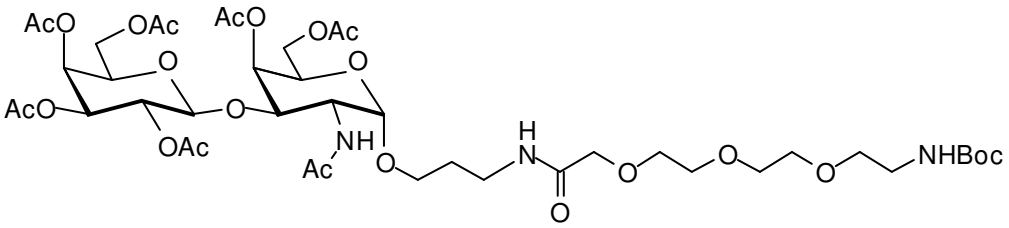

54

MALDI-MS (m/z) Calcd for $C_{42}H_{67}N_3O_{22}$ $[M + K]^+$: 1004.3853, found: 1004.5851.

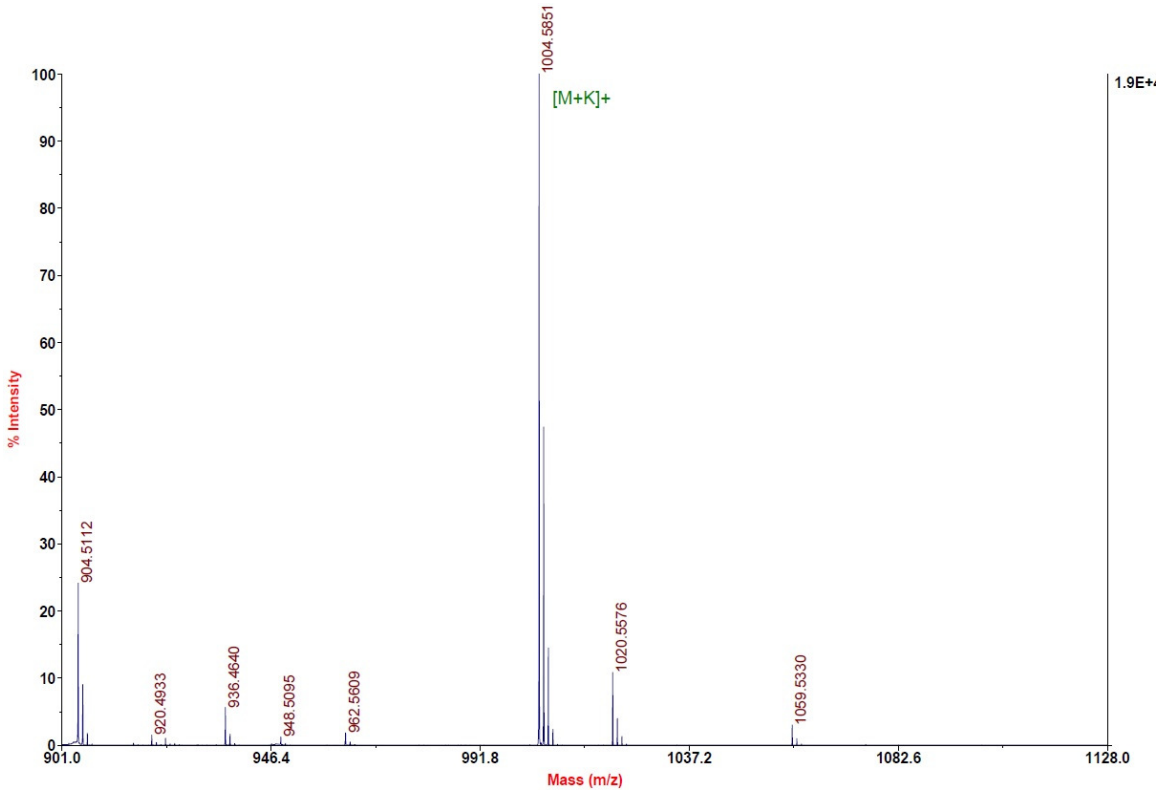

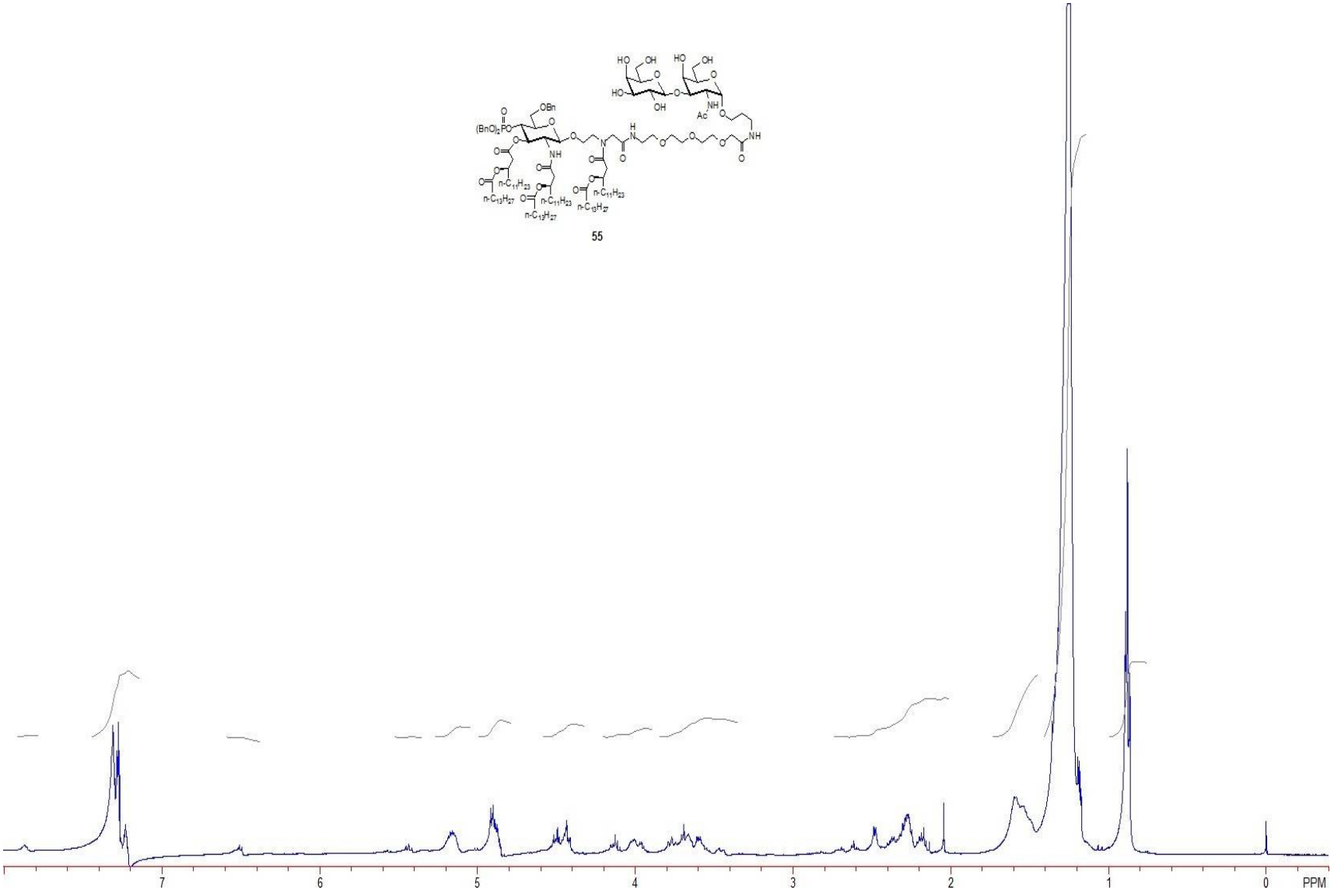
55
7
6
5
4
3
2
1
0
PPM

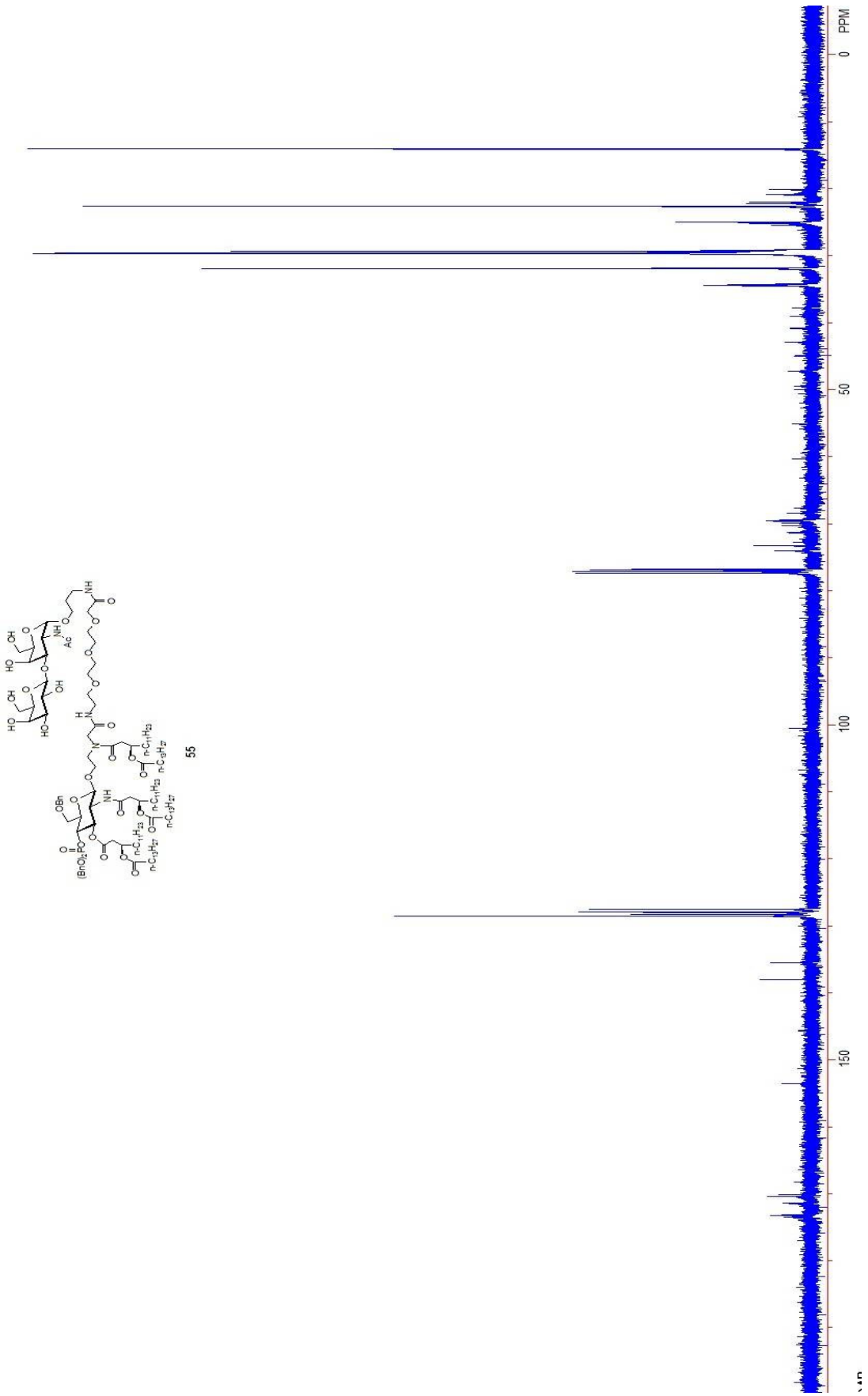
55
PPM
0
50
100
150

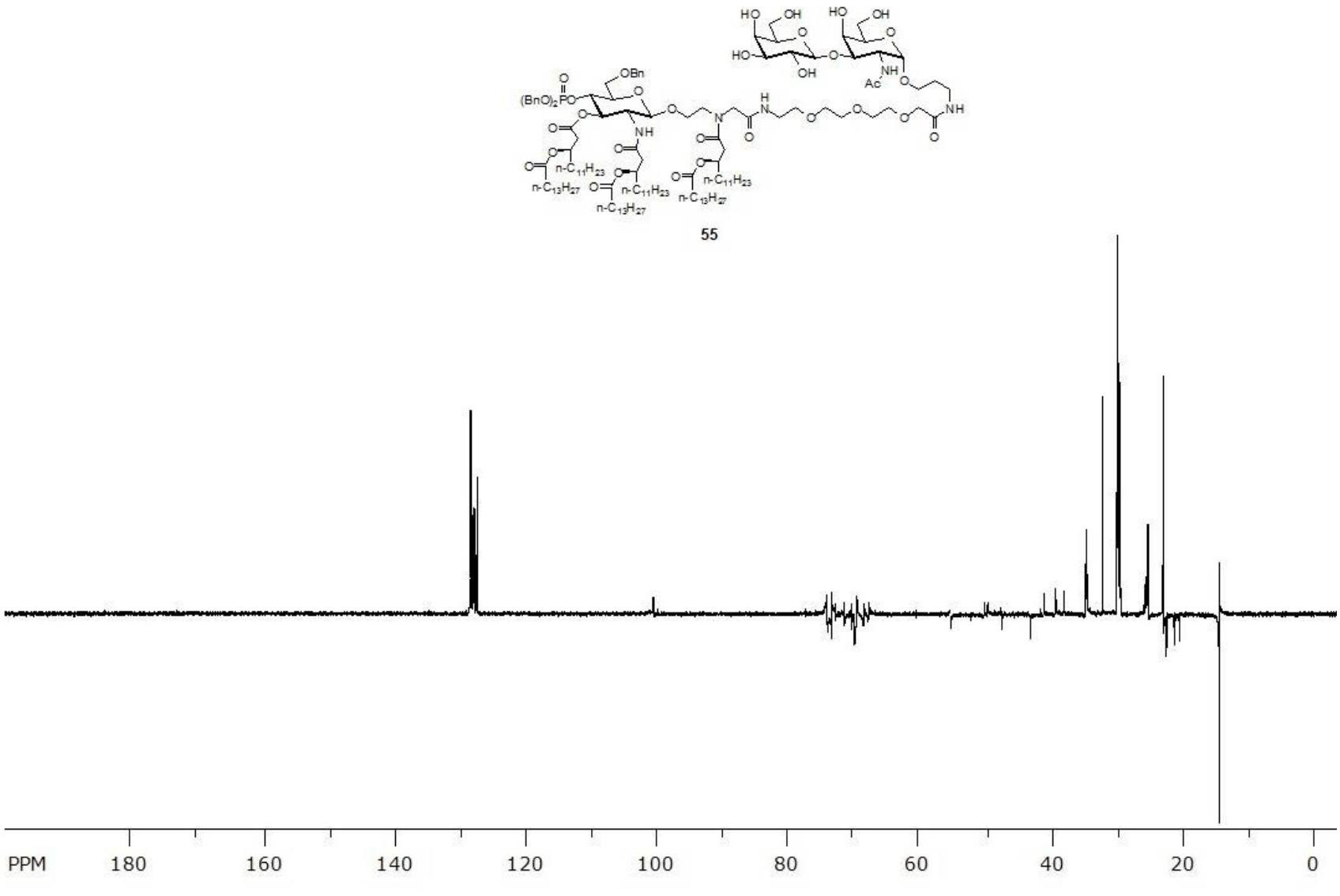
55
PPM
180
160
140
120
100
80
60
40
20
0

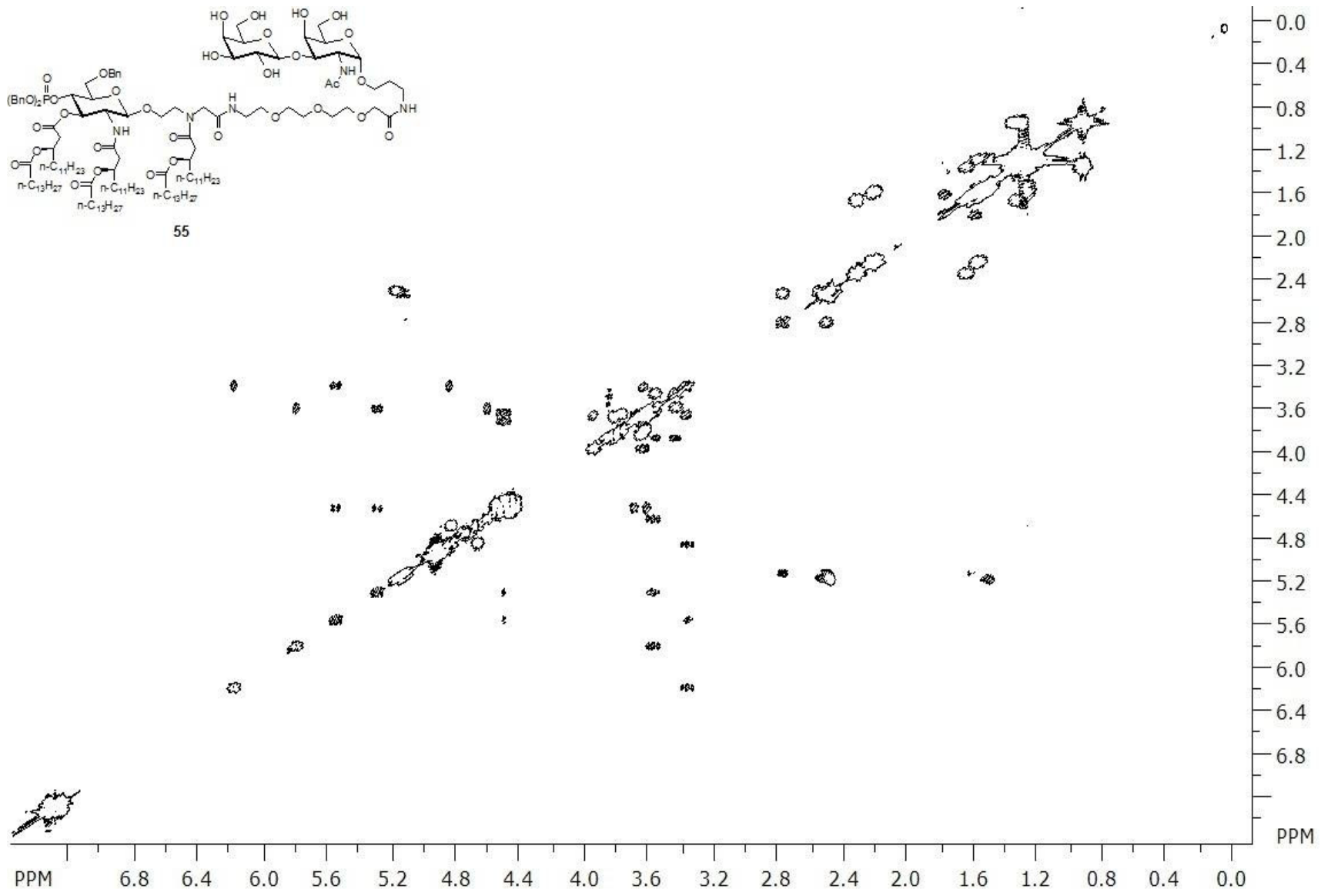
55
PPM
6.8
6.4
6.0
5.6
5.2
4.8
4.4
4.0
3.6
3.2
2.8
2.4
2.0
1.6
1.2
0.8
0.4
0.0

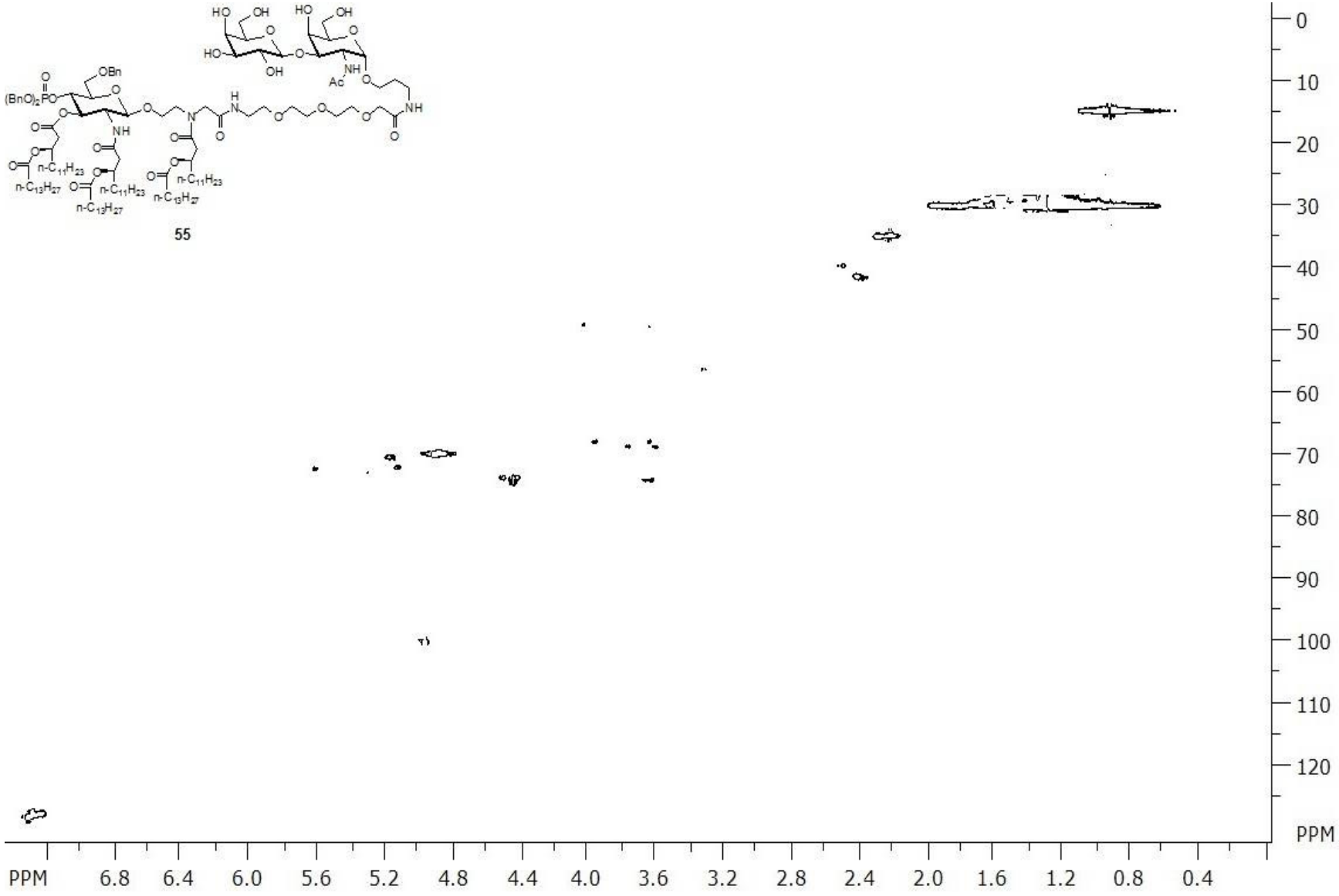
55
PPM
6.8
6.4
6.0
5.6
5.2
4.8
4.4
4.0
3.6
3.2
2.8
2.4
2.0
1.6
1.2
0.8
0.4
0
10
20
30
40
50
60
70
80
90
100
110
120
PPM

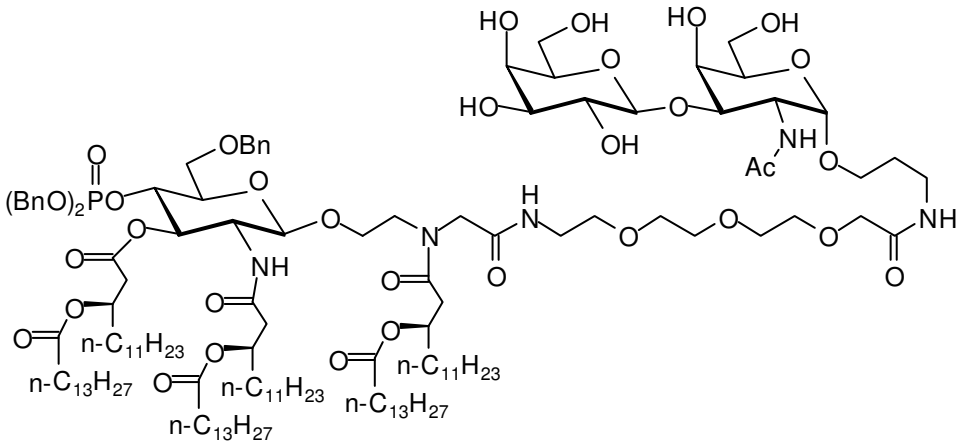

55

MALDI-MS (m/z) Calcd for $C_{140}H_{240}N_5O_{33}P$ $[M + Na]^+$: 2573.6891, found: 2573.6724.

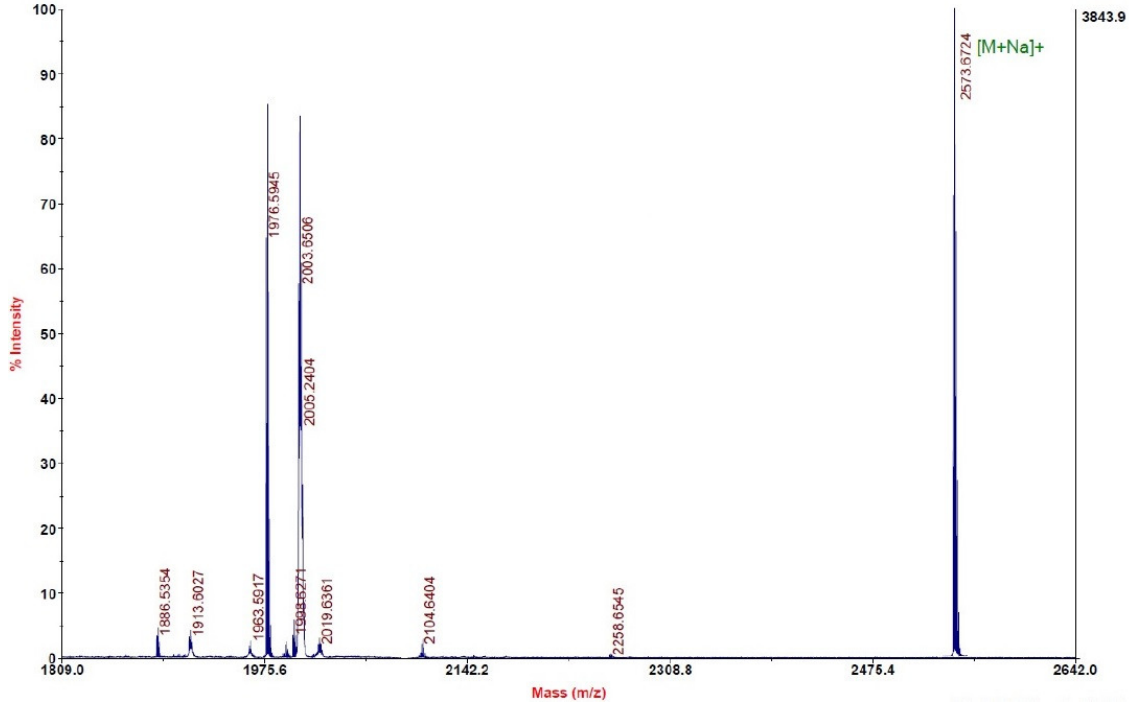

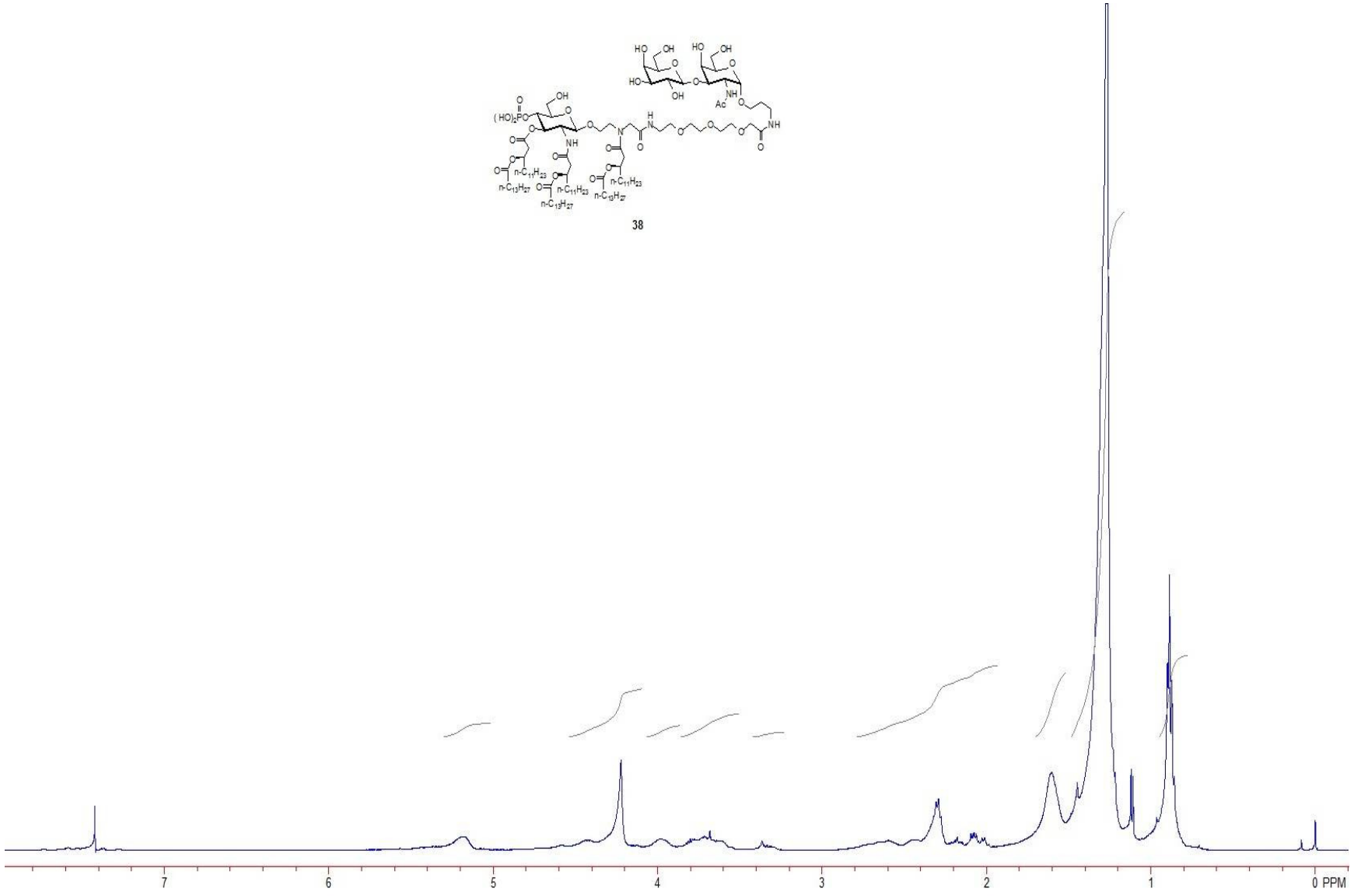
38
7
6
5
4
3
2
1
0 PPM

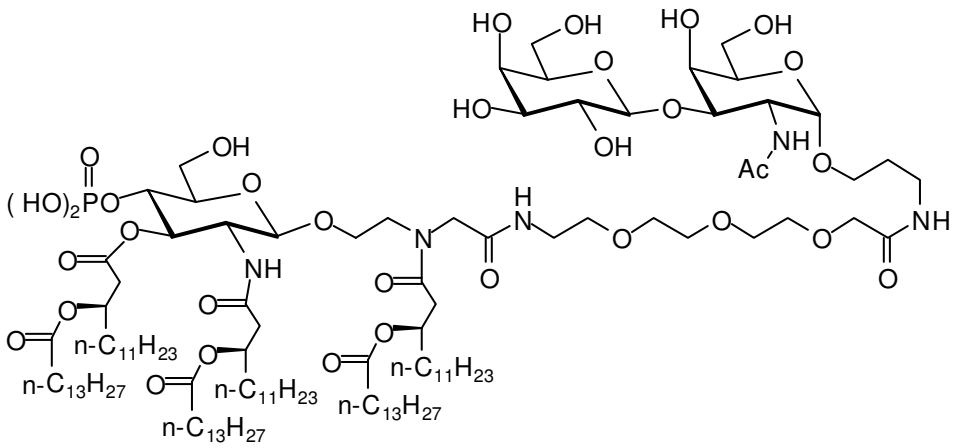

38

MALDI-MS (m/z) Calcd for $C_{119}H_{222}N_5O_{33}P$ $[M + Na]^+$: 2303.5483, found: 2303.5316.